Dabir S. Viswanath
Tushar K. Ghosh
Veera M. Boddu

Emerging Energetic Materials: Synthesis, Physicochemical, and Detonation Properties

Springer

Emerging Energetic Materials: Synthesis, Physicochemical, and Detonation Properties

Dabir S. Viswanath · Tushar K. Ghosh
Veera M. Boddu

Emerging Energetic Materials: Synthesis, Physicochemical, and Detonation Properties

Springer

Dabir S. Viswanath
Nuclear Science and Engineering Institute
University of Missouri
Columbia, MO
USA

and

Nuclear Engineering Teaching Laboratory
Cockrell School of Engineering
Austin, TX
USA

Tushar K. Ghosh
Nuclear Science and Engineering Institute
University of Missouri
Columbia, MO
USA

Veera M. Boddu
Environmental Processes Branch
US Army Engineer Research and Development Center
Champaign, IL
USA

and

Plant Polymer Research Unit, National Center for Agricultural Utilization Research
Agricultural Research Service, US Department of Agriculture
Peoria, IL
USA

ISBN 978-94-024-1199-7 ISBN 978-94-024-1201-7 (eBook)
https://doi.org/10.1007/978-94-024-1201-7

Library of Congress Control Number: 2017951437

© US Government (outside the USA) 2018
This work is subject to copyright. All rights are reserved by the Publisher, whether the whole or part of the material is concerned, specifically the rights of translation, reprinting, reuse of illustrations, recitation, broadcasting, reproduction on microfilms or in any other physical way, and transmission or information storage and retrieval, electronic adaptation, computer software, or by similar or dissimilar methodology now known or hereafter developed.
The use of general descriptive names, registered names, trademarks, service marks, etc. in this publication does not imply, even in the absence of a specific statement, that such names are exempt from the relevant protective laws and regulations and therefore free for general use.
The publisher, the authors and the editors are safe to assume that the advice and information in this book are believed to be true and accurate at the date of publication. Neither the publisher nor the authors or the editors give a warranty, express or implied, with respect to the material contained herein or for any errors or omissions that may have been made. The publisher remains neutral with regard to jurisdictional claims in published maps and institutional affiliations.

Printed on acid-free paper

This Springer imprint is published by Springer Nature
The registered company is Springer Science+Business Media B.V.
The registered company address is: Van Godewijckstraat 30, 3311 GX Dordrecht, The Netherlands

Preface

This monograph summarizes science and technology of select new generation high-energy and insensitive explosives. There is an enormous amount of information being generated and published in the open literature on different areas pertaining to civilian and military uses of these materials. The objectives of this monograph are to provide the professionals with comprehensive information on synthesis, physicochemical, and detonation properties of the explosives. Potential technologies applicable for treatment of contaminated waste streams from manufacturing facilities and environmental matrices are also included. This book provides the reader an insight into the theoretical and empirical models and experimental techniques currently being developed in the field of energetic materials. The material in this book should assist researchers involved in both sensitive and insensitive energetic materials, a program of the United States Department of Defense.

Physicochemical Measurements on Insensitive Munitions Compounds for Environmental Applications—Understanding the environmental impact of energetic materials is critical for their acceptance for use in weapons systems. Predicting their environmental distribution, biotransformation, and determining potential treatment processes assist both decision-makers and scientists in the development process. Combustion of explosives involves complex physicochemical changes and reaction mechanisms. Therefore, there is a need to have knowledge of accurate and good quality data on properties such as solubility, toxicity, enthalpies of formation and combustion, thermal properties, and a host of other properties. We have tried to put together as many properties available in the published literature. Since extensive testing to design high-energy insensitive munitions and formulations are expensive, this monograph should help researchers who use multiphysics modeling programs to achieve high-energy materials and formulations. Thermophysical properties collected in this monograph should be useful in 2-D numerical codes that will simulate slow and fast cook-off, and codes that simulate detonation properties.

This monograph has 11 chapters, and each chapter is devoted to one particular compound with the exception of Chap. 1. Chapter 1 deals with the measurements and estimations of several physical properties important to the characterization, screening, and utilization of energetic materials. It outlines different experimental methods of measurement of physical properties, and their limitations.

The remaining ten chapters are devoted to a set of new emerging energetic materials. Each chapter considers one energetic compound and enumerates the synthesis methods, structure, physical and chemical properties, decomposition and destruction, detonation characteristics, toxicity, explosive formulations, and detection of that compound. The compounds considered in this monograph are as follows: hexanitrohexaazaisowurtzitane (HNIW, CL-20), 1,1-diamino-2,2-dinitro ethylene (DADE, FOX-7), 2,4-dinitroanisole (DNAN), 5-nitro-2,4-dihydro-3H-1,2, 4-triazole-3-one (NTO), 1,3,3-trinitroazetidine (TNAZ), triacetone triperoxide (TATP), 1,3,5-triamino-2,4,6-trinitrobenzene (TATB), 1-azido-2-nitro-2-azapropane (ANAP), N-methyl-4-nitroaniline (MNA), and hexanitrostilbene (HNS). These compounds represent a cross section of sensitive high energetic materials such as TATP and insensitive energetic compounds that are used in different applications.

We have tried to present the current literature on these compounds, and bring together material scattered in different publications. The material presented in this monograph should supplement material found in several other books such as The Chemistry of Explosives by J. Akhavan, Propellants and Explosives by N. Kubota, Organic Chemistry of Explosives by J.P. Agrawal and R. Hodgson, High Energy Materials by J.P. Agrawal, Advanced Processing Technologies for Next-Generation Materials by T.M. Klapotke, Liquid Explosives by J. Liu, and others.

With great appreciation, we take this opportunity to thank the editors at Springer. The authors are thankful to the publishers for agreeing to our repeated requests to postpone submission of the manuscript. Special thanks are extended to Ms. Cynthia Feenstra for her coordination and patience in extending the deadline for submitting the manuscript. We also thank our family members for their support for realization of this book.

Columbia, MO, USA Dabir S. Viswanath
Columbia, MO, USA Tushar K. Ghosh
Peoria, IL, USA Veera M. Boddu

Contents

Chapter 1
Properties of Insensitive Energetic Materials and Their Measurement

Abstract The development of insensitive energetic materials with stability, high performance, reliability, safety, and low toxicity requires measurement and prediction of thermophysical and thermochemical properties. The measurement and estimation of properties such as the enthalpy of formation, density, detonation velocity, detonation pressure and sensitivity are used to screen potential energetic candidates. Experimental data are also needed to test prediction methods and molecular models. This chapter outlines experimental methods to measure some of the important properties. Different methods of determining a property and the theory associated have been outlined.

1.1 Introduction

There are a number of chemical and physical properties that are important to energetic materials [EM] for their characterization and comparison with each other, and a set of different properties particularly important to insensitive energetic materials [IEM]. Energetic materials by definition are high energy materials that detonate on shock, pressure, heat, and/or combustion. EM falls into three categories: propellants, explosives and pyrotechnics. A particular chemical may fall into one or the other category or more than one category. Explosives are further classified as primary and secondary explosives based on their susceptibility to initiation. Primary explosives are highly susceptible to detonation whereas secondary explosives are used as main charges. Secondary explosives can be further divided into two categories: melt-cast and plastic-bonded.

The design of future IEM and EM materials requires a sound knowledge of the chemistry and properties of the existing materials, since most of the new materials will be developed using the template of the existing materials. For instance, as the name itself suggests, energetic materials possess very high energy, and this can be made available if the material has a high enthalpy of formation. The use of existing IEM and EM materials to design and build weapons systems also requires a sound knowledge of several properties to achieve better performance, reduced

D.S. Viswanath et al., *Emerging Energetic Materials: Synthesis, Physicochemical, and Detonation Properties*, https://doi.org/10.1007/978-94-024-1201-7_1

vulnerability during transportation, reduced environmental impact in its manufacture and disposal, better shelf life, and their loading and packing into weapons delivery systems. It is therefore of interest to know the important physical and chemical properties of energetic materials, their experimental determination and prediction.

The main user of most of the explosives in the U.S. is the Department of Defense (DoD), which has developed standards and protocols for the measurement of various properties of explosives to qualify for their use by all departments and agencies under the DoD. These standards are given in "Department of Defense Test method Standard: Safety and Performance Tests for the Qualification of Explosives (High Explosives, Propellants, and Pyrotechnics), MIL-STD-1751A, 11 December 2001, Superseding MIL-STD-1751 (USAF), 20 August 1982 [1]. These qualifying properties and test procedures are also given in the implementing document for NATO STANAG 4170, "Principles and Methodology for the Qualification of Explosive Materials for Military Use," which has associated with it NATO Allied Ordnance Publication #7 (AOP-7), "Manual of Tests for the Qualification of Explosive Materials for Military Use" [2]. Certain test methods also implement NATO STANAGsAs. The test methods are arranged in groups according to the qualification data category. The numbering protocols for the groups are given in Table 1.1.

It may be noted that test groups under 1050, 1080, and 1110 are deleted from the current version.

Table 1.1 Numerical index of test methods (MIL-STD-1751A)

Test group	Qualification data category
1010	Impact sensitivity
1020	Friction sensitivity
1030	Electrostatic discharge sensitivity
1040	Explosive shock sensitivity
1060	Stability (Constant Temperature)
1070	Stability (Variable Temperature)
1090	Critical diameter
1100	Detonation velocity
1120	Flash point
1130	Detonability of fuel-air explosives
1140	Minimum pressure for vapor ignition
1150	Ignition sensitivity

1.2 Experimental Methods

The definition of some of these properties and their experimental determination are discussed in the following sections. The properties of interest are:

- Melting point (ASTM E794)
- Boiling point (ASTM D7169–11)
- Critical Properties
- Density (ASTM A572/A572 M–13a)
- Dipole moment (ASTM D3132-84(1996))
- Enthalpy of vaporization (ASTM E2071–00(2010))
- Enthalpy of formation ASTM D4612–08, ASTM D4809–13
- Solubility (ASTM E1148–02(2008), ASTM D1696-95(2011), ASTM D1110–84(2013), ASTM D7553–10
- Detonation velocity ASTM D2541–93(2001), ASTM D2541–93, ASTM D2539–93
- Detonation pressure
- Volatility and vapor pressure ASTM D5842–04(2009), ASTM D1837–11, ASTM D323–08
- Brisance UNE 31023:1994,
- Volume of products of explosion ASTM E1248–90(2009), ASTM E1226–12a
- Power, performance, and strength, ASTM D149–09(2013)
- Sensitivity and sensitivity to initiation ASTM D6600–00
- Decomposition ASTM E1641–13, ASTM E2550–11, ASTM D7876–13, ASTM D2879–10
- Detonation D-4814 (previously D-439), ASTM D-439/D-4814/EN228
- Toxicity (ASTM E1706)

1.3 Melting Point

The temperature at which a solid is in equilibrium with its liquid phase is called the **melting point**. Classical techniques can be used to determine melting point except for those materials which are highly sensitive, such as triacetone triperoxide (TATP). A common method for determining the melting point is the capillary tube method. In this method, fine powder of the compound is packed into the capillary tube to a depth of 1–2 mm. The capillary tube containing the sample is heated slowly, and the temperature at which the sample starts melting is noted. Often times, the melting of the compound is spotted visually. Several devices are available to measure melting points. These are: Thiele tube, Thomas-Hoover apparatus, and Mel-Temp system.

1.3.1 Thiele Tube

A Thiele tube for measurement of melting point is shown in Fig. 1.1. A silicon or mineral oil is used in the Thiele tube as the heat transfer medium and to maintain a constant temperature. The tube is filled to the base of the neck with oil. The capillary tube containing the sample is attached to a thermometer so that an accurate temperature measurement is obtained. The side arm of the Thiele tube is heated at a slow rate. The melting point is determined through visual observation. The Thiele tube can be used to measure melting point up to a temperature of 250 °C.

1.3.2 Thomas–Hoover Uni-Melt Device

The Thomas–Hoover Uni-Melt device, shown in Fig. 1.2, uses silicone oil as the heating medium. With the choice of a proper type of silicon oil, temperatures up to 300 °C are possible. The oil is heated electrically and stirred continuously to maintain a constant temperature. Depending on the design of the system, melting point of 5–7 samples can be obtained simultaneously.

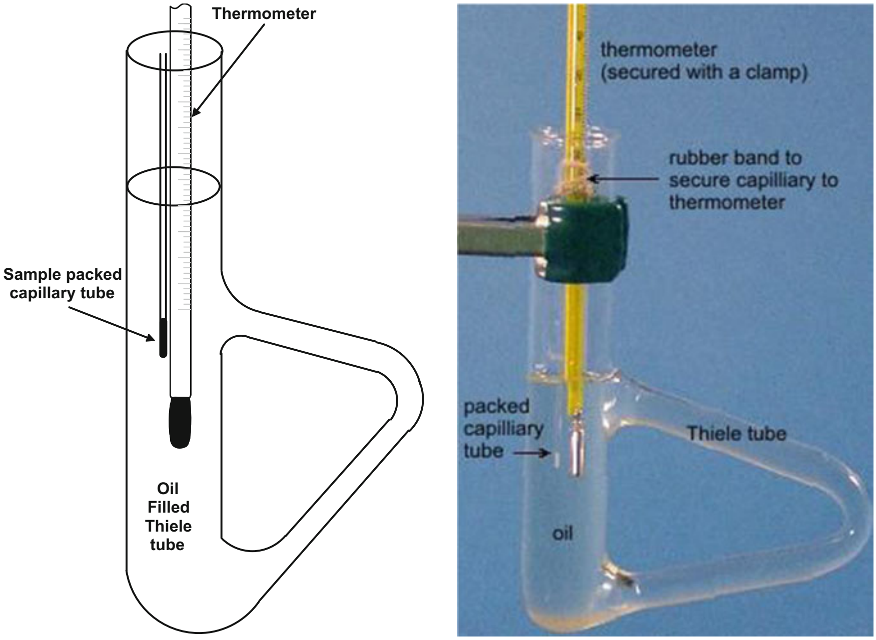

Fig. 1.1 A Thiele tube for measurement of melting point [3]

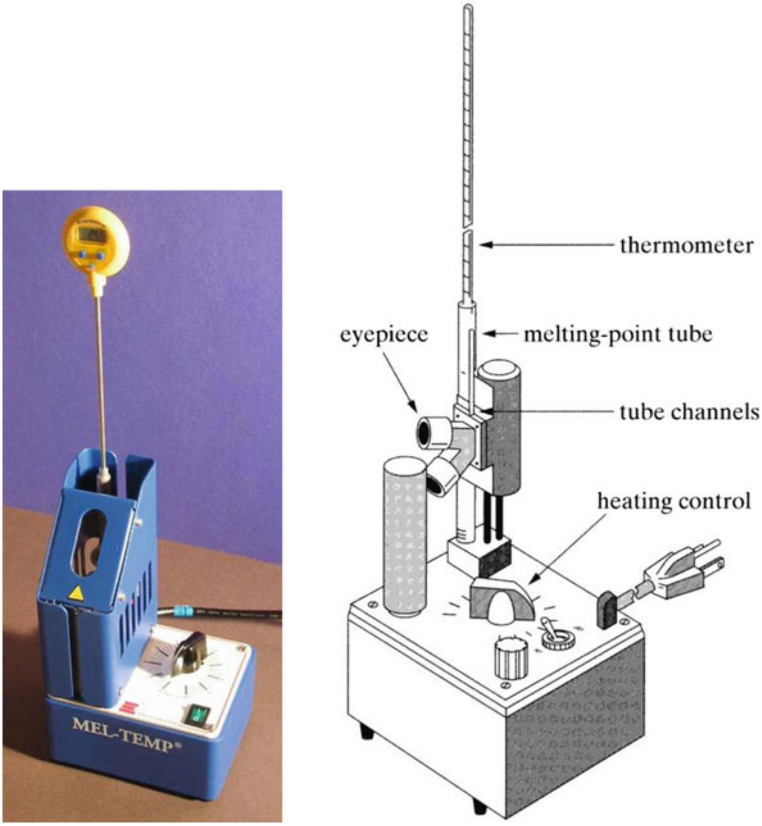

Fig. 1.2 A Thomas–Hoover Uni-Melt apparatus for melting point measurement [4, 5]

1.3.3 Mel-Temp Apparatus

The Mel-Temp apparatus for measurement of melting point is shown in Fig. 1.3. The uniform heating of the sample is accomplished using an aluminum block that is heated electrically. Several samples can be placed inside the aluminum block, which can be heated up to a temperature of 400 °C. The melting point is determined visually.

Fig. 1.3 A Mel-Temp apparatus for melting point measurement [6]

1.4 DSC/DTA Method

As described in the ASTM Standard E794-06, “The test method involves heating (or cooling) a test specimen at a controlled rate in a controlled environment through the region of fusion (or crystallization). The difference in heat flow (for DSC) or temperature (for DTA) between the test material and a reference material due to energy changes is continuously monitored and recorded. A transition is marked by absorption (or release) of energy by the specimen resulting in a corresponding endothermic (or exothermic) peak in the heating (or cooling) curve.” The operating temperature range is −120 to 600 °C for DSC and 25–1500 °C for DTA. Typical DSC curves for RDX and FX300 are shown in Fig. 1.4. The DSC curve for RDX, showed two sharp peaks. The peak at 205 °C indicates the phase change of RDX from solid to liquid, and can be designated as the melting point of RDX. The positive peak suggests an endothermic reaction. The negative (exothermic) peak at 240 °C is attributed to the decomposition of RDX. The DSC can be an important tool for assessment of the purity of a sample. As shown in Fig. 1.4b, The DSC curve (Fig. 1.4) for FX-300 that is a mixture of RDX, nitrocellulose and carbon, showed that the melting point of RDX shifted to 202 °C due to the presence of other compounds. Also, the decomposition peak shifted to 255 °C. Figure 1.5 shows a very strong DTA peat at 260 °C due to the decomposition of RDX. The TGA data indicated that almost 96% RDX decomposed in this temperature range.

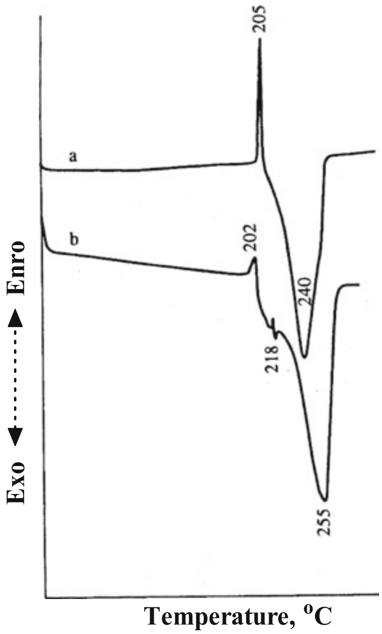

Fig. 1.4 DSC curves for RDX and FX-300. A 2 mg sample was used for both compounds. (Hussain G, Rees GJ (1995) Thermal decomposition of RDX and mixtures [7]

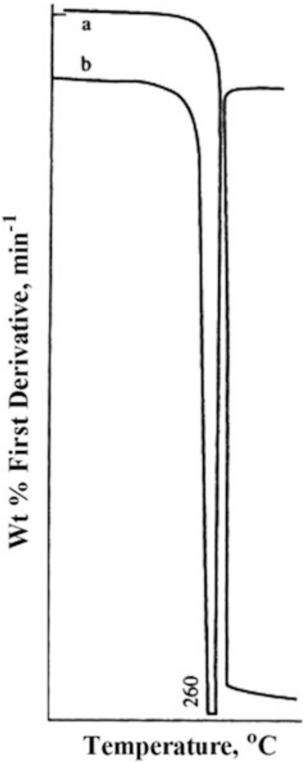

Fig. 1.5 DTA peat at 260 °C due to the decomposition of RDX [7]

1.5 Boiling Point

Most of the explosives decompose well before reaching the boiling point temperature. Therefore, the traditional method and apparatus cannot be used and as a result the boiling point of an explosive is not reported.

1.6 Critical Temperature, Volume, and Temperature

The direct determination of critical pressure, volume, and temperature of an explosive is challenging. Generally, a thermodynamic model involving the equation of state is used to estimate these values [8].

1.7 Density

The density of an explosive is expressed in a traditional manner: the mass of the explosive per unit volume (kg/m^3). Similarly, specific gravity is expressed as the ratio of the density of the explosive to the density of water under standard conditions. The specific gravity of commercial explosives ranges from 600 to 1700 kg/m^3.

For explosive materials, two other densities play an important role in their characterization:

- Package Density
- Loading Density

The package density refers to the density of an explosive as packaged in a cartridge or tube at the mixing plant. The unit for package density is still mass per unit volume (kg/m^3).

The loading density (*LD*) is defined as the mass of the explosive per unit length of the borehole at a specified borehole diameter. Therefore, *LD* can be mathematically expressed as follows:

$$LD = \frac{W}{L} \tag{1.1}$$

where, *W* is the mass of the explosive and *L* is the length of the loaded hole. For free running explosives, the unit used for loading density is often the pounds of explosives per foot of charge length in a given size borehole [or borehole size]. High loading density can reduce sensitivity by making the mass more resistant to internal friction. If density is increased to the extent that individual crystals are crushed, the explosive will become more sensitive. Denser explosives generally provide higher detonation velocities and pressures.

1.8 Detonation Velocity

The detonation velocity is the rate of propagation of the detonation wave through the mass of the explosive. The detonation velocity is considered to be the single most important property for evaluating an explosive. It may be measured either under confined or unconfined conditions. Although the measurement of the detonation velocity under confined conditions is more representative of the explosion, most manufacturers report the detonation velocity under unconfined conditions. The detonation velocity of an explosive is dependent on the density, chemical composition, particle size, charge diameter, and degree of confinement. Unconfined velocities are generally 70–80% of confined velocities.

The determination of detonation velocity is based on measuring the time required for the detonation wave to travel between two designated points (i.e., a certain distance). The method most often used is known as the Dautriche test method [9]. The basic arrangement of the Dautriche test system is shown in Fig. 1.6.

The explosive sample is placed in a confinement tube, which may or may not be enclosed in a steel tube. Two blasting cups, one at each end, are incorporated to mark the length of the column to be detonated. A detonation cord of known detonation velocity is connected to these blasting cups and passed across a lead plate as shown in Fig. 1.6. The center of the cord is marked in the lead plate. The detonation of the explosive is initiated by the detonator or booster. The detonation wave from this primary blast starts another detonation wave at the blast cup *A*, which starts travelling through the detonation cord. Another detonation wave starts

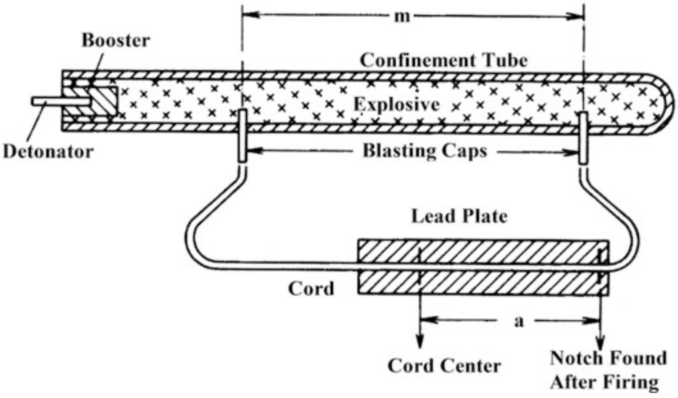

Fig. 1.6 Basic arrangements of the Dautriche test system [9]

at the second blast cup *B* as soon as the primary wave hits it. Two detonation waves colloids at some point on the lead plate and creates a notch. The distance between the center of the cord and this notch, a, is measured and is used to determine the detonation velocity using the following equation:

$$D_{sampie} = D_{cord} \frac{m}{2a} \tag{1.2}$$

where *D* sample is the detonation velocity of the test explosive, *D* cord is the detonation velocity of the detonation cord, which is known, m is the length of the charge or confinement tube (which is measured after placing the explosive in the tube), and a is defined earlier. The derivation of Eq. 1.2 has been given by several authors [10, 11]. The accuracy of the detonation velocity measured by the Dautriche method is around 4–5%.

Recently, several new methods have been proposed for more accurate measurement of the detonation velocity. These methods may be categorized into two classes: Electrical and Optical methods. These methods are discussed in details by several authors [12–14].

In the electrical method, different types of velocity probes are combined with an electronic counter or oscilloscope [15, 16]. The optical methods involve the use of various types of high speed cameras. [17–22].

1.9 Detonation Pressure

The detonation pressure is not measured directly; rather it is calculated from the detonation velocity. Detonation pressure is a function of the detonation velocity and density of an explosive. The National Park Services (NPS) developed a nomograph to find the approximate detonation pressure of an explosive if the detonation velocity and specific gravity are known [23]. The monograph is presented in Fig. 1.7.

Agrawal [24] presented the following equation for calculation of the detonation pressure (PDP):

$$P_{DP} = \frac{\rho D^2}{(\lambda + 1)} \tag{1.3}$$

where ρ is the density of the explosive, *D* is the detonation velocity, and λ is a constant, called the polytropic exponent of detonation products. The value of λ is approximately 3 for high explosives.

Agrawal [24] also described a more accurate method to experimentally determine the detonation pressure. The method is based on impedance mismatch technique. In this method, the detonation shock wave velocity in water is measured following detonation of the test explosive that is in contact with water. The equation

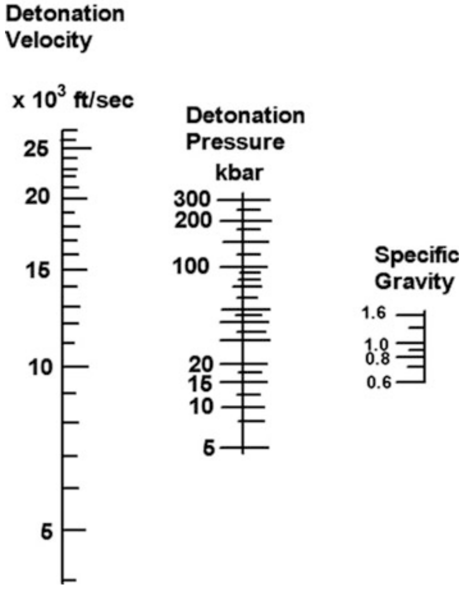

Fig. 1.7 A monograph for calculation of detonation pressure from known detonation velocity and specific gravity of the explosive

of state for water should be known. The equation for calculating the detonation pressure is given below:

$$P_{Dp} = \frac{P_W(\rho_W U_{SW} + \rho_X D)}{2\rho_W U_{PW}} \tag{1.4}$$

where,

P_W transmitted shock pressure in water = ρ_w U_{SW} U_{PW}
ρ_W density of water
U_{SW} transmitted shock velocity in water
U_{PW} particle velocity in water
ρ_X density of explosive
D detonation velocity of explosive

U_{SW} is obtained directly from the experimental measurement using the Aquarium technique. U_{PW} is related to U_{SW} by the following expression

$$U_{PW} = \frac{U_{SW} - 1.15}{1.85} \tag{1.5}$$

The basic experimental set-up for measurement of U_{SW} using Aquarium technique is shown in Fig. 1.8. In this method, the sample explosive charge is immersed in distilled water. The detonator and the booster are placed outside the water container, which may be made of glass. Following detonation of the charge, the shock wave, travels through the water changing its optical transparency. A high

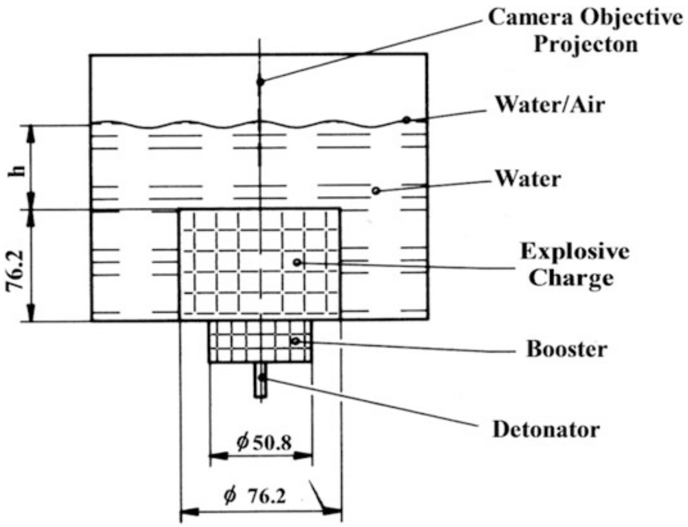

Fig. 1.8 Aquarium test [25]

speed camera located above the water surface records the propagation of the shock wave front as a function of time through water. A Plexiglas block may be replaced for water, which is also optically transparent (See Fig. 1.9).

A number of other techniques have been suggested to experimentally determine various detonation parameters that are essential for calculation of the detonation

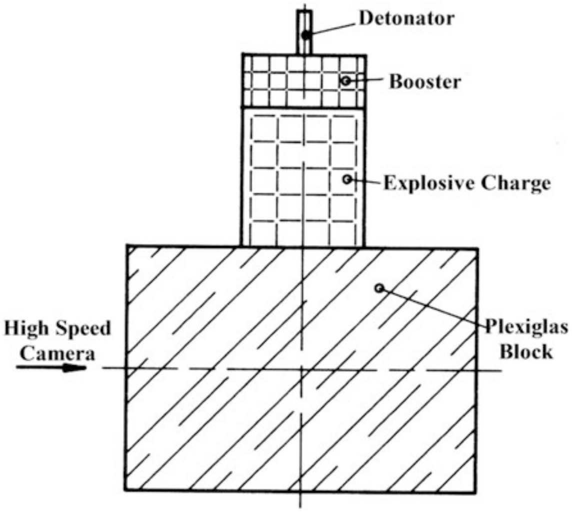

Fig. 1.9 Plexiglas test method [25]

pressure. These techniques include: Laser technique, Electromagnetic particle velocity gauge technique, Laser interferometry technique and Flash X-ray photography method. Several pressure gauges were also developed for direct measurement of detonation pressure, including Manganin pressure gauge and polyvinylfluoride-based pressure gauge [26–45].

1.10 Volatility

Volatility of a substance may be defined as the loss of mass per unit time at a certain temperature. For military explosives, researchers generally agreed on the following description: “Volatility, or the readiness with which a substance vaporizes, is an undesirable characteristic in military explosives. Explosives must be no more than slightly volatile at the temperature at which they are loaded or at their highest storage temperature. Excessive volatility often results in the development of pressure within rounds of ammunition and separation of mixtures into their constituents. Stability is the ability of an explosive to stand up under storage conditions without deteriorating. Volatility affects the chemical composition of the explosive such that a marked reduction in stability may occur, which results in an increase in the danger of handling. Maximum allowable volatility is 2 mL of gas evolved in 48 h”.

Although a standard method is not specified for the volatility measurement, a Thermo Gravimetric Analyzer (TGA) may be used to determine the volatility of explosives. From the mass loss measurement from the TGA at a certain temperature and with the knowledge of density, the volume of the gas may be calculated at a specified temperature.

1.11 Vapor Pressure

Methods for measuring vapor pressure can be divided into direct methods and indirect methods. In a direct method, the actual pressure of the pure vapor in equilibrium with liquid or solid is determined by using pressure gauges. The accuracy of the data will depend on the choice of the pressure gauge, sample purity, and assurance that the equilibrium condition has been achieved. In the indirect methods, the vapor pressure is calculated from other experimentally measured values or properties of the substances, which must have a theoretical relationship to the vapor pressure. The indirect methods are useful for low volatile substances and compounds that decompose before its boiling point.

1.11.1 Knudsen Effusion Method

One of the most used indirect-methods for the vapor pressure measurement of low-volatile substances is the Knudsen effusion method [46, 47]. In this method, a sample is placed in a small container with a pin-hole. The container with the sample is placed in a high vacuum and heated to a desired temperature. It is assumed that an equilibrium vapor pressure is established inside the container and molecules leave the container through pin-hole into the vacuum at a constant rate. If it is assumed that the mean free path (λ) of vapor molecules is long compared to the radius of the hole, the rate of molecules escaping through the hole would equal the rate at which molecules would strike an area of wall equal to the hole-area if the hole were closed. This assumption is valid for substances with a low vapor pressure which ensures a long mean free path. The derivation of an expression for calculation of vapor pressure from the Knudsen effusion method is given below.

The frequency of collisions of gas molecules with the wall per unit wall area is given by:

$$Z_{wall} = \frac{n\bar{c}}{4} \tag{1.6}$$

where n is the number density and $\bar{c}$ is the average speed of the molecule. (The number density is the ratio of the total number of gas molecules to the total gas volume).

The ideal gas law (using the number density and the number of particles) can be written as:

$$P = nkT \tag{1.7}$$

where, k is Boltzmann's constant. The average speed, $\bar{c}$, is given by:

$$\bar{c} = \sqrt{\frac{8kT}{\pi m}} \tag{1.8}$$

where m is the molecular mass.

If a hole of area is A, and assuming that the hole does not change the velocity and density distribution in the gas, the number of molecules (N) entering the hole in time θ can be expressed as:

$$N = Z_{wall}A\theta \tag{1.9}$$

Assuming that the same number of molecules is lost through the hole to the vacuum space permanently, the mass lost can be expressed as:

Table 1.2 Clausing factors for cylindrical holes

l/r	f
0.0	1.00
0.1	0.952399
0.2	0.909215
0.5	0.801271

$$\text{mass lost}, (g) = mN = m\, Z_{wall} A\theta \tag{1.10}$$

Substitution of Eqs. 1.6 and 1.7 through 1.10 gives the following expression for vapor pressure:

$$P = \frac{g}{A\theta}\sqrt{\frac{2\,\pi kT}{m}} = \frac{g}{A\theta}\sqrt{\frac{2\,\pi RT}{M}} \tag{1.11}$$

where R is the universal gas constant and M is the molar mass.

Equation 1.11 is valid for ideal situation, i.e., the pin-hole in the container has the zero length, which is not practical. Therefore, a molecule may enter the hole, strike the hole wall, and go back into the vapor space inside the container. In order to this into account, the effective area of the hole is multiplied by a correction factor, f, called the Clausing factor and depends on the ratio of hole length to hole radius. Iczkowski et al. [48] give the following Clausing factors for cylindrical holes (Table 1.2).

The Clausing factor can also be approximated by:

$$f = 1 - 0.5\left(\frac{1}{r}\right) + 0.2\left(\frac{1}{r}\right)^2 \tag{1.12}$$

where, l is the lid thickness. A schematic diagram of the apparatus is shown in Fig. 1.10.

The system is evacuated by a turbomolecular (turbo) pump and has a base pressure of 8×10^{-9} torr as read by an ion gauge. The apparatus is constructed of stainless steel with the exception of the lower half of the tube containing the Knudsen cell, which is made of copper to aid in heat transfer between the cell and the constant temperature bath. The temperature bath is filled with a light silicon oil and the temperature of the bath can be varied from 323–423 K. The apparatus was calibrated using benzoic acid as a standard.

1.11.2 Thermogravimetry Method for Vapor Pressure Determination

Thermogravimetry (TG) method is an indirect method for determination of the vapor pressure. In this method, an inert gas flows over the sample with known

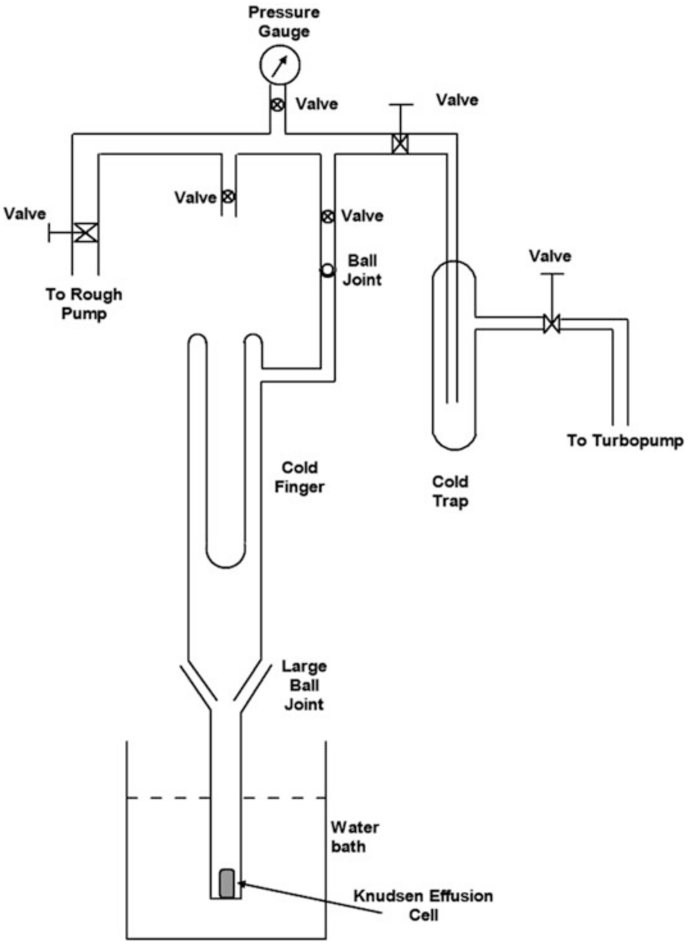

Fig. 1.10 Knudsen effusion methods for measurement of vapor pressure

surface area under a constant temperature. The free surface area of samples can be controlled and known by melting the sample in a 12.5 mm aluminum sample cup for the TG study. The vapor pressure is calculated from the mass loss at a constant rate using the Langmuir equation [49]. It is noted that all these vapor pressure calculations assumed that vapor pressure data obey the Clapeyron equation and required reliable vapor pressure data of a standard material.

Langmuir Equation

In 1913 Langmuir developed the following equation for the vaporization rate of tungsten as a function of temperature and vapor pressure. The Langmuir equation is given by:

$$\frac{dm}{dt} = p\alpha\sqrt{\frac{M}{2\,\pi\, RT}} \tag{1.13}$$

where

$\frac{dm}{dt}$ = rate of mass loss per unit area or sublimation rate per unit area

p	vapor pressure
α	vaporization coefficient
M	molecular weight
R	gas constant
T	absolute temperature

The Langmuir equation can be rearranged as follows for determination of α:

$$p = \left[\frac{dm}{dt}\sqrt{\frac{T}{M}}\right] \times [2\pi\alpha] \tag{1.14}$$

Equation 1.14 may be rewritten as follows:

$$p = v * k \tag{1.15}$$

or,

$$\ell n\, p = \ell n\, v + \ell n\, k \tag{1.16}$$

where, $v = \frac{dm}{dt}\sqrt{\frac{T}{M}}$, and $k = 2\,\pi\,\alpha$

Price [50] plotted known vapor pressure values of several standard materials (benzoic acid, benzophenone, phenanthrene, and acetamide) against their sublimation rates from a TG analysis in a log-log scale. A straight line resulted (See Fig. 1.11) suggesting that k is a universal constant; independent of the material.

Regression analysis for p and evaporation rate.

Gückel et al. [52–55] proposed the following relationship between the rate of mass loss and the vapor pressure of the substance.

$$\ell n\, p = C\,\ell n\left(\frac{dm}{dt}\right) + D \tag{1.17}$$

where constants C and D are calculated from the non-linear regression. They used twelve standard materials with their known vapor pressure data and their evaporation rate (obtained by gas chromatography experiment) and a straight line was reported when dm/dt was plotted against p in a log-log scale to determine universal constants C and D.

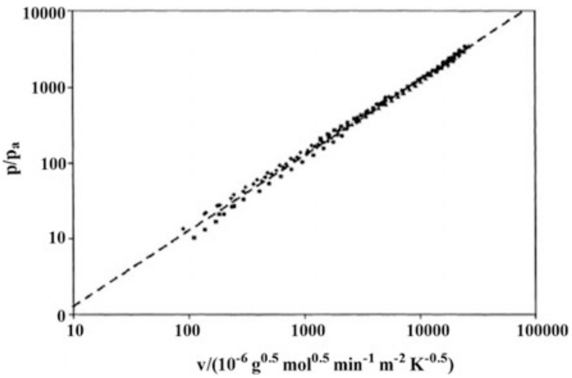

Fig. 1.11 Calibration curve made by Duncan and Price [51] showing a linear relationship between known vapor pressure (p) of benzoic acid (*filled diamond*), benzophenone (*filled triangle*), phenanthrene (*filled square*) and acetamide (*filled circle*) and their sublimation rate per unit area (v) from the gas chromatography experiment

1.11.3 Comparative Method

Phang et al. [56] modified the TG method for the vapor pressure estimation using only one substance of known vapor pressure. Thus, the need for the calibration curve of p vs. v was avoided. The Langmuir equation was rearranged as follows for two substances:

$$p = \left(\frac{dm/dt}{\left[\alpha\sqrt{\frac{M}{2\pi RT}}\right]}\right) = \left[\left(\frac{dm}{dt}\right)\sqrt{\frac{T}{M}}\right]\left[\frac{\sqrt{2\pi R}}{\alpha}\right] = v \cdot k \tag{1.18}$$

The Langmuir equations for a reference material or a standard material (subscript R) and for the sample investigated (subscript S) at the same temperature (T_1) can be expressed as:

$$\left(\frac{dm}{dt}\right)_R \sqrt{T_1} = \alpha M_R \left(\frac{1}{2\pi R}\right)^{1/2} p_R \tag{1.19}$$

$$\left(\frac{dm}{dt}\right)_S \sqrt{T_1} = \alpha M_S \left(\frac{1}{2\pi R}\right)^{1/2} p_S \tag{1.20}$$

Since α is a constant value depending on the TG system and its operating conditions, P_S can be simply evaluated from a pair of evaporation rate and vapor pressure data of the reference material as given below:

$$p_S = \left(\frac{M_R}{M_S}\right)^{1/2} p_R \left[\frac{(dm/dt)_s}{(dm/dt)_R}\right] \tag{1.21}$$

1.11.4 Vapor Pressure by Gas Chromatography Head Space Method

Head space method involves sealing a small amount of sample (about 10 mL) in a head space crimp top flat bottom vials fitted with septa to draw the sample using a syringe for gas chromatography analysis. The sample vials are allowed to equilibrate in an oven at various temperatures. A gas chromatograph oven may be used for this purpose. Following equilibration of the sample, the vapor that is in equilibrium with the liquid is drawn by the gas tight syringe and injected onto a gas chromatograph equipped with an appropriate column and detector. A calibration curve (peak area versus mg of the sample) should be prepared to determine the amount of sample in the vapor phase. The volume of gas was withdrawn through the septum of the equilibrated headspace vials is injected into the gas chromatograph and peak area is obtained. It is assumed that the vapor of the sample compound obeys the ideal gas law $[pV = (m/M)RT]$, the vapor pressure is calculated.

Vapor pressures of a low volatile substance, such as an explosive, can be determined from the retention time of that substance from a gas chromatography GC column, operating under isothermal conditions, if the retention time of several substances of known vapor pressures that have similar chemical structure (a homologous series) is available using the same gas chromatography column under the same isothermal conditions. The mathematical basis for this method is described below.

Jensen and Schall [57] noted that a relationship exists between the retention volume (V_R) and the retention time (t_R) for two substances eluted on a GC column under the same operating conditions:

$$\frac{V_{R1}}{V_{R2}} = \frac{t_{R1}}{t_{R2}} \tag{1.22}$$

The retention volume may be related to the vapor pressure by the following equation:

$$\frac{V_{R1}}{V_{R2}} = \frac{p_2^0}{p_1^0} \tag{1.23}$$

Substitution of Eq. 1.22 into Eq. 1.23 provides a relationship between the vapor pressure and retention time.

$$\frac{t_{R1}}{t_{R2}} = \frac{p_2^0}{p_1^0} \tag{1.24}$$

Equation 1.24 can be used to calculate the vapor pressure of Compound *2* if the retention times are known, as well as the vapor pressure of Compound *1*. However, a large error may result if the vapor pressure of Compound *1* is not very accurate. The accuracy may be increased if the vapor pressure data for several other compounds in the homologous series are known along with their latent heats. The Clausius-Clapeyron [58, 59] equation provides a relationship between the latent heat and vapor pressure of a compound.

$$\frac{dp^0}{dT} = \frac{L}{(V - v)T} \tag{1.25}$$

where,

T absolute temperature,
L latent heat per mole,
V vapor pressure per mole,
v liquid volume per mole

Since V is a function of temperature and pressure, a relationship among V, p and T is necessary for integration of Eq. 1.25. Assuming that the vapor obeys the perfect gas law and v is negligible compared to V, then the following expression results:

$$\frac{dp^0}{dT} = \frac{Lp^0}{RT^2} \tag{1.26}$$

Integration of Eq. 1.26 for compound 1 and 2, followed by some rearrangement, the following expression is obtained:

$$\ln p_1^0 = \frac{L_1}{L_2} \ln p_2^0 + C \tag{1.27}$$

Using Eqs. 1.24 and 1.27 can be expressed in terms of retention time as follows:

$$\ln\left(\frac{t_{R1}}{t_{R2}}\right) = \left(1 - \frac{L_1}{L_2}\right) \ln p_2 + C \tag{1.28}$$

For a homologous series, the ratio L_1/L_2 may be assumed to be a constant. Therefore, a plot of $\ell n\ (tr_1/tr_2)$ vs. $\ell n\ p_2$ should provide a straight line, from which the vapor pressure of the unknown compound can be obtained if its retention time under the same operating conditions is known.

1.12 Strength, Performance, and Brisance of Explosives

Brisance is "the shattering or crushing effect of an explosive measurable by the crushing of sand or the compression of a metal cylinder and dependent upon the rate of detonation and other factors". Several tests are performed to determine the strength, performance, and brisance of explosives. Isidor Trauzl was developed by 1885 [60]. These tests provide the information for an explosive regarding its ability to accomplish the task that is intended in the way of energy delivery.

1.12.1 Strength Tests

For determination of the strength of explosives, their performance and brisance, the following experimental methods are used [61]:

- Lead Block Test (also known as Trauzel Test) [62–92]
- Underwater Explosion Test [93–105]
- Ballistic motor test [106–121]

1.12.1.1 Lead Block Test

The Trauzl or lead block test is conducted to determine the strength of the explosive. Following detonation of the explosive charge, the volume increase of the cavity into which the detonation is carried out is determined. The basic configuration of the lead block is shown in Fig. 1.12.

The explosive charge, which may contain either 10 g or 10 cm^3 explosives (A constant volume of 10 cm^3 is recommended by the European Commission for the Standardization of the Tests of Explosives), is placed inside the cavity of the block together with the detonator. The cavity is stemmed by 500 μm diameter dry sand. The explosive charge is initiated and the expanded volume is determined. The strength of the explosive can be expressed as work done relative to a reference explosive and is expressed by the following expression:

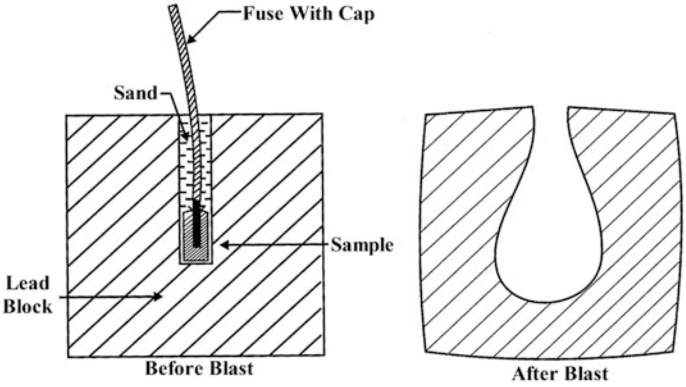

Fig. 1.12 Trauzl or lead block test configuration [122]

$$\frac{A_x}{A_{\text{Ammonit}-6}} = \frac{M_{\text{Ammonit}-6}}{M_x} \tag{1.29}$$

where, A_x and $A_{\text{Ammonit-6}}$ are the work done by the test explosive and the reference explosive, respectively, and Mx and $M_{\text{Ammonit-6}}$ are their masses, respectively.

1.12.1.2 Underwater Explosion Tests

This test method is used if the charge mass of less than 10 g has to be employed in the test. The strength of the explosive is determined from the energy release during underwater explosion. Generally, shock wave or bubble energy is measured. As shown in Fig. 1.13, the charge is placed inside a water-filled tank. A pressure gauge and a triggering gauge are also placed inside the tank at a predetermined distance from the charge.

The total energy released from explosion (E_T) is calculated as a sum of shock wave (E_S) and bubble energy (E_B) and can be written as:

$$E_T = E_S + E_B \tag{1.30}$$

The shock wave energy can be calculated from the following equation:

$$E_s = \frac{4\pi R^2}{M_B v_W \rho_W} k_1 k_C \int p^2 dt \tag{1.31}$$

where v_W is the velocity of sound in water, [specify T and P] ρ_W is the density of water, M_B is the mass of the charge, k_1 is the amplification factor, and k_c is the constant of integration.

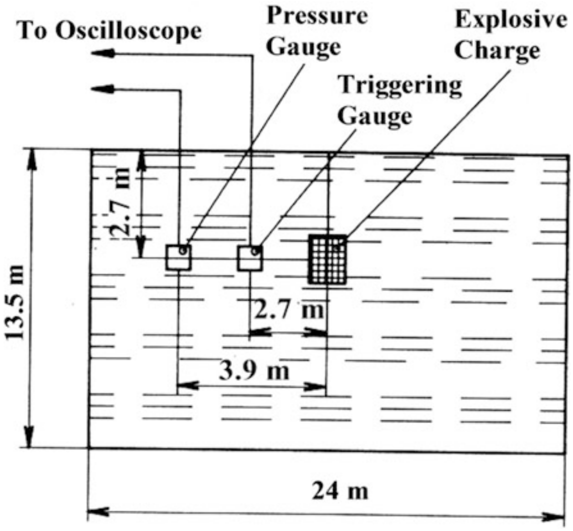

Fig. 1.13 Arrangement for the underwater explosion test to determine the strength of an explosive [123]

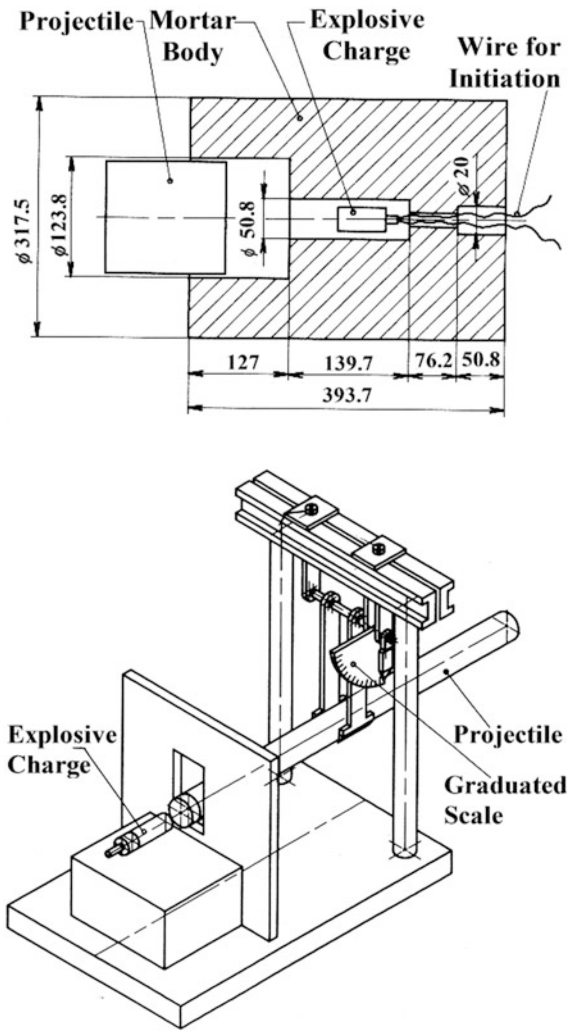

Fig. 1.14 Arrangement for ballistic motor test to determine the strength of the explosive [124]

The bubble energy is obtained from the following expression:

$$E_B = 2.5\frac{T^3}{M_R}(3.28H + 33.95)^{2.5} \tag{1.32}$$

and H is the depth of the explosive charge (expressed in meters).

1.12.1.3 Ballistic Motor Test

As shown in Fig. 1.14, a weight or a projectile is suspended from a pendulum axis. The explosive charge of a given mass in detonated in the motor cavity that enclosed the projectile. The maximum swing of the mortar is recorded following ejection of the projectile. The strength of the explosive is then calculated from the following expression:

$$E = \frac{A_X}{A_R} = \frac{1 - \cos\alpha}{1 - \cos\alpha_0} \times 100 \tag{1.33}$$

where A is the work done by the test sample (X) and the reference explosive (R), respectively. A is calculated from the experimental data using following equation:

$$A = M_M L(1 - \cos\alpha)\left(1 + \frac{M_M}{M_P}\right) \tag{1.34}$$

where M_M and M_P are the mass of the mortar and the projectile, respectively. L is the distance from the center of mass to the suspension axis, and α is the angle of the mortar swing. Figure numbers for the figure below.

1.12.2 Performance Tests

The most common tests for determination of performance of an explosive are double pipe and cylinder expansion tests.

1.12.2.1 Double Pipe Test [125, 126]

This test is used to determine the performance of the explosive under borehole conditions. Standard cartridges of different length of the explosive charges are placed inside a pipe that is equivalent to a borehole. The pipe loaded with the charge is placed on the top of a witness steel pipe. A heavy anvil supports the assembly as shown in Fig. 1.15a. Following the detonation, the dent on the witness pipe is determined as shown in Fig. 1.15b. A similar test is performed for a known explosive and the relative performance is determined.

1.12.2.2 Cylinder Expansion Test

The cylinder expansion test is performed to determine the Gurney energy, E_G, which is generally used to characterize the ability of an explosive to accelerate metals, and μ is the ratio between the masses of the cylinder and the explosive [127–175].

The Gurney energy is given by charge:

$$E_G = \frac{1}{2}\left(\mu v_m^2 + \frac{1}{2}\int v_g dV\right) \tag{1.35}$$

v_m is the velocity of the wall material and v_g is the velocity of the detonation materials. If it is assumed that the velocity of the detonation materials increase linearly in the expansion direction v_g may be expressed as:

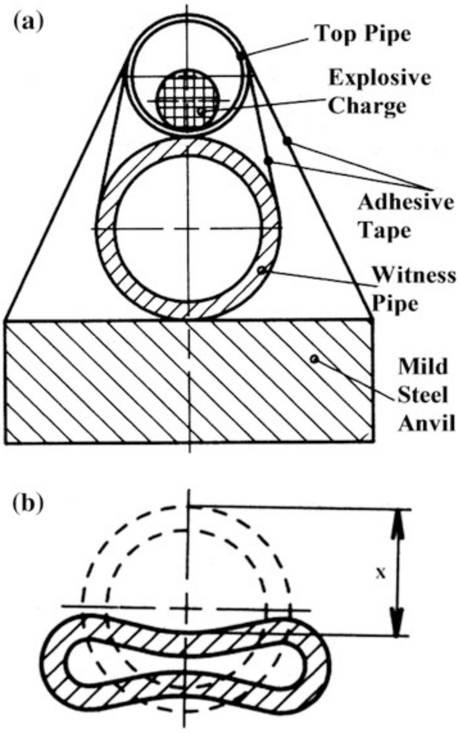

Fig. 1.15 Cross-sectional view of the arrangement of the double pipe test (**a**), and the determination of the dent of the witness plate following experimentation [125, 126]

$$v_g = \frac{v_m r}{r_m} \tag{1.36}$$

where r is the radius of the cylinder at any given time and r_m is the cylinder radius initially. Integration of Eq. 1.35 using Eq. 1.36 provides the following expression for Gurney energy.

$$E_G = \frac{1}{2}\left(\mu + \frac{1}{2}\right)v_m^2 \tag{1.37}$$

The wall velocity may be expressed by:

$$v_m = \frac{D}{2}\sqrt{\frac{1}{2\mu + 1}} \tag{1.38}$$

where D is the detonation velocity. The schematic of the experimental system for determination of v_m is shown in Fig. 1.16. The explosive charge is placed inside a copper cylinder. The detonation of the charge occurs at the end of the cylinder front by a detonator and booster. The expansion of the external radius of the cylinder is photographed using a high speed streak camera. The increase in the cylinder radius

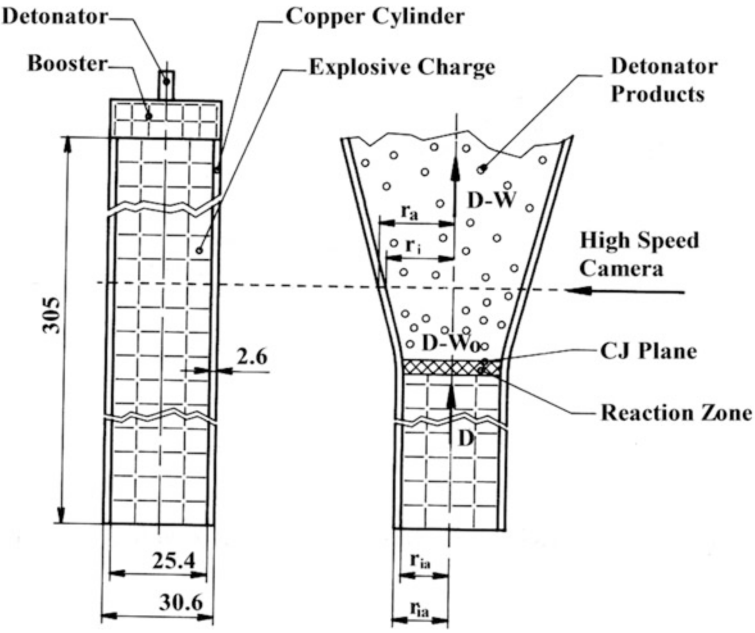

Fig. 1.16 A schematic representation of the cylinder expansion test before and after the test [214]

as the explosion progress is determined at a constant section of the cylinder. The external radius is plotted against time to obtain the expansion curve. From this curve, v_m is obtained using Eq. 1.38.

1.12.3 Brisance

Brisance (from the French meaning to "break") is a measure of the how rapidly the maximum pressure is attained when an explosion takes place, and denotes the shattering strength of the explosive. Brisance values are primarily employed in France and the Soviet Union. There are several methods for testing brisance, since no single brisance test is applicable for all explosives. Also, different tests can give different values for the same explosive. Brisance is experimentally determined by several methods:

- Sand Test [176–186]
- Plate-Dent Test [187–189]
- Lead Block Compression Test or Hess test [190–203]
- Kast test [204–211]

1.12.3.1 Sand Test

In the sand test, approximately 400 mg of the explosive are placed in 200 g of sand and detonated. Brisance is calculated from the amount of sand crushed by the explosive. This test tends to give the lowest values. Ottawa sand ASTM Standard which passes through No. 20 U.S. Standard Sieve and is retained on No. 30 U.S. Standard Sieve is used in the test. The sand testing system is shown in Fig. 1.17. About 80 g of sand is first poured in the cavity of the sand test bomb. It is leveled as much as possible. The capsule containing explosive, fuse, and detonator is placed in such a way that it just touches the sand. The rest of the 120 g sand is pour carefully into the cavity so that the position of the test capsule is not displaced from its position. The fuse is lighted and explosion occurs. Following detonation, the sand is sieved to determine what has become finer than 30 mesh. The same test is conducted for the detonator alone without the tested explosive. The amount of sand crushed below 30 mesh compared to the blank test is determined and the value is called brisance (determined by sand crushing test). The value is then compared to TNT to provide the relative value.

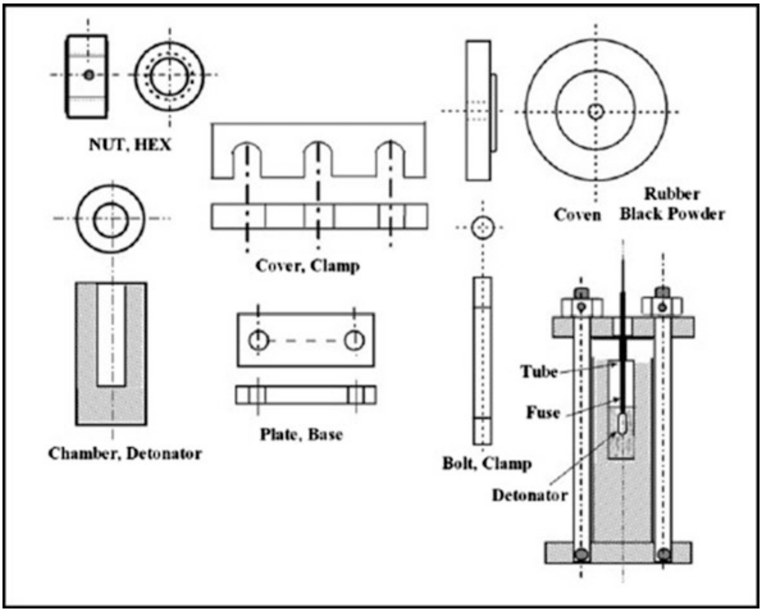

Fig. 1.17 The sand test assembly. US department of Defense (1962) Military standard Explosive: Sampling, inspection and testing. MIL-STD-650 [212]

1.12.3.2 Plate Dent Test

In the plate dent test, a sample of the explosive is detonated on a steel witness plate. The hemispherical deformation of the plate is determined that provides the brisance of the explosive. The relative brisance of the test explosive against a trinitrotoluene charge can also be obtained. The relative brisance may be expressed by:

$$B_r = \frac{Dent\,depth\,from\,test\,explosive}{Dent\,depth\,from\,trinitroluene} \times 100\% \tag{1.39}$$

Smith [213] suggested the following expression for calculation of dent depth for explosives with density in the range of 1.58–1.64 g/cm^3. The density of trinitrotoluene in about 1.63 g/cm^3.

$$h = 7.412\rho_0 - 5.375 \tag{1.40}$$

where h is the dent depth. The test methods currently used are in Figs. 1.18 and 1.19.

1.12.3.3 Hess Test

In this method the test explosive is placed on the top of a standard lead cylinder. The brisance is determined from the compression of the lead cylinder due to the shock wave originated by the detonation of the test explosives. The reduction of the height of the lead cylinder is related to the brisance. Often time, the relative brisance with respect to reference explosive, trinitrotoluene, is reported. The basic system is shown in Fig. 1.20. The deformation caused by the shock wave from the detonation is presented in Fig. 1.21.

Fig. 1.18 Set up for measuring brisance by plate dent method [214]

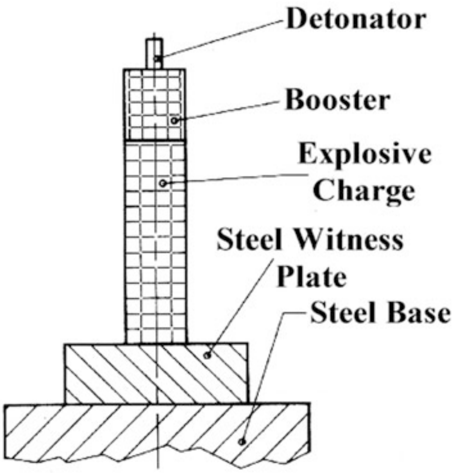

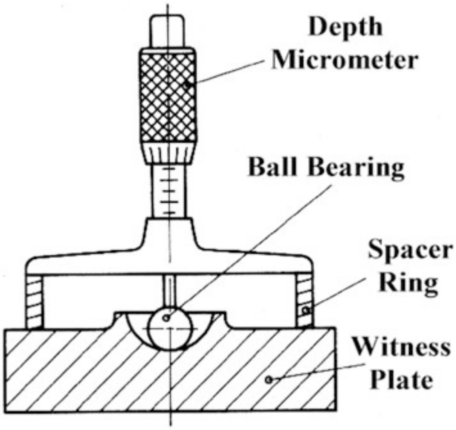

Fig. 1.19 Determination of the dent depth [214]

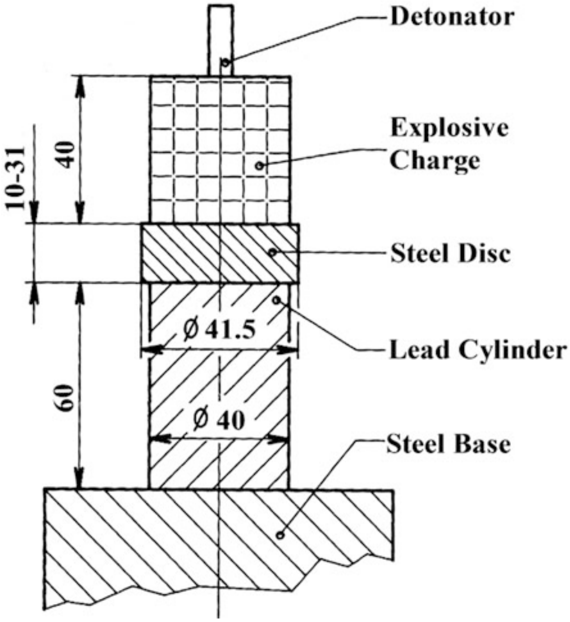

Fig. 1.20 The basic system for Hess test [214]

1.12.3.4 Kast Method

The Kast method involves compression of a copper crusher from the detonation of the test explosive. The copper crusher is separated from the charge by a steel piston, which transmit the energy from the explosive to the crusher. The brisance is determined from the decrease of the crusher height or units of crushing using Haid and Selle table. The units of crushing are given in Fig. 1.22.

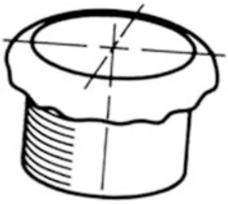

Fig. 1.21 The deformation of the lead block during Hess test [214]

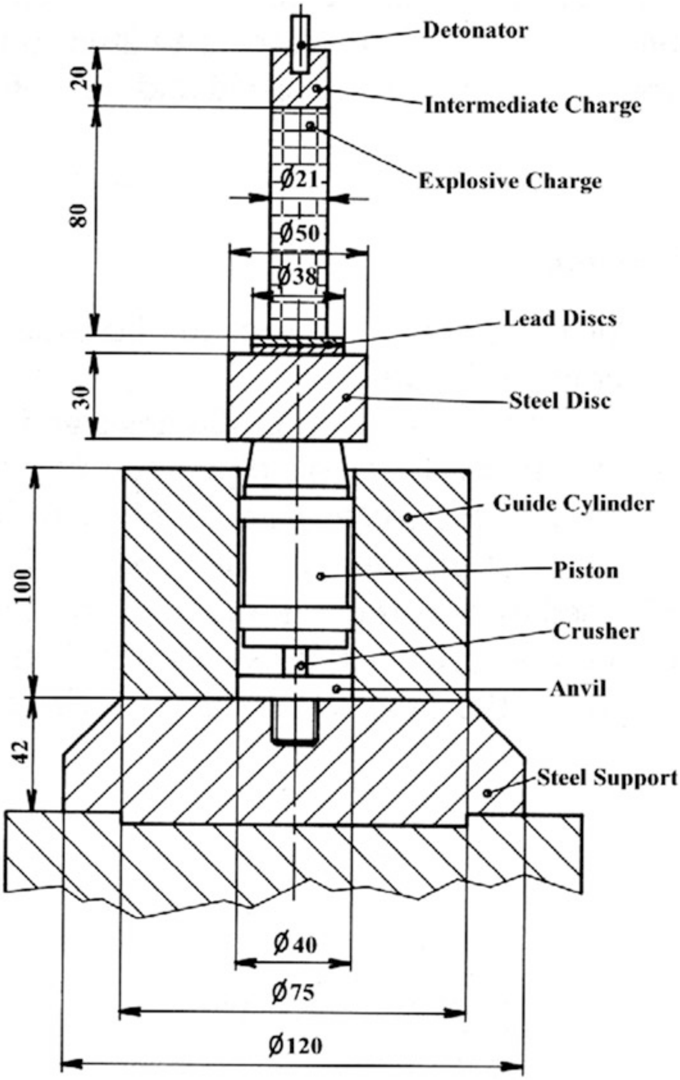

Fig. 1.22 Basic configuration of the apparatus for Kast's test [214]

1.13 Critical Diameter

The critical diameter of an explosive refers to the minimum physical diameter of a charge necessary to sustain its own detonation wave. The critical diameter is determined by detonating a series of charges of different diameters until sustaining of the detonation wave propagation is observed. One such test charge is shown in Fig. 1.23. This diameter ensures confidence and reliability that the explosive will detonate under all conditions that are specified for the particular explosive [215–244].

Fig. 1.23 Explosive charge configuration for determining critical diameter [245]

1.14 Chemical Decomposition

A chemical decomposition process may be defined as the rate at which the decomposition of an explosive occurs. The chemical decomposition of an explosive may take years, days, hours, or a fraction of a second. Depending on the objectives, the decomposition rate plays a crucial role in the choice of an explosive. For example, a slower process of decomposition may be desirable for long term storage and stability. However, two rapid forms of decomposition; deflagration and detonation, are of great interest to the users. (Group 1060, Test Methods, Chemical Stability, MIL-STD-1751A, Department Of Defense, Test Method Standard, Safety and Performance Test For the Qualification of Explosives (High Explosives, Propellants, and Pyrotechnics) [246].

1.15 Deflagration [247–256]

Deflagration may be defined as the decomposition of an explosive material in which a flame front propagates moves slowly through the explosive material, which is characteristic of low explosive materials. The flame front generally moves at a speed less that the speed of sound.

1.16 Detonation [257–276]

Detonation of an explosive may be described as a process in which the decomposition reaction propagates through the explosive at a supersonic speed. Various properties of detonation are described earlier in this chapter.

1.17 Sensitivity [277–300]

Sensitivity is an important parameter for an explosive. This refers to the ease with which an explosive material can be ignited or detonated. The main triggers are the shock, friction, and heat. Based on the mode of energy that needs to be supplied to ignite or detonate an explosive, sensitivity tests may be divided into three categories:

Mechanical Impulses: This includes impact, friction, and projectile impact. In impact test, sensitivity is expressed in terms of the distance through which a standard weight must be dropped to cause the material to explode. For friction tests, sensitivity is expressed in terms of what occurs when a weighted pendulum scrapes across the material (snaps, crackles, ignites, and/or explodes).

1.17.1 Shock Wave Tests

Thermal Impulses: Sensitivity is expressed in terms of the temperature at which flashing or explosion of the material occurs.

1.17.2 Mechanical Impulses

Various mechanical activities (or stimuli) can cause detonation of an explosive. These include impact, friction, firing pin impact, etc. For safe handling and storage of the explosive materials all these effects must be properly understood. The detonation of an explosive under mechanical stimuli is based on generation of heat from these activities. The mechanical energy imparted on the explosive from the dynamic action converts to heat energy causing local hot spots. If these hot spots have temperature above 700 K that is sustained for more than 300 μs in an area of diameter of 10 μm, the detonation can occur.

Several apparatus are designed for impact testing; however, all of them operate on the same principle—a weight is dropped (or a hammer falls on the explosive) on the test explosive. Because of this testing technique, all of these apparatus are called the Fallhammer Apparatus. The most common apparatus that are used for impact testing are: US Bureau of Explosive Impact Apparatus (BoE), US Bureau of Mines Impact Apparatus (BoM), Picatinny Impact Apparatus (PA), Bundesanstalt für Materialprüfung Apparatus (BAM).

The BoE apparatus, shown in Fig. 1.24, is capable of testing both solid and liquid samples. The explosive sample is confined in a 0.2 inch diameter by 0.1 inch long cylindrical cavity. An 8 lb weight [mass] is allowed to fall freely on a plunger and plug assembly from a maximum height of 33 inch directly, that is in contact with the test explosive charge. The sample cylinder rests on a die and anvil assembly.

About 10-mg sample is used in the test and is loaded onto the die. Either powdered sample or a solid wafer can be used in the test. The form of the test sample is an important property for evaluating the results. After placing the anvil and die, and the plug and plunger into their appropriate places, the drop weight is released from a predetermined height. A measurement is considered positive if either an audible report or flame is observed. A minimum of 25 tests are run to determine the 50% point using a Bruceton procedure.

When testing liquid explosives, one drop of the test liquid is placed in a copper cup which has been fixed in the cup positioning block. A special striker assembly is used for the test. The end of the striker should travel up to certain distance into the cup, but the positioning block should prevent the striker from actually touching the liquid in the cup. The bottom of the copper cup just touches the anvil when all the parts are assembled. This entire assembly is then placed in the same mechanism used for solid materials and tests are conducted in a similar manner.

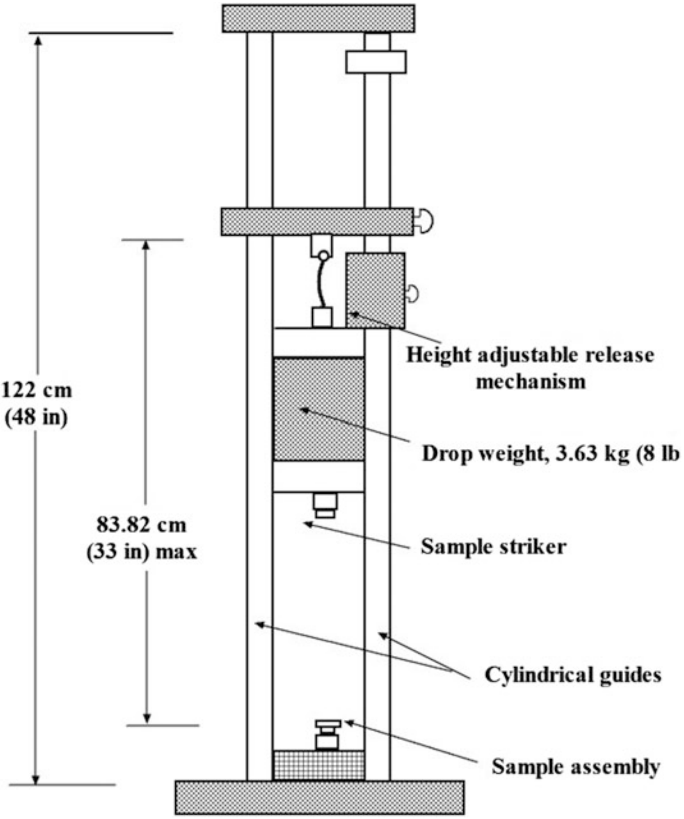

Fig. 1.24 Impact test apparatus from Bureau of explosive design (BOE) [300]

1.17.3 Friction Sensitivity

Friction is another stimulus for detonation of an explosive. The heat generated due to the friction between explosive particles or explosive-working surface can cause the detonation.

The pendulum friction device developed by the Bureau of Mines consists of a steel swinging shoe which is the bob of a pendulum. The apparatus is shown in Fig. 1.25. The friction between the shoe and anvil is controlled by controlling the number of swings of the pendulum. A specially designed anvil is used in the test. At the central portion of the anvil three parallel grooves are cut to prevent the test sample from being brushed off from the surface by swinging shoe. During the test, the test explosive charge is spread on the anvil surface. A steel shoe or one faced with red-hair fiber (called the “hard-fiber-faced shoe”) is used. A trigger is used to allow the shoe to be dropped upon the anvil from any desired vertical height ranging from 50 to 200 cm. The normal height of drop used is 100 cm. This test

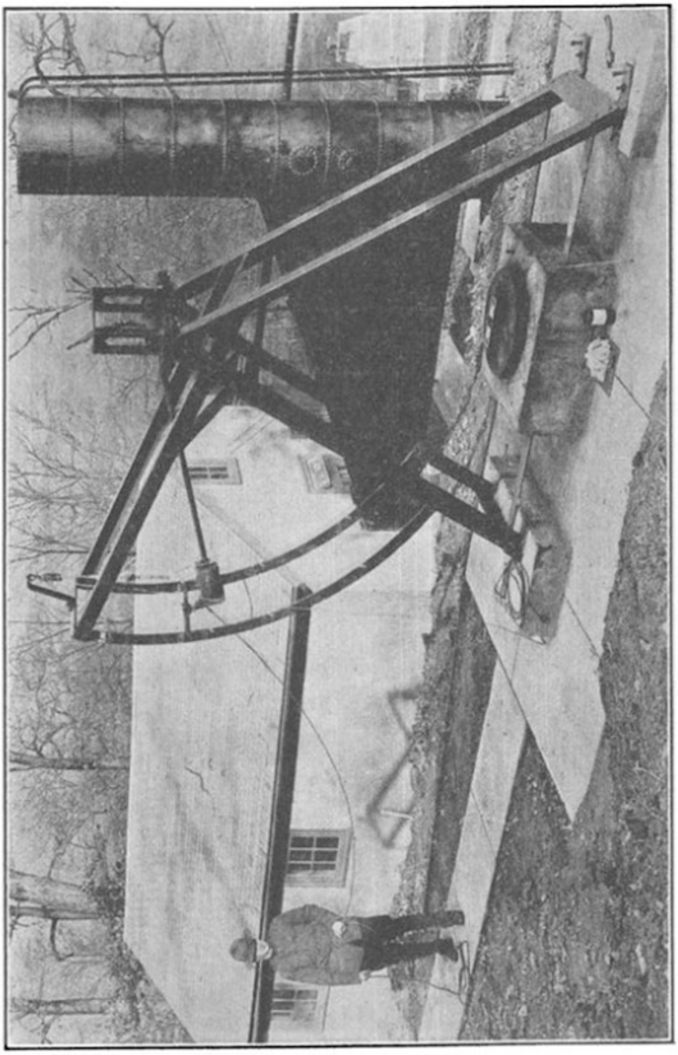

Fig. 1.25 A pendulum friction device (*Source* Munroe CE, Tiffany JE (1931) Physical testing of explosives at the bureau of mines explosives experiment station. Bruceton, PA. U.S. Dept. of Commerce, Bureau of Mines, Bulletin 346, pp. 78–84) [301]

should be conducted in a temperature controlled room so that the temperature of the anvil and shoe is 70 ± 5 F.

About 7 g of sample is spread evenly in and around the three grooves on the anvil plate. The apparatus is adjusted with loaded weights to provide about 18 ± 1 swings across the face of the anvil before coming to rest. The shoe is then released and the test result is noted. Twenty trials should be conducted using the steel shoe or fiber shoe. The test material using the steel shoe should not react in any of the twenty trials.

Other friction sensitivity tests that are most common include ABL Friction test (recommended by UN) and BAM friction test (recommended by both US DOD and UN).

1.17.4 ABL Tests [302–306]

The arrangement is shown in Fig. 1.26. In this method a thin uniform layer of the substance is placed under the wheel on the slidi337 ng anvil. A vertical compression force is applied under a non-rotating wheel, while the substance is moved in a horizontal direction on a sliding anvil. The maximum force to be used is 1800 lb (8000 N) and the minimum is 10 lb (44 N). A pendulum strikes the anvil and moves it at a known velocity, normally, the anvil slides 1 in (2.54 cm). The initial velocity is determined by calibration.

1.17.5 BAM Friction Test [307–309]

In this method, the friction is generated between two porcelain objects as shown in Fig. 1.27. A rough porcelain plate holds the sample that is moved electro-mechanically against a stationary porcelain pistil. A force normal to the plate is applied through the pistil and can be changed. The normal force at which 50% of initiations occur is used as the measure of the friction sensitivity.

Generally the sample is tested as received. For some explosives, a wetting agent is added for safe handling and transportation. This type of sample is tested with the minimum content of wetting agent. About 10 mg of the test sample is placed on the plate. The stationary porcelain cylinder is lowered to the top the sample by using the loading arm. A selected weight [mass] is attached to the arm to apply the force, which may vary from 4.9 to 353.2 N. The movement of the plate, or the stroke

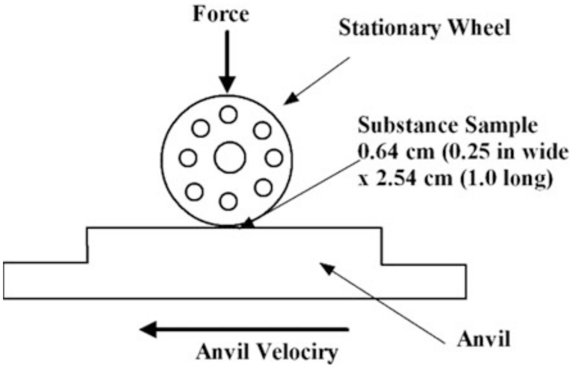

Fig. 1.26 The ABL test system [306]

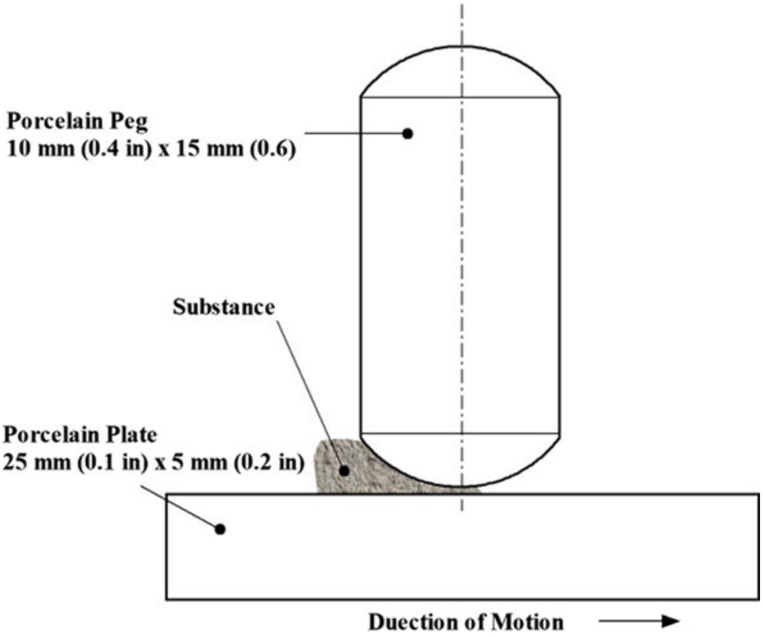

Fig. 1.27 The arrangement for creation of friction between the porcelain plate and pistil

length, is 10 mm forward and backward from the initial position. The occurrence of the initiation due to friction is determined from crackling sound, appearance of smoke, or by the characteristic burning smell.

Although both methods can be used in evaluating safety in transport, in other hazard assessments only the BAM test is specified (Fig. 1.28).

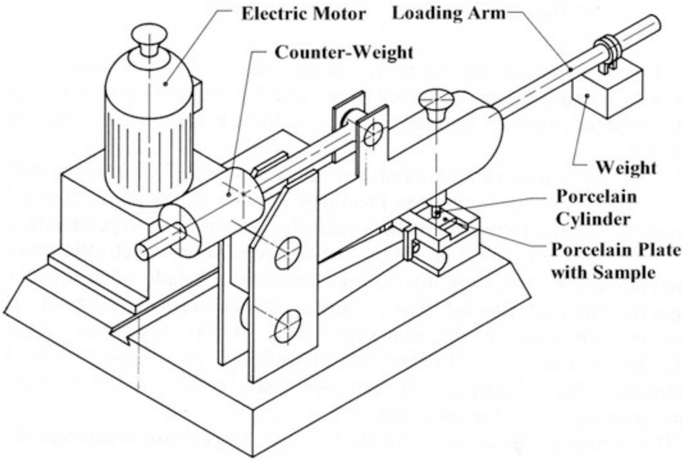

Fig. 1.28 A schematic diagram of the BAM apparatus [250]

1.18 Electrostatic Discharge (ESD) Test

This test refers to the amount of energy that is required to ignite explosives by electrostatic stimuli. A high potential needs to be applied to generate a spark between the test sample and the electrode. Figure 1.29 illustrates the working principle of an ESD testing device.

Samples are tested by varying the intensity of the released electrostatic discharge. The initiation point is determined whenever a flash, spark, burn, or specific noise is detected [310–312].

1.18.1 Gap Tests-Shock Wave [313–335]

The gap test is conducted to obtain the minimum shock wave pressure that can cause complete detonation of the explosive. The design of the experimental system depends on the size of the booster and the sample and is called either Small Scale Gap Test or Large Scale Gap Test system. The choice of the small or large scale gap test facility depends on the pressure and duration of positive phase of pressure of the generated shock wave. The determine the sensitivity to the shock wave, the complete detonation of the explosive charge must occur, which is generally indicated by the formation a clean hole in the steel witness plate that is 9.53 mm thick. A small scale gap test system is shown in Fig. 1.30.

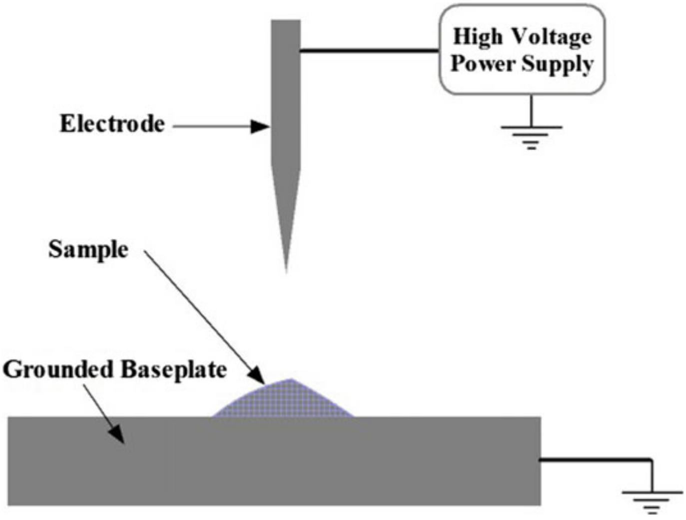

Fig. 1.29 Basic working principle of electrostatic discharge test system [310]

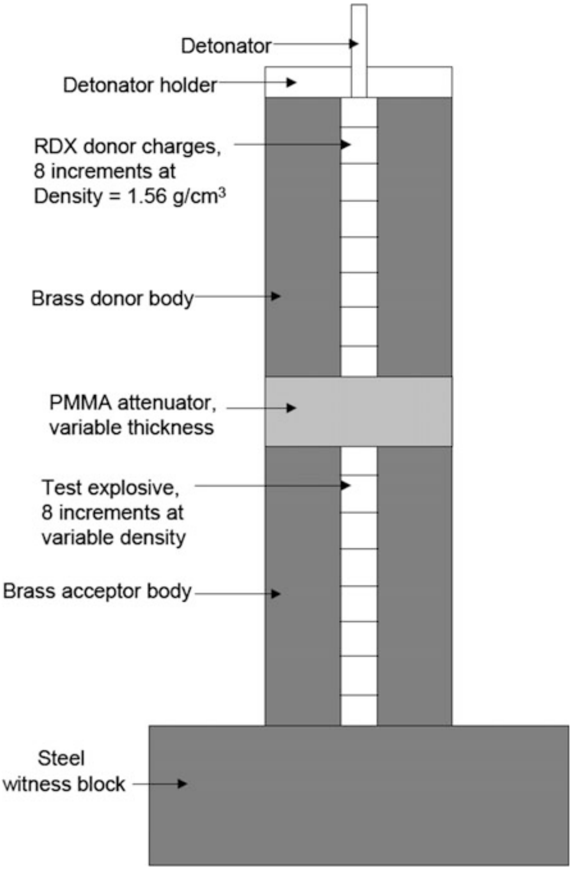

Fig. 1.30 Small scale gap test assembly. (*Source* Department Of Defense Test Method Standard. Safety and Performance Tests For The Qualification Of Explosives (High Explosives, Propellants, And Pyrotechnics) MIL-STD 1751A, 11 December 2001 SUPERSEDING, MIL-STD-1751(USAF), 20 August 1982 [246]

1.18.2 Thermal Sensitivity Test [336–341]

The best way to understand the sensitivity of an explosive to heat is to determine its ignition temperature, which is obtained by heating the sample of a given mass at a constant rate of temperature increase until the ignition occurs. Generally, 0.2 g of sample is placed in a test tube, which is heated in a liquid metal bath. Several samples may be tested simultaneously depending on the size of the bath and the electronics. A heating rate of 5 °C/min is recommended. The test tube containing the sample is placed in the bath when the temperature of the bath containing the sample is placed in the bath when the temperature of the bath reaches 100 °C. The time elapsed between immersion of the tube and the ignition is known as the induction period. The activation energy may be calculated from the knowledge of the induction period. The test assembly is shown in Fig. 1.31.

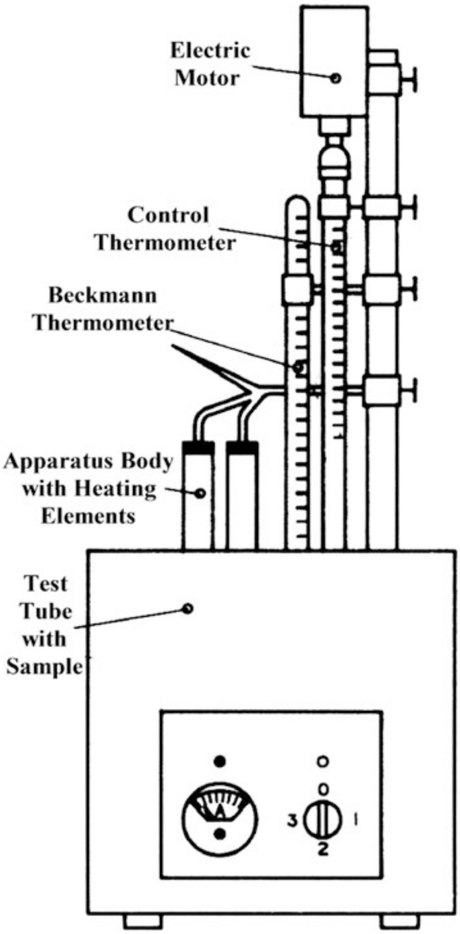

Fig. 1.31 Test assembly for determination of ignition temperature [246]

1.19 Stability

Stability of an explosive refers to the ability to store it without deterioration for a long period of time. The following factors generally affect the stability of an explosive:

Chemical constitution: The chemical compounds used for the formulation of the explosive may deteriorate or decompose to other compounds from exposure to atmospheric oxygen, heat, and moisture. The rate of the atmospheric decomposition will determine their stability or self life.

Temperature of storage: The temperature is one of the main parameters that affect the stability of the explosives most. Although the rate of decomposition of explosives increases with the increase of temperature, they should be stable at the temperature range of −10 to +35 °C.

Exposure to the sun: Exposure of explosives to sun should be avoided. The ultraviolet rays of the sun can decompose explosive compounds that contain nitrogen groups, affecting their stability.

Electrical discharge: Static or other electrical discharge may detonate an explosive under some circumstances. This is rather common to a number of explosives. As a result, the safe handling of explosives and pyrotechnics almost always requires electrical grounding of the operator.

References

1. Department of Defense (2001, December) Test method standard: safety and performance tests for the qualification of explosives (high explosives propellants and pyrotechnics). MIL-STD-1751A, 11 Superseding, MIL-STD-1751 (USAF), 20 August 1982
2. NATO STANAG 4170. Principles and Methodology for the Qualification of Explosive Materials for Military Use which has associated with it NATO Allied Ordnance Publication #7 (AOP-7) Manual of Tests for the Qualification of Explosive Materials for Military Use
3. Thiele, J (1907) Ein neuer Apparat zur Schmeltzpunktbestimmung, Berichte 40:996–997
4. LeFevre JW (2011) Measuring the melting points of compounds and mixtures: Tech 701. In: Jeffers J (ed) CER modular laboratory program in chemistry. http://www.cerlabs.com/experiments/10875407013.pdf
5. Organic Laboratory Techniques 4—University of Calgary. http://www.wwwchemucalgaryca.com/courses/351/laboratory/meltingpointpdf
6. Colepamer. www.coleparmer.com/Product/Electrothermal_Mel_Temp_Melting_Point_Apparatus_120_VAC/WU-03010-15
7. Hussain G, Rees GJ (1995) Thermal decomposition of RDX and mixtures. Fuel 74(2):273–277
8. Reid RC, Prausnitz JM, Poling BE (1972) The properties of gases & liquids. McGraw-Hill, New York, NY
9. Dautriche M (1907) The velocity of detonation in explosives. Compt Rend 143:641–644
10. Departmental of Defense (1970) Explosive sampling inspection and testing method T 1091. MIL-STD-650, Department of Defense, USA
11. Persson PA (1980) EXTEST international study group for the standardization of the methods of testing explosives. Prop Explos Pyrotech 5:23–28
12. Agrawal JP (2010) High Energy Materials Propellants Explosives Pyrotechnics. Wiley-VCH, Germany
13. Suceska M (1995) Test methods for explosives. Springer, The Netherlands
14. Kohler J, Meyer R (1993) Explosives. VCH Publishers, New York, NY, USA
15. Cook MA, Doran RL, Morris GJ (1955) Measurement of detonation velocity by dopplereffect at three-centimeter wavelength. J Appl Phys 16(4):426–428
16. Bussell T, Lam C (1994) An instrumentation system for the rapid measurement of run to detonation distances. Aeronautical and Maritime Research Laboratory, Australia, Report No DSTO-TR—0129
17. Ogata Y, Wada Y, Katsuyama K, Ma G-C (1995) Photographic measurement of the detonation velocity of explosives by high-speed camera and its comparison with other methods. Proc SPIE 2513:990
18. Benterou J, Udd E, Wilkins P, Roeske F, Roos E, Jackson D (2007) In-situ continuous detonation velocity measurements using fiber-optic bragg grating sensors. Report No UCRL-Proc-2331

19. Chan EM, Lee V, Mickan SP, Davies PJ (2005) Low-cost optoelectronic devices to measure velocity of detonation in smart structures devices and systems II. In: Al-Sarawi SF (ed) Proceedings of SPIE, vol 5649, Bellingham, WA
20. Prinse WC (2000) Development of fiber optic sensors at TNO for explosion and shock wave measurements. Proc SPIE 4183:748–758
21. van't Hof P (2006) Dynamic measurement of detonation pressure by use of a fiber bragg grating. proc SPIE, 6279
22. Cheng LK, van Bree J (2011) Fiber-optic sensors in explosion and detonation experiments. SPIE Newsroom, 1011: 17/212007050729
23. The National Park Services (NPS). U.S. Department of the Interior, USA. https://www.nps.gov/parkhistory/online_books/npsg/explosives/Chapter2.pdf
24. Agrawal JP, Hodgson RD (2007) Organic chemistry of explosives. Wiley-VCH Verlag GmbH
25. Suceska M (1995) Test methods for explosives (Shock Wave and High Pressure Phenomena). 1st edn. Springer
26. Adadurov GA, Dremin AN, Kanel GI (1969) Parameters of mach reflections in plexiglas cylinders. Zh Prikl Mekh Tekh Fiz 2:126–128
27. Bernecker RR, Clairmont AR Jr (1988) Shock initiation studies of cast plastic-bonded explosives. In: International annual conference on ICT 19th (Combust Detonation Phenom), 41/41-41/14
28. Biss MM (2013) Energetic material detonation characterization: a laboratory-scale approach. Propellants Explos Pyrotech 38(4):477–485
29. Chiang JC, Sanyal SK, Castanier LM, Brigham WE, Shah DO (1980) Foam as an agent to reduce gravity override effect during gas injection in oil reservoirs. Stanford Univ, p 89
30. Cook MA, Udy LL (1961) Calibration of the card-gap test. ARS J 31:52–57
31. Dorsett HE, Brousseau P, Cliff MD (2001) The influence of ultrafine aluminum upon explosives detonation. In: Proceedings of international pyrotech seminar 28th, pp 239–244
32. Dubovik AV, Voskoboinikov IM, Bobolev VK (1966) Role of forehead shock wave in low-speed detonation in liquid nitroglycerin. Fiz Goreniya Vzryva 4:105–110
33. Garg DD, Kamath PV (1979) Measurement of detonation pressure of explosive shocks. India Dep, Atomic Energy, pp 691–703
34. Heiss JF (1966) Pit-type rock salt dissolver tests in plexiglas models aimed at producing high-purity brine. Electrochem Technol 4(11–12):560–562
35. Hlinka JW (1975) Water model for the quantitative simulation of the heat and fluid flow in liquid-steel refractory systems. Met Soc pp 157–164
36. Ijsselstein RR (1984) A simple shock pressure transducer for measuring the performance of explosives and explosive devices. In: Proceedings of 12th symposium on explosion pyrotech, 3/89-83/95
37. Johnson JN (1982) Calculated shock pressures in the aquarium test. In: AIP conference on proceedings 78 (Shock Waves Condens Matter), pp 568–572
38. Lu S, Zhang J (1993) Simple method for determining the detonation pressure in industrial explosives. Baozha Yu Chongji 13(3):280–284
39. Majka M, Martinet J, Martin C, Berlot R (1969) Method of the temperature probe. Rev Gen Therm 8(87):251–261
40. Miller VF (1969) Selective chromium plating of Plexiglas. Soc Plast Eng Inc, pp 521–524
41. Novikov SS, Pokhil PF, Ryazantsev YS, Sukhanov LA (1969) Characteristic feature of the mechanism of combustion of condensed mixtures. Zh Fiz Khim 43(3):656–658
42. Sassa K, Ito I (1966) Measurement of detonation pressures of explosives by a modified aquarium technique. Kogyo Kayaku Kyokaishi 27(4):228–233
43. Slape RJ (1975) Detonation pressures of HNS I and II final report. Mason and Hanger-Silas Mason Co Inc, USA, p 18
44. Xu K, Yu DY, Xu YX, Zeng XF (1982) Effect of charge diameter on detonation pressure measured by aquarium technique. In: AIP Conference on proceedings 78 (Shock Waves Condens Matter) pp 573–577

45. Yakushev VV, Rozanov OK, Dremin AN (1968) The measurement of the polarization relaxation time in a shock wave. Zh Eksp Teor Fiz 54(2):396–400
46. Knudsen M (1909) Effusion and the molecular flow of gases through openings. Ann Physik 28:75–130
47. Knudsen M (1909) Experimental determination of the vapor Pressure of mercury at 0 and at higher temperatures. Ann Physik 29:179–193
48. Ickowski RP, Margrave JL, Robinson SM (1963) Clausing factor. J Phys Chem 67:229
49. Langmuir I (1916) The constitution and fundamental properties of solids and liquids part I: Solids. J Am Chem Soc 38(11):2221–2295
50. Price DM (2001) Vapor pressure determination by thermogravimetry. Thermochim Acta 253:367–368
51. Duncan M, Price MH (1998) Calorimetry of two disperse dyes using thermogravimetry. Thermochimica Acta 315: 19–24
52. Gückel W, Synnatschke G, Rittig R (1973) A method for determining the volatility of active ingredients used in plant protection. Pestic Sci 4: 137
53. Gückel W, Rittig FR, Synnatschke G (1974) A method for determining the volatility of active ingredients used in plant protection II. Applications to formulated products. Pestic Sci 5: 393
54. Gückel W, Kaüstel R, Lewerenz J, Synnatschke G (1982) A method for determining the volatility of active ingredients used in plant protection. Part III: The Temperature relationship between vapor pressure and evaporation rate. Pestic Sci 13: 161
55. Gückel W, Kaüstel R, Kroü R, Parg hl A (1995) A method for determining the volatility of active ingredients used in plant protection. Part IV: An Improved Thermogravimetric Determination Based on evaporation rate. Pestic Sci 45: 27
56. Phang P, Dollimore D, Evans SJ (2002) Thermochim Acta 392–393:119–125
57. Jensen DG, Schall ED (1966) Determination of vapor pressures of some phenoxyacetic herbicides by gas-liquid chromatography. J Agric Fd Chem 14:123–126
58. Clausius R (1850) Ueber die bewegende Kraft der Wärme und die Gesetze welche sich daraus für die Wärmelehre selbst ableiten lassen On the motive power of heat and the laws which can be deduced therefrom regarding the theory of heat. Annalen der Physik (in German) 155:500–524
59. Clapeyron MC (1834) Mémoire sur la puissance motrice de la chaleur. Journal de l'École polytechnique (in French) 23:153–190
60. Trauzl I (1885) La Dynamite. Harvard College Library, Boston
61. Gordon WE, Everett F, Bessie R, Lepper A (1955) Lead-block test for explosives. Ind Eng Chem 47(9):1794–1800
62. Ahrens H (1973) Nitropenta/potassium chloride reference curve for interpreting lead-block expansion results. Explosivstoffe 21(3):72–82
63. Ahrens H (1973) Quality of lead castings for the lead-block test and checking them by calibration with picric acid. Explosivstoffe 21(3):87–89
64. Bigourd J (1973) Bursting of blocks in the lead-block test. Explosivstoffe 21(3):82–84
65. Burlot E (1934) The lead block test for explosives. Mem artillerie franc 13:113–180
66. Chatel de Raguet de Brancion PML, Poinssot PLA, Legagneur PHMS (1967) Double-salt explosives stable toward firedamp. Societe d'Etudes et de Recherches pour l'Amelioration des Explosifs SERADEX, p 3
67. Comey AM, Holmes FB (1913) Methods for the determination of the effective strength of high explosives. In: 8th international of congress of applied chemistry (Separate)
68. Dautriche (1914) Two new types of grisoutines. Meml Poudres 17: 175–177
69. Dautriche H (1912) An explosive n with five per cent potassium nitrate. Z Gesamte Schiess-Sprengstoffwes 7:97
70. Dautriche H (1912b) An explosive n with five per cent potassium nitrate. Meml Poudres 16: 14-2069-70
71. Dautriche M (1909) Ammonium perchlorate explosives. Mem des poudres et salpetres. 14: 192-196206-133

72. Haeuseler E (1971) Choice of a method for determining the strength of explosives in the lead-block test. Explosivstoffe 19(5–6):76–82
73. Haeuseler E (1973) Problem of establishing the reference curve for the lead-block test. Explosivstoffe 21(3):71–72
74. Kast H, Haid A (1922) The explosibility of mercuric oxycyanide. Chem-Ztg 46:794–795
75. Kast H, Haid A (1922) The explosibility of mercuric oxycyanide. Z Gesamte Schiess-Sprengstoffwes 17:116–117
76. Kuznetsov VM, Shatsukevich AF (1978) Workability of explosives. Fiz Goreniya Vzryva 14(2):120–125
77. Langenscheidt F (1913a) The manufacture of tetranitromethylaniline. Arms Explos 21: 21-2236-27
78. Langenscheidt F (1913) The manufacture of tetranitromethylaniline. Z Gesamte Schiess-Sprengstoffwes 7:445–447
79. Le Roux A (1953) Explosive properties of tetramethyl ammonium nitrate. Meml Poudres 35:121–132
80. LeRoux A (1952) Explosive properties of the nitrate of monomethylamine. Meml Poudres 34:129–146
81. Medard L (1953) Explosive properties of nitroisobutanediol dinitrate. Meml Poudres 35:111–112
82. Mente WW (1909) Experiments with explosives regarding explosion of fire damp and coal dust. J Soc Chem Ind (London) 28:748
83. Moreau A, Grosborne P (1973) Tests concerning the evaluation of the initiating strength of detonators by the Hungarian method. Explosivstoffe 21(3):98–99
84. Naoum P, Aufschlager R (1924) Ammonium perchlorate. Z Gesamte Schiess-Sprengstoffwes 19:121–123
85. Neubner R (1928) The Trauzl (lead block) test. Z Gesamte Schiess-Sprengstoffwes 23: 1-553-5672-57125-129194-128
86. Porr K (1967, Jul 06) Fluid explosive mixtures from ammonium nitrate. Ger, DE 1244031 19670706, p 2
87. Reck W, Kiessetz C, Debik G (1962, Sep 03) Ammonium nitrate explosive. Patent DD 23657, p 2
88. Reidl HJ, Sauermilch W (1966, Jul 28) Castable high-capacity explosive mixtures. Wasag-Chemie A-G, DE 1221945, p 2
89. Stachlewska-Wroblowa A, Okon K (1961) Properties of tertiary phosphines II Electrophilic substitution reactions of triphenylphosphine oxides and its derivatives. Biul Wojsk Akad Tech im Jaroslawa Dabrowskiego 10(4):14–27
90. Sucharewsky M (1925) Accuracy of the Trauzl lead-block test for measuring explosive effect. Z ges Schiess-Sprengstoffw 20:26
91. Wang Y (2002) Description of lead nitride equivalent of detonator strength and its application in fuse design. Huogongpin 3:24–27
92. Wang Z-Z, Wang X-G, Xia B (2007) Study on power test method of industrial explosives. Huozhayao Xuebao 30(6): 24–26, 30
93. Aochi T, Matsunaga T, Nakayama Y, Iida M, Miyake A, Ogawa T (2000) Analysis of underwater explosion gas products of aluminum/potassium chlorate mixtures. Kayaku Gakkaishi 61(4):167–175
94. Aochi T, Miyake A, Ogawa T (1996) Underwater explosion test of Al/KClO3 pyrotechnic compositions. In: Proceedings of international pyrotech seminar 22nd, pp 23–34
95. Aochi T, Miyake A, Ogawa T, Matsunaga T, Nakayama Y, Iida M (1997) Underwater explosion characteristics of aluminum/potassium chlorate mixtures. Kayaku Gakkaishi 58 (5):202–210
96. Bjarnholt G (1980) Suggestions on standards for measurement and data evaluation in the underwater explosion test. Propellants Explos 5(2–3):67–74
97. Chi J, Ma B (1999) Underwater explosion wave by a TWT/RDX (40/60) spherical charge. Gaoya Wuli Xuebao 13(3):199–204

98. Hamashima H, Kato Y, Itoh S (2004) Determination of JWL parameters for non-ideal explosive. In: AIP conference on proceedings 706 (Pt 1 Shock Compression of Condensed Matter–2003 Part 1) pp 331–334
99. Hamashima H, Kato Y, Nadamitsu Y, Itoh S (2003) Determination of JWL parameters from underwater explosion test for ideal and non-ideal explosives. Sci Technol Energ Mater 64 (6):248–253
100. Matsunaga T, Iida M, Aochi T, Miyake A, Ogawa T, Hatanaka S, Miyahara A (1997) Explosive characteristics of report charges. In: Proceedings of international pyrotech seminar 23rd, pp 532–537
101. Murata K, Hatanaka S, Kato Y (2003) Risk assessment of pyrotechnic mixtures by underwater explosion test. In: Proceedings of international pyrotech seminar 30th (Europyro 2003, vol 2), pp 478–489
102. Paszula J, Maranda A, Paplinski A, Golabek B, Kasperski J (2005) An analysis of blast waves parameters and underwater explosion test of emulsion explosives and dynamites. University of Pardubice, pp 721–731
103. Ruyat Y, Nakayama Y, Matsumura T, Wakabayashi K, Okada K, Miyake A, Ogawa T Yoshida M (2004) Explosion strength of tri-n-butyl phosphate and fuming nitric acid (TBP/FNA) mixture evaluated by underwater explosion test. Sci Technol Energ Mater 65(1): 14–20
104. Sumiya F, Hirosaki Y, Kato Y, Wada Y, Ogata Y, Seto M Katsuyama K (2001) Characteristics of pressure wave propagation in emulsion explosives. In: Proceedings of annual conference of explosive blasting tech 27th (vol 2), 1–11
105. Sharon M, Boyles PE, Obney RH, Rast (1995, May 30) Miniscale ballistic motor testing method for rocket propellants. US 5419116 A
106. Dormans R, Nakka R (2006) "¼ Scale" ballistic evaluation motor (BEM). 1st static firing report rev. http://www.sugarshotorg.com/downloads/ssts_1st-BEM_test_reportpdf
107. Stephen WA, Warren TC, Humphrey JM, Levy S, Kroll WD (1974) Ballistic missile propellant evaluation test motor system (super bates). Air Force Rocket Propulsion Laboratory, USA, Ad/A-004 218
108. Fry RS (2001) Solid propellant test motor scaling chemical propulsion information agency. The Johns Hopkins University, Whiting School Of Engineering, Columbia Maryland, USA, DTIC Technical Report 2001, p 104
109. Rexford D, Atchley T, Sato SZ (1988, Jul 26) High strain capability ballistic test device for solid propellant rocket motors. A Morton Thiokol Inc, US 4759215
110. Brewczyk M, Rzazewski K, Clark CW (1997) Multielectron dissociative ionization of molecules by intense laser radiation. Phys Rev Lett 78(2):191–194
111. Cieslikowska M, Moskalewicz M, Wolszakiewicz T (2004) The examination of chosen ballistic parameters of igniter charge BKNO3 for igniters of solid propellant rocket motors. University of Pardubice, pp 456–463
112. Dundar D, Gullu M (2007) Use of alkyl hydantoin derivatives as binding materials in high-energy explosives propellants and undercoatings. Tubitak-Turkiye Bilimsel ve Teknik Arastirma Kurumu Turk, p 20
113. Frost DM, Cronin JB, Newton RU (2008) Have we underestimated the kinematic and kinetic benefits of non-ballistic motion? Sports Biomech 7(3):372–385
114. Johansson M, de Flon J, Petterson A, Wanhatalo M, Wingborg N (2006) Spray prilling of ADN and testing of ADN-based solid. Propellants. Eur Space Agency Spec Publ, SP SP-635 (3rd International Conference on Green Propellant for Space Propulsion and 9th International Hydrogen Peroxide Propulsion Conference 2006), johanssn/1-johanssn/6
115. Kovalev PI, Mikhalev AN, Podlaskin AB, Tomson SG, Shiryaev VA Isaev SA (1999) Investigation of the aerodynamic properties and flow field around hypervelocity objects in a ballistic test range. Tech Phys 44(12): 1402–1406
116. Labock N, Labock O (2009, Jan 15) Personal portable ballistic protection for motor vehicle occupants. USA PCT Int. Appl. (2009), WO 2009007972 A2

117. McFarland MJ, Palmer GR, Kordich MM, Pollet DA, Jensen JA Lindsay MH (2005a) Field validation of sound mitigation models and air pollutant emission testing in support of missile motor disposal activities. J Air Waste Manage Assoc 55(8): 1111–1121
118. McFarland MJ, Palmer GR, Rasmussen SL, Kordich MM, Pollet DA, Jensen JA, Lindsay MH (2006) Field verification of sound attenuation modeling and air emission testing in support of missile motor disposal activities. J Air Waste Manage Assoc 56 (7):1041–1051
119. Price EW (1952) Steady-state one-dimensional flow in rocket motors. J Appl Phys 23:142–146
120. Proebster M, Schmucker RH (1986) Ballistic anomalies in solid rocket motors due to migration effects. Acta Astronaut 13(10):599–605
121. Sandri Tussiwand G, Bandera Maggi F, De A, Luca LT (2007) Intrinsic structural-ballistic interactions in composite energetic materials Part I experiments. Hayastani Kim Handes 60 (2):186–200
122. Meyer R, Köhler J, Homburg A (2007) Expensive. Sixth, completely revised edition. Wiley-VCH, Germany
123. Satyavratan PV, Vedam R (1980) Some aspects of underwater testing method. Propellants Explos Pyrotech 5(2–3):62–66
124. Baum FA, Orlenko LI, Stanyukovich KP, Chelishev VI, Shooter BI (1975) Fizika goreniya i vzryva. Nauka, Moscow
125. Du Lownds CM, Plessis MP (1984) The double pipe test for commercial explosives I Description and results. Propellants Explos Pyrotech 9(6):188–192
126. Du Lownds CM, Plessis MP (1985) The double pipe test for commercial explosives II Numerical modeling and interpretation. Propellants Explos Pyrotech 10(1):5–9
127. Anderson PE, Cook P, Balas W, Davis A, Mychajlonka K (2010) An overview of combined effects explosives formulations. In: International annual conference on ICT 41st (Energetic Materials: for High Performance Insensitive Munitions and Zero Pollution), ander1/1-ander1/9
128. Borisov AA, Khomik SV, Mikhalkin VN (1991) Detonation of unconfined and semiconfined charges of gaseous mixtures. Prog Astronaut Aeronaut 133 (Dyn Detonations Explos: Detonations), pp 118–132
129. Broeckmann B (1998) Effective avoidance of ignition sparks electrostatic charging at pneumatic conveyors. Chem-Anlagen Verfahren 31(10):9496
130. Cudzilo S, Maranda A, Trzcinski WA (1997) Determination of energetic characteristics of ammonale 94/6 by using a cylinder test. In: International annual conference on ICT 28th (Combustion and Detonation), pp 104101–104109
131. Cudzilo S, Trzcinski WA (2001) A study on detonation characteristics of pressed NTO. J Energ Mater 19(1):1–21
132. Doherty RM, Simpson RL (1997) A comparative evaluation of several insensitive high explosives. In: International annual conference on ICT 28th (Combustion and Detonation), pp 3231–3223
133. Forbes JW, Glancy BC, Liddiard TP, Wilson WH (1998) Aquarium test evaluation of a pyrotechnic's ability to perform work in microsecond time frames. In: AIP conference on proceedings of 429 (Shock Compression of Condensed Matter–1997), pp 759–762
134. Fuch BE (1995) Picatinny arsenal cylinder expansion test and a mathematical examination of the expanding cylinder. Army Armament Res Dev Cent, Report (1995) (ARAED-TR-95014; Order No. AD-A300526), pp 31
135. Han C, Liu G, Dong Y, Feng J, Wang D, Hu H (1992) Expansion movement and fracture of a cylindrical shell due to internal explosion. North-Holland, pp 357–360
136. Hiroe T, Fujiwara K, Hata H, Yamauchi M, Tsutsumi K, Igawa T (2010) Explosively driven expansion and fragmentation behavior for cylinders spheres and rings of 304 stainless steel. Mater Sci Forum 638–642(Pt 2 THERMEC 2009), 1035–1040
137. Hiroe T, Fujiwara K, Kiyomura K (2004) The effect of wall configuration on deformation and fragmentation for explosively expanded cylinders of 304 stainless steel. Mater Sci

Forum 465–466. (Explosion Shock Wave and Hypervelocity Phenomena in Materials), pp 225–230

138. Hornberg H (1986) Determination of fume state parameters from expansion measurements of metal tubes. Propellants Explos Pyrotech 11(1):23–31
139. Hornberg H, Volk F (1989) The cylinder test in the context of physical detonation measurement methods. Propellants Explos Pyrotech 14(5):199–211
140. Jenkins CM, Horie Y, Lindsay CM, Butler GC, Lambert D, Welle E (2012) Cylindrical converging shock initiation of reactive materials. In: AIP Conference on proceedings of 1426 (Shock Compression of Condensed Matter–2011 Part 1), pp 197–200
141. Kamlet MJ, Short JM, Finger M, Helm F, McGuire RR, Akst IB (1983) The chemistry of detonations VIII Energetics relationships on the detonation isentrope. Combust Flame 51 (3):325–333
142. Koch E-C, Klapoetke TM (2012) Boron-based high explosives. Propellants Explos Pyrotech 37(3):335–344
143. Lang IF, Hung SC, Chen CY, Niu YM, Shiuan JH (1993) An improved simple method of deducing JWL parameters from cylinder expansion test. Propellants Explos Pyrotech 18 (1):18–24
144. Levkin VV (2005, Sep 27) Production method for power hydrogen and diamonds and device for its realization. Russia Russ, RU 2261223 C2
145. Lindsay CM, Butler GC, Rumchik CG, Schulze B, Gustafson R, Maines WR (2010) Increasing the utility of the copper cylinder expansion test. Propellants Explos Pyrotech 35 (5):433–439
146. Makhov MN (2007) Evaluation of the explosive performance of 12-dinitroguanidine. In: International annual conference on ICT 38th, 118/111-118/111
147. Mathieu JCE (1901, Jul 30) Carbureting apparatus for explosion-motors. U.S. US 679387 A
148. McGuire RR, Ornettas DL, Helm FH, Coon CL, Finger M (1982) Detonation chemistry: an investigation of fluorine as an oxidizing moiety in explosives. Lawrence Livermore Natl Lab, Livermore, CA, USA, ADA119092, p 38
149. Mitchell AR, Pagoria PF, Coon CL, Jessop ES, Poco JF, Tarver CM, Breithaupt RD, Moody GL (1994) Nitroureas 1 Synthesis scale-up and characterization of K-6. Propellants Explos Pyrotech 19(5):232–239
150. Murr LE, Foltz JV, Altman FD (1971) Deformation substructures and terminal properties of explosively-loaded thin-walled stainless-steel cylinders. Phil Mag 23(185):1011–1028
151. Murr LE, Wong GI, Foltz JV (1971) Comparison of residual defect structures and hardness in Inconel 600 following deformation by explosive shock loading cylindrical (explosive) expansion and cold-reduction. Mater Sci Eng 7(5):278–285
152. Nagayama K, Kubota S (2003) Equation of state for detonation product gases. J Appl Phys 93(5):2583–2589
153. Polyakov VN (1993) A new concept of estimation of fracture time and crack lengths in transmission pipelines. Inst Mater pp 1603–1609
154. Qingdong D, Bayi H, Changsheng H, Haibo H (1994) Expansion and fracture of AISI 1045 steel explosive-filled cylinders. J Phys IV 4(C8 International Conference on Mechanical and Physical Behaviour of Materials under Dynamic Loading 1994), C8-415–C418-420
155. Rumchik C, Nep R, Butler GC, Breaux B, Lindsay C (2012) The miniaturization and reproducibility of the cylinder expansion test. In: AIP conference on proceedings of 1426 (Shock Compression of Condensed Matter–2011 Part 1), pp 450–453
156. Sanchidrian JA, Lopez LM (2006) Calculation of the energy of explosives with a partial reaction model comparison with cylinder test data. Propellants Explos Pyrotech 31(1):25–32
157. Sanchidrian JA, Lopez LM, Segarra P (2008) The influence of some blasting techniques on the probability of ignition of firedamp by permissible explosives. J Hazard Mater 155 (3):580–589
158. Scovel CA, Menikoff R (2009) A verification and validation effort for high explosives at Los Alamos National Lab. In: AIP Conference on proceedings 1195 (Pt 1 Shock Compression of Condensed Matter–2009 Part 1), pp 169–172

159. Simpson RL, Urtiew PA, Ornellas DL, Moody GL, Scribner KJ, Hoffmann DM (1997) CL-20 performance exceeds that of HMX and its sensitivity is moderate. Propellants Explos Pyrotech 22(5):249–255
160. Stiel LI, Baker EL, Capellos C (2006) Study of detonation and cylinder velocities for aluminized explosives. In: AIP Conference on proceedings 845 (Pt 1 Shock Compression of Condensed Matter–2005 Part 1), pp 475–478
161. Stiel LI, Baker EL, Murphy DJ (2012) Equations of state of silicon boron and halogen species for accurate detonation calculations. Int J Energ Mater Chem Propul 11(2):149–163
162. Sun J, Kang B, Zhang H, Liu Y, Xia Y, Yao Y, Liu X (2011) Investigation on irreversible expansion of 135-triamino-246-trinitrobenzene cylinder. Cent Eur J Energ Mater 8(1):69–79
163. Tappan BC, Manner VW, Lloyd JM, Pemberton SJ (2012) Fast reactions of aluminum and explosive decomposition products in a post-detonation environment. In: AIP Conference on proceedings 1426 (Shock Compression of Condensed Matter–2011 Part 1), pp 271–274
164. Tarver CM, Tao WC, Lee CG (1996) Sideways plate-push test for detonating solid explosives. Propellants Explos Pyrotech 21(5):238–246
165. Trebinki R, Trzcinski WA (1999) Determination of an expansion isentrope for detonation products of condensed explosives. J Tech Phys (Warsaw) 40(4):447–504
166. Trzcinski WA (2001) Application of a cylinder test for determining energetic characteristics of explosives. J Tech Phys (Warsaw Pol) 42(2):165–179
167. Trzcinski WA, Cudzilo S (2006) Characteristics of high explosives obtained from cylinder test data. Hanneng Cailiao 14(1):1–7
168. Trzcinski WA, Cudzilo S, Szymanczyk L (1999) Determination of the detonation pressure from a water test. In: International annual conference on ICT 30th, 84/81-84/13
169. Victor AC (1996) A simple method for calculating sympathetic detonation of cylindrical cased explosive charges. Propellants Explos Pyrotech 21(2):90–99
170. Wesenberg DL, Forrestal MJ (1977) Dynamic expansion and fracture of stainless steel cylindrical shells. San Francisco, Calif., USA, 15–19 Aug 19776 INIS-MF–4543
171. Whittaker ML, Cutler RA, Anderson PE (2011) Boride-based materials for energetic applications. In: MRS online proceedings of library 1405 (Advances in Energetic Materials Research)
172. Wieland MS (2010) Gurney's journey—pipe-bomb fragments and fumes. In: Proceedings of annual conference on explos blasting tech 36th (vol 1), pp 293–305
173. Zhang H, Xu J, Liu Y, Huang H, Sun J (2013) Effects of crystal quality and preferred orientation on the irreversible growth of compact TATB cylindrical explosives. AIP Adv 3 (9): 092101/092101-092101/092108
174. Zimbal C, Nolde M (2010) Determination of the Gurney of civil used explosives. In: International annual conference on ICT 41st (Energetic Materials: for High Performance Insensitive Munitions and Zero Pollution) zimba1/1-zimba1/6 (1970) Improved smooth-blasting explosive cartridges, Nitro Nobel AB, p 3
175. Hornberg H (1986) Determination of fume state parameters from expansion measurements of metal tubes Propellants Explos Pyrotech 11(1): 23–31
176. Mitsui S, Watabe H, Yokogawa M, Katsuda T, Shigematsu K, Sugiyama N (1974) Liquid explosives containing nitroglycerin as the main ingredient. Kogyo Kayaku 35(3):127–132
177. Rinkenbach WH, Burton OE (1931) Explosive characteristics of tetracene. Army Ordnance 12:120–123
178. Roberts LN (1974) Liquid explosive for well fracturing. Talley-Frac Corp, May 2, 1972 p 9 US3659652 A
179. Sakurai T (1955) The brisance of explosives VIII Propagation of shock waves in air and powdery materials. J Ind Explosives Soc Japan 16:90–94
180. Trautmann W (1995) Low-brisance explosive for cladding and welding. Dynamit Nobel AG, Germany, p 3
181. Dsershkovich AA, Andreev KK (1930) The properties of the nitroglycerin isomers. Z Gesamte Schiess-Sprengstoffwes 25: 353-356400-353

182. Dubnov LV, Romanov AI (1962) Deflagration of permitted explosives in mines. Bezopasnost Truda v Prom 6(10):20–25
183. Edwards MR, Palmer ME (2003) Mitigation of comminution effects of explosives by particulate materials. J Appl Phys 93(5):2540–2543
184. Keshavarz MH, Seif F, Soury H (2014) Prediction of the Brisance of Energetic Materials. Propellants Explos Pyrotech Ahead of Print
185. Blinov IF, Svetlova LM (1963) Effect of the shell on the detonation capacity of some dinitrobenzenes. Teor Vzryvchatykh Veshchestv pp 550–557
186. Smith LC (1967) Brisance and a plate-denting test for estimation of detonation pressure. Explosivstoffe 15(6):4–130
187. Smith LC (1967) Brisance and a plate-denting test for estimation of detonation pressure. Explosivstoffe 15(5):10–106
188. Dynamit-Nobel A-G (1962) Ammonium nitrate explosives having improved sensitivity brisance and power. p 7
189. Ambrozek M, Baryla S, Guga J, Kurnatowski Z, Luszczak T (1988) Storage-stable hexogen-based plastic explosives. p 5 Abstracted and indexed from the unexamined application Zaklady Tworzyw Sztucznych “Nitron-Erg” Pol
190. Azarkovich AE (1970) Correlation between the laboratory characteristics of explosives and their explosive efficiency. Fiz-Tekh Probl Razrab Polez Iskop 3:64–69
191. Davydova EG (1948) Effect of moisture and sunlight on the explosive properties of TNT. Gorn Zh 122(5):24–25
192. Matyas R, Kuenzel M, Ruzicka A, Knotek P, Vodochodsky O (2015) Characterization of erythritol tetranitrate. Physical properties. Propellants Explos Pyrotech 40(2):185–188
193. Plucinski J, Smolenski D (1960) 246-Trinitro-3-methylnitraminotoluene (m-methyltetryl). Chem Stosowana 4:479–499
194. Ratner SB (1947) Properties of aluminum-containing explosives. Gorn Zh 121(5):21–25
195. Sakurai T, Takei I (1952) Brisance of explosives. J Ind Explosives Soc Japan 13:138–142
196. Smida T, Denkstein J, Kaderabek V (1978) Plastic gelatinized blasting explosive with high content of nitrates. Czech, p 3
197. Tamchyna V, Vetlicky B, Racek F, Mostak P (1984) Emulsion explosive. Czech, p 3
198. Urbanski T, Piskorz M, Maciejewski M, Cetner W (1959) Properties of tetranitromethane II The explosive properties of binary mixtures of tetranitromethane with some combustible or explosive substances. Biul Wojsk Akad Tech im Jaroslawa Dabrowskiego 8(42):37–41
199. Yokogawa M (1964) Combustibility of ammonium nitrate explosives Kogyo Kayaku Kyokaishi 25(3):156–159
200. Mitsui Shiro, Watabe Harusada, Yokogawa Mutsuo, Katsuda Takeshi; Shigematsu Kenji, Sugiyama Noboru (1974) Liquid explosives containing nitroglycerin as the main ingredient Kogyo Kayaku 35(3): 127–132
201. Azarkovich AE (1970) Correlation between the laboratory characteristics of explosives and their explosive efficiency. From Fiziko-Tekhnicheskie Problemy Razrabotki Poleznykh Iskopaemykh 3:9–64
202. Calvet E (1942) Brisance of explosives New tests of the practical determination of brisance. Ann faculte sci Marseille 16:3–13
203. Haid A, Koenen H (1930) The testing of blasting caps. Z Gesamte Schiess-Sprengstoffwes 25: 393-398433-399463-398
204. Haid A, Koenen H (1934) Explosive force and its determination II. Z Gesamte Schiess-Sprengstoffwes 29: 11-1437-19
205. Herlin C (1914) Brisance. Z Gesamte Schiess-Sprengstoffwes 8:448–452
206. Majrich A, Sorm F (1935) Brisance and its determination. Z Gesamte Schiess-Sprengstoffwes 30: 295-299337-240
207. Roth JF (1941) The explosive properties of mixtures of tetranitromethane and nitrobenzene: a contribution in support of the hydrodynamic theory. Z Gesamte Schiess- Sprengstoffwes 36: 4-628-3152-25

208. Smolenski D, Bogdal S, Glowiak B (1961) Preparation and properties of explosive m-hydroxytetryl salts. Zeszyty Nauk Politech Wroclaw Chem 7:3–9
209. Stadler R (1938) Analytical and technical explosive investigations on silver acetylide. Z Gesamte Schiess-Sprengstoffwes 33: 269-272302-265334-268
210. Urbanski T (1935) Determination of the brisance of explosives. Z Gesamte Schiess-Sprengstoffwes 30:68–71
211. Wohler L, Roth FJ (1934) The brisance of explosives. Z Gesamte Schiess-Sprengstoffwes 29: 9-1146-1874-17
212. US department of Defense (1962) Military standard Explosive: Sampling inspection and testing MIL-STD-650
213. Smith LC (1967) On Brisance, and a Plate-Denting Test for the Estimation of Detonation Pressure. Explosivstoffe 5(106) and (6)130
214. Suceska M (1995) Test methods for explosives. Springer Science + Business Media, LLC
215. Anshits AG, Anshits NN, Deribas AA, Karakhanov SM, Kasatkina NS, Plastinin AV, Reshetnyak AY, Silvestrov VV (2005) Detonation velocity of emulsion explosives with cenospheres. University of Pardubice, pp 175–179
216. Badners H, Leiber CO (1992) Method for the determination of the critical diameter of high-velocity detonation by conical geometry. Propellants Explos Pyrotech 17(2):77–81
217. Baklanov DI, Golub VV, Ivanov KV, Krivokopytov MS (2012) Transition of combustion into detonation within a channel with the diameter less than the critical diameter of the existence of stationary detonation. High Temp 50(2):238–243
218. Belov GV, Bakhrakh SM, Egorshin SP, Fedorova JG, Petrushin AV, Shaverdov SA, Jamolkin EL (2001) Initiation and parameters of trinitrotoluene explosion at impact by fragment. Elsevier Science BV pp 893–898
219. Borisov AA, Komissarov PV, Ibragimov RK, Silakova MA, Mailkov AE, Kudryashova EL (2004) Energies of initiation of detonation in propane- and kerosene-air mixtures by various sources. Torus Press Ltd, pp 54–59
220. Bowden M, Maisey MP, Knowles S (2012) Shock initiation of hexanitrostilbene at ultra-high shock pressures and critical energy determination. In: AIP conference on proceedings of 1426 (Shock Compression of Condensed Matter–2011 Part 1) pp 615–618
221. Debenham DF, Kosecki AP (1999) Shock initiation studies of composite gun propellants. In: International annual conference on ICT 30th 83/81-83/10
222. Dremin AN, Trofimov VS (1965) Nature of the critical diameter Symp (Int). Combust Proc 1964:839–843
223. Francois E, Sanders VE, Lloyd J, Mang J (2009) Shock sensitivity of diaminoazoxy furazan (DAAF) using an instrumented small scale gap test. In: International annual conference on ICT 40th (Energetic Materials) 17/11-17/10
224. Frankel MB, Milton B, Tarzana F, Harry A, Encino A, Glen D, Park CA, Gray JC (1980) Energetic monopropellant. United States Dept of the Air Force, Washington DC, USA, 4 297 152, Oct. 27, 1981, p 31
225. Hamate Y (2007) A computational study of microstructure effects on shock ignition sensitivity of pressed RDX. In: AIP Conference on proceedings of 955 (Pt 2 Shock Compression of Condensed Matter–2007 Part 2) pp 923–926
226. Haskins PJ, Cook MD (2007) Detonation failure in ideal and non-ideal explosives. In: AIP Conference on proceedings 955 (Pt 1 Shock Compression of Condensed Matter–2007 Part 1) pp 377–380
227. Higgins AJ, Pinard P, Yoshinaka AC, Lee JH, S (2001) Sensitization of fuel-air mixtures for deflagration-to-detonation transition. ELEX-KM Publishers, pp 45–62
228. Jette FX, Higgins AJ (2007) Critical diameter prediction for steady detonation in gasless metal-sulfur compositions. In: AIP Conference on proceedings 955 (Pt 1 Shock Compression of Condensed Matter–2007 Part 1) pp 385–388
229. Kato Y, Murata K (2008) Detonation propagation in packed bed of metal particles saturated with nitromethane. In: International annual conference on ICT 39th p 107/101-p107/108

230. Khomik SV, Gelfand BE, Knyazev MV (1994) Experimental determination of a critical diameter of detonation propagation in dust suspensions. Northeast Univ Press, pp 315–319
231. Kilmer EE (1978) Detonating cord failure in the F-111 aircraft crew module escape system. In: Proceedings of international pyrotech seminar 6th, pp 304–319
232. Klapoetke TM, Stierstorfer J (2008) Triaminoguanidinium dinitramide-calculations synthesis and characterization of a promising energetic compound. Phys Chem Chem Phys 10 (29):4340–4346
233. Knystautas R, Lee JH (1988) Detonation parameters for the hydrogen-chlorine system. Prog Astronaut Aeronaut 114(Dyn Explos) pp 32–44
234. Knystautas R, Lee JH Guirao CM (1982) The critical tube diameter for detonation failure in hydrocarbon-air mixtures. Combust Flame 48(1): 63–83
235. Knystautas R, Lee JHS, Moen IO, Guirao CM, Urtiew P (1981) Determination of critical tube diameters for acetylene-air and ethylene-air mixtures. Christian Michelsens Inst Vidensk Aandsfrihet, p 84
236. Lavrov VV, Afanasenkov AN, Shvedov KK (1997) On the experimental determination of a critical diameter and a critical detonation velocity. Publishing House of Ordnance Industry, pp 518–525
237. Maranda A, Paplinski A, Galezowski D (2003) Investigation on detonation and thermochemical parameters of aluminized. ANFO J Energ Mater 21(1):1–13
238. Maranda A, Szymanski R (2013) Testing of critical diameter and detonation velocity of mixtures of ammonium nitrate(V) and selected organic substances. Chemik 67(1):13–18
239. Matyas R, Zeman S, Trzcinski W, Cudzilo S (2008) Detonation performance of TATP/AN-based explosives. Propellants Explos Pyrotech 33(4):296–300
240. McKenney RL, Jr, Summers PG, Schomber PR, Whitney SD (1991) Small-scale testing of high bulk cubical and spherical nitroguanidine for comparative evaluation. In: International annual conference on ICT 22nd (Combust React Kinet) 2/1-2/15
241. Mendes R, Plaksin I, Campos J, Ribeiro J (2000) Double slapper initiation of the PBX. In: AIP conference on proceedings of 505 (Shock Compression of Condensed Matter Pt 2) pp 915–918
242. Michot C, Bigourd J (1978) Detonability of slurry blasting agents. Propellants Explos 3(1–2):30–33
243. Moen IO, Murray SB, Bjerketvedt D, Rinnan A, Knystautas R, Lee JH (1982) Diffraction of detonation from tubes into a large fuel-air explosive cloud. In: Symposium (Int) combust proceedings 19th, pp 635–644
244. Pawel D, Vasatko H, Wagner HG (1969) Influence of initial temperature of the limits of detonability. Goettingen Univ, p 71
245. UTEC Corp (2007) Explosive material critical diameter testing energetic materials business unit. http://www.utec-corp.com/index.php/energetic-materials/critical-diameter/
246. Department of Defense (1982) Group 1060 test methods chemical stability. USA, MIL-STD-1751A
247. Bola MS, Madan AK, Singh M, Vasudeva SK (1992) Expansion of metallic cylinders under explosive loading. Def Sci J 42(3):157–163
248. Kong X, Wu W, Li J, Liu F, Chen P, Li Y (2013) A numerical investigation on explosive fragmentation of metal casing using. Smoothed Particle Hydrodynamic method Mater Des 51:729–741
249. Stagg MS, Otterness RE (1995a) Effect of blasting practices on fragmentation: Full-scale results. In: Annual meeting Minn Sect SME proceedings of 68th 215–230
250. Stagg MS, Otterness RE (1995b) Screen analysis of full-scale production blasts. In: Proceedings of annual symposium explosive blasting Res 11th 298-313
251. Chen C-Y, Shiuan J-H, Lan IF (1994) The equation of state of detonation products obtained from cylinder expansion test. Propellants Explos Pyrotech 19(1):9–14
252. Chen H, Touchard GG Radke CJ (1996) A linearized double layer model for laminar flow electrification of hydrocarbon liquids in metal pipes. Institute of Electrical and Electronics Engineers pp 411-414

253. Craig BG, Johnson JN, Mader CL, Lederman GF (1978) Characterization of two commercial explosives. Los Alamos Scientific Laboratory Tech. Rep. USA, LA-7140 p 21
254. Cudzilo S, Maranda A Trzcinski WA (1997) Determination of energetic characteristics of ammonale 94/6 by using a cylinder test. In: International annual conference on ICT 28th (Combustion and Detonation) 104101-104109
255. Cudzilo S, Trzcinski WA (2000) A study on detonation characteristics of pressed NTO. In: International annual conference on ICT 31st (Energetic Materials) 77/71-77/14
256. Cudzilo S, Trzcinski WA (2001) A study on detonation characteristics of pressed NTO. J Energ Mater 19(1):1–21
257. Doherty RM, Short JM Kamlet MJ (1989) Improved prediction of cylinder test energies. Combust Flame 76(3-4): 297-306
258. Hamashima H, Kato Y, Nadamitsu Y, Itoh S, Haid A, Koenen H (1934) Explosive force and its determination II. Z Gesamte Schiess-Sprengstoffwes 29: 11-1437-19
259. Petel OE, Higgins AJ (2006) Comparison of failure thickness and critical diameter of nitromethane. In: AIP conference on proceedings of 845 (Pt 2 Shock Compression of Condensed Matter–2005 Part 2) pp 994–997
260. Petel OE, Mack D, Higgins AJ, Turcotte R, Chan SK (2007) Minimum propagation diameter and thickness of high explosives. J Loss Prev Process Ind 20(4–6):578–583
261. Reza A, McCarthy RL (1999) Measurements to determine the effect of selected additives on the detonability of ANFO mixtures. In Proceedings of annual conference on explosive blasting tech 25th (vol 2) pp 249–261
262. Swinton RJ, Bussell T, McVay L (1996) A critical diameter study of the Australian manufactured underwater explosive. Composition H6 Aeronautical Maritime Res Lab, AD A319313, Defence Science And Technology Organization Canberra (Australia) p 13
263. Titov VM, Sil'vestrov VV, Kravtsov VV, Stadnichenko IA (1976) Investigation of some cast TNT properties at low temperatures. Inst Hydrodynam, pp 36–46
264. Tsuchiya YN (1962) Crystal habit modification of ammonium nitrate III Application to ammonium nitrate-fuel oil explosives. Kogyo Kayaku Kyokaishi 23:78–83
265. Vidal P, Bouton E, Pagnanini L (2012) Modeling detonation in liquid explosives: The effect of the inter-component transfer hypothesis on chemical lengths and critical diameters. Combust Flame 159(1):396–408
266. Vidal P, Presles HN, Gustin JL, Calzia J (1993) Detonation failure diameters and detonation velocities of nitric acid acetic acid and water mixtures. J Energ Mater 11(2):135–153
267. Virchenko VA, Egorov AP, Fadeev AI (1993) The critical diameter of detonation of PETN single crystal. Hanneng Cailiao 1(2):17–22
268. Whelan DJ, Bocksteiner G (1995) Velocity of detonation charge diameter and critical diameter in unconfined RDX-driven heterogeneous explosives. J Energ Mater 13(1&2):15–34
269. Zenow L, Tkachenko EA, Brooks NB, Lansdale RL, Lewis GE (1967) Application of two-dimensional computations to the study of subcritical initiation and fadeout in a homogeneous explosive. Symp Combust 11:645–655 discussion 655-646
270. Wulfman DS, Sitton O, Nixon FT, Podzimek M, Worsey G, Beistel D, Worsey P, Burch D, Johnson M (1997) Reformulation of solid propellants and high explosives: an environmentally benign means of demilitarizing explosive ordnance. Can J Chem Eng 75(5):899–912
271. Nikitin VF, Dushin VR, Phylippov YG, Legros JC (2009) Pulse detonation engines: technical approaches. Acta Astronaut 64(2–3):281–287
272. Miyake A, Kobayashi H, Echigoya H, Arai H, Katoh K, Kubota S, Wada Y, Ogata Y, Ogawa T (2006) Combustion and detonation properties of ammonium nitrate and activated carbon mixtures. In: Proceedings of international pyrotech seminar 33rd pp 413–421
273. Shiromaru H, Kobayashi K, Mizutani M, Yoshino M, Mizogawa T, Achiba Y, Kobayashi N (1997) An apparatus for position sensitive TOF measurements of fragment ions produced by coulomb explosion. Phys Scr T T73 (8th International Conference on the Physics of Highly Charged Ions 1996) pp 407–409

274. Lemoine D, Cherin H, Jolibois P (1994) Determination of the sensitivity of liquid explosives submitted to mechanical threats. Int Annu Conf ICT 25th (Energetic Materials-Analysis Characterization And Test Techniques) 81/81-81/89
275. Plaksin IY, Shutov VI, Gerasimov VM, Gerasimenko VF, Morozov VG, Karpenko II Sokolov SS (1996) Evolution of explosion in TATB HE in the process of its expansion into a free space followed by impact against hard barrier. In: AIP Conference on Proceedings of 370 (Pt 2 Shock Compression of Condensed Matter–1995) pp 875–878
276. Santner E (1995) Comparison of wear and friction measurements of TiN coatings. Tribologia 26(1):7–29
277. Sapko MJ, Weiss ES, Watson RW (1989) Preferred explosives for blasting in the presence of combustible dusts. Can Inst Min Metall, USA, pp 49–61
278. Phillips JJ (2012) A modified type-12 impact sensitivity test apparatus for explosives. Propellants Explos Pyrotech 37(2):223–229
279. Le Roux JJPA (1990) The dependence of friction sensitivity of primary explosives upon rubbing surface roughness. Propellants Explos Pyrotech 15(6):243–247
280. Kubota S, Ogata Y, Wada Y, Saburi T, Nagayama K (2008) Behaviors of high explosive near the critical conditions for shock initiation of detonation. Mater Sci Forum 566 (Explosion Shock Wave and Hypervelocity Phenomena in Materials II) pp 15–22
281. Klapoetke TM, Krumm B, Nieder A, Richter O, Troegel D, Tacke R (2012) Silicon-containing explosives: syntheses and sensitivity studies of (Azidomethyl)- Bis (azidomethyl)- and Tris(azidomethyl)silanes. Z Anorg Allg Chem 638(7–8):1075–1079
282. Kerth J, Kuglstatter W (2001) Synthesis and characterization of 26-Diamino-35-dinitropyrazine-1-oxide (NPEX-1). In: International Annual Conference on ICT 32nd (Energetic Materials) 166/161-166/111
283. Peterson PD, Lee KY, Moore DS, Scharff RJ, Avilucea GR (2007a) The evolution of sensitivity in HMX-based explosives during the reversion from delta to beta phase. In: AIP Conference on Proceedings of 955 (Pt 2 Shock Compression of Condensed Matter–2007 Part 2) pp 987–990
284. Peterson PD, Avilucea GR, Bishop RL, Sanchez JA (2007b) Individual contributions of friction and impact on non-shock initiation of high explosives. In: AIP Conference on Proceedings of 955 (Pt 2 Shock Compression of Condensed Matter–2007 Part 2) pp 983–986
285. Miles G, Williams MR, Wharton RK, Train AW (1996) The development of an elevated temperature friction sensitiveness apparatus. In: International Annual Conference pn ICT 27th (Energetic Materials) pp 3131–3114
286. Matyas R, Selesovsky J, Musil T (2012) Sensitivity to friction for primary explosives. J Hazard Mater 213–214:236–241
287. Matyas R, Selesovsky J, Musil T (2012) Sensitivity to friction for primary explosives. J Hazard Mater 213–214:236–241
288. Mainiero RJ, Miron Y, Kwak SSW, Kopera LH, Wheeler JQ (1996) Impact thermal and shock sensitivity of molten TNT and of asphalt-contaminated molten TNT. In: Proceedings of annual conference on explosive blasting tech 22nd pp 179–197
289. Ishikawa K, Abe T, Kubota S, Wakabayashi K, Matsumura T, Nakayama Y, Yoshida M (2006) Study on the shock sensitivity of an emulsion explosive by the sand gap test. Sci Technol Energ Mater 67(6):199–204
290. Ling P, Sakata J, Wight CA (1996) Detonation chemistry of glycidyl azide polymer. Mater Res Soc Symp Proc 418(Decomposition Combustion and Detonation Chemistry of Energetic Materials) pp 363–371
291. Dundar D, Gullu M (2007) Use of alkyl hydantoin derivatives as binding materials in high-energy explosives propellants and undercoatings. Tubitak-Turkiye Bilimsel ve Teknik Arastirma Kurumu Turk, p 20
292. Alekseevskii EV, Musin YD (1945) Instrument for determination of ignition temperature and kinetics of oxidation of activated charcoal. Zh Prikl Khim (S-Peterburg Russ Fed) 18: 505–508

293. Bashkirov BG (1969) Determination of ignition temperature and duration of latent stage during the oxidation of sulfide deposits with the use of a linear function. Geol Razvedka Metody Izuch Mestorozhd Polezn Iskopaemykh pp 132–133
294. Edwards PW, Harrison RW (1930) Apparatus for the determination of ignition temperature of powder substances. Ind Eng Chem Anal Ed 2:344–345
295. Hu W, Yang H, Lu J, Zhang H, Zhang J, Liu Q, Yue G (2005) Determination of ignition temperature of coal by using thermogravimetry. In: Proceedings of international conference on fluid bed combust 18th pp 557–562
296. Simorova T (2007) The chosen methods of determination of ignition temperature of the wood dusts. University of Pardubice, pp 985–994
297. United Nations. Recommendations on the Transport of Dangerous Goods Tests and Criteria. United Natio United Nations Economic Commission for Europe Allied Ordnance Publication-7 (AOP-7) Annex 1 Description of Tests Used for the Qualification of Explosive. Materials for Military Use Recommendations on the Transport of Dangerous Goods: Manual of Tests and Criteria, United Nations, New York, USA
298. Department of Defense. TB 700-2 Explosives Hazard Classification Procedures Alsoknown as NAVSEAINST 80208B Air Force TO 11A-1-47 and DLAR 82201,s, Department Of Defense Ammunition And Explosives Hazard Classification Procedures New York, USA
299. Walker G R, Whitbread EG, Hornig DC (1966) Manual of Sensitiveness Tests Valcartier. Quebec Canada: Canadian Armament Research and Development Establishment Published for Tripartite Technical Cooperation Program (TTCP) Panel 0-2 (Explosives) Working Group on Sensitiveness, pp 46–50
300. NATO (1999) NATO STANAG 4489 Explosives impact sensitivity test(s) north atlantic treaty organization 1999-09-17
301. Munroe CE, Tiffany JE (1931) Physical Testing of Explosives at the Bureau of Mines Explosives Experiment Station, Bruceton, PA. U.S. Dept. of Commerce. Bureau of Mines, Bulletin 346:78–84
302. Dixon WJ, Massey FM Jr (1983) Introduction to statistical analysis, 4th edn. McGraw-Hill Co Inc, New York
303. Applied Mathematics Panel National Defense Research Committee (1944) Statistical Analysis for a New Procedure in Sensitivity Experiments. AMP Report No 101lR SRG-p No 40 July 1944
304. Becker KR (1972) Bureau of Mines Instrumented Impact Tester. Department of Interior Bureau of Mines Report of Investigations, USA, 7670
305. Dixon WJ, Mood AM (1948) Method for Obtaining and Analyzing Sensitivity Data. J Am Stat Assoc 43:109–126
306. Army Material Command (1971, January) Engineering design handbook explosive series properties of explosives of military interest. Washington DC, AMCP-706-177, p 26
307. Harris J (1982) Friction Sensitivity of Primary Explosives. ARLCD-TR-82012, Picatinny Arsenal, Dover, NJ, USA
308. Wharton RK, Harding JA (1994) A study of some factors that affect the impact sensitiveness of liquids determined using the BAM Fallhammer apparatus. J Hazard Mater 37(2):265–276
309. Wharton RK, Chapman D (1997) The relationship between BAM friction and rotary friction sensitiveness data for high explosives. Propellants Explos Pyrotech 22(2):71–73
310. Operating Manual for Model 150 ESD Sensitivity Tester Hercules Aerospace Company Allegan Ballistics Laboratory Rocket Center West Virginia
311. Kirshenbaum MS (1976) Response of Primary Explosives to Gaseous Discharges in an Approved Approaching Electrode Electrostatic Sensitivity Apparatus. PATR-4955 Picatinny Arsenal, Dover, N.J. USA
312. North Atlantic Treaty Organization (2001) NATO STANAG 4490 Explosives Electrostatic Discharge Sensitivity Test Large Scale
313. Price D, Clairmont AR Jr, Erkman JO (1974) The NOL large-scale gap test III. Compilation of Unclassified Data and Supplementary Information for Interpretation of Results Noltr 74-40, Naval Ordnance Lab, White Oak, MD, USA, AD 0780429

314. Erkman JO, Edwards DJ, Clairmont AR Jr, Price D (1973) Calibration of the NOL large-scale gap test; hugonoit data for polymethyl methacrylate NOLTR 73–15 April 1973. Naval Ordnance Laboratory, White Oak, Silver Spring, Maryland, USA
315. Walker GR, Whitbread EG, Hornig DC ed (1966) Manual of Sensitiveness Tests Valcartier. Quebec Canada: Canadian Armament Research and Development Establishment Published for Tripartite Technical Cooperation Program (TTCP) Panel 0-2 (Explosive) Working Group on Sensitiveness, pp 144–151
316. Ayres JN (1961) Standardization of the small scale gap test used to measure the sensitivity of explosives. NAVWEPS Report 7342 16 Naval Surface Warfare Center, White Oak, MD, USA
317. Price D, Liddiard TP Jr (1966) The small-scale gap test: calibration and comparison with the large scale gap test. NOLTR 66–87 7 Naval Surface Warfare Center, White Oak, MD, USA
318. Ayres JN, Montesi LJ, Bauer RJ (1973) Small-scale gap test (ssgt) data compilation:1959-1972: vo I Unclassified Explosives. NOLTR 73-132 26 Naval Surface Warfare Center, White Oak, MD, USA
319. Hampton LD, Blum GD (1965) Maximum likelihood logistic analysis of scattered go/no-go (quantal) data. NOLTR 64-238 26, Naval Surface Warfare Center, White Oak, MD, USA
320. Jaffe I, Beauregard RL, Amster AB (1960) The attenuation of shock in lucite. NAVORD 6876, Naval Ordnance Laboratory, White Oak, Maryland, USA, AD 241341
321. Liddiard TP, Price D (1987) The expanded large-scale gap test. NSWC TR 86-32, Naval Surface Weapons Center, Dahigren, Virginia, USA, AD A179406
322. Tasker DG, Baker RN (1992) Experimental calibration of the NSWC expanded large scale gap test. NSWC TR 92-54 ad A253813, Naval Surface Weapons Center, White Oak, Maryland, USA
323. Foster C (1983) Parsons and gunger “suppression of sympathetic detonation”. In: Proceedings of the 22nd explosive safety seminar, Houston, TX, USA
324. Glenn JG, Aubert SA, Gunger M E (1996) Development and calibration of a super large scale gap test. WL-TR-96-7039, Shalimar, FL, USA AD B213753
325. NATO, Standardization Agreement STANAGNATO STANAG 4488 Explosives shock sensitivity tests
326. Horst A (1987) The insensitive high explosives gap test. NSWC TR 86-058
327. Holmquist TJ (1988) Insensitive High Explosives Gap Test Data. NSWC Tr 88-282 Ad-A233 061 Strength And Fracture Characteristics OFHY-80, HY-1 00, And HY-130 Steels Subjected to Various Strains, Strain Rates,Temperatures, and Pressuresby, USA
328. Erkman JO, Edwards DJ, Clairmont AR, Jr, Price D (1973) Calibration of the nol large-scale gap test. Hugoniot Data for Polymethyl Methacrylate NOLTR 73–15, USA
329. Tan B, Long X, Peng R, Li H, Jin B, Chu S (2011) On the shock sensitivity of explosive compounds with small-scale gap test. J Phys Chem A 115(38):10610–10616
330. Koenig PJ, Mostert FJ (1998) A gap test driven by optimality statistics software. Propellants Explos Pyrotech 23(2):63–67
331. Yu X, Zheng M (2011) Influence of pad or air gap between the high explosive and flyer. University of Pardubice Institute of Energetic Materials, pp 404–411
332. Wolfson MG (1983) The MRL small scale gap test for the assessment of shock sensitivity of high explosives. Mater Res Lab. p 26
333. Trzcinski WA, Kutkiewicz M, Szymanczyk L (2005) The use of the gap test to investigate the shock to detonation transition in low-sensitivity explosives Part I—experimental approach. University of Pardubice, pp 840–846
334. Ruyat Y, Nakayama Y, Matsumura T, Wakabayashi K, Liu Z-Y, Kubota S, Nakahara T, Miyake A, Ogawa T, Yoshida M (2004) Card gap test of tri-n-butyl phosphate/fuming nitric acid mixture. Mater Sci Forum 465–466 (Explosion Shock Wave and Hypervelocity Phenomena in Materials) pp 319–324
335. Grant RL, Hanna NE, Van Dolah RW (1967) New gap-sensitivity methods for explosives. U S Bur Mines Rep Invest No 6974, p 17
336. Prokosch DW et al (1994) Chemical reactivity test for thermal stability. UCRL-JC-117941

337. McKenney RL Jr (1998) AFRL/MNME Technical Memorandum 98 60 Modified Vacuum Thermal Stability Apparatus
338. Knutson DT, Newman KE (1995) Processing and vulnerability evaluation of batch manufactured RDX. IHTR 1802, Indian Head Division Naval Surface Warfare Center Indian Head, MD, USA
339. Edwards PW, Harrison RW (1930) Apparatus for the determination of ignition temperature of powder substances. Ind Eng Chem Anal Ed 2:344–345
340. NATO STANAG 4515 Thermal Characterization of Explosives
341. ASTM (1986) E537-86 standard test method for assessing the thermal stability of chemicals by methods of differential thermal analysis. American Society for Testing and Materials, Philadelphia
342. Benchabane M (1993) The discontinuous vacuum stability test (DVST). J Energetic Materials 11(2):89–100

Additional Scholarly Articles for Further Reading

343. ASTM International (2006) Standard E 794-06: Standard test method for melting and crystallization temperatures by thermal analysis
344. ASTM D7169–11 Standard Test Method for Boiling Point Distribution of Samples with Residues Such as Crude Oils and Atmospheric and Vacuum Residues by High Temperature Gas Chromatography D6730 Test Method for Determination of Individual Components in Spark Ignition Engine Fuels by 100-Metre Capillary (with Precolumn) High-Resolution Gas Chromatography
345. ASTM A572 / A572 M–13a Standard Specification for High-Strength Low-Alloy Columbium-Vanadium Structural Steel A6/A6 M Specification for General Requirements for Rolled Structural Steel Bars Plates Shapes and Sheet Piling A36/A36 M Specification for Carbon Structural Steel A514/A514 M Specification for High-Yield-Strength Quenched and Tempered Alloy Steel Plate Suitable for Welding A588/A588 M Specification for High-Strength Low-Alloy Structural Steel up to 50 ksi 345 MPa Minimum Yield Point with Atmospheric Corrosion Resistance
346. ASTM D3132-84(1996) Withdrawn Standard: ASTM D3132-84(1996) Standard Test Method for Solubility Range of Resins and Polymers (Withdrawn 2005) Developed by Subcommittee: D0133 WITHDRAWN NO REPLACEMENT
347. ASTM E2071–00(2010) Standard Practice for Calculating Heat of Vaporization or Sublimation from Vapor Pressure Data
348. ASTM D4612–08 Standard Practice for Calculating Thermal Diffusivity of Rocks ASTM D4809–13 Standard Test Method for Heat of Combustion of Liquid Hydrocarbon Fuels by Bomb Calorimeter (Precision Method)
349. ASTM E1148-02(2008) Withdrawn Standard: ASTM E1148-02(2008) Standard Test Method for Measurements of Aqueous Solubility (Withdrawn 2013) ASTM D1696–95 (2011) Standard Test Method for Solubility of Cellulose in Sodium Hydroxide ASTM D1110 - 84(2013) Standard Test Methods for Water Solubility of Wood ASTM D7553–10 Standard Test Method for Solubility of Asphalt Materials in N-Propyl Bromide
350. ASTM D2541-93(2001) Withdrawn Standard: ASTM D2541-93(2001) Standard Test Method for Critical Diameter and Detonation Velocity of Liquid Monopropellants (Withdrawn 2003) Historical Standard: ASTM D2541-93 Standard Test Method for Critical Diameter and Detonation Velocity of Liquid Monopropellants SUPERSEDED ASTM D2539-93 Historical Standard: ASTM D2539-93 Standard Test Method for Shock Sensitivity of Liquid Monopropellants by the Card-Gap Test SUPERSEDED
351. ASTM D5842–04(2009) Standard Practice for Sampling and Handling of Fuels for Volatility Measurement ASTM D1837–11 Standard Test Method for Volatility of Liquefied

Petroleum (LP) Gases ASTM D323–08 Standard Test Method for Vapor Pressure of Petroleum Products (Reid Method)

352. UNE 31023:1994 Determination Of Explosive Brisance PowER (Hess MethoD)
353. ASTM E1248–90(2009) Standard Practice for Shredder Explosion Protection ASTM E1226–12a Standard Test Method for Explosibility of Dust Clouds
354. Specification D-4814 (previously D-439) D 7055-04 Practice for Preparation (by Abrasive Blast Cleaning) of Hot-Rolled Carbon Steel Panels for Testing of Coatings D 7072-04 Practice for Evaluating Accelerated Efflorescence of Latex Coatings
355. ASTM E1641–13 Standard Test Method for Decomposition Kinetics by Thermogravimetry Using the Ozawa/Flynn/Wall Method ASTM E2550–11 Standard Test Method for Thermal Stability by Thermogravimetry ASTM D7876–13 Standard Practice for Practice for Sample Decomposition Using Microwave Heating (With or Without Prior Ashing) for Atomic Spectroscopic Elemental Determination in Petroleum Products and Lubricants; ASTM D2879–10 Standard Test Method for Vapor Pressure-Temperature Relationship and Initial Decomposition Temperature of Liquids by Isoteniscope
356. ASTM D6600-00 Historical Standard: ASTM D6600-00 Standard Practice for Evaluating Test Sensitivity for Rubber Test Methods
357. ASTM D149–09(2013) Standard Test Method for Dielectric Breakdown Voltage and Dielectric Strength of Solid Electrical Insulating Materials at Commercial Power Frequencies

Chapter 2
Hexanitrohexaazaisowurtzitane (HNIW, CL-20)

Abstract Hexanitrohexaazaisowurtzitane, a nitroamine compound, has emerged as an important insensitive energetic material. This caged compound offers several interesting properties. This chapter discusses the properties and more importantly the formulations using CL-20.

2.1 Introduction

Hexanitrohexaazaisowurtzitane (HNIW), commonly known as CL-20, is 2,4,6,8,10,12-hexanitro-2,4,6,8,10,12-hexaazatetracyclododecane. It is a high-energy explosive compound and a polyazapolycyclic caged polynitramine. Structurally, it appears like two RDX molecules fused together. CL-20 is one of the most powerful explosives known today. Tests indicate that the formulations containing CL-20 have excellent stability, belong to hazard class 1.3, and environmentally friendly. It was first synthesized by Nielsen [1] in 1987 at the Naval Air Warfare Center, China Lake, CA, U.S.A. The strained/caged structure and high oxygen balance gives CL-20 a high density and high explosive power. The six N–NO_2 groups in CL-20 give a better oxidizer to fuel ratio and makes its performance better than RDX and HMX in specific impulse, detonation velocity, enthalpy of formation, and other parameters. It exists in five polymorphic forms, α, β, γ, ε, and ζ, and the existence of a polymorphic phase depends on the temperature and pressure. The ζ–form is formed at higher pressures. A sixth δ form has also been reported. Of these six forms, ε-polymorph has higher symmetry, thus morphologically more stable at room temperature and has the highest density (2.04 g/cm^3) than the other polymorphs. Of the six forms, only β, γ, and ε have been prepared in the pure form. CL-20 has many applications including in propulsion of strategic missiles, space launchers and for high-lethality warheads for smart and light weapons, such as Precision Guided Missiles, and Laser Guided Bombs. The cost of producing CL-20 is decreasing and is less than \$800 per kg as reported by the USA Navy Mantech Report of 2003 [2].

D.S. Viswanath et al., *Emerging Energetic Materials: Synthesis, Physicochemical, and Detonation Properties*, https://doi.org/10.1007/978-94-024-1201-7_2

2.2 Synthesis

The synthesis process may be divided into two steps. The first step involves the construction of the hexanitrohexaazaisowurtzitane cage, which is hexabenzylhexaazaisowurtzitane (HBIW). The chemical formula of HBIW is 2,4,6,8,10,12-hexabenzyl-2,4,6,12-hexaazatetracyclo[5, 5, 0, 05.9, 03.11] dodecane. HBIW is formed by the condensation reaction of glyoxal with benzylamine. Nielsen et al. [3] and Crampton et al. [4] suggested several derivatives of benzylamine to form cage. However, benzylamine provided the best yield for HBIW, about 80%. A number of solvents including acetonitrile, methanol, ethanol, and isopropyl alcohol have been tried to carry out the condensation reaction in the presence of an acid catalyst. However, acetonitrile is found to be the best solvent. The reaction can proceed in the temperature range of 0–25 °C [3]. Both organic and inorganic acids can be used as catalysts.

The second step involves nitrolysis. However, direct conversion of HBIW to CL-20 by nitrolysis cannot be carried out. The nitration of the phenyl rings is more favorable compared to the nitration of HBIW. Therefore, debenzylation of HBIW by catalytic hydrogenation prior to nitration is the preferred method. As a result, the functional groups associated with nitrogen atoms are substituted by the nitro groups.

The synthesis of CL-20 was first carried out by Nielsen and is described in the US Patent 5693794 [1]. Later Nielsen and his co-workers used a direct condensation of benzylamine with glyoxal. Crampton et al. [4] reported the synthesis of HNIW using the same route, which was the reaction of aldehydes with amines producing cage compounds. Both Nielsen et al. and Crampton et al. tried to find an alternative to benzalmine, but noted that the yield of HBIW was much lower. Debenzylation of HBIW is carried out in the presence of a catalyst. A variety of catalysts and nitrating agents have been explored. Nielsen and his co-workers used excess acetic anhydride for hydrogenation of HBIW forming 4,10-dibenzyl-2,6,8,12-tetraacetyl-2,4,6,8,10,12-hexaazaisowurtzitane (TADBIW) derivative. Several researchers employed Pd or Pd supported on carbon based catalyst in a variety of solvents for synthesis of HBIW derivatives. These include: Pd and Pd in formic acid as a solvent [5] H_2 and Pd/C in ethylbenzene [6], H_2, Pd/C, and acetic anhydride in the presence of N,N-dimethylacetamide [7]. However, the cost of palladium is an issue and should be optimized to lower the overall cost of synthesis. Other catalytic materials along with solvents used for synthesis are discussed below. Ou et al. [8] have substituted ethanol for acetonitrile. This not only reduces the cost but also the process is less toxic. In later papers, Ou et al. [9, 10] have described the synthesis of CL-20 using benyzlamine and glyoxal. Their method included the condensation with formic acid in acetonitrile to give CL-20. Methods of synthesis and properties of CL-20 a highly energetic polycyclic nitramine are surveyed (Figs. 2.1 and 2.2). Yet in another paper, Wang et al. [12] describe a one-pot synthesis of HNIW. The starting material in this case is tetraacetyldibenzylhexaaza-isowurtzitane (TADBIW).

Nielson et al. [13] and Latypov et al. [14] synthesized CL-20 via TADBIW conversion to tetraacetyldinitrosohexaazaisowurtzitane (TADNIW) using N_2O_4 or NOBF4 as catalyst. The resulting TADNIW was nitrated using NO_2BF_4. A yield of 90% was reported. However, reagents $NOBF_4$ and NO_2BF_4 are costly, which are also not environmental friendly. A mixture of nitric and sulfuric acids was used by Hamilton et al. [15] and Bellamy [16] to nitrate both TADAIW and TADFIW to CL-20. Zhao et al. used 95–99% nitric acid for TADAIW nitration. The optimized reaction parameters provided 85% yield of CL-20. Surapaneni et al. [17] also used 98% nitric acid in order to improve process economics for the synthesis of CL-20.

Qian et al. [18] developed a sono-chemical method for the synthesis of CL-20 starting with TADBIW. The described two synthesis schemes using ultrasound at 30–80 kHz frequency in their experiments and obtained yields varying from 40 to 90%. The experiments were carried out at 333.15 K, mostly at 60 kHz frequency, and 10:5:1 ratio of HNO_3, N_2O_4, and TADBIW in ionic liquids. Their two reaction schemes are shown in Figs. 2.3 and 2.4.

Qian et al. [19, 20] continued the use of N_2O_4 as a nitrating agent in their subsequent work and reported good yield of CL-20. Sung et al. [21] studied the reaction mechanism of nitration/nitrolysis of tetraacetylhexaazaisowurtzitane (TAIW) with the mixture of nitric acid and sulfuric acid. According to them, two free secondary amines of TAIW are nitrated first and then four acetyl groups of TAIW, which were dependent on temperature.

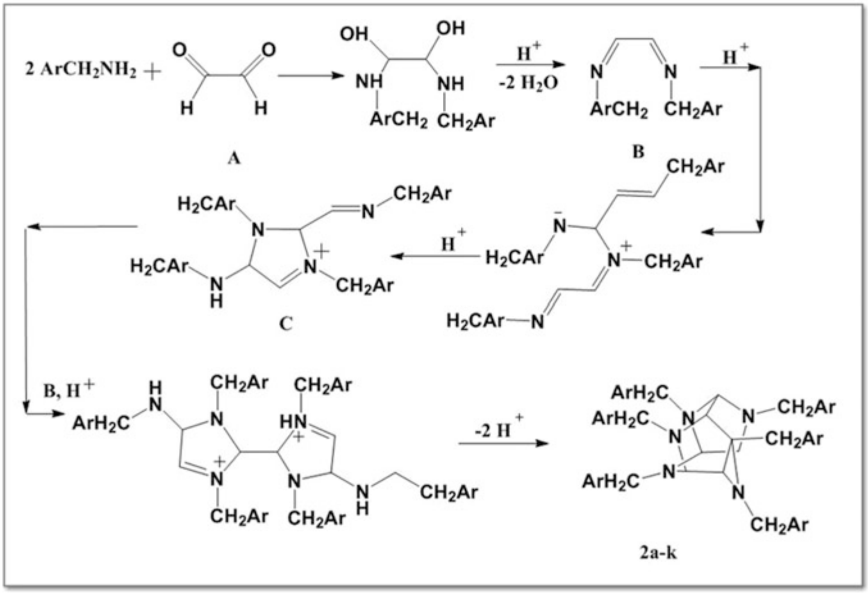

Fig. 2.1 Synthesis mechanism for this reaction is in scheme [11]. Ar = Ph (**a**), C_6H_4Me-p (**b**), C_6H_4Me-o (**c**), C_6H_4OMe-p (**d**), C_6H_4OMe-o (**e**), $C_6H_3(OMe)2.3,4$ (**f**), C_6H_4Pri-p (**g**), C_6H_4Cl-p (**h**), C_6H_4Cl-o (**i**), C_6H_4F-o (**j**), C_6H_4Br-o (**k**)

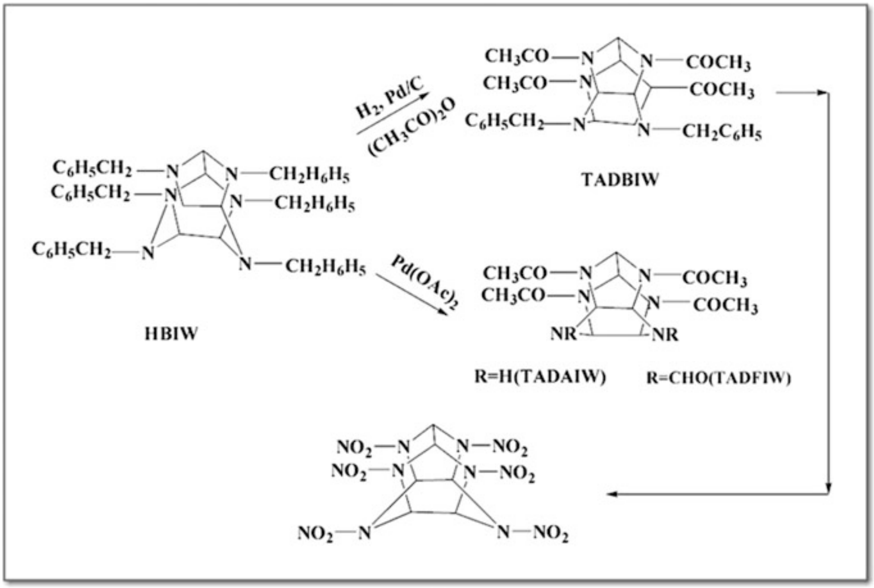

Fig. 2.2 Synthesis of hexanitrohexaazaisowurtzitane (CL-20) [3] and CL-20-based formulations

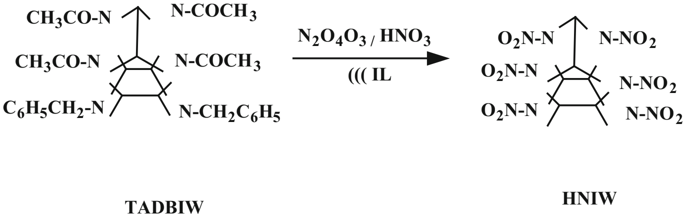

Fig. 2.3 Overall reaction scheme (Qian et al. [18, 20])

Gore et al. [22] described a method for synthesis of CL-20 from 2, 6, 8, 12-tetraacetyl-4, and 10-dibenzylhexaazaisowurtzitane using debenzylation followed by nitration. Reaction of TADBIW with cerium (IV) ammonium nitrate produced the debenzylated product, which on nitration with HNO_3/H_2SO_4 resulted in CL-20. Acetylation of the debenzylated and further nitration also resulted in CL-20. Kawabe et al. [23], and Cagnon et al. [24] patented their synthesis process for production of CL-20. Cagnon et al. synthesized hexanitrohexaaza- isowurtzitane, in a single reaction stage, by nitration of the substituted hexa- azaisowurtzitane derivative formed by reaction of the α, β-dicarbonyl derivative with the primary amine. They claimed that this route reduced the cost by eliminating the intermediate step of making HBIW and eliminating the expensive stage of catalytic hydrogenolysis. Kawabe et al. [23] used an expensive palladium catalyst.

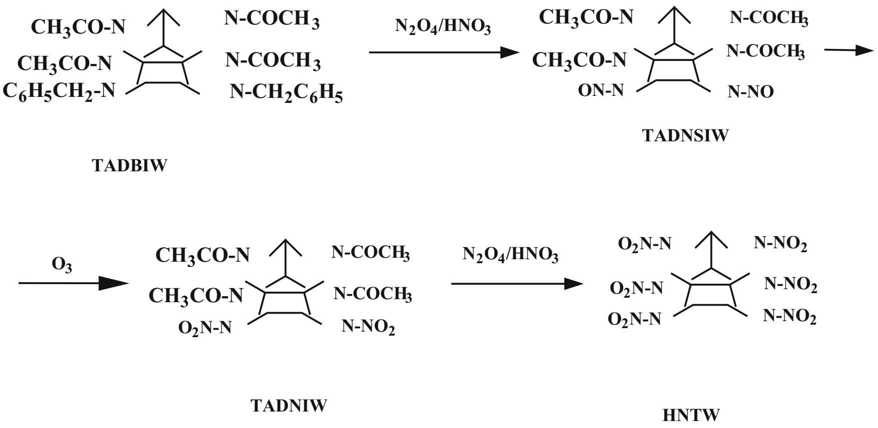

Fig. 2.4 Actual reaction scheme showing the intermediates [20]

In the one-pot synthesis process for HNIW described by Wang et al. [12] the starting material was TADBIW. A yield up to 82% and a purity of CL-20 up to 98% was claimed by the authors. This one pot method is based on the method described earlier by Latpov et al. [25]. This is a two stage process involving nitrosation followed by nitration in which 2,6,8,12-tetraacetyl-4,10-dibenzyl-2,4,6,8,10,12-hexaazaisowurtzitane is converted to 2,4,6,8,10,12-hexanitro- 2,4,6,8,10,12-hexaazaisowurtzitane, and it is claimed that the product is better than 95% pure. Pang et al. [26] describe a synthesis route in which hexabenzylhexaazaisowurtzitane is converted to HNIW and avoided the hydrogenolysis step. Although the route of oxidative debenzylation and acetylation is less expensive, the yield is less than the conventional process.

Chapman and Hollins [27] described the oxidation of hexa(1-pro-pentyl)hexaazaisowurtzitane [HPIW] by singlet oxygen. This synthesis route is a modified procedure suggested by Herve et al. [28], although they did not synthesize CL-20. They presented a general method for the synthesis of hexaazaisowurtzitane cages avoiding the condensation of benzylamines. Some of the compounds synthesized by these authors could act as precursors for the preparation of CL-20. The procedure consists of the synthesis of hexaallylhexaazaiso-wurtzitane, followed by its conversion to HPIW, and finally to HNIW. The authors present different routes to the synthesis of HPIW and different photooxidation routes to convert HPIW to HNIW.

The effect of several process variables and their optimization has been discussed by Mandal et al. [29]. Their study noted that for approximate 85% yield, optimized temperature range was 345–358 K, nitric acid concentration range from 98 to 92%, reaction time of 1 h, and temperature during the addition of TAIW into the mixed acid to be in the range of 298–313 K. To improve the particle size of CL-20, during the recrystallization process, the authors have studied the effect of parameters like addition rate of anti-solvent and rate of agitation and identified optimum conditions.

Purification, recrystallization, and nano particle synthesis of CL-20 have received a greater attention in recent years. The importance of different polymorphs and particle size in the use of CL-20 as an insensitive explosive have been discussed by several authors [30–34].

In an unusual study of crystal transition, Song et al. [21] have looked at the effect of solvents on crystal transformation. ε-CL-20 was recrystallized from pure (alcohol, dichloro-methane, acetone and ethyl acetate) and mixed (alcohol-acetone, alcohol-ethylacetate, dichloromethane-acetone, dichloromethane-ethyl acetate and acetone-ethyl acetate with different volume ratio) solvents. The resulting crystal forms were characterized by Fourier Transform Infrared Spectroscopy (FTIR) and Scanning Electron Microscope (SEM).

Several authors have reviewed the synthesis of CL-20. They are: Ou et al. [8, 9], Sysolyatin [11], Agrawal [35], and Nair et al. [36]. Chapman et al. [37] investigated the synthesis of CL-20 as a part of their work for SERDP. Their procedure does not involve benzylamine glyoxal condensation, a procedure followed by many investigators. A synthesis method starting from tetracetyldi-formylhexaazaisowurtzitane (TADFIW) has been described by Jin et al. [38] in which γ-HNIW was first produced and then was converted to ε-CL-20 in the solution in which nitration reaction occurred. The yield of ε-CL-20 was 91%, and the purity close to 99.5%. Duddu and Dave [39] proposed a method to transform all other polymorphs to ε-HNIW using acetic acid and ethyl acetate as mixed solvent, and n-hexane as nonsolvent.

2.2.1 Characterization of Polymorphs of CL-20

The ε-HNIW has the highest density among all other polymorphs and thermodynamically most stable at ambient conditions. As a result, the focus is to synthesize ε-HNIW with a maximum yield. Various properties of Cl-20 polymorphs are given in Table 2.1. As shown in Table 2.1, these polymorphs differ from each other in the spatial orientation of the nitro groups relative to the five- and six-membered rings of the cage, the type of the crystal packing and the number of molecules per unit cell [11].

Wardle and Hinshaw [40] discussed the formation of α-, β-HNIW, which mainly depended on the solution used for recrystallization or precipitation of HNIW. The α-HNIW was formed upon precipitation of HNIW with chloroform from its solutions in sulfolane. They noted the presence of β-HNIW when crude HNIW was recrystalized from benzene solution. However, β-HNIW is very unstable and coverts readily to γ-HNIW at 185 °C. γ-HNIW can also be synthesized by the nitrolysis of the diformyl derivative with nitric acid. Direct synthesis of δ-HNIW is not known. Although Wardle and Hinshaw initially reported that the heating of γ-HNIW at 230 °C changes it to δ-HNIW. Later, based on IR spectroscopic data, they suggested it was a structural modification rather than the formation of δ-HNIW, which is stable only at elevated pressures, and was detected during the

Table 2.1 Property and CL-20 polymorphs [11]

Property	Polymorph			
	α	β	γ	ε
Orientation of the NO_2 groups at the N(4) and N(10) Atoms	*exo, exo*	*exo, exo*	*exo, exo*	*exo, endo*
Number of molecules per unit cell	8	4	4	4
Space group	*Pbca*	$Pb2_{1a}$	$P2_{1/n}$	$P2_{1/n}$
Symmetry	Orthorhombic	Orthorhombic	Monoclinic	Monoclinic
Crystal habitus	Prisms	Needles	Plates	Prisms
Decomposition temperature, °C	260	260	260	260
Polymorphic transition temperature (and type), °C	–	185 (β→γ)	230 (γ→δ)	–
Density (g cm^{-3})	1.961 (2.001)[a]	1.985	1.916	2.04

[a] The value is given for the hemihydrate of the α Polymorph

equilibrium transformation of the γ-phase. Russel et al. [41] reported the presence of ζ-HNIW at a high pressure during a reversible phase transition of the γ-polymorph at a pressure of (0.7 ± 0.05) GPa.

Ciezak et al. [42] examined the high pressure transition of ε to γ-CL-20 at room temperature and at pressures up to 27 GPa. They obtained the vibrational spectra of polycrystalline material and their recorded Raman spectra are shown in Fig. 2.5.

Raman profiles shown are vertically scaled for the sake of clarity. The main region covered is from 200 to 1100 cm^{-1}, and the range between 1200 and 1400 cm^{-1} is omitted. The omission in this range is explained as dominance due to strong first-order scattering from the diamond anvils. The authors apparently omitted

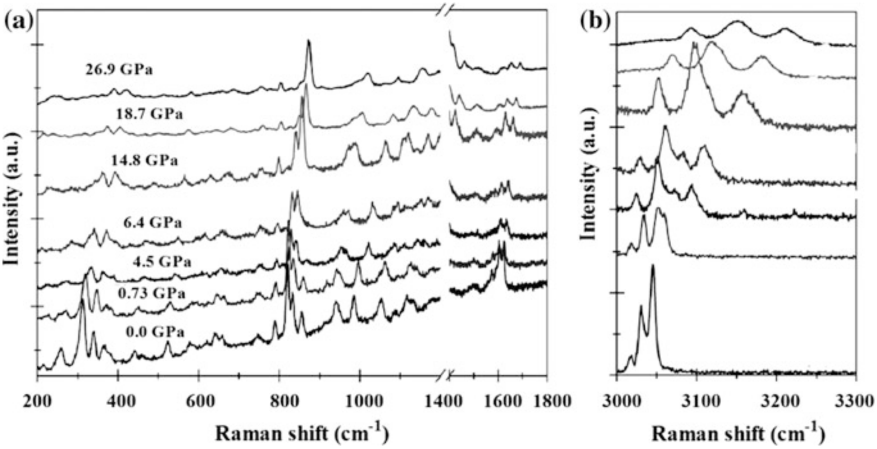

Fig. 2.5 Typical Raman spectra of CL-20 in the frequency range of 200–1800 cm^{-1} (**a**) and 3000–3300 cm^{-1} (**b**) [42]

the spectral region between 1800 and 3000 cm^{-1} as the vibrational intensity in this range was low. Based on their experimental data, they concluded that the $\varepsilon \rightarrow \gamma$ transition is purely conformational and that both the crystallographic space group and number of molecules per unit cell are retained. They also suggest the existence of $\gamma \rightarrow \delta$ transition at 18.7 GPa. It is clear that the spectra are pressure-induced, and the pressure effect is prominent in the 200–400 frequency range

Gump and Peiris [43] also investigated the phase transition as a function of pressure and temperature. They noted that ε-HNIW was stable under ambient pressure to a temperature of 120 °C. A phase transition to the γ-HNIW was observed at 125 °C and the γ-HNIW remained stable until thermal decomposition above 150 °C. The XRD measurements used to follow the phase transition are shown in Fig. 2.6. They fitted the pressure-volume data for the ε-HNIW phase at ambient and 75 °C by the Birch–Murnaghan formalism to obtain isothermal equations of state.

Turcotte et al. [44] explored the phase transitions using a DSC system. The DSC curve is shown in Fig. 2.7. They noticed the presence of two peaks. The peak at *Tp* = 162 ± 1 °C was assigned to a solid–solid phase transition from $\varepsilon \rightarrow \gamma$. The peak at 141 ± 1 °C could not be assigned to any polymorph as there was no reference of such a peak in the literature. Ghosh et al. [45] using raw CL-20 prepared ε-CL-20 and provide density, X-ray diffraction patterns, FTIR and Raman frequencies, DSC curve as a part of the characterization of ε-CL-20.

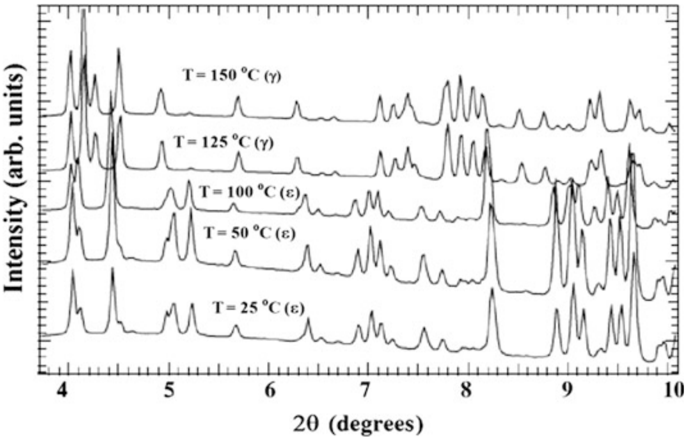

Fig. 2.6 Phase change from ε to γ upon heating at ambient pressure [43]

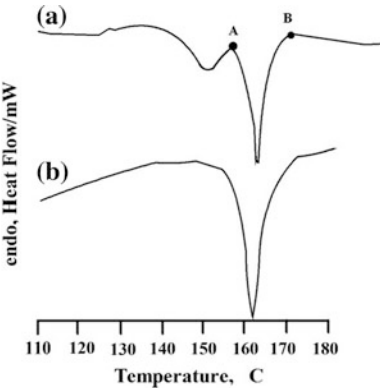

Fig. 2.7 Endothermic phase transition of CL-20: DSC, 5 °C min^{-1}, pinhole pan, in nitrogen: **a** 0.2 mg heated from 30 to 190 °C; **b** 5 mg with a 1 h isothermal step at 140 °C [44]

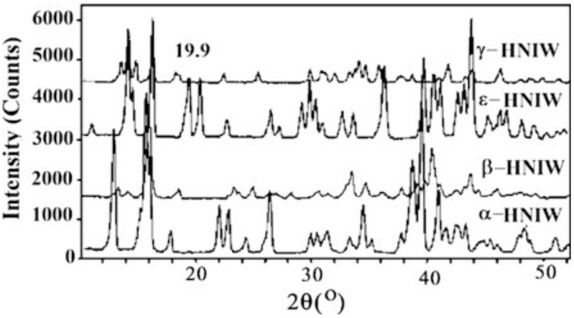

Fig. 2.8 XRD patterns of phase change of HNIW [47]

2.2.2 Diffraction Studies

The XRD pattern is a valuable information for identifying a compound and its polymorph. As discussed in the previous section (Fig. 2.8) the XRD was used to understand the transition of ε-HNIW to γ-HNIW. Meents et al. [46] investigated electron density of the ε-polymorph of CL-20 based on high-resolution X-ray single-crystal diffraction experiments at low temperature using synchrotron radiation. The crystals were made by recrystallization from a solution in which ε-HNIW was dissolved in propanol. Based on their experimental studies and model fitting, the authors discuss the chemical bonding and come to the conclusion that there is no evidence to support that electron-density maxima near the C–NO_2 bonds mapped on the electron-density isosurface can be correlated with impact sensitivities. The experimental results compared well with the DFT calculated bond-topological properties.

Chen et al. [47] studied in detail the XRD pattern of α-HNIW, β-HNIW, γ-HNIW, and ε-HNIW. The data are shown in Fig. 2.8 that covered 2θ from 10 to 50°. According to the authors, diffraction peaks for all four polymorph were not observed above 50°. There are more than 20 diffraction peaks in each XRD pattern of α-, β-, γ-, and ε-HNIW, respectively, some of which had overlapping peaks (Table 2.2).

Table 2.2 Important diffraction information of α-, β-, γ-, and ε-HNIW crystals [47]

Analytic	Crystallographic parameters	2θ (°)	D (hkl)	I%
ε-HNIW	Crystal system:	12.6	12.5	94.0
	Monoclinic	12.8	6.9	41.0
	Space group: P21/a	13.8	6.4	94
	a (nm) 1.3748	15.7	5.6	40
	b (nm) 1.2596	19.9	4.4	20
	c (nm) 0.8867	22.0	4.0	46
	α (°) 90	25.8	3.5	52
	β (°) 111.9	27.8	3.2	61
	γ (°) 90	29.9	3.0	47
α-HNIW	Crystal system:			
	Orthorhombic			
	Space group: Pbca	12.1	7.3	77.0
	a (nm) 0.9478	13.8	6.4	100
	b (nm) 1.3206,	15.1	5.9	36.0
	c (nm) 2.356	20.2	4.4	40
	α (°) 90	28.0	3.2	67.0
β-HNIW	Crystal system:			
	Orthorhombic			
	Space group: Pca21	13.6	6.5	89.0
	a (nm) 0.9652	13.7	6.5	100
	b (nm) 1.1644	24.2	3.7	21.0
	c (nm) 1.3002	28.3	3.2	28.0
γ-HNIW	Crystal system:	13.9	6.3	43.8
	Monoclinic	14.5	6.1	100
	Space group: P21/n	15.2	5.8	41.5
	a (nm) 1.3213	16.5	5.3	64.1
	b (nm) 0.8161	18.6	4.8	22.6
	c (nm) 1.4898	22.8	3.9	19.1
	α (°) 90	34.4	2.6	37.9
	β (°) 109.12	36.1	2.5	37.9
	γ (°) 90	42.1	2.1	40.0

2.3 Detection

The main focus on the detection of CL-20 is from water and soil. One of the issues related to its detection is the fragmentation and decomposition of CL-20 in the liquid medium including water. Cabalo and Sausa [48], by using a surface laser photo-fragmentation- fragment detection (SPF-FD) spectroscopy at ambient temperature and pressure, were able to detect various explosives including CL-20 in the concentration range of 1–15 ng/cm^2 at 1 atm and room temperature. They used a low power, 248-nm laser photo-fragments the target molecule on the surface of a substrate, and a low power, 226-nm laser ionizes the resulting nitric oxide fragment by resonance-enhanced multi-photon ionization by means of its A-X (0,0) transitions near 226 nm. The lower limit of detection for CL-20 was 7.1 ng/cm^2 at 248 nm. A HPLC coupled with a UV detector is used frequently to identify and quantify CL-20 in a solution. As noted by Larson et al. [49] the detection of CL-20 in a variety of environmental samples requires matrix-specific sample preparation, separation by reverse-phase high performance liquid chromatography, and ultraviolet detector. Also, most of these methods follow USEPA SW-846 Method 8330 for the determination of explosives in waters and soils. Using a chromatographic column and UV-VIS detector, Larson et al. separated and detected CL-20 from the solution [49]. The UV spectrum of CL-20 in acetonitrile is shown in Fig. 2.9.

A number of researchers have used a combination of HPLC and various other detectors to detect CL-20 [50, 51]. Anthony et al. [52] used EPA 8330A method to detect CL-20 in soil samples. The HPLC was equipped with a Supelcosil LC-CN column for separation of CL-20 and a Diode Array Detector set at 230 nm (lmax) was used for detection of CL-20. An ultra HPLC also appears to be promising for separation of energetic materials including Cl-20 [53]. Oehrle [54] used USEPA SW-846 Method 8330 for analysis of CL-20 in the presence of 14 nitroaromatics and nitramine. Along with HPLC, he used a photodiode array detection system for

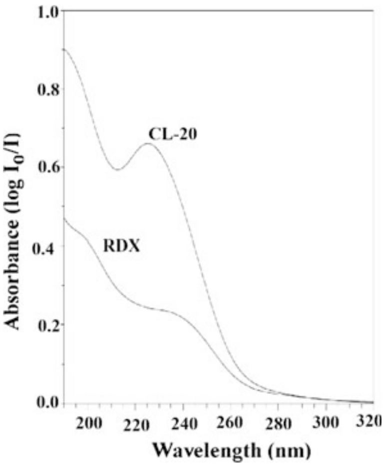

Fig. 2.9 Absorbance curve of 2.25 × 10^{-3} M RDX and CL-20 in the 190- to 290-nm range [48]

CL-20 peak identification. The analysis for CL-20 was accomplished in less than 30 min using an isocratic HPLC mobile phase of water and isopropanol.

Persson et al. [55] used a HPLC method for qualitative and quantitative analysis of a mixture of RDX, 2,4,6-TNT, 2,4-DNT, HMX, PETN, Tetryl, HNS, TNAZ and HNIW. A programmable multi-wavelength detector in the UVNIS range was used for detection of these explosives in less than 10 min. The detection limit for HNIW was was less than 5 ng.

NMR characterization has been carried out [56] and coupling constants have been determined. Agilent Technologies prposed a APCI LC/MS/MS based methods for deetction of TNT, RDX, and CL-20. According to them, CL-20 yields two intense product ions. The major product ion is m/z 154 or a loss of 319 mass units ($C_5H_5O_8N_9$). The mass spectrum is given in Fig. 2.10.

2.4 Physical and Thermal Properties

Physical, and thermal properties of CL-20 are given in Table 2.3. In addition to the data presented in this table, other properties such as solubility, vapor pressure, ideal gas heat capacity and entropy are also discussed in the following sections (Tables 2.4 and 2.5)

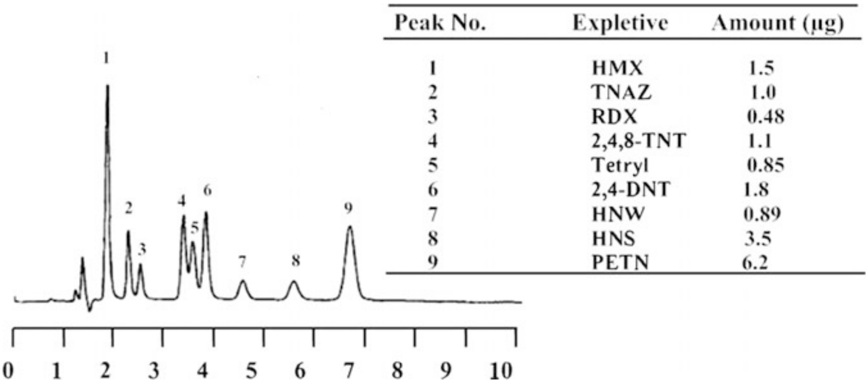

Peak No.	Expletive	Amount (μg)
1	HMX	1.5
2	TNAZ	1.0
3	RDX	0.48
4	2,4,8-TNT	1.1
5	Tetryl	0.85
6	2,4-DNT	1.8
7	HNW	0.89
8	HNS	3.5
9	PETN	6.2

Fig. 2.10 HPLC chromatogram for a nine compound explosive mixture (measurement parameters as in Table) [55]

Table 2.3 Properties of CL-20

CAS number	135285-90-4
IUPAC name	5,2,6-(Iminomethenimino)-1H-imidazo[4,5-b]pyrazine, octahydro-1,3,4,7,8,10-hexanitro-
Other names	2,4,6,8,10,12-Hexanitro-2,4,6,8,10,12-hexaazatetracyclododecane; 2,4,6,8,10,12-Hexanitrohexaazaisowurtzitane; CL 20; HNIW; Hexanitrohexaazaisowurtzitane; LX 19; RX 39AB; RX 39AC
Chemical structure	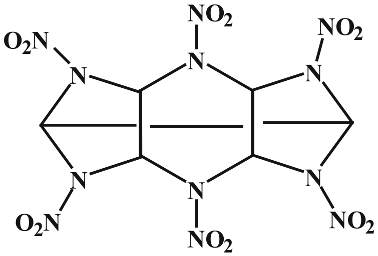
Molecular mass	438.23, Daltons
Density	2.04, g/cm^3 @ 298.15 K
Melting point	513 K [57]
Boiling point	862 K [57]
Acentric factor	2.347 [57]
Critical temperature	1058 K [57]
Critical pressure	48.9 bar [57]
Dipole moment	1.016 debye [58]
Enthalpy of fusion	13.7 [57] and 42.7 [59] kJ/mole
Enthalpy of formation (gas phase)	141.0 kcal/mole
Enthalpy of sublimation	150–170 kJ/mole
Enthalpy of vaporization	−311 kJ/mole
Aqueous solubility	3.86^{-3}; 2.91^{-3} g/l @ 298.15 K [60]
Log K_{OW}	1.92 [51] 1.375 and 4.14 {Predicted values}

Table 2.4 Enthalpy of combustion and formation [61]

Material	$\Delta H_{combustion}$ (10^6J/mo1)	$\Delta H_{formation}$ (10^3J/mol)
β-CL-20	−3.649	+431.0 ± 13
ε-CL-20	−3.596	+377.4 ± 13

Table 2.5 Enthalpy of detonation of CL-20 [61]

Material	ρ(g/cm^3)	J/g$^{(a)}$	J/cm^3	TMD$^{(b)}$J/J/cm^3
ε-CL-20	1.96 Expt.	6.234 ± 63	12,219 ± 123	12,717 ± 129
ε-CL-20	1.96 Calc.	6.029 ± 146	11,817 ± 286	12,301 ± 298

(a) 25 °C, $H_2O^{(liquid)}$

(b) TMD is the theoretical maximum density

2.4.1 Vapor Pressure

Only a few experimental vapor pressure data are reported in the literature. Greenlief et al. [62] obtained the data at the low pressure range using the Knudsen effusion method. The data are shown in Table 2.6.

Sinditskii et al. [63] while determining the kinetic parameters of combustion of four solid rocket propellant oxidizers and other energetic compounds also obtained the vapor pressure data including that of CL-20 above 600 K. Sinditskii et al. compiled the vapor pressure data for CL-20 from the literature (see Fig. 2.11), and noted significant differences in the reported values.

Both Greenlief et al. [62] and Sinditskii et al. [63] correlated the vapor pressure data according to a Clausius-Clapeyron type equations. The equations along with their best fit constants are given below:

$$\text{Solid: } \ell n P = 25.328 - \frac{17{,}715}{T}, (\text{for } 660\text{–}775\,\text{K})$$

$$\text{Liquid: } \ell n P = 19.337 - \frac{13{,}085}{T}, (\text{for } 775\text{–}960\ \text{K})$$

The equation provided by Greenlief is given below:

$$LnP = 9.552 - \frac{9087.9}{T}$$

This equation provided a maximum deviation of 5% and an average absolute deviation of 4%.

Boddu et al. [64] calculated the vapor pressure of CL-20 using an equation of state approach. However, their predicted values are an order of magnitude lower compared to our experimental data [62].

Table 2.6 Experimental vapor pressure data, P in Pascals. [62]

Temperature (K)	383.15	393.15	395.15	405.15	405.15
Vapor pressure (Pa)	7.067^{-07}	1.219^{-06}	1.528^{-06}	2.435^{-06}	2.659^{-06}

2.4.2 *Heat Capacity and Entropy Data*

Table 2.7 lists the ideal gas heat capacity and entropy values evaluated by Osmont et al. [65] based on Ab-Inito calculations.

2.5 Solubility

The aqueous solubility of CL-20 has been measured as a function of temperature by Monteil-Rivera et al. [51], and by Karakaya et al. [66]. Tables 2.8 and 2.9 list their data. The results from these two sets of data do not agree closely, and the difference between the two sets of data increased with the increase in temperature. This could be due to the analytical techniques used, the purity of the chemical, and the degree of conversion of ε-CL-20 to other phases, particularly the γ-phase. Holtz et al. [67]

Table 2.7 Ideal gas heat capacity and entropy [65]

T (K)	300	400	500	600	800	1000	1500
C_p^o (cal mol^{-1} K^{-1})	91.1	114.2	132.6	146.8	166.1	178.1	193.4
T (K)	2000	2500	3000	3500	4000	4500	5000
C_p^o (cal mol^{-1} K^{-1})	200.2	203.7	205.7	206.9	207.8	208.3	208.8
T (K)	300	400	500	600	800	1000	1500
S^o (cal mol^{-1} K^{-1})	167.3	196.8	224.3	249.8	295.0	333.4	409.0
T (K)	2000	2500	3000	3500	4000	4500	5000
S^o (cal mol^{-1} K^{-1})	465.7	510.8	548.2	580.0	607.7	632.2	654.2

Table 2.8 Aqueous solubility of CL-20 as a function of temperature [68]

Solubility of CL-20		
Temperature (°C)	(mg/L)	Mole fraction
4	2.27 (± 0.09)	9.33 10^{-8}
19.5	3.11 (± 0.06)	1.41 10^{-7}
25	4.33 (± 0.04)	178 10^{-7}
30	5.46 (± 0.02)	2.26 10^{-7}
35	6.69 (± 0.01)	2.86 10^{-7}
39	8.10 (± 0.06)	3.33 10^{-7}
45	11.30 (± 0.25)	4.64 10^{-7}
50	14.16 (± 0.47)	5.82 10^{-7}
55	17.37 (± 0.17)	7.14 10^{-7}
60	23.98 (± 0.41)	9.85 10^{-7}
65	32.36 (± 1.03)	1.33 10^{-6}
69	39.68 (± 0.25)	1.63 10^{-6}

Table 2.9 Aqueous solubility (*S*) of CL-20 as a function of temperature [68]

t (°C)	5	10	15	20	30	40	50	60
S (mg/L)	1.97	2.12	2.48	3.16	4.89	7.39	11.62	18.48

observed a transition in the solubility for CL-20 in different solvents. The solubility of Cl-20 in thirteen solvents—acetone, bis(fluorodinitroethy1) formal, ethanol, ethyldinitropentanoate, ethyl acetate, ethylene glycol, FM-1 (FM-1 is a liquid explosive composedof 25% FEFO, 25% bis(dinitropropy1) formal, and 50% fluorodinitroethyldinitropropylformal (by mole percent), methylene chloride, nitroglyceridtriacetin75/25 (NG/TA), nitroplasticizer (NP), triethyleneglycol dinitrate, trimethylolethane tri-nitrate, and water were measured. The solubility-temperature relation for each solvent was provided by them.

The solubility data collected by Monteil-Rivera et al. [51] are shown in Table 2.9 and graphically in Fig. 2.12. During measuremnets, the authors found that CL-20 decomposed in non-acidified water upon contact with glass containers to give NO_2^- (2 equiv.), N_2O (2 equiv.), and $HCOO^-$ (2 equiv.).

2.6 Decomposition and Destruction

Thermal Decomposition

Thermal decomposition of HNIW starts above 210 °C. Turcotte et al. [68] studied thermal behavior of CL-20 under various conditions using different techniques that included DSC, TG, Heat Flux Calorimetry, Accelerating Rate Calorimetry, and simultaneous TG-DTA-FTIR-MS analysis. NO_2 is the most significant product of the decomposition. Other compounds that are identified from FTIR included N_2O, CO_2, HCOOH, HNCO, H_2O, HCN, CO and NO. The gaseous products; CO_2, N_2O, NO_2, HCN, NO and CO are result of secondary decomposition reactions. They also noted that the heating rate and the purge gas used during heating had no effect on the decomposition products or the mass loss, which was between 80 and 98% of the initial mass. Korsounskii et al. [70] studied the thermal decomposition characteristics along with the kinetics for HNIW. As expected, the rate of mass loss of CL-20 was dependent on temperatures and found a final mass loss of about 80% in air within 200 min in the temperature range of 183–211 °C. In comparison, HMX did not show any decomposition at 220 °C within 200 min. Based on the IR spectrum, the authors conclude that the hemolytic cleavage of the N–NO_2 bond to be the primary cause of HNIW decomposition. The effect of particle size on thermal decomposition of CL-20 has been discussed by Dong et al. [71]. They compared the decomposition steps for isothermal and non-isothermal decomposition for 40 and 230 μm particles. The 230 μm particles decomposed in two steps under non-isothermal conditions, where as it was a one step decomposition for smaller particles. The main products identified using FTIR were NO,

N_2O, CO_2, and a small amount of NO_2 and $C_2N_2H_2$. During isothermal decomposition, the decomposition products from larger HNIW particles at 204 °C were same as that observed in the first step of the non-isothermal decomposition.

Several researchers focused on the decomposition kinetics and developed expressions for the reaction rates. Korsounskii et al. [70] found that the solid state decomposition follows first-order kinetics and that it is an autocatalytic decomposition. The thermogravimetry analysis in a narrow temperature range of 458–477 K resulted in an activation energy of 151.7 kJ/mol and a frequency factor of $10^{13.6}\ \mathrm{s}^{-1}$. The decomposition reaction rate is represented by:

$$\frac{dx}{dt} = k_1(1-\alpha) + k_2\alpha(1-\alpha)$$

$$\alpha = \frac{m_0 - m}{m_0 - m_\infty}$$

where m_0 is the weight of the starting sample, m is its weight at time t and m_∞ is the weight of the sample at the end of experiment and k_1 and k_2 are given by:

$$k_1 = 10^{20.5\pm0.8}\ \mathrm{e}^{\left(-\frac{53{,}400\pm1500}{RT}\right)}$$
$$k_2 = 10^{17.3\pm1.4}\ \mathrm{e}^{\left(-\frac{44{,}700\pm2900}{RT}\right)}$$

Bohn [72] provides a general model for isothermal decomposition of solid energetic materials, and verified his model with data on ε-CL-20. Kinetic parameters and Arrhenius parameters are developed. The following expression was suggested for approximation of the HNIW decomposition during which a mass loss of 0–11% would occur.

$$ML(t,T) = O + \frac{m_C}{m_A}\left[1 - M_{Ar}(t,T)\right] \times 100\%$$

The parameter, O, stands for an offset not caused by the decomposition of compound A.

Figure 2.13 shows some of the results of this study. The solid lines in Fig. 2.13 show the model calculations, and dots represent the experimental data over a range of temperatures and time. Based on the model and experimental data Bohn concludes that the thermal decomposition of HNIW is autocatalytic.

Qasim et al. [73] carried out theoretical computations using MOPAC [Molecular Orbital PACkage] quantum mechanical and classical force field mechanics to assess the type of bond degradation in CL-20. The FTIR and UV/FTIR were used to follow the decomposition of HNIW and the data were used for theoretical calculations, and concluded that the breakage of C–N bonds to be a plausible mechanism. In addition, they computed the dipole moment and enthalpies of formation. The values of the enthalpies of formation show that the PM3 model to be better than MNDO and AM1 models [73]. Qasim et al. [73] also reviwed the research work carried out to understand structural relationships and degradation mechanisms of current and a number of emerging explosives, including nitroaromatics, cyclic and cage cyclic nitramines, and a nitrocubane. The competitive degradation mechanisms by free radical oxidative, reductive and alkali hydrolysis were studied, that included, 2,4,6-trinitrotoluene (TNT); 1,3,5-trinitrobenzene (TNB); 2,4,6-trinitrophenol (TNP or picric acid); hexahydro-1,3,5-trinitro-1,3,5-triazine (RDX); octahydro-1,3,5,7-tetranitro-1,3,5,7-tetrazocine (HMX); 2,4,6,8,10,12-hexanitro- hexa-azoisowurtzitane (CL-20); and 2,4,6,8-tetranitro1,3,5,7-tetraaza-cubane (TNTAC), and octonitrocubane (ONC).

The thermal decomposition study of CL-20 (hexanitrohexaazaisowurtzitane) using pyrolysis GC/MS was carried out mainly by electron impact (EI) mode. Chemical ionization (CI) mode was used for further confirmation of identified species. Mass spectrum of CL-20 decomposition products predominantly revealed fragments with m/z 81 and 96 corresponding to $C_4H_5N_2^+$ and $C_4H_4N_2O^+$ ions, respectively. The total ion chromatogram (TIC) of CL-20 pyrolysis shows a peak within the first 2 min due to the presence of low molecular weight gases. Peaks corresponding to several other products were also observed including the atmospheric gases. Cyanogen formation (C_2N_2, m/z 52) observed to be enriched at the scan number 300–500. The low molecular mass range decomposition products formed by cleavage of C–N ring structure were found in majority. Additional structural information was sought by employing chemical ionization mode. The data generated during this study was instrumented in determining decomposition pathways of CL-20, and it is shown in Fig. 2.14 [76].

2.7 Hydrolysis of Hexanitrohexaazaisowurtzitane

HNIW can also be degraded through a hydrolysis reaction. Pavlov et al. [74] investigated the hydrolysis of the α, β, and ε polymorphs of 2,4,6,8,10,12-hexanitro-2,4,6,8,10,12-hexa azaiso-wurtzitane in dilute buffered aqueous solutions over a pH range of 4–10 and at 35, 43, 50, 58 and 65 °C, with starting concentrations of CL-20 at one half the solubility limit for the respective temperature. Figure 2.15 shows the hydrolysis rates at 50 °C at different pH values. In all cases, an overall first-order kinetic behavior was observed. The rate constants, half-lives, activation energies, and Arrhenius pre-exponential factors were determined. The latter was found to vary linearly with pH [74]. Specifically for each polymorph, the observed pseudo-first order hydrolytic rate constants at any pH and temperature in sub-solubility regions are as follows:

$$\frac{d[C_t]}{dt} = -k'[C_t]$$

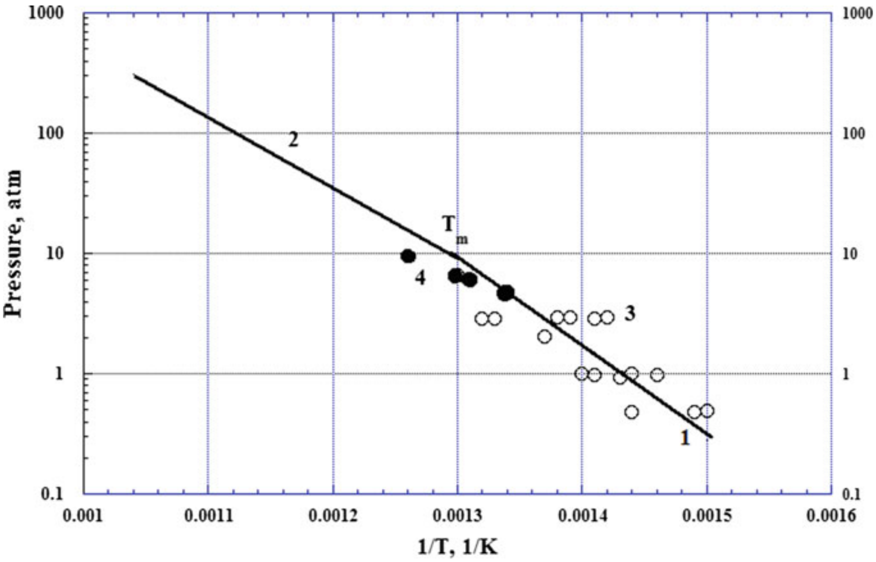

Fig. 2.11 Vapor pressure as a function of reciprocal temperature: vapor pressure above solid (*1*) and liquid CL-20 (*2*), and CL-20 surface temperatures [63]

$$k'_{\alpha} = \left(9.439 \times 10^{5} pH + 6.905 \times 10^{6}\right) \exp\left(-\frac{55748}{8.314 \times T}\right)$$

$$k'_{\beta} = \left(5.085 \times 10^{5} pH + 2.332 \times 10^{5}\right) \exp\left(-\frac{61530}{8.314 \times T}\right)$$

$$k'_{\varepsilon} = \left(6.662 \times 10^{4} pH + 4.875 \times 10^{5}\right) \exp\left(-\frac{56276}{8.314 \times T}\right)$$

Santiago et al. [75] studied the chemical remediation of soils containing CL-20 by alkaline hydrolysis. Their study is confined to lower concentration of CL-20, shorter time periods but at higher pH values compared to the study of Pavlov et al. [74]. From their results, alkaline hydrolysis appears to be faster, and removal greater than 90% was reported.

2.8 Biodegradation

Trott et al. [77] examined CL-20 in soil microcosms to determine its biodegradability. CL-20, after incubation with a variety of soils disappeared in all microcosms except in the controls in which microbial activity had been inhibited. CL-20 was degraded most rapidly in garden soil. After 2 days of incubation, about 80% of the initial CL-20 had disappeared. A CL-20-degrading bacterial strain, *Agrobacterium* sp. strain JS71, was isolated from enrichment cultures containing garden soil as an inoculum, succinate as a carbon source, and CL-20 as a nitrogen source. Growth experiments revealed that strain JS71 used 3 mol of nitrogen per mol of CL-20.

Jenkinks et al. [60] found that the half-life of CL-20 is dependent on the soil type. The rate of loss and estimation of the half-lives of several explosives were carried out by exposing them to three test soils. The mean concentrations obtained at each time period were plotted as the ℓn (C/Co) versus time (t), where C is the concentration at time t and Co is the initial concentration at time zero. Assuming, a first-order rate process, the half-life was determined using the following simple rate equation

$$\ell\mathrm{n}(C/Co) = -\mathrm{k}t$$

where k is the rate constant equal to the slope of the relationship. It may be noted that when the rate is first order, the half-life is independent of the starting concentration. Their finding is given in Table 2.10.

Crocker et al. [78] hypothesized that the biodegradation of cyclic nitramines such as CL-20 takes place by one or more of the mechanisms such as the formation of a nitramine free radical and loss of nitro functional groups, by the reduction of nitro functional groups, by direct enzymatic cleavage, by α-hydroxylation, and/or by hydride ion transfer. The intermediates formed by one or more of the pathways spontaneously decompose in water producing nitrite, nitrous oxide, formaldehyde, or formic acid as common end products. They summarize in a table the degrading bacteria and possible biochemical mechanisms for degradation of TNT, RDX, HMX, and CL-20, and show the pathways of degradation mechanism.

Both aerobic and anaerobic bacteria have been used to study the degradation of CL-20. Among the several bacteria used by the NRC Group of Canada, Phanerochaete chrysosporium and Irpex lacteus were found to degrade CL-20 [79]. Both *P. chrysosporium* and *I. lacteus* were able to remove almost all the nitramine after 25 days of incubation, and no CL-20 intermediates were detected. The proposed degradation pathway based on several publications [80, 81] by this group is shown in Fig. 2.16. They found that CL-20 transforms via an N-denitration mechanism, and putative doubly denitrated CL-20 inter–mediates and finally to the

Table 2.10 Half-life estimates (days) in three test soils [60]

Analyte	FG	CG	YTC
HMX	133	433	2310
TNAZ	<1	<1	<1
RDX	94	98	154
CL-20	69	267	144
NG	0.49	<1	<1
PETN	2.4	0.45	1.4

FG Fort Greely soil; *CG* Camp Guernsey soil; *YTC* Yakima Training Center soil

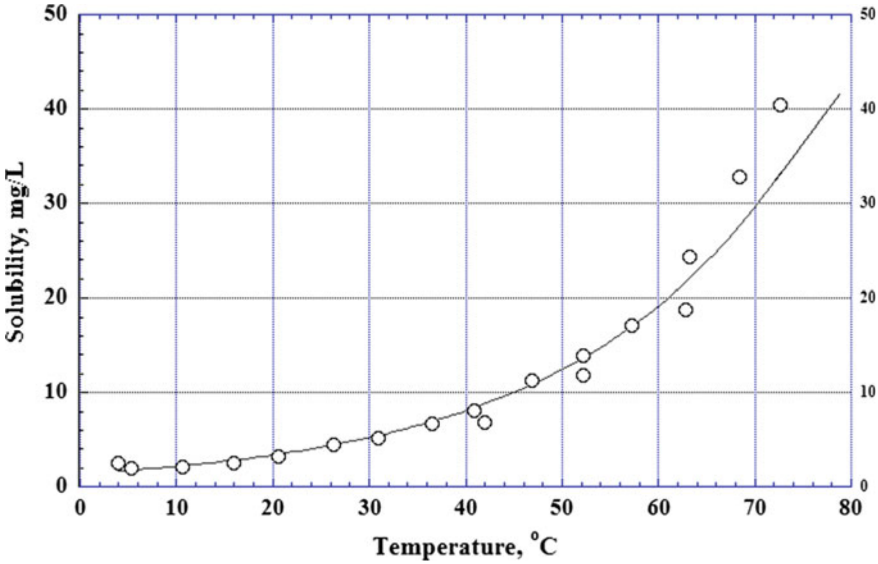

Fig. 2.12 Temperature-solubility of CL-20 in water

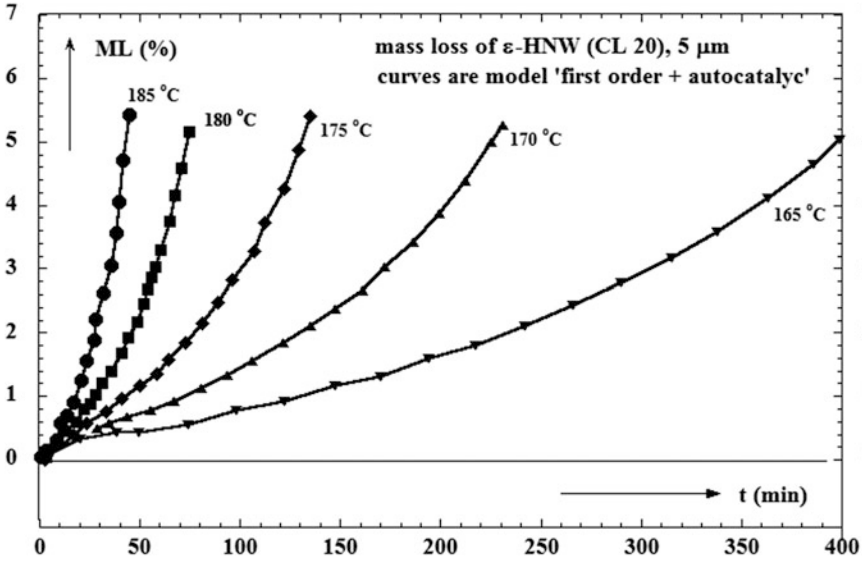

Fig. 2.13 Isothermal TGA data of ε-HNIW [72]

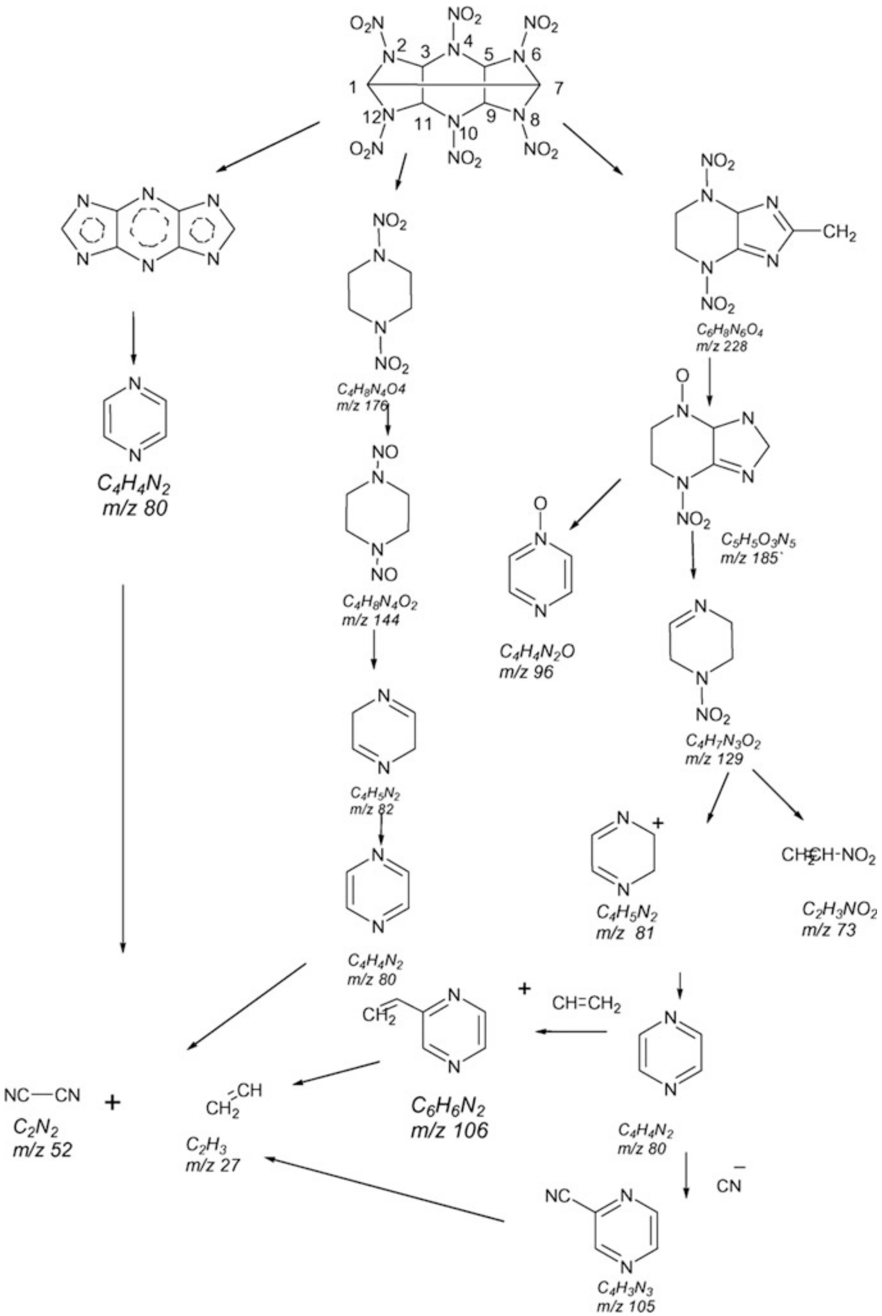

Fig. 2.14 Decomposition mechanism of CL-20 [76]

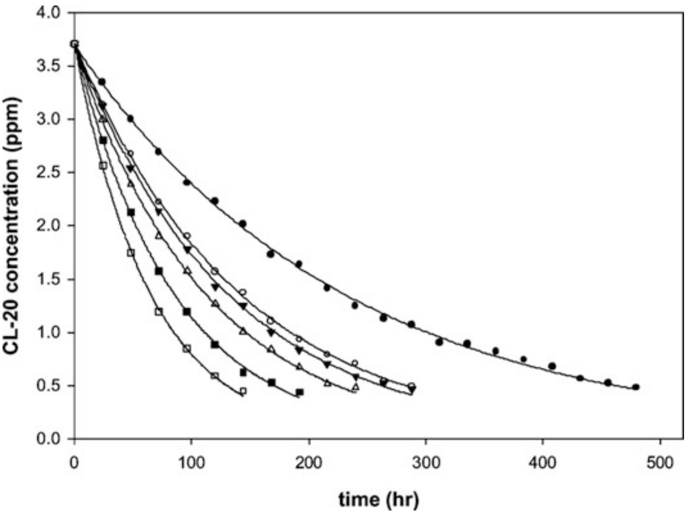

Fig. 2.15 Hydrolysis of α-CL-20 at 50 °C (●: data at pH 4; ○: data at pH 5.5; ▼: data at pH 7; Δ: data at pH 8; ■: data at pH 9; □: data at pH 10; —: exponential decay models) [74]

end products nitrous oxide (N_2O), formate ($HCOO^-$), ammonia (NH_3), and glyoxal (CHOCHO) as shown in Fig. 2.16 (Figs. 2.13, 2.14, and 2.15).

2.9 Spectroscopy

Kholod et al. [82] have carried out the B3LYP/6-31+G(d,p) level of theory studies to simulate IR and Raman spectra of different polymorphs of HNIW, and compared the theoretical values with experimental data of both IR and Raman spectra. They also found that the most stable conformers of CL-20, which correspond to experimentally obtained polymorphs, the pattern $\beta > \alpha$ and $\gamma > \varepsilon > \zeta$ for relative stability. Table 2.11 reproduced from their paper shows the assignments for IR and Raman, and experimental values. Experimental FTIR spectrum of a standard CL-20 sample obtained by Qasim et al. [83] as well as some characteristic bands in the experimental FTIR [84] spectra. Goede et al. [85] used FT-Raman to characterize the four stable phases of CL-20. They also report reported over the region from 0–4000 cm^{-1} and assigned the most predominant Raman. They use this method for detecting polymorphic impurities in ε-CL-20, and the detection level for polymorphic impurities was determined to be below 2%.

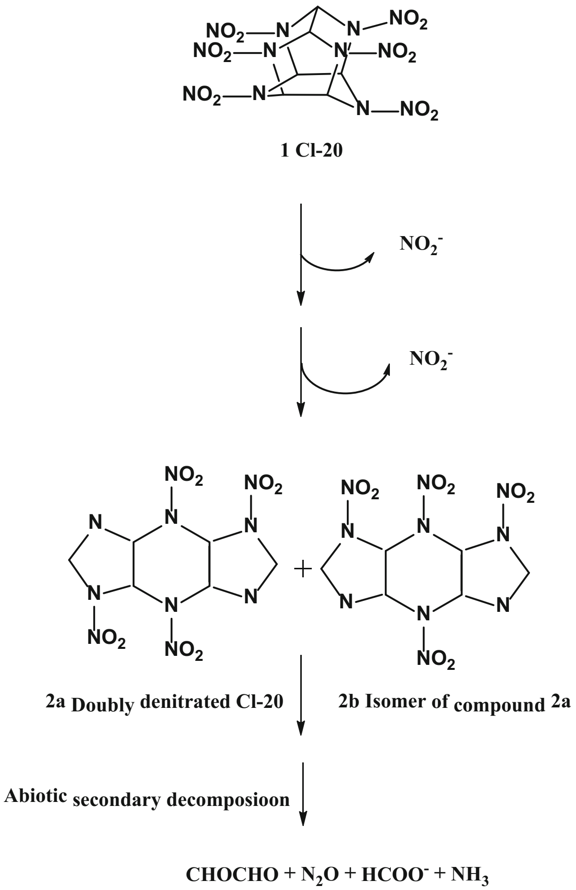

Fig. 2.16 Structure of CL-20 (*1*) and CL-20 denitration products (*2a* and *2b*) observed during treatment with FeO [79, 80] or with nitro-reductase [81]

2.10 Formulations and Detonation Characteristics

According to Simpson et al. [61] the explosive performance of ε-CL-20 is approximately 14% greater than HMX making it the most powerful explosive ever tested. They determined a number of detonation properties of CL-20 and compared with other explosives. Various detonation and morphological properties are summarized in Tables 2.12–2.17). They have also provided information on calorimetric and thermal properties, Jones-Wilkins-Lee equation of state to correlate the detonation parameters, and comparison with other explosive materials.

Table 2.11 Experimental and spectra of pure CL-20 polymorphs and the FTIR spectrum of a standard CL-20 sample [82]

		FTIR					Raman		
ε	α	β	γ	ζ	CL-20	ε	α	β	γ
		–		3038	3043 w	3048 vs	3058 s	3055 m	3062 m
				3031	3016 w	3031 m	3036 m	3045 m	3044 m
				1603	1605 s	3020 w	3028 m	3035 m	3035 w
				1568	1589 s		2924 w		
				1541	1566 s				
				1379	1381 w				
				1346					
				1332	1327 s				
				1284	1285 vs				
				1263	1265 vs				
				1229	1219 sh				
1191.7				1184		1190 m	1192 w	1188 w	1080 w
1182.5	1169.6	1178.6	1180.4		1180 w	1180 m	1170 m	1175 m	
	1168.1	1171.8							
		1154.4	1153	1161			1150 m	1155 m	1048 m
1139.2					1138 sh	1135 m		1130 w	
1125.1	1121.1		1106.1		1126 m	1125 s	1120 sh	1125 w	1020 w
1087.2	1119.8	1094.7	1080.4			1115 w			1105 m
1118.3					1088 m	1085 m	1095 vs	1090 vs	1083 m
	1094.9								
	1082								
	1078.3								
	1072.8							1060 s	
1051.6	1052.4	1052.3	1043.8	1038	1045 s	1055 vs	1054 s	1055 s	
1022.1						1010			1020 w
998.7	990.7	991.8					1000 s	1000 s	
980.9	989.2		970.6	970	980 m				
	953	959.2	958.8						
	951.7								
	949.1								
	947.7								

(continued)

Table 2.11 (continued)

		FTIR					Raman		
ε	α	β	γ	ζ	CL-20	ε	α	β	γ
944.4	945.2	944.9		946	941 s				
938.3			938.1						
913.2	904.3	907.7	909.4	904	910 sh w				
900.3			938.1						
883.8	881.7	882.9	879.2	875	883 s				
855.4	860.2	835.4	858.3		856 m	857 w	861 w	854 w	861 w
831.6	835.4		834.4	833	829 m	832 m	842 m	835 m	849 m
820.2	825.3		831.7		818 m	820 s	825 w		836 w
				800		791 w	895 w	805 w	895 w
	764.9	766.8	764.1	770	764.9			792 w	
758.2	757.7		755.8	755	756 s	755 w	762 w	763 w	762 w
751.4	751.1								
744.5	746.5	746.4	741	745	741 s				
738.2									
723.9	718	718.9	719.5		721 s				
705.1					706 sh				
					660 sh				
							283 w	284 w	287 w
						267 w			270 w

Table 2.12 Small scale safety test results

Material	Impact(a) (cm)	Friction(b) (kg)	Spark(c)	CRT(d) (cm^3/g)
β-CL-20(e)	14	6.4	no rxn	0.24
ε-CL-20(f)	12–16	6.4–7.2	no rxn	0.16
ε-CL-20(g)	17	6.4	no rxn	0.10
ε-CL-20(h)	21	6.2	no rxn	na

(a) 2.5 kg Type 12 tool with 35 mg pressed samples
(b) Julius-Peters-Berlin 21 friction machine. One reaction in ten tries
(c) Ten tries at 1 J with 510 R in line resistance
(d) 22 h at 120 ”C under 1 atm He
(e) LLNL synthesized CL-20
(f) Aerojet synthesized CL-20. The median value is approximately 15 cm
(g) Thiokol synthesized CL-20
(h) Thiokol synthesized CL-20. Ground by NAWC, China Lake, to 3-5 pm

Table 2.13 Heats of combustion and formation [61]

Material	$\Delta H_{combustmn}$ (10^6 J/mo1)	$\Delta H_{formatlon}$ (10^3 J/mol)
β-CL-20	−3.649	+431.0 ± 13
ε-CL-20	−3.596	+377.4 ± 13

Table 2.14 Calorimetric heat of detonation of CL-20 [61]

Materials	p (g/cm^3)	J/g$^{(a)}$	J/cm^3	J/cm^3 at TMD$^{(b)}$
ε-CL-20 experimental	1.96	6.234 ± 63	12,219 ± 123	12,717 ± 129
ε-CL-20 experimental estimated from products	1.96	6.029 ± 146	11,817 ± 286	123,013 ± 298

Table 2.15 Performance characteristics of explosive components [86]

Substance	ΔH_f (kcal/kg)	Q (g/cm^3)	D_{calc} (m/s)	P_{cj} (GPa)	ΔE at $V/V_9 = 6.5$ (kj/cm^3)	V_{gas} at 1 bar (cm^3/g)
TNT	−70.5	1.654	6881	19.53	−5.53	738
RDX	72.0	1.816	8977	35.14	−8.91	903
HMX	60.5	1.910	9520	39.63	−9.57	886
PETN	−407.4	1.778	8564	31.39	−8.43	852
TATB	−129.38	1.937	8114	31.15	−6.94	737
HNS	41.53	1.745	7241	23.40	−6.30	709
NTO	−237.8	1.930	8558	31.12	−6.63	768
TNAZ	45.29	1.840	9006	36.37	−9.39	877
CL-20	220.0	2.044	10065	48.23	−11.22	827

Table 2.16 Insensitive munitions properties of and new energetic materials [86]

Substance	Friction sensitivity (N)	Impact sensitivity (Nm)	Deflagration point (°C)
TNT	353	15	300
RDX	120	7.4	230
HMX	120	7.4	287
CL-20	54	4	228

The materials data sheet from Société nationale des poudres et explosifs, France (SNPE) lists the following properties for CL-20:
Deflagration temperate: 220–225 °C
Decomposition temperate: 213 °C
Maximum Decomposition temperate: 249 °C
Heat of Decomposition: 2300 J/g
Detonation velocity: 9650 m/s (experimental value)
Vacuum test, 193 h at 100 °C: 0.4 cm^3/g

2.11 CL-20 Based Formulations

Various CL-20 based formulations are available for use in both propellants and explosives. A large number of CL-20-based plastic bonded explosives (PBXs) are developed to enhance the explosive powers, and the burning rate in the case of propellants. Nair et al. [87] carried out thermal and sensitivity studies on CL-20

Table 2.17 Properties of CL-20 Polymorphs [86]

Property	γ-CL-20	α-CL-20	β-CL-20	ε-CL-20	HMX
Density (g/cm^3)	1.92	1.97	1.99	2.04	1.91
Detonation velocity (m/s)	9380	9380	9380	9660	9100
Phase transition temperate (°C)	260	170	163	177	280

Table 2.18 Density and velocity of detonation of selected CL-20-based PBXs [87–90]

Composition	Density (g/cm^3)	Detonation velocity [mm/(μ sec)]
96% CL-20; 1% Hy Temp; 3% DOA	1.901	9.018
96% HMX; 1% Hy Temp; 3% DOA	1.792	8.748
RX-39-AA&AB: 95.5–95.8% CL-20; estane	1.942 ± 0.001	9.208
PBXC-19: 95% CL-20; EVA	1.896 ± 0.002	9.083
PATHX-1: 88–95% CL-20; estane	1.868–1.944	8.89–9.37
PATHX-2: 92–95% CL-20; estane	1.869–1.923	8.85–9.22
PATHX-3: 85–94% CL-20; estane	1.871–1.958	8.91–9.50
LX-19: 95% CL-20; estane	1.959	9.44
LX-14: 95% HMX; estane	1.835	8.79
PBXCLT-1:49-70% CL-20; 48-27% energetic material HNJ and 3% polymeric binder PVB	1.906	8.384–9.102
PBXCL-1: 97% CL-20; 3% PVB	1.921	9.102
66.8–72.1% CL-20; HTPB	1.648–1.710	8.325–8.470
66.8–72.1% HMX; HTPB	1.575–1.618	8.030–8.107
32% CL-20; 48% TEX; 20% HTPB	1.595	
32% HMX; 48% TEX; 20% HTPB	1.560	

coated with several polymers—Ethylene vinyl acetate (EVA), copolymer of polybutylene terephthalate polyether glycol (hytrel), polyurethane-ester-MDI (Estane), hexafluoropropylene vinylidine fluoride copolymer (Viton) and polyurethane (PU). Their results are given in Table 2.18 [87–90].

As shown in Table 2.18, CL-20 based formulations have 12–15% higher velocity of detonation compared to the corresponding HMX based formulations. CL-20 is also found to be a superior alternative to RDX and HMX for applications in low signature rocket propellants. CL-20 based propellants showed a 35–110% higher burning rates than those of HMX-based propellants. Golfier et al. [91] noted that the Isp of CL-20–glycidyl azide polymer (GAP) propellants is 251 s, compared to 242 s for the corresponding RDX-based propellant.

Li and Brill [92] discuss nanostructured energetic compounds of CL-20. They found that the cryogel method enabled them to load up to 90% of CL-20 (by mass) in energetic polymer matrices composed of single precursors of GAP polyol, NC, and THMNM and their mixed precursors. One of the objectives for development of

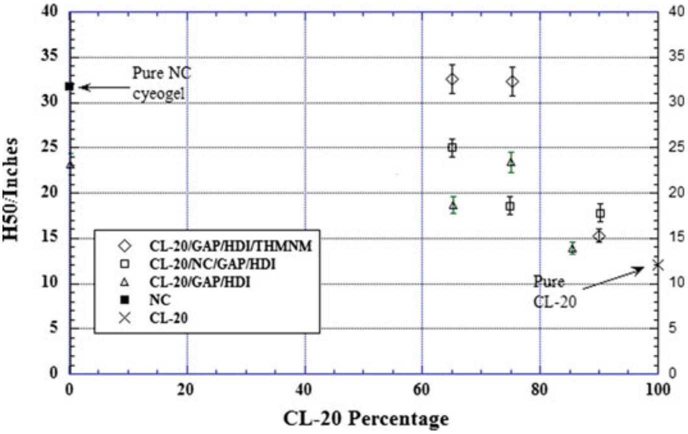

Fig. 2.17 Drop weight impact test data of energetie polymer gels and composite energetie gels CL-20 in the 50–70% by weight rang appear to have a notable reduction in scnsitivy [92]

Table 2.19 Burning rates of CL-20-incorporating rocket propellants [69, 91–93]

Composition	Burning rate (mm/sec)	n
60% CL-20; 40% PGA	11.5–23 (7–15 MPa)	0.92
60% HMX; 40% PGA	6–11 (7–15 MPa)	0.89
60% CL-20; 40% GAP 1	3.4–27.2 (7–15 MPa)	0.94
60% HMX; 40% GAP	7.2–13.6 (7–15 MPa)	0.91
60% CL-20; 40% GAP	20.0–32.4	0.48
(catalyzed)	(7–20 MPa)	
60% RDX; 40% GAP	14.6–21.4	0.37
(catalyzed)	(7–20 MPa)	
70% CL-20; 20% GAP;	15	0.57
10% BDNPF/A	(7 MPa)	

Note n is the exponent in the power law of the burning rate, PGA is polyglycol adipate, and GAP is a glycidyl azide polymer

this product was to reduce the sensitivity of the formulations. The sensitivity determine by the drop test is shown in Fig. 2.17 (Table 2.19).

Mueller [94] has studied several formulations of CL-20 and RDX with nitrocellulose, BDNPA/F, EPX, and a stabilizer, and compared the properties of these two explosives. Mueller has presented thermodynamic and chemical stability data along with 40-mm gun simulation data as a function of temperature.

Besides using CL-20 as an explosive, it is also used as a propellant. It is being tested as an alternative to ammonium perchlorate in missile and space applications. Golfier et al. [89] found that CL-20 propellants offer 7% superior I_{sp} (251 s) compared to RDX-based formulations. Weiser et al. [95] found that the CL-20/glycidylazide polymer-(GAP) propellants exhibit burning rates twice those of

HMX/GAP propellants. Attempts have been made to ballistically modify CL-20 formulations, but specific information about the modifiers is not available. Nair et al. [96] have studied CL-20 based composites as double-based propellants. With corporate 17.5% aluminum based on their theoretical evaluation of I_{sp}. In another paper, Thepenier and Fanblanc [97] compare the characteristics of several compounds and show the superiority of CL-20 with respect to density, enthalpy of formation, and oxygen balance. In addition this paper provides information on a wide variety of fields from new raw materials (energetic binders, plasticizers, oxidizers) through new propellants and new processes to new tools for designing grains. Unlike many other propellants, the CL-20 propellant exhaust is free of lead, acids, and aluminum oxide emissions. The absence of halogens like in ammonium perchlorate makes CL-20 products of combustion more environmentally friendly.

2.12 Toxicity

Kuperman et al. [98, 99] have reported the Enchytraeid Reproduction Test, and found that toxicities for *E. crypticus* adult survival and juvenile production significantly increased in weathered and aged treatments compared with toxicity in freshly amended soil, based on 95% confidence intervals. The EC50 and EC20 values for juvenile production were 0.3 and 0.1 mg kg^{-1} for CL-20 freshly amended into soil, and 0.1 and 0.035 mg kg^{-1}, respectively, for weathered and aged CL-20 treatments.

2.13 Conclusion

CL-20 has attracted a great deal of attention in the recent years as a powerful insensitive explosive. Current literature search revealed that several countries are working on this explosive mainly on the synthesis, scale-up, and cost reduction. There is little work on properties, detection, toxicity, and remediation of contaminated sites should this be made in large quantities.

References

1. Nielsen AT (1997) Caged polynitramine compound. US Patent 5693794
2. USA Navy Manteca (2004) Report of 2003. Dept of Navy, Fiscal Year 2003 Rpt
3. Nielsen AT, Nissan RA, Vanderah DJ, Coon CL, Gilardi RD, George CF, Lippen-Anderson JF (1990) Polyazapolycyclics by condensation of aldehydes with amines 2 Formation of 2,4,6,8,10,12-Hexabenzyl-2,4,6,8,10,12-hexaazatetra – cyclo [55000] dodecanes from glyoxal and benzylamines. J Org Chem 55(5):1459–1466

4. Crampton MR, Hamid J, Millar R, Ferguson G (1993) Studies of the synthesis, protonation and decomposition of 2,4,6,8,10,12-hexabenzyl-2,4,6,8,10,12-hexaazatetracyclo[55005,903,11]dodecane (HBIW). J Chem Soc Perkin Trans 2(5):923–929
5. Edwards WW, Wardle RB (1998) Process for making 2,4,6, 8,10,12- hexanitro- 2,4,6,8,10, 12-hexa azatetracyclo 550 0 5,9 0 3,11] –dodecane. EP 1153025 A2 (WO2000052011A2), US Patent 5739325
6. Kodama T (1994) Preparation of hexakis (trimethylsilylethylcarbamyl) hexaazaisowurtzitane. JP06321962A
7. Kodama T, Tojo M, Ikeda M (1996) Acylated hexaazaisowurtzitane derivatives and process for producing the same. WO9623792A1
8. Ou Y-x, Xu Y-j, Liu L-h, Zheng F-p, Wang C, Chen J-t (1999) Comparison of acetonitrile process with ethanol process for synthesis of hexabenzylhexaazaisowurtzitane. Hanneng Cailiao 7(4):152–155
9. Ou Y, Xu Y, Chen B, Liu L, Wang C (1999) Synthesis of hexanitrohexaazaisowurtzitane from tetraacetyldiformylhexaazaisowurtzitane. Proc Int Pyrotech Semin 26th:406–411
10. Ou Y, Meng Z, Liu J (2007) Advance in high energy density compound CL-20-developments of synthesis route and production technologies of CL-20. Huagong Jinzhan 26 (6):762–768
11. Sysolyatin SV, Lobanova AA, Chernikova YT, Sakovich GV (2005) Methods of synthesis and properties of hexanitrohexaazaisowurtzitane. Russ Chem Rev 74(8):757–764. doi:10.1070/RC2005v074n08ABEH001179
12. Wang C, Ou Y-X, Chen B-R (2000) One pot synthesis of hexabenzylhexaazaiso-wurtzitane. Beijing LigongDaxueXuebao 20(4):521–523
13. Nielsen AT, Chafin AP, Christian SL, Moore DW, Nadler MP, Nissan RA, Vanderah DJ (1998) Synthesis of polyazapolycyclic caged polynitramines. Tetrahedron 54(39):11793–11812. doi:10.1016/S0040-4020(98)83040-8
14. Larson SL, Felt DR, Davis JL, Escalon L (2002) Analysis of CL-20 in environmental matrices: water and soil. J Chromatogr Sci 40(4):201–206. doi:10.1093/chromsci/404201
15. Hamilton RS, Sanderson AJ, Wardle RB, Warner KF (2000) Studies of the crystallization of CL-20. International Annual Conference of ICT [Institut ChemischeTechnologie], 31st (Energetic Materials), 21/1–21/8
16. Bellamy AJ (1995) Reductive debenzylation of hexabenzylhexaazaisowurtzitane. Tetrahedron 51(16):4711–4722
17. Surapaneni R, Damavarapu R, Kumar RA, Dave PR (2000) Process improvements in CL-20 manufacture. International Annual Conference of ICT, 31st (Energetic Materials), 108/1–108/4
18. Qian H, Ye Z-W, Lv C-X (2007) Efficient and facile synthesis of hexanitrohexaaza-isowurtzitane (HNIW) for high energetic materials. Lett Org Chem 4(7):482–485
19. Qian H, Chunxu LV, Zhiwen YE (2008) Synthesis of CL-20 by clean nitrating agent dinitrogen pentoxide. J Indian Chem Soc 85(4):434–439
20. Qian H, Ye Z-W, Lu C-X (2008) Synthesis of CL-20 via nitration and nitrolysis of 2,6,8,12-tetraacety l-2,4,6,8,10,12-hexaazaisowurtzitane with N_2O_5/HNO_3. Yingyong Huaxue 25(3):378–380
21. Song ZW, Yan QL, Li XJ, Qi XF, Lim M (2010) Crystal transition of CL-20 in different solvents. Chin J Energ Mater 6:648–653
22. Gore GM, Sivabalan R, Nair UR, Saikia A, Venugopalan S, Gandhe BR (2007) Synthesis of CL-20: By oxidative debenzylation with cerium (IV) ammonium nitrate (CAN). Indian J Chem, Sect B: Org Chem Incl Med Chem 46B(3):505–508
23. Kawabe S, Miya H, Kodama T, Miyake N (2007) Process for the preparation of 1,3,5,7-tetranitro-1,3,5,7-tetraazacyclooctane. US 6297372 B1, EP 0547735
24. Cagnon G, Eck G, Herve G, Jacob G (2007) Method for making new polycyclic polyamides as precursors for energetic polycyclic polynitramine oxidizers. US Patent 7279572

25. Latypov NV, Wellmar U, Goede P, Bellamy AJ (2000) Synthesis and Scale-Up of 2,4,6,8,10,12-Hexanitro-2,4,6,8,10,12-hexaazaisowurtzitane from 2,6,8,12-Tetraacetyl-4,10-dibenzyl-2,4,6,8,10,12- hexaazaisowurtzitane (HNIW, CL-20). Org Proc Res Dev 4(3):156–158
26. Pang S-P, Yu Y-Z, X-Q Zhao () A novel synthetic route to hexanitrohexa- azaisowurtzitane. Propellants, Explosives, Pyrotechnics 30(6):442–444
27. Chapman RD, Hollins RA (2008) Benzylamine-Free, heavy-metal-free synthesis of CL-20 via hexa(1-propenyl)hexaazaisowurtzitane. J Energ Mater 26(4):246–273
28. Herve G, Jacob G, Gallo R (2006) Preparation and structure of novel hexaazaisowurtzitane cages. Chem Eur J 12(12):3339–3344
29. Mandal AK, Pant CS, Kasar SM, Soman T (2009) Process Optimization for Synthesis of CL-20. J Energ Mater 27(4):231–246. doi:10.1080/07370650902732956
30. Lu L, Xu B, Ma Z, Yue H, Mu W, Ou Y (2007) New method for synthesis and crystallizing of HNIW in nitric acid. In: Huang P, Wang Y, Li S (eds) 2007 Science Press, Proc Intl Autumn Seminar on Propellants, Explosives and Pyrotechnics, 7th, Xi’an, China, Oct 23–26, pp 64–65
31. Wang J, Li J, An C, Hou C, Xu W, Li X (2012) Study on ultrasound- and spray-assisted precipitation of CL-20. Propellants, Explos, Pyrotech 37(6):670–675
32. van der Heijden AEDM, Bouma RHB (2004) Crystallization and characterization of RDX, HMX, and CL-20. Cryst Growth Des 4(5):999–1007
33. Bellamy AJ (2003) A simple method for the purification of crude hexanitrohexaaza-isowurtzitane (HNIW or CL20). Propellants, Explos, Pyrotech 28(3):145–152
34. Degirmenbasi N, Peralta-Inga Z, Olgun U, Gocmez H, Kalyon DM (2006) Recrystallization of CL-20 and HNFX from solution for rigorous control of the polymorph type: part II, experimental studies. J Energ Mater 24(2):103–139. doi:10.1080/07370650600672090
35. Agrawal JP (2011) High Energy Materials. Wiley, Weinheim, Germany
36. Nair UR, Sivabalan R, Gore GM, Geetha M, Asthana SN, Singh H (2005) Hexanitrohexaazaisowurtzitane (CL-20) and CL-20-based formulations (Review). Combust Explosion Shock Waves 41:121–132
37. Chapman RD, Hollins RA, Groshens TJ, Nissan DA (2006) Benzylamine-Free, heavy-metal-free synthesis of CL-20. SERDP seed Prohect WP-1518
38. Jin S, Shu Q, Chen S, Shi Y (2007) Preparation of e-HNIW by a one-pot method in concentrated nitric acid from tetraacetyldiformylhexaazaisowurtzitane. Propellants, Explos, Pyrotech 32(6):468–471
39. Duddu R, Dave PR (1999) Processes and Compositions for Nitration of N-Substituted Isowurtzitane Compounds. Paten WO9957104, USA
40. Wardle RB, Hinshaw JC (2000) Synthesis and reactions of hexaazaisowurtzitane-type compounds in synthesis of hexanitrohexaazaisowurtzitane (HNIW) explosive. In: Cordant Technologies Inc, USA, Division of US Ser No 292 028, pp 8
41. Russell TP, Miller PJ, Piermarini GJ, Block S (1992) High-pressure phase transition in γ-hexanitrohexaazaisowurtzitane. J Phys Chem 96(13):5509–5512
42. Ciezak JA, Jenkins TA, Liu Z (2007) Evidence for a high-pressure phase transition of ε-2,4,6,8,10,12-hexanitrohexaazaisowurtzitane (CL-20) using vibrational spectroscopy. Propellants, Explos, Pyrotech 32(6):472–477. doi:10.1002/prep200700209
43. Gump JC, Peiris SM (2008) Phase transitions and isothermal equations of state of epsilon hexanitrohexaazaisowurtzitane (CL-20). J Appl Phys 104(8):083509/1–083509/5. doi:10.1063/1.2990066
44. Turcotte R, Vachon M, Kwok QSM, Wang R, Jones DEG (2005) Thermal study of HNIW (CL-20). Thermochim Acta 433:105–115
45. Ghosh M, Venkatesan V, Sikder AK, Sikder N (2012) Preparation and characterisation of ε-CL-20 by solvent evaporation and precipitation methods. Def Sci J 62(6):390–398
46. Meents A, Dittrich B, Johnas SKJ, Thome V, Weckert EF (2008) Charge-density studies of energetic materials: CL-20 and FOX-7. Acta Crystallogr B 64(Pt 1):9–42
47. Chen H, Chen S, Li L, Jin S (2008) Quantitative determination of e-phase in polymorphic HNIW using diffraction patterns. Propellants, Explos, Pyrotech 33:467–471

48. Cabalo JB, Sausa RC (2005) Explosive residue detection by laser surface photo-fragmentation–fragment detection spectroscopy: II *In Situ* and Real-time Monitoring of RDX, HMX, CL20, and TNT, by an Improved ion probe. Report ARL-TR-3478
49. Larson SL, felt DR, Escalon L, JD Davis, Hansen LD (2001) Analysis of CL-20 in environmental matrices water and soil. ERDC/EL TR-01-21
50. Liu Y, Chen S, Luo S (2000) HPLC method for analysis of CL-20 in explosive mixture. Huaxue Yanjiu Yu Yingyong 12(4):446–448
51. Monteil-Rivera F, Paquet L, Deschamps S, Balakrishnan VK, Beaulieu C, Hawari J (2004) Physico-chemical measurements of CL-20 for environmental applications Comparison with RDX and HMX. J Chromatogr A 1025(1):125–132. doi:10.1016/jchroma200308060
52. Anthony JS, Davis EA, Haley MV, Kolakowski JE, Kurnas CW, Phillips CT, Simini M, Kuperman RG, Checkai RT (2004) HPLC determination of hexanitrohexaazaisowurtzitane (CL 20) in soil and aqueous matrices. US Army Res Dev Eng Command Edgewood chem Bio Center, ECBE-TR, p 403
53. Makarov A, LoBrutto R, Christodoulatos C, Jerkovich A (2009) The use of ultra high-performance liquid chromatography for studying hydrolysis kinetics of CL-20 and related energetic compounds. J Hazard Mater 162(2–3):1034–1040. doi:10.1016/jjhazmat200805157
54. Oehrle SA (1994) Analysis of CL-20 and TNAZ in the presence of other nitroaromatic and nitramine explosives using HPLC with photodiode array (PDA) detection. J Energ Mater 12 (4):22–211. doi:10.1080/07370659408018651
55. Persson B, Ostmark H, Bergman H (1997) An HPLC method for analysis of HNIW and TNAZ in an explosive mixture. Propellants, Explos, Pyrotech 22(4):238–239
56. Agilent Technology, LC/MS Application Note, April 2004
57. Toghiani RK, Toghiani H, Maloney SW, Boddu VM (2008) Prediction of physicochemical properties of energetic materials. Fluid Phase Equilib 264:86–92
58. Qasim MM, Furey J, Fredrickson HL, Szecsody J, McGrath C, Bajpai R (2004) Semiempirical predictions of chemical degradation reaction mechanisms of CL-20 as related to molecular structure. Struct Chem 15(5):493–499. doi:10.1023/B:STUC000003790727898f5
59. Zeman S, Jalovy Z (2000) Heats of fusion of polynitro derivatives of polyazaisowurtzitane. Thermochim Acta 345(1):31–38
60. Jenkins TF, Bartolini C, Ranney TA (2003) Stability of CL-20,TNAZ, HMX, RDX,NG, and PETN in moist, unsaturated soil. ERDC/CRREL TR-03-7
61. Simpson RL, Urtiew PA, Ornellas DL, Moody GL, Scribner KJ, Hoffmann DM (1997) CL-20 performance exceeds that of HMX and its sensitivity is moderate. Propellants, Explos, Pyrotech 22(5):249–255
62. Greenlief CM, Ghosh TK, Viswanath DS, Boddu VM (2010) Vapor Pressure of Hexanitrohexaazaisowurtzitane (HNIW, CL-20). Report to Leonard Wood Institute, LWI-101.1, MO, USA
63. Sinditskii VP, Egorshev VY, Berezin MV, Serushkin VV, Milekhin YM, Gusev SA, Matveev AA (2003) Combustion characteristics of the high-energy cage hexanitrohexaaza-isowurtzitane nitramine. Khim Fiz 22(7):69–74
64. Boddu VM, Maloney SW, Toghiani RK, Toghiani H (2010) Prediction of physicochemical properties of energetic materials for identification of treatment technologies for waste streams. U.S. Army Engineer Research and Development Center, ERDC/CERL TR-10-27
65. Osmont A, Catoire L, Gökalp I, Yang V (2007) Ab initio quantum chemical predictions of enthalpies of formation, heat capacities, and entropies of gas-phase energetic compounds. Combust Flame 151:262–273
66. Karakaya P, Sidhoum M, Christodoulatos C, Nicolich S, Balas W (2005) Aqueous solubility and alkaline hydrolysis of the novel high explosive hexanitrohexaazaisowurtzitane (CL-20). J Hazard Mater 120(1–3):183–191
67. von Holtz E, Ornellas D, Foltz MF, Clarkson JE (1994) The solubility of ε-CL-20 in selected materials. Propellants, Explos, Pyrotech 19:206–212

68. Turcotte R, Vachon M, Kwok QSM, Wang R, Jones DEG (2005) Thermal study of HNIW (CL-20). Thermochim Acta 433(1–2):105–115
69. Highsmith T, Johnston H (2004) Continuous process for preparing alkoxynitroarenes. ALLIANT TECHSYSTEMS INC., MINNESOTA, US 10/338,767, USA
70. Korsounskii BL, Nedel'ko VV, Chuk anov NV, Larikova TS, Volk F (2000) Kinetics of thermal decomposition of hexanitrohexaazaisowurzitane, Russ Chem Bull 49:812–817
71. Ding T, Yang H, Zhang Y (2013) Thermal decomposition of CL-20/RDX mixed system. Huaxue Tuijinji Yu Gaofenzi Cailiao 11(6):84–86
72. Bohn MA (2002) Kinetic description of mass loss data for the assessment of stability, compatibility and aging of energetic components and formulations exemplified with ε-CL20. Propellants, Explos, Pyrotech 27(3):125–135
73. Qasim MM, Moore B, Taylor L, Honea P, Gorb L, Leszczynski J (2007) Structural characteristics and reactivity relationships of nitroaromatic and nitramine explosives—a review of our computational chemistry and spectroscopic research. Int J Mol Sci 8:1234–1264
74. Pavlov J, Christodoulatos C, Sidhoum M, Nicolich S, Balas W, Koutsospyros A (2007) Hydrolysis of hexanitrohexaazaisowurtzitane (CL-20). J Energ Mater 25(1):1–18
75. Santiago L, Felt DR, Davis JL (2007) Chemical remediation of an ordnance-related compound: thealkaline hydrolysis of CL-20. ERDC/El TR-07-18 Report
76. Naik NH, Gore GM, Gandhe BR, Sikder AK (2008) Studies on thermal decomposition mechanism of CL-20 by pyrolysis gas chromatography-mass spectrometry (Py-GC/MS). J Hazard Mater 159(2–3):5–630
77. Trott S, Nishino SF, Hawari J, Spain JC (2003) Biodegradation of the nitramine explosive CL-20. Appl Environ Microbiol 69(3):1871–1874
78. Crocker FH, Indest KJ, Fredrickson HL (2006) Biodegradation of the cyclic nitramine explosives RDX, HMX, and CL-20. Appl Microbiol Biotechnol 73(2):274–290; Fournier D, Monteil-Rivera F, Halasz A, Bhatt M, Hawari J (2006) Degradation of CL-20 by white-rot fungi Chemosphere 63(1):175–181
79. Balakrishnan VK, Monteil-Rivera F, Gautier MA, Hawari J (2004) Sorption and stability of the polycyclic nitramine explosive CL-20 in soil. J Environ Qual 33(4):1362–1368
80. Balakrishnan VK, Monteil-Rivera F, Halasz A, Corbeanu A, Hawari J (2004) Decomposition of the Polycyclic Nitramine Explosive, CL-20, by Fe0. Environ Sci Technol 38(24):6861–6866
81. Bhushan B, Paquet L, Spain JC, Hawari J (2003) Biotransformation of 2,4,6,8,10,12-hexanitro-2,4,6,8,10,12-hexaazaisowurtzitane (CL-20) by denitrifying Pseudomonas sp strain FA1. Appl Environ Microbiol 69(9):5216–5221
82. Kholod Y, Okovytyy S, Kuramshina G, Qasim M, Gorb L, Leszczynski J (2007) An analysis of stable forms of CL-20: a DFT study of conformational transitions, infrared and Raman spectra. J Mol Struct 843(1–3):14–25
83. Qasim M, Fredrickson H, Honea P, Furey J, Leszcznski J, Okovytyy S, Szecsody J, Kholod Y (2005) Prediction of CL-20 chemical degradation pathways, theoretical and experimental evidence for dependence on competing modes of reaction. SAR QSAR Environ Res 16:495–515
84. Foltz MF (1994) Thermal stability of ε-hexanitrohexaazaisowurtzitane in an Estane formulation. Propellants, Explos, Pyrotech 19(2):63–69
85. Goede P, Latypov NV, Oestmark H (2004) Fourier transform Raman Spectroscopy of the four crystallographic phases of α, β, γ and ε 2,4,6,8,10,12-hexanitro-2,4,6,8,10,12-hexaazatetracyclo[55005,903,11]dodecane (HNIW, CL-20). Propellants, Explos, Pyrotech 29(4):205–208
86. Ulrich TF (2005) Energetic materials: particle processing and characterization. Wiley, New York
87. Nair UR, Gore GM, Sivabalan R, Satpute RS, Asthana SN, Singh H (2004) Studies on polymer coated CL-20-the most powerful explosive J Polym Mater 21(4):377–382

88. Nair UR, Sivabalan R, Gore GM, Dudek K, Marecek P, Vavra P (2000) Laboratory testing of HNIW mixtures. Proc. 31st Int Conf ICT, Karlsruhe, June 27–30 (2000), pp 110/1–110/6
89. Mezger MJ, Nicholich SM, Geiss DA et al (1999) Performance and hazard characterzation of CL-20 formulations. In: Proceedings of 30th International Annual Conference of ICT, Karlsruhe, June 29–July 2 (1999), pp. 4/1–4/14
90. Tian Y, Xu R, Zhou Y, Nie F (2001) Study on formulation of CL-20. In: Procecings of 4th International Autumn Seminar on Propellants, Explos, Pyrotech Shaoxing, China, pp 43–47
91. Golfier M, Graindorge H, Longevialle Y, Mace H (1998) New energetic molecules and their applications in the energetic materials. In: Proceedings of 29th International Annual Conf. of ICT, Karlsruhe, 30 June–3 July 1998, pp 3/1–3/17
92. Li J, Brill TB (2006) Nanostructured energetic composites of CL-20 and binders synthesized by sol gel methods. Propellants, Explos, Pyrotech 31:61–69
93. Wagstaff DC (2002) Desensitization of energetic materialsby energetic plasticizer, Brit. UK Pat. Appl GB 2374867 A1, 30 October 2002
94. Mueller D (1999) New gun propellant with CL-20. Propellants, Explos, Pyrotech 24(3):176–181. doi:10.1002/(SICI)1521-4087(199906)24:03<176:AID-PREP176>30CO;2-4
95. Weiser V, Eisenreich N, Eckl W, Eisele S, Menke K (2000) Burning behavior of CL-20/GAP and HMX/GAP rocket propellants. In: International Annual Conference on ICT 31st (Energetic Materials), pp 144/141–144/146
96. Nair UR, Gore GM, Sivabalan R, Divekar CN, Asthana SN, Singh H (2004) Studies on advanced CL-20-based composite modified double-base propellants. J Propul Power 20 (5):952–955; Thepenier J, Fanblanc G (2001) Acta Austronautica, 38:245
97. Thepenier J, Fanblanc G (2001) Advanced technologies available for future solid propellant grains. Acta Austronautica 48(5–12):245–255
98. Kuperman RG, Checkai RT, Simini M, Phillips CT, Anthony JS, Kolakowski JE, Kumas CW, Davis EA (2006) U S Army Research, Development and Engineering., ECBC-TR-485
99. Kuperman RG, Checkai RT, Simini M, Phillips CT, Anthony JS, Kolakowski JE, Davis EA (2006) Toxicity of emerging energetic soil contaminant CL-20 to potworm Enchytraeus crypticus in freshly amended or weathered and aged treatments. Chemosphere 62(8):1282–1293

Additional Scholarly Articles for Further Reading

100. Agrawal JP, Walley SM, Field JE (1998) A high-speed photographic study of the impact initiation of hexanitro-hexaaza-isowurtzitane and nitrotriazolone. Combust Flame 112(1/2):62–72. doi:10.1016/S0010-2180(97)81757-9
101. Aldoshin SM, Aliev ZG, Goncharov TK (2014) Crystal structure of 2,4,6,8,10,12-hexanitro-2,4,6,8,10,12-hexaazaisowurtzitane solvate with ε-caprolactam. J Struct Chem 55(4):709–712. doi:10.1134/S0022476614040179
102. Aldoshin SM, Aliev ZG, Goncharov TK, Korchagin DV, Milekhin YM, Shishov NI (2011) New conformer of 2,4,6,8,10,12-hexanitro-2,4,6,8,10,12-hexaazaisowurtzitane (CL-20). Crystal and molecular structures of the CL-20 solvate with glyceryl triacetate. Russ Chem Bull 60(7):1394–1400. doi:10.1007/s11172-011-0209-5
103. Aldoshin SM et al (2014) Crystal structure of cocrystals 2,4,6,8,10,12-hexanitro-2,4,6,8,10,12-hexaazatetracyclo[5.5.0.05.9.03.11]dodecane with 7H-tris-1,2,5-oxadiazolo(3,4-b:3′,4′-d:3″,4″-f)azepine. J Struct Chem 55(2):327–331. doi:10.1134/S0022476614020206
104. Alnemrat S, Hooper JP (2013) Predicting temperature-dependent solid vapor pressures of explosives and related compounds using a quantum mechanical continuum solvation model. J Phys Chem A 117(9):2035–2043. doi:10.1021/jp400164j

105. Alnemrat S, Hooper JP (2014) Predicting solubility of military, homemade, and green explosives in pure and saline water using COSMO-RS. Propellants, Explos, Pyrotech 39 (1):79–89. doi:10.1002/prep.201300071
106. Ammon HL (2008) Updated atom/functional group and atom_code volume additivity parameters for the calculation of crystal densities of single molecules, organic salts, and multi-fragment materials containing H, C, B, N, O, F, S, P, Cl, Br, and I. Propellants, Explos, Pyrotech 33(2):92–102. doi:10.1002/prep.200700054
107. Amwele HR, Papirom P, Chukanhom K, Beamish FHW, Petkam R (2015) Acute and subchronic toxicity of metal complex azo acid dye and anionic surfactant oil on fish Oreochromis niloticus. J Environ Biol 36(1):199–205, 7p
108. Andelkovic-Lukic M (2000) New high explosive—polycyclic nitramine hexanitrohexaaza-isowurtzitane (HNIW, CL-20). Naucno-Teh Pregl 50(6):60–64
109. Anderson SR, am Ende DJ, Salan JS, Samuels P (2014) Preparation of an energetic-energetic cocrystal using resonant acoustic mixing. Propellants, Explos, Pyrotech 39(5):637–640 doi:10.1002/prep.201400092
110. Atwood AI et al (1999) Burning rate of solid propellant ingredients, part 1: pressure and initial temperature effects. J Propul Power 15(6):740–747. doi:10.2514/2.5522
111. Paromov AE, Sysolyatin SV, Gatilov YV (2016) An acid-catalyzed cascade synthesis of oxaazatetracyclo [5.5.0.0^{3,11}.0^{5,9}]dodecane derivatives. J Energ Mater. doi:10.1080/07370652.2016.1194499
112. Atwood AI et al (1999) Burning rate of solid propellant ingredients, part 2: determination of burning rate temperature sensitivity. J Propul Power 15(6):748–752. doi:10.2514/2.5523
113. Aubuchon CM, Rector KD, Holmes W, Fayer MD (1999) Nitro group asymmetric stretching mode lifetimes of molecules used in energetic materials. Chem Phys Lett 299(1):84–90. doi:10.1016/S0009-2614(98)01241-X
114. Balakrishnan VK, Halasz A, Hawari J (2003) Alkaline Hydrolysis of the cyclic nitramine explosives RDX, HMX, and CL-20: new insights into degradation pathways obtained by the observation of novel intermediates. Environ Sci Technol 37(9):1838–1843. doi:10.1021/es020959h
115. Balakrishnan VK, Monteil-Rivera F, Gautier MA, Hawari J (2004) Sorption and stability of the polycyclic nitramine explosive CL-20 in soil. J Environ Qual 33(4):1362–1368. doi:10.2134/jeq2004.1362
116. Balakrishnan VK, Monteil-Rivera F, Halasz A, Corbeanu A, Hawari J (2004) Decomposition of the polycyclic nitramine explosive, CL-20, by FeO. Environ Sci Technol 38(24):6861–6866. doi:10.1021/es049423h
117. Bardai G, Sunahara GI, Spear PA, Martel M, Gong P, Hawari J (2005) Effects of dietary administration of CL-20 on Japanese Quail Coturnix coturnix japonica. Arch Environ Contam Toxicol 49(2):215–222. doi:10.1007/s00244-004-0231-9
118. Bardai GK et al (2006) In vitro degradation of hexanitrohexaazaisowurtzitane (CL-20) by cytosolic enzymes of Japanese quail and the rabbit. Environ Toxicol Chem 25(12):3221–3229. doi:10.1897/06-068R.1
119. Bayat Y et al (2013) Synthesis of 2,4,6,8,10,12-Hexanitro-2,4,6,8,10,12-hexaazaisowurtzitane using Melaminium-tris(hydrogensulfate) by a Simple One-pot Nitration Procedure. Propellants, Explos, Pyrotech 38(6):745–747. doi:10.1002/prep.201300034
120. Bayat Y, Mokhtari J, Farhadian N, Bayat M (2012) Heteropolyacids: an efficient catalyst for synthesis of CL-20. J Energ Mater 30(2):124–134. doi:10.1080/07370652.2010.549539
121. Bayat Y, Pourmortazavi SM, Ahadi H, Iravani H (2013) Taguchi robust design to optimize supercritical carbon dioxide anti-solvent process for preparation of 2,4,6,8,10,12-hexanitro-2,4,6,8,10,12-hexaazaisowurtzitane nanoparticles. Chem Eng J 230:432–438 doi:10.1016/j.cej.2013.06.100
122. Bayat Y, Soleyman R, Zarandi M (2015) Synthesis and characterization of novel 2,4,6,8,10,12-hexanitro-2,4,6,8,10,12-hexaazaisowurtzitane (2,4,6,8,10,12-hexanitro-2,4,6,8,10,12-hexaazatetracyclo dodecane based nanopolymer-bonded explosives by microemulsion. J Mol Liq 206:190–194. doi:10.1016/j.molliq.2015.02.019

123. Bazaki H, Kawabe S, Miya H, Kodama T (1998) Synthesis and sensitivity of hexanitrohexaaza-isowurtzitane (HNIW). Propellants, Explos, Pyrotech 23(6):333–336. doi:10.1002/(SICI)1521-4087(199812)23:6<333:AID-PREP333>3.0.CO;2-X
124. Behler KD, Pesce-Rodriguez R, Cabalo J, Sausa R (2013) Infrared spectroscopy and density functional theory of crystalline β-2,4,6,8,10,12-hexanitrohexaaziosowurtzitane (β CL-20) in the region of its C-H stretching vibrations. Spectrochim Acta, Part A 114:708–712. doi:10.1016/j.saa.2013.05.075
125. Behrens R (2005) Thermal decomposition processes of energetic materials in the condensed phase at low and moderate temperatures. Adv Ser Phys Chem 16(Overviews of Recent Research on Energetic Materials):29–73
126. Bhushan B, Halasz A, Hawari J (2004) Nitroreductase catalyzed biotransformation of CL-20. Biochem Biophys Res Commun 322(1):271–276. doi:10.1016/j.bbrc.2004.07.115
127. Bhushan B, Halasz A, Spain JC, Hawari J (2004) Initial reaction(s) in biotransformation of CL-20 is catalyzed by salicylate 1-monooxygenase from Pseudomonas sp. strain ATCC 29352. Appl Environ Microbiol 70(7):4040–4047. doi:10.1128/AEM.70.7.4040-4047.2004
128. Bhushan B, Halasz A, Thiboutot S, Ampleman G, Hawari J (2004) Chemotaxis-mediated biodegradation of cyclic nitramine explosives RDX, HMX, and CL-20 by Clostridium sp. EDB2. Biochem Biophys Res Commun 316(3):816–821. doi:10.1016/j.bbrc.2004.02.120
129. Bolton O, Simke LR, Pagoria PF, Matzger AJ (2012) High power explosive with good sensitivity: A 2:1 cocrystal of CL-20:HMX. Cryst Growth Des 12(9):4311–4314. doi:10.1021/cg3010882
130. Bonin PML, Bejan D, Radovic-Hrapovic Z, Halasz A, Hawari J, Bunce NJ (2005) Indirect oxidation of RDX, HMX, and CL-20 cyclic nitramines in aqueous solution at boron-doped diamond electrodes. Environ Chem 2(2):125–129. doi:10.1071/EN05006
131. Boudreau AE, Hoatson DM (2004) Halogen variations in the paleoproterozoic layered mafic-ultramafic intrusions of East Kimberley, Western Australia: implications for platinum group element mineralization. Econ Geol 99(5):1015–1026
132. Bresler PI (1966) Gas analyzer for determination of chlorine concentrations in gas mixtures. Zavod Lab 32(6):7–766
133. Bunte G, Pontius H, Kaiser M (1999) Analytical characterization of impurities or byproducts in new energetic materials. Propellants, Explos, Pyrotech 24(3):149–155. doi:10.1002/(SICI)1521-4087(199906)24:03<149:AID-PREP149>3.0.CO;2-4
134. Byrd EFC, Chabalowski CF, Rice BM (2007) An Ab initio study of nitromethane, HMX, RDX, CL-20, PETN, and TATB. Science Press, pp 696–700
135. Byrd EFC, Rice BM (2006) Improved prediction of heats of formation of energetic materials using quantum mechanical calculations. J Phys Chem A 110(3):1005–1013
136. Byrd EFC, Rice BM (2007) Ab initio study of compressed 1,3,5,7-tetranitro-1,3,5,7-tetraazacyclooctane (HMX), cyclotrimethylenetrinitramine (RDX), 2,4,6,8,10,12-hexanitrohexaazaisowurzitane (CL-20), 2,4,6-trinitro-1,3,5-benzenetriamine (TATB), and pentaerythritol tetranitrate (PETN). J Phys Chem C 111(6):2787–2796. doi:10.1021/jp0617930
137. Bywater WG, Coleman WR, Kamm O, Merritt HH (1945) Synthetic anticonvulsants. Preparation and properties of some benzoxazoles. J Am Chem Soc 67:7–905. doi:10.1021/ja01222a008
138. Campbell JA, Szecsody JE, Devary BJ, Valenzuela BR (2007) Electrospray ionization mass spectrometry of hexanitrohexaazaisowurtzitane (CL-20). Anal Lett 40(10):1972–1978. doi:10.1080/00032710701484459
139. Chambers RD, Musgrave WKR, Urben PG (1975) Chlorination of perfluorodiazines. J Fluorine Chem 5(3):6–275. doi:10.1016/S0022-1139(00)82489-6
140. Chan RKS, Anselmo KJ, Reynolds CE, Worman CH (1978) Diffusion of vinyl chloride from PVC packaging material into food simulating solvents. Polym Eng Sci 18(7):6–601. doi:10.1002/pen.760180709
141. Chang C-L, Lee J-S, Hsu C-K, Shieh B (2001) Thermal decomposition properties of CL-20 and NTO. Proc NATAS Annu Conf Therm Anal Appl 29th:685–690

142. Chapman RD, Hollins RA (2008) Benzylamine-Free, heavy-metal-free synthesis of CL-20 via hexa(1-propenyl)hexaazaisowurtzitane. J Energ Mater 26(4):246–273. doi:10.1080/07370650802182385
143. Chernyshev EA, Mironov VF, Petrov AD (1960) New method of preparation of organosilicon monomers by high temperature condensation of alkenyl chlorides, aryl chlorides, and olefins with hydrosilanes. Izv Akad Nauk SSSR, Ser Khim:2147–2156
144. Chung K-H, Kil H-S, Choi I-Y, Chu C-K, Lee I-M (2000) New precursors for hexanitrohexaazaisowurtzitane (HNIW, CL-20). J Heterocycl Chem 37(6):1647–1649. doi:10.1002/jhet.5570370640
145. Clawson JS, Anderson KL, Pugmire RJ, Grant DM (2004) 15 N NMR Chemical Shift Tensors of Substituted Hexaazaisowurtzitanes: The Intermediates in the Synthesis of CL-20. J Phys Chem A 108(14):2638–2644. doi:10.1021/jp0373999
146. Collet C, Dervaux M, Werschine M (2011) B2514A: a novel enhanced blast explosive. Proc Int Pyrotech Semin 37th(EUROPYRO 2011):72–84
147. Crocker FH, Indest KJ, Fredrickson HL (2006) Biodegradation of the cyclic nitramine explosives RDX, HMX, and CL-20. Appl Microbiol Biotechnol 73(2):274–290. doi:10.1007/s00253-006-0588-y
148. Crocker FH, Thompson KT, Szecsody JE, Fredrickson HL (2005) Biotic and abiotic degradation of CL-20 and RDX in soils. J Environ Qual 34(6):2208–2216. doi:10.2134/jeq2005.0032
149. DeTata D, Collins P, McKinley A (2013) A fast liquid chromatography quadrupole time-of-flight mass spectrometry (LC-QToF-MS) method for the identification of organic explosives and propellants. Forensic Sci Int 233(1–3):63–74. doi:10.1016/j.forsciint.2013.08.007
150. Divekar CN, Sanghavi RR, Nair UR, Chakraborthy TK, Sikder AK, Singh A (2010) Closed-vessel and thermal studies on triple-base gun propellants containing CL-20. J Propul Power 26(1):120–124. doi:10.2514/1.40895
151. Doriath G (1995) Energetic insensitive propellants for solid and ducted rockets. J Propul Power 11(4):82–870. doi:10.2514/3.23912
152. Dorofeeva OV, Suntsova MA (2015) Enthalpy of formation of CL-20. Comput Theor Chem 1057:54–59. doi:10.1016/j.comptc.2015.01.015
153. Dubovik AV, Kozak GD, Aleshkina EA (2007) Theoretical estimation of explosion hazard of NTO, FOX-7, TNAZ, and CL-20. University of Pardubice, pp 484–495
154. Dumas S, Gauvrit JY, Lanteri P (2012) Determining the polymorphic purity of ε-CL20 contaminated by other polymorphs through the use of FTIR spectroscopy with PLS regression. Propellants, Explos, Pyrotech 37(2):230–234. doi:10.1002/prep.200900090
155. Dziura R, Kazimierczuk R, Skupinski W, Pienkowski L, Grzelczyk S (2003) Reductive debenzylation in synthesis of hexanitrohexaazaisowurtzitane (HNIW, CL-20). Organika:31–43
156. Elbeih A, Zeman S, Jungova M, Vavra P (2013) Attractive nitramines and related PBXs. Propellants, Explos, Pyrotech 38(3):379–385. doi:10.1002/prep.201200011
157. Fournier D, Monteil-Rivera F, Halasz A, Bhatt M, Hawari J (2006) Degradation of CL-20 by white-rot fungi. Chemosphere 63(1):175–181. doi:10.1016/j.chemosphere.2005.06.052
158. Gar KA (1958) Field trials of 65% chlorten. Org Insektofungitsidy i Gerbitsidy:208–230
159. Geetha M, Nair UR, Sarwade DB, Gore GM, Asthana SN, Singh H (2003) Studies on CL-20: The most powerful high energy material. J Therm Anal Calorim 73(3):913–922
160. Ghosh M et al (2014) Probing crystal growth of ε- and α-CL-20 polymorphs via metastable phase transition using microscopy and vibrational spectroscopy. Cryst Growth Des 14(10):5053–5063. doi:10.1021/cg500644w
161. Ghule VD, Jadhav PM, Patil RS, Radhakrishnan S, Soman T (2010) Quantum-chemical studies on hexaazaisowurtzitanes. J Phys Chem A 114(1):498–503. doi:10.1021/jp9071839
162. Gnirke AU, Weidle UH (1998) Investigation of prevalence and regulation of expression of progression associated protein (PAP). Anticancer Res 18(6A):4363–4369
163. Gnirke AU, Weidle UH (1998) Investigation of prevalence and regulation of expression of progression associated protein (PAP). Anticancer Res 18(6A):4363–4369

164. Goede P, Latypov NV, Oestmark H (2004) Fourier transform Raman Spectroscopy of the four crystallographic phases of α, β, γ and ε 2,4,6,8,10,12-hexanitro-2,4,6,8,10,12-hexaazatetracyclo[5.5.0.05,9.03,11]dodecane (HNIW, CL-20). Propellants, Explos, Pyrotech 29(4):205–208 doi:10.1002/prep.200400047
165. Golofit T, Zysk K (2015) Thermal decomposition properties and compatibility of CL-20 with binders HTPB, PBAN, GAP and polyNIMMO. J Therm Anal Calorim 119(3):1931–1939. doi:10.1007/s10973-015-4418-2
166. Gong P, Sunahara GI, Rocheleau S, Dodard SG, Robidoux PY, Hawari J (2004) Preliminary ecotoxicological characterization of a new energetic substance, CL-20. Chemosphere 56 (7):653–658. doi:10.1016/j.chemosphere.2004.04.010
167. Granito C, Schultz HP (1963) Decarboxylation studies. II. Preparation of alkyl phenyl ketones. J Org Chem 28:81–879. doi:10.1021/jo01038a521
168. Greenberg BL, Kalyon DM, Erol M, Mezger M, Lee K, Lusk S (2003) Analysis of slurry-coating effectiveness of CL-20 using grazing incidence x-ray diffraction. J Energ Mater 21(3):185–199. doi:10.1080/716100383
169. Groom CA, Halasz A, Paquet L, D'Cruz P, Hawari J (2003) Cyclodextrin-assisted capillary electrophoresis for determination of the cyclic nitramine explosives RDX, HMX and CL-20. Comparison with high-performance liquid chromatography. J Chromatogr, A 999(1–2):17–22 doi:10.1016/S0021-9673(03)00389-3
170. Hakansson K, Coorey RV, Zubarev RA, Talrose VL, Hakansson P (2000) Low-mass ions observed in plasma desorption mass spectrometry of high explosives. J Mass Spectrom 35 (3):337–346
171. Hawari J, Deschamps S, Beaulieu C, Paquet L, Halasz A (2004) Photodegradation of CL-20: insights into the mechanisms of initial reactions and environmental fate. Water Res 38 (19):4055–4064. doi:10.1016/j.watres.2004.06.032
172. Hoffmann RW, Sieber W, Guhn G (1965) Decomposition of 1,2,3-benzothiadiazole 1,1-dioxide. Chem Ber 98(11):8–3470
173. Hultquist ME et al (1951) N-Heterocyclic benzenesulfonamides. J Am Chem Soc 73:66–2558. doi:10.1021/ja01150a042
174. Isayev O, Gorb L, Qasim M, Leszczynski J (2008) Ab initio molecular dynamics study on the initial chemical events in nitramines: thermal decomposition of CL-20. J Phys Chem B 112(35):11005–11013. doi:10.1021/jp804765m
175. Kaste PJ, Rice BM (2004) Novel energetic materials for the future force: the army pursues the next generation of propellants and explosives. AMPTIAC Q 8(4):85–89
176. Keshavarz MH, Yousefi MH (2008) Heats of sublimation of nitramines based on simple parameters. J Hazard Mater 152(3):929–933. doi:10.1016/j.jhazmat.2007.07.067
177. Kholod Y et al (2006) Are 1,5- and 1,7-dihydrodiimidazo[4,5-b:4',5'-e]pyrazine the main products of 2,4,6,8,10,12-hexanitro-2,4,6,8,10,12-hexaazaisowurtzitane (CL-20) alkaline hydrolysis? A DFT study of vibrational spectra. J Mol Struct 794(1–3):288–302. doi:10.1016/j.molstruc.2006.02.061
178. Kholod Y, Kosenkov D, Okovytyy S, Gorb L, Qasim M, Leszczynski J (2008) CL-20 photodecomposition: Ab initio foundations for identification of products. Spectrochim Acta, Part A 71A(1):230–237. doi:10.1016/j.saa.2007.12.021
179. Kim J-H, Park Y-C, Yim Y-J, Han J-S (1998) Crystallization behavior of hexanitrohexaazaisowurtzitane at 298 K and quantitative analysis of mixtures of its polymorphs by FTIR. J Chem Eng Jpn 31(3):478–481. doi:10.1252/jcej.31.478
180. Kim J-H, Park Y-C, Yim Y-J, Han J-S (1998) Crystallization behavior of hexanitrohexaazaisowurtzitane at 298 K and quantitative analysis of mixtures of its polymorphs by FTIR. J Chem Eng Jpn 31(3):478–481. doi:10.1252/jcej.31.478
181. Klapotke TM, Ang H-G (2001) Estimation of the crystalline density of nitramine (N-NO_2 based) high energy density materials (HEDM). Propellants, Explos, Pyrotech 26(5):221–224. doi:10.1002/1521-4087(200112)26:5<221:AID-PREP221>3.0.CO;2-T
182. Klapötke TM, Witkowski TG (2016) Covalent and Ionic Insensitive High-Explosives. Propellants, Explos, Pyrotech 41:470–483. doi:10.1002/prep.201600006

183. Knox-Holmes B (1993) Biofouling control with low levels of copper and chlorine. Biofouling 7(2):66–157. doi:10.1080/08927019309386250
184. Koslik P, Stas J, Wilk Z, Zakrzewski A (2007) Research of high explosives based on RDX, HMX and CL-20 in the small scale underwater test examination. Cent Eur J Energ Mater 4 (3):3–13
185. Koutsospyros A, Christodoulatos C, Panikov N, Malcheva O, Karakaya P, Nicolich S (2004) Environmental relevance of CL-20: preliminary findings. Water Air Soil Pollut Focus 4(4–5):459–470. doi:10.1023/B:WAFO.0000044818.76609.e9
186. Li H, Shu Y, Gao S, Chen L, Ma Q, Ju X (2013) Easy methods to study the smart energetic TNT/CL-20 co-crystal. J Mol Model 19(11):4909–4917. doi:10.1007/s00894-013-1988-4
187. Li J, Brill TB (2007) Kinetics of solid polymorphic phase transitions of CL-20. Propellants, Explos, Pyrotech 32(4):326–330. doi:10.1002/prep.200700036
188. Lizlovs EA, Bond AP (1975) Effect of low-temperature aging on corrosion resistance of chromium-molybdenum (18Cr-2Mo) titanium-stabilized ferritic stainless steel. J Electrochem Soc 122(5):93–589. doi:10.1149/1.2134271
189. Maksimowski P, Skupinski W, Szczygielska J (2013) Comparison of the crystals obtained by precipitation of CL-20 with different chemical purity. Propellants, Explos, Pyrotech 38 (6):791–797. doi:10.1002/prep.201300064
190. Marvin KW, Fujimoto W, Jetten AM (1995) Identification and characterization of a novel squamous cell-associated gene related to PMP22. J Biol Chem 270(48):16–28910. doi:10.1074/jbc.270.48.28910
191. Mathieu J, Stucki H (2004) Military high explosives. Chimia 58(6):383–389. doi:10.2533/000942904777677669
192. Meents A, Dittrich B, Johnas SKJ, Thome V, Weckert EF (2008) Charge-density studies of energetic materials: CL-20 and FOX-7. Acta Crystallogr Sect B: Struct Sci 64(4):519. doi:10.1107/S0108768108017497
193. Millar DIA et al (2012) Crystal engineering of energetic materials: Co-crystals of CL-20. CrystEngComm 14(10):3742–3749. doi:10.1039/c2ce05796d
194. Molt RW, Bartlett RJ, Watson T, Bazante AP (2012) Conformers of CL-20 explosive and ab initio refinement using perturbation theory: implications to detonation mechanisms. J Phys Chem A 116(49):12129–12135. doi:10.1021/jp305443h
195. Monteil-Rivera F et al (2009) Fate of CL-20 in sandy soils: degradation products as potential markers of natural attenuation. Environ Pollut 157(1):77–85
196. Naik NH, Gore GM, Gandhe BR, Sikder AK (2008) Studies on thermal decomposition mechanism of CL-20 by pyrolysis gas chromatography-mass spectrometry (Py-GC/MS). J Hazard Mater 159(2–3):630–635. doi:10.1016/j.jhazmat.2008.02.049
197. Namasivayam C, Kanagarathinam A (1992) Distillery wastewater treatment using waste iron (3+)/chromium(3+) hydroxide sludge and polymer flocculants. J Environ Sci Health, Part A A 27(7):37–1721
198. Nedelko VV et al (2000) Comparative investigation of thermal decomposition of various modifications of hexanitrohexaazaisowurtzitane (CL-20). Propellants, Explos, Pyrotech 25 (5):255–259. doi:10.1002/1521-4087(200011)25:5<255:AID-PREP255>3.0.CO;2-8
199. Oehrle SA (1996) Analysis of nitramine and nitroaromatic explosives by micellar electrokinetic capillary chromatography (MECC). J Energ Mater 14(1):47–56. doi:10.1080/07370659608216057
200. Ogata Y, Kawasaki A, Nakagawa K (1964) Kinetics of the formation of benzoguanamine from dicyandiamide and benzonitrile. Tetrahedron 20(12):61–2755. doi:10.1016/S0040-4020(01)98493-5
201. Okovytyy S, Kholod Y, Qasim M, Fredrickson H, Leszczynski J (2005) The Mechanism of Unimolecular Decomposition of 2,4,6,8,10,12-Hexanitro-2,4,6,8,10,12-hexaazaisowurtzitane. A computational DFT study. J Phys Chem A 109(12):2964–2970. doi:10.1021/jp045292v
202. Patel AR, Oneto JF (1963) Basic 1,3-dioxolanes. J Pharm Sci 52(6):92–588. doi:10.1002/jps.2600520618

203. Paulin A, Jobson BA, Vukcevic S (1981) Chlorination of alumina-containing materials in fluidized bed. Trav Com Int Etude Bauxites, Alumine Alum 16:70–161
204. Peralta-Inga Z, Degirmenbasi N, Olgun U, Gocmez H, Kalyon DM (2006) Recrystallization of CL-20 and HNFX from solution for rigorous control of the polymorph type: part I, mathematical modeling using molecular dynamics method. J Energ Mater 24(2):69–101. doi:10.1080/07370650600672082
205. Pivina T, Korolev V, Khakimov D, Petukhova T, Ivshin V, Lempert D (2012) Computer simulation of decomposition mechanisms for CL-20, hydrazine, and their binary system. Propellants, Explos, Pyrotech 37(4):502–509. doi:10.1002/prep.201100098
206. Reeves CC Jr, Miller WD (1978) Nitrate, chloride and dissolved solids, Ogallala aquifer, west Texas. Ground Water 16(3):73–167. doi:10.1111/j.1745-6584.1978.tb03218.x
207. Robidoux PY et al (2004) Acute and chronic toxicity of the new explosive CL-20 to the earthworm (Eisenia andrei) exposed to amended natural soils. Environ Toxicol Chem 23 (4):1026–1034. doi:10.1897/03-308
208. Sandor A (1964) Thermionic emission from barium-coated ultrapure nickel in the emission microscope. J Electron Control 17(4):91–377. doi:10.1080/00207216408937712
209. Sandor A (1964) Thermionic emission from barium-coated ultrapure nickel in the emission microscope. J Electron Control 17(4):91–377. doi:10.1080/00207216408937712
210. Sausa RC, Cabalo JB (2012) The detection of energetic materials by laser photoacoustic overtone spectroscopy. Appl Spectrosc 66(9):993–998. doi:10.1366/12-06699
211. Schefflan R, Kovenklioglu S, Kalyon D, Redner P, Heider E (2006) Mathematical model for a fed-batch crystallization process for energetic crystals to achieve targeted size distributions. J Energ Mater 24(2):157–172. doi:10.1080/07370650600672058
212. Sikder AK, Sikder N, Gandhe BR, Agrawal JP, Singh H (2002) Hexanitrohexaazaisowurtzitane or CL-20 in India: synthesis and characterisation. Def Sci J 52(2):135–146
213. Sinditskii VP, Burzhava AV, Sheremetev AB, Aleksandrova NS (2012) Thermal and combustion properties of 3,4-bis(3-nitrofurazan-4-yl)furoxan (DNTF). Propellants, Explos, Pyrotech 37(5):575–580. doi:10.1002/prep.201100095
214. Sinditskii VP, Egorshev VY, Serushkin VV, Filatov SA, Chernyi AN (2012) Combustion mechanism of energetic binders with nitramines. Int J Energ Mater Chem Propul 11(5):427–449. doi:10.1615/IntJEnergeticMaterialsChemProp.2013005557
215. Singh H (2005) Current trend of R&D in the field of high energy materials: an overview. Explosion 15(3):120–132
216. Sivabalan R, Gore GM, Nair UR, Saikia A, Venugopalan S, Gandhe BR (2007) Study on ultrasound assisted precipitation of CL-20 and its effect on morphology and sensitivity. J Hazard Mater 139(2):199–203. doi:10.1016/j.jhazmat.2006.06.027
217. Souers PC et al (2001) Detonation energies from the cylinder test and CHEETAH V3.0. Propellants, Explos, Pyrotech 26(4):180–190 doi:10.1002/1521-4087(200110)26:4<180::AID-PREP180>3.0.CO;2-K
218. Steinmetz I, Rott L, Boer C (1966) Enrichment of ground waters with surface waters. Hidrobiologia 7:195–201
219. Strigul N, Braida W, Christodoulatos C, Balas W, Nicolich S (2005) The assessment of the energetic compound 2,4,6,8,10,12-hexanitro-2,4,6,8,10,12-hexaazaisowurtzitane (CL-20) degradability in soil. Environ Pollut 139(2):353–361. doi:10.1016/j.envpol.2005.05.002
220. Suzuki J et al (1984) Performance of Shimadzu clinical chemistry analyzer CL-20. Shimadzu Hyoron 41(4):45–229
221. Szecsody JE, Girvin DC, Devary BJ, Campbell JA (2004) Sorption and oxic degradation of the explosive CL-20 during transport in subsurface sediments. Chemosphere 56(6):593–610. doi:10.1016/j.chemosphere.2004.04.028
222. Talawar MB et al (2006) Effect of organic additives on the mitigation of volatility of 1-nitro-3,3’-dinitroazetidine (TNAZ): Next generation powerful melt castable high energy material. J Hazard Mater 134(1–3):8–18. doi:10.1016/j.jhazmat.2003.10.008
223. Talawar MB, Sivabalan R, Polke BG, Nair UR, Gore GM, Asthana SN (2005) Establishment of process technology for the manufacture of dinitrogen pentoxide and its utility for the

synthesis of most powerful explosive of today—CL-20. J Hazard Mater 124(1–3):153–164. doi:10.1016/j.jhazmat.2005.04.021

224. Tappan AS, Basiliere M, Ball JP, Snedigar S, Fischer GJ, Salton J (2010) Linear actuation using milligram quantities of CL-20 and TAGDNAT. Propellants, Explos, Pyrotech 35 (3):207–212. doi:10.1002/prep.201000025
225. Tappan BC, Brill TB (2003) Thermal decomposition of energetic materials 86. Cryogel synthesis of nanocrystalline CL-20 coated with cured nitrocellulose. Propellants, Explos, Pyrotech 28(5):223–230 doi:10.1002/prep.200300009
226. Thiboutot S, Brousseau P, Ampleman G, Pantea D, Cote S (2008) Potential use of CL-20 in TNT/ETPE-based melt cast formulations. Propellants, Explos, Pyrotech 33(2):103–108. doi:10.1002/prep.200700223
227. Tian Q et al (2013) Thermally induced damage in hexanitrohexaazaisowurtzitane. Cent Eur J Energ Mater 10(3):359–369
228. Tomas-Alonso F, Rubio AM, Alvarez R, Ortuno JA (2013) Dynamic potential response and SEM-EDX studies of polymeric inclusion membranes based on ionic liquids. Int J Electrochem Sci 8(4):4955–4969
229. Urbelis JH, Young VG, Swift JA (2015) Using solvent effects to guide the design of a CL-20 cocrystal. CrystEngComm 17(7):1564–1568. doi:10.1039/C4CE02285H
230. Van der Heijden AEDM (1998) Crystallization and characterization of energetic materials. Curr Top Cryst Growth Res 4:99–114
231. van der Heijden AEDM, Bouma RHB, van der Steen AC (2004) Physicochemical parameters of nitramines influencing shock sensitivity. Propellants, Explos, Pyrotech 29 (5):304–313. doi:10.1002/prep.200400058
232. van der Heijden AEDM, Bouma RHB, van der Steen AC (2004) Physicochemical parameters of nitramines influencing shock sensitivity. Propellants, Explos, Pyrotech 29 (5):304–313. doi:10.1002/prep.200400058
233. Viswanath DS, Reinig M, Ghosh TK, Boddu VM (2010) Vapor pressure of nitro compounds, vol Pt. 1. University of Pardubice, Institute of Energetic Materials, pp 306–309
234. Viswanath JV, Venugopal KJ, Rao NVS, Venkataraman A (2016) An overview on importance, synthetic strategies and studies of 2,4,6,8,10,12-hexanitro-2,4,6,8,10,12-hexaazaisowurtzitane (HNIW). Defence Technol 12(5), October 2016, pp 401–418
235. Volk F, Bathelt H (1997) Influence of energetic materials on the energy-output of gun propellants. Propellants, Explos, Pyrotech 22(3):120–124. doi:10.1002/prep.19970220305
236. Volk F, Bathelt H (1995) Influence of energetic materials on the energy-output of gun propellants. Am Defense Preparedness Assoc: 82–89
237. von Holtz E, Ornellas D, Foltz MF, Clarkson JE (1994) The solubility of ε-CL-20 in selected materials. Propellants, Explos, Pyrotech 19(4):12–206. doi:10.1002/prep.19940190410
238. Wu Y, Ou Y, Liu Z, Liu J, Meng Z, Chen B (2004) Theoretical studies on the possible conformers and properties of tetranitrodiazidoacetylhexaazaisowurtzitane (TNDAIW). Sci China, Ser B: Chem 47(5):414–419. doi:10.1360/04yb0046
239. Xing X et al (2015) Thermal decomposition behavior of hexanitrohexaazaisowurtzitane and its blending with BTATz (expand) and Al by microcalorimetry. J Therm Anal Calorim: Ahead of Print. doi:10.1007/s10973-015-4431-5
240. Yazici R, Kalyon D (2005) Microstrain and defect analysis of CL-20 crystals by novel x-ray methods. J Energ Mater 23(1):43–58. doi:10.1080/07370650590920287
241. Zhang C et al (2014) Evident hydrogen bonded chains building CL-20-based cocrystals. Cryst Growth Des 14(8):3923–3928. doi:10.1021/cg500796r
242. Zhang P, Guo X-Y, Zhang J-Y, Jiao Q-J (2014) Application of liquid paraffin in castable CL-20-based PBX. J Energ Mater 32(4):278–292. doi:10.1080/07370652.2013.862318
243. Zubarev RA, Hakansson P, Hakansson K, Talrose VL (1998) Matrix assisted particle desorption techniques: use of explosive matrixes. Adv Mass Spectrom 14:B061920/1–B061920/8

Chapter 3
FOX-7 (1,1-Diamino-2,2-Dinitroethylene)

Abstract FOX-7 (1,1-diamino-2,2-dinitroethylene) was first synthesized in 1998 by the FOA Defense Research Establishment (Sweden). Synthesis of the FOX-7 and its structural, spectroscopic, and explosive properties are described in this chapter. The chemical reactivity of FOX-7 towards nucleophilic substitution (transamination), electrophilic substitution, and acid-base properties, thermal behavior (phase transformations and thermal decomposition, molecular structure and physical properties, other energetic molecules that are structurally related to FOX-7 are also summarized in this chapter.

3.1 Introduction

1,1-diamino-2,2-dinitroethylene, (better known as DADE or FOX-7), is a relatively new explosive with a high performance and low sensitivity. It is a high energy density material with low friction and low impact sensitivity. FOX-7 was synthesized first in 1998 by the defense establishment in Sweden, and derives the name FOX-7 because the Swedish Defense Research Agency is known as FOI, and *I* being replaced by *X* to convey that it is an eXplosive as in RDX and HMX. It has a large activation barrier for detonation. Its detonation characteristics are similar to that of RDX, but its sensitivity is lower than TNT. It is structurally similar to several other energetic compounds but much simpler to synthesize. The chemical structure of FOX-7 along with RDX and HMX is shown in Fig. 3.1. These unique combinations of properties arise because of the structure of FOX-7 with molecular packing consisting of strong hydrogen bonding, and the layered packing indicative of weak van der Waals interactions.

FOX-7 is classified as an insensitive high explosive. FOX-7 is thermally stable with an activation energy of 56 kcal/mole compared to 40 kcal/mole for RDX and 35 kcal/mole for HMX [1]. FOX-7 is a symmetric molecule with a simple crystal

D.S. Viswanath et al., *Emerging Energetic Materials: Synthesis, Physicochemical, and Detonation Properties*, https://doi.org/10.1007/978-94-024-1201-7_3

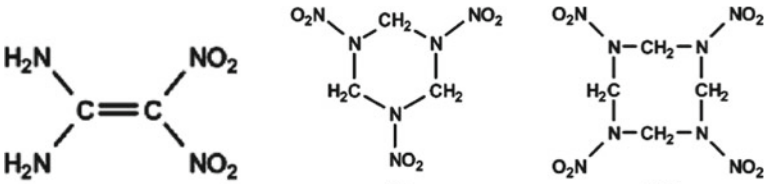

II

III

(a) FOX-7 (b) RDX (c) HMX

Fig. 3.1 Chemical structure of 1,1-Diamino-2,2-dinitroethylene (FOX-7)

structure, which makes it easier to model compared to many other energetic materials. It is slightly soluble in common organic solvents and water, but readily dissolves in dipolar aprotic solvents such as dimethyl sulfoxide, N,N-dimethyl formamide and 1-methyl-2-pyrrolidinone.

FOX-7 exists in three forms depending upon the temperature [2]. Solid FOX-7 is trimorphic with the α-phase stable on heating up to 388 K, the β-phase from 388 to 435 K, and the γ-phase from about 435 K until thermal decomposition at 504 K [3]. The thermal behavior of DADE has been studied by several researchers [1, 4–6].

3.2 Synthesis

FOX-7 was first synthesized by Latypov et al. [7] by reacting 2-(dinitro- methylene)-4,5-imidazolidinedione with aqueous ammonia solution. They also studied the synthesis of FOX-7 by nitration of 4,6-dihydroxy-2-methylpyrimidine, followed by hydrolysis of the resulting intermediate 2-dinitromethylene-5,5-dinitropyrimidine-4,6-dione [8]. Jalovy et al. [9] synthesized FOX-7 by the hydrolysis of 2-dinitrodinitromethylene)-4,5-imidazolidinedione. Swedish Defense Establishment [10] used 2-methyl-pyrimidine-4,6-di-one is the method currently used for the production of FOX-7 on a production scale. Ostmark et al. [11] at have studied various properties that affect the sensitivity of DADE. In addition, Lochert [6] described three different methods followed by the Swedish Defense Establishment for the synthesis of DADE. These three reactions are shown in Fig. 3.2.

The first reaction path produced a highly sensitive intermediate and concluded to be non-preferable synthesis path for producing DADE. The second path was satisfactory, but the yield was rather low, about 38%. This second reaction path was scaled up in the laboratory to produce about 50 g of DADE. Lochert [6] carried out a cost analysis for this synthesis route and reported that the cost of production of DADE by the new route can be half of the cost of the commercial product at that time. Based on the analysis, Lochert [6] estimated that it costs AU$ 2930 to make

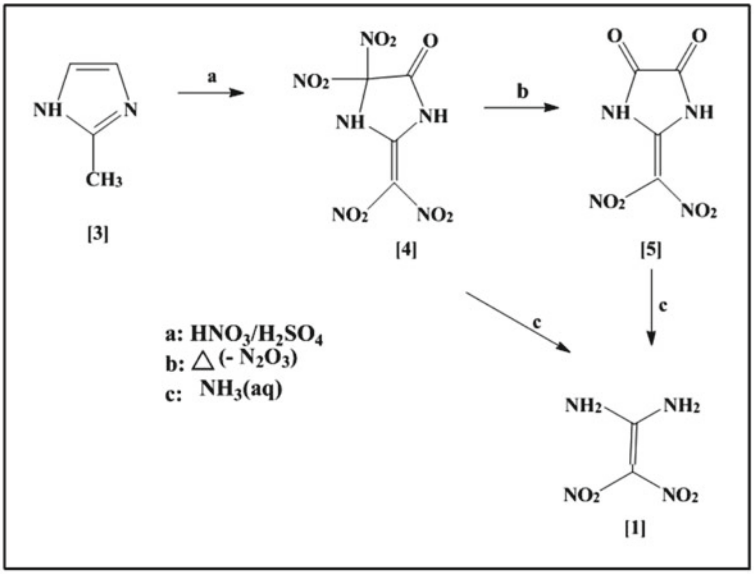

Reaction Path 1

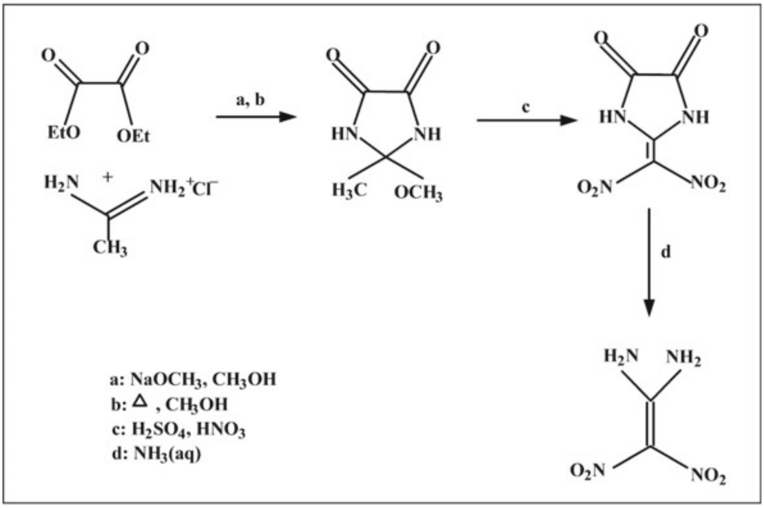

Reaction Path 2

Fig. 3.2 Three reaction paths followed by FOI for synthesis of DADE [6]

1 kg of DADE, and cost of the commercial product at that time was AU$ 5800/Kg. The chemicals and the quantities used in the cost calculation are given in Table 3.1.

During laboratory scale experimentation, another problem was encountered; frothing of the solution [5, 6, 12–15]. To avoid this problem, a third synthesis route was developed, which also provided higher yield (Table 3.2).

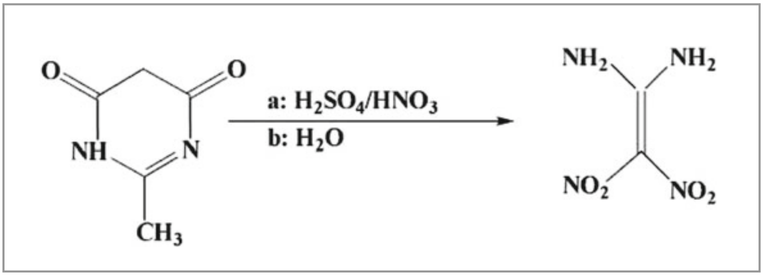

Reaction Path 3

Fig. 3.2 (continued)

Table 3.1 Amounts of various materials estimated for production of 50 g of FOX-7 via FOI reaction path 2 [6]

Item	Amount required
Methanol	7500 mL
Sodium Methoxide (30%)	1070 mL
Acetamidine Hydrochloride	168 g
Diethyl Oxalate	258 g
Hydrochloric Acid	375 mL
Sulfuric Acid	940 mL
Nitric Acid	205 mL
Ammonia	190 mL

Trzcinski et al. [16] synthesized DADE by following the method suggested by Chylek et al. [17], which was a modification of the method proposed by Latypov et al. [8]. In this process, DADE was synthesized via 2-methylpyrimidine-4,6 (3H,5H-dione (1), which was prepared by the condensation of acetamidine hydrochloride with diethyl malonate as shown in Fig. 3.3. The process was similar to that used by the Sweden Defence Establishment [1]. The final product, DADE, was obtained by nitration and hydrolysis. The authors provided a detailed explanation of the reaction paths, the crystallization process using water/ N-methyl-2-pyrrolidone mixture, the particle size distribution of the finished product, and SEM micrographs. The size and distribution of particles depended on the crystallization process, which is discussed in the following section.

Figure 3.4 shows two different synthesis schemes used by Anniyappan et al. [5]. In the first method, they nitrated 2-methylimidazol (7) with mixed acid to yield intermediate 2-dinitromethylene-4,4-dinitro-5-imidazolidinone, (8) that decomposed at room temperature to give the compound (6), which was converted to FOX-7 by amination.

Temperature control was important in the nitration step. The product was isolated as a solid. The product yield was low (<15%). In the second method, acetamidine hydrochloride (9) was reacted with diethyl oxalate (10) to give a mixture of 2-methoxy-2-methyl-4,5 imidazolidinedione (11) and 2-methyl-4,5-imidazolidinedione (12). This

Table 3.2 A summary of various synthesis routes explored by researchers

<table>
<tr><th>Authors</th><th>Synthesis Route</th><th>Yield</th></tr>
<tr><td>Cai et al. [12]</td><td>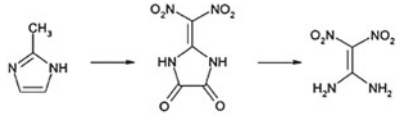
1 2
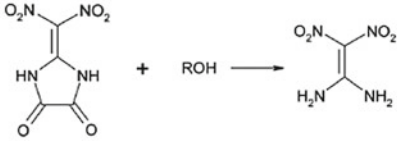
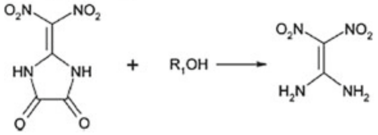
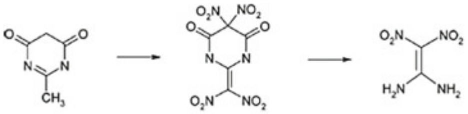
2</td><td>13%</td></tr>
<tr><td>Cai et al. [14]</td><td>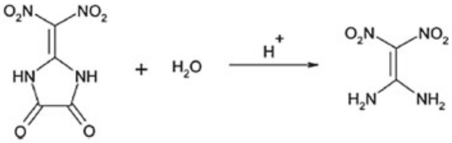
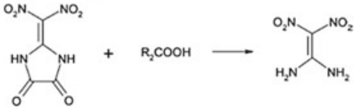
a Carboxylic acid (200 ml), 2-(dinitromethylene)-4,5-imidazolidinedione (0.01 mol), reaction 30 min, T = 25 °C.</td><td>81.1%
<table><tr><th>cardoxylic acid (%)</th><th>yield of 2</th></tr><tr><td>Formic acid</td><td>94.6</td></tr><tr><td>Acetic acid</td><td>95.8</td></tr><tr><td>Propanoic acid</td><td>95.8</td></tr><tr><td>n-butanoic acid</td><td>96.6</td></tr><tr><td>Formic acid</td><td>94.6</td></tr></table></td></tr>
</table>

product mixture11 and 12 or 11 alone was nitrated by mixed acid to from 2-(dinitromethylene)-4,5-imidazolidinedione (6) which was subsequently converted to FOX-7 as shown in Fig. 3.4. They describe other methods in their paper, and also the preparation of salts of DADE. Table 3.2 shows a summary of synthesis processes used by various researchers.

The synthesis of FOX-7 by transacylation reactions based on the hydrolysis and methanolysis has been reported by Dewey [18]. The report contains environmental fate and transport parameters for several compounds such as AP, ADNA, ADNDNA, DNNC, and HCO. The same results, as has been reported by Dewey,

Table 3.2 (continued)

	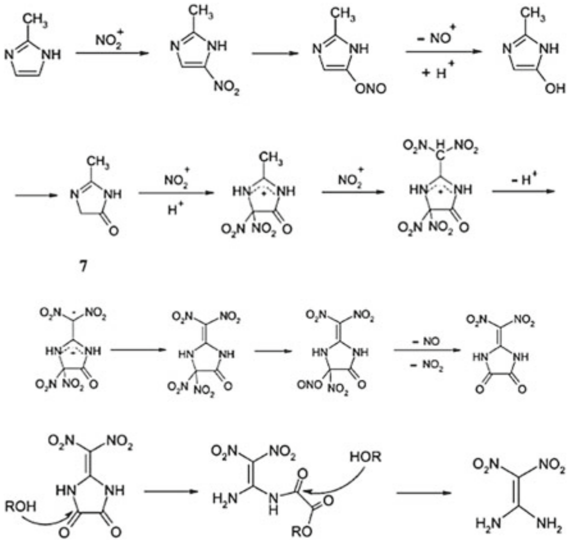
Lochert [6]	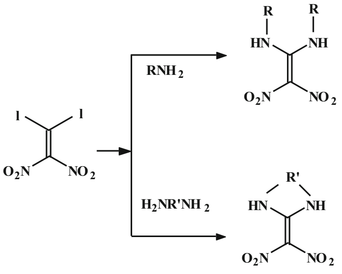 R, R' = alkyl, aryl
Anniyappan.et al [5]	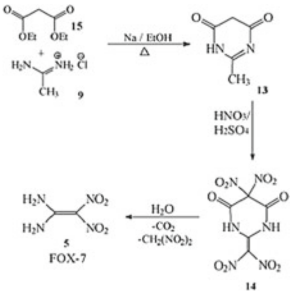

have also been reported by Clausen et al. [19]. There appears to be some discrepancies as for instance the melting point is reported as 478-543 K based on the work of different investigators. This is a classic example of the discrepancies in values of physical properties existing for different explosives.

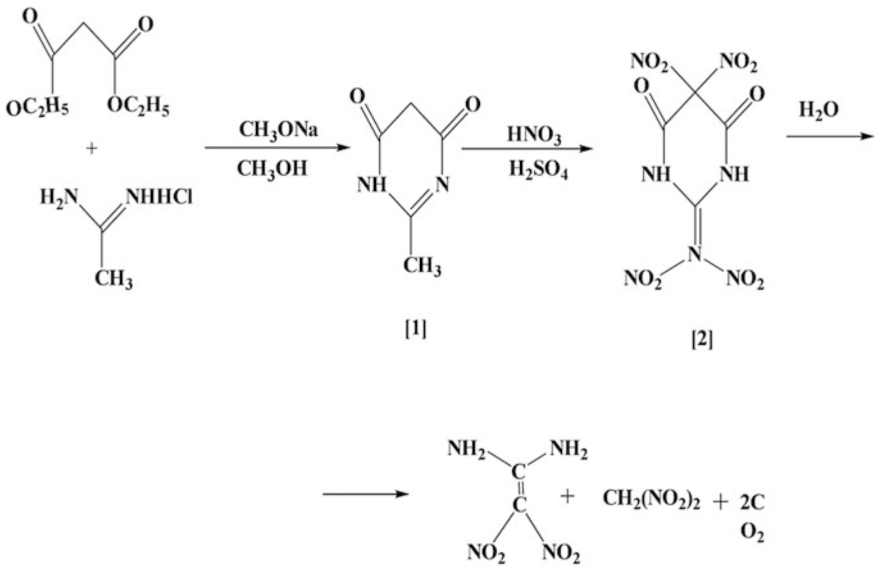

Fig. 3.3 Reaction scheme of coworkers [16]

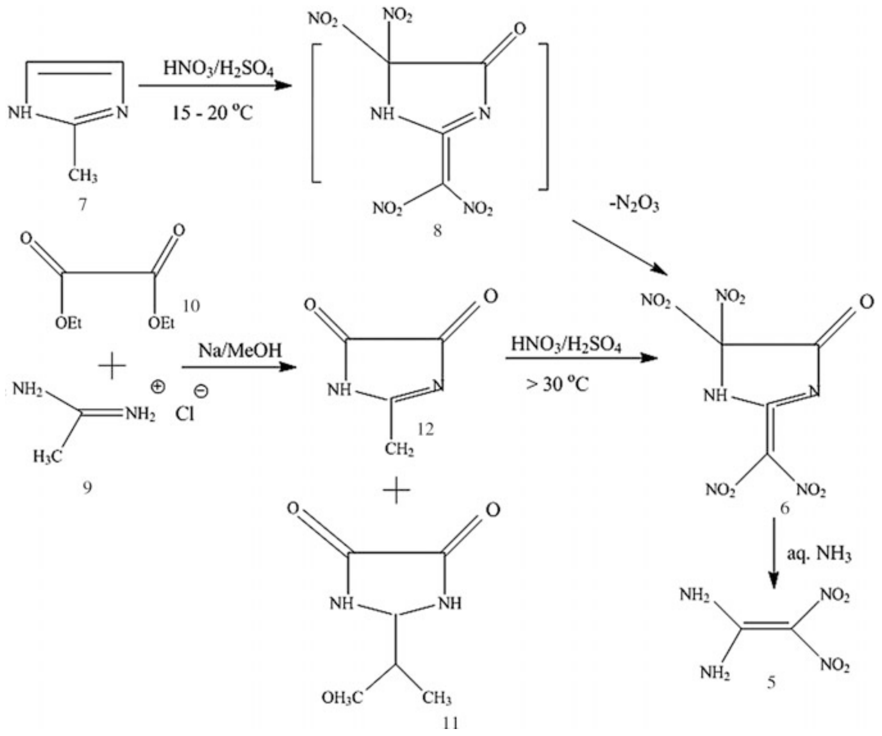

Fig. 3.4 Different routes for the synthesis of FOX-7 [5]

Zhou et al. [20] describe the synthesis procedure starting with 2-methylimidazole. They also determined density (1.885 g cm^{-3}) detonation velocity (8047 m s^{-1} at ρ = 1.696 g cm^{-3}), friction sensitivity of 10% (3.92 MPa, 90°), impact sensitivity of 6% (10 kg, 25 cm), H_2O of 89.1 cm (5 kg), vacuum stability test of 0.14 mL/5 g (100 °C, 48 h), explosion temperature of 285 °C (5 s delay).

In the recent years, Cai et al. [12–15] have used different synthesis routes, scaled up the preparation to 7 kg/batch, and compared the properties with other explosives.

Bladek et al. used thin layer chromatography to monitor FOX-7 during its synthesis [21]. The analytical parameters involved in quantitative determination are examined. The authors also examined the effect of water concentration and found an improvement in the yields during the nitration step. Orzechowski et al. [22] discuss crystallization of from DMF, DMSO, and DMSO + water. They also provide the solubility of FOX-7 in these two solvents from 293 to 363 K. They synthesized FOX-7 by reacting dioctylmalonate with acetamidine hydrochloride in thesolution of sodium methylate, and nitration of obtained 2-methylpyrimidyne 4,6 (3H,5H)-dione. Several examples of the crystallization step are provided together with SEM photomicrographs and particle size distribution, and conclude that the best results in terms of particle size and density were obtained using a mixture of DMSO + water as the solvent.

Goh et al. [23, 24] who discussed the synthesis starting from 2-methylpyrimidyne 4,6-dione and report yields close to 80%; of Goh and Kim [25] who discussed the nitration of 4,6-Dihydroxy -2-methylpyrimidine using dichloromethane as a solvent, and on hydrolysis of the nitrated product, 4,6-dihydroxy-5,5-dinitro-2-(dinitromethylene)-2,5-dihydro pyrimidine, report yields of 90%. The reactions were carried out at temperatures between 293 and 313 K and hydrolysis time of 2 h. They also discuss different schemes of nitration, and ratio of reactants used, and other reaction parameters, and of Bellamy [26] who summarized the discovery, synthesis, structure, and isomers together with an account of spectroscopic and explosive properties, and chemical reactions of FOX-7.

3.3 Crystallization/Recrystallization

Particle size, along with crystal quality and morphology, play an important role in determining the sensitivity of an explosive. The size of the crystals affects the packing density, and, therefore, the performance. The crystals should have minimum defects to maximize its detonation properties. As a result, a number of recrystallization techniques were proposed that can reliably produce crystals of desirable size in a consistent manner. The parameters that affect the crystal shape, size, and its particle size distribution include: solvent type, cooling rate, stirring rate, and method of stirring, such as sonic method with different frequencies.

Trzcinski et al. [16] used a mixture of water/N-methyl-2-pyrrolidone in a ratio of 75/25 and a cooling rate of 0.3 K/min to recrystallize DADE. They used vigorous mechanical stirring during the recrystallization process. Particles of diameter in the range of 100 to 600 μm with a normal distribution were obtained. The particle diameter ranged from 2 to 18 μm with a peak around 7 μm when DADE was recrystallized from NMP into water at an ambient temperature. The FOX-7 crystals are shown in Fig. 3.5 and their size distribution is presented in Fig. 3.6.

Orzechowski et al. [22] discuss crystallization of DADE from DMF, DMSO, and DMSO+water solvent. They also provide the solubility of FOX-7 in these two solvents from 293 to 363 K. Teipel et al. [27] evaluated several solvents and solvent/anti-solvent mixture for recrystallization of DADE. They noted that solvent has significant effect on particle shape, surface texture, size and yield. Solvents used in their study included N-methyl pyrrolidinone (NMP), NMP/water mixtures and N, N-dimethyl formamide (DMF), γ-butyrolactone (GBL) and acetonitrile. The mean particle size varied from one run to another run, leading them to conclude that standard cooling-type recrystallization processes are not a preferable approach. Depending on the solvent used, different types of morphologies of recrystallized DADE were observed: rhombic, flat, or rectangular. Several researchers tried to optimize the process parameters that can produce the best crystals in a consistent manner. The parameters were optimized in terms of solvents, stirring rate and cooling rate, and the use of anti-solvent. The goal was to produce near spherical particles or particles that can provide the best packing density.

Solvents used for the recrystallization not only affected the particle sizes and morphology, but also the detonation properties. Fuhr and Mikonsaari [28] showed that not only yield of FOX-7 depended on the choice of solvent, but also the impact and friction sensitivity. Their results are given in Table 3.3.

Several researchers have suggested the use of sonication using ultrasound as a stirring method during recrystallization process. Ultrasonic cavitation induces nucleation providing a dominant mechanism of crystal inception. A better control over the crystal size and morphology was achieved. The particle sizes of DADE produced from different solvent when 20 kHz ultrasound was applied are given in Table 3.4 [29]. The application of ultrasound appeared to improve crystal quality in comparison to traditional recrystallization. The frequency of the ultrasound affected

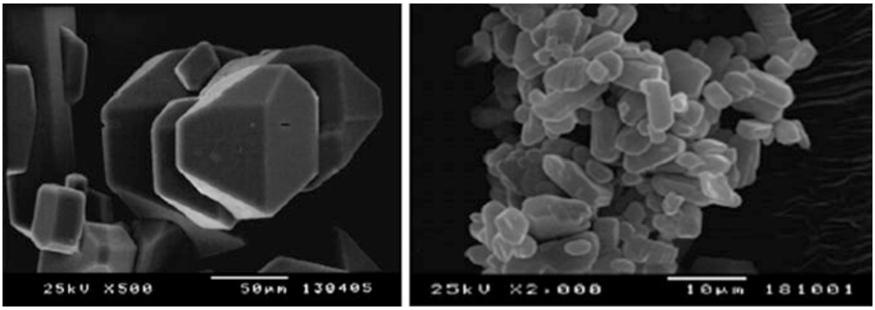

Fig. 3.5 FOX-7 crystals prepared by recrystallization method are shown in two magnification scale [16]

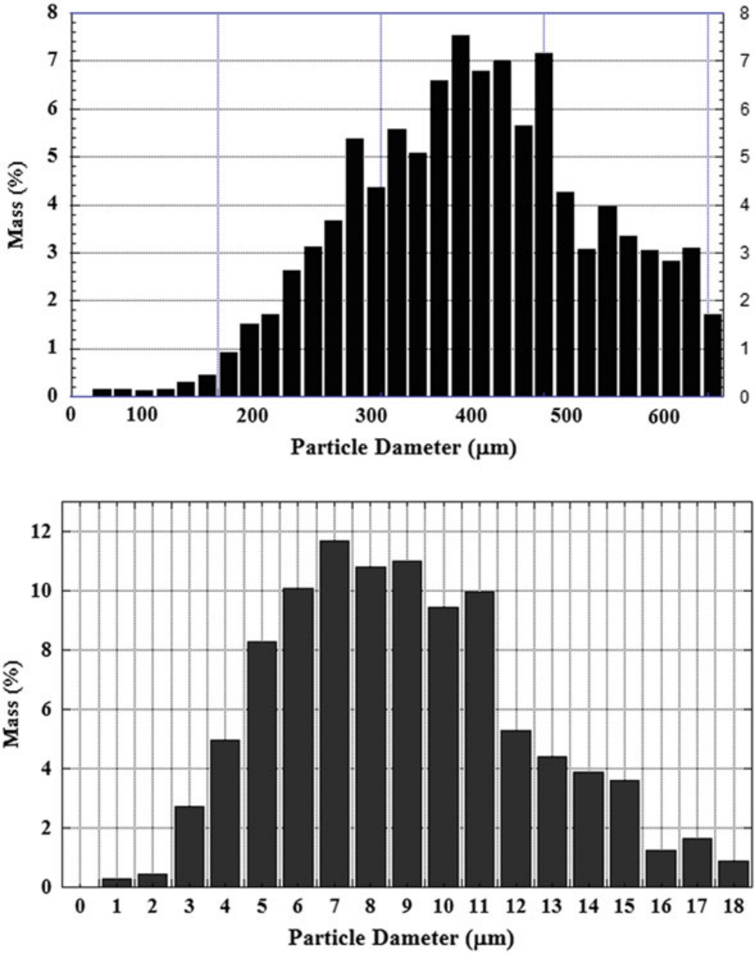

Fig. 3.6 Particle size distribution of FOX-7 crystals following their recrystallization [16]

Table 3.3 Properties of the recrystallized FOX-7 [28]

FOX-7	NMP/water	NMP/water+antisolvent
Mean particle size (µm)	213	273
Span (90/10)	1.445	0.506
Rate of yield	50%	80%
Impact sensitivity (N m)	25	35
Friction sensitivity (N)	240	192

the particle size and is explained in Table 3.5. The SEM micrographs of particles [29] produced under three conditions are given in Fig. 3.7. Less agglomeration or twinning, and more spherical shape were noted.

Table 3.4 Effect of solvent on the recrystallization of FOX-7 from various solvents using 20 kHz ultrasound for production of 3 g materials [29]

Solvent	Particle size (µm)			Morphology
	d (0.1)	d (0.5)	d (0.9)	
NMP/H_2O (50:50)	10	29	66	Sharp blocks
GBL	7	16	30	Rounded plates
DMF	3	11	25	Rounded oblongs
DMF/H_2O (75:25)	12	35	78	Sharp blocks
Acetonitrile	30	59	103	Rounded blocks

Table 3.5 Effect of frequency of ultrasound on FOX-7 recrystallization [29]

Expt.	Method	Particle size (mm)					Morphology
	Application of ultrasound	Scale (g)	Cooling rate (^{o}C/min)	d (0.1)	d (0.5)	d (0.9)	
#1	None	10	0.5	113	278	543	Blocky, jagged
#2	None	100	2.0	86	213	445	Blocky
#3	45 kHz continuous	10	0.5	30	59	105	Rounded, rhombic
#4	45 kHz continuous	10	1.0	–	<601	–	Blocky
#5	45 kHz continuous, with surfactant	10	0.5	45	95	183	Rhombic
#6	45 kHz pulsed at 15 min intervals	100	0.5	48	98	186	Smooth, rhombic
#7	20 kHz continuous	100	0.5	65	105	170	Blocky
#8	20 kHz continuous	100	2.0	27	59	121	Blocky

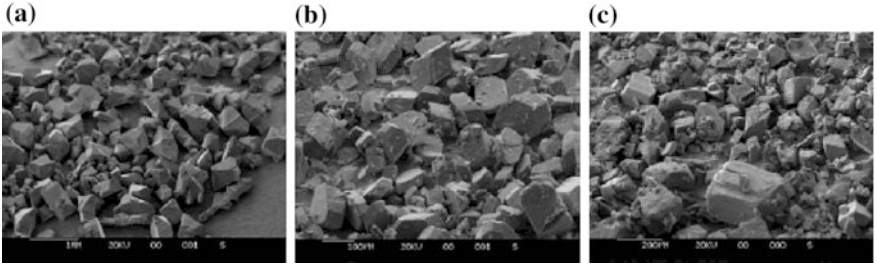

Fig. 3.7 SEM images of FOX-7 (**a**) No ultrasound (**b**) 45 kHz ultrasound (**c**) 20 kHz ultrasound [29]

They [29] synthesized FOX-7 by reacting dioctylmalonate with acetamidine hydrochloride in the solution of sodium methylate, and nitration of obtained 2-methylpyrimidyne 4,6(3H,5H)-dione. Several examples of the crystallization step are provided together with SEM photomicrographs and particle size distribution, and conclude that the best results in terms of particle size and density were obtained using a mixture of DMSO + water as the solvent.

3.4 Structure

3.4.1 Polymorphic Forms

FOX-7 has three polymorphic forms: α, β, and γ. Evers et al. [3] found that the α and β polymorphic transformation in FOX-7 to be first order transition with the crystal symmetry changing from monoclinic to orthorhombic with a decrease in density from 1.86 to 1.82 g cm^{-1} and a $\Delta H \sim 584$ J mol^{-1}. The molecules in the crystal are arranged in a wave-like structure similar to the (0001) basal-plane of graphite, and the crystal structure determined by Evers et al. is shown in Fig. 3.8.

Crawford et al. [2] studied transformation of α and β phases to γ-FOX-7 using a DSC over a temperature range of 380–450 K. They noted that the transformation to γ-form takes place around 435 K, and was found to be stable up to 504 K. There are small differences in physicochemical properties between the α-monoclinic to β-orthorhombic phase compared to the trimorphic γ-phase. The authors prepared γ-FOX-7 by slowly heating β-FOX-7. The authors have also carried out a detailed

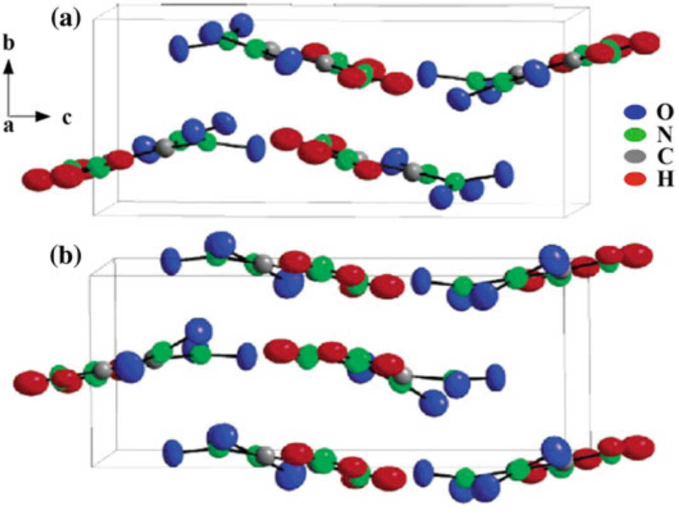

Fig. 3.8 Crystal structure of FOX-7 [3]

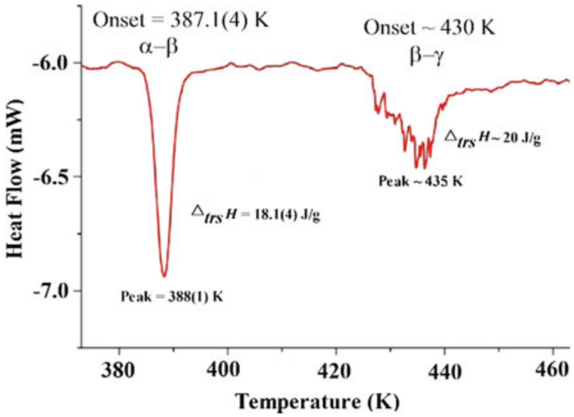

Fig. 3.9 DSC of FOX-7 between 373 and 463 K with endotherms showing the α–β and β–γ phase transitions at 388(1) K and ~435 K [2]

study of the structure of the γ-phase. The paper provides lattice parameters as a function of temperature, DSC over a temperature range of 380–450 K, unit cell volumes for the three phases, and other useful information.

Welch [30] using data from DSC measurements showed that the polymorphic transformations is temperature dependent and can transform from α to β at 388 K and β to γ around 435 K (see Fig. 3.9). In addition, Welch also provides detailed crystallographic data for α, β, and γ phases.

3.4.2 Crystal Structure

The molecules in the crystal are arranged in a wave-like structure similar to the (0001) basal-plane of graphite. This may be due to the extensive intermolecular hydrogen bonding within the layers and ordinary van der Waals interactions between the layers. The wave like structure was determined by Evers et al. [3] and is shown in Fig. 3.8. Further study of the crystal structure was carried out by a number of researchers using x-ray diffraction technique and other spectrometric method such as the Raman spectrometry.

Bemm and Ostmark [31] carried out a general x-ray diffraction studies of FOX-7 to determine the crystal parameters. Although, they did not identify any polymorphic phase for their sample, later Zhao and Liu [32] indicated that the data was for α-phase. These parameters are given in Table 3.6.

Crawford et al. [2] carried out a detailed study of the structure of the β and γ-phase and provided lattice parameters at various temperature. They prepared single crystal of β and γ-FOX-7 to study the diffraction pattern. The results are given in Table 3.7.

Zhao and Liu [32] calculated various lattice parameters for α-phase using the density functional theory (DFT) within local density approximation (LDA) as well as generalized gradient approximation (GGA) to simulate the structural and

Table 3.6 Crystal lattice parameters [31]

$C_2H_4N_4O_4$	Mo Kα radiation
$M_r = 148.09$	$\lambda = 0.71073$ Å
Monoclinic $P2_1/n$	Cell parameters from 3831 reflections
a = 6.941 (1) Å	$\theta = 3.4$-25.9°
b = 6.569 (1) Å	$\mu = 0.181\ \mathrm{mm}^{-1}$
c = 11.315 (2) Å	T = 173 (2) K
$\beta = 90.55$ (2)°	Prismatic
V = 515.9 (1) $Å^3$	0.30 × 0.30 × 0.20 mm
Z = 4	Yellow
$D_1 = 1.907\ \mathrm{Mg\ m}^{-3}$	
D_m not measured	

Table 3.7 Crystallographic data for select explosives

Properties	FOX-7	RDX	HMX	γ-FOX-7
T (K)	403	413	423	200
Phase	β	β	β	γ
Crystal system	Orthorhombic	Orthorhombic	Orthorhombic	Monoclinic
Space group	$P2_12_12_1$	$P2_12_12_1$	$P2_12_12_1$	$P2_1/n$
a (pm)	698.6 (1)[a]	698.6 (1)	698.6 (1)	1335.4 (3)
b (pm)	666.0 (2)	667.1 (2)	668.6 (2)	689.5 (1)
c (pm)	1167.4 (3)	1168.1 (3)	1168.7 (3)	1205.0 (2)
β (°)				111.102 (8)
$V\ (10^6\ \mathrm{pm}^3)$	543.1 (2)	544.4 (2)	545.9 (2)	1035.0 (3)
Z	4	4	4	8
$D_{calc}\ (\mathrm{g\ cm}^{-3})$	1.811 (1)	1.807 (1)	1.802 (1)	1.901 (1)
Reflections				
Measured	2897	2913	2902	3620
Unique	1127	1127	1137	2021
R(σ)	0.0289	0.0296	0.0282	0.0602
$R(F_o)$	0.0592	0.0600	0.0575	0.1118[b]
$R_w(F_o^2)$	0.1784	0.1858	0.1749	0.3387[b]
GOF	1.096	1.118	1.117	1.116
Highest rest electron density[c]	+0.31/−0.24	+0.33/−0.22	+0.28/−0.24	0.63/−0.58

Obtained from single crystal investigations [2]

[a] Experimental uncertainties in parentheses

[b] The high R-values result from the two phase transitions performed on the single crystal, first α/β at 390 K, second β/γ at 440 K and then quenching to 200 K

[c] In $e/10^6\ \mathrm{pm}^3$

Table 3.8 Attice parameters and unit cell volume of α-phase crystalline FOX-7 [32]

	a (Å)	b (Å)	c (Å)	α (°)	β (°)	γ (°)	V (Å)^3
Exp. [3]	6.94	6.56	11.31	90.0	90.55	90.0	515.9
Exp. [4]	6.94	6.64	11.34	90.0	90.61	90.0	522.3
Exp. [8]	6.93	6.62	11.23	90.0	89.48	90.0	514.6
Exp. [9]	6.92	6.55	11.27	90.0	90.06	90.0	511.2
LDA	6.74	6.18	11.05	90.0	90.69	90.0	460.5
GGA	7.19	7.54	11.49	90.0	91.96	90.0	623.0
Mean	6.96	6.83	11.27	90.0	91.32	90.0	535

Table 3.9 Selected bond lengths (nm) and bond angle (°) [33] Bond length

Bond length					
C(1)—C(2)	0.1492(2)	N(4)—C(2)	0.1376(2)	O(4)—N(4)	0.12525(18)
N(1)—C(1)	0.1342(2)	O(1)—N(3)	0.12586(19)	N(5)—C(3)	0.1315(2)
N(2)—C(1)	0.1277(2)	O(2)—N(3)	0.12469(18)	N(6)—C(3)	0.1325(2)
N(3)—C(2)	0.1360(2)	O(3)—N(4)	0.12375(19)	N(7)—C(3)	0.1321(2)
Bond angle					
N(1)–C(1)–N(2)	121.1(2)	N(3)–C(2)–N(4)	121.86(16)	O(4)–N(4)–C(2)	116.17(15)
N(1)–C(1)–C(2)	115.21(18)	O(1)–N(3)–C(2)	116.47(15)	O(3)–N(4)–O(4)	120.28(15)
N(2)–C(1)–C(2)	123.61(18)	O(2)–N(3)–C(2)	123.23(15)	N(5)–C(3)–N(6)	121.4(2)
N(3)–C(2)–C(1)	119.87(16)	O(1)–N(3)–O(2)	120.30(15)	N(5)–C(3)–N(7)	119.87(19)
N(4)–C(2)–C(1)	118.20(16)	O(3)–N(4)–C(2)	123.55(15)	N(7)–C(3)–N(6)	118.75(19)

electronic properties of FOX-7 crystal under high-pressure up to 4 GPa. Their calculated lattice parameter data are shown in Table 3.8 along with the experimental data from four researchers. A good agreement of the experimental data with the theory was reported.

Xu et al. [33] used B3LYP, HF and MP2 methods to elucidate the crystal structure. They reported the bond lengths and bond angles between various atoms within the structure. This information is useful in determining the reactivity of FOX-7. For example, FOX-7 can react with some nucleophiles and strong alkalis to obtain new energetic compounds. The bond lengths and bond angles between various atoms within the structure are given in Table 3.9.

3.5 Thermophysical Data

A limited number of experimental data for fundamental properties of FOX-7 are available in the literature. This may be due to the difficulties in conducting experiments with FOX-7 due its sensitivity and decomposition characteristics.

The experimental data for fundamental properties are given in Table 3.10. The lack of experimental data due to difficulties associated with conducting experiments led several researchers to use various thermodynamic model and approaches to estimate these properties. Dewey [18] used EPI (Estimation Program Interface) Suite^{TM} to estimate various fundamental properties of FOX-7. EPI (Estimation Program Interface) Suite^{TM} is a publicly available Windows$^{®}$ based suite of physical/chemical property and environmental fate estimation models developed by the US Environmental Protection Agency (EPA). EPI Suite is comprised of individual chemical/physical estimating modules; each designed to estimate a specific physical or chemical property of a given structure. The estimated values of various properties of FOX-7 by the EPI suite are given in Table 3.11.

Table 3.10 Values for some fundamental properties of FOX-7 [34]

Bioconcentration factor	1.0
Boiling point (°C)	194.6 ± 40.0
Density (g/cm^3)	1.688 ± 0.06 @ 298.15 K and 760 torr
Enthalpy of vaporization (kJ/mol)	43.08 ± 3.0
Flash point (°C)	71.5 ± 27.3
K_{oc}	1.0 @ pH = 1
Vapor pressure	0.438 torr @ 298.15 K

Table 3.11 Summary of FOX-7 literature values and EPI Suite input and output [18, 34]

Molecular formula	$C_2H_4N_4O_4$ Molecular weight (g/mol)		148.08
	Literature value	SMILES only	SMILES and MP
Physical state			
Melting point (°C)	205.0	83.37	83.37
Boiling point (°C)	NA	287.51	287.51
Solubility, Water (mg/L)	NA	1.0^{6}	1.0^{6}
Partion coefficients			
Log K_{ow}	NA	−2.86	−2.86
K_{oc}	NA	30.6	30.6
Vapor Pr. (mm Hg, 25 °C)	NA	0.00104	4.70^{-5}
Henry's Law Constant (atm-m^3/mole)	NA	1.43^{-12}	1.43^{-12}
Half-life in Air (hr)	NA	5.85	5.85
Half-life in Water (hr)	NA	360	360
Half-life in Soil (hr)	NA	360	360
Half-life in Sediment (hr)	NA	1440	1440
Daphnid LC_{50} (mg/L)	NA	2073.6	2073.6
Density (g/cm^3)	1.86	1.87 [6]	
Enthalpy of formation (kcal/mole)	−32 [6]		

Kim et al. [35] proposed a simplified model based on molecular surface electrostatic potentials to predict the densities of high energetic molecules in the solid state, and compared with experimental values. Their value varied from 1.752 to 1.803 g cm^{-3} depending on the regression technique used, where as the experimental value is 1.883 g cm^{-3} [6].

Xu et al. [36] determined specific heat of γ-FOX-7 both experimentally and theoretically. A Micro-DSCIII apparatus (SETARAM, France) was used for continuous measurement of the specific heat. They used 442.37 mg of sample and a heating rate of 0.15 °C min^{-1} from 10 to 80 °C. The heat capacity was calculated from the following expression on a continuous basis:

$$C_p = \frac{A_s - A_b}{m \times \beta}$$

where C_p is the specific heat capacity, A_s and A_b are the heat flows of the sample and blank, m_s is the amount of the sample, and β is the heating rate.

For theoretical determination of the specific heat, they first obtained the optimized parameters for the crystal structure using a software and obtained the frequencies at various temperatures. Then various thermodynamic properties were calculated based on the statistical thermodynamic methods. Their measured specific heat and calculated values are presented in Table 3.12.

As can be seen from the table, the calculated values are always lower than the experimental values by 18.36–21.49%, which they attributed to the consideration of only gas-phase molecule in the calculation process. The authors stated that molecules at the solid phase should be considered for better estimation of the specific heats.

Table 3.12 Experimental and theoretical specific heat, Units: J mol^{-1} K^{-1} [36]

Temperature (K)	Specific heat	
	Experimental	Theoretical
283.0	266.6	217.7
288.0	272.0	220.1
293.0	277.1	222.5
298.0	281.9	224.9
303.0	286.4	227.4
308.0	290.7	229.8
313.0	294.7	232.2
318.0	298.4	234.6
323.0	301.8	237.0
328.0	305.0	239.5
333.0	307.9	241.9
338.0	310.5	244.3
343.0	312.8	246.7
348.0	314.9	249.1
353.0	316.7	251.5

They also fitted the experimental data to the following temperature dependent expression:

$$C_p = -2.3346 + 2.0290 \times 10^{-2}T - 2.6476 \times 10^{-5}T^2, \quad (283K \langle T \langle 353K)$$

where C_p is in $J\,g^{-1}K^{-1}$.

Zerilli and Kuklja [37] carried out Ab Initio calculations to estimate various thermodynamic properties of FOX-7. They calculated a complete equation of state from first principles in the temperature range of 0–400 K and for specific volumes from 61 to 83 cm^3/mol. The properties calculated by them included pressure-volume data, heat capacity as a function of temperature at different specific volumes, and bulk modulus. They compared the pressure-volume data at 300 K with the experimental data reported by Peiris et al. [38] Figs. 3.10, 3.11, 3.12, 3.13 and 3.14 show various computed values.

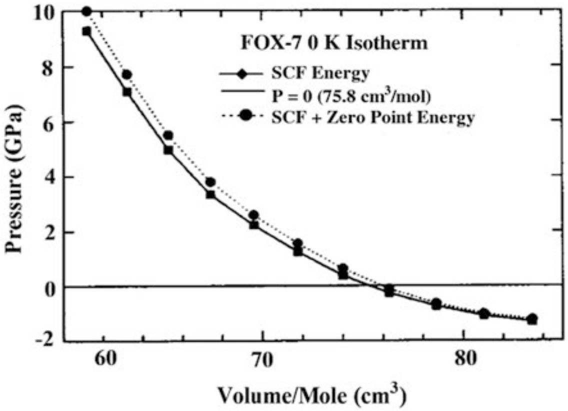

Fig. 3.10 Pressure-volume relation at 0 K calculated with HartreeFockself-consistent field energy including vibrational. Mode zero point energy [37]

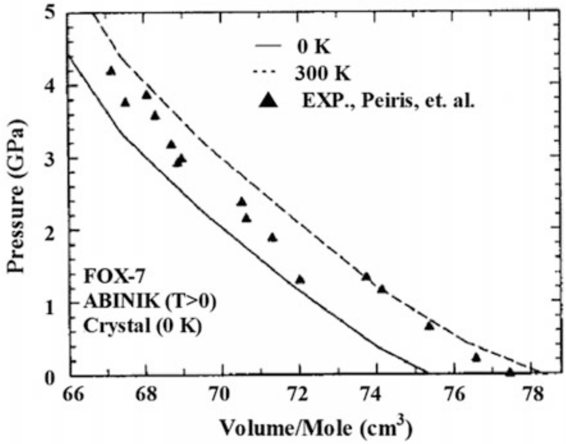

Fig. 3.11 Calculated 300 K isotherm compared to experimental data of Peiris et al. [37]

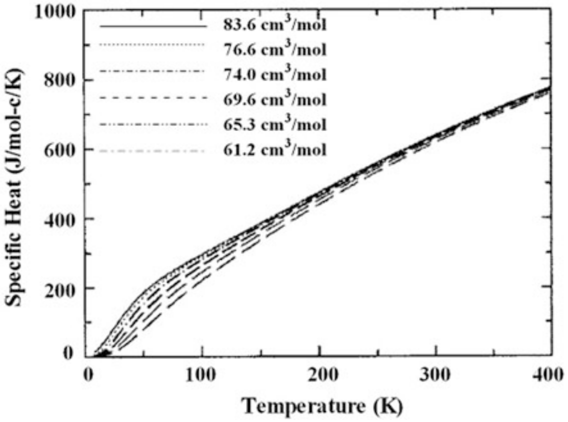

Fig. 3.12 Calculated specific heat as a function of temperature for different cell volumes [37]

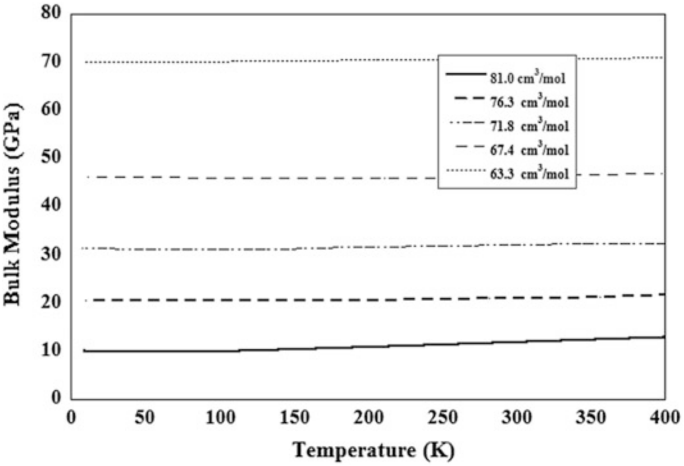

Fig. 3.13 Calculated bulk modulus as function of temperature for different cell volumes [37]

Charge density calculations have been carried out by Meents et al. [39, 40] from single crystal diffraction studies. The results of comparison of theoretical and experimental electrostatic potentials do not show any correlation of electron density with impact sensitivities.

Sun et al. [41] used the density functional theory to calculate various fundamental properties of FOX-7. These included specific heats, entropies, and also applied correction to enthalpies. The interaction between FOX-7 and water was also evaluated to study the dimmers of FOX-7. Table 3.13 lists the thermodynamic properties of FOX-7 calculated by Sun et al.

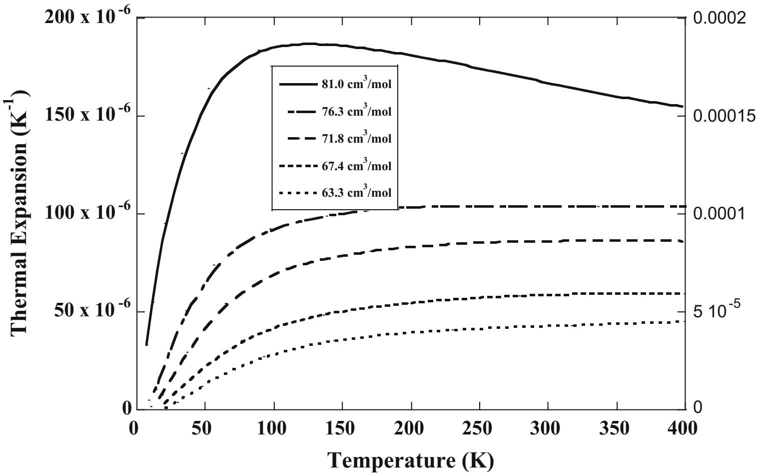

Fig. 3.14 Calculated thermal expansion for different cell volumes [37]

Table 3.13 Thermodynamic properties [41]

Temp (K)	C_p^o	S_T^o (J/mol/K)	H_T^o (kJ/mol)
200	114.57	345.50	14.15
298.15	152.46	398.55	27.32
500	208.92	491.86	64.25
700	242.90	568.02	109.71

3.5.1 Solubility of FOX-7

The characteristics of FOX-7 synthesized by above methods depend on the crystallization step. Solvents and solubility of FOX-7 in these solvents are an important factor on the selection of the solvent. Fuhr and Mikonsaari [28] studied the crystallization of FOX-7 using n-methyl pyrrolidone (NMP), dimethylformamid (DMF) and mixtures of NMP/water [28, 29]. The solubility data of FOX-7 in these solvents are shown in Fig. 3.15.

The crystallization process is temperature dependent. The temperature should be maintained constant during the crystallization process to obtain uniform shape and size of the particles. The partial molal enthalpies of FOX-7 in DMSO at 298.15 K, kinetics of dissolution, and other thermodynamic properties have been measured and discussed by Xing et al. [42]. They noted that the dissolution of FOX-7 in DMSO is an exothermic process. Therefore, the enthalpy change during the dissolution process should be known. They provided the partial molal enthalpies of FOX-7 in DMSO at 298.15 K and kinetics of dissolution. The partial molal enthalpies are given in Table 3.14.

Xing et al. [42] suggested an empirical expression for calculation of enthalpies of dissolution and is given below:

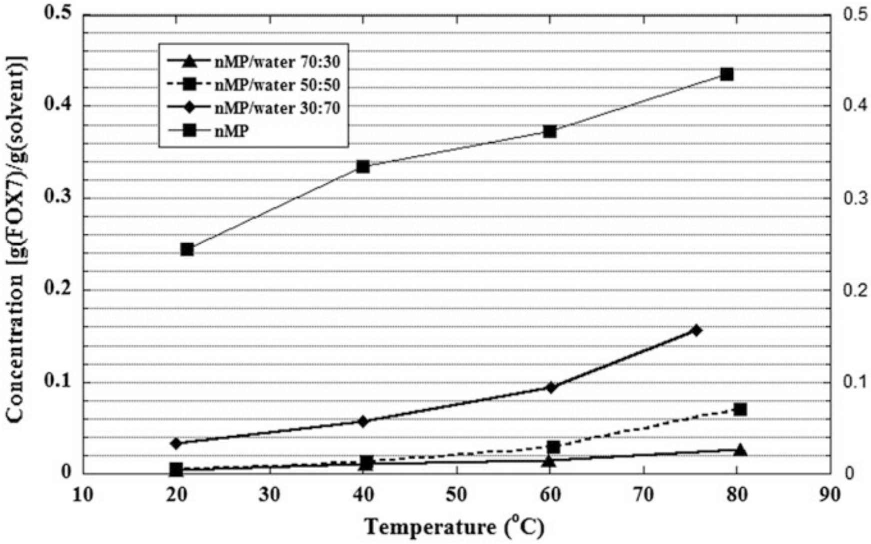

Fig. 3.15 Solubility of FOX-7 in NMP and NMP-water mixtures [29]

Table 3.14 The enthalpies of dissolution of FOX-7 in DMSO [42]

$b \times 10^2$ (mol/kg)	$b^{1/2}$	$\Delta_{diss}H$ (kJ/mol)		$\Delta_{diss}\ H_{partial}$ (kJ/mol)	$\Delta_{diss}\ H_{apparent}$ (kJ/mol)
		Found	Calculated		
2.14	0.146	−8.64	−8.58	−18.04	−16.48
2.50	0.158	−8.81	−8.80	−17.28	−16.66
3.00	0.173	−8.83	−8.79	−15.71	−16.60
3.18	0.178	−8.73	−8.72	−15.04	−16.56
3.68	0.192	−8.38	−8.37	−12.98	−16.22

$$\Delta_{\text{diss}}H = 8.2146 - 207.343\,b^{1/2} + 629.7194\,b$$

where b represents the concentration of the solution after FOX-7 dissolved in DMSO.

3.6 Detection

There appears to be very little attention paid to the detection of FOX-7. From the homeland security point of view, it will be necessary to detect it at very low concentrations. Majano et al. [43] studied detection of FOX-7 by stabilizing it in the pores of MFI-type nanocrystals. The presence of FOX-7 was determined using XRD, IR, and Raman spectroscopy. Although this method may be useful in laboratory setting, the detection of field sample may not be feasible. The immobilization of field samples into the pores of MFI-type nanocrystals may not be feasible.

Ottis and Benova [44] applied UV spectroscopy and HPLC for analysis of FOX-7 determination of FOX-7 and its precursors used for its synthesis. All experiments were conducted using acetone solutions with a concentration of 0.3 g/L, and 10 µL samples of the solutions were applied on the start line of chromatoplates (band width 4 mm). Normal and reversed phase systems were used. They were able to separate various compounds using a two-step elution process, which were: Step 1: methanol/dichloromethane (3:2 v/v), range of elution–2 cm, and Step 2: carbon tetrachloride/acetonitrile (3:2 v/v), range of elution–6 cm. The chromatograph is shown in Fig. 3.16. They also developed a calibration curve for the quantification purpose.

Dorsett [45] studied fragmentation of FOX-7 in an electron impact mass spectrometer (EIMS). EIMS involves ionizing molecules in a sample by bombarding with electron. Each molecule exhibits its distinct mass/charge (*m*/*z*) ratio of the resulting fragments. The known fragmentation pattern may be used to identify

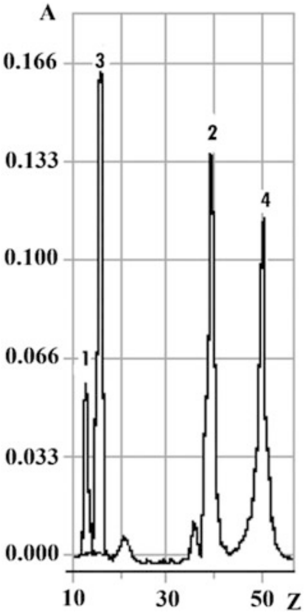

Fig. 3.16 A chromatograph of a mixture of compounds containing FOX-7 Chromatogram of the analytes: (*1*) 2-methylpyrimidine-4,6(1H,5H)-dione; (*2*) 2-dinitromethylene-5,5-dinitropyrimidine-4,6(1H,3H)-dione; (*3*) 2-methyl-5-nitropyrimidine-4,6(1H,5H)-dione; (*4*) FOX-7; A, absorbance [a.u.]; z, range of elution [mm] [44]

Table 3.15 EI-MS spectra for FOX-7 subjected to 20 and 70 eV electron impact energies [45]

M/z	20 eV peak int (%)	70 eV peak int (%)	Possible species
18	n/a	20.0	H_2O
27	n/a	4.9	HCN
28	n/a	33.2	CO, N_2
29	n/a	6.0	
30	n/a	32.5	NO
41	–	4.9	
42	3.5	16.2	
43	13.3	100.0	$C(NH)(NH_2)$, CNO
44	100.0	80.0	$C(NH_2)_3$, CO_2
45	37.3	1.9	
46	0.7	7.9	NO_2
53	–	12.8	
54	0.6	3.4	
55	–	9.1	
60	24.1	<0.5	
69	–	33.2	
70	–	6.4	
72	–	9.1	
86	–	21.9	
88	25.2	<0.5	$C(NO)(NO_2)$
89	1.0	<0.5	
130	–	<0.2	
148	21.2	69.4	FOX-7
149	1.5	12.5	FOX-7 + H

1 eV = 1.602×10^{-19} J = 23.06 kcal/mol

FOX-7 in a sample. The fragmentation of FOX-7 depends on the electron beam strength. The major m/e peaks observed in 70 and 20 eV spectra are given in Table 3.15.

3.7 Decomposition and Destruction

As the temperature is increased above 200 °C, decomposition, without melting, begins to occur. The thermal behavior of FOX-7 at temperatures below 200 °C has already been described above.

Sinditskii et al. [46] carried out thermal decomposition studies and found that the burning rate of FOX-7 is slower than RDX. The initial stages of decomposition, revealed that FOX-7 to be more thermally stable than RDX.

The authors suggested that the decomposition of FOX-7 depends on its purity and also on the presence of crystalline phases in the sample. They noted that when a sample of FOX-7 is consisted of two phases, part crystalline and part amorphous, the amorphous phase decomposes first as indicated by the first DSC peak leaving the original crystalline part. The relative amounts of these two phases are dependent on the synthesis process conditions.

The products formed during decomposition of FOX-7 have been studied by a number of researchers using FTIR (Fourier Transform Infrared Spectroscopy) and laser-induced breakdown spectroscopy (LIBS). The FTIR analysis showed the presence of CO_2, HCN, N_2O, NO_2, HOCN, H_2O and NO during the first stage of decomposition as suggested by selected ion flow tube mass spectrometry (SIFT-MS), while HNO_2 and HCOOH are produced in the second decomposition. The apparent activation energies for the two steps are reported as 238.3 and 322.4 kJ mol^{-1}, respectively.

Civis et al. [47] used a combination of laser-induced breakdown spectroscopy (LIBS) and SIFT-MS to study the decomposition of γ-FOX-7. They observed several atomic transitions and molecular electronic bands in the LIBS emission spectra of the FOX-7 during decomposition. Based on the decomposition products, they suggested a decomposition path, which is shown in Fig. 3.17.

Civis et al. [47] identified directly H_2O, NH_3, HCN from their experimental results (HNC isomer could not be distinguished by SIFT-MS), and NO, CO, and HONO stable molecules from theoretical calculation. CO molecules cannot be detected by SIFT-MS. They also reported that production of two molecules of N_2, CO, and H_2O from the FOX-7 molecule is exothermic (117 kcal/mol). In addition, they also observed C_2H_5OH in a relatively high concentration (several parts per million. The formation mechanism of ethanol is proposed in Scheme 1 as a reaction path in which the structure (D) does not fragment directly to CO, HNC, and NH_2 but where only the C–N bonds dissociate (Fig. 3.18).

3.8 Spectroscopy

The understanding of the spectroscopic properties of FOX-7 is important for the analysis and development of detection systems. Dorsett [45] used B3LYP functional in conjunction with Dunning's correlation consistent basis sets cc-pVDZ and aug-cc-pVDZ3 for calculating geometric parameters and compared with available experimental data. Besides geometric parameters and vibrational frequencies, the author also evaluated configurational energies and enthalpies of various reaction species and are given in Tables 3.16 and 3.17.

Welch [30] investigated the spectroscopic behavior of FOX-7 using DSC, temperature resolved Raman spectroscopy, powder and single crystal X-ray diffraction studies. The DSC data agreed well with the literature data. Raman

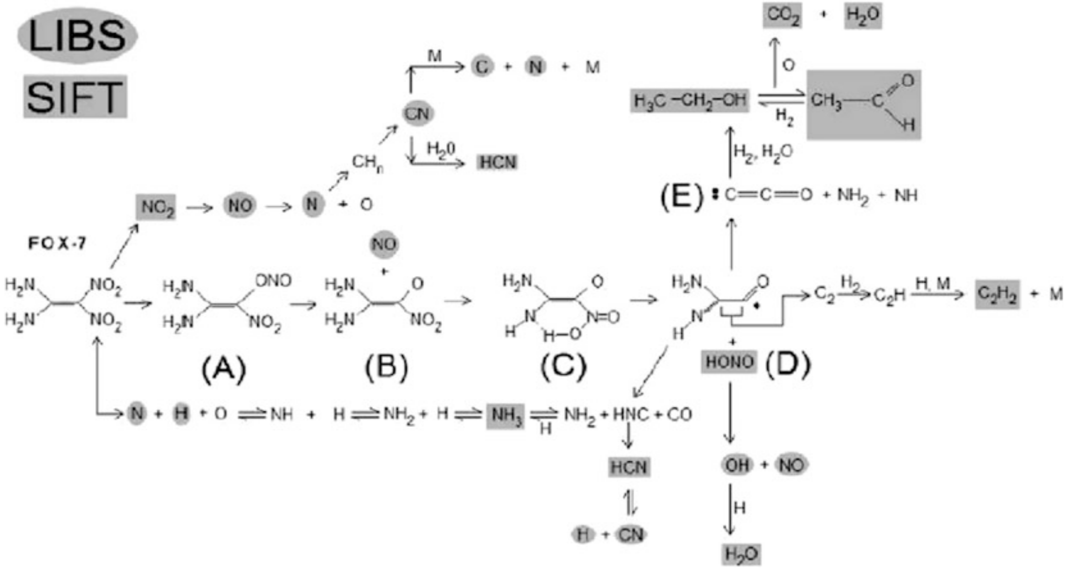

Fig. 3.17 The thermal decomposition path for FOX-7 [47]

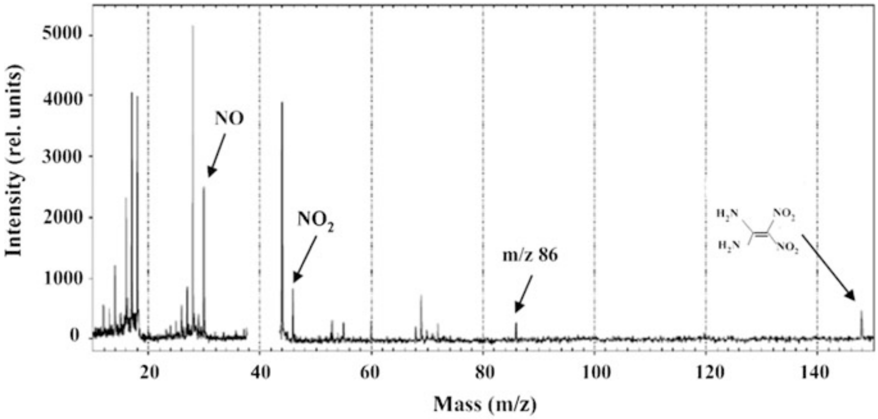

Fig. 3.18 CO$_2$-Laser induced thermal decomposition mass spectrum FOX-7, 100 W 80 MS (The region m/z 38 and 42 is entirely dominated by solvent peaks and has therefore been removed) [47]

Table 3.16 Selected geometric parameters for FOX-7 (Å, degrees) [45]

Parameter	Expt. [13]	Calc.	Parameter	Expt. [13]	Calc.
C=C	1.456	1.430	N–H(t)	0.88, 0.87	1.008
C–NH$_2$	1.319, 1.325	1.344	N–H(s)	0.84	1.018
C–NO$_2$	1.399, 1.426	1.433	N–O(t)	1.252, 1.242	1.255
O(s)–H(s)	1.97, 2.03	1.790	N–O(s)	1.249, 1.242	1.222
<H$_2$N–C–NH$_2$	118.4	117.7	<O–N–O	120.9, 121.0	122.4
<O$_2$N–C–NO$_2$	116.3	116.9	<H(t)–N–C	121.0, 121.1	120.3
<H$_2$N–C=C	120.7, 120.8	121.1	<H(s)–N–C	119.8, 121.9	117.0
<O$_2$N–C=C	119.8, 123.9	121.6	<O(s)–N–C	118.6, 118.9	117.9
<H–N–H	118.3, 118.1	122.2	<O(t)–N–C	120.1, 120.4	119.7
<H$_2$N–C=C–NO$_2$	172.9, 177.8	169.2			
<H(t)–N–C–C	−179.6, −178.3	−170.4	<O(t)–N–C–C	171.0,143.6	156.0
<H(s)–N–C–C	0.5, 10.1	2.1	<O(s)–N–C–C	−5.8, −34.3	−21.7

T terminal bond (bond nearly parallel to C=C axis), *s* side bond

spectra of α, β, and γ FOX-7 are shown in Figs. 3.19 and 3.20. Detailed explanation of the spectra and the transitions that occur from one phase to another have been discussed by Welch [30].

Majano et al. [43] have also contributed to IR, Raman, NMR and XRD of FOX-7 in MFI-type nanocrystalline zeolites.

Table 3.17 Vibrational normal modes [45]

Freq	Type	Freq	Type
61	C=C stretch + NO_2 scissor	806	NO_2–C–NO_2 scissor + N–O stretch
88	NH_2–C–NH_2 rock + N–H(t) stretch	870	N–O(s) stretch + N–O(t) oop rock
114	NH_2–C–NH_2 rock + N–H(t) stretch	1068	C–NH_2 torsion + N–H(s) stretch
212	C=C stretch + N–H(t) stretch	1083	C–NH_2 torsion + N–H(s) stretch
266	N–H(t) stretch	1149	NH_2–C–NH_2 bend
296	C–N stretch + N–H(t) stretch	1214	C–NH_2 torsion + C–NO_2 stretch
335	C–N stretch	1272	C–NO_2 bend
376	N–H(t) stretch	1341	C–NO_2 bend + N–H(t) oop rock
387	N–H(t) stretch	1481	N–H(s) stretch + NH_2–C–NH_2 bend
442	NH_2 torsion + N–H stretch	1519	C–NH_2 stretch + N–H oop rock
465	C=C stretch + NO_2–C–NO_2 scissor	1565	N–H(s) stretch + C–NH_2 bend
471	C=C torsion	1602	C–N stretch + NO_2 stretch
610	C–NH_2 torsion + C–N stretch	1624	NH_2–C–NH_2 bend + C–NH_2 bend
643	N–H(s) stretch + NH(s) rock	1632	C–NH_2 bend
690	C=C stretch + NH_2–C–NH_2 scissor	3446	C–NH_2 bend + C–NH_2 rock
751	NO_2–C–NO_2 rock + N–O stretch	3460	C–NH_2 bend + C–NH_2 rock
751	N–H(s) stretch + NH(s) rock	3681	N–H(t) rock
771	C=C stretch + NO_2–C–NO_2 scissor	3683	N–H(t) rock

Frequencies in wavenumbers (cm^{-1})

t terminal bond; *s* side bond; *oop* out of plane

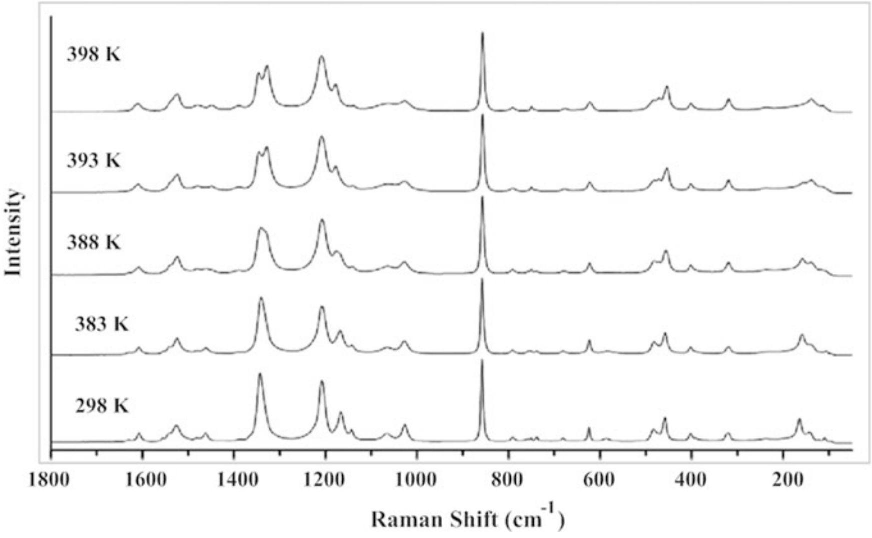

Fig. 3.19 Raman spectra of α- and β-FOX-7 over the temperature range 298–398 K [29]

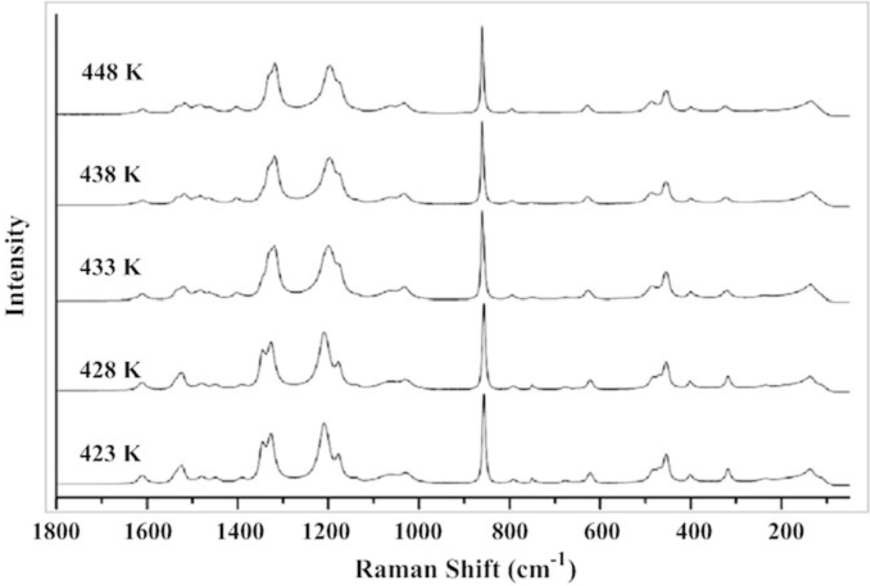

Fig. 3.20 Raman spectra of β- and γ-FOX-7 over the temperature range 423–448 K [29]

3.9 Detonation Properties

Detonation properties of FOX-7 measured by various researchers and their comparison with other explosives are complied in Table 3.18. Although FOX-7 has the detonation pressure and velocity similar to that of RDX, it is much less sensitive as indicated by the drop weight test and friction test. For a better understanding of the detonation characteristics of FOX-7, its detonation properties are compared with other explosives in Table 3.19. Anniyappan et al. [5] also compared the detonation properties of FOX-7 with several other explosives and the results are given in the same Table 3.19. They included the thermal stability properties and compared with RDX, TEX, and TATB. Although it is less stable thatn TEX and TATB, but it is more stable compared to RDX. Latypov et al. [4], besides synthesizing DADE, carried out sensitivity tests and compared them with RDX. Their results are shown in Table 3.18.

Table 3.18 Comparison of FOX-7 with RDX

	RDX	DADE
Dropweight test (cm)	38	126
Friction test (N)	120	>350
Detonation pressure[a] (GPa)	34.63	33.96
Detonation velocity[a] (m/s)	8869	8930

[a] Calculated values

Table 3.19 Explosive properties of FOX-7 in comparison with RDX, TEX and TATB

Properties	FOX-7	RDX	TEX	TATB
Detonation velocity (m/s)[a]	9090	8800	8749	8108
Detonation pressure (GPa)[a]	36.6	34.7	36.5	31.1
Drop weight test (cm)	126	38	177	170
Friction test (kg)	>36	12	>36	>36
Thermal stability (°C)	240	215	285	287

[a]Calculated values by Cheetah v 2.0

Table 3.20 Sensitivity test data for three batches of FOX-7 synthesized by two different research group and its comparison with RDX data [49]

Test	FOX-7 (Bofors 20017011)[c]	FOX-7 (Bofors 20017002)[d]	FOX-7 (DSTO)[e]	RDX
Rotter impact (F of I)	100	100	110–140	80
BAM friction (N)	240	240	168–288	~120
ESD[a], Ignition (J)	4.5	4.5	4.5	4.5
ESD[a], No Ignition (J)	0.45	0.45	0.45	0.45
VTS[b] (mL/g)	0.28	–	<0.1	<0.1
Temp of Ignition (°C)	217	–	226	223
Beckford fuse	Ignition	–	Fails to ignition	Fails to ignition
Train test	Ignition	–	Ignition	Ignition

[a]Electrostatic discharge
[b]Vacuum thermal stability (perfumed at 100 °C for 48 h)
[c]Bofors, not recrystallized
[d]Bofors, recrystallized
[e]Synthesizes at DSTO, not recrystallized

Trzcinski et al. [16] have measured detonation velocity, detonation pressure, and calorimetric heat of explosion as well as the accelerating ability.

Theoretical study of Sorescu et al. [48] reveals that Fox-7 can be adsorbed on aluminum and oxidized aluminum surfaces. The adsorption of FOX-7 on aluminum surface provides an energy of 69.5 kcal/mol compared to the aluminum surface.

Chen et al. [49] studied the sensitivity of FOX-7 using DSC-TG combination, and found the friction sensitivity to be 68% or less and impact sensitivity to be more than 25 J (Table 3.20).

Charge density calculations have been carried out by Meents et al. [39] from single crystal diffraction studies. The results of comparison of theoretical and experimental electrostatic potentials do not show any correlation of electron density with impact sensitivities.

3.10 Cylinder Test

The cylinder test was conducted by several researchers and their findings are discussed below. Karlsson et al. [1] used a copper cylinder of 300 mm in length and 30.2 mm in diameter, and a shell thickness of 2.52 mm. The charge was FOX-7 containing 1.5 w% wax and had a density of 1.756 g/cm^3. Their experimental cylinder is shown in Fig. 3.21. The detonation velocity was estimated to 8.335 ± 0.025 mm/µs. They used a HI-Dyna2d modeling for comparison with the experimentally derived cylinder wall motion. The calculated and experimental values are presented in Fig. 3.22. Also, the of detonation velocity calculated using CHETTA, BKWC, gave a velocity of 8.266 mm/µs, which is in good agreement with the experimental value.

Trzcinski et al. [16] estimated t.he detonation energy from the cylinder test data. They used a cylinder of same dimension as Karlsson et al. [1] to conduct the test. The test results are given in Fig. 3.23. They recorded a detonation velocity of 8325 ± 50 m/s, Gurney energy of 3540 ± 100 j/g, and Gurney velocity of 2660 ± 40 m/s for FOX-7.

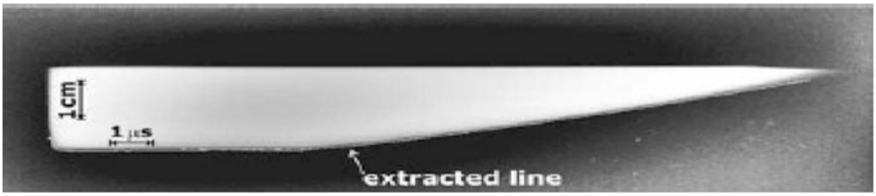

Fig. 3.21 Radial expansion of the cylinder wall during cylinder test of FOX-7 [1]

Fig. 3.22 Radial velocity along the wall during the cylinder test of FOX-7 [1]

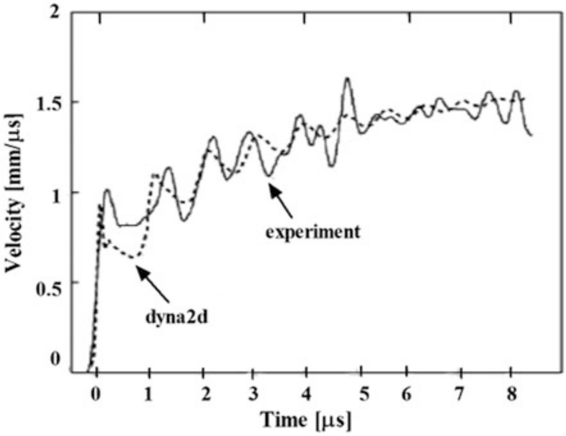

The data from the cylinder test was used to determine the detonation pressure using the Jones, Wilkins and Lee equation of the isentrope. The equation can be written as:

$$p = Ae^{-R_1 V} + Be^{-R_2 V} + CV^{(-1-\varpi)}$$

where A, B, C, R_1, R_1 and ω are constants for a given explosive, $V = \mathrm{v}/\mathrm{v}_0$, $\mathrm{v} = 1/\rho_0$. The constants for the JWL equation are given in Table 3.21.

A comparison among various computational methods is also provided by them. The computational methods included the JWL isentrope calculation, the CHEETAH(BKWC) code, and a constant isentrope (g = 3.22). The comparison is shown in Fig. 3.24. The detonation parameters provided by Trzcinski et al. [16] are given in Table 3.22.

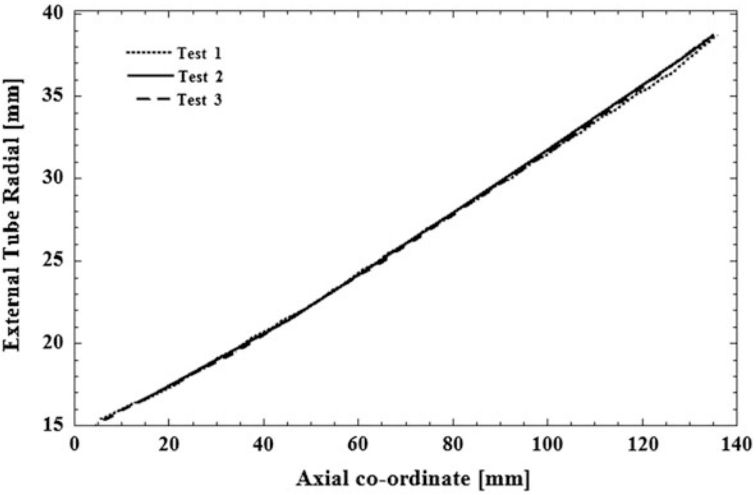

Fig. 3.23 Radial displacement of the external surface of the tube versus an axial co-ordinate [16]

Table 3.21 JWL isentrope of DADNE [50]

Explosive characteristics	JWL isentrope constants
ρ_0 = 1780 kg/m^3	A = 1414.339 GPa
D = 8325 m/s	B = 21.6637 GPa
γ_{CJ} = 3.35	C = 1.23412 GPa
p_{CJ} = 28.4 GPa	R_1 = 5.54
E_0 = 8.9 GPa	R_2 = 1.51
	ω = 0.32

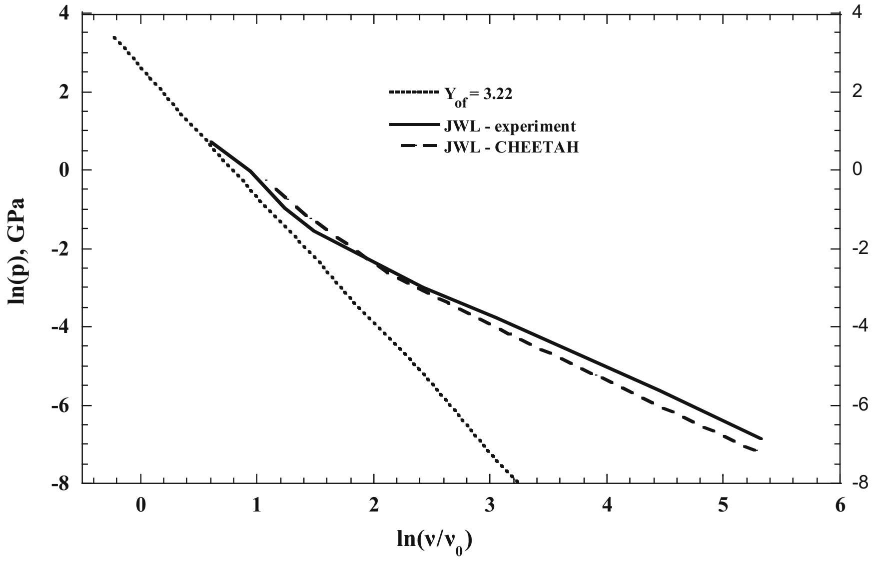

Fig. 3.24 Constant γ and JWL isentropes for detonation products of DADE [16]

Table 3.22 Experimental and calculated detonation properties of DADE [16]

Test no	*D* (m/s)	γ	P_{CI}	*Dt*	γ_i	$P_{CJ,t}$
1	8405	3.31	29.2	8453	3.335	29.34
2	8375	3.39	28.4			

Table 3.23 CHEETAH QRX080 JWL constants [50]

JWL parameter	Value
A (GPa)	545.35
B (GPa)	5.97
C (GPa)	1.08
R_1	4.09
R_2	1.06
ω	0.3143

Cullis and Townsley [50] used CHEETAH to estimate the JWL parameters for a FOX-7 formulation that contained 95% FOX-7 and 5% binder (Table 3.23).

The detonation velocity predicted by CHEETAH was 8.434 km/s, which was greater than the average value obtained experimentally, which was 8.28 km/s.

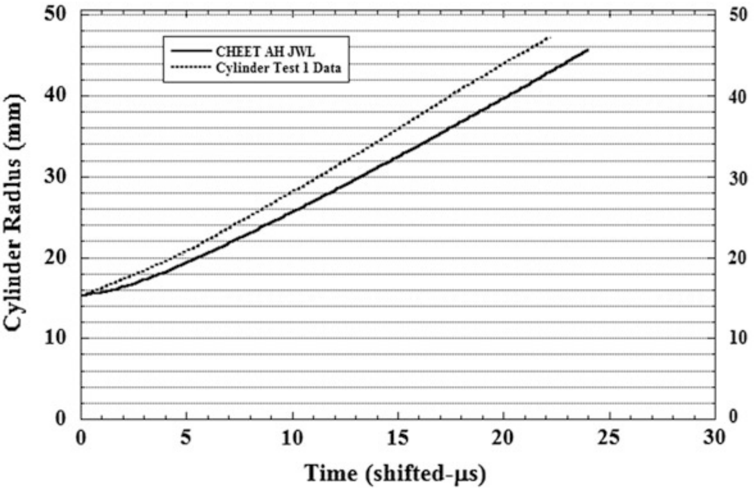

Fig. 3.25 Cylinder wall expansion predicted from CHEETA for QRX080 using JWL equation [50]

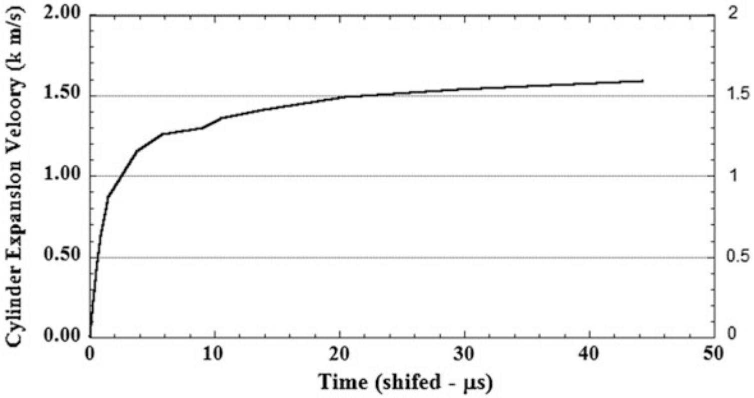

Fig. 3.26 Cylinder wall velocity predicted by using CHEETAH with JWL equation [50]

Using the CHEETAH QRX080 JWL constants and modeling the cylinder test using the DYNA2D hydrocode gave the predictions for the cylinder wall motion in terms of radial expansion with time (see Fig. 3.25) and cylinder wall velocity (see Fig. 3.26).

3.11 FOX-7 Formulation

A mixture of FOX-7 with another explosive can enhance the detonation properties of the mixture. A number of researchers have carried the formulation of FOX-7 and noted that some properties can be changed significantly. Karlsson et al. [1] have carried out detonation and sensitivity measurements of their formulation of FOX-7 with a composite called Lis-2. The impact and friction sensitivity of this formulation and its components is summarized in Table 3.24. A plastic bound explosive based on FOX-7 and an energetic binder was prepared and designated as LIS-2. The energetic binder consisted of polyGLYN, Bu-NENA and H12MDI. Table 3.25 shows the composition of the formulation. This formulation showed no friction sensitivity but it was more sensitive to impact than its respective components. The formulation did not propagate to detonation during a detonation test in steel tubes with a diameter of 25 mm, however the formulation did react violently during slow heating (3.3 °C/h). It ignited at 220 °C and burned without damage to the test container (bomb) or the surroundings.

Powala et al. [51] carried out Gap-test, sensitivity, and detonation velocity measurements on PBX explosives of FOX-7, HMX, and RDX, and different compositions of the explosives. In addition they carried out theoretical calculations of detonation characteristics of mixtures of FOX-7 with HMX or RDX. The PBX explosives contained 5% of PTFE. Table 3.26 shows part of their results.

Table 3.24 Impact and friction sensitivity of FOX-7 composition and its components [1]

Sample	Drop height[a] (cm)	Min. load (N)
FOX-7 (recryst., 250–355 μm)	79	–
FOX-7 (recryst., <70 μm)	63	–
Binder[b]	159	–
LIS-2 (70% FOX-7)	40	>340

[a] The highest drop height where no reaction occurs. Drop weight = 2 kg

[b] The composition of the binder is shown in Table 3.25

Table 3.25 Composition of the formulation (LIS-2) [1]

Component	Amount (weight)
FOX-7 (250–355 μm)	50%
FOX-7 (<70 μm)	20%
PolyGlyN	21%
Bu-NENA	5%
H_{12}MDI (Desmodur-W)	4%
DBTDL	Cat. Amounts

Cured for 24 h at 50 °C

Table 3.26 Detonation velocity of several FOX-7 formulation

95% explosives 5% PTFE	100% RDX 0% FOX-7	80% RDX 20% FOX-7	60% RDX 40% FOX-7	40% RDX 60% FOX-7	20% RDX 80% FOX-7	0% RDX 100% FOX-7
Detonation velocity (m/s)	8200	8290	8230	8200	8180	8200
Density (g/cm^3)	1.72	1.75	1.78	1.80	1.82	1.84
95% explosives 10% PTFE	100% RDX 0% FOX-7	80% RDX 20% FOX-7	60% RDX 40% FOX-7	40% RDX 60% FOX-7	20% RDX 80% FOX-7	0% RDX 100% FOX-7
Detonation velocity (m/s)	8500	8360	8300	8260	8150	8200
Density (g/cm^3)	1.82	1.82	1.82	1.83	1.84	1.85

3.12 Conclusion

FOX-7 has attracted a great deal of attention since its synthesis in 1998. Its evaluation is underway, however, various properties are scattered throughout the literature. A review of information available on DADE in the literature shows that its detonation properties are similar to RDX, but it is less sensitive than RDX. Various explosive properties suggests that a number of formulation is possible with FOX-7 to meet a variety of specialized applications. There is much more information particularly in Chinese journals. The fact that FOX-7 is an ethene, and the two electrons contribute to its reactivity should be useful in developing other insensitive explosive of higher performance. In spite of the information available on its synthesis and different formulations, there is a paucity of information on its physicochemical and thermochemical properties.

References

1. Karlsson S, Östmark H, Eldsäter C, Carlsson T, Bergman H, Wallin S, Pettersson A (2002) Detonation and sensitivity properties of FOX-7 and formulations containing FOX-7. Swedish Defence Research Agency Report, Revised
2. Crawford MJ, Evers J, Goebel M, Klapoetke TM, Mayer P, Oehlinger G, Welch JM (2007) γ-FOX-7: structure of a high energy density material immediately prior to decomposition. Propellants, Explos, Pyrotech 32:478–495
3. Evers J, Klapoetke TM, Mayer P, Oehlinger G, Welch J (2006) α- and β-FOX-7, polymorphs of a high energy density material, studied by X-ray single crystal and powder investigations in the temperature range from 200 to 423 K. Inorg Chem 45(13):4996–5007. Also The three ambient pressure polymorphs of FOX-7, New Trends in Research of Energetic Materials, 2007, 368-375, Pardubice, Czech Republic, April 25–27, 2007
4. Fan XZ, Li JZ, Liu ZR (2007) Thermal behavior of 1,1-diamino-2,2-dinitroethylene. J Phys Chem A 111:13291–13295

5. Anniyappan M, Talawar MB, Gore GM, Venugopalan S, Gandhe BR (2006) Synthesis, characterization and thermolysis of 1,1-diamino-2,2-dinitroethylene (FOX-7) and its salts. J Hazard Mater 137(2):812–819
6. Lochert IJ (2001) FOX-7- A new insensitive explosive. Weapons Systems Divisio Aeronautical and Maritime Research Laboratory, DSTO-TR-1238, Australia
7. Latypov NV, Bergman J, Langlet A, Wellmar U, Bemm U (1998) Synthesis and reactions of 1,1-Diamino-2,2-dinitroethylene. Tetrahedron 54:11525–11536
8. Latypov NV, Johansson M, Holmgren E, Sizova EV, Sizov VV, Bellamy AJ (2007) On the Synthesis of 1,1-Diamino-2,2-dinitroethene (FOX-7) by Nitration of 4,6-Dihydroxy-2-methylpyrimidine. Org Process Res Dev 11(1):56–59
9. Jalovy Z, Marecek P, Dudek K, Weidlich T (2001) Synthesis and properties of 1,1-Diamino-2,2-dinitroethene, New Trends in Research of Energetic Materials. In Ed S Zeman Proceeding Seminar, 4th, Pardubice, Czech Republic, April 11–12, pp 151–161
10. Wahigren K, ed (2004) FOI Weapons and Protection Division, Annual Report, p 11
11. Ostmark H, Bergman H, Bemm U, Goede P, Holmgren E, Johansson M, Langlet A, Latypov NV, Pettersson A, Pettersson M-L, Wingborg N, Vorde C, Stenmark H, Karlsson L, Hihkio M (2001) 2,2-dinitro-ethene-1,1-diamine (FOX-7) - properties, analysis and scale-up Int Annu Conf ICT 32nd(Energetic Materials):26/1–26/21 12
12. Cai HQ, Shu YJ, Yu WF, Li JS, Cheng BB (2004) Study on synthesis of FOX-7 and its reaction mechanism. ActaChim Sinica 62(3):295–301
13. Cai HQ, Shu YJ, Yu WF, Zeng GY (2004) Cheng BB Research development of 1,1-diamino-2, 2 dinitroethylene. HannengCailiao 12:124–128
14. Cai HQ, Shu YJ, Huang H, Cheng BB (2004) Li JS Study on Reactions of 2-(Dinitromethylene)-4,5 imidazolidinedione. J Org Chem 69:4369–4374
15. Cai HQ, Shu YJ, Cheng BB, Bi-Bo (2005) Improved method for synthesis of FOX–7. YingyongHuaxue 22(1):95–98
16. Trzcinski WA, Cudzilo S, Chylek Z, Szymanczyk L (2008) Detonation properties of 1,1-diamino-2,2-dinitroethene (DADNE). J Hazard Mater 157(2–3):605–612. doi:10.1016/jjhazmat200801026
17. Chylek Z, Pietrzyk S (2007) Effect of water on preparation of 1,1-diamino-2,2-dinitroethene (FOX-7). Biuletyn Wojskowej Akademii Technicznej 56(2):297–305
18. Dewey MA (2007) Synthesis, evaluation, and formulation studies on new oxidizers as alternatives to ammonium perchlorate in DoD missile propulsion Applications, ATK Launch Systems, SERDP Project WP1403, 23 April 2007
19. Clausen JL, Clough S, Gray M, Gwinn P (2007) Experimental screening assessment of perchlorate replacements, ERDC/CRREL TR-07-12, August 2007
20. Zhou C, Zhou Y, Huang X (2005) Wang X Synthesis and properties of 1,1-diamino-2,2-dinitroethylene. HuozhayaoXuebao 28(2):65–67
21. Bladek J, Pietrzyk S, Cudzilo S, Chylek Z (2009) Application of thin layer chromatography for monitoring of FOX–7 synthesis, propellants, explosives. Pyrotechnics 34(4):321–325
22. Orzechowski A, Powała D, Florczak B, Maranda A, Nowaczewski J (2006) Optimization of crystallization of 1,1-Diamino-2-2dinitroethylene, Proc New Trends in Research of Energetic Materials, Pardubice, Czech Republic 2006, Apr 19–21, 2006, 693–700
23. Goh EM, Cho JR, Kim JK (2005) Safe and convenient pilot scale process of 1,1–Diamino–2,2-dinitroethylene, American Chemical Society, p IEC-025, 230th ACS National Meeting, Washington, DC, Aug 28–Sept 1
24. Chung KH, Goh EM, Cho JR (2005) Synthetic modification and scale-up process for 1,1–diamino–2,2-dinitroethene (FOX-7). In: International Annual Conference ICT 36th (Energetic Materials), 52/1–52/13
25. Goh EM, Kim HS (2010) The scale up process improvement of 1,1-Diamino-2,2-dinitroethane (DADNE) New Trends in Research of Energetic Materials. In: Proceeding 10th Seminar, Pardubice, Czech Republic, Apr 21–23, 2010, 495–500
26. Bellamy AJ (2007) FOX-7 (1,1-diamino-2,2-dinitroethene) Struct Bonding (Berlin, Ger) 125 (High Energy Density Materials):1–33. doi:10.1007/430_2006_054

27. Teipel U, Fuhr I, Hartlieb K, Kjellstroem A, Eldsaeter C (2004) Crystallization of 1,1-diamino-2,2-dinitro-ethylene (FOX-7). In: International Annual Conference ICT 35th:51/1–51/11
28. Fuhr I, Mikonsaari I (2004) Production and characterization of insensitive explosive. In: Proceedings of the 2004 Insensitive Munitions and Energetic Materials Symposium, San Francisco, USA, November 14–17, 2004
29. Daniel MA, Davies PJ, Locher IJ (2010) FOX-7 for Insensitive Boosters. Weapons Systems Division, Defence Science and Technology Organisation. Australia, DSTO-TR-2449
30. Welch J (2008) Low sensitivity energetic materials. PhD Dissertation, Ludwig-Maximilians-UniversitätMünchen
31. Bemm U, Ostmark H (1998) 1, 1 - Diamino - 2, 2 - dinitroethylene: a novel energetic material with infinite layers in two dimensions. Acta Cryst Sect C C54:1997–1999
32. Zhao J, Liu H (2008) High-pressure behavior of crystalline FOX-7 bydensity functional theory calculations. Compu Mater Sci 42:698–703
33. Xu KZ, Chang CR, Song JR, Zhao FQ, Ma HX, Lu XQ, Hu RZ (2008) Preparation, crystal structure and theoretical calculation (FOX-7). Chinese of J Chem 26(3):495–499
34. Calculated using Advanced Chemistry Development (ACD/Labs) Software V819 for Solaris (1994–2008 ACD/Labs) Science Finder
35. Kim CK, Cho SG, Kim CK, Park H-Y, Zhang H, Lee HW (2008) Prediction of densities for solid energetic molecules with molecular surface electrostatic potentials. J Comput Chem 29:1818–1824
36. Xu K, Song J, Zhao F, Ma H, Gao H, Chang C, Ren Y, Hu R (2008) Thermal behavior, specific heat capacity and adiabatic time-to-explosion of G(FOX-7). J Hazard Mater 158(2–3):333–339. doi:10.1016/jjhazmat200801077
37. Zerilli FJ, Kuklja MM (2007) Ab-Initio equation of state of a organic molecular crystal: 1,1-Diamino-2,2-dinitroethylene. J Phys Chem A 111:1721–1725
38. Peiris SM, Wong CP, Zerilli FJ (2004) Equation of state and structural changes in diaminodinitroethylene under compression. J Chem Phys 120(17):8060–8066
39. Meents A, Dittrich B, Johnas SKJ, Thome V, Weckert EF (2008) Charge-density studies of energetic materials: CL-20 and FOX-7 Acta Crystallogr. Sect B: Struct Sci 64(1):42–49. doi:10.1107/S0108768107055292
40. Meents A, Dittrich B, Johnas SKJ, Thome V, Weckert EF (2008) Charge-density studies of energetic materials: CL-20 and FOX-7 Acta Crystallogr. Sect B: Struct Sci 64(4):519. doi:10.1107/S0108768108017497
41. Sun X-Q, Ju X-H, Xu X-J, Fan X-W (2007) J Chinese Chem Soc 54:1451–1456
42. Xing XL, Xue L, Zhao FQ, Gao HX, Hu RZ (2009) Thermochemical properties of 1,1-diamino–2,2–dinitroethylene (FOX-7) in dimethyl sulfoxide (DMSO). Thermochim Acta 491(1–2):35–38
43. Majano G, Mintova S, Bein T, Klapotke TM (2007) Confined detection of high-energy-density materials. J Phys Chem C111:6694–6699
44. Ottis J, Benova B (2007) Determination of FOX - 7 purity by UV spectroscopy, New Trends in Research of Energetic Materials, Proc 10thSeminar, Pardubice, Czech Republic, Apr 25–27, 2007, (Pt 2), 831-835, 2007
45. Dorsett H (2000) Computational Studies of FOX-7, A New Insensitive Explosive. Weapons Systems Divisions, Aeronautical and Maritime Research Laboratory, Australia, DSTO-TR-1054
46. Sinditskii VP, Levshenkov AI, Egorshev VY, Serushkin VV (2003) Study on combustion and thermal decomposition of 1,1-diamino-2,2-dinitroethylene (FOX-7) Proc Int Pyrotech Semin 30th(Europyro 2003, Volume 1):299–311
47. Civis M, Civis S, Sovova K, Dryahina K, Spanel P, Kyncl M (2011) Laser ablation of FOX-7: proposed mechanism of decomposition. Anal Chem (Washington, DC, US) 83(3):1069–1077. doi:10.1021/ac1028769

48. Sorescu DC, Boatz JA, Thompson DL (2003) First principles calculations of the adsorption of nitromethane and 1,1-Diamino-2,2-dinitroethylene (FOX-7) Molecules on the Al(111) Surface. In: Proceedings of the 2003 User Group Conference, IEEE, 2003
49. Chen ZE, Li ZY, Yao N, Lei, Wang D (2010) Safety property of FOX-7 and HTPB propellants. Chin J Energ Mater 18:316–319
50. Cullis IG, Townsley R (2011) The potential of FOX-7 explosive in insensitive munition design J Appl Mech 78(5):051012/1–051012/8
51. Powala D, Orzechowski A, Paplinski A, Maranda (2009) Some properties of PBX containing FOX-7. In: Proceeding New Trends in Research of Energetic Materials, Pardubice, Czech Republic 2009, Apr 1–3, 2009, 781–786, 2009

Additional Scholarly Articles for further Reading

52. Artemenko AG et al (2011) QSAR analysis of the toxicity of nitroaromatics in Tetrahymena pyriformis: structural factors and possible modes of action. SAR QSAR Environ Res 22(5–6):575–601. doi:10.1080/1062936X.2011.569950
53. Artsob H et al (1986) Arbovirus infections in several Ontario mammals, 1975–1980. Can J Vet Res 50(1):42–46
54. Bellamy AJ, Latypov NV, Goede P (2002) Transamination reactions of 1,1-diamino-2,2-dinitroethene (FOX-7). J Chem Res, Synop (6):257, 641–661. doi:10.3184/030823402103172103
55. Borges I Jr (2014) Electronic and ionization spectra of 1,1-diamino-2,2-dinitroethylene, FOX-7. J Mol Model 20(3):2095
56. Buszewski B, Michel M, Cudzilo S, Chylek Z (2009) High performance liquid chromatography of 1,1-diamino-2,2-dinitroethene and some intermediate products of its synthesis. J Hazard Mater 164(2–3):1051–1058. doi:10.1016/j.jhazmat.2008.09.018
57. Cheng K-F, Liu M-H, Chen C, Hong Y-S (2010) Computational optimum conditions for FOX-7 synthesis–A comparative synthesis route. J Mol Struct: THEOCHEM 957(1–3):6–14. doi:10.1016/j.theochem.2010.06.02
58. Chtragadda K, Vargeese AA (2017) A kinetics investigation on the nitro-nitrite rearrangement mediated thermal decomposition of high temperature monoclinic phase of 1,1-Diamino-2,2-Dinitroethylene (γ-Fox-7). J Chem Sci 129:281. doi:10.1007/s12039-016-1220-z
59. de Klerk WPC, Popescu C, van der Heijden AEDM (2003) Study on the decomposition kinetics of FOX-7 and HNF. J Therm Anal Calorim 72(3):955–966
60. Dreger ZA, Stash AI, Yu Z, Chen Z,Tao Y, Gupta YM (2016) High-pressure crystal structures of an insensitive energetic crystal: 1,1-Diamino-2,2-dinitroethene. J Phys Chem C 120:1218–1224
61. Dubovik AV, Kozak GD, Aleshkina EA (2007) Theoretical estimation of explosion hazard of NTO, FOX-7, TNAZ, and CL-20. University of Pardubice, pp 484–495
62. Ek S, Eldsaeter C, Goede P, Holmgren E, Tryman R, Latypov N (2005) Synthesis and characterisation of 2,2-dinitro-1,3-propanediol-based plasticisers. Cent Eur J Energ Mater 2 (4):33–45
63. Evers J, Klapoetke TM, Mayer P, Oehlinger G, Welch J (2006) α- and β-FOX-7, polymorphs of a high energy density material, studied by X-ray single crystal and powder investigations in the temperature range from 200 to 423 K. Inorg Chem 45(13):4996–5007. doi:10.1021/ic052150m
64. Florczak B (2008) A comparison of properties of aluminized composite propellants containing HMX and FOX-7. Cent Eur J Energ Mater 5(3–4):103–111
65. Garg S, Gao H, Parrish DA, JnM Shreeve (2011) FOX-7 (1,1-Diamino-2,2-dinitroethene): Trapped by Copper and Amines. Inorg Chem 50(1):390–395. doi:10.1021/ic102136r
66. Ghanta S (2016) Theoretically predicted Fox-7 based new high energy density molecules. J Mol Struct 1118:28–33

67. Ghule VD, Deswal S, Devi A, Kumar TR (2016) Computer-Aided Design of Energetic Tris (tetrazolyl)amine Derivatives and Salts. Ind Eng Chem Res 55(4):875–881. doi:10.1021/acs.iecr.5b04587
68. Herrmann M, Foerter-Barth U, Kempa PB (2009) Size/strain diffraction peak broadening of the energetic materials FOX-7, RDX and ADN. Cent Eur J Energ Mater 6(2):183–193
69. Herve G, Jacob G, Latypov N (2005) The reactivity of 1,1-diamino-2,2-dinitroethene (FOX-7). Tetrahedron 61(28):6743–6748. doi:10.1016/j.tet.2005.05.010
70. Huang B, et al (2010) Fabrication of FOX-7 quasi-three-dimensional grids of one-dimensional nanostructures via a spray freeze-drying technique and size-dependence of thermal properties. J Hazard Mater 184(1–3):561–566. doi:10.1016/j.jhazmat.2010.08.072
71. Jones DEG, Vachon MCR, Wang R, Kwok QSM (2004) Preliminary studies on the thermal properties of FOX-7. In: Proceeding NATAS Annu Conf Therm Anal Appl 32nd:105.17.703/1–105.17.703/15
72. Kempa PB, Herrmann M (2006) Temperature resolved X-ray diffraction for the investigation of the phase transitions of FOX-7. Part Part Syst Charact 22(6):418–422. doi:10.1002/ppsc.200501006
73. Landerville AC, Conroy MW, Budzevich MM, Lin Y, White CT, Oleynik II (2010) Equations of state for energetic materials from density functional theory with van der Waals, thermal, and zero-point energy corrections. Appl Phys Lett 97(25):251908/1–251908/3 doi:10.1063/1.3526754
74. Liu M-H, Cheng K-F, Chen C, Hong Y-S (2011) Computational study of FOX-7 synthesis in a solvated reaction system. Int J Quantum Chem 111(9):1859–1869. doi:10.1002/qua.22472
75. Lochert IJ (2001) DSTO advances in the evaluation of FOX-7. In: Proceeding International Pyrotechnics Seminar, vol 28, pp479–489
76. Luo J, et al. (2010) Syntheses and thermal behaviors of Rb(FOX-7)·H2O and Cs(FOX-7)·H2O. Bull Korean Chem Soc 31(10):2867–2872. doi:10.5012/bkcs.2010.31.10.2867
77. Mandal AK, Pandey RK, Asthana SN, Kulkarni A, Kulkarni BD (2011) Modeling and simulation of micro reactor with nitration of 2-methyl-4,6-dihydroxy-pyrimidine. Sci Technol Energ Mater 72(1–2):9–20
78. Meents A, Dittrich B, Johnas SKJ, Thome V, Weckert EF (2008) Charge-density studies of energetic materials: CL-20 and FOX-7. Acta Crystallogr, Sect B: Struct Sci 64(4):519. doi:10.1107/S0108768108017497
79. Muthurajan H, Sivabalan R, Talawar MB, Venugopalan S, Gandhe BR (2006) Computer code for the optimization of performance parameters of mixed explosive formulations. J Hazard Mater 136(3):475–481. doi:10.1016/j.jhazmat.2006.01.066
80. Sorescu DC, Boatz JA, Thompson DL (2001) Classical and Quantum-Mechanical Studies of Crystalline FOX-7 (1,1-Diamino-2,2-dinitroethylene). J Phys Chem A 105(20):5010–5021 doi:10.1021/jp010289m
81. Teipel U (2006) Product design of particulate energetic materials. Mater Sci Technol 22 (4):414–421. doi:10.1179/174328406X91113
82. Trzciński W, Belaada A (2016) 1,1-Diamino-2,2-dinitroethene (DADNE, FOX-7) – Properties and Formulations (a Review). Central Eur J Energ Mater 13(2):527–544

Chapter 4
2,4 Dinitroanisole (DNAN)

Abstract DNAN was historically used as an explosive in warheads containing Amatol 40 and is currently being investigated as a replacement for 2,4,6-Trinitrotoluene (TNT) in melt-cast insensitive munitions (IM) formulations. Alternatives with suitable chemical and physical properties have been sought. 2,4-Dinitroanisole (DNAN) is a promising alternative that prima facie appears to possess adequate properties and, by virtue of reduced sensitivity, may enable the development of a new class of low sensitivity melt-cast formulations for use in Insensitive Munitions (IM). This chapter provides an overview of DNAN including its synthesis, characterization, and basic properties. In addition, the sensitivity and explosive properties of various DNAN-based formulations (containing RDX and/or NTO) are discussed.

4.1 Introduction

Dinitroanisole [DNAN] finds applications in various fields such as synthesis of dyes, insecticide, and explosive formulations. It is a less sensitive explosive and can be handled and transported with less stringent conditions. Because of these properties, DNAN is being tested by the Military Industry as a replacement for 2,4,6-trinitrotoluene (TNT) in explosive formulations. For example, Picatinny Arsenal, USA is developing a range of DNAN based explosive formulations typically referred to as the "PAX explosives". DNAN appears to promise a new class of low sensitive melt-cast formulations. It was during World War II that DNAN was used along with ammonium nitrate and RDX as an explosive by name Amatol 40. The recent interest in DNAN stems from the fact that it can be used as an ingredient in less-sensitive melt-cast formulations than TNT, and it is classified as a Class 4.1 flammable solid. Because of this classification it is subject to less stringent international transportation requirements than Class 1 materials. DNAN is a stable compound and has a much higher melting point compared to TNT. It is cheaper to manufacture compared to TNT and is also less toxic. It is soluble in ethanol, ether,

D.S. Viswanath et al., *Emerging Energetic Materials: Synthesis, Physicochemical, and Detonation Properties*, https://doi.org/10.1007/978-94-024-1201-7_4

acetone, and benzene, and highly soluble in pyridine. Recently DNAN has been used with oxidizers for incendiary and armor-piercing munitions [1].

4.2 Synthesis

The synthesis of DNAN has evolved over the years. Although DNAN can be prepared by a number of methods starting with different raw materials, some the processes need harsh experimental conditions and, involves toxic raw materials, and generates hazardous wastes. However, current routes use less harsh conditions, and addresses environmental concerns. The main synthesis methods use chlorobenzene, phenol, 1-chloro-2,4-dinitrobenzene (DNCB), and anisole as the starting raw materials.

The reaction path when chlorobenzene is used as the starting raw material is shown in Fig. 4.1. In this process, chlorobenze is first nitrated using a mixture of sulfuric and nitric acid at 313 K forming DNCB.

DNCB next reacts with sodium hydroxide in the presence of methanol (CH_3OH) under ambient conditions producing DNAN (Fig. 4.2). The reaction involves simple nucleophilic aromatic substitution of the highly labile chloro substituent with a methoxide anion. However, under the experimental conditions, CH_3OH and NaOH also produce hydroxide nucleophile leading to formation of other chloro-derivatives. As a result, both the yield and the purity of the product are low. Davies and Provatas [2] raised a similar concern for this route for production of DNAN.

Direct nitration of phenolic compounds is typically highly exothermic and difficult to control and therefore is not a preferable route. Slater-Blanc et al. [3] suggested several alternate paths to avoid the direct nitration path. Following nitration of phenol, the product 1-hydroxyl-2,4-dinitrobenzene undergoes methylation to pro-dice DNAN. The reaction path is shown in Fig 4.3.

Another route for preparing DNAN is the nitration of anisole directly. The reaction pathway is shown in Fig. 4.4. One of the disadvantages of this route is the formation of both 2,4- and 2,6-dinitroanisole. DNAN has also been prodiced by nitration of p-nitro- and o-nitroanisole.

Researchers have pursued variation of one of these methods for the preparation of DNAN. Barnett et al. [4] synthesized nitroanisoles by boiling 1-chloro-2, 4-dinitrobenzene with sodium methoxide in methanol to study the reaction rates.

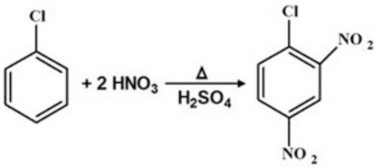

Fig. 4.1 Nitration of chlorobenzene to 1-chloro-2,4-dinitrobenzene (DNCB) [4]

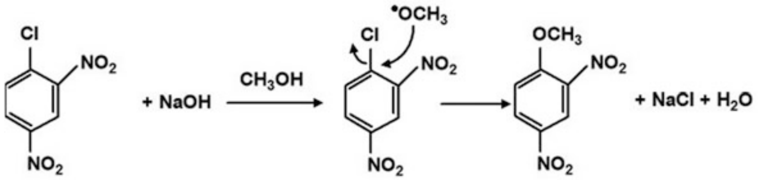

Fig. 4.2 Synthesis of DNAN from chlorobenzene [2]

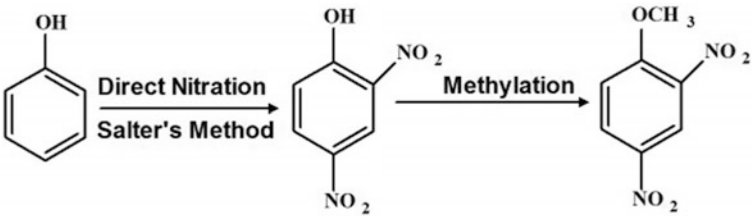

Fig. 4.3 Synthesis of DNAN from phenol [3]

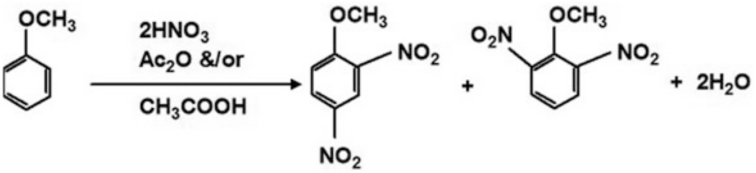

Fig. 4.4 DNAN from direct nitration of anisole [3]

The analysis of kinetics of the reaction showed that the specific reaction rate constant, *k*, varied as a function of the percentage of sulfuric acid in the nitration mixture. The $\log_{10}k$ values varied from −3.8 to 1.0 over a concentration range of 55–72 mass% of sulfuric acid.

Dey et al. [5] carried out a detailed study for preparation of DNAN and studied the effect of various parameters on the yield of DNAN. They used 2,4-dinitrochlorobenzene as the starting raw materials. Table 4.1 shows the effect of various constituents on the yield of DNAN.

Davies and Provatas [2] provide a detailed description of the synthesis of DNAN from DNCB. They used sodium hydroxide instead of sodium methoxide in the synthesis of DNAN. The labile chlorine is methoxylated with methanol in the presence of sodium. Holleman and Wilhelmy [6] also used the nitration of DCNB route for the preparation of 2-4 and 2-6 dinitroanisoles, and used carbon disulfide extraction process for separation.

A continuous process for the preparation of DNAN by the nitration of nitroanisole has been described by Xu et al. [7]. The authors used 2-nitroanisole,

Table 4.1 Effect of various parameters on the yield of DNAN when using 2,4-dinitrochlorobenzene as the starting material [5]

2,4-dinitrochlorobenzene	NaOH	95% methyl alcohol	Duration of heating	2,4-dinitroanisole (gms)	(%)	(mp)	2,4-dinitrophenol
20	6	150	6	13.7	70	68	27.7%
20	5	150	6	16.1	82.3	78–80	16.0%
20	4	150	6	18.8	96.1	86	
160	32	1200	6	153.0	97.8	86	
20	4	150	4	18.9	96.6	83	
20	4	150		19.2	98.2	81	

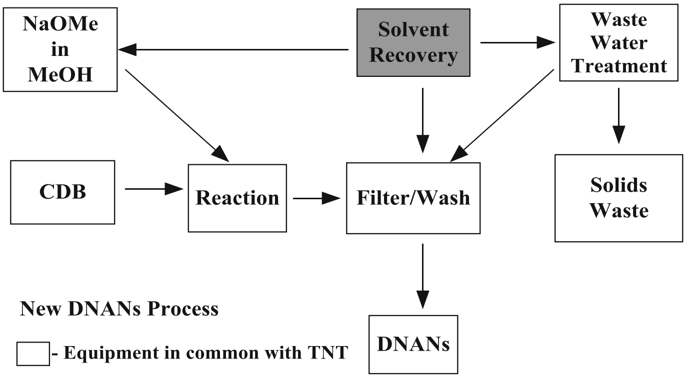

Fig. 4.5 New dinitroanisole process (ATK process) [8]

4-nitroanisole, and their mixtures as raw materials. The reactions appear to have been conducted at low pressures.

Alliant Techsystems [8] have the capability to make DNAN, CL-20, NTO, and TEX. In this process, the starting material is 1-chloro-2,4-dinitro benzene (DNCB). The process equipment is similar to that of TNT except for the solvent recovery system. The production rate is 5–10 lb/h. A schematic diagram of the process is shown in Fig. 4.5.

An interesting process using Phase Transfer Catalyst (PTC) is provided by Xia et al. [9]. They used triethyl benzyl ammonium chloride as the PTC, and found a reaction temperature of 329 K, mass ratio of catalyst to 2,4-dinitrochlorobenzene of 1:100 and a time of adding sodium hydroxide of 30 min as the best conditions. The product was characterized by FT IR and HPLC methods.

The phenomenon of rate enhancement of a reaction between chemical species located in different phases (immiscible liquids or solid and liquid) by addition of a small quantity of an agent (called the ‘phase-transfer catalyst’) that extracts one of the reactants, most commonly an anion, across the interface into the other phase so that reaction can proceed. These catalysts are salts of ‘onium ions’ (e.g. tetraalkylammonium salts) or agents that complex inorganic cations (e.g. crown ethers). The catalyst cation is not consumed in the reaction although an anion exchange does occur [10].

4.3 Structure

Two stable polymorphic forms of DNAN exist; 2-4, Dinitroanisole and 2-6, Dinitroanisole. However, only 2-4, Dinitroanisole exhibits explosive properties. Nyburg et al. [11], and Malinovskii et al. [12] have shown that 2-4, Dinitroanisole exhibits a monoclinic structure. They have determined the crystal unit cell parameters, and provide information on bond angles and bond distances. Xue et al. [13]

Table 4.2 Structural parameters of 2-4, dinitroanisole [11]

Parameters	Values
Monoclinic, $P2_1/n$	
a	8.772 (2)
b	12.645 (2)
c	15.429 (4) Å
β	81.89 (2)°
V	1694 $Å^3$
Z	8
D_x	1.56 g/cm^3
λ ($MoK\alpha_1$)	0.7093 Å
μ	1.26 cm^{-1}

found a polymorphic modification of 2-4, Dinitroanisole with similar bond lengths but some different torsional bond angles. They found that both modifications crystallize in P21/n, but have different molecular packing. The data provided by Nyburg et al. [11] are tabulated in Table 4.2.

Detailed information on bond angels and bond lengths are proved by Nyburg et al. [11].

4.3.1 Spectral Data

The NMR spectrum for DNAN can be obtained from Wiley Subscription Services Inc. [14] and is given in Fig. 4.6. The NMR spectrum is useful in checking the purity of the substance.

The spectrum was taken using a Varian HA-60 in Chloroform-d (865-49-6) and Tetramethylsilane (75-76-3) was used as the standard.

The IR spectrum was obtained from the Integrated Spectral Database System of Organic Compounds, National Institute of Advanced Industrial Science and Technology (Japan). The spectrum is shown in Fig. 4.7.

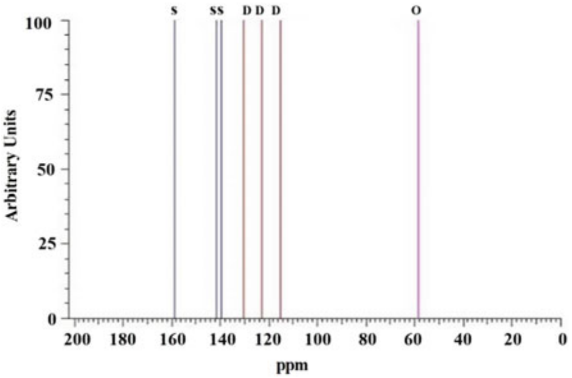

Fig. 4.6 NMR spectrum [14]

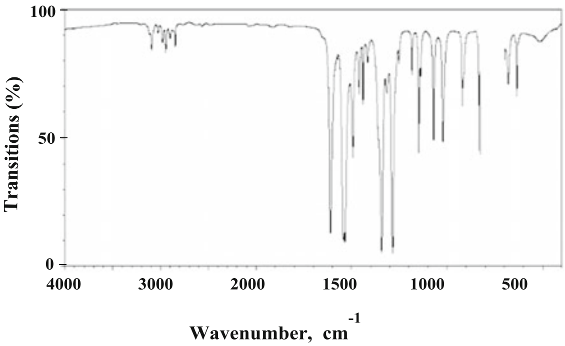

Fig. 4.7 IR absorption spectrum [15]

4.4 Physical and Chemical Properties

Various chemical and physical properties of DNAN are listed in Table 4.3.

4.4.1 Solubility in Various Media

Boddu et al. [21] determined solubility of DNAN both in water and in the presence of different concentrations of electrolytes. They also reported octanol-water partition coefficient and Henry's law constant as a function of temperature. Their data are presented in Tables 4.4. The DNAN used for this study was received from the Ordance Systems, Kingsport, Tennessee, U.S.A. The concentration of DNAN in different media was determined by HPLC with an UV detector at 254 nm. Extra precautions were taken to avoid recrystallization when measuring the concentration. Their apparatus for the determination of Henry's law constants is shown in Fig. 4.8 and the data are tabulated in Table 4.4.

Tables 4.5 and 4.6 show data on solubility and octanol-water partition coefficients.

QSPR model is extensively used to predict the solubility of military, pharmaceutical, and various other types of molecules. Boddu et al. [21, 22] used QSPR model and the model predictions are compared with the results from EPI Suite. The EPI suite predicts properties at 298.15 K. The EPI predictions are much different from the experimental data of Boddu et al. [22]

Potoff [23] has made model predictions based on Lennard-Jones 6-12 potential with a columbic term for partial charges. Potoff states "the vapor liquid coexistence curves, vapor pressures, boiling points and critical points were determined for a

Table 4.3 Some properties of 2,4-dinitroanisole

Properties	Values	References
Synonyms	DNAN; Anisole, 2,4-dinitro; 1-Methoxy-2,4-dinitrobenzene; 2,4-Dinitroanisol; 2,4-Dinitrophenyl methyl ether; Dinitroanisole; Benzene, 1-methoxy-2,4-dinitro-	
CAS number	119-27-7	
Structural formula	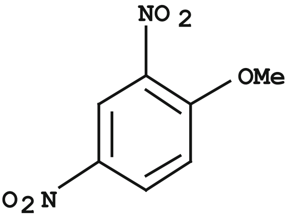	
Force field analysis	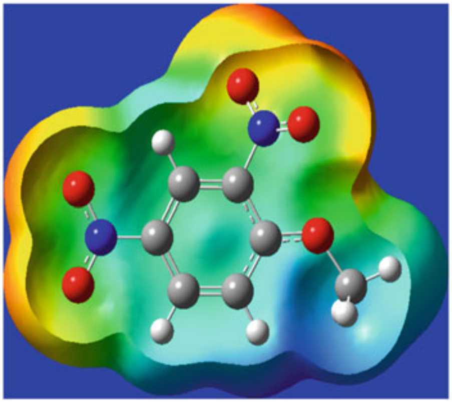	
Empirical formula	$C_7H_6N_2O_5$	
Molecular mass	g mol^{-1}, 198.13	
Density	g/mL, 1.336 [CRC]	
Molar volume	cm^{3}mol^{-1}, 137 ± 3.0 at 293 K and 760 Torr	[16]
Boiling point	479.15 K at 12 mm Hg	[17]
	588 K	[18]
	592.77 K	[19]
Melting point	367.65 K	[17]
	359.9 K	[18]
Flash point	180.5 ± 24.3 °C	[16]
Critical temperature	806 K	[18]
Critical pressure	39.9 bar	[18]
Dipole moment	3.83 Debye	[21]
Acentric factor	0.858	[22]
Vapor pressure	0.000145 mm Hg and	[18]
	0.000138 mm Hg	[16]
	0.0000895 @ 298.15 K	[17]

(continued)

Table 4.3 (continued)

Properties	Values	References
Enthalpy of fusion	19.91 kJ/mol	[19]
Velocity of detonation	5320 m/s	
Detonation pressure	9.5 GPa	

Temperature (K)	298.15	308.15	318.15	
Log Kow	1.612 ± 0.014	1.549 ± 0.013	1.472 ± 0.025	
Log Kow	1.38	1.70	1.92	[18]
Koc	169 at pH 1 and 298.15 K			[16]
Vapor pressure	8.59E-5 Torr @ 25 °C, 0.000138 mm Hg @ 25 °C			[16, 17]
Enthalpy of vaporization	57.21 ± 3.0 $\mathrm{kJmol^{-1}}$			[16]
Aqueous solubility	0.14	0.159 $\mathrm{g\ L^{-1}}$ @ 298.15 K		[18]
Bioconcentration factor (BCF)	9.1 $\mathrm{g\ L^{-1}}$ @ 25 °C	4.14 °C		[16, 20]
Dermal permeability coefficient (Kp)	0.74 $\mathrm{\mu g\ cm^{-2}\ hr^{-1}}$			[2]

Table 4.4 Henry's law constant (kH) as a function of temperature [21]

Temperature (K)	298.15	308.15	318.15
$\mathrm{m^3\ Pa\ mol^{-1}}$ (kH)	1.366	1.397	1.442

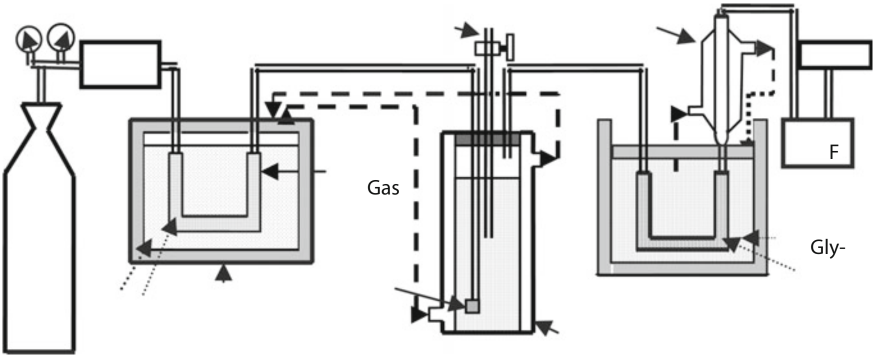

Fig. 4.8 Experimental setup for the determination of Henry's Law constant [21]

Table 4.5 Aqueous solubility of DNAN (S, mg/L) in the presence of NaCl and $CaCl_2$ salts at different temperatures

Vol.% of salt solution	Temperature (K)		
	298.15	308.15	318.15
0	276.2 ± 2.5	399.2 ± 4.0	560.0 ± 5.0
1% NaCl	267.1 ± 2.5	388.6 ± 3.0	527.2 ± 5.0
5% NaCl	233.5 ± 2.5	320.1 ± 2.5	437.2 ± 4.0
10% NaCl	190.7 ± 2.5	240.0 ± 2.5	321.4 ± 2.5
1% $CaCl_2$	268.1 ± 2.5	388.8 ± 3.0	537.5 ± 5.0
5% $CaCl_2$	249.0 ± 2.5	333.5 ± 3.0	463.5 ± 4.0
10% $CaCl_2$	224.2 ± 2.5	276.7 ± 2.5	378.7 ± 3.0

Table 4.6 Octanol-water partition coefficients at different temperatures [22]

Temperature (K)	298.15	308.15	318.15
Log Kow	1.612 ± 0.014	1.549 ± 0.013	1.472 ± 0.025

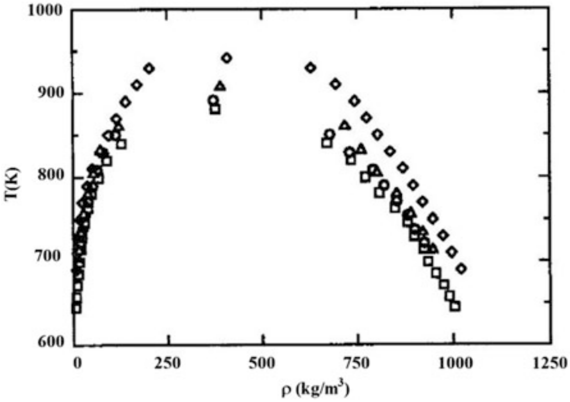

Fig. 4.9 Co-Existence plot for DNAN. IC model (*diamond*); 4C model (*triangle*); 6C model (*circle*); 10C model (*square*) [23]

series of force fields for DNAN. These force fields are denoted IC, 4C, 6C and 10 °C, corresponding to the original partial charges derived from a CHELPG analysis of HF/6-31 g + (d,p) ab initio calculations and 4, 6 and 10% reductions from these values, respectively". Figures 4.9 and 4.10, reproduced from Potoff's report, show the two-phase coexistence curve and vapor pressure data.

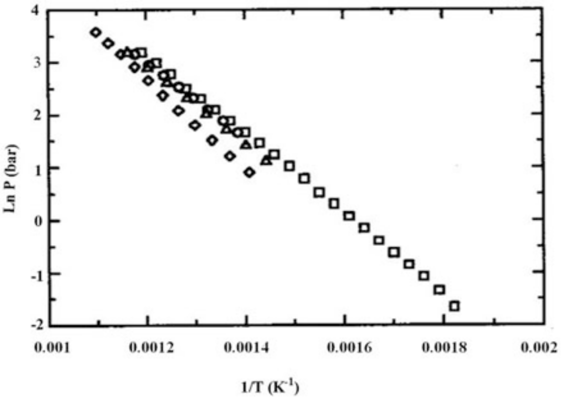

Fig. 4.10 Vapor pressure plot for DNAN. IC model (*diamond*); 4C model (*triangle*); 6C model (*circle*); 10C model (*square*) [23]

4.4.2 Vapor Pressure

Highsmith and Johnston [24] in their work on synthesis of DNAN carefully followed the time-temperature-pressure variation. They also computed the vapor pressure of DNAN using a ChemCad model and their values shown graphically is reproduced in Fig. 4.11. Potoff [23] values are in the range of 555–900 K where as Highsmith and Johnston [24] values range from 300 to 423 K.

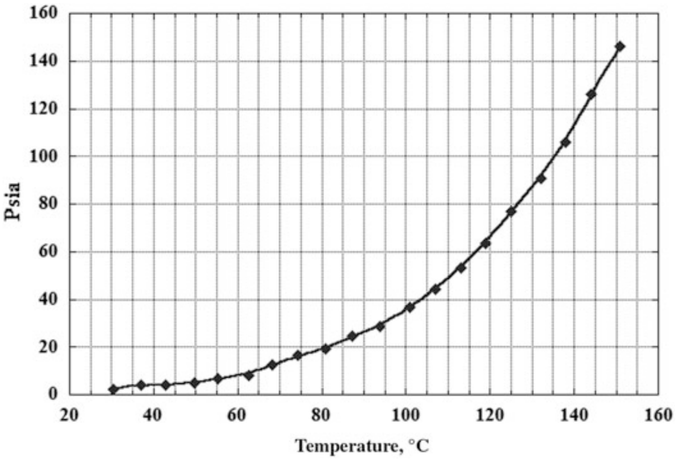

Fig. 4.11 Temperature-vapor pressure calculated [24]

Table 4.7 Solubility of RDX in DNAN [2]

Temperature (K)	373	383	393
Solubility (g/100 g)	11	17	20

4.5 Detonation Characteristics

The performance of DNAN is about 10% less compared to TNT [2] but it is highly insensitive. Its ignition temperature is about 347 °C compared to 306 °C for TNT. The velocity of detonation and other detonation characteristics are included.

4.6 Decomposition

Desvergnes [25] studied the hydrolysis of DNAN and found that it formed 2,4-dinitrophenol and methanol

$C_6H_3CH_3O(NO_2)_2 + H_2O \rightarrow C_6H_3OH(NO_2)_2 + CH_3OH.$

However in a recent study, Bausinger and Preuss [26] did not observe such a hydrolysis and conclude that DNAN is stable. This allowed them to carry out analysis based on liquid chromatography.

Boddu et al. [27] have studied degradation of DNAN on nanoparticles of magnesium and zinc oxide as catalysts. The have identified that degradation occurs through ring cleavage, hydroxylation, amination and denitration. The transformation products were identified through HPLC, LC-MS, FTIR and ^{1}H-NMR studies. The transformation products are shown in Fig. 4.12. The approximate composition of the products are also shown in Fig. 4.12.

Zhao et al. [28] have also identified 2,4-diaminoanisole from their hydrogenation studies of DNAN on palladium catalysts. These studies indicate that degradation and transformation products can be controlled using the catalyst and redox conditions.

4.7 Biodegradation/Biotransformations

Biodegradation studies are important for treatment of wastewaters generated from manufacture and also to understand the fate of DNAN in soils and slurries. Both aerobic and anaerobic degradation studies have been reported. Perreault et al. [29] have reported aerobic transformation of soils and slurries supplemented with carbon and nitrogen sources. They found that DNAN was completely transformed in 34 days while complete biotransformation (co-meblism) in soils is observed in 8 days by *Bacillus* Sp. (strain *Bacillus* 1 G). HPLC and LC-MS analysis of

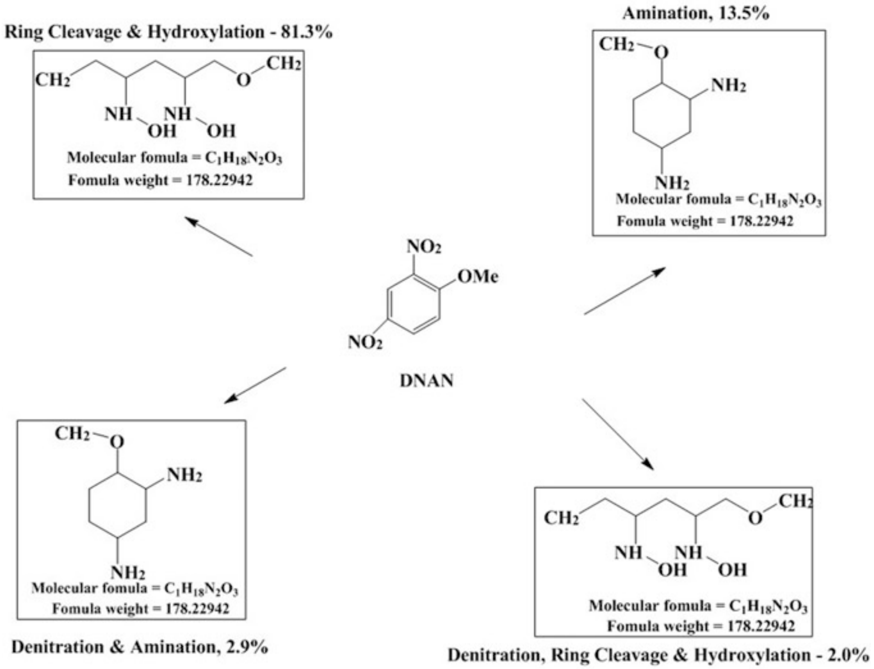

Fig. 4.12 Degradation of 2,4 dinitroanisole on MgO and ZnO nanostructures [27]

transformation products show the formation of 2-amino-4-nitroanisole as the major end product following the regioselective reduction of the ortho-nitro group. The authors have identified various intermediate compounds arylnitroso and arylhydroxylamino derivatives. Secondary reaction products involving these intermediates formed azoxy- and azo-dimers. Acetylated and demethylated products were also observed (Fig. 4.13). Platten et al. [30] have studied biotransformation of DNAN in aqueous systems using anaerobic fluidized-bed bioreactors. They have used ethanol as the electron donor. They also report that DNAN transformed into diaminonitrosol, and formation of azocompounds after exposure to air.

Figure 4.14 shows the dimers formation.

4.8 Detection

Schechter and Haller [31] discuss a calorimetric procedure for detection and estimation of DNAN which is rapid and accurate. Further this method gives a linear calibration curve. A HPLC method has been described by Chow et al. [32] in a recent paper. They analyzed samples containing 0.02–1000 ppm of DNAN in the

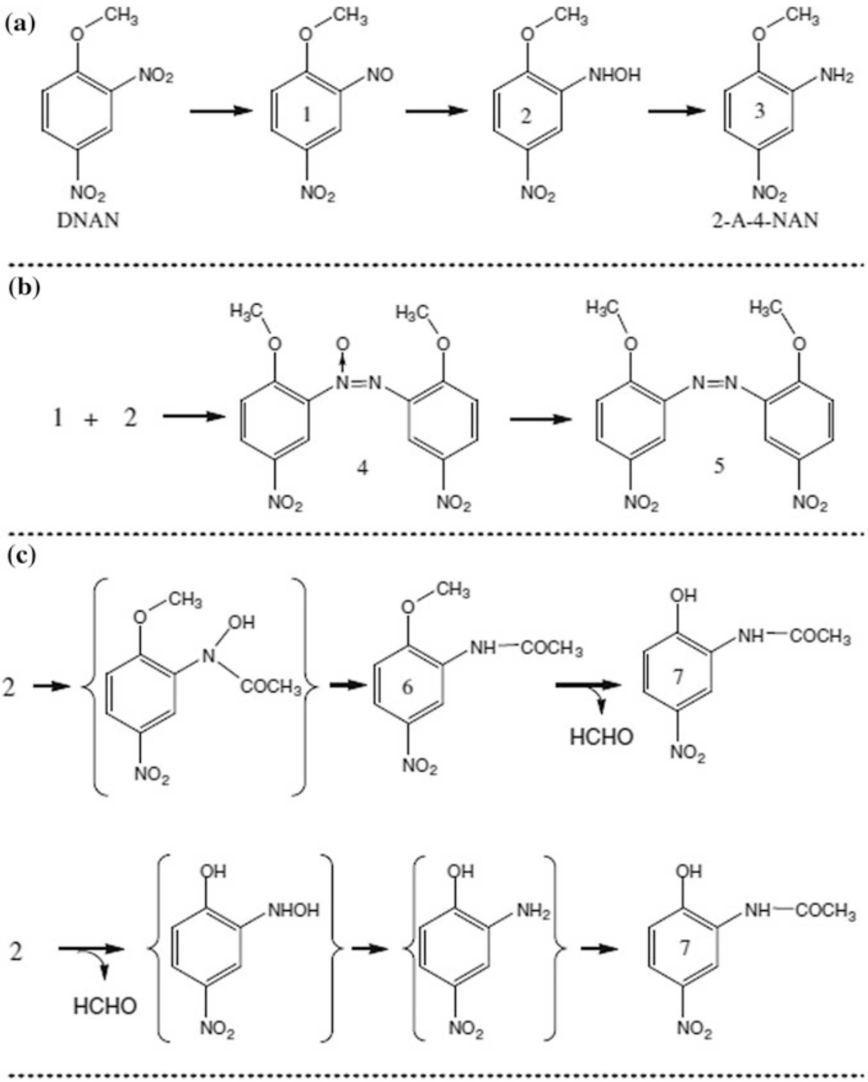

Fig. 4.13 Proposed degradation routes of 2,4-DNAN with Baxillus 13 G. path **a** Primary transformation routes of DNAN by Bacillus 13G; path **b** Production of azoxy- and azo-compounds (4 and 5, respectively) from compound 1 and 2; path **c** proposed secondary transformation routes of compound 2 to produce acetylated compounds (compounds in brackets were not detected) [30]

presence of 16 other explosives. Chow et al. [32], evaluated and modified the U.S. EPA Method 8330 the analysis of DNAN and MNA by HPLC technique in various aqueous media in the presence and absence of the 14 energetic compounds.

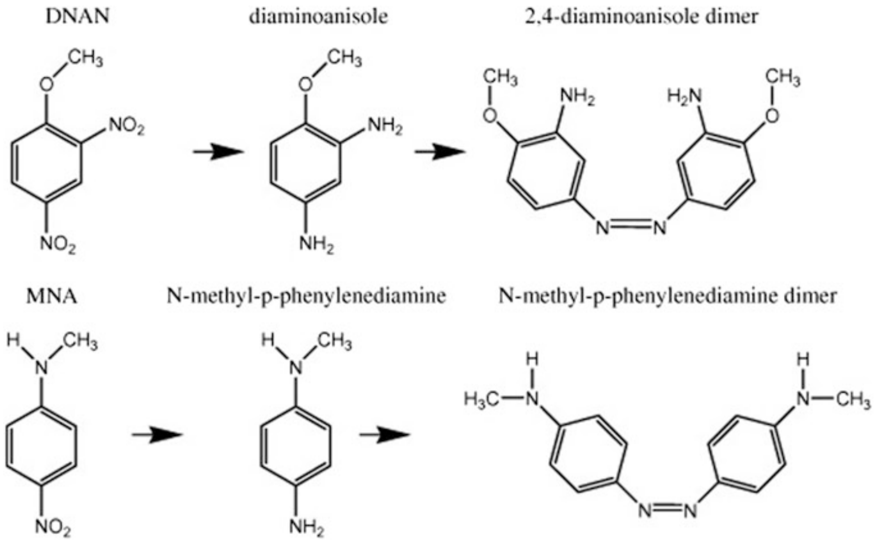

Fig. 4.14 Chemical structures of 2,4-dinitroanisole (DNAN) and N-methyl paranitro aniline (MNA) and their transformation products, diaminoanisole, N-methyl-p-phenylenediamine, and their dimers [30]

They the optimized method to separate all 14 energetic compounds from DNAN and MNA using a tertiary mobile phase of water-methanol-acetonitrile (68:28:4) in an isocratic run of 35 min.

4.9 Formulation Using DNAN

Davies and Provatas [2] further provide an extensive review of the characterization and formulation of DNAN with other explosives such as RDX. Two DNAN/RDX formulations, namely ARX- 4027 (60/40 RDX/DNAN + 0.25% MNA) incorporating RS-RDX (ARX-4027 M1) and non-RS-RDX (ARX-4027 M2) have been studied. This has led to the study of the solubility of RDX in DNAN [2], and is discussed later in this report. Davies and Provatas [2] have carried out extensive study of these formulations. Table 4.7 shows the solubility of RDX in DNAN.

Wilson [33] provides density, velocity of detonation, and other useful information on some formulations including PAX-21 and PAX-41. The data on some of these formulations are shown in Table 4.8.

In addition to the above PAX formulations, several other formulations are tested by the army. The PAX, OSX, and other formulations contain DNAN as one of the components replacing TNT. Zhang and Dong [34] provide a review of 2,4-dinitroanisole(DNAN)-based melt-castable explosives, including its synthesis, properties, thermal characteristics, and compatibility with other materials.

Table 4.8 Comparison of DNAN formulations [33]

Material	TMD	VOD (%)	LSGT	DSC MP	Effluxviscosity	Onset (° C)
	(g.cm$^{-3)}$	Comp. B	Cards	Exotherm	(sec) @96C	
TNT	1.654	84	133	–	–	
COMP B	1.76329	100	207	80/215		–
PAX-21	1.72857	83	161	89/193		4.8–8.6
PAX-33	1.73614	89	144	88/207		8.7
PAX-34	1.76098	83	104	87/245		8.5
OSX-7	1.74835	95	118	92/215	15	
OSX-CAN	1.59437	84	131	93/225		5.9
1043-03	1.76937	103	144	95/229		9.2

LGST large scale gap test

References

1. Nielson DB, Ashcroft BN, Doll DW (2005) Incendiary and armor-piercing munitions containing metal fuels, oxidizer, and Class 1.1 explosives (USA). US Pat Appl Publ (2005), US 2005199323 A1 20050915
2. Davies PJ, Provatas A (2006) Characterization of 2,4-Dinitroanisole: an ingredient for use in low sensitivity melt cast formulations. Australian Government, Department of Defense Report DSTO-TR-1904
3. Salter-Blanc AJ, Bylaska EJ, Johnston HJ, Tratnyek PG (2015) Predicting reduction rates of energetic nitroaromatic compounds using calculated one-electron reduction potentials. Environ Sci Technol 49(6):3778–3786. doi:10.1021/es505092s
4. Barnett JW, Moodie RB, Schofield K, Weston JB, Coombes RG, Golding JG, Tobin GD (1977) Electrophilic aromatic substitution part 162 the nitration of anisole, o-methylanisole, and p-methylanisole in aqueous sulphuric acid. J Chem Soc Perkin Trans 248–255
5. Dey BB, Govindachari TR, Udupa HK (1946) Preparation of 4-chloro-2-nitroanisole, 4-chloro-2-nitrophenetole, 2,4-dinitroanisole, and 2,4-dinitro–phenetole. J Sci Indus Res, Sect B: Phys Sci 5B(3):37–40
6. Holleman F, Wilhelmy G (1902) Preparation of the dinitrophenols and dinitroanisoles, and certain of their physical properties. Recl Trav Chim Pays-Bas 21:432–447
7. Xu W, Duan Y, Liu X (2006) Faming Zhuanli Shenqing Gongkai Shuomingshu. Chinese Patent 1861564 and 1861565
8. Holt P, Johnston G, Sanderson AJ, Wesson P, Worthington J (2004) Development of an efficient and green TNT manufacturing process. IM/EM Technical Symposium, San Francisco, CA, 15–17 November
9. Xia X-Z, Xu Z-L, Li F, Zhao G-S (2010) Study on the synthesis of 2,4-dinitroanisole with TEBA as phase transfer catalys. Huaxue Shijie 51(3):162–164
10. Muller P (1994) Glossary of terms used in physical organic chemistry (IUPAC Recommendations 1994). Pure Appl Chem 66(5):1077–1184
11. Nyburg SC, Faerman CH, Prasad L, Palleros D, Nudelman N (1987) Structures of 2,4-dinitroanisole and 2,6-dinitroanisole. Acta Crystallogr C 43:686–689
12. Malinovskii ST, Fonar MS, Simonov YA, Dvorkin AA, Ganin EV, Luk'yanenko NG, Musienko GS (1992) Crystal and molecular structures of the host-guest type of complex of 18-crown-6 with 24-dinitroanisole and 2–4-dinitroanisole in the free state. Kristallografiya (Crystallogr Rep) 37:671–673

13. Xue G, Gong C-R, Chen H-Y (2007) Crystal structure of 2,4-dinitroanisole C7H6N2O5 Z. Kristallogr 222:321–322
14. Greenberg D (2006) Spectral data were obtained from Wiley Subscription Services, Inc. (US). Wiley STM Databases, Wiley Launches, Wiley Registry of Mass Spectral Data, 8th edn
15. Yamaji T, Saito T, Hayamizu K, Yanagisawa M, Yamamoto O (2017) Integrated spectral database system of organic compounds, National Institute of Advanced Industrial Science and Technology, Spectrum ID: NIDA8188). (Japan) http://sdbs.db.aist.go.jp
16. Calculated using Advanced Chemistry Development (ACD/Labs) Software V904 for Solaris (1994–2008 ACD/Labs)
17. Syracuse research corporation database
18. Toghiani RK, Toghiani H, Maloney SW, Boddu VM (2008) Prediction of physicochemical properties of energetic materials. Fluid Phase Equilib 264:86–92
19. Chakka S, Boddu VM, Maloney SW, Damavarapu R, Paper Presented At the AIChE Meeting
20. Mehrotra NK, Shukla JP, Saxena MC (1967) Relaxation times and dipole moments of some substituted benzenes having hydroxyl, methoxy, or ethoxy groups. Indian J Pure Appl Phys 5(2):61–63
21. Boddu VM, Abburi K, Fredricksen AJ, Maloney SW, Damavarapu R (2009) Equilibrium and column adsorption studies of 2,4-dinitroanisole (DNAN) on surface modified granular activated carbons. Environ Technol 30(2):173–181
22. Boddu VM, Abburi K, Maloney SW, Damavarapu R (2008) Thermophysical properties of an insensitive munitions compound, 2,4-dinitroanisole. J Chem Eng Data 53:1120–1125
23. Potoff J (2007) Prediction of environmental impact of high-energy materials with atomistic computer simulations. Annual Report, Contract Number W9132–06-2-2027
24. Highsmith TK, Johnston HE (2004) Continuous process for preparing alkoxynitroarenes. US Patent 0133046
25. Desvergnes L (1994) Sur quelques proprie´ te´ s physiques des de´ rive´ s nitre´ s. Monit Scient 14(5 series):249–257
26. Bausinger T, Preuss J (2008) Stability of nitroaromatic specialty explosives in reversed-phase liquid chromatographic systems. J Hazard Mater
27. Boddu VM, Abburi K, Maloney SW, Damavarapu R (2010) Physicochemical property measurements on insensitive munitions compounds for environmental applications. CRC Press, Boca Raton, pp 139–160
28. Zhao X, Chen X, Chen L (1997) Hydrogenation of 2,4–dinitroanisole in liquid phase. Jingxi Huagong 14(5):41–43 (in Chinese)
29. Perreault NN, Manno D, Halasz A, Thiboutot S, Ampleman G, Hawai J (2012) Biodegradation 23:287–295
30. Platten WE, Bailey D, Suidan MT, Maloney SW (2010) Chemosphere 81:11
31. Schechter S, Haller HL (1944) Colorimetric determination of 2,4-dinitroanisole. Ind Eng Chem Anal Ed 16:325
32. Chow TM, Wilcoxon MR, Piwoni MD, Maloney SW (2009) Analysis of new generation explosives in the presence of U.S. EPA method 8330 energetic compounds by high-performance liquid chromatography. J Chromatogr Sci 47(1):40–43. doi:10.1093/chromsci/47.1.40
33. Wilson AE (2006) BAE Systems. http://www.imemg.org/res/imemts2006_Wilson_3B.ppt.pdf
34. Zhang G, Dong H (2010) Review on melt-castable explosives based on 2,4-dinitroanisole. Chinese Journal of Energetic Materials Institute of Chemical Materials, CAEP, Mianyang, China

Additional Scholarly Articles for further Reading

35. Ahn SC, Cha DK, Kim BJ, Oh S-Y (2011) Detoxification of PAX-21 ammunitions wastewater by zero-valent iron for microbial reduction of perchlorate. J Hazard Mater 192 (2):909–914. doi:10.1016/j.jhazmat.2011.05.104
36. Ahn SC, Hubbard B, Cha DK, Kim BJ (2014) Simultaneous removal of perchlorate and energetic compounds in munitions wastewater by zero-valent iron and perchlorate-respiring bacteria. J Environ Sci Health Part A Toxic/Hazard Subst Environ Eng 49(5):575–583. doi:10.1080/10934529.2014.859455
37. Arnett CM, Rodriguez G, Maloney SW (2009) Analysis of bacterial community diversity in anaerobic fluidized bed bioreactors treating 2,4-dinitroanisole (DNAN) and n-methyl-4-nitroaniline (MNA) using 16S rRNA gene clone libraries. Microbes Environ 24(1):72–75
38. Bhatnagar N, Kamath G, Potoff JJ (2013) Prediction of 1-octanol-water and air-water partition coefficients for nitro-aromatic compounds from molecular dynamics simulations. Phys Chem Chem Phys 15(17):6467–6474. doi:10.1039/c3cp44284e
39. Boddu VM, Abburi K, Fredricksen AJ, Maloney SW, Damavarapu R (2009) Equilibrium and column adsorption studies of 2,4-dinitroanisole (DNAN) on surface modified granular activated carbons. Environ Technol 30(2):173–181. doi:10.1080/09593330802422993
40. Boddu VM, Maloney SW (2012) Physical properties of insensitive munitions compounds for developing wastewater treatment technologies, vol 3. Air and Waste Management Association, pp 1958–1965
41. Capela D et al (2001) Analysis of the chromosome sequence of the legume symbiont Sinorhizobium meliloti strain 1021. Proc Natl Acad Sci USA 98(17):9877–9882. doi:10.1073/pnas.161294398
42. Casjens S, Huang WM (1993) Linear chromosomal physical and genetic map of Borrelia burgdorferi, the Lyme disease agent. Mol Microbiol 8(5):967–980. doi:10.1111/j.1365-2958.1993.tb01641.x
43. Cayrou C, Turenne C, Behr MA, Drancourt M (2010) Genotyping of Mycobacterium avium complex organisms using multispacer sequence typing. Microbiology 156(3):687–694. doi:10.1099/mic.0.033522-0
44. Chakka S, Boddu VM, Maloney SW, Toghiani RK, Damavarapu R (2009) Vapor pressures and melting points of select munitions compounds. American Institute of Chemical Engineers, pp chakk1/1-chakk1/9
45. Chauhan S, Tyagi JS (2011) Analysis of transcription at the oriC locus in Mycobacterium tuberculosis. Microbiol Res 166(6):508–514. doi:10.1016/j.micres.2010.10.005
46. Chiaramello AE, Zyskind JW (1990) Coupling of DNA replication to growth rate in Escherichia coli: a possible role for guanosine tetraphosphate. J Bacteriol 172(4):2013–2019
47. Cho E, Ogasawara N, Ishikawa S (2008) The functional analysis of YabA, which interacts with DnaA and regulates initiation of chromosome replication in Bacillus subtilis. Genes Genet Syst 83(2):111–125. doi:10.1266/ggs.83.111
48. Choung K-K, Estiva E, Bremer H (1981) Genetic and physiological characterization of a spontaneous mutant of Escherichia coli B/r with aberrant control of deoxyribonucleic acid replication. J Bacteriol 145(3):1239–1248
49. Cirz RT, O'Neill BM, Hammond JA, Head SR, Romesberg FE (2006) Defining the Pseudomonas aeruginosa SOS response and its role in the global response to the antibiotic ciprofloxacin. J Bacteriol 188(20):7101–7110. doi:10.1128/JB.00807-06
50. Clark MA, Baumann L, Baumann P (1998) Sequence analysis of a 34.7-kb DNA segment from the genome of Buchnera aphidicola (endosymbiont of aphids) containing groEL, dnaA, the atp operon, gidA, and rho. Curr Microbiol 36(3):158–163. doi:10.1007/PL00006760
51. Costales-Nieves C, Boddu VM, Maloney SW, Chakka S, Damavarapu R, Viswanath DS (2010) SPARC prediction of physical properties of explosive compounds. American Institute of Chemical Engineers, pp a291/1-a291/17

52. Coulouarn C, Aumasson R, Lamy-Bracq P, Bulot S (2014) Evaluation of melt-cast explosive compositions based on TNT and DNAN NEXTER Munitions. Int Annu Conf ICT 45th Energetic Materials: Particles, Processing, Applications): Coulouarn/1-Coulouarn/13, 13 pp
53. Cuddy MF, Poda AR, Chappell MA (2014) Estimations of Vapor Pressures by Thermogravimetric Analysis of the Insensitive Munitions IMX-101, IMX-104, and Individual Components. Propellants, Explos, Pyrotech 39(2):236–242. doi:10.1002/prep.201300069
54. Dodard SG et al (2013) Ecotoxicological assessment of a high energetic and insensitive munitions compound: 2,4-Dinitroanisole (DNAN). J Hazard Mater 262:143–150. doi:10.1016/j.jhazmat.2013.08.043
55. Fischer D, Klapoetke TM, Stierstorfer J (2014) Oxalylhydrazinium nitrate and dinitrate—efficiency meets performance. J Energ Mater 32(1):37–49. doi:10.1080/07370652.2012.750697
56. Golius A, Isayev O, Gorb L, Hill FC, Leszczynski J (2014) Energetic compounds as environmental contaminants: theoretical studies. American Chemical Society, p TOXI-118
57. Grau H, Gandzelko A, Samuels P (2014) Solubility determination of raw energetic materials in molten 2,4-dinitroanisole. Propellants, Explos, Pyrotech 39(4):604–608. doi:10.1002/prep.201300083
58. Hawari J et al (2015) Environmental fate of 2,4-dinitroanisole (DNAN) and its reduced products. Chemosphere 119:16–23. doi:10.1016/j.chemosphere.2014.05.047
59. Hoyt N et al (2013) Biomarkers of oral exposure to 3-nitro-1,2,4-triazol-5-one (NTO) and 2,4-dinitroanisole (DNAN) in blood and urine of rhesus macaques (Macaca mulatta). Biomarkers 18(7):587–594. doi:10.3109/1354750X.2013.829522
60. Kennedy AJ et al (2015) Inter- and intraspecies chemical sensitivity: A case study using 2,4-dinitroanisole. Environ Toxicol Chem 34(2):402–411. doi:10.1002/etc.2819
61. Kitcher E, Pavlov J, Koutsospyros A, Christodoulatos C, Braida W (2013) Reaction mechanism of the reductive removal of NTO and DNAN from IM wastewater using bimetals. American Chemical Society, p ENVR-238
62. Li Y, Hsieh W-P, Mahmudov R, Huang CP (2011) Treatment of ammunition wastewater using ultrasonic Fenton (US-Fenton) process. American Institute of Chemical Engineers, pp 399a/1–399a/16
63. Liang J, Olivares C, Field JA, Sierra-Alvarez R (2013) Microbial toxicity of the insensitive munitions compound, 2,4-dinitroanisole (DNAN), and its aromatic amine metabolites. J Hazard Mater 262:281–287. doi:10.1016/j.jhazmat.2013.08.046
64. Linker BR et al (2015) Adsorption of novel insensitive munitions compounds at clay mineral and metal oxide surfaces. Environ Chem 12(1):74–84. doi:10.1071/EN14065
65. Liu R, Zhang T, Liu Y, Yang L, Zhou Z (2013) Evaporation characteristics of low-melting nitrocompounds by isothermal thermogravimetry. J Therm Anal Calorim 112(3):1523–1532. doi:10.1007/s10973-012-2665-z
66. Liu R, Zhang T, Yang L, Zhou Z Researches on vapor pressure and thermal decomposition of low-melting explosives. In, 2013. University of Pardubice, Institute of Energetic Materials, p 441–449
67. Liu R, Zhang T, Zhou Z, Yang L (2014) Volatilization interference in thermal analysis and kinetics of low-melting organic nitro compounds. RSC Adv 4(19):9810–9818. doi:10.1039/c3ra47218c
68. Lopez-Canut V, Roca M, Bertran J, Moliner V, Tunon I (2011) Promiscuity in alkaline phosphatase superfamily. Unraveling evolution through molecular simulations. J Am Chem Soc 133(31):12050–12062. doi:10.1021/ja2017575
69. Lotufo GR, Biedenbach JM, Sims JG, Chappell P, Stanley JK, Gust KA (2015) Bioaccumulation kinetics of the conventional energetics TNT and RDX relative to insensitive munitions constituents DNAN and NTO in Rana pipiens tadpoles. Environ Toxicol Chem 34(4):880–886. doi:10.1002/etc.2863
70. Mu R, Shi H, Yuan Y, Karnjanapiboonwong A, Burken JG, Ma Y (2012) Fast separation and quantification method for nitroguanidine and 2,4-dinitroanisole by ultrafast liquid

chromatography-tandem mass spectrometry. Anal Chem 84(7):3427–3432. doi:10.1021/ac300306p

71. Mudryy R (2011) Solidification modeling of DNAN based explosive compositions. Int Annu Conf ICT 42nd(Energetic Materials):111/1–111/11
72. Muscat D et al (2000) In-source decay of hyperbranched polyesteramides in matrix-assisted laser desorption/ionization time-of-flight mass spectrometry. J Am Soc Mass Spectrom 11 (3):218–227. doi:10.1016/S1044-0305(99)00141-5
73. Niedzwiecka JB, Millerick KA, Galloway S, Schlautman MA, Finneran KT (2014) Microbially mediated 2, 4-dinitroanisole (DNAN) degradation. American Chemical Society, p ENVR-48
74. Olivares C, Liang J, Abrell L, Sierra-Alvarez R, Field JA (2013) Pathways of reductive 2,4-dinitroanisole (DNAN) biotransformation in sludge. Biotechnol Bioeng 110(6):1595–1604. doi:10.1002/bit.24820
75. Platten WE III, Bailey D, Suidan MT, Maloney SW (2010) Biological transformation pathways of 2,4-dinitro anisole and N-methyl paranitro aniline in anaerobic fluidized-bed bioreactors. Chemosphere 81(9):1131–1136. doi:10.1016/j.chemosphere.2010.08.044
76. Platten WE, III, Bailey D, Suidan MT, Maloney SW (2013) Treatment of energetic wastewater containing 2,4-dinitroanisole and N-methyl paranitro aniline. J Environ Eng 139 (1):104–109. doi:10.1061/(ASCE)EE.1943-7870.0000592
77. Provatas A, Wall C (2011) Thermal testing of 2,4-dinitroanisole (DNAN) as a TNT replacement for melt-cast explosives. Int Annu Conf ICT 42nd(Energetic Materials):6/1–6/12
78. Richard T, Weidhaas J (2014) Biodegradation of IMX-101 explosive formulation constituents: 2,4-dinitroanisole (DNAN), 3-nitro-1,2,4-triazol-5-one (NTO), and nitroguanidine. J Hazard Mater 280:372–379. doi:10.1016/j.jhazmat.2014.08.019
79. Richard T, Weidhaas J (2014) Dissolution, sorption, and phytoremediation of IMX-101 explosive formulation constituents: 2,4-dinitroanisole (DNAN), 3-nitro-1,2,4-triazol-5-one (NTO), and nitroguanidine. J Hazard Mater 280:561–569. doi:10.1016/j.jhazmat.2014.08.042
80. Russell AL, Seiter JM, Coleman JG, Winstead B, Bednar AJ (2014) Analysis of munitions constituents in IMX formulations by HPLC and HPLC-MS. Talanta 128:524–530. doi:10.1016/j.talanta.2014.02.013
81. Saad R, Radovic-Hrapovic Z, Ahvazi B, Thiboutot S, Ampleman G, Hawari J (2012) Sorption of 2,4-dinitroanisole (DNAN) on lignin. J Environ Sci 24(5):808–813. doi:10.1016/S1001-0742(11)60863-2
82. Salter-Blanc AJ, Bylaska EJ, Johnston HJ, Tratnyek PG (2015) Predicting reduction rates of energetic nitroaromatic compounds using calculated one-electron reduction potentials. Environ Sci Technol 49(6):3778–3786. doi:10.1021/es505092s
83. Salter-Blanc AJ, Bylaska EJ, Ritchie JJ, Tratnyek PG (2013) Mechanisms and kinetics of alkaline hydrolysis of the energetic nitroaromatic compounds 2,4,6-trinitrotoluene (TNT) and 2,4-dinitroanisole (DNAN). Environ Sci Technol 47(13):6790–6798. doi:10.1021/es304461t
84. Scott AM, Burns EA, Hill FC (2014) Theoretical study of adsorption of nitrogen-containing environmental contaminants on kaolinite surfaces. J Mol Model 20(8):1–13. doi:10.1007/s00894-014-2373-7
85. Scott AM, Burns EA, Hill FC (2014) Theoretical study of adsorption of nitrogen-containing environmental contaminants on kaolinite surfaces. J Mol Model 20(8):2373
86. Scott AM, Burns EA, Lafferty BJ, Hill FC (2015) Theoretical predictions of thermodynamic parameters of adsorption of nitrogen containing environmental contaminants on kaolinite. J Mol Model 21(2):1–16. doi:10.1007/s00894-015-2577-5
87. Scott AM, Burns EA, Lafferty BJ, Hill FC (2015) Theoretical predictions of thermodynamic parameters of adsorption of nitrogen containing environmental contaminants on kaolinite. J Mol Model 21(2):21

88. Shen J et al (2013) Pretreatment of 2,4-dinitroanisole (DNAN) producing wastewater using a combined zero-valent iron (ZVI) reduction and Fenton oxidation process. J Hazard Mater 260:993–1000. doi:10.1016/j.jhazmat.2013.07.003
59. Sokkalingam N, Ketko MH, Potoff JJ (2010) Physical property prediction of energetic materials from molecular dynamics simulation. CRC Press, Boca Raton, pp 37–62
90. Souza BS et al (2009) Hydrolysis of 8-quinolyl phosphate monoester: kinetic and theoretical studies of the effect of lanthanide ions. J Org Chem 74(3):1042–1053. doi:10.1021/jo801870v
91. Stanley JK, Lotufo GR, Biedenbach JM, Chappell P, Gust KA (2015) Toxicity of the conventional energetics TNT and RDX relative to new insensitive munitions constituents DNAN and NTO in Rana pipiens tadpoles. Environ Toxicol Chem 34(4):873–879. doi:10.1002/etc.2890
92. Sviatenko L et al (2014) Comprehensive investigations of kinetics of alkaline hydrolysis of 2,4,6-trinitrotoluene, 2,4-dinitrotoluene, and 2,4-dinitroanisole. Environ Sci Technol 48(17):10465–10474. doi:10.1021/es5026678
93. Taylor S, Park E, Bullion K, Dontsova K (2015) Dissolution of three insensitive munitions formulations. Chemosphere 119:342–348. doi:10.1016/j.chemosphere.2014.06.050
94. Trzcinski WA, Cudzilo S, Dyjak S, Nita M (2012) A comparison of sensitivity and performance characteristics of melt-pour explosives with TNT and DNAN binder. University of Pardubice, Institute of Energetic Materials, pp 893–901
95. Tsendra O et al (2014) Adsorption of nitrogen-containing compounds on the (100) α-quartz surface: Ab Initio cluster approach. J Phys Chem C 118(6):3023–3034. doi:10.1021/jp406827h
96. Verbenko VN, Kuznetsova LV, Luchkina LA, Klopov NV (2009) Mutation in the cspH–cspG gene cluster enhances expression of heat-shock proteins and SOS repair system of Escherichia coli. Russ J Genet 45(9):1047–1054. doi:10.1134/S102279540909004X
97. Walsh MR et al (2013) Characterization of PAX-21 insensitive munition detonation residues. Propellants, Explos, Pyrotech 38(3):399–409. doi:10.1002/prep.201200150
98. Walsh MR et al (2014) Energetic residues from the detonation of IMX-104 insensitive munitions. Propellants, Explos, Pyrotech 39(2):243–250. doi:10.1002/prep.201300095
99. Walsh MR, Walsh ME, Ramsey CA, Brochu S, Thiboutot S, Ampleman G (2013) Perchlorate contamination from the detonation of insensitive high-explosive rounds. J Hazard Mater 262:228–233
100. Xiao L-B et al (2014) Thermochemical properties of 2,4-dinitroanisole in N-methyl pyrrolidone and dimethyl sulfoxide. J Therm Anal Calorim 118(3):1755–1761. doi:10.1007/s10973-014-4042-6
101. Xing X et al (2012) Specific heat capacity, thermal behavior, and thermal hazard of 2,4-dinitroanisole. Propellants, Explos, Pyrotech 37(2):179–182. doi:10.1002/prep.201000077
102. Xu Z, Hao J, Braida W, Strickland D, Li F, Meng X (2011) Surface-enhanced Raman scattering spectroscopy of explosive 2,4-dinitroanisole using modified silver nanoparticles. Langmuir 27(22):13773–13779. doi:10.1021/la202560t
103. Zabihi-Mobarakeh H, Nezamzadeh-Ejhieh A (2015) Application of supported TiO_2 onto Iranian clinoptilolite nanoparticles in the photodegradation of mixture of aniline and 2,4-dinitroaniline aqueous solution. J Ind Eng Chem: Ahead of Print. doi:10.1016/j.jiec.2014.12.003

Chapter 5
5-Nitro-2,4-Dihydro-3H-1,2,4-Triazole-3-One (NTO)

Abstract NTO is a very attractive explosive due to its insensitivity, thermal and mechanical stability. NTO can be used to prepare melt-cast explosives (NTO-TNT mixture) as well as pressed explosives with thermoplastic binder and cast PBX charges for Insensitive Munitions. In this chapter, various synthesis processes and physico-chemical properties of NTO are discussed. A number of formulations along with there explosive properties are presented and compared with neat NTO and TNT. The toxicity, biodegradation, and detection techniques are also discussed in this chapter.

5.1 Introduction

Both 5-Nitro-2,4-dihydro-3H-1,2,4-triazole-3-one and 3-Nitro-2,4-dihydro-3H-1,2,4-triazole-5-one are abbreviated as NTO and are considered as a potential insensitive replacement for RDX in various explosive formulations. 5-Nitro-2,4-dihydro-3H-1,2,4-triazole-3-one and 3-Nitro-2,4-dihydro-3H-1,2,4-triazole-5-one are isomers, and, therefore, have similar properties. NTO is a low sensitive material and has been in use since 1980s. Its performance is slightly less than RDX, but either similar or superior to other explosives. However, the high yields and the availability of raw materials coupled with its excellent properties have made NTO a preferred material compared to TATB, RDX and HMX. NTO is thermally stable and exhibits low sensitivity to radiation damage and other stimuli. Therefore, it is relatively easy to transport and store.

5.2 Synthesis

The first reported synthesis of NTO appears to be by Manchot and Noll [1], which was followed by Chipen et al. [2]. Several synthesis routes have been developed during 1980s. Synthesis of NTO is a two step process. In the first step triazol-3-one

D.S. Viswanath et al., *Emerging Energetic Materials: Synthesis, Physicochemical, and Detonation Properties*, https://doi.org/10.1007/978-94-024-1201-7_5

(TO) is produced. In the second step TO undergoes nitration to produce NTO. Attempts were made to produce TO by reacting acetone semicarbazone with formic acid, semicarbazide hydrochloride (SC) with formic acid or with triethylorthoformate [3]. However, the best method for synthesis of TO was found to be via reaction of SC with formic acid.

Smith and Cliff [3] discussed various procedures for synthesis of NTO, and gave details of a method adopted by Australian researchers. The simplest method appears to be the condensation of SC with formic acid forming triazolone, followed by nitration to TO forming NTO. Reactions are shown in Fig. 5.1.

As pointed out by Smith and Cliff [3], this reaction takes place at a very desirable temperature of 338 K with yields approaching 80%. A detailed study of the kinetics of nitration of 1,2,4-triazol-5-one using 70–100% nitric acid has been undertaken by Zbarsky and Yudin [4]. It is interesting to note that the yield of NTO did not depend on temperature in the range of 273–303 K and the reaction time, which was independent of both the initial acid concentration in the range from 90 to 98% HNO_3 and the ratio of HNO_3 to triazol-3-one (TO) in the range of 4–8 mol HNO_3 per mole TO. They also reported that the yield dropped significantly in 98% HNO_3 if the HNO_3 to TO ratio was greater than 10. Mukundan et al. [5] followed the same synthesis route and obtained pure NTO with 80% yield by crystallization from water. Singh et al. [6] used the same reaction scheme but used 70% nitric acid for nitration of TO to NTO.

The Defence Science & Technology Organisation Aeronautical and Maritime Research Laboratory of Australia [7] used a similar scheme for preparation of NTO. In their one-pot synthesis route, formic acid and SC mixed at ambient temperature

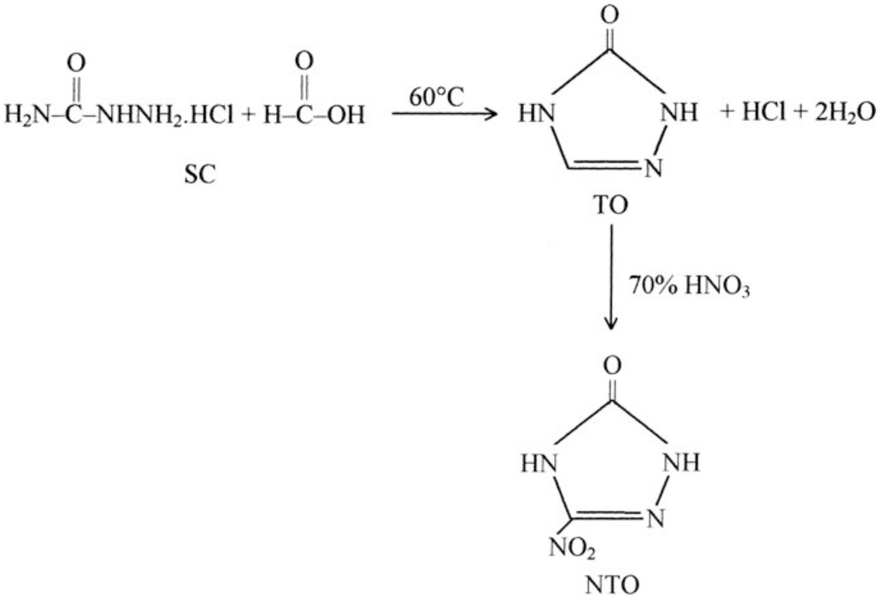

Fig. 5.1 Reaction scheme for the synthesis of NTO

in the ratio of 8:3 (formic acid:SC). The intermediate compound was obtained by stirring the mixture at 338 K. The nitration was carried out using a mixture of neat nitric acid and 98% sulfuric acid (5:1 ratio). The final product NTO was obtained by recrystallization from hot water with a 77% yield.

Li [8] also employed the one-pot synthesis route for preparation of NTO. In his process, cyclocondensation of semicarbazide with formic acid followed by nitration provided an yield of 76.8% NTO. Kim et al. described [9] the preparation of NTO by mixing 1,2,4-triazol-5-one with a mixture of 98% sulfuric acid and 70% nitric acid in a reactor at 298 K., and then raising the temperature to 308–318 K. The temperature was maintained in this range to generate a crystal nucleus of 3-nitro-1,2,4-triazol-5-one and the reaction was completed by heating the reaction mixture to 333–343 K.

Spears et al. [7] reviewed the preparation of NTO by various researchers who used different ratios of semicarbazide, formic acid, nitric acid, and mixtures of sulfuric and nitric acid under different experimental conditions. The yields varied from 36 to 75% based on semicarbazide. These reaction schemes for the preparation of NTO from TO summarized by Spears et al. [7] are given in Fig. 5.2.

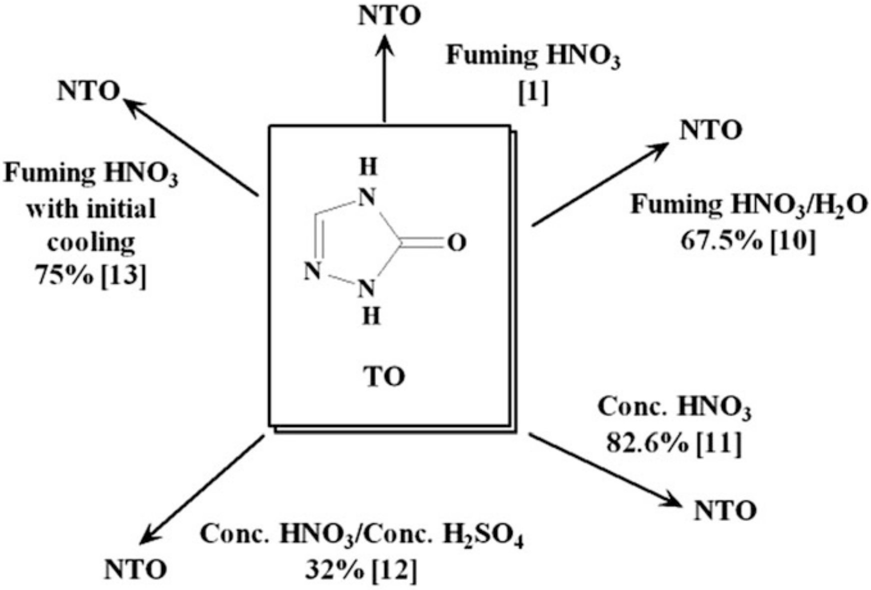

[10] Chipen GI, Bokalder RP, Grinshtein VYa (1966) 1,2,4-Triazol-3-one and its Nitro and Amino Derivatives. Chemistry of Heterocyclic Compounds 2(1):79-83

[11] Lee K-Y, Coburn MD (1985) 3-Nitro-1,2,4-triazol-5-one, a less sensitive explosive. Los Alamos National Laboratory Report No LA-10302-MS

[12] Kroger CF, Miethchen R, Frank H, Soemer M, Pilz S (1969) 1, 2, 4-triazoles. 17. nitration and bromination of 1, 2, 4-triazolones. chemische berichte 102(3):755

[13] Katritzky R, Ogretir C (1982) The Kinetic Nitration and Baskity of 1,2,4-Triazol-5-ones. Chimica Acta Tureica 10:137-146

Fig. 5.2 Methods for synthesis of NTO from TO [7, 13]

The nanosize particles offer lower sensitivity to various stimuli and can enhance performance of energetic materials. Yang et al. [14] prepared NTO nano particles using spray freezing technique from 90% pure neat NTO. Several techniques including scanning electron and atomic force microscopy, X-ray diffraction, thermogravimetric analysis, and differential and scanning calorimetry were used to characterize the particles. The results show that NTO particles have an elongated shape with a size of 70–90 nm. The SEM obtained by the authors is shown in Fig. 5.3, and the thermogravimetric and DSC results in Fig. 5.4. The DSC data showed the decomposition of nanoparticles in the temperature range of 513–543 K that is 16 K lower than the microsize particles. The TGA data also showed that the mass loss of nanoparticles started at a temperature 40 K lower than microparticles, suggesting that nanoparticles are more sensitive than micro-size particles.

Wang et al. [15] employed a reverse microemulsion of solvent evaporation method to prepare nanoparticles of NTO. An n-alkanol was used as a co-surfactant. The mass ratio between surfactant and co-surfactant was 7:1 and the water content of the solution was 24%. The experiment was carried out at 298–303 K under a vacuum between −0.6 and −0.85 MPa. The particle size of NTO produced by this method was in the range of 10–30 nm.

Several authors have reviewed the literature for the synthesis of NTO. Ma et al. [16], along with the review of the synthesis process, also discussed various properties of NTO. These included crystal structure, thermal behaviors, toxicity and various compounds of NTO with alkali, alkaline earth, transition metals and rare

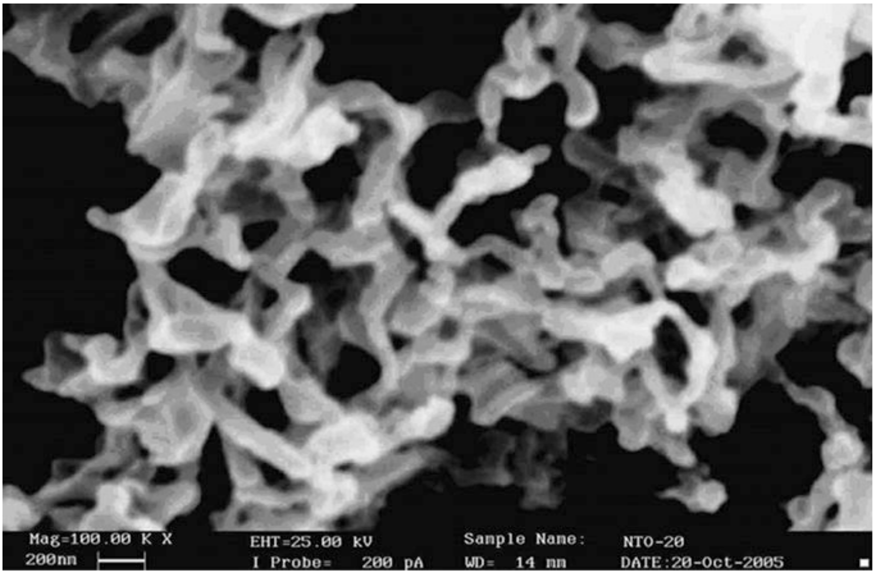

Fig. 5.3 Scanning electron micrograph of nano-NTO (with permission from [14])

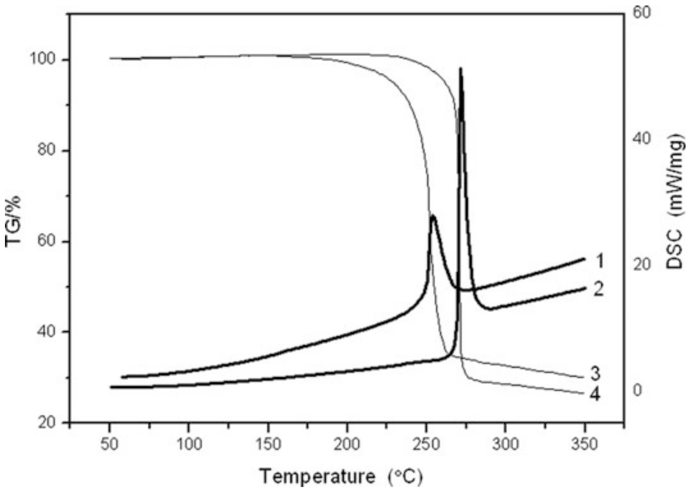

Fig. 5.4 Thermal analysis results of micro-NTO and nano-NTO. (*1* DSC curve of nano-NTO; *2* DSC curve of micro-NTO; *3* TG curve of nano-NTO; *4* TG curve of micro-NTO) (with permission from [14])

earth metals. Smith and Cliff [3] reviewed NTO based explosive formulations. They also discussed various chemical and physical properties of NTO, and explosive characteristics.

5.3 Structure

Crystalline NTO exists in two polymorph forms—α and β, with α being the dominant polymorph and more stable. The different forms are obtained by using different crystallization techniques.

Lee and Gilardi [17] prepared α-NTO by slow cooling of a hot solution of NTO in water, followed by refrigeration. The crystals appear as long needles. For preparation of β-NTO, recrystallization from methanol or a mixed ethanol/dichloromethane solvent was employed. They noted that β-NTO prepared this way remained stable for six month after which it decomposed. As noted by Lee and Gilardi [17], β-NTO can also be prepared by cooling from a hot aqueous solution of NTO, but large enough quantities could not be obtained by this method. They studied the XRD patterns of both α and β polymorphs of NTO and provided the lattice parameters. The lattice parameters are shown in Table 5.1 and the XRD pattern in Fig. 5.5. Bolotina et al. [18] also studied the crystal structure of the metastable α form at 298 K, and that of β-NTO as a function of temperature from 100 to 298 K [19]. Their results are compared in the same Table 5.1. Both the research groups obtained similar results.

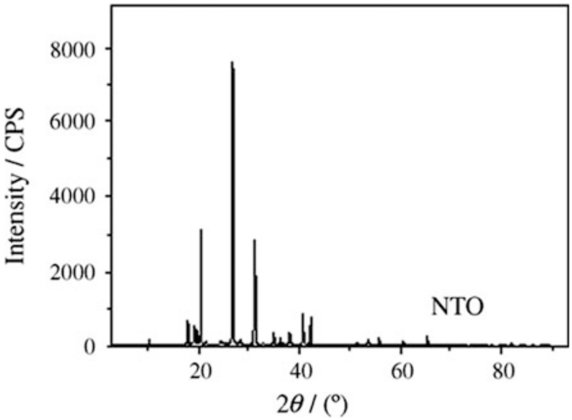

Fig. 5.5 XRD pattern of NTO [20]

Table 5.1 Lattice parameters of α and β polymorphs of NTO [18]

Crystal polymorph	α	β
Space group	P1	$P2_1/C$
Unit cell	Triclinic, 8 molecules/cell	Monoclinic, 4 molecules/cell
a (Å)	5.12	9.236
b (Å)	10.30	5.513
c (Å)	17.9	9.107
α (°)	106.7	
β (°)	97.7	100.77
γ (°)	90.2	
Density (g/cm^3)	1.92	1.878

The work of Bolotina et al. [19] with β-form revealed some interesting information. Although the β-form is solid from 100 to 298 K, the density of the β-form varied from 1.926 at 100 K to 1.876 at 298 K.

5.4 Properties

Various physical and chemical properties of NTO are summarized in Table 5.2. A detailed discussion of some of these properties is provided in the following sections.

5.4.1 *Heat Capacity and Entropy*

Osmont et al. [26] computed the ideal gas heat capacity and entropy using B3LYP/6-31G(d,p)//B3LYP/6-31G(d,p) technique based on the density function theory.

Table 5.2 Chemical and physical properties of NTO

Common chemical formula	5-Nitro-2,4-dihydro-3H-1,2,4-triazole-3-one
Other names	5-oxy-3-nitro-1,2,4-triazol-5-(ONTA); 5-nitro-2,4-dihydro-3H-1,2,4-triazol-3-one (NTO)
CAS no.	932-64-9 [NTO 3, 5]
Empirical formula	$C_2H_2N_4O_3$
Structural formula	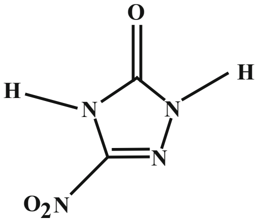
Molecular mass	130
Density (gcm^{-3})	1.93 [21]; 2.46 [22];1.911 [23]
Molar volume (cm^{3}mol^{-1})	52.7 ± 7.0 [22]
Boiling point (K)	568 [23]
Melting point (K)	539.35 [23] 543 [21]; 546 [24] 547.9 [24]
Auto-ignition temperature (K)	538.2 [24]
Critical temperature (K)	829 [23]
Critical pressure	86.0 [23]
Acentric factor	0.798 [23]
Log Kow	0.82; −1.19 [23]
Koc	1.0 to 4.24 @ pH 10 to 1 [22]
pKa	3.67 [1]; 3.78 [4] 4.7 ± 020 [22]
	−2.09 ± 0.20 [18] Basic
Vapor pressure	log P = −1.375 ± 0.656 [22] Liquid: ln P = 14.82 − 9914.4/T pressure in MPa [24] Solid: lnP = −12984.4/T + 20.48 [24]
Enthalpy of formation (kJmol^{-1})	−59.83 [24]; −117.21 [21]; −100.7 [25]; −30.927 kcal mol^{-1} [7]
Enthalpy of formation (gas phase), (kcal/mol)	−0.9 [22]; −3.2 and −5.7 [7]
Enthalpy of combustion (kJmol^{-1})	−943.4 to −995.7 [20]
Enthalpy of vaporization (kJmol^{-1})	82.4 [20]
Enthalpy of sublimation (kJmol^{-1})	110.5 [23]
Enthalpy of fusion (kJmol^{-1})	28.0 [20]; 20.17 [19]; 27 [23]; 92.8 [24]
Enthalpy of explosion (kJ/mol)	4100; 409.2 [25]
Specific energy (kJ/mol)	122.9 [25]
Heat capacity (J g^{-1} k^{-1})	1.46 [24]
LD$_{50}$ rats and mice (g/kg)	5
Velocity of detonation (ms^{-1})	8564 [2]
Aqueous solubility (g/l)	7.56; 9.97 @ 25 °C [1]; 49 [26]; in acetone 18 g/l; in DMSO 625 g/l [26]

Table 5.3 Ideal gas heat capacity and entropy [26]

Heat capacity			
Temperature (K)	C_p (cal mol^{-1} K^{-1})	Temperature (K)	C_p (cal mol^{-1} K^{-1})
300	28.1	2000	58.1
400	34.2	2500	59.2
500	39.1	3000	59.9
600	42.9	3500	60.3
800	48.1	4000	60.6
1000	51.4	4500	60.8
1500	55.9	5000	61.0
Entropy			
Temperature (K)	S (cal mol^{-1} K^{-1})	Temperature (K)	S (cal mol^{-1} K^{-1})
300	85.2	2000	172.4
400	94.2	2500	185.5
500	102.4	3000	196.3
600	109.9	3500	205.6
800	123.0	4000	213.7
1000	134.1	4500	220.8
1500	156.0	5000	227.3

The harmonic oscillator rigid rotator approximation was used in these calculations. They found that the contribution due to harmonic molecular motions, in particular internal rotations, is negligible. The values of the heat capacity and entropy calculated at various temperatures are given in Table 5.3.

Li et al. [27] proposed the following equation for calculation of specific heat capacity of NTO in the temperature range of 283–353 K.

$$C_P = 0.2806 + 2.7103 \times 10^{-3} T \tag{5.1}$$

They used the standard molar heat capacity of NTO as 141.53 J/mol/K at 298.15 K and then using the Cp–temperature data, thermodynamic functions (enthalpy, entropy and Gibbs free energy) of NTO between 283 and 353 K, relative to the standard temperature 298.15 K, the heat capacities were determined.

5.4.2 *Solubility*

NTO is soluble in a number of solvent including water, acetone, and acetonitrile. The solubility data of NTO in various solvent compiled by Smith and Cliff [3] is given in Table 5.4.

Table 5.4 Solubility in different solvents [3]

Solvent	Temperature (°C)	Solubility (g/100 ml)
Water	4.85	0.72
	18.95	1.28
	43.3	2.60
	100	∼10
Acetone	18.95	1.68
Ethyl acetate	18.95	0.28
Dichloromethane	18.95	<0.02

Table 5.5 Experimental mole fraction solubility x of NTO in water [28]

Mole fraction (x)	Temperature (K)	Mole fraction (x)	Temperature (K)
0.001 383	284.65	0.012 308	351.85
0.002 762	307.05	0.013 657	356.05
0.004 137	319.65	0.015 002	358.45
0.005 508	327.95	0.016 344	361.95
0.006 875	334.85	0.017 682	364.25
0.008 239	340.55	0.019 016	366.75
0.009 599	345.45	0.020 347	367.55
0.010 956	349.65		

Kim et al. [28] measured the density and solubility of NTO in water over a range of temperature. The purity of NTO is stated to be better than 99.93 mol% and the accuracy of mass measurements was better than ±0.0001 g, and that of mole fractions was better than $\pm 2 \times 10^{-4}$. Both the solubility and density of NTO was reported as the mole fraction of NTO in water. Their data on solubility and density of NTO in water are shown in Tables 5.5 and 5.6.

Kim et al. [28] also correlated the solubility data to an exponential equation and is given below:

$$x = 1.429 \times 10^{-7} e^{0.0322} \tag{5.2}$$

where, x is the solubility, and T is temperature in K.

The suggested correlation for density calculation is as follows:

$$\rho = 1166.74 + 427.75x - 0.5508T + 5.9576xT \tag{5.3}$$

where ρ is in (kg/m^3), T is in K and x is the mole fraction. The data predicted by these two correlations are compared with the experimental data in Figs. 5.6 and 5.7.

Zbarsky and Yudin [4] studied the solubility of NTO in water and water-nitric acid mixtures. They measured the solubility during both cooling cycle (leading to crystallization of NTO from the solution) and heating cycle (disappearance of the

Table 5.6 Experimental densities for xNTO+ $(1 - x)H_2O$ [28]

$10^2\ x$	T (K)	ρ (kg/m^3)	$10^2\ x$	T (K)	ρ (kg/m^3)
0.2762	308.15	1003.3	0.5508	363.15	981.1
0.2762	313.35	1000.8	0.5508	368.15	978.5
0.2762	318.15	997.9	0.8239	333.15	1003.2
0.2762	323.15	995.2	0.8239	338.15	1000.8
0.2762	328.15	992.5	0.8239	343.15	998.3
0.2762	333.15	989. 8	0.8239	348.15	995.8
0.2762	338.15	987.0	0.8239	353.15	993.7
0.2762	343.15	984.1	0.8239	358.15	990.9
0.2762	348.15	981.6	0.8239	363.15	988.3
0.2762	353.15	979.1	0.8239	368.15	985.8
0.2762	358.15	976.4	1.0956	343.15	1003.9
0.2762	363.15	973.7	1.0956	348.15	1002.1
0.2762	368.15	971.0	1.0956	353.15	999.9
0.5508	328.15	999.4	1.0956	358.15	997.6
0.5508	333.15	996.4	1.0956	363.15	995.2
0.5508	338.15	993.8	1.0956	368.15	992.8
0.5508	343.15	990.6	1.3657	353.15	1006.5
0.5508	348.15	988.0	1.3657	358.15	1004.2
0.5508	353.15	985.9	1.3657	363.15	1001.9
0.5508	358.15	984.0	1.3657	368.15	999.6

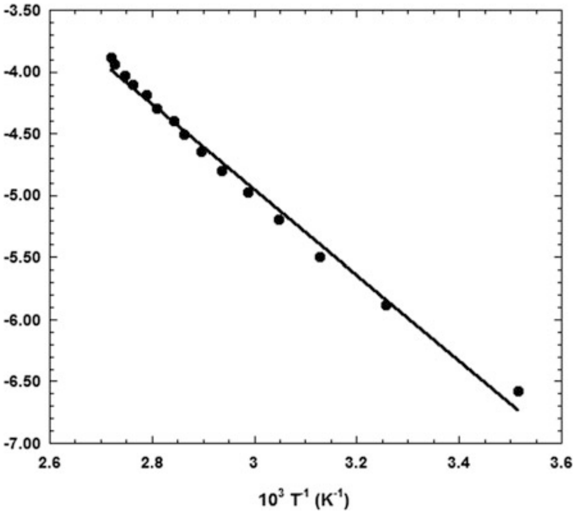

Fig. 5.6 Mole fraction of NTO (in natural log scale) as a function of reciprocal of temperature [28]

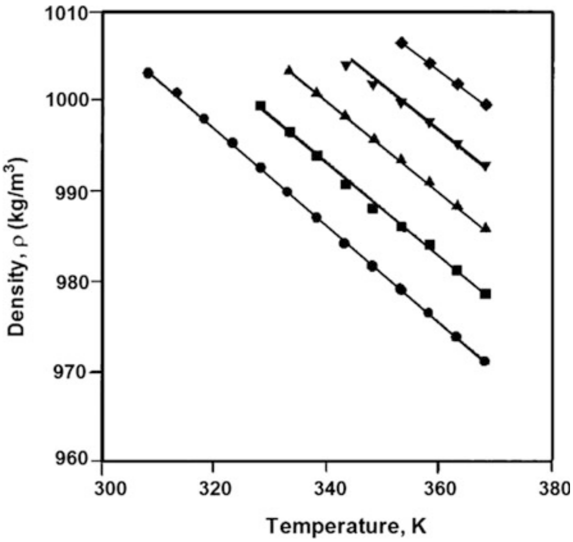

Fig. 5.7 Density of NTO aqueous solutions as a function of mole fraction *x*: (*filled circle*) x = 0.002 762, (*filled square*) x = 0.005 508, (*filled up triangle*) x = 0.008 249, (*filled down triangle*) x = 0.010 956, (*filled diamond*) x = 0.013 657 [28]

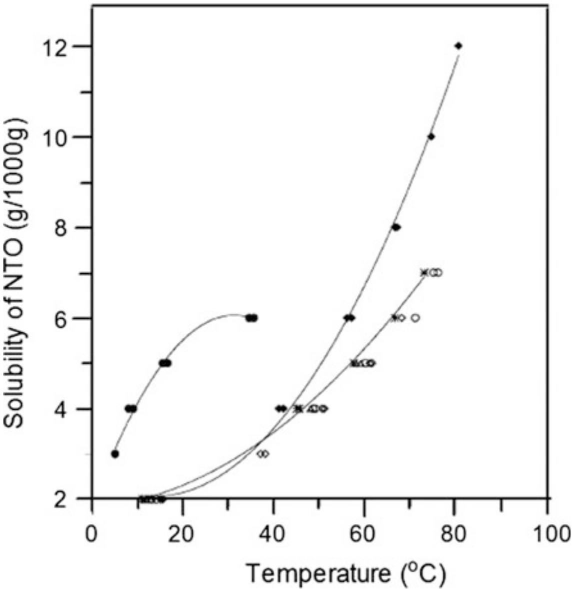

Fig. 5.8 Solubility of NTO in different concentrations of nitric acid. *Asterisk*: 33.3% HNO_3; *white diamond*: 51.8% HNO_3; *white circle*: 61.0% HNO_3; *white triangle*: 69.1% HNO_3; *filled circle*: 80.5% HNO_3; *filled diamond*: water. With permission from [4]

solid crystal from the solution). They correlated the mole fraction of NTO in the solution according to the Shreader equation and evaluated the enthalpy of dissolutions during cooling and heating. Figures 5.8 and 5.9 show the solubility data at different temperatures and concentrations of nitric acid. The results indicate that the solubility increases with temperature as expected but is independent of concentration.

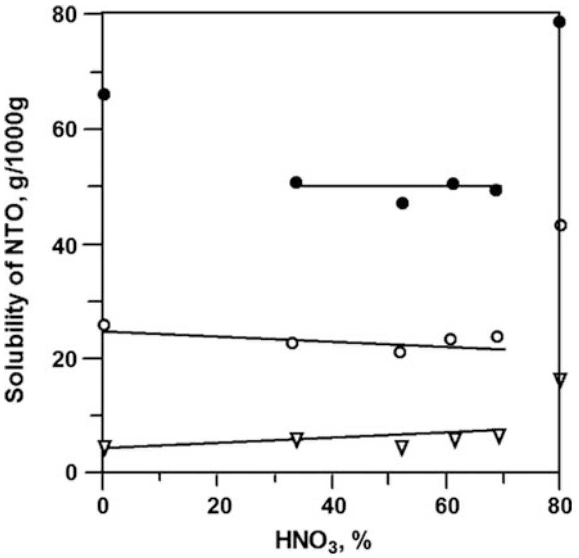

Fig. 5.9 Solubility of NTO in nitric acid at different temperatures. *White triangle*: 0 °C; *white circle*: 40 °C; *filled circle*: 70 °C. With permission from [4]

A number of researchers have used variations of the density function theories for estimation of various properties of NTO. These include estimation of thermodynamic properties [29], study of dimer and their energetics [30], study of NTO-water interactions [31], study of NTO-ammonia interactions [32], and determination of structural parameters.

5.4.3 Vapor Pressure of NTO

Sinditskii et al. [24] reported a limited number of experimental vapor pressure data of NTO. They also calculated the NTO vapor pressure above the liquid and solid phases from the heat of sublimation and taking into account the equality of the vapor pressure above the liquid and solid phases at the melting point. Their experimental and predicted vapor pressure data are given in Fig. 5.10. They proposed following expressions for estimation of the vapor pressure.

The expression for calculating vapor pressure above the liquid is given by:

$$\ln P = 14.82 - \frac{9914.4}{T} \tag{5.4}$$

The expression for calculating vapor pressure above the solid is given by:

$$\ln P = 20.48 - \frac{12984.4}{T} \tag{5.5}$$

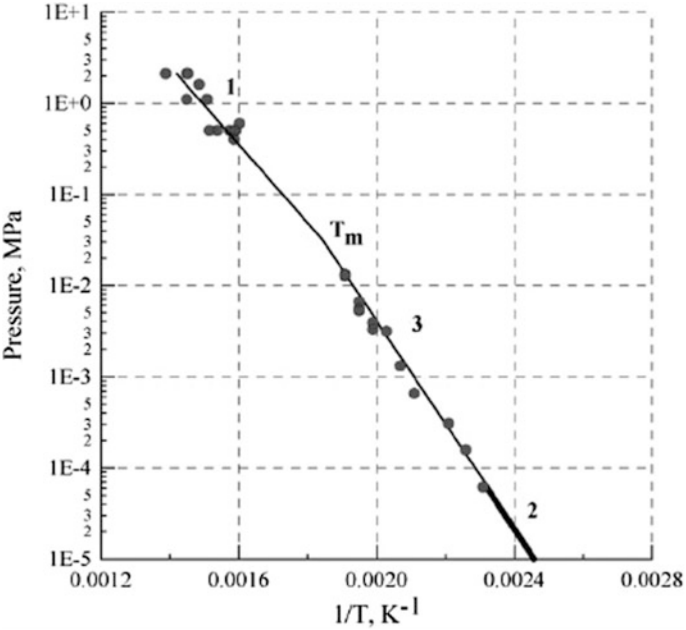

Fig. 5.10 Vapor pressure as a function of reciprocal temperature: *1* (*points* and *line*)—NTO surface temperature, *2* (*line*)—vapor pressure above solid NTO, calculated from [8], *3* (*points*)—initial vapor pressures of NTO in glass Bourdon gauge in experiments on NTO decomposition. With permission from [24]

The calculated vapor pressure data from these two expressions are also given in Fig. 5.10 for comparison.

5.5 Decomposition and Destruction

NTO can be destructed thermally, chemically by reacting it with other compounds, photochemically, and through biological degradation. Generally, the thermal decomposition process depends on temperature and pressure. However, other factors, such as phase change during decomposition, can alter the reaction path ways. As a result, there are significant disagreements among researchers on the decomposition reaction pathways and consequently on decomposition reaction rates. Singh et al. [6] provided an excellent review of the thermolysis and mechanism of NTO degradation. These decomposition pathways may be described as follows:

1. First step involving the thermal decomposition of NTO in which the C–NO_2 bond breaks. This can happen by direct thermal activation [33, 34] or catalysis by H atom transfer and loss of HONO [35].

2. Decomposition by producing CO_2 and N_2O [36, 37].
3. Decomposition by producing CO_2 and N_2 as gaseous products [38].
4. Decomposition by producing small amount of NO_2 and HONO [38].
5. No production of NO_2 or HONO [39].

Rothgery et al. [33] studied the thermal decomposition of NTO using DSC, TGA-MS, and ARC. Based on the analysis of the decomposition products, they suggested the following decomposition reaction:

$$\begin{aligned} C_2H_2N_4O_3\,(s) \rightarrow & \frac{1}{6}C_2H_3O(s) + \frac{1}{6}H_2O(l) + \frac{1}{3}CO_2(g) \\ & + \frac{1}{3}N_2O(g) + \frac{3}{2}CO(g) + \frac{4}{3}N_2(g) + \frac{1}{6}NO(g) + \frac{7}{12}H_2(g) \end{aligned} \tag{5.6}$$

Prabhakaran et al. [37] also studied the thermal decomposition of NTO using TGA, DTA, IR, DSC, XRD and hot stage microscopy. The gaseous product evolved during the decomposition was analyzed by IR. The compounds that were identified in the gas phase included CO_2, NO_2, NO and N_2O in larger amounts. However, small amounts of CO and HCN were also detected.

Meredith et al. [40] reviewed the decomposition pathways that are proposed by several researchers. Ostmark et al. [41, 42] suggested that the decomposition is initiated through the loss of NO_2 group, whereas Oxley et al. [35] noted that HONO group was lost first (Figs. 5.11 and 5.12).

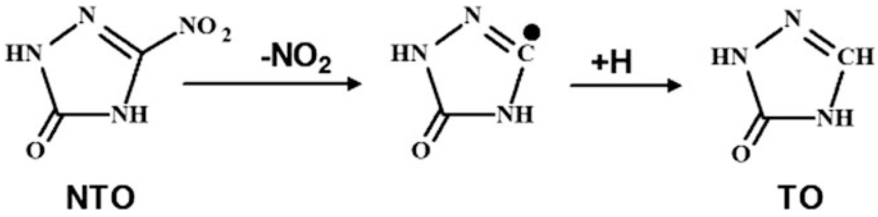

Fig. 5.11 NTO decomposition path suggested by Ostmark et al. [41]

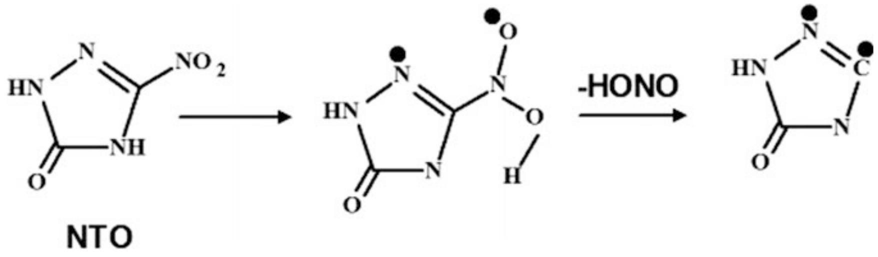

Fig. 5.12 NTO decomposition path suggested by Oxley et al. [35]

The decomposition pathways suggested by Beardall et al. [43] involved ring opening as shown in Fig. 5.13.

A migration of nitro group followed by breakdown of the triazole ring, as shown in Fig. 5.14, was the proposed decomposition pathway by Oxley et al. [44].

Menapace et al. [45] studied thermochemical and photochemical decomposition of NTO and per deuterio NTO (NTO-d_2) using electron paramagnetic resonance (EPR) and high performance liquid chromatography (HPLC). They identified several intermediates. The EPR data during photochemical decomposition of NTO (NTO-d_2)/acetone (acetone-d_6) solutions at room temperature showed the presence of NTO hydroxy nitroxide radicals. The NTO nitro group abstracts hydrogen atoms from other NTO species and/or acetone forming these radicals. The reaction pathway for the above concept in which NO_2 group on NTO removes hydrogen atoms from other NTO species and/or from acetone is shown in Fig. 5.15.

The decomposition of NTO can be accomplished from its aqueous and methanol solutions. Oxley et al. [35] prepared solutions containing 4 wt% NTO in water and in methanol and observed decompositions of NTO to be first order (up to 70% conversion) in the temperature range of 240–280 °C. The decomposition rates were generally faster than those of neat NTO. However, 50 mg of solid NTO decomposed four times faster than those of 100 mg NTO in water or in methanol solution. The concentration of NTO in water or in methanol had negligible effect on exhibited the decomposition rate at 260 °C. They also reported higher

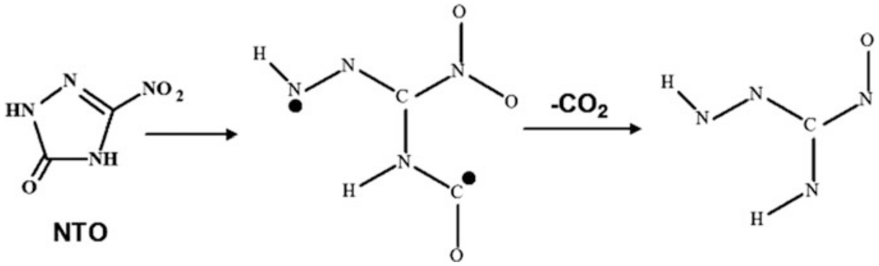

Fig. 5.13 Decomposition of NTO through ring opening [43]

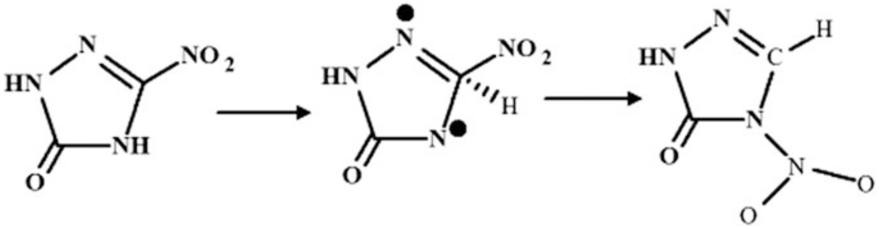

Fig. 5.14 Migration of NO_2 group during decomposition of NTO [44]

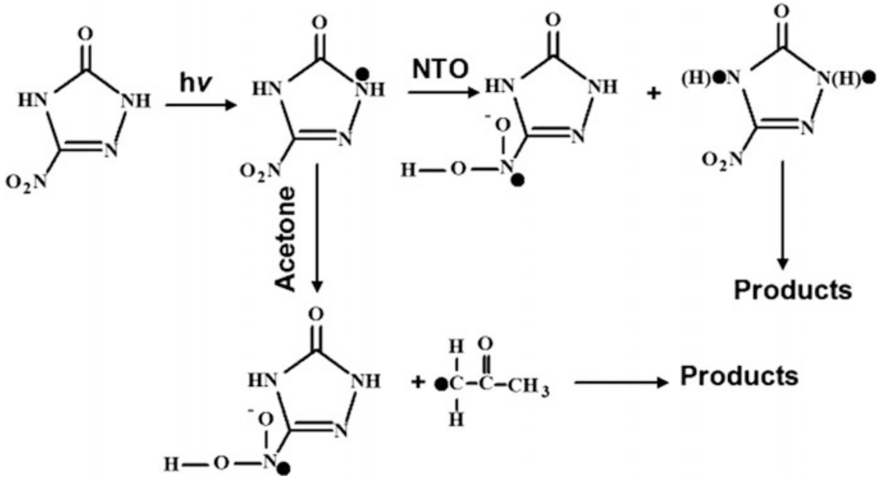

Fig. 5.15 Thermo and photochemical destruction of NTO

decomposition rate in the presence of either NO_2, NH_3, nitric acid, 50 wt% ammonium nitrate or TO.

Interestingly, Zbarsky and Yudin [4] noted that NTO can also be decomposed in 100% nitric acid. They noted that at HNO_3 concentrations of 98–100%, the decomposition rate of N-NTO was higher than the rate of NTO formation.

5.5.1 Laser Induced Decomposition

In this method, solid samples of NTO were decomposed using 7 ns pulses from a Nd:YAG laser (Quantel 660-50) applied normal to the surface of the pellet at 266 nm wavelength. The gaseous products released during decomposition are detected using 118 nm single-photon ionization in a time-of-flight mass spectrometer [46]. The decomposition products are given in Table 5.7.

Table 5.7 Identification of products following laser-induced decomposition of NTO [46]

Observed (m/z)	Proposed product
56	from 84?
71	CN_3OH
83–85	C_2N_3OHx, $x = 1–3$
100	$C_2N_3O_2H_2$
101	$C_2N_3O_2H_3$
114	$C_2N_4O_2H_2$
130	NTO, $C_2N_4O_3H_2$

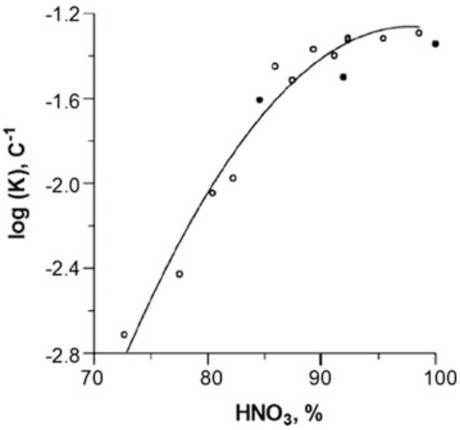

Fig. 5.16 Rate constant for NTO formation at 25 °C during nitration reaction. *Filled circle*: from N-NTO; *white circle*: from TO. With permission from [4]

Table 5.8 Parameters of the Arrhenius equation for triazol-3-one nitration and NTO decomposition. [4]

Reaction	HNO_3(%)	A (s^{-1})	E (kJ/mol)
Nitration	77.9	1.06e13	86.0
Nitration	89.27	1.13e12	76.5
Nitration	100	2.02e10	66.8
Destruction	100	6.89e12	78.5

5.6 Nitration Kinetics

Zbarsky and Yudin [4] studied the kinetics of nitration of N-NTO and TO to NTO. The reaction followed first-order reaction in both the cases, and was found to be dependent on both the concentration and temperature. Figure 5.16 shows the dependence of rate constant on the concentration of HNO_3 at 25 °C, and the Arrhenius parameters are shown in Table 5.8. The Arrhenius equation is written as follows:

$$\ln k = \ln A - \frac{E}{RT} \tag{5.7}$$

5.7 Decomposition Kinetic Rates

A number of studies focused on determining the decomposition rate of NTO. Most of the researchers agreed on a first-order reaction rate. Kondrikov et al. [47] studied thermal decomposition of NTO/3-5 in the temperature range of 473–533 K. According to them, the overall decomposition reaction includes two distinct stages:

Table 5.9 Arrhenius parameters reported by various researchers for first order decomposition rate equation [47]

E (kcal/mol)	ln A (S^{-1})	T (°C)	Method	References
40.7	26.9	100–137	NO Chemiluminescence	[49]
44.8	38.3	229–246	ITGA, Avrami-Erofeev Equation	[37]
49.3	47.6	195–210	IR	[37]
50.2	44.5	229–246	ITGA[a]	[37]
78.1	67.0	220–280	HPLC	[50]
87.5 ± 1.8	77.8[b]	225–245	HPLC	[45]
120.4	112.1	266–280	DSC	[51]

[a] TGA data in Ref. [37] recalculated using second order rate model in Ref. [45]
[b] Calculated from data given in Ref. [45]

the fast first-order decomposition and the subsequent autocatalytic reaction. Oxley et al. [35] also reported a similar observation. The noted that the decomposition reaction followed the first-order reaction up to 20% decomposition, and it was autocatalytic after 50% conversion. The first order rate constants were calculated using only the first 20% of the decomposition data. Arrhenius parameters reported by various researchers for the first order reaction vary widely from each other. The parameters are given in Table 5.9.

Vakul'skaya et al. [52] studied the tautomerism in their work on the electro-chemical reduction of NTO. This study sheds light on the mechanism of breakup of NTO and the radical formation. This study and their earlier studies [53, 54] should be useful in assessing the formation of compounds during NTO degradation.

The manufacture of NTO contaminates various process streams during its manufacturing and generates industrial wastes that need to be remediated before discharging to the environment. Generally the recovery of NTO from these streams is not economical due to its low concentration in the streams. The degradation of NTO to less harmful chemicals is desirable. Besides thermal degradation, photo-catalytic or biodegradation is a promising method. However it is important to assess the products of such degradation as NTO involves the reduction of the nitro group, which can be accompanied by the formation of toxic intermediates such as primary amines and hydroxylamines.

5.8 Photocatalytic Degradation

Campion et al. [55] noted complete destruction of 150 mg/L of NTO in 3 h when the solution was irradiated at 290 nm in the presence of 0.4 g/L of TiO_2. They did not observe significant photo-degradation of NTO in the absence of the catalyst. They also applied Fenton reaction for degradation of NTO. In this reaction, a

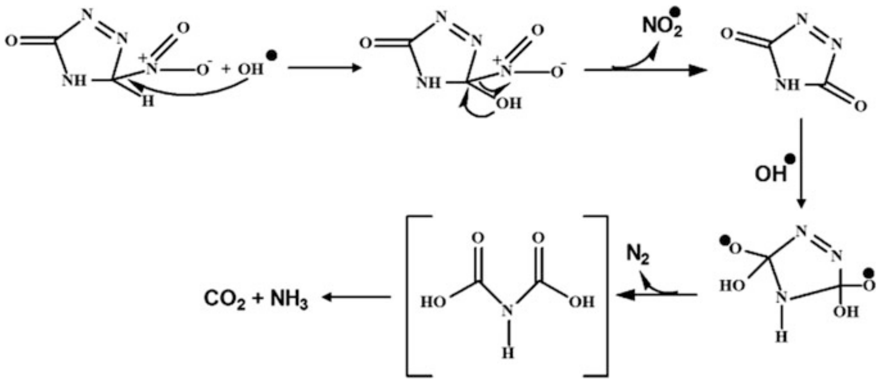

Fig. 5.17 Mechanism for degradation of NTO by hydroxyl radical ($OH^{\cdot}$) as proposed by Campion et al. [55]

mixture of a ferrous salt and hydrogen peroxide is used to degrade NTO. The reaction mechanism hypothesized by Campion et al. [55] is shown in Fig. 5.17. The Fenton reaction converted NTO to CO_2, nitrates and probably ammonium ions. No harmful intermediates were detected. A mixture of 1% H_2O_2 and 80 mg/L of $FeSO_4$ degraded 150 mg/L NTO in 5 min.

5.9 Biodegradation of NTO

Selected microorganisms can degrade NTO from industrial waste streams. Campion et al. [56] used a *Bacillus licheniformis* strain, isolated from the contaminated solutions, to biodegradation NTO from a 15 g/l solution. The biodegradation process proceeded through the nitro-reduction of NTO, followed by the ring cleavage of the formed primary amine 5-amino-1,2,4-triazol-3-one (ATO). The final biodegraded products included carbon dioxide (40%), urea and a polar compound, assumed to be hydroxyurea. The assumed biodegradation path is shown in Fig. 5.18.

Sarlauskas et al. [57] studied the enzymatic reduction of NTO and ANTA relevant to their cytotoxicity. Three mechanisms were studied that included oxyhemoglobin oxidation and single- and two-electron reduction by flavoenzymes. The

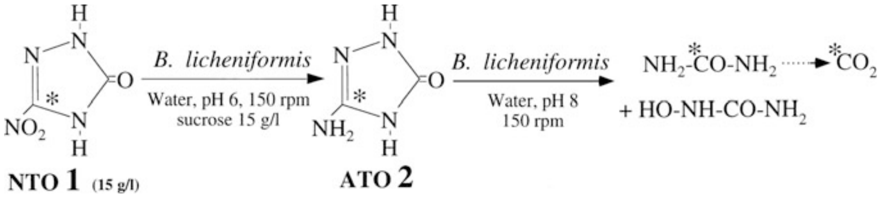

Fig. 5.18 Mechanism for biodegradation of NTO

direct oxidation converted oxyhemoglobin into methemoglobin. The single-electron reduction involved flavoenzymes dehydrogenases-electrontransferases NADPH: cytochrome P-450 reductase (P-450R) and ferredoxin: NADP+reductase (FNR) that facilitated the free radical formation of nitroaromatic compounds and their redox cycling. The two-electron reduction was carried out using rat NAD (P)H: quinone oxidoreductase (DT-diaphorase, NQO1) and *Enterobacter cloacae* NAD(P)H-: nitroreductase (NR). These enzymes reduce nitroaromatics to the corresponding hydroxylamines.

5.10 Spectroscopic Analysis of NTO

The IR and Raman spectra are important tools for analysis and identification of chemical compounds. Hiyoshi et al. [58] have obtained the IR and Raman spectra and their assignments for NTO. These spectra are shown in Fig. 5.19 and wavelengths at which the peaks are observed are given in Table 5.10.

They also recorded Raman and IR spectra for NTO labeled with isotopes ^{15}N, ^{13}C, and deuterium (D). The Ab initio calculations showed a close agreement between the predicted values and experimental data.

Lewis et al. [59] obtained Stokes the Raman Spectra of NTO with 785 and 830 nm excitation. They used commercial samples obtained from the Federal

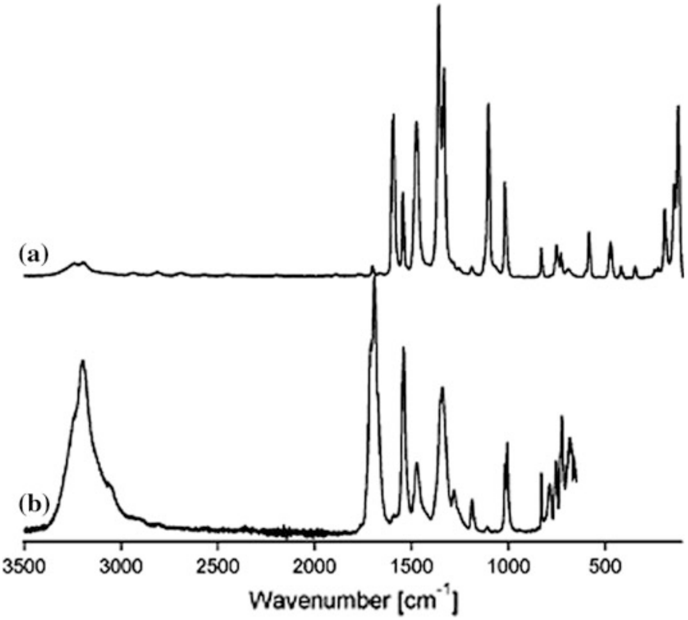

Fig. 5.19 IR and Raman spectra of NTO. **a** Raman spectrum was taken at 532 nm (~1 mW), with resolution of 2–5 cm^{-1}. **b** IR spectrum with a resolution of 1 cm^{-1} [58]

Table 5.10 Wave number of NTO for Raman and IR shifts for Fig. 5.19

Peak locations during Raman shift (cm^{-1})		Peak locations in IR spectrum (cm^{-1})	
146	1009 sh	682	1340
192	1018	723	1355 sh
227	1104	731	1473
243	1190	750 sh	1541
347	1255	755	1546 sh
418	1286	762 sh	1590 vw
473	1332	787	1600
585	1360	829	1674 sh
600	1475	948	1691
691	1545	1006	1712
729	1548 sh	1018	3198
742 sh	1702	1109	3242
751	3192	1188	
830	3241	1280	

sh shoulder, *vw* very weak
All frequencies in cm^{-1}

Bureau of Investigation to explore the suitability of this method for a rugged, portable spectrometer that can be employed in the field. Based on their findings they concluded that the Fourier transform (FT)-Raman is the preferred method for fluorescence-free analysis of explosive materials in the laboratory, and 830 nm excitation should be used for a field-portable instrument. The Raman spectra obtained for several explosives including NTO at various excitations are given in Fig. 5.20. It may be noted there are significant difference in these spectra that may be utilized to distinguish NTO from other explosives. For NTO, the excitation at 785 and 830 nm did not make any difference between the two spectra.

5.11 Detonation Characteristics

Various detonation properties of NTO are provided in the following tables along with the methods used for their determination.

5.11.1 Vacuum Stability Test

The vacuum stability test data showed NTO is fairly stable up to a temperature of 150 °C. The experiments were carried out in the temperature range of 100–150 °C by a number of researchers. The maximum amount of gas evolved in this temperature range was reported to be 1.45 cm^3/g. The data are given in Table 5.11.

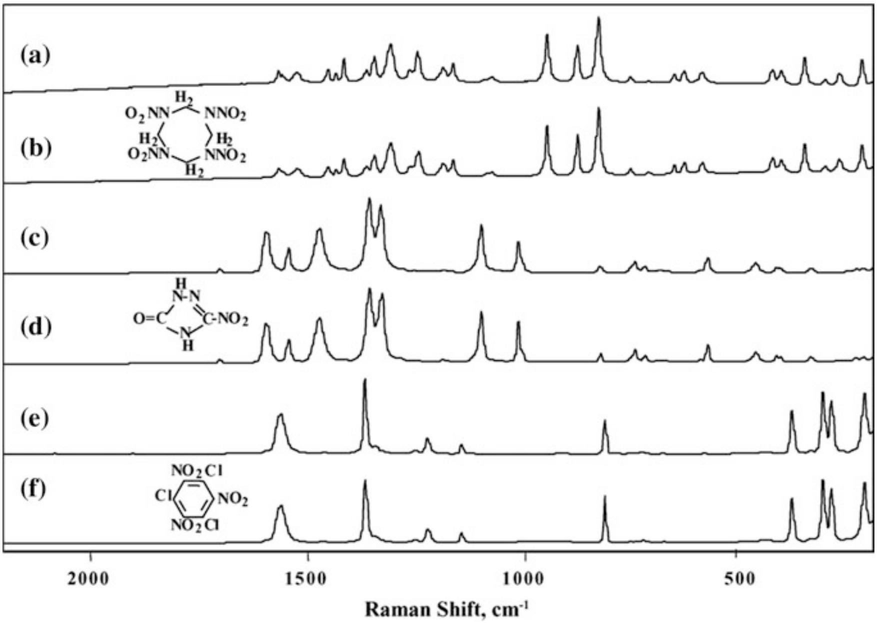

Fig. 5.20 Raman spectra of HMX, NTO, and TCNB over the spectral range 200–2200 cm^{-1}: **a** HMX, 785 nm; **b** HMX, 830 nm; **c** NTO, 785 nm; **d** NTO, 830 nm; **e** TCNB, 785 nm and **f** TCNB, 830 nm [59]

Table 5.11 Vacuum stability test data

Material	Temperature (°C)	Duration (h)	Gas evolved (cm^3/g)	References
NTO	100	48	0.2	[60–63]
NTO	100	193	1.45	[61]
NTO	110	20	0.06	[65]
NTO	120	40	0.0	[7]
NTO	120	48	0.3	[60–62]
NTO	130	193	1.45	[64]
NTO	150	193	1.7	[64]
NTO	150	200	Stable	[66, 67]

5.11.2 Impact Sensitiveness

The impact sensitiveness of NTO is shown in Table 5.12. The data indicates that NTO is less sensitive compare to other explosives such as RDX, HMX, and PETN. The sensitivity of NTO for impact is the subject of a study by Agrawal et al. [68] who used high-speed photographic technique.

Table 5.12 Results from impact sensitivity tests

Test method	Result	References
Julius Peter apparatus results (J)	22	[64]
Rotter impact (Figure of sensitivity[a])	80–90	[7]
Rotter impact (Figure of sensitivity[b])	316	[63, 69]
US drop impact type 12 (cm)	>280	[60–62, 70]
US drop impact type 12B (cm)	293	[60, 61, 71]
US impact sensitivity H_{50} (cm)	92	[72, 73]
30 kg Hammer, Non-reaction height (m)	>4	[64, 74, 75]

[a] RDX Reference of [80] used
[b] RDX Reference of [100] used

Table 5.13 BAM friction sensitivity test results

Researchers	Test Data	References
SNPE data (N)	>353	[74, 75]
South Africa data (N)	>353	[63, 69]
SNPE data (N)	>353	[64]

5.11.3 Friction Sensitivity Tests

The tests were carried out using BAM Friction test protocols by two laboratories. Both of them reported similar values. The BAM friction test data for NTO showed it to be less sensitive to friction compared to PETN, RDX, and HMX and similar to TNT and TATB. The data for NTO is shown in Table 5.13.

5.11.4 Electrostatic Discharge Sensitivity

The sensitivity of NTO to electrostatic discharge has been measured in several laboratories. The data are given in Table 5.14, which indicate that NTO is comparable to RDX and TNT.

5.11.5 Thermal Sensitivity

Ignition temperature is an important factor for explosives as it determines the storage and handling of the materials. NTO was found to ignite at a much higher temperature than PETN, RDX, and HMX. It is almost the same as TNT, but it is more sensitive than TATB. The temperature of ignition of NTO measured by various groups is given in Table 5.15.

Table 5.14 Electrostatic sensitivity test results

Research groups	Test results	References
Australian data (J)	>4.5	[3]
South Africa data (J)	15	[63, 69]
SNPE data (J)	>0.726	[76, 77]
Czech data (J) [96]	8.98	[78]
US data (3 mil, J)	0.91	[60–62]
US data (10 ml, J)	3.40	[60, 64]

Table 5.15 Ignition temperature

Research groups	Temperature	Values (°C)	References
SNPE	Temperature of ignition	280	[64, 74, 75]
MRL	Temperature of ignition	258	[7]
	Henkin critical temperature	237	[60–62, 71]
	Henkin critical temperature	216	[79]

5.11.6 *Shock Sensitivity*

Becuwe and Delclos [64] measured the shock sensitivity of NTO using a Large Scale Gap Test. They used a number of 0.19 mm polymethylmethacrylate attenuation discs to determine the shock sensitivity of NTO and several other explosives. The shock sensitivity of NTO was 260. The results indicated that NTO is less sensitive compared to PETN, RDX, and HMX and more sensitive than TATB.

5.12 Detonation Velocity

The detonation velocity report by various groups for NTO is given in Table 5.16. The data showed that the detonation velocity of NTO was less than that of RDX and HMX, but it was higher than TATB, whereas it has a similar detonation velocity as PETN.

Table 5.16 Detonation velocity of NTO

Research group	Detonation velocity (m/s)	References
French data	8510	[64, 74, 75]
Czech data	8590	[80]
American data	8560	[72]

Doherty and Simpson [72] also used the CHETA software to predict the detonation velocity, whereas Becuwe and Delclos [75] used the Kamlet and Jacobs method [81]. Both the groups reported good agreement with the experimental data.

5.13 Detonation Pressure

Plate dent tests were used to determine the detonation pressure of NTO [60–62]. Tests were conducted with NTO charges of different Theoretical Maximum Density (TMD). The BKW equation of state was used for prediction of detonation pressures. The experimental and calculated detonation pressures for these charges are given in Table 5.17.

5.14 Formulations

A low sensitive mixture with high detonation properties is highly desirable. The low sensitivity of NTO to various mechanical stimuli makes it an ideal material for explosive formulation with other high performance explosives such an RDX, HMX, and TNT. A number of NTO based formulations have been proposed by various groups. They are summarized in Table 5.18. Following the formulation of the explosives, their detonation properties were measured and also predicted using known software such as CHETA. These detonation properties are listed in Tables 5.19 and 5.20.

Based on both experimental and estimated data it appears that NTO based explosive formulation has potential to meet the needs of the ADF and Insensitive Munitions. Also, these formulations can improve storage, handling, and transportation of them. However, large scale charges should be tested to confirm their performance and response to various stimuli.

Table 5.17 Detonation pressure for NTO at various charge densities. Both measured and calculated values from BKW equation of state are reported [60–62]

Charge density (g/cm3)	Charge diameter (cm)	Pressure (GPa)	
		Measure	Calculated
1.93 (100% TMD)	–	–	34.9
1.781 (92.2% TMD)	4.13	27.8	28.4
1.853 (96% TMD)	4.13	26.0	31.6
1.782 (92.3% TMD)	2.54	24.0	28.4
1.855 (96.1% TMD)	2.54	Failed	31.6
1.759 (91.1% TMD)	1.27	25.0	27.1
1.824 (94.5% TMD)	1.27	Failed	–

Table 5.18 Composition of various formulations using NTO

Designation	NTO	TNT	RDX	HMX	AP	Aluminum	Additives	Energetic Plasticizer	Binder	References
TNTO	50	50					–		–	[82]
TNTO/D2	52	42					–		6 (D2 Wax)	[82]
TNTO/OD2	52	42					–		6 (OD2 Wax)	[82]
TNTO O	38	40					16 (Aluminium)		6 (D2 Wax)	[82]
TNTO I	42	34					19 (Aluminium)		5 (D2Wax)	[82]
TNTO II	42	32					19 (Aluminium)		7 (D2 Wax)	[82]
TNTO III	42	30					19 (Aluminium)		9 (D2Wax)	[82]
AFX-644 (TNTO IV)	40	30					20 (Aluminium)		10 (D2Wax)	[82]
AFX-645	48	32					12 (Aluminium)		8 (1-800 Ganex)	[83]
GD-1	65	35					–		–	[84, 85]
GD-2	35	35					30 (HMX)		–	[84, 85]
South African 1	40	60					–		–	[63, 69]
South African 2	25	50					25 (RDX)		–	[63, 69]
B 2214	72		–	12	–	–			16 (HTPB)	[64, 86–92]
B 2225	#		#	–	-	–			14.5 (HTPB)	[76]
B 2233	31		–	6	28	10			15 (HTPB)	[93]
B 2245	8		12	–	43	25			12 (HTPB)	[87]
B 2248	46		–	42	-	–			12 (HTPB)	[87, 92, 94]
B 3017	74		–	–	-	–			26 (Energetic)	[90, 94]
B 3021	50		25	–	-	–			25 (Energetic)	[87, 90, 94, 95]
PBXW-121	63		10	–	-	15			12 (HTPB)	[96]
PBXW-122	47		5	–	20	15			13 (HTPB)	[97, 98]
PBXW-124	27		20	–	20	20			13 (HTPB)	[98]
PBXW-125	22		20	–	20	26			12 (HTPB)	[98]

(continued)

Table 5.18 (continued)

Designation	NTO	TNT	RDX	HMX	AP	Aluminum	Additives	Energetic Plasticizer	Binder	References
PBXW-126	22		20	–	20	26			12 (Polyurethane)	[98, 99]
CPX 412	50	30					–	10 (K10)	10 (PolyNIMMO)	[100]
CPX 413	45	35					–	10 (K10)	10 (PolyNIMMO)	[92, 100, 101]
CPX 450	40	20					20 (Aluminium)	10 (K10)	10 (PolyNIMMO)	[102]
CPX 455	40	20					20 (Aluminium)	10 (K10)	10 (PolyNIMMO)	[102]
CPX 458	30	30					20 (Aluminium)	10 (K10)	10 (PolyNIMMO)	[102]
CPX 459	20	40					20 (Aluminium)	10 (K10)	10 (PolyNIMMO)	[102]
CPX 460	27.5	27.5					25 (Aluminium)	10 (K10)	10 (PolyNIMMO)	[102]
GD-3	12	12					–	–	16 (HTPB)	[84, 85]
GD-5	43	43					–	10 (BDNPA/F)	7 (PGA)	[84, 85]
HX 310	47	47					10 NG	–	18 (HTPB)	[92]
CHN-037							–	–	24 (GAP)	[103]
GD-9	47.5	47.5							2.5 (Cariflex 1101)	[84, 85]
GD-10	48.8	48.8							2.4 (Cariflex 1101)	[84, 85]
GD-11	48	48							4 (Cariflex 1101)	[84, 85]
GD-12	48	48							4 (Cariflex 1101)	[84, 85]
GD-13	48	48							2/2 (Hy Temp/DOA)	[84, 85]
GD-14	48	48							4 (Estane)	[84, 85]
French 1	55.5	37							7/0.5 (KelF/Graphite)	[74, 86]

Table 5.19 Modification using surfactants

Formulation	Density (g/cm^3)	Velocity of detonation (m/s)	Critical diameter (mm)	Volume of gas evolved (cm^3/g)	$H_{50\%}$ (cm)	BAM friction (N)	Electrostatic discharge (J)	Impact sensitivity (F of I)	References
TNTO	1.74	7340	16	0.09	91.5	41.2	0.062		[82, 83, 104]
TNTO/D2	1.54	6470	<25	0.29	>200.5	53.0	0.062		[82, 83, 104]
TNTO/OD2	1.61	6900	<25	–	>200.5	–	–		[82, 83, 104]
TNTO O				0.21	>200.5	41.2	0.040		[82, 83, 104]
TNTO I	1.76	6670	25–51	–	>200.5	–	–		[82, 83, 104]
TNTO II	1.74	6840	32–35	0.35	>200.5	53.0	0.040		[82, 83, 104]
TNTO III					>200.5	–	–		[82, 83, 104]
AFX-644	1.70	6960	41–43	0.37	>200.5	60.8	0.040		[82, 83, 104]
GD-1	1.750	7510	–	–		–			[84, 85]
GD-2	1.761	7870	–	–		–			[84, 85]
South Africa Sample: NTO/TNT (40/60)						>353	170	276	[63, 69]
South Africa Sample: NTO/RDX/TNT (25/25/50)						>353	170	186	[63, 69]
B 2214	1.63	7495	35 (confined) 65 (unconfined)						[64, 87, 89, 90, 92]
B 2245	1.81	5150	–						[87]
B 2248	1.70	8130	11						[92]
B 3017	1.75	7780	10–15						[88, 90]

(continued)

Table 5.19 (continued)

Formulation	Density (g/cm^3)	Velocity of detonation (m/s)	Critical diameter (mm)	Volume of gas evolved (cm^3/g)	$H_{50\%}$ (cm)	BAM friction (N)	Electrostatic discharge (J)	Impact sensitivity (F of I)	References
B 3021	1.77	8100	<10						[88, 90]
GD-3	–	6838	–						[84, 85]
GD-5	–	8035	–						[84, 85]
HX 310	1.57	7750	<10						[92]
CPX 412	1.66	7200	–						[100]
CPX 413	1.74	8150	10						[92, 100]
CPX 450	1.85	7762	–						[102]
CPX 458	1.85	7676	–						[102]
CPX 459	1.86	7761	–						[102]
CPX 460	1.88	6420	–						[102]
GD-9		8280				192	0.320		[84, 85]
GD-10		8352				192	0.180		[84, 85]
GD-11		8187				–	–		[84, 85]
GD-12		8174				252	–		[84, 85]
GD-13		8275				252	–		[84, 85]
GD-14		8268				213	–		[84, 85]

Table 5.20 Materials, friction sensitivity tests

Type of tests	Materials						References
	NTO	PETN	HMX	RDX	TNT	TATB	
Impact sensitivity tests							
Julius Peter apparatus CSI test (J)	22	–	5	4.5	30	–	[12]
Rotter impact (Figure of insensitivity)	80–90	40	60	80	106–115	–	[3]
Rotter impact (Figure of insensitivity)	316	–	–	100	221	–	[84, 86]
US drop impact type 12 (cm)	>280	12	26	22	148	>320	[9–11, 91]
US drop impact type 12B (cm)	293	16–32	28–38	41	–	–	[9, 10, 92]
US impact sensitivity H_{50} (cm)	92	13–16	32	28	80	>177	[89, 90]
30 kg Hammer: non reaction height (m)	>4	0.5	0.5	1	>4	>4	[12, 93, 94]
BAM friction sensitivity tests							
SNPE data	>353	125	175	133	~353	>353	[93, 94]
South African data (N)	>353	–	–	247	>353	–	[84, 86]
SNPE data	>353	–	100	113–174	300	–	[12]
Electrostatic discharge sensitivity							
Australian data	>4.5			4.5	–		3
South African data (J)	15			0.225	0.138		[85, 86]
SNPE data (J)	>0.726			–	–		[5, 6]
Czech data (J)	8.98			2.49	6.85		[96]
US data (3 mil, J)	0.91			0.22	–		[9, 11]
US data (10 mil, J)	3.40			0.55	–		[9, 11]
Thermal sensitivity ignition tests							
Ignition temp (SNPE), C	280	190	270	220	290	350	[12, 93, 94]
Ignition temp (MRL), C	258	149	–	216	240	–	[3]
Henkin critical temp, C	237	175	210	219.6	261	–	[9–11, 92]
Henkin critical temp, C	216	–	–	–	–	–	[62]

(continued)

Table 5.20 (continued)

Type of tests	Materials						References
	NTO	PETN	HMX	RDX	TNT	TATB	
Shock sensitivity test							
SNPE results (No. of discs)	260	330	305	310		190	[12, 93, 94]
Detonation velocity							
French data (m/s)	8510	8500	9100	8850		8000	[12, 93, 94]
Czech data (m/s)	8590	8930	9130	8890		–	[96]
American data (m/s)	8560	–	9300	8930		8100	[89]

Trzcinski and Szymanczyk [105] determined detonation characteristics of several mixtures containing NTO with TNT, RDX, and HMX. Their comparison of the experimental data with CHEETAH predictions reveals good agreement. Results show that as the percentage of NTO increases, detonation velocities decrease, and with lower percentage TNT detonation velocity increases.

5.15 Toxicity

The synthesis of NTO involves release of significant amount of NTO into the atmosphere as wastewater that generally contains 10–15 g/L of NTO. Therefore, understanding of NTO's toxicological effect is of great interest. London and Smith [106] at Los Alamos National Laboratories conducted the following tests to provide a preliminary assessment of its toxicity: (1) acute oral toxicity, (2) primary skin irritation, (3) skin sensitization, and (4) eye (conjunctival) instillation. The following conclusions were made from the preliminary tests. The LD_{50} values for NTO for mice and rats when administered orally are found to be are greater than 5 g/kg that is considered to be slightly toxic or practically non-toxic in both species. It is a mild irritant to rabbit skin. NTO does not induce sensitization in the intradermal guinea pig assay and the rabbit eye test is considered negative; however, transient conjunctival and corneal irritation did result from the NTO exposure in several animals and one developed a chronic anterior uveitis.

Sarlauskas et al. [107] studied the mechanisms of toxicity of NTO following their reactions with the single-electron transferring flavoenzymes NADPH: cytochrome P-450 reductase and ferredoxin: NADP+reductase, two-electron transferring flavoenzymes mammalian NAD(P)H: quinone oxidoreductase (DT-diaphorase), and *Enterobacter cloacae* NAD(P)H: nitroreductase, and their reactions with oxyhemoglobin. The results show NTO to be mildly toxic.

Reddy et al. [108] investigated the genotoxicity of NTO, using several genotoxicity tests, including the Ames test, Chinese Hamster Ovary (CHO) cell chromosome aberration test, L5178Y TK+/− mouse lymphoma mutagenesis test and rat micronucleus test. These studies reveal that NTO was not genotoxic in either in vitro or in vivo tests and suggest a low risk of genetic hazards associated with exposure.

5.16 Detection

The general technique for detecting NTO appears to be through the detection of decomposition products. This procedure was adopted by Tabrizchi and Ilbeigi [109], and by Garland et al. [46]. An ion mobility spectrometer (IMS) was used by Tabrizchi and Ilbeigi [109] to detect and identify NTO from the gas phase. In Fig. 5.21 the positive ion mobility spectrum of NTO is shown along with the background spectrum and the NO_2 spectrum. Although the decomposition products of NTO in the temperature range of 180–250 °C contain CO_2, CO, NO_2, NO,

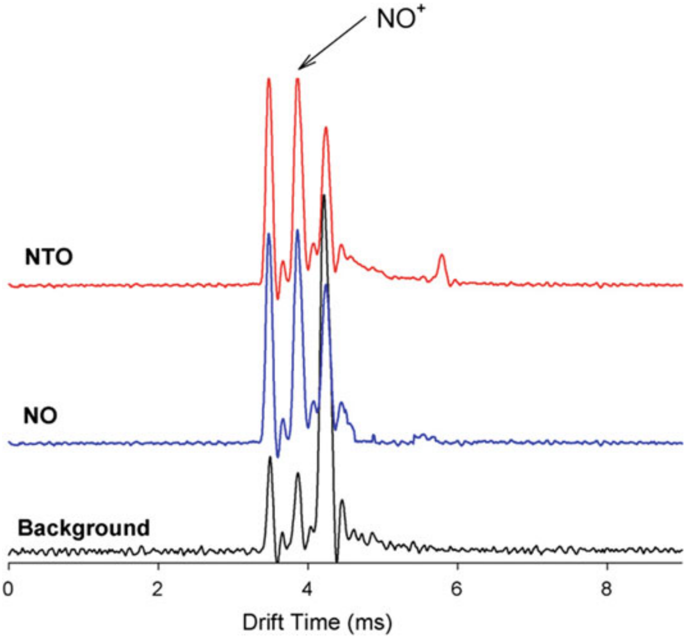

Fig. 5.21 Detection of decomposition products by an ion mobility spectrometer [46]

Fig. 5.22 Mass spectrum of the products from laser induced decomposition of NTO in a time-of-flight mass spectrometer. Laser fluence: 380 mJ/cm^2; Delay between the decomposition and ionization lasers: 55 μs

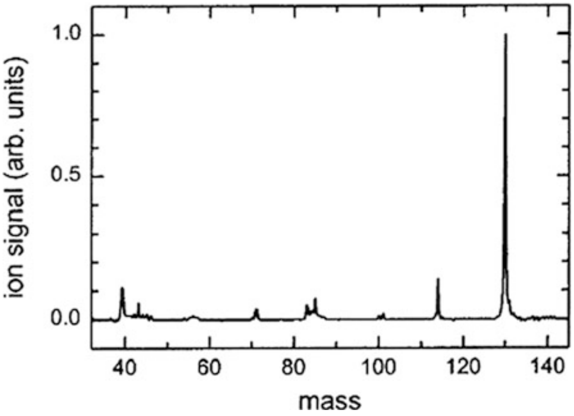

HONO, H_2O, N_2, CH_2O, and N_2O, only NO, NO_2, and HONO increased the NO^+ peak. This NO^+ peak may be used to identify NTO.

As discussed earlier, Garland et al. [46] studied laser-induced decomposition of NTO. The decomposition products are given earlier in Table 5.7. Following decomposition, they used a Time-of-Flight mass spectrometry to detect the decomposition products. The spectrum is shown in Fig. 5.22. The large peak at 130 m/z is for NTO/$C_2N_4O_3H_2$ which can be used to detect NTO directly.

Oehrle [110] outlines a capillary electrophoretic method for the analysis of NTO in presence of several other explosives. Oehrle [110] claims capillary electrophoresis (CE) is better than HPLC technique particularly in the presence of explosives other than TNT. CE is found to have high resolution and speed in the analysis of both neutral compounds and ions whereas HPLC methods for analyzing NTO mixtures give reasonable results for NTO and TNT. Figure 5.23 shows the number compounds that could be analyzed by CE.

Mass spectra of NTO can be used to detect NTO as it showed distinct pattern during thermal decomposition. The spectrum is shown in Fig. 5.24. According to

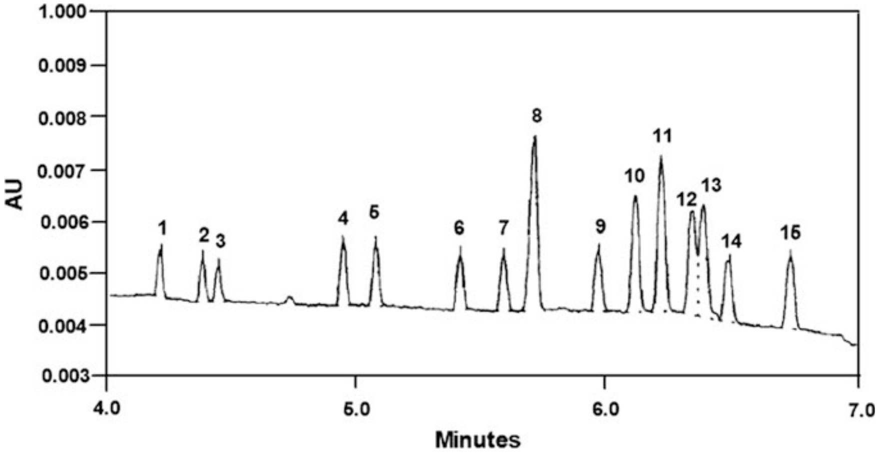

Fig. 5.23 Electropherogram of NTO in the presence of 14 other nitramine and nitroaromatic explosives. Peaks: *1* = HMX (10 mg/l); *2* = RDX (10 mg/l); *3* = TNB (10 mg/l); *4* = DNB (10 mg/l); *5* = NB (10 mg/l); *6* = TNT (l0 mg/l); *7* = Tetryl (10 mg/l); *8* = NTO (15 mg/l); *9* = 2,4 DNT (10 mg/l); *10* = 2,6-DNT; *11* = 3-NT; *12* = 4-NT; *13* = 3-NT; *14* = 2-Am-4,6-DNT [10 mg/l]; and *15* = 4-Am-2,6-DNT (10 mg/l)

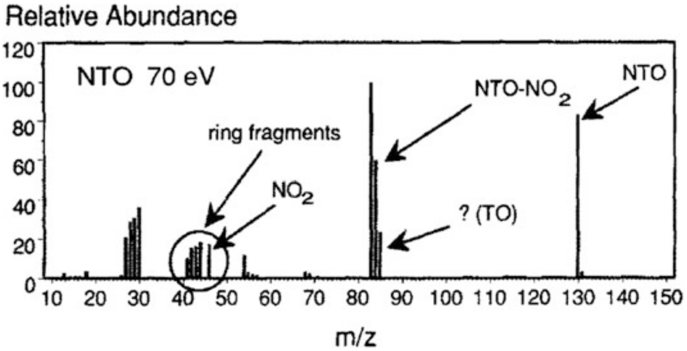

Fig. 5.24 Fragmentation of NTO during mass spectrometry

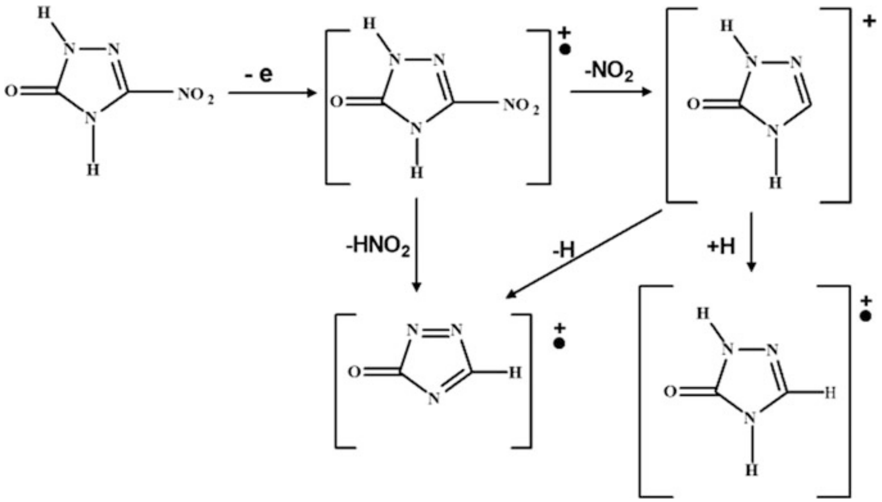

Fig. 5.25 Fragmentation of NTO during mass spectrometry

Ostmark, three distinct zone was observed: the molecular ion (m/z 130) for undecomposed NTO, the azole ring (m/z 83, 84, and 85), and the azole ring fragmentation (m/z 41, 42, 43, and 44). The fragmentation pattern is given in Fig. 5.25. The fragmentation pattern can be used to detect NTO from its mixtures.

5.17 Conclusion

NTO has attracted attention as a possible replacement for RDX and similar energetic materials in various military propellants and explosives. Large scale production of NTO will lead to environmental concerns, but economical degradation methods are not available. In addition there are no cost effective detection techniques. Both detection and degradation need various physical and chemical properties which are lacking.

References

1. von M Manchot, Noll R (1905) Ueber Derivate des Triazols (On the derivatives of triazols). Justus Liebigs Annalen de Chemie 343:1–27
2. Chipen GI, Bokalder RP, Grinshtein VY (1966) 1, 2, 4-triazol-3-one and its nitro and amino derivatives. Chem Heterocycl Compds 2(1):110–116
3. Smith MW, Cliff MD (1999) NTO-based formulations: a technology review. DSTO-TR-0796

4. Zbarsky VL, Yudin NV (2005) Kinetics of the synthesis of NTO in nitric acid. Propellants Explos Pyrotech 30(4):298–302
5. Mukundan T, Purandare GN, Nair JK, Pansare SM, Sinha RK, Singh H (2002) Explosive nitrotriazolone formulates. Defence Sci J 52(2):127–133
6. Singh G, Kapoor IPS, Tiwari SK, Felix PS (2001) Studies on energetic compounds part 16 chemistry and decomposition mechanisms of 5-nitro-2,4dihydro-3H-1,2,4-triazole-3-one (NTO). J Hazard Mater B 81:67–82
7. Spears RJ, Louve CN, Wolfson MG (1989) A preliminary assessment of NTO as an insensitive high explosive. MRL-TR-89-19 DSTO
8. Li J (1998) One-pot synthesis of 3-nitro-1,2,4-triazol-5-one. Beijing Ligong Dexue Xuebao 18(4):518–519
9. Kim HS, Goh EM, Park BS (2003) Preparation method of 3-nitro-1,2,4-triazol-5-one by a process minimizing heat generation during crystallization. US Patent 6583293
10. Chipen GI, Bokalder RP, Grinshtein VYa (1966) 1,2,4-triazol-3-one and its nitro and amino derivatives. Chem Heterocycl Compd 2(1):79–83
11. Lee K-Y, Coburn MD (1985) 3-nitro-1,2,4-triazol-5-one, a less sensitive explosive. Los Alamos National Laboratory Report No LA-10302-MS
12. Kroger CF, Miethchen R, Frank H, Soemer M, Pilz S (1969) 1, 2, 4-triazoles. 17. nitration and bromination of 1, 2, 4-triazolones. chemische berichte 102(3):755
13. Katritzky R, Ogretir C (1982) The kinetic nitration and basicity of 1,2,4-triazol-5-ones. Chim Acta Tureica 10:137–146
14. Yang G, Nie F, Li J, Guo Q, Qiao Z (2007) Preparation and characterization of nano-NTO explosive. J Energ Mater 25:35–47
15. Wang D, Zhang J, Wang J, Wang B (2007) Preparation of nanometer NTO by W/O microemulsion. Huogongpin 14(1):9–11
16. Ma H, Song J, Hu R (2006) A review on 3-nitro-1, 2, 4-triazol-5-one and its salts. Huozhayao Xuebao 29(6):9–15
17. Lee KY, Gilardi R (1993) Structure and properties of energetic materials. Material Research Society, Pittsberg, PA, p 237; Lee KY, Gilardi R (1993) Mater Res Soc Symp Proc 296:237
18. Bolotina N, Kirschbaum K, Pinkerton AA, Alan A (2005) Energetic materials: a-NTO crystallizes as a four component triclinic twin. Acta Crystallogr Struct Sci B 61(5):577–584
19. Bolotina NB, Zhurova EA, Pinkerton AA (2003) crystal structure. J Appl Cryst 36:280–285
20. Yi J-H, Zhao F-Q, Gao H-X, Xu S-Y, Wang M-C, Hu R-Z (2008) Preparation, characterization, non-isothermal reaction kinetics, thermodynamic properties, and safety performances of high nitrogen compound: Hydrazine 3-nitro-1,2,4-triazol-5-one complex. J Hazard Mater 153:261–268
21. Badgujar DM, Talawar MB, Asthana SN, Mahulikar PP (2008) Advances in science and technology of modern energetic materials: an overview. J Hazard Mater 151:289–305
22. Calculated using Advanced Chemistry Development (ACD/Labs) Software V814 for Solaris 1994–2008 (ACD/Labs)
23. Toghiani RK, Toghiani H, Maloney SW, Boddu VM (2008) Prediction of physicochemical properties of energetic materials. Fluid Phase Equilib 264(1–2):86–92
24. Sinditskii VP, Smirnov SP, Yu EV (2007) Thermal decomposition of NTO: an explanation of the high activation energy. Propellants, Explos, Pyrotech 32(4):277–287
25. Volk F, Bathelt H (2002) Performance parameters of explosives: equilibrium and non-equilibrium reactions. Propellants, Explos, Pyrotech 27:136–141
26. Osmont A, Catoire L, Gökalp I, Yang V (2007) Ab initio quantum chemical predictions of enthalpies of formation, heat capacities, and entropies of gas-phase energetic compounds. Combust Flame 151:262–273
27. Li ZN, Ma HX, Song JR, Zhao FQ, Xu KZ, Hu RZ (2008) Specific heat capacity, thermodynamic properties and adiabatic time-to-explosion of NTO. Chin J Explos Propellants No 3

28. Kim KJ, Kim MJ, Lee JM, Kim SH, Kim HS, Park BS (1998) Solubility, density, and metastable zone width of the 3-nitro-1,2,4-triazol-5-one + water system. J Chem Eng Data 43:65–68
29. Liu MH, Chen C, Hong YS, Liu CW (2005) Polyparametric modification equation for estimating thermodynamic properties of energetic nitro compounds. Theor Chem Acc 113 (1):35–41
30. Xiao HM, Ju XH, Xu LN, Fang GY (2004) A density-functional theory investigation of 3-nitro-1,2,4-triazole-5-one dimers and crystal. J Chem Phys 121:12523–12531
31. Fang GY, Xu LN, Hu XG, Li XH, Xiao HM, Ju XH, Gong XD (2005) Density functional theory study of the interaction between 3-nitro-1, 2, 4-triazol-5-one and water. J Theor Comput Chem 4(3):849–856
32. Fang GY, Xu LN, Hu XG, Li XH (2005) Density functional theory study of the interaction between 3-nitro-1, 2, 4-triazol-5-one and ammonia. Int J Quantum Chem 105(2):148–153
33. Rothgery EF, Audette DE, Wedlich RC, Csejka DA (1991) The study of the thermal decomposition of 3-nitro-1,2,4-triazol-5-one (NTO) by DSC, TGA-MS, and ARC. Thermochim Acta 185(2):235–243
34. Brill TB, Brush PJ, Patil DG (1993) Thermal decomposition of energetic materials 58. Chemistry of ammonium nitrate and ammonium dinitramide near the burning surface temperature. Combust Flame 92(1–2):178–186
35. Oxley JC, Smith JL, Zhou Z, McKenney RL (1995) Thermal decomposition studies on NTO and NTO/TNT. J Phys Chem 99:10383–10391
36. Garland NL, Ladouceur HD, Nelson HH (1997) Laser-induced decomposition of NTO. J Phys Chem A 101:8508–8512
37. Prabhakaran KV, Naidu SR, Kurian EM (1994) XRD, spectroscopic and thermal analysis studies on 3-nitro-l,2,4-triazol-5-one. Thermochim Acta 241:199–212
38. Ostmark H, Bergman H, Aquist G, Langlet A, Persson B Decomposition of NTO: some initial observations. In: Proceedings of the 16th international pyrotechnics seminar, Jönköping, Sweden, p 874
39. Williams GK, Palopoli SF, Brill TB (1994) Thermal decomposition of energetic materials 65. Conversion of insensitive explosives (NTO, ANTA) and related compounds to polymeric melon-like cyclic azine burn-rate suppressants. Combust Flame 98:197
40. Meredith C, Russell TP, Mowrey RC, McDonald JR (1998) Decomposition of 5-nitro-2,3-dihydro-3H-1,2,4-triazol-3-one (NTO): energetics associated with several proposed initiation routes. J Phys Chem A 102:471–477
41. Ostmark H (Nov 1991) Thermal decomposition of NTO FOA. Report D-2017823 National Defense Research Establishment: Sundbyberg, Sweden
42. Ostmark H, Bergman H, Åqvist G (1993) The chemistry of 3-mtro-1,2,4-triazol-5-one (NTO): thermal decomposition. Thermochim Acta 213(1):165–175
43. Beardall DJ, Botcher TR, Wight CA (1996) Explosive thermal decomposition mechanism of NTO. Mater Res Soc Symp Proc 418:379–384
44. Oxley JC, Smith JL, Yeager KE, Rogers E, Dong XX (1996) NTO decomposition studies. In: Brill TB, Russell TP, Tao WC, Wardle RB (eds) MRS decomposition, combustion, & detonation chemistry of energetic materials 418:135. https://doi.org/10.1557/PROC-418-135
45. Menapace JA, Marlin JE, Bruss DR, Dascher RV (1991) Photochemical and thermochemical decomposition of 3-nitro-1,2,4-triazol-5-one and predeuterio-3-nitro-1,2,4-triazol-5-one in neat and mixed systems. J Phys Chem 95(14):5509–5517
46. Garland NL, Ladouceur HD, Nelson HH (1997) Laser-induced decomposition of NTO. J Phys Chem A 101:8508–8512
47. Kondrikov BN, Smirnov P, Minakin AV, Doherty RM (2004) Chemical kinetics of the thermal decomposition of NTO. Propellants, Explos, Pyrotech 29(1):27–33
48. Brill TB, Gongwer PE, Williams GK (1994) Thermal decomposition of energetic materials 66 kinetic compensation effects in HMX, RDX, NTO. J Phys Chem 98:12242–12247

49. Ostmark H, Bergman H, Aqrist G, Langlet A, Persson B (June 1991) Decomposition of NTO: some initial observations. In: Sixteenth international pyrotechnics seminar, Jonkijping, Sweden, pp 874–886
50. Oxley JC, Zhou Z, Smith JL, McKenney RL (March 21–24 1994) Thermal decomposition studies on NTO and NTO/TNT. In: Proceedings of the ADPA international symposium on energetic materials technology international symposium on energetic materials technology, meeting #450, Florida, USA, 21–24 March, American Defense Preparedness Association, pp 155–165
51. Yi X, Hu R, Wang X, Fu X, Zhu C (1991) Thermal behaviour of 3-nitro-1,2,4-triazol-5-one and its salts. Thermochim Acta 189:283–296
52. Vakul'skaya TI, Titova, IA, Dolgushin, GV, Loppyrev, VA (2005) Free radicals in various C-amination reactions of 1-methyl-4-nitropyrazole. Magnetic Resonance in Chemistry 43:1023–1027
53. Vakul'skaya TI, Rakhmatulina TN, Pevzner MS, Kofman TP, Lopyrev VA (1987) EPR and polarography of nitroazoles. 6. 3-Nitro-1,2,4-triazoles. Chem Heterocycl Comp 23(3):287–291
54. Lopyrev VA, Larina LI, Sosonkin IM, Vakul'skaya TI, Kalb GL, Shibanova EF (1985) EPR and polarography of nitroazoles. 5. First step in the electrochemical reduction of 2-substituted 5(6)-nitrobenzimidazole using a rotating platinum ring-disk electrode. Chem Heterocycl Comp 21:688 (Translated from Khim. Geterotsikl Soedin 21(6):827–832 (June 1985); Chemosphere 38(7):1561–1570)
55. Campion LL, Giannotti C, Ouazzani J (1999) Photocatalytic degradation of 5-nitro-1,2,4-triazol-3-one NTO in aqueous solution of TiO_2. Comparison with Fenton oxidation. Chemosphere 38(7):1561–1570
56. Campion LL, Vandais A, Ouazzani J (1999) Microbial remediation of NTO in aqueous industrial wastes FEMS. Microbiol Lett 176:197–203
57. Sarlauskas J, Nemeikaite-Ceniene A, Anusevicius Z, Miseviciene L, Maroziene A, Markevicius A, Cenas N, Naturforsch Z (2004) Enzymatic redox properties of novel nitrotriazole explosives implications for their toxicity. 59(5–6):399–404
58. Hiyoshi RI, Kohno Y, Nakamura J (2004) Vibrational assignment of energetic material 5-Nitro-2,4-dihydro-1,2,4-triazol-3-one (NTO) with labeled isomers. J Phys Chem A 108:5915–5920
59. Lewis ML, Lewis IR, Griffiths PR (2005) Raman spectrometry of explosives with a no-moving-parts fiber coupled spectrometer: a comparison of excitation wavelength. Vib Spectrosc 38:17–28
60. Lee K-Y, Coburn MD (1985) 3-nitro-l,2,4-triazol-5-one, a less sensitive explosive. LA-10302-MS Los Alamos National Laboratory Los Alamos, USA
61. Lee K-Y, Coburn MD (1988) 3-nitro-l,2,4-triazol-5-one, a less sensitive explosive. US Patent 4,733,610
62. Lee K-Y, Chapman LB, Coburn MD (1987) 3-nitro-l,2,4 triazol-5-one, a less sensitive explosive. J Energ Mater 5:27–33
63. Barnard PW, Fouche FC, Bezuidenhout HC (1997) Less sensitive TNT based formulations. In: Australasian explosive ordnance symposium (Parari '97) 3rd Canberra, Australia, 12–14
64. Becuwe A, Delclos A (1993) Low-sensitivity explosive compounds for low vulnerability warheads. Propellants, Explos, Pyrotech 18:1–10
65. Marecek P, Pokornä J, Vävra P (1998) A study of some insensitive explosives. In: International conference of ICT 29th Karlsruhe Federal Republic of Germany 30 June–3 July, Fraunhofer-Institut Für Chemische Technologie Berghausen, Bundesrepublik, Deutschland 52(l):52(5)
66. Graham KJ, Williams EM, Lynch RD, Floyd TG, Struck SR (1994) Reducing the sensitivity of high-performance warhead fills. In: Insensitive munitions technology symposium, meeting #471, Virginia, USA 6–9 June, American Defense Preparedness Association, pp 541–563
67. Sanderson AJ (1997) A draft sheet for 3-nitro-l,2,4-triazol-5-one. The NIMIC Coordinated Characterisation Program

68. Agrawal JP, Walley SM, Field JE (1998) A high-speed photographic study of the impact initiation of hexanitro hexaaza isowurtzitane and nitrotriazolone. Combus Flame 112:62–72
69. Fouche FC, van Schalkwyk GC (1996) TNT-based insensitive munitions. In: International conference of ICT 27th Karlsruhe Federal Republic of Germany, 25–28 June, Fraunhofer-Institut Für Chemische Technologie Berghausen, Bundesrepublik, Deutschland 69(1):69(12)
70. Hall TN, Holden JR (1988) Navy explosives handbook explosive effects and properties, part III properties of explosives and explosive compositions. NSWC MP 88-116 White Oak Laboratory Naval Surface Warfare Centre, Maryland, USA
71. Popolato A, Forsberg HC, Gritzo LA (1957). In: Popolato A (ed) Handbook of properties of some explosives of interest to GMX-division. May 24, 1957 (CRD)
72. Doherty RM, Simpson RL (1997) A comparative evaluation of several insensitive high explosives. In: International conference of ICT 28th Karlsruhe Federal Republic of Germany, 24–27 June, Fraunhofer-Institut Für Chemische Technologie Berghausen, Bundesrepublik, Deutschland 32(l):32(23)
73. Dobratz BM (1981) LLNL explosives handbook properties of chemical explosives and explosive simulants. Lawrence Livermore National Laboratory, California, USA
74. Becuwe A, Delclos A (1987) L'Oxynitrotriazole et son Utilisation et tant Qu'Explosif Insensible. In: International conference of ICT 18th Karlsruhe Federal Republic of Germany, 1–3 July, Fraunhofer-Institut Für Chemische Technologie Berghausen, Bundesrepublik, Deutschland 27(1):27(14)
75. Becuwe A, Delclos A (1987) Oxynitrotriazole and it's use as insensitive explosive. In: Jing D (ed) International symposium on pyrotechnics and explosives 1st Beijing China 12–15 Oct, China Academic Publishers Beijing China 255–261
76. Sanderson AJ (1994) A programme and data for the characterisation of new ingredients for energetic materials. The NIMIC Coordinated Characterisation Programme 110:57–62
77. Sanderson AJ (1997) A draft sheet for 3-nitro-l,2,4-triazol-5-one. The NIMIC Coordinated Characterisation Program
78. Zeman V, Zeman S (1997) Relationship between the electric spark sensitivity and detonation velocities of some polynitro compounds. In: International conference of ICT 28th Karlsruhe Federal Republic of Germany, 24–27 June, Fraunhofer-Institut Für Chemische Technologie Berghausen, Bundesrepublik, Deutschland 67(1):67(10)
79. Aubert SA, Corley JD, Glenn JG (1993) Development of TNTO composite explosives. WL-TR-92-7073 Wright Laboratory Eglin Air Force Base, Florida, USA
80. Zeman V, Zeman S (1997) Relationship between the electric spark sensitivity and detonation velocities of some polynitro compounds. In: International conference of ICT 28th Karlsruhe Federal Republic of Germany, 24–27 June, Fraunhofer-Institut Für Chemische Technologie Berghausen, Bundesrepublik, Deutschland 67(1):67(10)
81. Kamlet MJ, Jacobs SJ (1968) Chemistry of detonations I a simple method for calculating detonation properties of C-H-N-O explosives. J Chem Phys 48(1):23–35
82. Aubert SA, Corley JD, Glenn JG (1993) Development of TNTO composite explosives. WL-TR-92-7073 Wright Laboratory, Eglin Air Force Base, Florida, USA
83. Corley JD, Stewart AC (1995) Fuzed insensitive general purpose bomb containing AFX-645. Final Report WL-TR-95-7019 Wright Laboratory, Eglin Air Force Base, Florida, USA
84. Hammer JO, Skjold E, Kildal SK, Gjersoe R, Mathieu J, Berger B, Mäder P, Bircher HR (1997) Formulation of NTO based compositions. In: Insensitive munitions and energetic materials technology symposium event #854, Florida, USA, 6–9 Oct, National Defense Industrial Association
85. Bircher HR, Mathieu J, Berger B, Mäder P, Skjold E, Kildal SK, Gjersoe R, Hammer JO (1997) Vulnerability and performance of NTO based high explosives. In: Insensitive munitions and energetic materials technology symposium event #854, Florida, USA, 6–9 Oct, National Defense Industrial Association

86. Becuwe A, Isler J (1997) Extremely insensitive detonating substances (EIDS) for 16 munitions applications. In: Insensitive munitions and energetic materials technology symposium event #854, Florida, USA 6–9 Oct, National Defense Industrial Association
87. Becuwe A, Delclos A, Isler J (1995) EIDS high explosives for 16 munitions. In: International symposium on energetic materials technology meeting #680, Arizona, USA, 24–27 Sept, American Defense Preparedness Association,pp 119–124
88. Becuwe A, Delclos A, Donzel G, Golfier M (1997) Improvements in NTO based PBXs a new powerful and insensitive class of PBX. In: Insensitive munitions and energetic materials technology symposium event #854, Florida, USA, 6–9 Oct, National Defense Industrial Association
89. Becuwe A, Delclos A (1989) Use of oxynitrotriazole to prepare an insensitive high explosive. In: Symposium (international) on detonation 9th HI Oregon, USA, 28 Aug–l Sept, pp 871–876
90. Becuwe A, Delclos A, Donzel G, Golfier M (1998) Improvements in NTO based PBXs. In: International conference of ICT 29th Karlsruhe Federal Republic of Germany, 30 June–3 July, Fraunhofer-Institut Für Chemische Technologie Berghausen, Bundesrepublik, Deutschland 95(l):95(5)
91. Quidot M, Hamaide S, Groux J, Gimenez P, Isler JC (1993) Fragment impact initiation of cast PBXs in relation with shock sensitivity tests. In: International detonation symposium 10th Massachusetts, USA, 12–16, July Office of Naval Research, Virginia, USA, pp 113–121
92. Lamy P, Leiber C-O, Cumming AS, Zimmer M (1996) Air senior national representative long term technology project on insensitive high explosives (IHEs) studies of high energy insensitive high explosives. In: International conference of ICT 27th Karlsruhe Federal Republic of Germany, 25–28ÜI June, Fraunhofer-Institut Für Chemische Technologie Berghausen, Bundesrepublik, Deutschland 1(1):1(14)
93. Nouguez B (1994) Dual formulation warheads: a mature technology. In: Insensitive munitions technology symposium meeting #471, Virginia, USA, 6–9 June, American Defense Preparedness Association, pp 280–287
94. Becuwe A, Delclos A, Donzel G, Golfier M (1997) Improvements in NTO based PBXs a new powerful and insensitive class of PBX. In: Insensitive munitions and energetic materials technology symposium event #854, Florida, USA, 6–9 Oct, National Defense Industrial Association
95. Kayser V, Boussufe R, Kihm JF, Deneuville P, Pascal S (1994) Use of cast PBX in insensitive high performance shaped charges. In: Insensitive munitions technology symposium meeting #471, Virginia, USA, 6–9 June, American Defense Preparedness Association, pp 574–584
96. Spear RJ, Dagley IJ, Whitty P (1994) Options for future RAAF GP bombs meeting IM and/or HD 16 criteria. DSTO-CIC-0001 Aeronautical and Maritime Research Laboratory, Melbourne, Australia
97. Senn MR, Newman KE, Wise TE, Jones WS (1990) Chemicals and processing assessment of candidate explosives for the advanced bomb family. IHTR-1370 Naval Ordnance Station Indian Head, USA
98. Wilson LT, Reedal DR, Simpson BM (1997) Comparison of PBXW-126 and PBXC-129 for use in large fragmenting warheads. In: Insensitive munitions and energetic materials technology symposium event #854, Florida, USA, 6–9 Oct, National Defense Industrial Association
99. Murphy MJ, Simpson RL, Urtiew PA, Souers PC, Garcia F, Garza RG (1995) Reactive flow model development for PBXW-126 using modern nonlinear optimisation methods. In: Schmidt SC, Tao WC (eds) Conference of the American physical society topical group on shock compression of condensed matter, American Institute of physics conference proceedings 370 Washington, USA, 13–18 Aug, AIP Press, New York, USA, pp 417–420
100. Cumming AS, Gaulter SE, Leach CJ (1994) The formulation of an insensitive high explosive based on HMX, NTO and PolyNIMMO. In: Insensitive munitions technology

symposium meeting #471, Virginia, USA, 6–9 June, American Defense Preparedness Association, pp 376–382
101. Cumming AS (1997) Part 1—focus area reports. Technical panel WTP-4 energetic materials and propulsion technology. Volume III, UK, 14–18 April, The Technical Cooperation Program, pp 97–99
102. Leach CJ, Garaty BJ, Cox KJ (1997) Progress in aluminised IHE. The Technical Cooperation Program Technical panel W-4 energetic materials and propulsion technology. In: 22nd meeting, United Kingdom, 14–18 April, pp 1–8
103. Mclntosh G (1997) Effect of 245 GHz microwave radiation on diverse explosives. DREV-TM-9702 Defence Research Establishment Valcartier, Quebec, Canada
104. Aubert SA (1994) Characterisation of the hydrodynamic performance properties of NTO and TNTO composite explosives. WL-TR-94-7037 Wright Laboratory, Eglin Air Force Base, Florida, USA
105. Trzcinski WA, Szymanczyk L (2005) Detonation properties of low-sensitivity NTO-based explosives. Energ Mater 23:151–168
106. London JE, Smith DM (1985) A toxicological study of NTO. Report No LA-10533-MS UC-48
107. Sarlauskas J, Nemeilaite-Ceniene A, Anusevicius Z, Miseviciene L, Maroziene A, Markevicius A, Cenas N (2004) Enzymatic redox properties of novel nitrotriazole explosives implications for their toxicity. Z Naturforsch 59c:399–404
108. Reddy G, Song J, Kirby P, Lenta EM, Crousea LCB, Johnson MS (2011) Genotoxicity assessment of an energetic propellant compound, 3-nitro-1,2,4-triazol-5-one (NTO). Mutation Res 719:35–40
109. Tabrizchi M, Lbeigi VI (2010) Detection of explosives by positive corona discharge ion mobility spectrometry. J Hazard Mater 176:692–696
110. Oehrle SA (1997) Analysis of 3-nitro- 1,2,4-triazole-5-one (NTO) in explosive mixtures by capillary electrophoresis. Propellants Explos Pyrotech 22:1–3

Additional Scholarly Articles for Further Reading

111. Amandurdyeva AD, Saraev VV, Kuz'mina NE, Golod EL (2004) Adamantylazoles: VIII. Acid-catalyzed adamantylation of 1,2,4-triazol-5-ones. Russ J Gen Chem 74(8):1277–1281. doi:10.1007/s11176-005-0151-z
112. Andes FS, III (1974) Identification of kinetic performance losses of NTO/MMH. Air Force Rocket Propulsion Laboratory, 45 pp
113. Asahi H, Inabe T (1994) Charge-transfer complexes of 1,4,5,8-naphthalenetetrones and 1,4,9,10-anthracenetetrones. Novel acceptors for electrically conducting materials. Chem Mater 6(10):1875–1879. doi:10.1021/cm00046a050
114. Asahi H, Inabe T (1995) Novel conductive charge-transfer complexes of 1,4,5,8-naphthalenetetrone (NTO) and 1,4,9,10-anthracenetetrone (ATO). Synth Met 70 (1–3):1117–1118. doi:10.1016/0379-6779(94)02780-3
115. Bak A, Maranda A, Nowaczewski J, Szerszen M (2006) Some properties of high explosive mixtures of low sensitivity to external stimuli. Cent Eur J Energ Mater 3(3):53–64
116. Barnes MW, Deppert TM, Taylor RD (1996) Gas-generating compositions using dicyanamide salts as fuel. US5544687A
117. Beard BC, Sharma J (1993) Early decomposition chemistry of NTO, (3-nitro-1,2,4-triazol-5-one). J Energ Mater 11(4–5):325–343. doi:10.1080/07370659308019715
118. Becuwe A, Delclos A, Isler J (1995) EIDS high explosives for 1.6 munitions. American Defense Preparedness Association, pp 119–124
119. Bhatnagar N, Kamath G, Potoff JJ (2013) Prediction of 1-octanol-water and air-water partition coefficients for nitro-aromatic compounds from molecular dynamics simulations. Phys Chem Chem Phys 15(17):6467–6474. doi:10.1039/c3cp44284e

120. Boddu VM, Maloney SW (2012) Physical properties of insensitive munitions compounds for developing wastewater treatment technologies, vol 3. Air & Waste Management Association, pp 1958–1965
121. Bolotina N, Kirschbaum K, Pinkerton AA (2005) Energetic materials: α-NTO crystallizes as a four-component triclinic twin. Acta Crystallogr, Sect B: Struct Sci B 61(5):577–584. doi:10.1107/S0108768105022792
122. Bolotina NB, Zhurova EA, Pinkerton AA (2003) Energetic materials: variable-temperature crystal structure of β-NTO. J Appl Crystallogr 36(2):280–285. doi:10.1107/S002188980300092X
123. Borro-Escribano B, Martinez-Alpuente I, Blanco AD, Torrente J, Fernandez-Manjon B, Matesanz R (2013) Application of game-like simulations in the Spanish Transplant National Organization. Transplant Proc 45(10):3564–3565
124. Botcher TR, Beardall DJ, Wight CA, Fan L, Burkey TJ (1996) Thermal decomposition mechanism of NTO. J Phys Chem 100(21):8802–8806. doi:10.1021/JP952984Y
125. Brill TB, Zhang TL, Tappan BC (2000) Thermal decomposition of energetic materials 74. Volatile metal isocyanates from flash pyrolysis metal-NTO and metal-picrate salts and an application hypothesis. Combust Flame 121(4):662–670. doi:10.1016/S0010-2180(99)00172-8
126. Can Z, Uezer A, Tekdemir Y, Ercag E, Tuerker L, Apak R (2012) Spectrophotometric and chromatographic determination of insensitive energetic materials: HNS and NTO, in the presence of sensitive nitro-explosives. Talanta 90:69–76. doi:10.1016/j.talanta.2011.12.077
127. Catoire L, Chaumeix N, Paillard C (2004) Chemical kinetic model for monomethylhydrazine/nitrogen tetroxide gas-phase combustion and hypergolic ignition. J Propul Power 20(1):87–92. doi:10.2514/1.9234
128. Chakka S, Boddu VM, Maloney SW, Damavarapu R (2008) Prediction of physicochemical properties of energetic materials via EPI suite. American Institute of Chemical Engineers, pp 437/1–437/10
129. Chakka S, Boddu VM, Maloney SW, Toghiani RK, Damavarapu R (2009) Vapor pressures and melting points of select munitions compounds. American Institute of Chemical Engineers, pp chakk1/1–chakk1/9
130. Chang C-R et al (2008) Molecular structure, theoretical calculation and thermal behavior of DAG (NTO). Chin J Chem 26(9):1549–1554. doi:10.1002/cjoc.200890280
131. Chang CW, Wong YM, Chang TC, Chen C (1997) AM1 study of ammonium 3-nitro-1,2,4-triazole-5-onate (ANTO). Propellants, Explos, Pyrotech 22(4):240–241
132. Ciezak JA, Trevino SF (2005) Theoretical and experimental study of the inelastic neutron scattering spectra of β-5-nitro-2,4-dihydro-3H-1,2,4-triazol-3-one. J Mol Struct: THEOCHEM 732(1–3):211–218. doi:10.1016/j.theochem.2005.07.022
133. Ciller JA, Serna FJ, Quintana JR (1992) Thermal characterization of mixtures of nitrotriazolone with HMX and RDX. J Energ Mater 10(4–5):251–265. doi:10.1080/07370659208018925
134. Coburn MD, Lee KY (1990) Picryl derivatives of 5-nitro-2,4-dihydro-3H-1,2,4-triazol-3-one. J Heterocycl Chem 27(3):575–577. doi:10.1002/jhet.5570270318
135. Cortial S, Chaignon P, Sergent D, Dezard S, Ouazzani J (2012) Dehydrogenation, oxidative denitration and ring contraction of N, N-dimethyl-5-nitrouracil by a Bacillus nitroreductase Nfr-A1. J Mol Catal B Enzym 76:1–8. doi:10.1016/j.molcatb.2011.11.014
136. Cronin MP, Day AI, Wallace L (2007) Electrochemical remediation produces a new high-nitrogen compound from NTO wastewaters. J Hazard Mater 149(2):527–531. doi:10.1016/j.jhazmat.2007.08.007
137. Crouse LCB, Lent EM, Leach GJ (2015) Oral toxicity of 3-nitro-1,2,4-triazol-5-one in rats. Int J Toxicol 34(1):55–66. doi:10.1177/1091581814567177
138. Cuddy MF, Poda AR, Chappell MA (2014) Estimations of vapor pressures by thermogravimetric analysis of the insensitive munitions IMX-101, IMX-104, and individual components. Propellants, Explos, Pyrotech 39(2):236–242. doi:10.1002/prep.201300069

139. Cudzilo S, Trzcinski WA (2001) A study on detonation characteristics of pressed NTO. J Energ Mater 19(1):1–21. doi:10.1080/07370650108219390
140. Cumming AS (1995) Characteristics of novel United Kingdom energetic materials. American Defense Preparedness Association, pp 69–74
141. Daimon Y, Terashima H, Koshi M (2014) Chemical kinetics of hypergolic ignition in N2H4/N2O4-NO2 gas mixtures. J Propul Power 30(3):707–716. doi:10.2514/1.B35004
142. Dauerman L, Fraser W (1970) Preignition products from propellants at simulated high altitude conditions (Comment). Combust Sci Technol 2(4):177–178. doi:10.1080/00102207008952246
143. De Paz JLG, Ciller J (1993) On the use of AM1 and PM3 methods on energetic compounds. Propellants, Explos, Pyrotech 18(1):33–40. doi:10.1002/prep.19930180107
144. Deguchi K, Kanno K, Miyagawa H (1976) Application of the natural transition orbital (NTO) method to excited states. Chem Phys Lett 39(1):169–173. doi:10.1016/0009-2614(76)85222-0
145. Delpeyroux D, Charrue P, Simonetti P (1998) Calculation of the energetic performances of explosives: prediction of the heat of formation. High Temp - High Pressures 30(5):625–628. doi:10.1068/htec351
146. Dlott DD, Hambir S, Franken J (1998) The new wave in shock waves. J Phys Chem B 102(12):2121–2130. doi:10.1021/JP973404V
147. Ebrahimbeiki Chimeh A, Montazer M, Rashidi A (2013) Conductive and photoactive properties of polyethylene terephthalate fabrics treated with nano TiO_2/nano carbon blacks. Carbon 64:559. doi:10.1016/j.carbon.2013.07.080
148. Elijosiute E, Jankunaite D, Eicher-Lorka O (2015) TD-DFT study of the electronic absorption spectra of iron(III) monoisothiocyanate. Polyhedron 90:41–46. doi:10.1016/j.poly.2015.01.034
149. Ellis GJ, Bezuidenhout HC (1999) Determination of the detonation energy and some of the energetic characteristics of various NTO-based formulations. In: International Annual Conference ICT 30th:63/1–63/10
150. Fan L, Dass C, Burkey TJ (1996) Synthesis and thermal decomposition of 15 N-labeled NTO. J Labelled Compd Radiopharm 38(1):87–94. doi:10.1002/(SICI)1099-1344(199601)38:1<87:AID-JLCR819>3.0.CO;2-I
151. Fang G, Xu L, Hu X, Li X (2008) DFT study of the interaction between 3-nitro-1,2,4-triazole-5-one and hydrogen fluoride. J Hazard Mater 160(1):51–55. doi:10.1016/j.jhazmat.2008.02.082
152. Festoff BW (ed) (1990) NATO ASI series. Series A, life sciences, vol 191: serine proteases and their serpin inhibitors in the nervous system: regulation in development and in degenerative and malignant disease. In: Proceedings of a NTO advanced research workshop on regulation of extravascular fibrinolysis in nervous system development and disease, Held 2–8 July 1989, Plenum Press, Marater, Italy
153. Finch A, Gardner PJ, Head AJ, Majdi HS (1991) The enthalpies of formation of 1,2,4-triazol-5-one and 3-nitro-1,2,4-triazol-5-one. J Chem Thermodyn 23(12):1169–1173. doi:10.1016/S0021-9614(05)80150-8
154. Finch A, Gardner PJ, Head AJ, Majdi HS (1993) The standard enthalpies of formation of the ammonium and silver salts of 3-nitro-1,2,4-triazol-5-one. Thermochim Acta 213(1–2):17–22. doi:10.1016/0040-6031(93)80003-S
155. Franken J, Hambir SA, Dlott DD (1998) Ultrafast spectroscopy of laser-driven shock waves in molecular materials. Mol Cryst Liq Cryst Sci Technol, Sect A 314:25–36. doi:10.1080/10587259808042453
156. Grau H, Gandzelko A, Samuels P (2014) Solubility determination of raw energetic materials in molten 2,4-dinitroanisole. Propellants, Explos, Pyrotech 39(4):604–608. doi:10.1002/prep.201300083
157. Guillemin JP, Menard Y, Brunet L, Bonnefoy O, Thomas G (2008) Development of a new mixing rheometer for studying rheological behaviour of concentrated energetic suspensions. J Non-Newtonian Fluid Mech 151(1–3):136–144. doi:10.1016/j.jnnfm.2007.12.007

158. Guillemin J-P, Brunet L, Bonnefoy O, Thomas G (2007) A flow time model for melt-cast insensitive explosive process. Propellants, Explos, Pyrotech 32(3):261–266. doi:10.1002/prep.200700028
159. Hahma A (1995) On the combustion of Al under detonation; experimental and theoretical studies. American Defense Preparedness Association, pp 153–159
160. Halcy M, Kuperman RG, Checkai RT (2009) Aquatic toxicity of 3-nitro-1,2,4-triazol-5-one. DIR, ECBC, pp 2, 7–27
161. Harding JT, Fry V, Tuffias RH, Kaplan RB (1987) Oxidation resistance of CVD (chemical vapor deposition) coatings. Ultramet, 29 pp
162. Hare DE et al (1996) Ultrafast dynamics of shock waves and shocked energetic materials. Mater Res Soc Symp Proc 418(Decomposition, Combustion, and Detonation Chemistry of Energetic Materials):337–348
163. Hayashi R, Kowhakul W, Susa A, Koshi M (2009) Detection of explosives using a vacuum ultraviolet ionization time-of-flight mass spectrometry (VUV-TOFMS). Sci Technol Energ Mater 70(3):62–67
164. He B, Nie W, Feng S, Su L, Zhuang F (2013) Effects of NTO oxidizer temperature and pressure on hypergolic ignition delay and life time of UDMH organic gel droplet. Propellants, Explos, Pyrotech 38(5):665–684. doi:10.1002/prep.201200160
165. He B, Nie W, He H (2012) Unsteady combustion model of no metalized organic gel fuel droplet. Energy Fuels 26(11):6627–6639. doi:10.1021/ef300990d
166. Hidding B, Pfitzner M, Bruno C, Simone D (2008) Silanes/H2O2: a high-performance synthetic bipropellant for chemical space propulsion. J Propul Power 24(1):150–153. doi:10.2514/1.30346
167. Hiyoshi RI, Brill TB (2002) Thermal decomposition of energetic materials 83. Comparison of the pyrolysis of energetic materials in air versus argon. Propellants, Explos, Pyrotech 27(1):23–30. doi:10.1002/1521-4087(200203)27:1<23::AID-PREP23>3.0.CO;2-B
168. Hiyoshi RI et al (2006) Effect of pressure on the vibrational structure of insensitive energetic material 5-nitro-2,4-dihydro-1,2,4-triazole-3-one. J Phys Chem A 110(32):9816–9827. doi:10.1021/jp063142+
169. Hoyt N et al (2013) Biomarkers of oral exposure to 3-nitro-1,2,4-triazol-5-one (NTO) and 2,4-dinitroanisole (DNAN) in blood and urine of rhesus macaques (Macaca mulatta). Biomarkers 18(7):587–594. doi:10.3109/1354750X.2013.829522
170. Irfan I, Sawangjaroen N, Bhat AR, Azam A (2010) New dioxazole derivatives: synthesis and effects on the growth of *Entamoeba* histolytica and *Giardia* intestinalis. Eur J Med Chem 45(4):1648–1653. doi:10.1016/j.ejmech.2009.12.051
171. Ishikawa Y, McQuaid MJ (2007) Reactions of NO_2 with CH3NHNH and CH3NNH2: a direct molecular dynamics study. J Mol Struct: THEOCHEM 818(1–3):119–124. doi:10.1016/j.theochem.2007.05.014
172. Jadhav HS, Talawar MB, Dhavale DD, Asthana SN, Krishnamurthy VN (2005) Synthesis, characterization and thermolysis of 2,4-dihydro -2,4,5-trinitro-3H-1,2,4-triazol-3-one (DTNTO): a new derivative of 3-nitro-1,2,4-triazol-5-one (NTO). Indian J Eng Mater Sci 12(5):467–471
173. Jokela K, Kalsch I (2004) Decontamination of MMH- and NTO/MON-propellant tanks. Eur Space Agency, [Spec Publ] SP SP-555(Space Propulsion 2004):157–161
174. Joo Y-H, Gao H, Zhang Y, JnM Shreeve (2010) Inorganic or organic azide-containing hypergolic ionic liquids. Inorg Chem 49(7):3282–3288. doi:10.1021/ic902224t
175. Jung J-W, Kim K-J (2011) Effect of supersaturation on the morphology of coated surface in coating by solution crystallization. Ind Eng Chem Res 50(6):3475–3482. doi:10.1021/ie102099a
176. Keshavarz MH, Pouretedal HR, Semnani A (2007) Novel correlation for predicting impact sensitivity of nitroheterocyclic energetic molecules. J Hazard Mater 141(3):803–807. doi:10.1016/j.jhazmat.2006.07.046

177. Keshavarz MH, Sadeghi H (2009) A new approach to predict the condensed phase heat of formation in acyclic and cyclic nitramines, nitrate esters and nitroaliphatic energetic compounds. J Hazard Mater 171(1–3):140–146. doi:10.1016/j.jhazmat.2009.05.118
178. Kim KJ (2000) Spherulitic crystallization of 3-nitro-1,2,4-triazol-5-one in water + N-methyl-2-pyrrolidone. J Cryst Growth 208(1–4):569–578. doi:10.1016/S0022-0248(99)00408-X
179. Kim K-J, Kim H-S (2008) Agglomeration of NTO on the surface of HMX particles in water-NMP solvent. Cryst Res Technol 43(1):87–92. doi:10.1002/crat.200710946
180. Kim K-J, Kim M-J, Lee J-M, Kim S-H, Kim H-S, Park B-S (1998) Experimental solubility and density for 3-nitro-1,2,4-triazol-5-one + C1 to C7 1-alkanols. Fluid Phase Equilib 146 (1, 2):261–268. doi:10.1016/S0378-3812(98)00182-4
181. Kim YH, Lee K, Koo KK, Shul YG, Haam S (2002) Comparison study of mixing effect on batch cooling crystallization of 3-nitro-1,2,4-triazol-5-one (NTO) using mechanical stirrer and ultrasound irradiation. Cryst Res Technol 37(9):928–944. doi:10.1002/1521-4079(200209)37:9<928:AID-CRAT928>3.0.CO;2-R
182. Knowles PJ (1972) Helium absorption into nitrogen tetroxide (NTO) and Aerozine-50 (A-50). J Spacecr Rockets 9(9):708–709. doi:10.2514/3.61782
183. Kohno Y, Takahashi O, Saito K (2001) Theoretical study of initial decomposition process of NTO dimer. Phys Chem Chem Phys 3(14):2742–2746. doi:10.1039/b101745o
184. Krause G (2012) Volume-dependent self-ignition temperatures for explosive materials. Propellants, Explos, Pyrotech 37(1):107–115. doi:10.1002/prep.201100007
185. Krzmarzick MJ, et al. (2015) Biotransformation and Degradation of the Insensitive Munitions Compound, 3-nitro-1,2,4-triazol-5-one (NTO), by Soil Bacterial Communities. Environ Sci Technol. Ahead of Print. doi:10.1021/acs.est.5b00511
186. Kulkarni PB, Purandare GN, Nair JK, Talawar MB, Mukundan T, Asthana SN (2005) Synthesis, characterization, thermolysis and performance evaluation studies on alkali metal salts of TABA and NTO. J Hazard Mater 119(1–3):53–61. doi:10.1016/j.jhazmat.2004.12.014
187. Kulkarni PB et al (2005) Studies on salts of 3-nitro-1,2,4-triazol-5-one (NTO) and 2,4,6-trinitroanilino benzoic acid (TABA): potential energetic ballistic modifiers. J Hazard Mater 123(1–3):54–60. doi:10.1016/j.jhazmat.2005.04.010
188. Le Campion L, Adeline MT, Ouazzani J (1997) Separation of NTO related 1,2,4-triazole-3-one derivatives by a high performance liquid chromatography and capillary electrophoresis. Propellants, Explos, Pyrotech 22(4):233–237. doi:10.1002/prep.19970220410
189. Le Campion L, Delaforge M, Noel JP, Ouazzani J (1998) Metabolism of 14C-labeled 5-nitro-1,2,4-triazol-3-one (NTO): comparison between rat liver microsomes and bacterial metabolic pathways. J Mol Catal B Enzym 5(1–4):395–402. doi:10.1016/S1381-1177(98)00103-9
190. Le Campion L, Giannotti C, Ouazzani J (1999) Photocatalytic degradation of 5-nitro-1,2,4-triazol-3-one (NTO) in aqueous suspension of TiO_2 comparison with Fenton oxidation. Chemosphere 38(7):1561–1570. doi:10.1016/S0045-6535(98)00376-2
191. Lee JS, Jaw KS (2006) Thermal decomposition properties and compatibility of CL-20, NTO with silicone rubber. J Therm Anal Calorim 85(2):463–467. doi:10.1007/s10973-005-7325-0
192. Li D, Haneda H, Hishita S, Ohashi N (2005) Visible-light-active nitrogen-containing TiO_2 photocatalysts prepared by spray pyrolysis. Res Chem Intermed 31(4–6):331–341. doi:10.1163/1568567053956653
193. Lin H, Zhu S-G, Zhang L, Peng X-H, Chen P-Y, Li H-Z (2013) Intermolecular interactions, thermodynamic properties, crystal structure, and detonation performance of HMX/NTO cocrystal explosive. Int J Quantum Chem 113(10):1591–1599. doi:10.1002/qua.24369
194. Linker BR et al (2015) Adsorption of novel insensitive munitions compounds at clay mineral and metal oxide surfaces. Environ Chem 12(1):74–84. doi:10.1071/EN14065
195. Liu Z, Wu Q, Zhu W, Xiao H (2015) Vacancy-induced initial decomposition of condensed phase NTO via bimolecular hydrogen transfer mechanisms at high pressure: a DFT-D study. Phys Chem Chem Phys 17(16):10568–10578

196. Long GT, Brems BA, Wight CA (2002) Thermal activation of the high explosive NTO: sublimation, decomposition, and autocatalysis. J Phys Chem B 106(15):4022–4026. doi:10.1021/jp012894v
197. Ma H et al (2009) Preparation, non-isothermal decomposition kinetics, heat capacity and adiabatic time-to-explosion of NTO·DNAZ. J Hazard Mater 169(1–3):1068–1073. doi:10.1016/j.jhazmat.2009.04.057
198. McMillen DF, Erlich DC, He C, Becker CH, Shockey DA (1997) Fracture-induced and thermal decomposition of NTO using laser ionization mass spectrometry. Combust Flame 111(3):133–160. doi:10.1016/S0010-2180(97)00100-4
199. Muthurajan H, Sivabalan R, Talawar MB, Asthana SN (2004) Computer simulation for prediction of performance and thermodynamic parameters of high energy materials. J Hazard Mater 112(1–2):17–33. doi:10.1016/j.jhazmat.2004.04.012
200. Najafi M, Samangani AK (2011) Non-isothermal kinetic study of the thermal decomposition of melamine 3-nitro-1,2,4-triazol-5-one salt. Propellants, Explos, Pyrotech 36(6):487–492. doi:10.1002/prep.201000153
201. Nandi AK, Singh SK, Kunjir GM, Singh J, Mandal AK, Pandey RK (2013) Assay of the intensive high explosive 3-nitro-1,2,4-triazol-5-one (NTO) by acid-base titration. Cent Eur J Energ Mater 10(1):113–122
202. Nazari A, Montazer M, Dehghani-Zahedani M (2013) Nano TiO_2 as a new tool for mothproofing of wool: protection of wool against *Anthrenus verbasci*. Ind Eng Chem Res 52 (3):1365–1371. doi:10.1021/ie302187c
203. Nouguez B, Mahe B, Vignaud PO (2009) Cast PBX related technologies for IM shells and warheads. Sci Technol Energ Mater 70(6):135–139
204. Oestmark H, Bergman H, Aqvist G (1993) The chemistry of 3-nitro-1,2,4-triazol-5-one (NTO): thermal decomposition. Thermochim Acta 213(1–2):165–175. doi:10.1016/0040-6031(93)80014-2
205. Osmont A, Catoire L, Klapotke TM, Vaghjiani GL, Swihart MT (2008) Thermochemistry of species potentially formed during NTO/MMH hypergolic ignition. Propellants, Explos, Pyrotech 33(3):209–212. doi:10.1002/prep.200700213
206. Oxley JC, Smith JL, Rogers E, Dong XX (1997) NTO decomposition products tracked with 15 N labels. J Phys Chem A 101(19):3531–3536. doi:10.1021/JP9640078
207. Oxley JC, Smith JL, Yeager KE (1995) Synthesis of 15 N-labeled isomers of 5-nitro-2,4-dihydro-3H-1,2,4-triazol-3-one (NTO). J Energ Mater 13(1&2):93–105. doi:10.1080/07370659508019345
208. Oxley JC, Smith JL, Zhou Z, McKenney RL (1995) Thermal decomposition studies on NTO. International Annual Conference ICT 26th(Pyrotechnics):28/1–28/15
209. Oxley JC, Smith JL, Zhou Z, McKenney RL (1995) Thermal decomposition studies on NTO and NTO/TNT. J Phys Chem 99(25):10383–10391. doi:10.1021/j100025a047
210. Piotrowski T, Fraczak M, Buczkowski D, Paplinski A, Maranda A (2006) The ranking of explosives by use of material indices as proposed in the Temclev-Ex method. Cent Eur J Energ Mater 3(1–2):3–17
211. Powala D, Orzechowski A, Maranda A, Nowaczewski J, Lorek A (2004) Researches on new crystalline form of some insensitive high explosives in PBX. Cent Eur J Energ Mater 1 (1):63–73
212. Prabhakaran KV, Naidu SR, Kurian EM (1994) XRD, spectroscopic and thermal analysis studies on 3-nitro-1,2,4-triazol-5-one. Thermochim Acta 241(1–2):199–212. doi:10.1016/0040-6031(94)87018-7
213. Quinn MJ Jr, Bannon DI, Jackovitz AM, Hanna TL, Shiflett AA, Johnson MS (2014) Assessment of 3-nitro-1,2,4-triazol-5-one as a potential endocrine disrupting chemical in rats using the Hershberger and uterotrophic bioassays. Int J Toxicol 33(5):367–372. doi:10.1177/1091581814548729
214. Russell AL, Seiter JM, Coleman JG, Winstead B, Bednar AJ (2014) Analysis of munitions constituents in IMX formulations by HPLC and HPLC-MS. Talanta 128:524–530. doi:10.1016/j.talanta.2014.02.013

215. Salvador CAV, Costa FS (2006) Vaporization lengths of hydrazine fuels burning with NTO. J Propul Power 22(6):1362–1372. doi:10.2514/1.18348
216. Sarangapani R, Ramavat V, Reddy S, Subramanian P, Sikder AK (2015) Rheology studies of NTO-TNT based melt-cast dispersions and influence of particle-dispersant interactions. Powder Technol 273:118–124. doi:10.1016/j.powtec.2014.12.013
217. Sarangapani R, Ramavat V, Reddy TS, Patil RS, Gore GM, Sikder AK (2014) Effect of particle size and shape of NTO on micromeritic characteristics and its explosive formulations. Powder Technol 253:276–283. doi:10.1016/j.powtec.2013.11.029
218. Schoenman L (1995) 4000°F materials for low-thrust rocket engines. J Propul Power 11 (6):1261–1267. doi:10.2514/3.23967
219. Schwarzenbach D, Kirschbaum K, Pinkerton AA (2006) Order-disorder twinning model and stacking faults in alpha-NTO. Acta Crystallogr B 62(Pt 5):944–948
220. Schwarzenbach D, Kirschbaum K, Pinkerton AA (2006) Order-disorder twinning model and stacking faults in α-NTO. Acta Crystallogr, Sect B: Struct Sci B 62(5):944–948. doi:10.1107/S0108768106024761
221. Scott AM, Burns EA, Hill FC (2014) Theoretical study of adsorption of nitrogen-containing environmental contaminants on kaolinite surfaces. J Mol Model 20(8):1–13. doi:10.1007/s00894-014-2373-7
222. Scott AM, Burns EA, Lafferty BJ, Hill FC (2015) Theoretical predictions of thermodynamic parameters of adsorption of nitrogen containing environmental contaminants on kaolinite. J Mol Model 21(2):21
223. Shekhar H (2012) Studies on empirical approaches for estimation of detonation velocity of high explosives. Cent Eur J Energ Mater 9(1):39–48
224. Shukla MK, Hill F (2014) Dissociative adsorption of 5-nitro-2,4-dihydro-3h-1,2,4-triazol-3-one (NTO) on aluminum-terminated (0001) surface of α-alumina as predicted from plane-wave density functional theory. J Phys Chem C 118 (1):310–319. doi:10.1021/jp408661h
225. Sinditskii VP et al (2009) Evaluation of decomposition kinetics of energetic materials in the combustion wave. Thermochim Acta 496(1–2):1–12. doi:10.1016/j.tca.2009.07.004
226. Singh G, Felix SP (2003) Studies of energetic compounds, part 29: effect of NTO and its salts on the combustion and condensed phase thermolysis of composite solid propellants, HTPB-AP. Combust Flame 132(3):422–432. doi:10.1016/S0010-2180(02)00479-0
227. Singh G, Felix SP (2003) Studies on energetic compounds. Part 32: crystal structure, thermolysis and applications of NTO and its salts. J Mol Struct 649(1–2):71–83. doi:10.1016/S0022-2860(02)00717-2
228. Singh G, Kapoor IPS, Felix SP, Agrawal JP (2002) Studies on energetic compounds part 23: preparation, thermal and explosive characteristics of transition metal salts of 5-nitro-2,4-dihydro-3H-1,2,4-triazole-3-one (NTO). Propellants, Explos, Pyrotech 27 (1):16–22. doi:10.1002/1521-4087(200203)27:1<16:AID-PREP16>3.0.CO;2-W
229. Singh G, Kapoor IPS, Mannan SM, Tiwari SK (1998) Studies on energetic compounds Part 7 thermolysis of ring-substituted arylammonium salts of 3-nitro-1,2,4-triazole-5-one (NTO). J Energ Mater 16(2 & 3):101–118. doi:10.1080/07370659808217507
230. Singh G, Kapoor IPS, Mannan SM, Tiwari SK (1998) Studies on energetic compounds. Part 6. Synthesis of ring-substituted arylammonium salts of 3-nitro-1,2,4-triazol-5-one(NTO). J Energ Mater 16(1):31–43. doi: 10.1080/07370659808216092
231. Singh G, Kapoor IPS, Tiwari SK (2000) Studies on energetic compounds (part 18): preparation and kinetics of thermolysis of alkaline earth metal salts of 5-nitro-2,4-dihydro-3H-1,2,4-triazole-3-one (NTO). Indian J Chem Technol 7(5):236–241
232. Singh G, Kapoor IPS, Tiwari SK, Felix SP, Ninan KN, Varghese TL (2002) Studies on energetic compounds. Part 15: transition metal salts of NTO as potential energetic ballistic modifiers for composite solid propellants. J Energ Mater 20(4):309–327. doi:10.1080/07370650208244826

233. Singh G, Kapoor IPS, Tiwari SK, Prem FS (2000) Studies on energetic compounds. Part 12. Preparation and thermolysis of transition metal salts of 5-nitro-2,4-dihydro-3H-1,2,4-triazol-3-one (NTO). Indian J Eng Mater Sci 7(3):167–171
234. Singh G, Prem Felix S (2002) Studies on energetic compounds 25. An overview of preparation, thermolysis and applications of the salts of 5-nitro-2,4-dihydro-3H-1,2,4-triazol-3-one (NTO). J Hazard Mater 90(1):1–17. doi:10.1016/S0304-3894(01)00349-1
235. Singh G, Prem Felix S (2003) Studies on energetic compounds Part 36: evaluation of transition metal salts of NTO as burning rate modifiers for HTPB-AN composite solid propellants. Combust Flame 135(1–2):145–150. doi:10.1016/S0010-2180(03)00156-1
236. Stanley JK, Lotufo GR, Biedenbach JM, Chappell P, Gust KA (2015) Toxicity of the conventional energetics TNT and RDX relative to new insensitive munitions constituents DNAN and NTO in Rana pipiens tadpoles. Environ Toxicol Chem 34(4):873–879. doi:10.1002/etc.2890
237. Sutton NV, Dubb HE, Bell RE, Lysyj I, Neale BC (1965) Chemical analysis of corrosive oxidizers. II. Instrumental analysis of nitrogen tetroxide. Advan Chem Set 54:231–236
238. Teipel U, Krober H, Krause HH (2001) Formation of energetic materials using supercritical fluids. Propellants, Explos, Pyrotech 26(4):168–173. doi:10.1002/1521-4087(200110)26:4<168:AID-PREP168>3.0.CO;2-X
239. Tuerker L, Atalar T (2006) Quantum chemical study on 5-nitro-2,4-dihydro-3H-1,2,4-triazol-3-one (NTO) and some of its constitutional isomers. J Hazard Mater 137(3):1333–1344. doi:10.1016/j.jhazmat.2006.05.015
240. Tuerker L, Bayar CC (2012) NTO-picryl constitutional isomers-A DFT study. J Energ Mater 30(1):72–96. doi:10.1080/07370652.2010.543005
241. Underwood CJ, Wall C, Provatas A, Wallace L (2012) New high nitrogen compounds azoxytriazolone (AZTO) and azotriazolone (azoTO) as insensitive energetic materials. New J Chem 36(12):2613–2617. doi:10.1039/c2nj40800g
242. Van der Heijden AEDM (1998) Crystallization and characterization of energetic materials. Curr Top Cryst Growth Res 4:99–114
243. Vaullerin M, Espagnacq A, Blaise B (1998) Reparametrization of the BKW equation of state for the triazoles and comparison of the detonation properties of HMX, TNMA, and NTO by means of ab-initio and semiempirical calculations. Propellants, Explos, Pyrotech 23(2):73–76. doi:10.1002/(SICI)1521-4087(199804)23:2<73:AID-PREP73>3.0.CO;2-M
244. Vaullerin M, Espagnacq A, Morin-Allory L (1998) Prediction of explosives impact sensitivity. Propellants, Explos, Pyrotech 23(5):237–239. doi:10.1002/(SICI)1521-4087(199811)<237:AID-PREP237>3.0.CO;2-#
245. Wallace L, Cronin MP, Day AI, Buck DP (2009) Electrochemical method applicable to treatment of wastewater from nitrotriazolone production. Environ Sci Technol 43(6):1993–1998. doi:10.1021/es8028878
246. Walsh MR et al (2014) Energetic residues from the detonation of IMX-104 insensitive munitions. Propellants, Explos, Pyrotech 39(2):243–250. doi:10.1002/prep.201300095
247. Walsh MR et al (2013) Characterization of PAX-21 insensitive munition detonation residues. Propellants, Explos, Pyrotech 38(3):399–409. doi:10.1002/prep.201200150
248. Williams GK, Brill TB (1995) Thermal decomposition of energetic materials. 68. Decomposition and sublimation kinetics of NTO and evaluation of prior kinetic data. J Phys Chem 99(33):12536–12539. doi:10.1021/j100033a027
249. Xie Y, Hu R, Wang X, Fu X, Zhu C (1991) Thermal behavior of 3-nitro-1,2,4-triazol-5-one and its salts. Thermochim Acta 189(2):283–296
250. Xie Y, Hu R, Yang C, Feng G, Zhou J (1992) Studies on the critical temperature of thermal explosion for 3-nitro-1,2,4-triazol-5-one (NTO) and its salts. Propellants, Explos, Pyrotech 17(6):298–302
251. Yang G, Nie F (2006) Preparation and characterization of core/shell structure of HMX/NTO composite particles. Sci Technol Energ Mater 67(2):77–81

252. Yau AD, Byrd EFC, Rice BM (2009) An investigation of KS-DFT electron densities used in atoms-in-molecules studies of energetic molecules. J Phys Chem A 113(21):6166–6171. doi:10.1021/jp9010845
253. Ye S, Tonokura K, Koshi M (2003) Energy transfer rates and impact sensitivities of crystalline explosives. Combust Flame 132(1/2):240–246. doi:10.1016/S0010-2180(02)00461-3
254. Yim W-L, Z-f Liu (2001) Application of Ab initio molecular dynamics for a priori elucidation of the mechanism in unimolecular decomposition: the case of 5-nitro-2,4-dihydro-3H-1,2,4-triazol-3-one (NTO). J Am Chem Soc 123(10):2243–2250. doi:10.1021/ja0019023
255. Yun S-S, Kim J-K, Kim C-H (2006) Lanthanide complexes of some high energetic compounds, crystal structures and thermal properties of 3-nitro-1,2,4-triazole-5-one (NTO) complexes. J Alloys Compd 408–412:945–951. doi:10.1016/j.jallcom.2004.11.087
256. Zbarsky V, Basal A, Yudin N, Zhilin VF (2003) Study on solubility of 2,4-dihydro-3H-1,2,4-triazol-3-one and 5-nitro-2,4-dihydro-3H-1,2,4-triazol-3-one in diluted acid. International Annual Conference ICT 34th:139/1–139/8
257. Zeman S (1997) Kinetic compensation effect and thermolysis mechanisms of organic polynitroso and polynitro compounds. Thermochim Acta 290(2):199–217. doi:10.1016/S0040-6031(96)03078-X
258. Zeman S (2003) New aspects of impact reactivity of polynitro compounds. Part IV. Allocation of polynitro compounds on the basis of their impact sensitivities. Propellants, Explos, Pyrotech 28(6):308–313. doi:10.1002/prep.200300021
259. Zhang TL, Hu RZ, Li FP (1994) Structural characterization and thermal decomposition mechanisms of alkaline earth metal (Mg, Ca, Sr, and Ba) salts of 3-nitro-1,2,4-triazol-5-one. Thermochim Acta 244(1–2):185–194
260. Zhu W et al (2015) Shaping single-crystalline trimetallic Pt-Pd-Rh nanocrystals toward high-efficiency C-C splitting of ethanol in conversion to CO_2. ACS Catal 5(3):1995–2008. doi:10.1021/cs5018419
261. Zhurova EA, Pinkerton AA (2001) Chemical bonding in energetic materials: beta-NTO. Acta Crystallogr B 57(Pt 3):359–365
262. Zhurova EA, Pinkerton AA (2001) Chemical bonding in energetic materials: β-NTO. Acta Crystallogr, Sect B: Struct Sci B 57(3):359–365. doi:10.1107/S0108768100020048
263. Zhurova EA, Tsirelson VG, Stash AI, Yakovlev MV, Pinkerton AA (2004) Electronic energy distributions in energetic materials: NTO and the biguanidinium dinitramides. J Phys Chem B 108(52):20173–20179. doi:10.1021/jp0470997

Chapter 6
Hexanitrostilbene (HNS)

Abstract This chapter summarizes the properties of 2, 2′, 4, 4, 6, 6′ hexanitrostilbene (HNS) relative to more common thermally stable explosives. The very fine crystalline HNS material, purified by extraction of impurities, is designated as HNS-I. HNS-II is a larger particle-size, higher bulk-density, free-flowing material obtained by recrystallization of HNS-I.

6.1 Introduction

2, 2′, 4, 4, 6, 6′ hexanitrostilbene, HNS, [also known as JD-X] is a heat resistant explosive and has been used extensively in space applications. It was used on the Apollo spaceship program for stage operation. It is less sensitive compared to other compounds such as tetryl. It is used in military applications for detonating fuses. HNS exists in two polymorphs HNS I and HNS II. HNS I appears as thin fluffy plates where as HNS II exists in orthorhombic crystalline form. There are minor differences in the properties of these two polymorphs, but the yield of HNS II is too small to be of commercial use. Another form HNS IV has been by produced from HNS II [1]. While HNS I and II are used in mild detonating fuses, HNS IV is used as an initiator. HNS has been used in the manufacture of new booster explosives [2] such as LX-15 (RX-26-AS) for some time. It is a heat-resistant explosive with a low vapor pressure, high vacuum stability and a melting point between 316 and 321 °C. Neyer [1] has reported the explosive properties of HNS-IV. The USA military standard MIL-E-82903 is very specific of how HNS IV is made from HNS I. It states “HNS-IV shall be crash precipitated from HNS-II which was recrystallized from HNS-I conforming to WS 5003. HNS-II must be prepared by recrystallization from an organic solvent system (i.e., Dimethylformamide—DMF certified) by the process approved by the contracting agency. HNS-IV shall be a superfine particle size material with a surface area of 5.0–25.0 square meters per gram (m/g). HNS-I is a high explosive synthesized by a “one-step” process from trinitrotoluene (TNT).”

D.S. Viswanath et al., *Emerging Energetic Materials: Synthesis, Physicochemical, and Detonation Properties*, https://doi.org/10.1007/978-94-024-1201-7_6

6.2 Synthesis

Shipp [3] is credited for synthesizing HNS first by reacting tri-nitrobenzyl bromide with alcoholic potash. Although Reich et al. [4] used a similar synthesis route before Shipp, it was found out that the compound Reich et al. synthesized was 2, 2′, 4, 4, 6, 6′ hexanitrobibenzyl. Shipp confirmed the product to be HNS by performing spectral and elemental analysis. The reaction path used by Shipp is shown below (Fig. 6.1). Shipp reported an over-all yield of 40–45%.

Shipp and Kaplan [5] modified the original process of Shipp and also discussed the reaction mechanisms. The modified reaction scheme is shown in Fig. 6.2.

Shipp [6] was issued a patent based on the above synthesis route. In this process HNS is prepared by reacting 2,4,6-trinitrotoluene (TNT) with a 5% aqueous sodium hypochlorite solution in the presence of tetrahydrofuran (THF) and methanol (MeOH) as solvents. TNT is chlorinated producing trinitrobenzyl chloride, which subsequently reacts with NaOH producing a mixture of HNS and HNBiB that precipitates out as crystals. However, Kayser [7] noted that a combined yield of HNS and HNBiB is less than 50% with the remainder of the material forming a red-tar fraction. Approximately 98% of the HNS can be recovered in the crystalline form from the product stream. However, several by-products and unreacted TNT have been found trapped within the HNS crystals. The byproducts include HNBiB, Anil, PiOH, PiCHOH, $PiCH_2Cl$, chloropicrin, PiCOOH, PiCl, PiCHO, TNB, and unreacted TNT.

Several attempts have been made to develop simple methods employing comparatively cheaper and less toxic solvents to get better yields of HNS. Similar experiments with different concentrations of sodium hypochlorite at different *pH* and solvent systems were attempted. The overall reaction schemes are shown

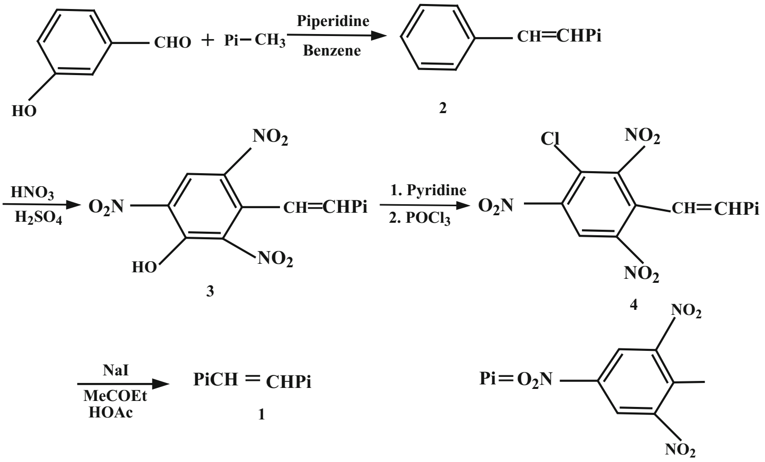

Fig. 6.1 Reaction path chemical structure of HNS [3]

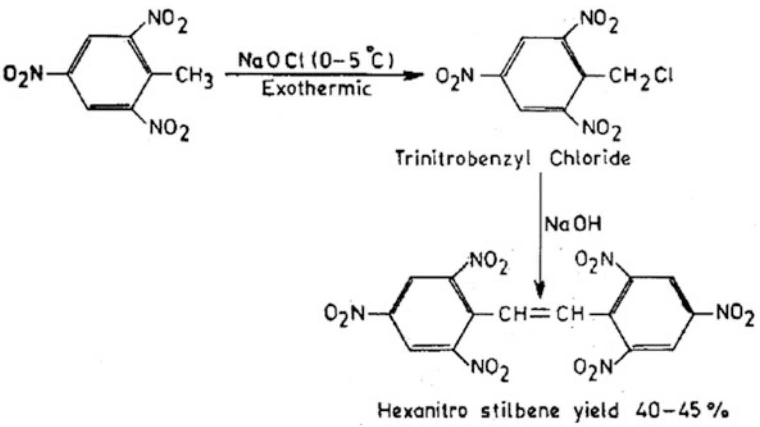

Fig. 6.2 Shipp process 2, 2′, 4, 4, 6, 6′ hexanitrostilbene stilbene yield [5]

below. Synthesis routes for HNS have been surveyed by Singh and Singh [8] and shown in Fig. 6.3.

Sodium hypochlorite, calcium hypochlorite or potasium hypochlorite in concentrations varying from 5 to 12% were used in the synthesis of HNS and 42% yield was obtained. Procedures for the preparation of 2,4,6 trinitrobenzyl chloride with 85% yield and 2, 2′, 4, 4′, 6, 6′ hexanitrobibenzyl with 79% yield were reported. Later on three modifications of Shipp process were reported.

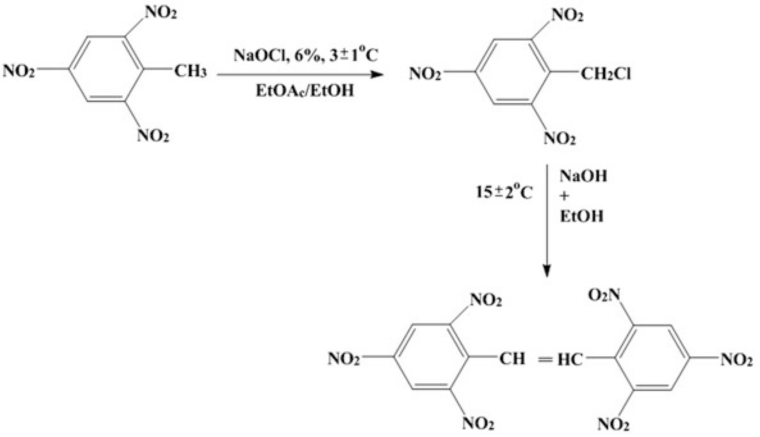

Fig. 6.3 Synthesis of Hexanitrostilbene overall reaction can be depicted TBRL (Terminal Ballistics Research Laboratory) process [8]

6.2.1 UK Laboratory HNS Process

This report [9] describes the separation, characterization, and analysis of the products which the Shipp hexanitrostilbene (HNS) process yields. In this process, trinitrotoluene (TNT), dissolved in a mixture of tetrahydrofuran (THF) and methanol (MeOH), is reacted with commercial bleach (NaOCl) to form HNS (Fig. 6.4). Hexanitrostilbene has been tested in silver and aluminum detonating cords. These cords were loaded with the explosive precipitated both from organic solvents and acid solvents at two different density ranges (detonation velocities). Thermal stability is reflected as changes in detonation velocity as a function of temperature and time of exposure.

6.2.2 Kompolthy Process

Kompolthy et al. [10], [Hungarian Pat. T/9639 No. VE-719 (CO6 f 9/04, Fig. 6.5)], developed a new procedure based on the air oxidation of TNT. They also observed that the preparation of HNS from TNT could be done in two steps as follows. Shipp and Kaplan [5] showed that TNT could be converted to HNBB or HNS using sodium hypochlorite under varied conditions, but they did not demonstrate any procedure for converting HNBB to HNS. Shipp and Kaplan obtained a 79% yield of HNBB from TNT. Kompolthy et al. obtained an 82% yield of HNBB and reported yields of 76–91% of HNS from HNBB using dimethylformamide or dimethylsulfoxide as solvents in a reaction mixture containing methanol, potassium hydroxide, copper sulfate and pyridine. This Kompolthy et al. work has been repeated by others but yields of only 25–40% of HNS have been obtained. There is, therefore, a need for a process for the production of HNS in high reproducible yields.

In the synthesis of HNS, the yield depends on the concentration of the alkali and there appears to be an optimum concentration. Some modifications have been made to these processes in the UK [9] and Kompolthy et al. [11, 12]. Several other processes, including continuous processes, have been described both in open and patented literature. HNS is made industrially using the Schipp and Kaplan process [5]. Singh and Malhotra [13] have surveyed the literature on HNS up to 1983.

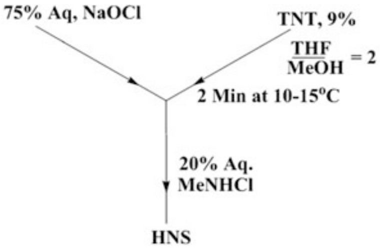

Fig. 6.4 U. K. Laboratory HNS Process [9]

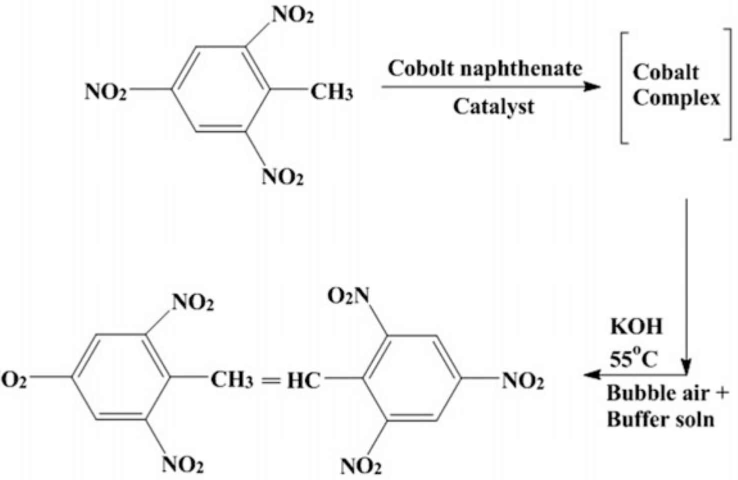

Fig. 6.5 Kompolthy-Hungarian process [10]

Sleadd et al. [14] and Morris et al. [15] disclosed processes for the production of HNS which essentially consisted of oxidative coupling of TNT in the presence of air, methanolic potassium hydroxide solution, a polar aprotic solvent and optionally a catalyst consisting of anhydrous copper sulphate or cobalt naphthenate (Fig. 6.6). The first unequivocal synthesis of HNS was disclosed in U.S. Pat. No. 3,505,413 [3].

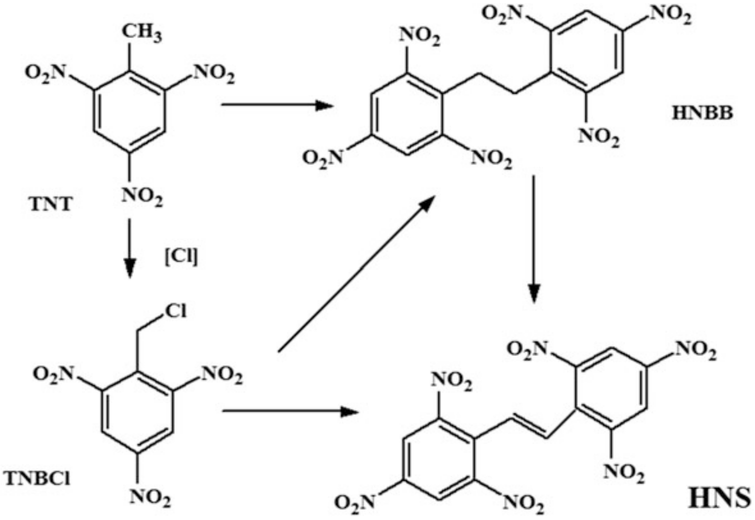

Fig. 6.6 Synthesis of HNS [14, 15]

Several modifications in starting materials, catalysts, and process parameters have been used, and these as tabulated by Morris et al. [15] are shown below along with original references.

- Shipp [6]: NaOCl, THF, MeOH
- Kompolthy et al. [10]: Co/Cu complex, O_2, Base, Polar Aprotic Solvent (PAS)
- Duffin et al. [16]: Carboxylate base, O_2, PAS
- Duffin et al. [17]: $CuCl_2$, Carboxylate base, PAS
- Kompolthy et al. [12]: HNBB, O_2, Copper complex, Base, PAS
- Gilbert [19]: HNBB, O_2, Copper complex, Base, PAS
- Sollott [20]: TNBCl, THF, Methanol, Base.
- Duffin et al. [18]: HNBB, Carboxylate base, O_2, PAS.

Morris et al. [21] carriedout improvements for scale-up of HNS. This is a two step process consisting of:

1. Vary Shipp conditions to maximize HNBB—No THF, higher temperature, added base
2. Use Gilbert process to convert HNBB to HNS—DMSO, copper amine complex and air as the oxidant.

Bellamy [22] reaction scheme is shown in (Fig. 6.7). One can envisage that HNS is formed by self-condensation of TNBCl (reaction between TNBCl and its conjugate base B), via R-chlorohexanitrobibenzyl, whilst HNBB is formed by cross condensation of TNBCl with the conjugate base of TNT (A), the mode of addition generating conditions which favor one or the other of these two products. In less controlled mixing regimes both products are likely to be formed. In the batch synthesis of HNS, the reaction occurs in essentially two stages.

Golding and Hayes [23] used Schipp synthesis and studied the effects of time, temperature, pH, solvent composition and mode of TNT addition on the yield of HNS. They found the reaction to be highly susceptible to variations in process conditions, particularly the type of base and water concentrations. A British patent by Golding et al. [24] describes the synthesis of HNS by the oxidation of TNT using curic (II) and Co (III) salts. Various solvents including DMF, pyridine, N-methylpyrrolidone, hexamethylphosphoramide, dioxane, N,N-dimethylacetamide, DMSO, HMPA, di-Me propylene urea, dimethylethylene urea were used. Gilbert [19] used different oxidizing agents in particular copper (II) compounds, halogenating agents, quinones, and air or oxygen, in the synthesis of HNS. The reactions were carried out in basic medium with a proper solvent.

Bellamy [25] scaled up the synthesis of HNS from 2.5 to 25 g of TNT reactant. The author used the same reaction time but varied the diameter of the stirrer by a factor of two. The variation of the ratio of NaOCl to TNT (0.5–1.2) and the concentration of reactants were also investigated. Various conditions for the after-reaction period (2 h) were explored on the basis of the author's work with a batch reactor, including (i) no pH control, (ii) pH control using aq. H_2SO_4 and NaOH solutions, and (iii) pH control using aq. RNH_3Cl and RNH_2 solutions. Under

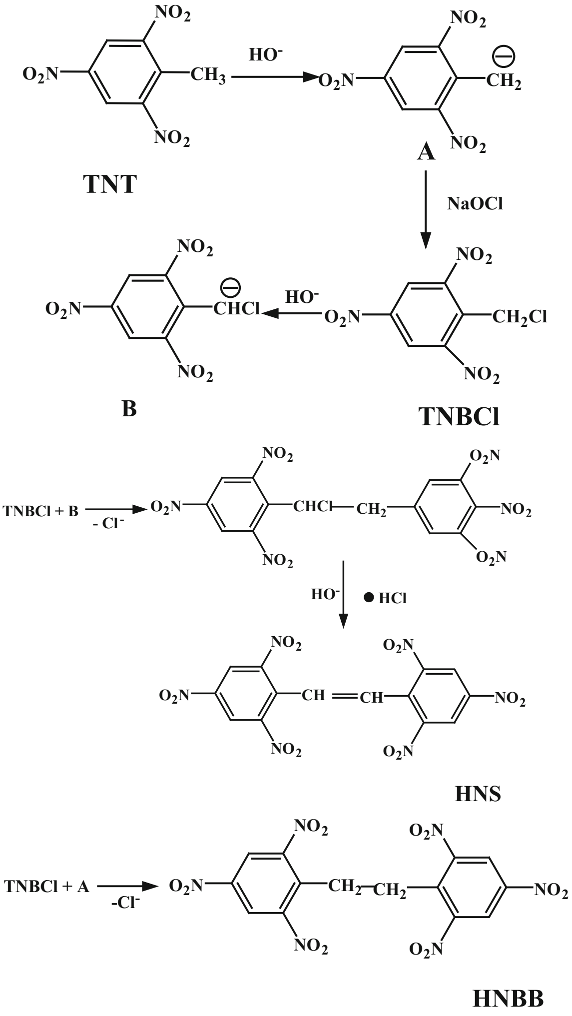

Fig. 6.7 Synthesis of HNS by Bellamy [22]

most of the conditions investigated the author reports better yields and selectivity. The intermediate in the Schipp synthesis is α-chloro-2,2′,4,4′,6,6′-hexanitrobibenzyl. An NMR of this compound has been presented by Bellamy [25]. Lu [26] describe a two-step process starting with TNT via an intermediate hexylnitrobibenzyl and further oxidation. They claim good conversion of TNT and yield of HNS. The effects of solvents in their synthesis has been described in a separate communication [27].

Orechowski et al. [28] have paid particular attention to obtain cubic crystals in their attempt to synthesize HNS. Various parameters affecting the formation and growth of crystals were investigated. They used tetrahydrofurane as the solvent and N,N,N,-tertbutylamineammonium chloride as the phase transfer catalyst. A combination of solvents and 100% fuming nitric acid was used for crystallization, and the crystal density was 1.74 g/cm^3. Prior to this study, Dacons [29] studied the crystallization of HNS. A continuous method for the preparation of HNS from TNT and crystallization using nitric acid is the subject of a study by Emeury [30]. It is reported that this method yielded crystals of 6.2 m diameter melting at 317 °C, and had a detonation velocity of 6900 ms^{-1} when used with 5% poly (tetra fluoro-ethylene). A patent filed for the U.K. Defense Department describes a process for the production of HNS by catalytic oxidation of TNT using a cupric or a cobalt salt [31]. Yet another method of synthesis is the conversion of 4,6-trinitrobenzyl chloride to 2,2′,4,4′,6,6′-hexanitrostilbene by nitrogen bases such as amines instead of sodium hydroxide [20]. Higher yields are reported in this route. An interesting place where HNS IV is made is at Perkin Elmer Optoelectronics [1].

6.3 Structure

Gerard and Hardy [32] reported that HNS is monoclinic with space group $P2_1/c$, with $a = 22.326(7)$, $b = 5.5706(9)$, $c = 14.667(2)$ Å, and $\beta = 110.04(1)°$; D_m (exptl.) = 1.74(1) and D_x(calcd.) = 1.745(1) g/cm^3 for Z = 4 final R = 0.051 for 2345 reflections. The atomic coordinates are given. Two different molecules have a symmetry center either in 2(*d*) o ri n2 (*c*). Their benzene planes are parallel and 1.298 and 1.428 Å apart, respectively. The NO_2 groups are twisted in at 5.51–48.64° with respect to the C-rings. The molecules are tilted with regard to the axes and make a herringbone pattern. Molecular stacking gives the shortest intermolecular distances. A structural comparison between HNS and TNT is made.

Chang et al. [33] state that TNT and HNS are monoclinic, space group P21/c, with a 21.230(5) and 22.083(6), b 6.081(2) and 5.554(1), c 14.958(5) and 14.634(3) Å., and β =110.12(2) and 108.45(2)°; Z = 4, resp. The structures were solved by direct methods and refined by block-diagonal full-matrix least-squares to R = 0.037 and 0.050, resp. The thermal-expansion coefficients are given. The bond lengths and angles are described.

Wang et al. [34] have performed theoretical computations on the electronic structure of HNS and its derivatives. They also correlated detonation velocities, molecular volumes, densities detonation pressures, and bond dissociation energies of HNS and its derivatives with various factors such as oxygen balance, number of nitro groups, and other parameters.

A recent paper by Shu et al. [35] has dealt with the crystal structure and thermal expansion of HNS in the temperature range of 303–513 K. They also computed the theoretical densities of HNS in this temperature range, and present XRD patters. The lattice parameters followed linear relations with temperature, and the density followed the relation

$$\rho = 1.7509 - 2.8032 \times 10^{-4} T$$

Table 6.1 Lattice parameters of HNS [35]

T (°C)	a (Å)	b (Å)	c (Å)	*β* (°)	Volume (Å^3)	Density (g/cm^3)	Rwpa (%)
30	22.3472	5.5753	14.6698	110.05	1716.98	1.7418	8.44
60	22.3927	5.5851	14.6740	110.00	1724.51	1.7342	8.21
90	22.4400	5.5961	14.6798	109.96	1732.67	1.7260	8.33
120	22.4915	5.6076	14.6864	109.92	1741.49	1.7172	8.68
150	22.5382	5.6174	14.6889	109.88	1748.94	1.7099	9.07
180	22.5931	5.6300	14.6947	109.83	1758.29	1.7008	9.55
210	22.6501	5.6431	14.7015	109.79	1768.10	1.6914	10.29
240	22.7062	5.6542	14.7025	109.74	1776.61	1.6833	11.08
210	22.6465	5.6422	14.6987	109.79	1767.19	1.6923	10.23
180	22.5928	5.6308	14.6954	109.83	1758.58	1.7006	9.68
150	22.5403	5.6190	14.6891	109.87	1749.63	1.7093	9.03
120	22.4833	5.6059	14.6796	109.91	1739.58	1.7191	8.80
90	22.4370	5.5960	14.6740	109.95	1731.85	1.7268	8.39
60	22.3901	5.5855	14.6684	110.00	1723.83	1.7348	8.34
30	22.3450	5.5757	14.6640	110.043	1716.34	1.7424	8.21

The data on crystal parameters, according to Shu et al. are shown in Table 6.1. The authors give the initial parameters used to generate the Rietveld refinement data shown in Table 6.1.

The XRD patterns shown in Fig. 6.8 indicate no phase changes but mere expansion.

Table 6.2 lists some thermochemical properties of HNS.

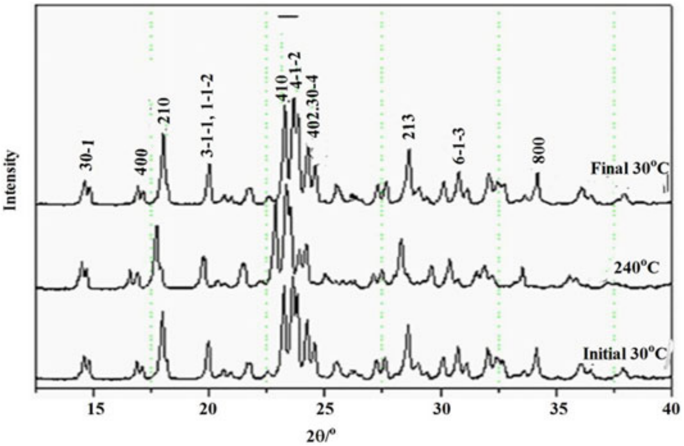

Fig. 6.8 XRD patterns phase changes of HNS at various temperatures [35]

Table 6.2 Some properties of HNS

HNS	Hexanitrodiphenylethylene, 1,2bis-(2,4,6-trinitrophenyl)-ethylene, 1,1′-(1,2-ethenediyl)bis-(2,4,6-trinitrobenzene)	
CA name	Benzene, 1,1′-(1,2-ethenediyl)bis[2,4,6-trinitro-	
CAS No.	20062-22-0	
Empirical formula	$C_{14}H_6N_6O_{12}$	
Structural formula	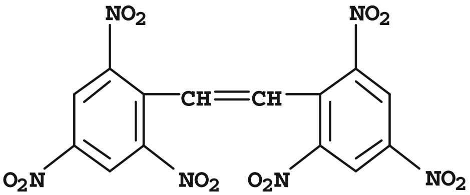	
Molecular mass (g mole^{-1})	450.15	
Density (g cm^{-3})	1.74 @ 25 °C 1.847 @ 20 °C	[36, 37]
Molar volume (cm^3 mol^{-1})	243.6 ± 3.0, 293.15 K and 760 Torr	[37]
Boiling point (°C)	578 ± 50	[37]
Melting point (°C)	316; 317	[23]
Flash point (°C)	275.4 ± 22.9	[37]
Crystal:	Orthorhombic; Unit cell: a = 22.13, b = 5.57, c = 14.67 Å	
K_{ow}	112	[21]
K_{oc}	86 [17]; 383	[37]
logP	2.218 ± 0.744, Temp: 25 °C	[37]
Vapor pressure	Pa (20 °C) 1.33×10^{-7}	
Vapor pressure equation	$\log_{10} P = 14.19 - \frac{43\,010}{4.576 \times T}$ with T in K and P in Torr	
Henry's law constant	2.7×10^{-9} atm m^3/mL	[38]
Aqueous solubility	mg/L [20/25 °C] 0.22	[38]
Molar solubility (4.9×10^{-7} mol/L) @ 25 °C	pH 1	[37]
Enthalpy of combustion (k cal/mol)	−1535.34 ± 1.08	[39]
Enthalpy of formation (s) (k cal/mol)	−13.89	[39]
Enthalpy of formation (g) (K cal/mol)	29.2 69.0	[39, 40]
Enthalpy of sublimation (K cal/mol)	43.01	[41]
Enthalpy of vaporization (K cal/mol)	19.9	[37]
Enthalpy of detonation (K cal/mol)	494.9	[42]
Heat capacity C_p in		[43]

(continued)

[cal/(g °C)]	$C_p = 0.201 + (1.27 \times 10^{-3})\,T - (2.36 \times 10^{-6})\,T^2$ $47 < T < 220$; T in °C	
Diffusion in air (m^2/s) [20 °C]	4.5×10^{-6}	[38]
Diffusion in water (m^2/s) [20 °C]	3.9×10^{-10}	[38]
K_{oc}	383 @ pH 10 and 25 °C	[37]
Bioconcenration	28.6 for pH 1 to 10 @ 25 °C	[37]

6.4 Polymorphism

HNS exists in four forms—HNS I, HNS II, HNS III and HNS IV. However the properties of I and II do not differ very much, and the yields of HNS II are low. HNS I, HNS II, and HNS IV are the most useful forms. Singh and Malhotra [13] have compared the properties, and some of the properties are shown in Table 6.3.

The vapor pressure of HNS measured by Rosen and Dickinson [41] are tabulated in Table 6.4. They used the Langmuir method to collect the data, and fitted the data to Clausius-Clapeyron type relation

$$Log_{10}P = 14.19 - \frac{43,010}{4.576T}$$

where T is in K, and P in Torr.

Table 6.3 Comparison of properties of HNS I and II [13]

	HNS I	HNS II
Shape of the crystal	Plate like	Dense orthorhombic
Melting point (K)	589.15	592.15
Bulk density (g/cm^3)	0.32–0.45	0.45–1.0
DSC on set of exotherm (K)	588.15	598.15
Velocity of detonation (m/sec) [density = 1.70]	7000	7000
Autoignition point (K)	598.15	598.15
Enthalpy of combustion (k J g/mole)	6500	6500
Impact sensitivity 50% height, cm NOL-ERL	44	61

Table 6.4 Vapor pressure as a function of temperature [36]

Temperature (°C)	VP($\times 10^{-7}$), Torr
161.4	0.396
166.4	0.592
177.3	2.15
185.8	4.97
206.3	39.4

Table 6.5 Solubility [9] of HNS (g/100 ml of solvents) at various temperatures in °C

Solvent	30	40	60
Nitrobenzene	0.059	0.072	0.094
Ethyl-methylketone	0.035	0.052	0.061
Acetone	0.064	0.075	0.131
Methanol	0.003	0.006	0.008
Dimethylformarnide	1.312	1.703	2.198
Acetonitrile	0.043	0.064	0.084
Cyclohexanone	0.118	0.156	0.206

Solubility of energetic materials such as HNS is necessary for purification by crystallization. Singh and Malhotra [13] provide the solubility values listed in Table 6.5.

Williams and Kuklenz [44] have determined temperature-dependent solubility of HNS in ten solvents and solvent blends using the Tyndall effect. The solubilities of HNS at 25 °C were used to determine the three-component Hansen solubility parameters [HSP] ($\delta_D = 18.6$, $\delta_P = 13.5$, $\delta_H = 6.1$ MPa$^{1/2}$) and the radius of the solubility sphere ($R_0 = 5.8$ MPa$^{1/2}$). The HSP determined for HNS using group-additivity ($\delta_D = 21.0$, $\delta_P = 13.3$, and $\delta_H = 8.6$ MPa$^{1/2}$) also correctly predicted the optimum solvents for this explosive. Table 6.6 shows the values of HSPs for various solvents. Ideal gas heat capacity and entrory [30] are included in (Table 6.7).

Table 6.6 Hansen Solubility Parameters (HSPs) of HNS in various solvents

Solvent system	δ_D/MPa$^{1/2}$	δ_P/MPa$^{1/2}$	δ_H (MPa$^{1/2}$)	g/100 mL	R_{ED}
NMP	18.0	12.3	7.2	1.940	0.440
DMF	17.4	13.7	11.3	1.310	1.000
DMF (1)	17.4	13.7	11.3	1.237	1.000
DMSO	18.4	16.4	10.2	1.210	0.816
DMF (2)	17.4	13.7	11.3	1.126	1.000
NMP + 5% Water	17.9	12.5	9.0	0.569	0.631
4-Butyrolactone	19.0	16.6	7.4	0.541	0.498
Propylene carbonate	20.0	18.0	4.1	0.475	0.841
25% ACN + 75% DMF	16.9	14.8	10	0.452	0.943
NMP + 2.5% Water	17.9	12.4	8.1	0.261	0.523
Acetophenone	19.6	8.6	13	0.195	1.000
50% ACN + 50% DMF	16.4	15.9	8.7	0.175	1.000
Cyclohexanone	17.8	6.3	5.1	0.124	1.329
75% ACN + 25% DMF	15.8	16.9	7.4	0.069	1.152
1,2-dimethoxyethane	15.4	6.0	6.0	0.064	1.754
ACN	15.3	18.0	6.1	0.062	1.369
bis(2-methoxyethyl)ether	15.8	6.1	9.2	0.056	1.736

(continued)

Table 6.6 (continued)

Solvent system	δ_D/MPa$^{1/2}$	δ_P/MPa$^{1/2}$	δ_H (MPa$^{1/2}$)	g/100 mL	R_{ED}
p-Dioxane	19.0	1.8	7.4	0.047	2.031
Methylethyl ketone	16.0	9.0	5.1	0.044	1.270
Ethyl acetate	15.8	5.3	7.2	0.037	1.773
ACN	15.3	18.0	6.1	0.035	1.369
Methyl formate	15.3	8.4	10.2	0.030	1.653
Ethyl formate	15.5	7.2	7.6	0.024	1.606
n-Propyl formate	15.5	7.1	8.6	0.017	1.652
2-Methoxy ethanol	16.2	9.2	16.4	0.014	2.089
Ethoxy benzene	18.4	4.5	4.0	0.011	1.614
1,2-Dichloroethane	19.0	7.4	4.1	0.007	1.135
Dichloromethane	18.2	6.3	6.1	0.006	1.289
Ethyl lactate	16.0	7.6	12.5	0.006	1.780
3-Methylphenol	18.0	5.1	12.9	0.004	1.880
2-Chloroethanol	16.9	8.8	17.2	0.003	2.142
Chlorobenzene	19.0	4.3	2.1	0.002	1.734
2-Ethoxy ethanol	16.2	9.2	14.3	0.002	1.813
2-Propanol	15.8	6.1	16.4	0.002	2.387
NMP + 10% Water	17.8	12.7	10.7	<0.001	0.882
Chloroform	17.8	3.1	5.7	0.001	1.838
Cyclohexanol	17.4	4.1	13.5	0.001	2.108
Ethanol	18.8	8.8	19.4	0.000	2.377
Methanol	15.1	12.3	22.3	0.000	2.991
Solute	δ_D/MPa$^{1/2}$	δ_P/MPa$^{1/2}$	δ_H (MPa$^{1/2}$)	R_0/MPa$^{1/2}$	F
HNS	18.9	13.9	6.1	6.0	0.9824

Table 6.7 Ideal gas heat capacity and entropy [30]

T (K)	300	400	500	600	800	1000	1500
Cpo (cal mol^{-1} K^{-1})	101.7	124.2	142.4	156.6	176.2	188.5	204.5
T (K)	2000	2500	3000	3500	4000	4500	5000
Cpo (cal mol^{-1} K^{-1})	211.6	215.3	217.4	218.7	219.6	220.2	220.7
T (K)	300	400	500	600	800	1000	1500
So (cal mol^{-1} K^{-1})	195.7	228.1	257.9	285.2	333.2	373.9 453.9	
T (K)	2000	2500	3000	3500	4000	4500	5000
So (cal mol^{-1} K^{-1})	513.8	561.4	600.9	634.5	663.8	689.7 712.9	

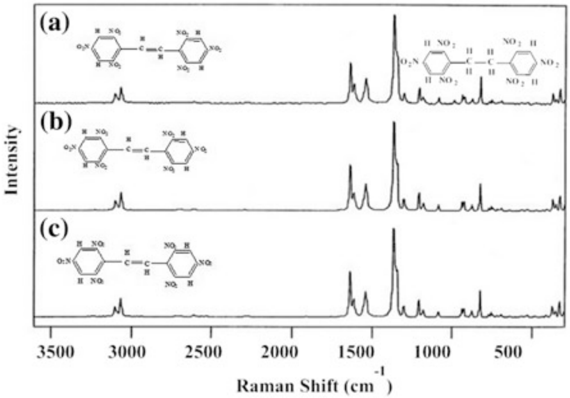

Fig. 6.9 Raman spectra of the HNS containing explosives in nitro-aromatic Group A recorded with 1064-nm laser excitation over the Raman shift range 300 ± 3600 cm^2 (**a**) HNS 1 HNBiB, (**b**) HNS II, and (**c**) HNS Super® ne

6.5 Spectra

Lewis et al. [45] used Fourier Transform Raman spectroscopy to measure the spectra of several nitro-containing explosives including HNS. Figure 6.9 shows their results collected using a 1064 nm laser excitation. Of the two HNS compounds, HNS Superfine composed of particle sizes of less than 1 μm, and HNS II is composed of particle sizes of 100 ± 300 μm. These different particle sizes lead to changes in melting points. The spectra of these compounds appear to be similar with slight band shifts.

6.6 Sensitivity

The sensitivity of HNS depends on the density as expected. Clement and Rudolf [46] have carried out gap tests on HNS with density varying from 165 to 1.70 gcm^{-3}. They were able to achieve these densities by making pellets at different pressures varying from 2 to 4.3 kbar.

References

1. Neyer BT, Cox L, Stoutenborough T, Tomasoski R (2003) HNS-IV explosive properties and characterization tests. 39th AIAA/ASME/-SAE/ASEE Joint Propulsion Conference and Exhibit AIAA-2003-5138, Huntsville AL July 20–24, 2003
2. Golopol HA, Fields DB, Moody GL (1977) A new booster explosive. LX-15, Rev. 1, NTIS Report UCRL-52175, March 18, 1977
3. Shipp KG (1964) Reactions of α-substituted polynitrotoluenes. i. synthesis of 2,2′,4,4′,6,6′-hexanitrostilbene. J Org Chem 29(9):2620–2623

4. Reich S, Wetter O, Widmer M (1912) Über das 2.4.6-trinitro-benzylbromid und seine derivate. Ber Dtsch Chem Ges 45(3):3055–3061
5. Shipp KG, Kaplan LA (1966) Reactions of α-substituted polynitrotoluenes. ii. the generation and reactions of 2,4,6-trinitrobenzyl anion. J Org Chem 31:857–861
6. Shipp KG (1970) Hexanitrostilbene. US Pat 3 505 413 A
7. Kayser EG (1983) An investigation of the Shipp hexanitrostilbene (HNS) process. J Energy Mater 1(4):325–348
8. Singh B, Singh H (1982) Synthesis of 2,2′,4,4′,6,6′-hexanitrostilbene. Def Sci J 31(4):305–308
9. Kilmer EE (1979) Hexanitrostilbene—survey of processes of synthesis and sources of procurement. Proc Symp Explos Pyrotech 10th: Paper No 6–7 pp
10. Kompolthy T, Bencz G, Deres J, Hajos L (1975) A Process for the preparation of 2,2′,4,4′,6,6′-hexanitrostilbene. 28 April 1975. Hung. Teljes, HU 9639 19750428
11. Kompolthy T, Bencz G, Deres J, Hajos L (1975) Process for production 2,2′,4,4′,6,6′-hexanitrostilbene. Hungarian Patent HU167394, 28 Oct 1975
12. Kompolthy T, Deres J, Hajos LL (1976) 2,2′,4,4′,6,6′-hexanitrostilbene. Chem Abstr 84:58886
13. Singh B, Malhotra RK (1983) Hexanitrostilbene and its properties. Def Sci J 33(2):165–176
14. Sleadd B, Greer P, Mueller G, Owens J (2007) Process improvement studies for scale-up of hns at holston army ammunition plant. NDIA insensitive munitions & energetic materials technology symposium 2007, BAE SYSTEMS OSI, Holston Army Ammunition Plant
15. Morris J, Clark G, Price D (2009) Process improvement studies for scale-up of hns at holston army ammunition plant. BAE SYSTEMS OSI, Holston Army Ammunition Plant
16. Duffin HC, Golding P, Jaweera-Bandar AM (1986) Production of hexanitrostilbene (HNS). US 4626606 A Dec 2, 1986
17. Duffin HC, Golding P, Wells CHJ (1998) A Parametric study of the synthesis of 4, 4H, 5, 5H, 7, 7H-Hexanitro-1, 1H-Binaphthyl. Propellants Explosives, …, 217.148.94.129
18. Duffin HC, Golding P, Jaweera-Bandara AM (1985) Production of hexanitrostilbene (hns). Secr Defence Brit, February 13, 1985: EP0132990-A2 (2 worldwide citation)
19. Gilbert EE (1980) The preparation of hexanitrostilbene from hexanitrobibenzyl. Propellants Explos 5(6):168–172
20. Sollott GP (1982) Conversion of 2,4,6-trinitrobenzyl chloride to 2,2′,4,4′,6,6′-hexanitrostilbene by nitrogen bases. J Org Chem 47(12):2471–2474
21. Morris J, Price D, Tucker N, Dye T, Kelly T (2015) BAE systems energetics pilot plant. Insensitive munitions & energetic material technology symposium 2015, BAE Systems Ordnance Systems Inc. Holston Army Ammunition Plant, Kingsport TN, USA
22. Bellamy AJ (2010) Synthesis of Hexanitrostilbene (HNS) using a kenics static mixer. Org Process Res Dev 14(3):632–639
23. Golding P, Hayes GF (1979) Studies on the synthesis of 2,2′,4,4′,6,6′-hexanitrostilbene. Propellants Explos 4(6):115–120
24. Golding P, Jayaweera-Bandara AM, Duffin HC, Charles H (1988) Production of hexanitrostilbene (HNS) from trinitrotoluene oxidation by transition metal compound. EP 1988-904587
25. Bellamy AJ (2010) Identification of α-chloro-2,2′,4,4′,6,6′-hexanitrobibenzyl as an impurity in hexanitrostilbene. J Energ Mater 28(1):1–16
26. Lu M, Sun R, Lu C, Hui J (1994) New method for synthesis of hexanitrostilbene. Nanjing Ligong Daxue Xuebao 5:8–11
27. Lu M (1994) Solvent effect on the reaction in two-step synthesis of hexanitrostilbene. Hanneng Cailiao 2(2):31–35
28. Orzechowski A, Powala D, Maranda A, Pawlowski W (2005) Crystallization of hexanitrostilben. New trends in research of energetic materials Proceedings 8th Seminar Pardubice Czech Republic, 2005 Apr 19–21, 2:687–694

29. Dacons JC (1981) Recrystallization of hexanitrostilbene from nitric acid and water. US Patent 4260837
30. Emeury JML (1980) Hexanitrostilbene for pyrotechnic applications. Eur Space Agency. [Spec Publ] ESA SP, (ESA SP-144 Explos Pyrotech-Appl Spat) 63–68
31. Golding P, Jayaweera-Bandara A, Duffin H (1988) Production of hexanitrostilbene (HNS). US 5023386 A, Brit UK Pat 2205312 16 pp
32. Gerard F, Hardy A (1988) Structure of 2,2′,4,4′,6,6′-hexanitrostilbene, HNS, a comparison with 2,4,6-trinitrotoluene, TNT. Acta Crystallo graphica Section C: Crystal Structure Communications C 44(7):1283–1287
33. Chang HC, Tang CP, Chen YJ, Chang CL (1987) Molecular structures of 2,4,6-trinitrotoluene (TNT) and 2,2′,4,4′,6,6′-hexanitrostilbene (HNS). Internationale Jahrestagung-Fraunhofer-Institut fuer Treib- und Explosiv- stoffe 18th (Technol Energ Mater) 51/1-51/13
34. Wang G-X, C-h Shi, X-d Gong, H-m Xiao (2009) Theoretical investigation on structures, densities, detonation properties, and the pyrolysis mechanism of the derivatives of HNS. J Phys Chem A 113(7):1318–1326
35. Shu X, Tian Y, Song G, Zhang H, Kang B, Zhang C, Liu Y, Liu X, Sun J (2011) Thermal expansion and theoretical density of 2,2′,4,4′,6,6′-hexanitrostilbene. J Mater Sci 46(8):2536–2540
36. Meyer R, Kohler J, Homburg A (2002) Explosives. 5th ed Wiley–VCH
37. Calculated using Advanced Chemistry Development (ACD/Labs) Software V904 for Solaris (1994–2008) (ACD/Labs)
38. Environment Agency (2000) Collation of. toxicological data and development of guideline values for expansion substances. R&D Project Record P5-036/01, Bristol, 2000
39. Martantz S, Armstrong GT (1968) Heats of combustion of trans-stilbene and trans-2,2′,4,4′,6,6′-hexanitrostilbene (HNS). J Chem Eng Data 13:118–121
40. Osmont A, Catoire L, Gökalp I, Yang V (2007) Ab initio quantum chemical predictions of enthalpies of formation, heat capacities, and entropies of gas-phase energetic compounds. Combust Flame 151:262–273
41. Rosen JM, Dickinson C (1969) Vapor pressures and heats of sublimation of some high melting organic explosives. J Chem Eng Data 14:120–124
42. Ornellas DL (1982) Calorimetric determinations of the heat and products of detonation for explosives: October 1961 to April 1982. Rep UCRL-52821, LLNL, USA
43. Department Of The Army Technical Manual (1984) Military Explosives, TM 9-1300-214 Department of Army, September 1984
44. Williams DL, Kuklenz KD (2009) A determination of the hansen solubility parameters of hexanitrostilbene (HNS). Propellants, Explos, Pyrotech 34(5):452–457
45. Lewis IR, Daniel NW Jr, Griffiths PR (1997) Interpretation of raman spectra of nitro-containing explosive materials: Part I: Group frequency and structural class membership. Appl Spectros 51:1854–1867
46. Clement D, Rudolf K (2006 Apr 19–21) Hexanitrostilbene—density dependent sensitivity. New Trends in Research of Energetic Materials Proc 9th Seminar Pardubice Czech Republic 540–543

Additional Scholarly Articles for Further Reading

47. Achuthan CP, Samudre SS, Gharia JS (1984) Hexanitrostilbene—a heat-resistant explosive. J Sci Ind Res 43(4):197–199
48. Aziz A, Cartwright M, Hill CJ (1996) Thermal stability of the crystallization nucleant: 2,4,6-trinitrotoluene, TNT, and 2,2′,4,4′,6,6′-hexanitrostilbene. HNS. J Therm Anal 47 (6):1617–1628. doi:10.1007/BF01980908

49. Bellamy AJ, Brzoska E (2003) Contamination of explosive materials with N-methylpyrrolidin-2-one (NMP). J Energ Mater 21(1):43–55. doi:10.1080/07370650305583
50. Bellamy AJ, Price TP, Mahon MF, Drake R, Mansell J (2005) Crystal structure of the 1:1 adduct of hexanitrostilbene and dioxane. J Energ Mater 23(1):33–41. doi:10.1080/07370650590920278
51. Can Z, Uezer A, Tekdemir Y, Ercag E, Tuerker L, Apak R (2012) Spectrophotometric and chromatographic determination of insensitive energetic materials: HNS and NTO, in the presence of sensitive nitro-explosives. Talanta 90:69–76. doi:10.1016/j.talanta.2011.12.077
52. Cartwright M, Collett GC (1993) Effect of additives on the nucleation of TNT. J Energy Mater 11(3):167–193. doi:10.1080/07370659308227809
53. Cartwright M, Hill CJ (1995) Thermal investigation of the crystallization nucleant formed between 2,4,6-trinitrotoluene, (TNT) and 2,2′,4,4′,6,6′-hexanitrostilbene (HNS). J Therm Anal 44(5):1021–1036. doi:10.1007/BF02547530
54. Casetta B, Garofolo F (1994) Characterization of explosives by liquid chromatography/mass spectrometry and liquid chromatography/tandem mass spectrometry using electrospray ionization and parent-ion scanning techniques. Org Mass Spectrom 29(10):517–525. doi:10.1002/oms.1210291002
55. Chen L-Z, Zhou F-R, Wang J-L (2014) Solubilities of 2,4,6-Trinitrotoluene in Methanol and Binary Mixtures of Methanol + Water from 293.15 to 333.15 K. J Solution Chem 43 (12):2163–2169. doi:10.1007/s10953-014-0263-3
56. Clement D, Rudolf KP (2007) The shock initiation threshold of HNS as a function of its density. Propellants, Explos, Pyrotech 32(4):322–325. doi:10.1002/prep.200700035
57. da Silva G, Iha K, Cardoso AM, Mattos EC, Dutra RdCL (2010) Study of the thermal decomposition of 2,2′,4,4′,6,6′-hexanitrostilbene. J Aerosp Technol Manage 2(1):41–46
58. Du Z, Zhang R, Fu D, Tong H, Li F (2012) Study on cook-off test of HNS at constant temperatures. Procedia Eng 45:580–583. doi:10.1016/j.proeng.2012.08.207
59. Fourmigue M, Boubekeur K, Batail P, Renouard J, Jacob G (1998) Light-induced detonant materials: charge-transfer complexes of tetrathiafulvalene (TTF) with hexanitrostilbene (HNS) and tetraazidoquinone (TAZQ) and their associated C-H···O hydrogen-bonded networks. New J Chem 22(8):845–850. doi:10.1039/a709257a
60. Gallo AE, Tench N (1984) Commissioning of a production plant for hexanitrostilbene. J Hazard Mater 9(1):5–11. doi:10.1016/0304-3894(84)80002-3
61. Golding P, Hayes GF (1983) A parametric study of the synthesis of 2,2′,4,4′,6,6′-hexanitrostilbene from trinitrotoluene and sodium hypochlorite. Propellants, Explos, Pyrotech 8(2):35–39. doi:10.1002/prep.19830080202
62. Huang P, Shi W (2011) Study on terahertz time-domain spectroscopy of HNS by sample measure and quantum chemistry calculation. Propellants, Explos, Pyrotech 36(6):513–518. doi:10.1002/prep.201010041
63. Kaur J, Arya VP, Kaur G, Gupta YP, Verma MM, Lata P (2010) Determination of solvent contamination and characterization of ultrafine HNS particles after solvent recrystallization. Propellants, Explos, Pyrotech 35(5):487–493. doi:10.1002/prep.200800094
64. Kaur J, Arya VP, Kaur G, Lata P (2013) Evaluation of the thermomechanical and explosive properties of bimodal and hybrid polymer bonded explosive (PBX) compositions based on HNS and HMX. Cent Eur J Energy Mater 10(3):371–391
65. Kilmer EE (1968) Heat-resistant explosives for space applications. J Spacecraft Rockets 5 (10):1216–1219. doi:10.2514/3.29452
66. Kony M, Dagley IJ, Whelan DJ (1992) Deuterium isotope effects on the rates of thermal decomposition of 2,2′,4,4′,6,6′-hexanitrostilbene in the condensed phase. J Phys Chem 96 (20):8001–8006. doi:10.1021/j100199a034
67. Lee J-S, Hsu C-K, Chang C-L (2002) A study on the thermal decomposition behaviors of PETN, RDX, HNS and HMX. Thermochim Acta 392–393:173–176. doi:10.1016/S0040-6031(02)00099-0

68. Liu G-h, Ye Z, Li H, Che R, Cui L (2012) Biological treatment of hexanitrostilbene (HNS) produced wastewater using an anaerobic-aerobic immobilized microbial system. Chem Eng J (Amsterdam, Neth) 213:118–124. doi:10.1016/j.cej.2012.09.115
69. Liu R, Zhang T, Zhou Z, Yang L, Yu W (2015) Nanoscale Effect on Thermal Decomposition of 2,2′,4,4′,6,6′-hexanitrostilbene by Dynamic Pressure Measuring Thermal Analysis. J Energ Mater 33(1):34–50. doi:10.1080/07370652.2013.877103
70. Lu T, Yao K, Mao Y, Xu J, Wang P, Lu M (2013) A Novel and Efficient Synthesis of Hexanitrostilbene by N-Hydroxyphthalimide/FeCl2-Catalyzed Aerobic Dehydrogenation of Hexanitrobibenzyl. J Energ Mater 31(3):217–223. doi:10.1080/07370652.2012.710870
71. Lu T-t, Lu M (2012) Efficient 2,2,6,6-tetramethylpiperidine-1-oxyl/iron catalyzed aerobic dehydrogenation of hexanitrobibenzyl to hexanitrostilbene. J Chin Chem Soc (Weinheim, Ger) 59(7):899–903. doi:10.1002/jccs.201100473
72. Minier LM, Oxley JC (1990) Thermolysis of nitroarenes: 2,2′,4,4′,6,6′-hexanitrostilbene. Thermochim Acta 166:241–249. doi:10.1016/0040-6031(90)80185-2
73. Mohan VK, Field JE (1984) Impact initiation of hexanitrostilbene. Combust Flame 56 (3):269–277. doi:10.1016/0010-2180(84)90061-0
74. Oxley JC, Smith JL, Yue J, Moran J (2004) Hypergolic reactions of TNT. Proc NATAS Annu Conf Therm Anal Appl 32nd:113.17.583/1–113.17.583/7
75. Parry MA, Thorpe BW (1979) The role of HNS (2,2′,4,4′,6,6′-hexanitrostilbene) in the grain modification of TNT. J Cryst Growth 47(4):541–550. doi:10.1016/0022-0248(79)90137-4
76. Philp DK, Thorpe BW (1976) Nucleation of 2,4,6-trinitrotoluene by 2,2′,4,4′,6,6′-hexanitrostilbene. J Cryst Growth 35(2):133–138
77. Qian W, Shu Y, Li H, Ma Q (2014) The effect of HNS on the reinforcement of TNT crystal: a molecular simulation study. J Mol Model 20(10):1–7. doi:10.1007/s00894-014-2461-8
78. Rieckmann T, Volker S, Lichtblau L, Schirra R (2001) Investigation on the thermal stability of hexanitrostilbene by thermal analysis and multivariate regression. Chem Eng Sci 56 (4):1327–1335. doi:10.1016/S0009-2509(00)00355-9
79. Rieckmann T, Volker S, Lichtblau L, Schirra R (2001) Thermal decomposition of hexanitrostilbene at low temperatures. J Anal Appl Pyrolysis 58–59:569–587. doi:10.1016/S0165-2370(00)00177-7
80. Selig W, Schroyer B, Silveira VG, Smathers ER (1972) Charge transfer complexes of 2,2′,4,4′,6,6′ hexanitrostilbene (HNS). Explosivstoffe 20(11–12):204–218
81. Setchell RE (1984) Grain-size effects on the shock sensitivity of hexanitrostilbene (HNS) explosive. Combust Flame 56(3):343–345
82. Setchell RE, Taylor PA (1988) A refined equation of state for unreacted hexanitrostilbene. J Energy Mater 6(3–4):157–199. doi:10.1080/07370658808012553
83. Shui M et al. (2013) Photothermal decomposition of HNS at 532 nm. Opt (Munich, Ger) 124 (23):6115–6118. doi:10.1016/j.ijleo.2013.04.089
84. Sitzmann ME, Foti SC (1975) Solubilities of explosives. Dimethylformamide as general solvent for explosives. J Chem Eng Data 20(1):53–55. doi:10.1021/je60064a032
85. Sun Y et al (2013) Laser-induced decomposition of 2,2′,4,4′,6,6′-hexanitrostilbene at 263, 527 and 1053 nm. Asian J Chem 25(8):4247–4250. doi:10.14233/ajchem.2013.13914
86. Sun Y, Xu T, Shu Y, Zhong F (2013) UV-induced photodecomposition of 2, 2′, 4, 4′, 6, 6′-hexanitrostilbene (HNS). Mater Sci-Pol 31(3):306–311. doi:10.2478/s13536-013-0105-9
87. Taylor RE, Groot H, Donaldson AB (1983) Thermal diffusivity of hexanitrostilbene (HNS) high explosive. Therm Conduct 16:251–260
88. Teipel U, Mikonsaari I (2002) Size reduction of particulate energetic material. Propellants, Explos, Pyrotech 27(3):168–174. doi:10.1002/1521-4087(200206)27:3<168:AID-PREP168>3.0.CO;2-D
89. Wang G, Gong X, Xiao H (2013) A theoretical study on the vibrational spectra and thermodynamic properties for the derivatives of HNS with -CH3, -N3, and -NF2 groups. Adv Mater Res (Durnten-Zurich, Switz) 742:202–208. doi:10.4028/www.scientific.net/AMR.742.202

90. Wang G-X, Gong X-D, Liu Y, Xiao H-M (2013) A theoretical study on the infrared spectra, thermodynamic functions, and detonation parameters for the -CN, -NC, -NNO2, and -ONO2 derivatives of HNS. J Theor Comput Chem 12(1):1250095/1–1250095/14. doi:10.1142/S0219633612500952
91. Wang J et al (2009) Prefilming twin-fluid nozzle assisted precipitation method for preparing nanocrystalline HNS and its characterization. J Hazard Mater 162(2–3):842–847. doi:10.1016/j.jhazmat.2008.05.107
92. Waschl J, Richardson D (1991) Effect of specific surface area on the sensitivity of hexanitrostilbene to flyer plate impact. J Energy Mater 9(4):269–282. doi:10.1080/07370659108018628
93. Waschl JA (1996) Temperature effects on the performance of a complete explosive device. J Energy Mater 14(3 & 4):153–171. doi:10.1080/07370659608216062
94. Zengguo F, Boren C (1994) Studies on reactions of polynitrostilbenes with sodium azide. J Energy Mater 12(4):237–247. doi:10.1080/07370659408018653
95. Zhu W, Shi C, Xiao H (2009) Density functional theory study of high-pressure behavior of crystalline hexanitrostilbene. J Mol Struct: THEOCHEM 910(1–3):148–153. doi:10.1016/j.theochem.2009.06.029

Chapter 7
N-Methy-4-Nitroaniline (MNA)

Abstract N-Methyl-4-nitroaniline (MNA) is used as an additive to lower the melting temperature of energetic materials in the synthesis of insensitive explosives. This chemical is commonly used as an intermediate in the synthesis of dyes, antioxidants, pharmaceuticals and gasoline, in gum inhibitors, poultry medicines, and as a corrosion inhibitor.

7.1 Introduction

N-Methyl-4-nitroaniline is a stabilizer which enhances the service life of double-base and minimum smoke propellants. The use of MNA as a stabilizer has been discussed Provatas and Davies [1]. They considered RDX/MNA and DNAN/MNA fortheir vacuum thermal stability tests, and obtained temperature of ignition for these mixtures. They also provide the DSC of pure components and mixtures. Some defence standards for MNA have been issued by the Ministry of Defence UK [2]. Padmanabhan et al. [3] carried out methylation of several aromatic amines, and obtained 20% yields of MNA. The spectral characteristics of n(NH) absorption bands of ‘free’ N-methyl-4-nitroaniline with various proton acceptors were determined within the temperature range 285–350 K [4].

In Table 7.1, proton acceptors are specified along with enthalpy, entropy, and equilibrium constants for the complex. α is the slope of the enthalpy-spectral shift relation.

7.2 Solvents

The effect of solvent mixtures on the electronic spectra of MNA has been studied by Seifried and Bekárek [5]. Table 7.2 shows the wave numbers for the stated mixture of solvents. In Table 7.2, wave numbers are in (cm^{-1}. 10^3). Extensive data are reported in the paper.

D.S. Viswanath et al., *Emerging Energetic Materials: Synthesis, Physicochemical, and Detonation Properties*, https://doi.org/10.1007/978-94-024-1201-7_7

Table 7.1 Thermodynamic properties of MNA complexes [4]

Proton	α	$-\Delta H_{calc}$	$-\Delta H_{exp}$	ΔS	K_{298}
Acceptor		(kcal $mole^{-1}$)	(kcal $mole^{-1}$)	(cal $mole^{-1}$ K^{-1})	(dm^3 mol^{-1})
CH_3CN	6.2	4.0	4.1	12.3	2.1
THF		3.9	4.5	13.1	3.0
DMF		6.8	7.1	18.8	12.1
DMSO		7.7	8.5	22.5	21.4
HMPA		9.6	9.3	23.9	39.1

Table 7.2 Effect of solvents on electronic spectra of MNA [5]

Hexane + acetone						
vol.%	0	20	40	60	80	100
Wave No.	24.75	23.98	23.81	23.70	23.64	23.41
Cyclohexanol + ethanol						
vol.%	0	20	40	60	80	100
Wave No.	29.22	26.74	26.46	26.32	26.25	26.09

7.3 Physical Properties

Two publications, Toghiani et al. [6] and Boddu et al. [7], provide information on thermophysical properties of MNA. Toghiani et al. used estimation procedures to evaluate physical properties where as Boddu et al. provide experimental data on aqueous solubility (S_w), octanol–water partition coefficient (K_{ow}), and Henry's law constant (K_H). Their data along with other data are shown in Table 7.3.

7.4 Solubility

The experimental aqueous solubility data of Boddu et al. [7] as a function of temperature in different media are presented in Table 7.4.

The predicted solubility data of Togiani et al. [6] is shown in Fig. 7.1. A comparison of the experimental data of Boddu et al. [7] with the predicted data of Toghiani et al. [6] shows that they differ by orders of magnitude, and points to the fact that the predicted data have to be carefully analyzed before they are used for any purpose.

7.5 Spectrum

The IR absorption spectrum is shown in Fig. 7.2, and NMR in Fig. 7.3.

Table 7.3 Some properties of N-Methy-4-nitroaniline

Name	N-Methy-4-nitroaniline	
Other names: Aniline, N-methyl-p-nitro- (6CI,7CI,8CI); 4-(Methylamino)nitrobenzene; 4-Nitro-N-methylaniline; Methyl(4-nitrophenyl)amine; N-Methyl-4-nitroaniline; N-Methyl-4-nitrobenzenamine; N-Methyl-p-nitraniline; N-Methyl-p-nitroaniline; N-Monomethyl-p-nitroaniline; NSC 5390; p-(Methylamino)nitrobenzene; p-Nitro-N-methylaniline		
CAS Number:	100-15-2	
Structural formula:	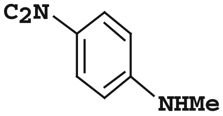	
Empirical Formula:	$C_7\ H_8N_2O_2$	
Molecular Mass (g mole^{-1})	152.15	
Density (g/cm^3)	1.26	
Molar Volume, cm^3/mol @ 298.15 K and 760 Torr	120.7 ± 3.0	
Boiling point (K)	527; 563.75	[6], [8]
Melting point	423.15	[6]
Flash point (K)	402.65 ± 22.6	[8]
Critical temperature (K)	748	[6]
Critical pressure (bar)	41.7	[6]
Acentric factor	0.659	[6]
Log K_{ow}	2.04; 1.47; 1.574; 0.807	[6]
	2.1028 ± 0.0209 @ 298.15 K	[7]
	1.9846 ± 0.0305 @ 308.15 K	[7]
	1.9377 ± 0.0146 @ 318.15 K	[7]
Enthalpy of fusion (kJmol^{-1})	18.85	[6]
Enthalpy of vaporization (kJmol^{-1})	53.00 ± 3.0	[8]
Vapor pressure, Torr @ 298.15 K	2.05×10^{-3}	[8]
Aqueous solubility, mg l^{-1} @ 298.15 K	1.17; 0.347	[6]
	971.3 (Ideal solubility)	[6]
Henry's Law Constant:		

(continued)

Table 7.3 (continued)

Name	N-Methy-4-nitroaniline	
K_H (M^3 Pa mol^{-1})	0.6100 @ 298.15 K	[7]
	0.5566@ 308.15 K	[7]
	0.5160@ 318.15 K	[7]
K_H (dimentionless g/aq)	2.46×10^{-4} @ 298.15 K	[7]
	2.25×10^{-4} @ 308.15 K	[7]
	2.08×10^{-4} @ 318.15 K	[7]
pKa (Most Basic @ 298.15 K)	0.56 ± 0.12	[8]
Koc in the pH range of 1–10 @ 298.15 K	225–306	[8]
Bioconcentration factor @ pH 1.0–10	15.3–20.9	[8]

Table 7.4 Aqueous solubility in presence of NaCl and $CaCl_2$ salts at different temperatures [7]

Medium	Solubility (mg/L)		
	298.15 K	308.15 K	318.15 K
Water	85.42 ± 0.85	111.51 ± 1.12	141.93 ± 1.42
1% NaCl	79.49 ± 0.80	96.65 ± 0.97	128.17 ± 1.28
5% NaCl	63.69 ± 0.64	75.51 ± 0.76	113.96 ± 1.14
10% NaCl	49.56 ± 0.50	58.22 ± 0.58	76.28 ± 0.76
1% $CaCl_2$	82.82 ± 0.83	104.99 ± 1.05	134.81 ± 1.35
5% $CaCl_2$	72.30 ± 0.72	95.03 ± 0.95	117.29 ± 1.17
10% $CaCl_2$	60.62 ± 0.61	85.84 ± 0.86	101.28 ± 1.01

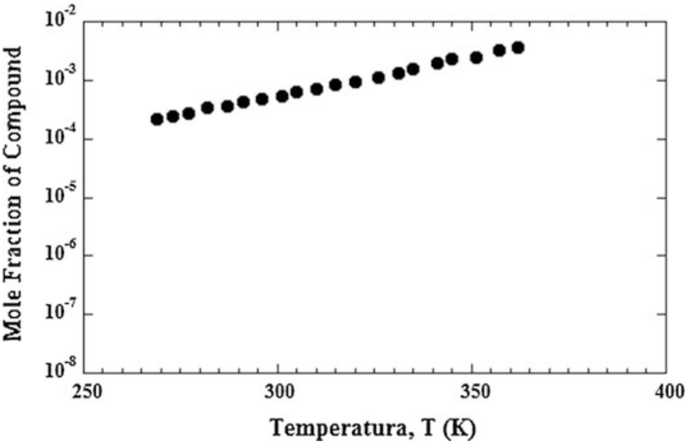

Fig. 7.1 Solubility as a function of temperature [6]

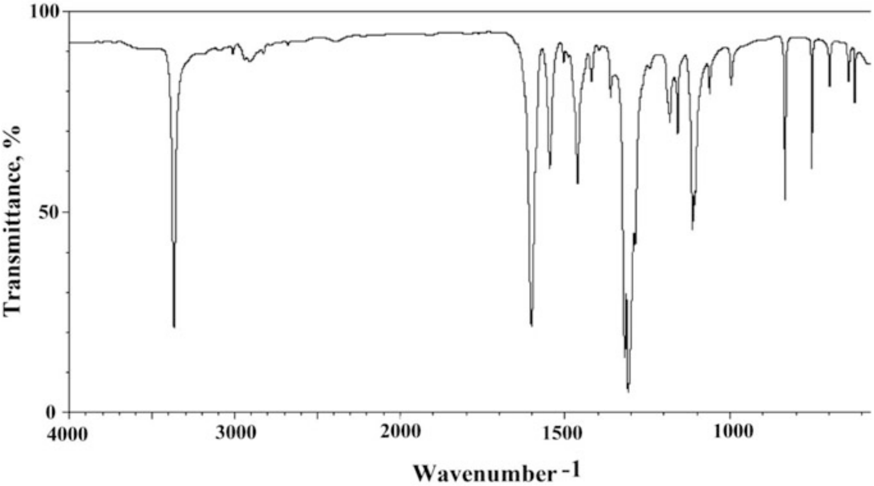

Fig. 7.2 IR Spectra of MNA (Source: Integrated Spectral Database System of Organic Compounds, data were obtained from the National Institute of Advanced Industrial Science and Technology, Japan)

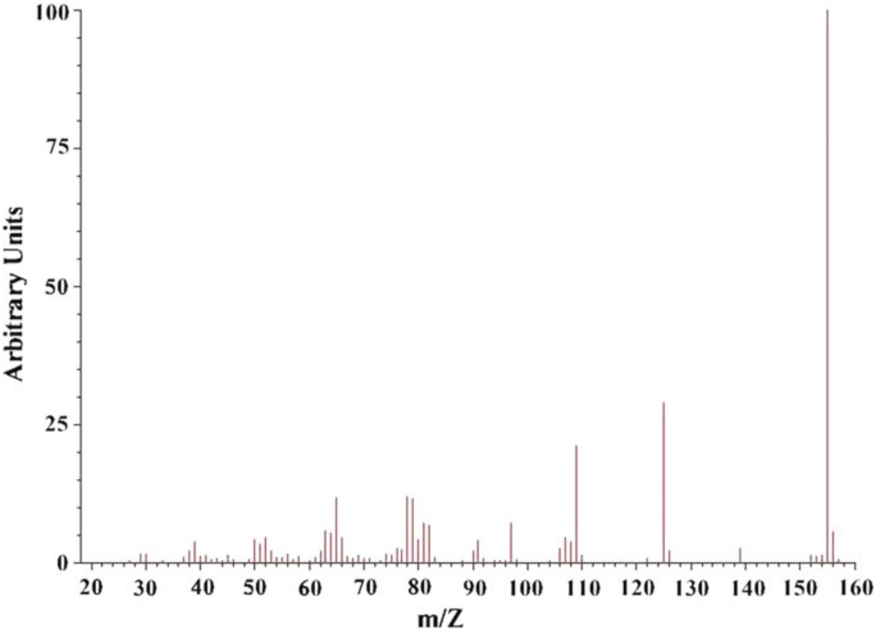

Fig. 7.3 NMR spectrum. Source: Spectral data were obtained from Wiley Subscription Services, Inc. (US)

References

1. Provatas A, Davies PJ (1998) DNAN—A Replacement for TNT in Melt-Cast Formulations. Australian Melt-cast Research and Development, Explosives & Pyrotechnics Group, Weapons Systems Division, Defence Science and Technology Organisation, EDINBURGH SA
2. Ministry of Defence (1990) N-METHYL-4-NITROANILINE. UK 68–37 Issue 2, 23 March 1990
3. Padmanabhan S, Laxma RN, Durant GJ (1997) A convenient one pot procedure for N-methylation of aromatic amines using trimethyl orthoformate. Synth Commun 27(4):691–699
4. Borisenkoa VE, Yu A, Zavjalovaa TG, Tretjakovaa ZS, Kozlovaa A, Koll J (2004) Thermodynamic properties of the hydrogen bonded complexes between N-substituted anilines and proton acceptors. Molecular Liquids 109:125–135
5. Seifried R, Bekárek V (1998) Solvent effect of mixed solvents on the electronic spectra of N-methyl-2-nitroaniline and N-methyl-4-nitroaniline. Acta Universitatis Palackianae Olomucensis FACULTAS RERUM NATURALIUM 1998 CHEMICA 37
6. Toghiani RK, Toghiani H, Maloney SW, Boddu VM (2008) Prediction of physicochemical properties of energetic materials. Fluid Phase Equilib 264:86–92
7. Boddu VM, Krishnaiah A, Maloney SW, Damavarapu R (2008) Physicochemical properties of an insensitive munitions compound, N-methyl-4-nitroaniline (MNA). J Hazardous Materials 155:288–294
8. Calculated using Advanced Chemistry Development (ACD/Labs) Software V8.14 for Solaris (1994–2008 ACD/Labs)

Additional Scholarly Articles for Further Reading

9. Abraham MH, Duce PP, Morris JJ, Taylor PJ (1987) Hydrogen bonding Part 2 Equilibrium constants and enthalpies of complexation for 72 monomeric hydrogen-bond acids with N-methylpyrrolidinone in 1,1,1-trichloroethane. J Chem Soc, Faraday Trans 1 83(9):2867–81 doi:10.1039/f19878302867
10. Ahmed A, Sandler SI (2012) Solvation free energies and hydration structure of N-methyl-p-nitroaniline. J Chem Phys 136(15):154505
11. Bailey RT, Cruickshank FR, Pavlides P, Pugh D, Sherwood JN (1991) Organic materials for nonlinear optics: interrelationships between molecular properties, crystal structure, and optical properties. J Phys D Appl Phys 24(2):135–145. doi:10.1088/0022-3727/24/2/009
12. Basque P, Ritcey AM (1994) Langmuir-Blodgett films from a cellulose derivative containing N-methyl-4-nitroaniline. Polym Mater Sci Eng 71:488–489
13. Benchabane M (1993) Gas evolution analysis III Chemical compatibility study of GAP based propellant by the DVST. J Energ Mater 11(2):119–34. doi:10.1080/07370659308018643
14. Boddu VM, Maloney SW (2012) Physical properties of insensitive munitions compounds for developing wastewater treatment technologies. In: Air & Waste Management Association, vol 3. p 1958–1965
15. Buncel E, Rajagopal S (1989) Solvatochromic studies of novel azo merocyanine dyes. The π*azo scale of solvent polarity. J Org Chem 54(4):798–809. doi:10.1021/jo00265a017
16. Damman P, Vallee R, Dosiere M, Toussaere E, Zyss J (2001) Oriented crystallization of NLO organic materials. Synth Met 124(1):227–232. doi:10.1016/S0379-6779(01)00459-3
17. Dezern JF (1988) Synthesis and characterization of BTDA-based poly(amide imides). J Polym Sci Part A: Polym Chem 26(8):2157–2169. doi:10.1002/pola.1988.080260813
18. Drago RS (1992) Extension of the unified scale of solvent polarities to acceptor probes: concerns about β-π* parameters. J Org Chem 57(24):6547–6552. doi:10.1021/jo00050a033
19. Eilmes A (2014) Solvatochromic probe in molecular solvents: implicit versus explicit solvent model. Theor Chem Acc 133(9):1–13. doi:10.1007/s00214-014-1538-x
20. Elliot MS, Smith FJ, Fraser AM (2000) Synthetic procedures yielding targeted nitro and nitroso derivatives of the propellant stabilisers diphenylamine, N-methyl-4-nitroaniline, and N, N'-diethyl-N, N'-diphenylurea. Propellants Explos Pyrotech 25(1):31–36. doi:10.1002/(SICI)1521-4087(200001)25:1<31:AID-PREP31>3.0.CO;2-Z
21. Ferguson G, Glidewell C, Low JN, Skakle JMS, Wardell JL (2001) Hydrogen bonding in C-methylated nitroanilines: the three-dimensional framework structure of 2-methyl-4-nitroaniline. Acta Crystallogr, Sect C: Cryst Struct Commun C 57(3):315–316. doi:10.1107/S0108270100019405
22. Fife TH, Bembi R (1993) Metal ion promoted hydroxide ion and water catalyzed hydrolysis of amides. Effects of the acyl group and the leaving group. J Am Chem Soc 115(24):11358–11363. doi:10.1021/ja00077a039
23. Gajda K, Daszkiewicz Z, Kozubek E, Ejsmont K, Zarychta B (2014) Theoretical multipolar atom model transfer in nitro-derivatives of n-methylaniline. Cryst Growth Des 14(11):5737–5748. doi:10.1021/cg500984p
24. Garofalo A et al (2010) Design, synthesis, and dna-binding of n-alkyl(anilino)quinazoline derivatives. J Med Chem 53(22):8089–8103. doi:10.1021/jm1009605
25. Hayashi S (1999) Differential broadening caused by dipolar interaction with 1H in 13C MAS NMR signals split by residual dipolar interaction with 14N. Magn Reson Chem 37 (11):843–851
26. Hayata K, Yanagawa K, Koshiba M (1990) Field analysis of the Cherenkov doubling of infrared coherent radiation utilizing an organic crystal core bounded by a glass capillary. J Appl Phys 68(12):6033–6043. doi:10.1063/1.346915
27. Kanoun MB, Botek E, Champagne B (2010) Electrostatic modeling of the linear optical susceptibilities of 2-methyl-4-nitroaniline, m-nitroaniline, 3-methyl-4-nitropyridine N-oxide

and 2-carboxylic acid-4-nitropyridine-1-oxide crystals. Chem Phys Lett 487(4–6):256–262. doi:10.1016/j.cplett.2010.01.021

28. Kanoun MB, Champagne B (2011) Calculating the second-order nonlinear optical susceptibilities of 3-methyl-4-nitropyridine N-oxide, 2-carboxylic acid-4-nitropyridine-1-oxide, 2-methyl-4-nitroaniline, and m-nitroaniline crystals. Int J Quantum Chem 111(4):880–890. doi:10.1002/qua.22852
29. Keswani CL, Weber DJ (1967) Thin-layer chromatography of substituted nitroanilines and related compounds. J Chromatogr 30(1):130–135. doi:10.1016/S0021-9673(00)84121-7
30. Khan F, Pal D, Ghosh A, Cameotra SS (2013) Degradation of 2,4-dinitroanisole (DNAN) by metabolic cooperative activity of Pseudomonas sp. strain FK357and Rhodococcus imtechensis strain RKJ300. Chemosphere 93(11):2883–2888. doi:10.1016/j.chemosphere.2013.09.005
31. Ko C-J et al (2013) Nitroanilines enhancing the holographic data storage characteristics of the 9,10-phenanthrenequinone-doped poly(methyl methacrylate) photopolymer. J Appl Polym Sci 127(1):643–650. doi:10.1002/app.37835
32. Kobeissi M, Yazbeck O, Chreim Y (2014) A convenient one-pot synthesis of polysubstituted pyrroles from N-protected succinimides. Tetrahedron Lett 55(15):2523–2526. doi:10.1016/j.tetlet.2014.03.021
33. Kodiyath R et al (2013) Assemblies of silver nanocubes for highly sensitive SERS chemical vapor detection. J Mater Chem A 1(8):2777–2788. doi:10.1039/c2ta00867j
34. Kumar VMMJ, Shameer H, Jayadevaiah KV, Jayachandran E, Sreenivasa GM (2009) Synthesis, characterization and biological evaluation of thiazolidinone derivatives as potential antimicrobial agents. J Chem Pharm Sci 2(2):128–131
35. Lebegue N, Gallet S, Flouquet N, Carato P, Giraudet S, Berthelot P (2004) Synthesis of 4-methoxybenzylamino derivatives of dibenzothiadiazepine dioxide. Heterocycles 63 (11):2457–2463. doi:10.3987/COM-04-10095
36. Longo M, Cavallaro A (1996) Determination of aromatic amines at trace levels by derivatization with heptafluorobutyric anhydride and gas chromatography - electron-capture negative-ion chemical ionization mass spectrometry. J Chromatogr A 753(1):91–100
37. Nesterov VN, Timofeeva TV, Borbulevych OY, Antipin MY, Clark RD (2000) A combinatorial chemistry approach to new materials for non-linear optics. I. Five schiff bases. Acta Crystallogr, Sect C: Cryst Struct Commun C56(8):971–975. doi:10.1107/S0108270100002845
38. Nunes N, Elvas-Leitao R, Martins F (2014) UV-Vis spectroscopic study of preferential solvation and intermolecular interactions in methanol/1-propanol/acetonitrile by means of solvatochromic probes. Spectrochim Acta, Part A 124:470–479. doi:10.1016/j.saa.2014.01.021
39. Ojo IAO, Ajayi I, Akingbohungbe AE, Adereti A (2006) The synthesis and assessment of some benzyl anilinomethyl sulfides as insecticides. Int J Chem (Calcutta, India) 16(1):21–28
40. Patel KD, Patel CN, Patel GM (2014) Synthesis and antidiabetic activity of novel 4-substituted-N-[phenyl(2,4,5-triphenyl-1H-imidazol-1-yl)methyl]benzenamine. Inventi Impact: Med Chem(4):142–145, 4 pp
41. Pavlat P, Hlavac J, Bekarek V (1998) Solvent effect on electronic and vibrational spectra of N-methyl-2-nitroaniline and N-methyl-4-nitroaniline. Chem Pap 52(4):226–229
42. Pavlat P, Hlavac J, Bekarek V (1997) Solvent effect on electronic and vibrational spectra of N-methyl-2-nitroaniline and N-methyl-4-nitroaniline. In: Vydavatelstvo STU, p 111–112
43. Platten WE 3rd, Bailey D, Suidan MT, Maloney SW (2010) Biological transformation pathways of 2,4-dinitro anisole and N-methyl paranitro aniline in anaerobic fluidized-bed bioreactors. Chemosphere 81(9):1131–1136
44. Sena VLM, Srivastava RM, de Simone CA, da Cruz Goncalves SM, Silva RO, Pereira MA (2007) Conventional and microwave-assisted reaction of N-(hydroxymethyl)phthalimide with arylamines: synthesis of N-[(arylamino)methyl] phthalimide derivatives. J Braz Chem Soc 18 (6):1224–1234
45. Smiataczowa K, Maj K, Widernik T, Nesterowicz M (1998) Basicity of N-arylglucopyranosylamines in methanol. Pol J Chem 72(3):587–594

46. Sophy KB, Shedge SV, Pal S (2008) Noniterative Density Functional Response Approach: Application to Nonlinear Optical Properties of p-Nitroaniline and Its Methyl-Substituted Derivatives. J Phys Chem A 112(44):11266–11272
47. Steinmetz FP et al (2014) Methods for assigning confidence to toxicity data with multiple values—Identifying experimental outliers. Sci Total Environ 482–483:358–365
48. Stephens J, Gebre T, Batra AK, Aggarwal MD, Lal RB (2003) Microhardness studies on organic crystals. J Mater Sci Lett 22(3):179–180
49. Tayebee R, Rezaei Seresht E, Jafari F, Rabiei S (2013) Simple Methodology for the Aerobic N-Methylation of Substituted Anilines Catalyzed by Zirconium Oxychloride Octahydrate, ZrOCl2·8H2O. Ind Eng Chem Res 52(32):11001–11006
50. Turker L (2013) Detonation velocity—a molecular aspect. Adv Chem Model 4:223–236
51. Vijay Kumar MMJ et al (2009) N-substituted-thiazolidinones: synthesis and characterization of new novel anti-inflammatory agents. Int J Pharm Sci 1(1):42–54
52. Vijay Kumar MMJ, Jayadevaiah KV, Nagaraja TS, Shameer H, Jayachandran E, Sreenivasa GM (2009) Synthesis, characterization and anthelmintic activity of novel N-substituted thiazolidinones. J Chem Pharm Sci 2(4):277–280
53. Watanabe T, Yamamoto H, Hosomi T, Miyata S (1991) New molecular design for noncentrosymmetric crystal structures: lambda shape molecules for frequency doubling. NATO ASI Ser, Ser E 194(Org. Mol. Nonlinear Opt. Photonics):151–9
54. Yonehara H, Kang W-B, Kawara T, Pac C (1994) Synthesis and second-harmonic generation properties of 2-(4-nitroanilino)-1,3,5-triazine derivatives. J Mater Chem 4(10):1571–1577
55. Zheng X et al (2007) Analgesic agents without gastric damage: Design and synthesis of structurally simple benzenesulfonanilide-type cyclooxygenase-1-selective inhibitors. Bioorg Med Chem 15(2):1014–1021
56. Zhou J, Chen S (1998) Manufacture of N-methyl-4-nitroaniline as explosive stability detecting standard. Huozhayao Xuebao 21(3):30–35

Chapter 8
1-Azido-2-Nitro-2-Azapropane (ANAP)

Abstract Thermodynamic and explosive properties of 1-azido-2-nitro-2-azapropane (ANAP) have been determined in a combined computational *ab initio* and EXPLO5 (Becker—Kistiakowsky—Wilson equation of state, BKW EOS) study. The enthalpy of formation of ANAP in the liquid phase, heat of detonation, detonation pressure and detonation velocity of ANAP were calculated. ANAP compounds were characterized using vibrational (IR and Raman) and multinuclear NMR spectroscopy, elemental analysis and low-temperature single crystal X-ray diffraction. ANAP represents a covalently bound liquid energetic material which contains both a nitramine unit and an azide group in the molecule.

8.1 Introduction

1-azido-2-nitro-2-azapropane, ANAP, is a colorless liquid which is stable but explodes in the presence of a flame. It has friction sensitivity of 120 N and an impact sensitivity of 1 J.

8.2 Synthesis

Klapotke et al. [1] describe a two-step synthesis of ANAP. In the first step, trimethyl-hexahydro-triazine was converted into 1-chloro-2-nitro-2-azapropane which is treated with sodium azide to yield ANAP.

U.S. Patent 3883374 [2] describes a method of preparation of ANAP. The patent gives the following details which are reproduced. Two hundred and fifty mL of redistilled dioxane and 62.4 g of trioxylmethylene were placed in a 1 L three necked flask having a gas inlet tube, a mechanical stirrer, a thermometer and a drying tube. Dry HCl gas was passed into the mixture until it was almost clear.

D.S. Viswanath et al., *Emerging Energetic Materials: Synthesis, Physicochemical, and Detonation Properties*, https://doi.org/10.1007/978-94-024-1201-7_8

The addition of HCl was stopped and the temperature of the reaction mixture was allowed to drop to 35 °C before 39.6 g of dry, powdered methyl nitramine has added. The rate of addition was such that the temperature did not rise above 40 °C. After the addition was complete, the passage of HCl was resumed and continued for 3 h. The reaction mixture was allowed to stand for 13 h at ambient temperature. The solvent was then removed on a rotary evaporator. The product was a greenish-yellow oil.

15.7 g of the oil was dissolved in 100 mL of acetone in a beaker and the beaker was immersed in an ice-salt bath. A solution of 25.2 g of sodium azide in 75 mL of water was added with mechanical stirring. The reaction mixture was blanketed with dry nitrogen during this operation and the temperature was maintained below 10 °C.

After standing 64 h the reaction mixture was extracted with ether and the extract was dried over $MgSO_4$. The ether was evaporated leaving a greenish-yellow product in an amount equivalent to an 80% yield. Distillation under reduced pressure gave a clear liquid [3, 4]. Table 8.1 lists the structure and other names of ANAP while Table 8.2 lists some physical properties of ANAP.

Table 8.1 Structure and other names of ANAP

Name	ANAP
CAS No.	55680-29-0
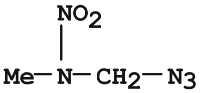 $\mathrm{Me{-}}\overset{\overset{\displaystyle NO_2}{|}}{N}\mathrm{{-}CH_2{-}N_3}$	
Empirical formula	$C_2H_5N_5O_2$
CA index name	Methanamine, 1-azido-N-methyl-N-nitro-
Other names	2-Nitrazapropyl azide

Table 8.2 Physical properties of 1-azido-2-nitro-2-azapropane (ANAP)

Molecular mass	131.11	
Crystal system	Orthorhombic	[2]
Boiling/Decomposition temperature (K)	433–453	[1]
Enthalpy of vaporization (kJ mol^{-1})	39.7 ± 0.8	
Density (g cm^{-3})	1.493	[2]
Refractive index, nm	1.4828 Wave length: 589.3	
Enthalpy of formation (kJ mol^{-1})	(l) ΔH_f^o = ANAP(l) = +297.1	[2]
Enthalpy of detonation (Q_v) (kJ kg^{-1})	−6088	[2]
Detonation pressure (P) (GPa)	23.8	[2]
Detonation temperature (K)	4092	[2]
Detonation velocity (D) (ms^{-1})	8033	[2]

References

1. Klapotke TM, Steemann FX, Suceska M (2008) Computed thermodynamic and explosive properties of 1-Azido-2-nitro-2-azapropane (ANAP). Propellants, Explos, Pyrotech 33 (3):213–218
2. Rosher R (1975) Double-base propellant containing organic azide. The United States of America as represented by the Secretary of the Navy (Washington DC) US 3883374
3. Boese R, Klapotke TM, Meyer P, Verma V (2006) Synthesis and characterization of 1-Azido-2-Nitro-2-Azapropane and 1-Nitrotetrazolato-2-Nitro-2-Azapropane. Propellants, Explos, Pyrotech 31(4):263–268
4. Klapotke TM, Mayer P, Schulz A, Weigand1 JJ (2005) 5-Diamino-4-methyltetrazolium dinitramide. 2032 9 J. Am Chem Soc 127:2032–2033

Additional Scholarly Articles for Further Reading

5. Dorofeeva OV, Ryzhova ON, Suntsova MA (2013) Accurate prediction of enthalpies of formation of organic azides by combining g4 theory calculations with an isodesmic reaction scheme. J Phys Chem A 117(31):6835–6845. doi:10.1021/jp404484q
6. Heeb G, et al. (2007) New energetic materials for nitrocellulose based propellants. Int Annu Conf ICT 38th:101/1-101/13
7. Pjatakov NF, Shlyapochnikov VA, Cherskaya NO, Vjyunova IB (1995) Intermolecular interactions of nitramines. Proc Int Pyrotech Semin 21st:698–712
8. Rosher R (1975) Organic azides. US3873579A
9. Stepanov RS, Kruglyakova LA (1999) Thermal decomposition of polyfunctional azido compounds. Int Annu Conf ICT 30th:47/1-47/8
10. Stepanov RS, Kruglyakova LA, Astachov AM (2007) Thermal decomposition of high energy compound azidonitramines. Cent Eur J Energ Mater 4(1–2):151–156
11. Unterhalt B, Leiblein F (1979) Nitramines, XII: N-Fluoromethyl- and N-azidomethyl-N-alkylnitramines. Arch Pharm (Weinheim, Ger) 312(2):159–64

Chapter 9
1, 3, 5-Triamino-2, 4, 6-Trinitrobenzene (TATB)

Abstract This chapter reviews the research and development work on 1, 3, 5-Triamino-2, 4, 6-trinitrobenzene (TATB), and TATB-based formulations. Syntheses, analytical methods, thermophysical properties, performance, formulations, and toxicological and safety of TATB are included in this chapter.

9.1 Introduction

There has been a renewed interest in the synthesis and characterization of new energetic materials during the past two to three decades. This is due in part to find materials of better performance but also to reduce the loss of lives and property due to accidental explosions that could occur during the different stages of explosive preparation, manufacture, formulations, load assemble and package operations, and use.

Military is focused to minimize the collateral damage to all sites other than the targeted sites. Determining the fate of these chemicals in the environment is also as important. Detecting hidden explosives requires extremely accurate data on vapor pressure for development of sensors.

Accurate predictive methods for testing and fielding of new energetic materials to minimize the cost and time associated with an experimental program are required. In the present collecion of properties, it has become evident that models currently used to predict properties are far from satisfactory. For example, prediction of crystal density paves the way in predicting detonation velocities. Enthalpies of formation and sublimation are critical in assessing the potential energy release and performance in a gun or a warhead.

Studying syntheses pathways, reaction mechanisms and products, exhaust plume signature, etc. require accurate physicochemical properties.

Among the various insensitive high explosives 1, 3, 5-Triamino-2, 4, 6-trinitrobenzene, commonly known as TATB, is an attractive insensitive explosive as it satisfies the safety requirements at high temperatures and its resistance to

D.S. Viswanath et al., *Emerging Energetic Materials: Synthesis, Physicochemical, and Detonation Properties*, https://doi.org/10.1007/978-94-024-1201-7_9

accidental initiation and explosion. In addition it readily forms eutectics with other explosives such as 1,3,5,7-tetranitro-1,3,5,7-tetra azacyclooctane (HMX), trinitrotoluene (TNT), and several others. This paper should be viewed as a companion review to the excellent review by Dobratz [1]. TATB is perhaps the most thermo-resistant insensitive explosive known to date. Although TATB contains an amino group, it is much more stable compared to a nitro compound such as trinitrobenzene.

The potential of TATB as an insensitive explosive was realized during the 1960s. TATB is used in modern nuclear warheads in the military and deep oil well explorations in the civilian community, and as a reagent in the manufacture of liquid crystal displays. It is used extensively in the USA. In recent years it is the preferred conventional secondary high explosive in nuclear weapons [2].

Dobratz [1] cites Jackson and Wing as the earliest workers to mention TATB in 1888, although it was left to Flurscheim and Holmes [3] to synthesize pure TATB by ammoniation of pentanitroaniline. Many processes yield TATB with a small percentage of chlorine but recent attempts to make chlorine-free TATB have been documented. TATB exhibits both in monoclinic and triclinic crystal structures and is classified as a heat resistant explosive.

9.2 Synthesis and Manufacture

The current industrial method is to nitrate 1, 3, 5-trichlorobenzene to give 1, 3, 5-trichloro-2, 4, 6-trinitrobenzene. Nitration is carried out at 423 K using a mixture of nitric and sulfuric acids. It is reacted with ammonia in a toluene medium to yield the product. One method of synthesis of TATB has been described in Fig. 9.1. The current cost of TATB prohibits its use for civilian applications but new routes for its synthesis could reduce the cost of production. One such route is patented by Mitchell et al. [4] who used picramide as the starting material. Bellamy et al. [5] have described a new route starting with 1, 3, 5-trihydroxy benzene for the synthesis of TATB. Although the direct nitration of 1, 3, 5-trihydroxy benzene can be carried out, Bellamy et al. have suggested a number of modifications. The authors give details of the above syntheses methods, claim improved yields and report other starting materials. They also show their synthesis of TATB by vicarious nucleophilic substitutions. In all the syntheses methods, the low solubility of TATB has posed a problem.

Thiokol Corporation has set up a pilot-plant for the production of TATB as described by Dressen et al. [6]. This process is based on the synthetic route proposed by Bellamy et al. [5]. The overall process yield was 81%. The syntheses routes are shown in Figs. 9.1 and 9.2. A similar synthesis method as shown in Fig. 9.3 was followed by researchers at Pantex to reduced chlorine contamination. Aniline was used as a starting material to synthesize 1, 3, 5-trichlorobenzene by Urbansky and Vasudeva [7] in their attempts to synthesize TATB. TNT was the

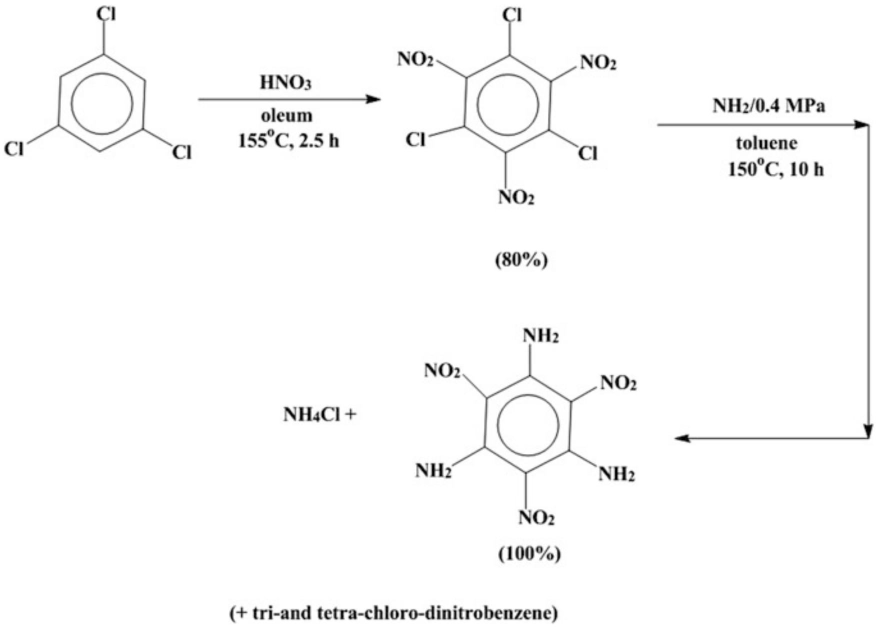

Fig. 9.1 Synthesis of TATB using 1, 3, 5-trichlorobenzene. Reproduced from Ref. [5]

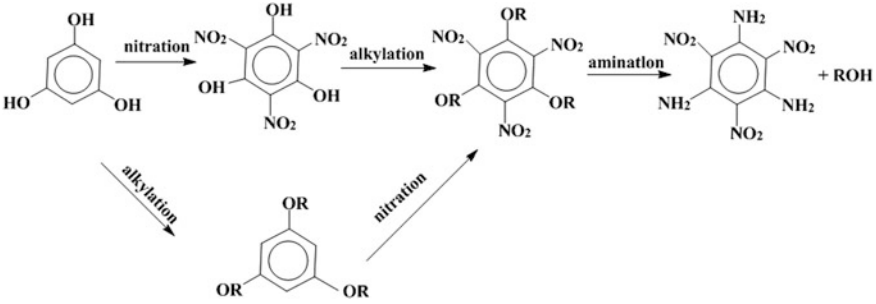

Fig. 9.2 New synthesis of TATB. Reproduced from Ref. [5]

starting material for Atkins et al. [8] to form 2,3,4,5,6-pentanitroaniline using H_2S and NH_4OH, which was converted to TATB after adding NH_3, toluene, and CCl_4. High purity TATB was synthesized by Ott and Benzinger [9] by ammonolysis of 3,5-dichloro-2,4,6-trinitroanisole in toluene at room temperature.

Recently Yang et al. [10] have prepared nano particles by amination of TCTNB [1, 3, 5-trichloro-2, 4, 6-trinitrobenzene] in toluene medium. The surface area of the particles was 22 m^2/g and pore diameter 1.7 nm. X-ray Diffraction (XRD) patterns of nano and micron sized TATB are shown in Fig. 9.4. XRD studies showed that the particles are about 60 nm in size. The size of these particles may be small for

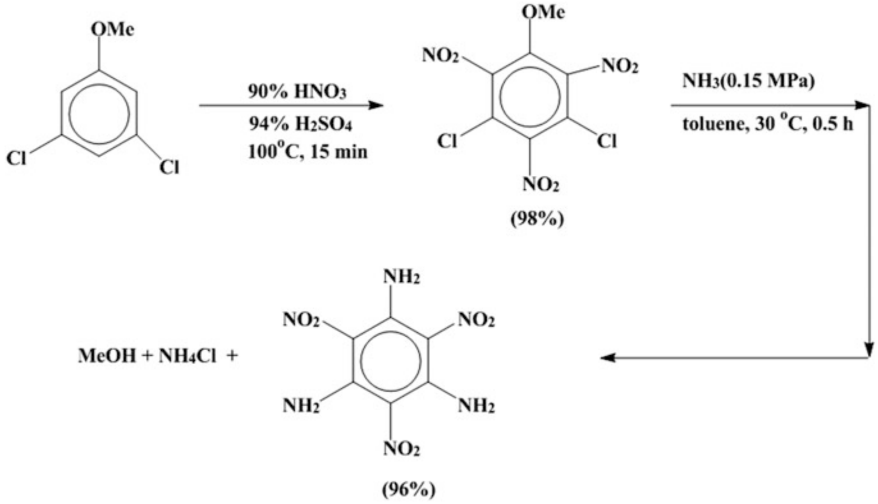

Fig. 9.3 Modified synthesis of TATB. Reproduced from Ref. [5]

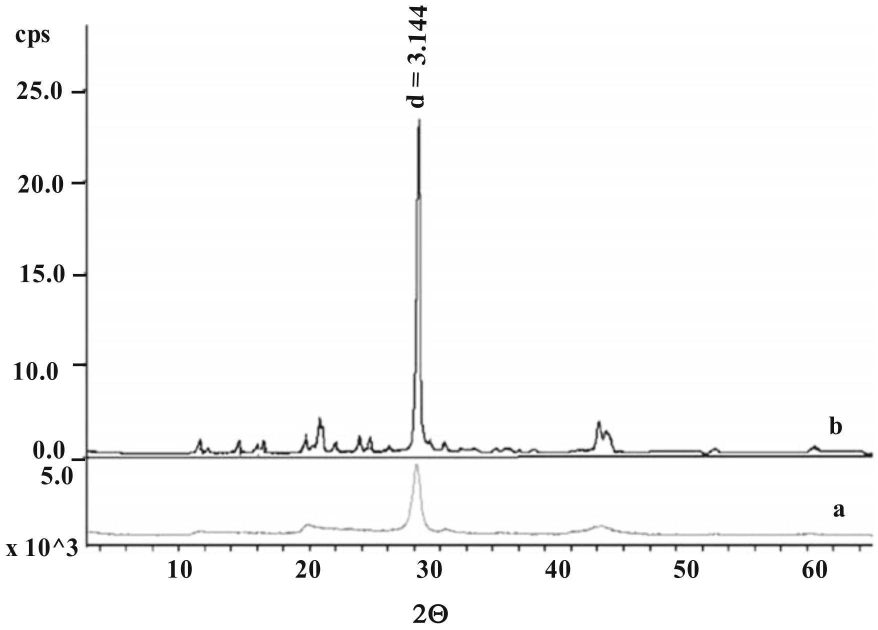

Fig. 9.4 XRD diagram of nano TATB (**a**) and micron TATB (**b**). Reproduced from Ref. [10]

certain formulations, and by changing the experimental parameters it is possible to obtain larger particles. Nevertheless, nano particles would give higher surface energy and higher detonation energy.

Pagoria et al. [11] and Agrawal [12] provide excellent reviews of the synthesis of several energetic explosive materials. These two reviews complement one another in discussing the current state of knowledge in the synthesis of explosive and propellant materials.

9.3 Structure

TATB has a simple ring structure with long C–C bonds and short C–N bonds with six fractured hydrogen bonds. Agrawal [12] states that there is strong evidence of inter-and intramolecular hydrogen bonds. These strong hydrogen bonds induce a strong dipole-dipole van der Waals-Keesom force and affect properties such as boiling and melting points which are evident in TATB. X-ray diffraction studies have indicated two molecules per unit cell and extensive O–N and N–H hydrogen bonding, and a layered structure. This gives rise to polarity and dispersion forces, and affects solvation and physical properties.

TATB is a planar molecule with a triclinic centrosymmetric lattice. Based on the structures shown in Fig. 9.5, Huang et al. [13] evaluated the vibrational frequencies, and the assignments are shown in Table 9.1. Except for the weak bands all other bands have been verified in the experimental spectrum.

A more detailed assignment of vibrational frequencies has been carried out by Liu et al. [14]. The simulated infrared spectra agree well with the experimental data shown in Fig. 9.6.

These two studies indicate that there is a conformational change in TATB from crystalline phase to gas phase possibly due to intermolecular hydrogen bonding. The assignments made by Liu et al. [14] agree more closely with experimental data. Kolb and Rizzo [15] used the same structure in their evaluation of thermal expansion of TATB crystal.

TATB undergoes structural changes on heating as observed by Son et al. [16]. This is similar in nature to what one observes with HMX where a phase change occurs from β to δ. Son et al. observed second harmonic generation both in transmission through a thin layer of powdered crystal and in reflection from the surface of a pressed polycrystalline pellet. The results were also confirmed by XRD.

The Differential Scanning Calorimetry (DSC) thermogram [17] in Fig. 9.7 shows that TATB exothermic decomposing temperature lies between 360 and 390 °C indicating its excellent thermal stability and heat resistance. This shows how some of the properties of nitro explosives can be improved with the introduction of other groups such as amino groups as in the case of TATB. The products of decomposition of TATB appear to be HCN, CO_2, NO_2, and H_2O with approximate activation energy of 150 kJ/mol [18]. It is likely that C=C homolysis occurs in the form of ring scission leading to these products.

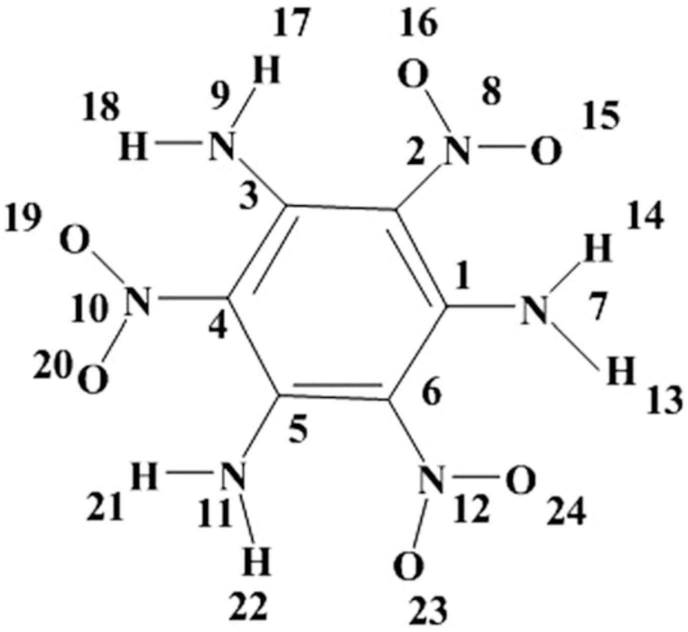

Fig. 9.5 The equilibrium geometry of TATB [13]

Table 9.1 Summary of assignment of vibrational modes (cm^{-1}) [13]

Symmetrical N–H stretching	3220.9
Unsymmetrical N–H stretching	3322.5
Unsymmetrical N–O stretching	1571.3
Symmetrical N–O stretching	1235.6
C–N stretching [Amino group]	1613.1; 779.56
C–N’ stretching [Nitro group]	1321.5
Skeletal stretching [Ring]	1448.4; 1181.2; 1031.4
Weak bands	932.54; 539.32; 741.48

9.4 Crystal Properties

Crystal density is important information used to predict the performance of known and unknown energetic materials. The experimental lattice parameters [19] are: a (Ao) = 9.01; b = 9.028; c = 6.812; $\alpha = 108.58$ deg; $\beta = 91.82$; $\gamma = 119.97$; space group: P1. The crystal structure of TATB has been calculated based on Ab Initio method by Byrd and Rice [20]. Among the different methods used by the authors, it appears that the Perdew-Wang 91 theory gives better estimates of volumes with pressure in comparison with experimental data. A crucial point in such predictions is the inclusion of dispersion forces in the model as they play an important role.

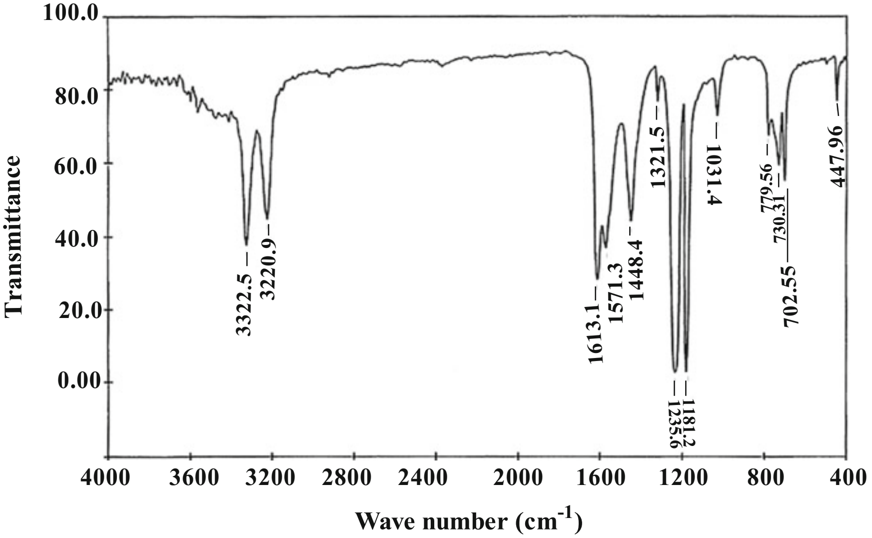

Fig. 9.6 Experimental IR spectrum of TATB [14]

Fig. 9.7 DSC profile of TATB. [17]

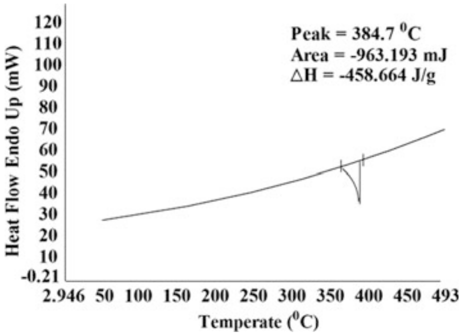

Kolb and Rizzo [15] have carried out X-ray crystallographic studies from 214 to 377 K to monitor the cell constants of triclinic and monoclinic forms of TATB. The calculated cell volumes are shown in Table 9.2. The authors have carried out linear regression analysis on the data and found the anisotropic volume coefficient of thermal expansion to be 30.4×10^{-5} K^{-1}. The unit cell constants are also tabulated in their paper.

Table 9.2 Experimental cell volume for TATB as a function of temperature [15]

Triclinic form		C-Centered monoclinic form	
Temp (°C)	Vol (A^3)	Temp (°C)	Vol (A^3)
−59 ± 3	434.5	−57 ± 1	875.2
−45 ± 3	436.2	−47 ± 2	874.1
−36 ± 1	436.3	−34 ± 2	877.3
−26 ± 1	437.4	−23 ± 2	878.5
−13 ± 3	438.7	−12 ± 1	880.2
11 ± 2	441.6	1 ± 1	883.0
23 ± 1	442.9	12 ± 1	885.5
35 ± 1	447.0	23 ± 1	889.8
44 ± 1	446.7	35 ± 1	895.1
54 ± 1	447.7	45 ± 1	896.7
65 ± 1	449.5	57 ± 2	899.1
76 ± 1	451.9	67 ± 1	901.4
83 ± 1	453.4	76 ± 1	903.0
94 ± 1	454.7	86 ± 1	908.3
104 ± 1	456.2	95 ± 1	910.9

9.5 Physical and Thermodynamic Properties

Table 9.3 provides a list of the general physical properties of TATB [21–28]. This list reveals the disagreement in the values of some of the properties and the need for more accurate values.

9.6 Thermodynamic Properties

Rosen and Dickinson [23] measured vapor pressures and enthalpies of sublimation of high melting explosives including TATB. These authors have made careful measurements of temperatures and pressures but failed to mention the purity of TATB used. The impurities in TATB include amino- and chloro-compounds of dinitrobenzene. The vapor pressure of TATB reported in the literature [23, 26, 29] is summarized in Table 9.4.

The least squares fit of the vapor pressures to the Antoine type equation is given by

$$Log_{10}P = 14.6777 - \left[\frac{60261.2}{6.87372 \times T}\right]$$

Table 9.3 Physical properties of TATB

CAS number	3058-38-6	
Empirical formula	$C_6H_6N_6O_6$	
Molecular mass (Daltons)	258.1	
Enthalpy of formation (kJ/kg)	−541.4	[21]
Enthalpy of explosion [H_2O] (kJ/kg)	3062	[21]
Enthalpy of sublimation (kJ/mol)	180.3 168.2 168.1	[22] [23] [24]
Crystal density (g/cm^3)	1.93	[21]
Melting point (K), Melts above 573 K but decomposes above	623.15 712	[21] [25]
Decomposition temperature (K)	594–599 623.15	[25] [26]
Enthalpy of fusion (kJ/mol)	43.0	[25]
Critical temperature (K)	913	[25]
Critical pressure (bar)	56.5	[25]
Acentric factor	1.802	[25]
Aqueous solubility @ 25°C:	0.16 0.197 2.5	[25]
Log K_{ow}	−1.5 −0.44 4.74	[25]
Volume coefficient of thermal expansion [crystal]	30.4×10^{-5} K^{-1} [214–377 K]	[15]
Crystal heat capacity at 293 K J/g °C	1.38 1.09	[28] [27]
Thermal conductivity (J/cms °C)	8.0×10^{-3}	[28]

Table 9.4 Vapor pressure of TATB

t (°C)	P × 10^7 torr	References
129.3	0.740	[23]
136.2	1.88	[23]
150.0	9.82	[23]
161.4	32.25	[23]
166.4	45.8	[23]
177.3	167.0	[23]
177.3	167.0	[26]
175.0	240.0	[29]
200.0	2100.0	[29]

where T is in K and is different from the fit given by Rosen and Dickenson. Vapor pressure data are very important in predicting the properties of any substance and also in its detection. This table shows the need to generate accurate vapor pressure data. As reported by Agrawal [12, 30] the boiling point of TATB is not well defined, and it is insoluble in most of the solvents except sulfuric acid. It starts decomposing close to the melting point.

Osmont et al. [31] have carried out theoretical evaluation of standard state enthalpy of formation at 298.15 K, and heat capacities and entropy in the temperature range of 300–5000 K for various energetic compounds. Their value of enthalpy of formation is −0.7 kcal/mol^{-1}. Ideal gas heat capacity data are shown in Table 9.5, and entropy values in Table 9.6.

9.7 Solubility

Talawar et al. [17] have tabulated the solubility of TATB in different solvents at room temperature. The values are tabulated in Table 9.7. These are calculated values but the authors do not mention the method of calculation. They also document the DSC and Thermogravimetric Analysis (TGA) profiles, and mechanical properties of TATB/Polymer-Bonded Explosive (PBX) formulations.

Selig [32] has discussed methods of measuring solubility of extremely low soluble materials and measured the solubility of TATB in various solvents. Selig [32] reports the solubility of TATB in sulfuric acid-water mixtures as reproduced in Table 9.8.

During their study on recrystallization, Foltz et al. [33, 34] measured the solubility of TATB in dimethyl sulfoxide (DMSO). The measurements were carried out gravimetrically. The values at 294.35 and 418.65 K were 0.47 and 6.80 g/L, respectively. The authors also use larger particles from approximately 60 to 220 μm

Table 9.5 Calculated C_p^0 (cal mol^{-1} K^{-1}) in the temperature range of 300–1500 K [31]

Temp (K)	300	400	500	600	800	1000	1500
Heat capacity (cal mol^{-1} K^{-1})	60.3	74.8	86.1	94.9	106.9	114.7	125.4
Temp (K)	2000	2500	3000	3500	4000	4500	5000
Heat capacity (cal mol^{-1} K^{-1})	130.5	133.3	134.9	136.0	136.7	137.1	137.5

Table 9.6 Calculated S_0 (cal mol^{-1} K^{-1}) in the temperature range of 300–1500 K [31]

Temp (K)	300	400	500	600	800	1000	1500
Entropy (cal mol^{-1} K^{-1})	129.8	149.2	167.2	183.7	212.8	237.6	286.4
Temp (K)	2000	2500	3000	3500	4000	4500	5000
Entropy (cal mol^{-1} K^{-1})	323.3	352.8	377.2	398.1	416.3	432.5	446.9

Table 9.7 Solubility of TATB in various solvents at 298.15 K [17]

Solvent	Solubility (ppm)
Methanesulfonic acid	820
Hexamethylphosphortriamide	150
Ethanesulfonic acid	120
DMSO	70
Hexafluroacetone sesquihydrate	68
N-Methyl-2-pyrrolidone	58
N,N-Dimethylacetamide	33
DMF	27
Tetramethylurea	26
Dimethyl methylphosphonate	22
N,N-Dimethyl propionamide	16
Conc. Nitric acid	14
3-Methylsulfone	13
Pyridine	12
Trimethylphosphate	11
Acetone	3
Acetonitrile, Acetic anhydride	1
Trifluoroacetic acid, Acetic acid	1

Table 9.8 Solubility of TATB in sulfuric acid:water mixtures [32]

H_2SO_4:H_2O	Acid (vol. %)	(g TATB/100 mL)
1:1	50	>0.02
2:1	66.7	<0.02
4:1	80	−0.24
5.67:1	85	−0.32
7:1	87.5	>1.28
9:1	90	−3.84
Concentrated	100	>24.0

for use in different formulations. The enthalpy of detonation of TATB is calculated to be 3.267 against an experimental value of 3.062 kJ/g [35].

9.8 Performance

Kennedy et al. [36] describe methods of preparing TATB in the range of 1.2–6 μm and dent profiles in detonation-spreading spot-size tests. The density of the different particles tested varied from 1.693 to 1.810 g/cm^3. The results indicate that particle morphology and crystal structure influence the sensitivity of TATB. Similar tests have also been conducted by Tran et al. [37]. Some detonation characteristics of TATB, based on watershock measurements, are listed in Table 9.9 [38].

Table 9.9 Detonation characteristics [38]

Density (g/cm^3)	Detonation Vel. (m/s)	Detonation Pr. (kBar)	Detonation energy (cal/gm)
1.80	7,658	259.4	829
1.50	6,555	174.6	808

Table 9.10 Comparison of SDA.FOR algorithm with Mader values [39, 40]

	Density	PCJ (Mbar)		TCJ (K)		DCJ (m/s)	
	g/cm^3	BKW	SDA	BKW	SDA	BKW	SDA
TATB	1.895	0.326	0.325	1887	1890	8411	8365

Mader [39] used the Becker-Kistiakowsky-Wilson (BKW) equation of state model to calculate the detonation velocity of TATB as a function of density. His calculations using 1,3,5-trinitro-1,3,5-triazacyclohexane (RDX) parameters and assuming carbon as either graphite or diamond do not show good agreement with experimental data.

Based on the Chapman-Jouguet theory, Borg et al. [40] wrote a code -SDA. FOR- to perform chemical equilibrium calculations for detonation of explosives, and compared their results with the values obtained by Mader for TATB. Table 9.10 shows the comparison. They also show some results for other explosives and other models.

Becuwe and Delclos [41] compare the sensitivities of nitrotriazolene (NTO), TATB, RDX, HMX and pentaerythritol tetranitrate (PETN), and show that TATB undergoes spontaneous ignition at a higher temperature compared to other explosives. According to Chevalier et al., [42] the velocity of detonation is higher for HMX compared to TATB but the axial curvature is higher for TATB for any given diameter. They have measured the velocity of detonation for different compositions of TATB.

9.9 TATB Formulations

TATB is combined with other explosives and polymers to produce formulations with varying properties such as densities, velocities of detonation, and impact sensitivity. These formulations make the explosive less sensitive to shock and at the same time impart desirable properties. Hallam [43], and Kolb and Pruneda [44] have discussed the bonding of TATB with Kel-F 800 and the effect of solvents, and found that different polymers did not change the character of the TATB surface energies. Pruneda et al. [45] have discussed the combination of TATB with Kel-F 800 using various solvents in order to increase the binding of TATB with the polymer. The performance of TATB + HMX bonded with Kel-F 800 polymer is shown in Table 9.11. The review by Rainwater et al. [46] is recommended.

Table 9.11 TATB/HMX based PBXs and their properties

Composition	TATB	HMX	Kel-F 800	Density	VOD	Impact sensitivity
	Mass%	Mass%	Mass%	g/cm^3	m/s	cm
PBX-9502	95	0	5	1.895	7706	–
X-0344	71.25	23.75	5	1.894	8046	–
PBX-9501	0	95	5	1.832	8802	–
–	0	90	10	1.869	–	<30

9.10 Conclusions

This paper together with the papers referenced herein provides a survey of the properties of TATB and its formulations. The values of the properties listed in this paper reveal that there are discrepancies in the reported values, and the prediction models are far from satisfactory. There is a need to collect accurate experimental data and develop better models. This would be useful not only in the case of TATB but for all insensitive explosives.

References

1. Dobratz BM (1995) The insensitive high explosive triaminotrinitrobenzene (TATB). Development and Characterization-1888 to 1994 Report LA-13104-H, Los Alamos National Laboratory, Los Alamos NM, USA
2. Agrawal JP, Hodgson RD (2007) Organic chemistry of explosives. Wiley, Hoboken NJ
3. Flurscheim B, Holmes EL (1929) CCCXCIX Pentanitroaniline. J Chem Soc (London) 304 L Hexaminobenzene 334
4. Mitchell AR, Pagoria PF, Schmidt RD (1997) US Patent No 5,569,783, 29 Oct 1996; 5,633,406, 27 May 1997; 6,069,277, 30 May 2000
5. Bellamy AJ, Ward SJ, Golding P (2002) Synthesis of ammonium diaminopicrate (ADAP), a new secondary explosive. Propellants Explos Pyrotech 27(2):59–61
6. Druce RL, Souers PC, Chow C, Roeske F Jr, Vitello P, Hrousis C (2005) Detonation in TATB hemispheres. Propellants Explos Pyrotech 30(2):95–100. doi:10.1002/prep.200400089
7. Urbansky T, Vasudeva SK (1978) Heat resistant explosives. J Scientific Ind Res 37:221–280
8. Atkins RL, Hollins RA, Wilson WS (1986) Synthesis of polynitro compounds hexa-substituted benzenes. J Org Chem 51:3261–3266
9. Ott RG, Benzinger TM (1991) Preparation of 1,3,5-trizmino-2,4,6-trinitrobenzene. J Energetic Mater 5:343 US Patent No 4,997,987
10. Yang G, Nie F, Huang H, Zhao L, Pang W (2006) Preparation and characterization of nano-TATB explosive. Propellants Explos Pyrotech 31:390
11. Pagoria PF, Lee GS, Mitchell AR, Schmidt RD (2002) A review of energetic materials synthesis. Thermochim Acta 384:187
12. Agrawal JP (1998) Recent trends in high-energy materials. Progr Energy Combustion Sci 24:1–30
13. Huang Z, Chen B, Gao G (2005) IR vibrational assignments for TATB from the density functional B3LYP/6-31G(d) method. J Mol Struct 752:87

14. Liu H, Zhao J, Ji G, Wei D, Gong Z (2006) Vibrational properties of molecule and crystal of TATB: A comparative density functional study. Phys Lett A 358:63
15. Kolb JR, Rizzo HF (1979) Growth of 1,3,5-Triamino-2,4,6-trinitrobenzene (TATB) I anisotropic thermal txpansion. Propellants Explos Pyrotech 4:10
16. Son SF, Asay BW, Henson BF, Sander RK, Ali AN, Zielinski PM, Phillips DS, Schwarz RB, Skidmore CB (1999) Dynamic observation of a thermally activated structure change in 1,3,5-triamino-2,4,6-trinitrobenzene (TATB) by second harmonic generation. J Phys Chem B 103(26):5434–5440. doi:10.1021/JP983307H
17. Talawar MB, Agarwal AP, Anniyappan M, Gore GM, Asthana SN, Venugopalan S (2006) Method for preparation of fine TATB (2–5 μm) and its evaluation in plastic bonded explosive (PBX) formulations. J Hazard Mater 137(3):1848–1852. doi:10.1016/j.jhazmat.2006.05.031
18. Makashir PS, Kurian EM (1996) Spectroscopic and thermal studies on the decomposition of 1,3,5-triamino-2,4,6-trinitrobenzene. J Therm Anal 46:225
19. Cady HH, Larson AC (1965) The crystal structure of 1,3,5-triamino-2,4,6-trinitrobenzene. Acta Crystallogr 18(3):485–496. doi:10.1107/S0365110X6500107X
20. Byrd EFC, Rice BM (2009) Improved prediction of heats of formation of energetic materials using quantum mechanical calculations. [Erratum to document cited in CA144:256621]. J Phys Chem A 113(19):5813. doi:10.1021/jp806520b
21. Meyer R, Kohler J, Homburg A (2002) Explosives, 5th edn. Wiley-VCH, Weinheim Germany, p 344
22. Garza RG (1979) A thermogravimetric study of TATB and two TATB-based explosives. Report UCRL-82723 Lawrence Livermore National Laboratory, Livermore CA, USA
23. Rosen JM, Dickinson C (1969) Vapor pressures and heats of sublimation of some high-melting organic explosives. J Chem Eng Data 14(1):120–124. doi:10.1021/je60040a044
24. Stephenson RM, Malanowski S (1987) Handbook of the thermodynamics of organic compounds. Elsevier, New York
25. Toghiani RK, Toghiani H, Maloney SW, Boddu VM (2008) Prediction of physicochemical properties of energetic materials. Fluid Ph Eq 64:86
26. Solovyev VP, Selezenev AA, Aleinikov AY, Lashkov VN, Postnikov AY (2007) Calculation and experimental determination of the HE dependence specific heat versus temperature. In University of Pardubice, pp 299–306
27. Jones DA, Parker RP (1994) Simulation of cookoff results in a small scale test. Report DSTO-TR-0090 DSTO Aeronautical and Maritime Research Laboratory, Melbourne, Australia
28. Beard BC, Sharma J (1993) Surface chemical characterization methods applied to energetic materials. Mater Res Soc Symp Proc 296(Structure and Properties of Energetic Materials):257–268 (Boston MA 1992) DH Liebenberg, RW Armstrong, JJ Gilman (eds) Materials Research Society, Pittsburgh PA
29. F Nie, G Yang, G Zheng, Z Qiao, H Huang (2007) Proc NTREM Conference, Pardubice. p 452, April 25–27
30. Agrawal JP (2005) Some new high energy materials and their formulations for specialized spplications. Propellants Explos Pyrotech 30:316
31. Osmont A, Catoire L, Gökalp I, Yang V (2007) Ab initio quantum chemical predictions of enthalpies of formation, heat capacities, and entropies of gas-phase energetic compounds. Combust Flame 151:262
32. Selig W (1977) How to Estimate the Solubility of an Insoluble Compound: 1,3,5-Triamino-2,4,6-Trinitrobenzene (TATB). Report UCID-17412-Rev. 1, 1977. Estimation of the Solubility of 1,3,5-Triamino-2,4,6-Trinitrobenzene (TATB) in Various Solvents, Report UCID-17412, 1977, Lawrence Livermore National Laboratory, Livermore CA, USA

33. Foltz MF, Ornellas DL, Pagoria PF, Mitchell AR (1996) Recrystallization and solubility of 1,3,5-triamino-2,4,6-trinitrobenzene in dimethyl sulfoxide. J Mater Sci 31(7):1893–1901. doi:10.1007/BF00372205
34. Foltz MF, Maienschein JL, Green LG (1996) Particle size control of 1,3,5-triamino-2,4,6-trinitrobenzene by recrystallization from DMSO. J Mater Sci 31 (7):1741–1750. doi:10.1007/BF00372187
35. Keshavarz MH (2007) Quick estimation of heats of detonation of aromatic energetic compounds from structural parameters. J Hazard Mater 143:549
36. Kennedy JE, Lee KY, Spontarelli T, Stine JR (1998) Los Alamos, Report LA-UR-98-2525
37. Tran TD, Pagoria PF, Hoffman DMN, Cunningham B, Simpson RL, Lee RS, Cutting JL (2002) http://www.intdetsymporg/detsymp2002/PaperSubmit/FinalManuscript/pdf/Tran-238pdf
38. Department of Army (1984 September) Military explosives, TM 9-1300-214, pp 8–72
39. Mader CL (2008) Numerical modeling of explosive and propellants. CRC Press, New York NY
40. Borg RAJ, Kemister G, Jones DA (1995 October) DSTO-TR-0226. Aeronautical and Maritime Research Laboratory, Melbourne, Australia
41. Becuwe A, Delclos A (1993) Low-sensitivity explosive compounds for low vulnerability warheads. Propellants Explos Pyrotech 18(1):1–10. doi:10.1002/prep.19930180102
42. Chevalier JM, Carion N, Protat JC, Redasse JC (1993) Propagation phenomena on the detonation wave front. Phys Rev Lett 71(5):712–714. doi:10.1103/PhysRevLett.71.712
43. Hallam JS (1976) TATB formulation study. Univ California, UCID-17087, p 28
44. Kolb JR, Pruneda CO (1979) Surface chemistry and energy of untreated and thermally treated TATB and plastic-bonded TATB composites. Lawrence Livermore National Laboratory, UCRL-82623 CONF-790632-9
45. Pruneda CO, Bower JK, Kolb JR (1980) Polymeric coatings effect on energy and sensitivity of high explosives. Org Coat Plast Chem 42:588–594
46. Rainwater KA, Lightfoot JM, Richardson RB (1988) Literature review of the lifetime of DOE materials: aging of plastic bonded explosives and the explosives and polymers contained therein. Report ANRCP-1998-12, Amarillo National Resource Center for Plutonium, San Antonio TX, USA

Additional Scholarly Articles for Further Reading

47. Adriaanse C (2010) Security: colorful response to TATP explosives. Chem Ind 21:9 (London, UK)
48. Al-Jalili TAR, Shah HN (1988) Protoheme, a dispensable growth factor for Bacteroides fragilis grown by batch and continuous culture in a basal medium. Curr Microbiol 17(1):13–18
49. Almog J, Klein A, Tamiri T, Shloosh Y, Abramovich-Bar S (2005) A field diagnostic test for the improvised explosive urea nitrate. J Forensic Sci 50(3):582–586
50. Amani M, Chu Y, Waterman KL, Hurley CM, Platek MJ, Gregory OJ (2012) Detection of triacetone triperoxide (TATP) using a thermodynamic based gas sensor. Sens Actuators B 162(1):7–13
51. Andrews G, Lewis D, Notey J, Kelly R, Muddiman D (2010) Part I: characterization of the extracellular proteome of the extreme thermophile Caldicellulosiruptor saccharolyticus by GeLC-MS2. Anal Bioanal Chem 398(1):377–389
52. Armitt D, Zimmermann P, Ellis-Steinborner S (2008) Gas chromatography/mass spectrometry analysis of triacetone triperoxide (TATP) degradation products. Rapid Commun Mass Spectrom 22(7):950–958

53. Ball R (2013) Thermal oscillations in the decomposition of organic peroxides: identification of a hazard, utilization, and suppression. Ind Eng Chem Res 52(2):922–933. doi:10.1021/ie301070d
54. Banerjee S, Mohapatra SK, Misra M, Mishra IB (2009) The detection of improvised nonmilitary peroxide based explosives using a titania nanotube array sensor. Nanotechnology 20(7):075502
55. Bellamy AJ (1999) Triacetone triperoxide: its chemical destruction. J Forensic Sci 44 (3):603–608
56. Benson SJ, Lennard CJ, Maynard P, Hill DM, Andrew AS, Roux C (2009) Forensic analysis of explosives using isotope ratio mass spectrometry (IRMS)—preliminary study on TATP and PETN. Sci Justice 49(2):81–86
57. Brady JE, Smith JL, Hart CE, Oxley J (2012) Estimating ambient vapor pressures of low volatility explosives by rising-temperature thermogravimetry. Propellants Explos Pyrotech 37(2):215–222. doi:10.1002/prep.201100077
58. Brady JJ, Judge EJ, Levis RJ (2010) Identification of explosives and explosive formulations using laser electrospray mass spectrometry. Rapid Commun Mass Spectrom 24(11):1659–1664
59. Brauer B, Dubnikova F, Zeiri Y, Kosloff R, Gerber RB (2008) Vibrational spectroscopy of triacetone triperoxide (TATP): anharmonic fundamentals, overtones and combination bands. Spectrochim Acta A Mol Biomol Spectrosc 71(4):1438–1445
60. Brauer CS, Barber J, Weatherall JC, Smith BT, Tomlinson-Phillips J, Wooten A (2011) Characterization of peroxide-based explosives using Raman spectroscopy: isotopic analysis and DFT calculations of triacetone triperoxide (TATP). Proc SPIE 8019:80190H/1-80190H/6 (Sensors, and command, control, communications, and intelligence (C3I) technologies for homeland security and homeland defense X)
61. Brautigam CA, Deka RK, Schuck P, Tomchick DR, Norgard MV (2012) Structural and thermodynamic characterization of the interaction between two periplasmic Treponema pallidum lipoproteins that are components of a TPR-protein-associated TRAP transporter (TPAT). J Mol Biol 420(1–2):70–86
62. Bry A, Frenois C, Nony S, Forzy A, Hairault L (2009) Sampling importance for the detection of explosives vapors by laboratory techniques. Actual Chim 334:28–35
63. Bulatov V, Reany O, Grinko R, Schechter I, Keinan E (2013) Time-resolved, laser initiated detonation of TATP supports the previously predicted non-redox mechanism. Phys Chem Chem Phys 15(16):6041–6048
64. Bulatov V, Reany O, Grinko R, Schechter I, Keinan E (2013) Time-resolved, laser initiated detonation of TATP supports the previously predicted non-redox mechanism. Phys Chem Chem Phys 15(16):6041–6048
65. Buttigieg GA, Knight AK, Denson S, Pommier C, Bonner Denton M (2003) Characterization of the explosive triacetone triperoxide and detection by ion mobility spectrometry. Forensic Sci Int 135(1):53–59
66. Cagan A, Schmidt H, Rodriguez JE, Eiceman GA (2010) Fast gas chromatography-differential mobility spectrometry of explosives from TATP to Tetryl without gas atmosphere modifiers. Int J Ion Mobility Spectrom 13(3–4):157–165
67. Capua E, Cao R, Sukenik CN, Naaman R (2009) Detection of triacetone triperoxide (TATP) with an array of sensors based on non-specific interactions. Sens Actuators B 140(1):122–127
68. Cerna J, Bernes S, Canizo A, Eyler N (2009) 3,3,6,6,9,9-Hexaethyl-1,2,4,5,7,8-hexaoxacyclononane at 296 K. Acta Crystallogr Sect C: Cryst Struct Commun 65(11):o562–o564
69. Chen J, Wu W, McNeil AJ (2012) Detecting a peroxide-based explosive via molecular gelation. Chem Commun (Camb) 48(58):7310–7312
70. Chen N-C, Wu S-H, Wang C-H, Tsai C-L, Huang Y-T, Shih H-M (2014) Thermal hazard assessment of triacetone triperoxide (TATP) using differential scanning calo-rimetry (DSC). J Appl Fire Sci 23(4):423–434. doi:10.2190/AF.23.4.d

71. Chou H-H, Shih H-H, Cheng C-H (2010) Triptycene derivatives as high-Tg host materials for various electrophosphorescent devices. J Mater Chem 20(4):798–805. doi:10.1039/B918188A
72. Climent E et al (2013) Selective, sensitive, and rapid analysis with lateral-flow assays based on antibody-gated dye-delivery systems: the example of triacetone triperoxide. Chemistry 19 (13):4117–4122
73. Contini AE, Bellamy AJ, Ahad LN (2012) Taming the beast: measurement of the enthalpies of combustion and formation of triacetone triperoxide (TATP) and diacetone diperoxide (DADP) by oxygen bomb calorimetry. Propellants Explos Pyrotech 37(3):320–328. doi:10.1002/prep.201100100
74. Cooper JK, Grant CD, Zhang JZ (2013) Experimental and TD-DFT study of optical absorption of six explosive molecules: RDX, HMX, PETN, TNT, TATP, and HMTD. J Phys Chem A 117(29):6043–6051
75. Corfield R (2006) Was TATP lethal liquid? Chem Ind 16:4 (London, UK)
76. Costales-Nieves C, Boddu VM, Maloney SW, Chakka S, Damavarapu R, Viswanath DS (2010) SPARC prediction of physical properties of explosive compounds. In American institute of chemical engineers, pp a291/1–a291/17
77. Cotte-Rodriguez I, Chen H, Cooks RG (2006) Rapid trace detection of triacetone triperoxide (TATP) by complexation reactions during desorption electrospray ionization. Chem Commun (Camb) 9:953–955
78. Cotte-Rodriguez I, Hernandez-Soto H, Chen H, Cooks RG (2008) In situ trace detection of peroxide explosives by desorption electrospray ionization and desorption atmospheric pressure chemical ionization. Anal Chem 80(5):1512–1519 (Washington, DC, US) doi:10.1021/ac7020085
79. Crowson A, Cawthorne R (2012) Quality assurance testing of an explosives trace analysis laboratory–further improvements to include peroxide explosives. Sci Justice 52(4):217–225
80. Damour PL, Freedman A, Wormhoudt J (2010) Knudsen effusion measurement of organic peroxide vapor pressures. Propellants Explos Pyrotech 35(6):514–520. doi:10.1002/prep.200900083
81. DeCamp DL, Lim S, Colman RF (1988) Reaction of pyruvate kinase with the new nucleotide affinity labels 8-[(4-bromo-2,3-dioxobutyl)thio]adenosine 5’-diphosphate and 5’-triphosphate. Biochemistry 27(20):7651–7658. doi:10.1021/bi00420a012
82. DeGreeff L, Rogers DA, Katilie C, Johnson K, Rose-Pehrsson S (2015) Technical note: headspace analysis of explosive compounds using a novel sampling chamber. Forensic Sci Int 248:55–60
83. Denekamp C, Gottlieb L, Tamiri T, Tsoglin A, Shilav R, Kapon M (2005) Two separable conformers of TATP and analogues exist at room temperature. Org Lett 7(12):2461–2464
84. Dobrokhotov V et al (2012) Toward the nanospring-based artificial olfactory system for trace-detection of flammable and explosive vapors. Sens Actuators B 168:138–148
85. Dubnikova F et al (2005) Decomposition of triacetone triperoxide is an entropic explosion. J Am Chem Soc 127(4):1146–1159. doi:10.1021/ja0464903
86. Dubnikova F, Kosloff R, Oxley JC, Smith JL, Zeiri Y (2011) Role of metal ions in the destruction of TATP: theoretical considerations. J Phys Chem A 115(38):10565–10575
87. Dubnikova F, Kosloff R, Zeiri Y, Karpas Z (2002) Novel approach to the detection of triacetone triperoxide (TATP): its structure and its complexes with ions. J Phys Chem A 106 (19):4951–4956
88. Dunayevskiy I, Tsekoun A, Prasanna M, Go R, Patel CKN (2007) High-sensitivity detection of triacetone triperoxide (TATP) and its precursor acetone. Appl Opt 46(25):6397–6404
89. Efremenko I, Zach R, Zeiri Y (2007) Adsorption of explosive molecules on human hair surfaces. J Phys Chem C 111(32):11903–11911
90. Egorshev VY, Sinditskii VP, Smirnov SP (2013) A comparative study on two explosive acetone peroxides. Thermochim Acta 574:154–161

91. Eren S, Uezer A, Can Z, Kapudan T, Ercag E, Apak R (2010) Determination of peroxide-based explosives with copper(II)-neocuproine assay combined with a molecular spectroscopic sensor. Analyst 135(8):2085–2091 (Cambridge, UK)
92. Espinosa-Fuentes EA, Pacheco-Londono LC, Barreto-Caban MA, Hernandez-Rivera SP (2012) Novel uncatalyzed synthesis and characterization of diacetone diperoxide. Propellants Explos Pyrotech 37(4):413–421. doi:10.1002/prep.201000130
93. Evans HK, Tulleners FAJ, Sanchez BL, Rasmussen CA (1986) An unusual explosive, triacetonetriperoxide (TATP). J Forensic Sci 31(3):1119–1125
94. Ewing RG, Waltman MJ, Atkinson DA (2011) Characterization of triacetone triperoxide by ion mobility spectrometry and mass spectrometry following atmospheric pressure chemical ionization. Anal Chem 83(12):4838–4844 (Washington DC, US)
95. Ezoe R, Imasaka T, Imasaka T (2015) Determination of triacetone triperoxide using ultraviolet femtosecond multiphoton ionization time-of-flight mass spectrometry. Anal Chim Acta 853:508–513
96. Fan W, Young M, Canino J, Smith J, Oxley J, Almirall JR (2012) Fast detection of triacetone triperoxide (TATP) from headspace using planar solid-phase microextraction (PSPME) coupled to an IMS detector. Anal Bioanal Chem 403(2):401–408
97. Fang X, Ahmad SR (2009) Detection of explosive vapour using surface-enhanced Raman spectroscopy. Appl Phys B: Lasers Opt 97(3):723–726
98. Felix-Rivera H, Ramirez-Cedeno ML, Sanchez-Cuprill RA, Hernandez-Rivera SP (2011) Triacetone triperoxide thermogravimetric study of vapor pressure and enthalpy of sublimation in 303–338 K temperature range. Thermochim Acta 514(1–2):37–43
99. Fialkov AB, Moragn M, Amirav A (2011) A low thermal mass fast gas chromatograph and its implementation in fast gas chromatography mass spectrometry with supersonic molecular beams. J Chromatogr A 1218(52):9375–9383
100. Fidler Albo RL et al (2010) Degradation of triacetone triperoxide (TATP) using mechanically alloyed Mg/Pd. Propellants Explos Pyrotech 35(2):100–104
101. Fitzgerald M, Bilusich D (2011) Sulfuric, hydrochloric, and nitric acid-catalyzed triacetone triperoxide (TATP) reaction mixtures: an aging study. J Forensic Sci 56(5):1143–1149
102. Fitzgerald M, Bilusich D (2012) The identification of chlorinated acetones in analyses of aged triacetone triperoxide (TATP). J Forensic Sci 57(5):1299–1302
103. Fujiyama-Novak JH, Gaddam CK, Das D, Vander Wal RL, Ward B (2013) Detection of explosives by plasma optical emission spectroscopy. Sens Actuators B 176:985–993
104. Gaft M, Nagli L (2008) UV gated Raman spectroscopy for standoff detection of explosives. Opt Mater 30(11):1739–1746 (Amsterdam, The Netherlands)
105. Gerber M, Walsh G, Hopmeier M (2014) Sensitivity of TATP to a TASER electrical output. J Forensic Sci 59(6):1638–1641
106. Germain ME, Knapp MJ (2008) Turn-on fluorescence detection of H_2O_2 and TATP. Inorg Chem 47(21):9748–9750
107. Girotti S et al (2011) A quantitative chemiluminescent assay for analysis of peroxide-based explosives. Anal Bioanal Chem 400(2):313–320
108. Giubileo G, Colao F, Puiu A (2012) Identification of standard explosive traces by infrared laser spectroscopy: PCA on LPAS data. Laser Phys 22(6):1033–1037
109. Giubileo G, Puiu A (2010) Photoacoustic spectroscopy of standard explosives in the MIR region. Nucl Instrum Methods Phys Res, Sect A 623(2):771–777
110. Gu H, et al. (2010) Geometry-independent neutral desorption device for the sensitive EESI-MS detection of explosives on various surfaces. Analyst 135(4):779–788 (Cambridge, UK) doi:10.1039/b921579d
111. Haroune N, Crowson A, Campbell B (2011) Characterisation of triacetone triperoxide (TATP) conformers using LC-NMR. Sci Justice 51(2):50–56
112. Hilton CK, Krueger CA, Midey AJ, Osgood M, Wu J, Wu C (2010) Improved analysis of explosives samples with electrospray ionization-high resolution ion mobility spectrometry (ESI-HRIMS). Int J Mass Spectrom 298(1–3):64–71

113. Hiyoshi RI, Nakamura J, Brill TB (2007) Thermal decomposition of organic peroxides TATP and HMTD by T-jump/FTIR spectroscopy. Propellants Explos Pyrotech 32(2):127–134
114. Huestis DL, Mullen C, Coggiola MJ, Oser H (2008) Laser-ionization mass spectrometry of explosives and chemical warfare simulants. Sel Top Electron Syst 48:417–423 (Spectral sensing research for water monitoring applications and science and technology for chemical, biological and radiological defense)
115. Huestis DL, Mullen C, Coggiola MJ, Oser H (2008) Laser-ionization mass spectrometry of explosives and chemical warfare simulants. Int J High Speed Electron Syst 18(1):159–165
116. Jensen L, Mortensen PM, Trane R, Harris P, Berg RW (2009) Reaction kinetics of acetone peroxide formation and structure investigations using Raman spectroscopy and X-ray diffraction. Appl Spectrosc 63(1):92–97
117. Jian F, Qiao Y, Yu H, Zhuang R (2007) Hydrogen peroxide biosensor based on the electrochemistry of the myoglobin-TATP composite film. Anal Lett 40(14):2664–2672. doi:10.1080/00032710701588572
118. Junqueira JRC, de AWR, Salles MO, Paixao TRLC (2013) Flow injection analysis of picric acid explosive using a copper electrode as electrochemical detector. Talanta 104:162–168
119. Katz G, Zybin S, Goddard WA III, Zeiri Y, Kosloff R (2014) Direct MD simulations of terahertz absorption and 2D spectroscopy applied to explosive crystals. J Phys Chem Lett 5 (5):772–776. doi:10.1021/jz402801m
120. Kessel R (1991) An end to TATP in the UK. Hastings Cent Rep 21(6):3
121. Kozole J et al (2012) Characterizing the gas phase ion chemistry of an ion trap mobility spectrometry based explosive trace detector using a tandem mass spectrometer. Talanta 99:799–810
122. Kozole J, Levine LA, Tomlinson-Phillips J, Stairs JR (2015) Gas phase ion chemistry of an ion mobility spectrometry based explosive trace detector elucidated by tandem mass spectrometry. Talanta 140:10–19. doi:10.1016/j.talanta.2015.03.001
123. Krishna BV, Misra VN, Mukherjee PS, Sharma P (2002) Microstructure and properties of flame sprayed tungsten carbide coatings. Int J Refract Met Hard Mater 20(5–6):355–374. doi:10.1016/S0263-4368(02)00073-2
124. Kuzmin VV, Solov'ev MYe, Tuzkov YB, Kozak GD (2008) Forensic investigation of some peroxides explosives. Cent Eur J Energ Mater 5(3–4):77–85
125. Latendresse CA, Fernandes SC, You S, Zhang HQ, Euler WB (2013) A fluorometric sensing array for the detection of military explosives and IED materials. Anal Methods 5(20):5457–5463. doi:10.1039/c3ay40293b
126. Lazic V, Palucci A, Jovicevic S, Carpanese M (2011) Detection of explosives in traces by laser induced breakdown spectroscopy: differences from organic interferents and conditions for a correct classification. Spectrochim Acta Part B 66(8):644–655. doi:10.1016/j.sab.2011.07.003
127. Lazic V, Palucci A, Jovicevic S, Poggi C, Buono E (2009) Analysis of explosive and other organic residues by laser induced breakdown spectroscopy. Spectrochim Acta Part B 64B (10):1028–1039. doi:10.1016/j.sab.2009.07.035
128. Li X, Zhang Z, Tao L (2013) A novel array of chemiluminescence sensors for sensitive, rapid and high-throughput detection of explosive triacetone triperoxide at the scene. Biosens Bioelectron 47:356–360. doi:10.1016/j.bios.2013.03.002
129. Li X, Zhang Z, Tao L (2013) A novel microarray chemiluminescence method based on chromium oxide nanoparticles catalysis for indirect determination of the explosive triacetone triperoxide at the scene. Analyst 138(5):1596–1600 (Cambridge, UK) doi:10.1039/c3an00084b
130. Lin H, Suslick KS (2010) A colorimetric sensor array for detection of triacetone triperoxide vapor. J Am Chem Soc 132(44):15519–15521
131. Lu D, Cagan A, Munoz RAA, Tangkuaram T, Wang J (2006) Highly sensitive electrochemical detection of trace liquid peroxide explosives at a Prussian-blue 'artificial-peroxidase' modified electrode. Analyst 131(12):1279–1281

132. Lubczyk D, Grill M, Baumgarten M, Waldvogel SR, Muellen K (2012) Scaffold-optimized dendrimers for the detection of the triacetone triperoxide explosive using quartz crystal microbalances. ChemPlusChem 77(2):102–105
133. Lubczyk D, Siering C, Loergen J, Shifrina ZB, Muellen K, Waldvogel SR (2010) Simple and sensitive online detection of triacetone triperoxide explosive. Sens Actuators B 143 (2):561–566
134. MacCrehan W, Moore S, Hancock D (2011) Development of SRM 2907 trace terrorist explosives simulants for the detection of semtex and triacetone triperoxide. Anal Chem 83 (23):9054–9059 (Washington DC, US) doi:10.1021/ac201967m
135. MacCrehan W, Moore S, Schantz M (2012) Reproducible vapor-time profiles using solid-phase microextraction with an externally sampled internal standard. J Chromatogr A 1244:28–36
136. Malashikhin S, Finney NS (2008) Fluorescent signaling based on sulfoxide profluorophores: application to the visual detection of the explosive TATP. J Am Chem Soc 130(39):12846–12847
137. Mamo SK, Gonzalez-Rodriguez J (2014) Development of a molecularly imprinted polymer-based sensor for the electrochemical determination of triacetone triperoxide (TATP). Sensors 14(12):23269–23282. doi:10.3390/s141223269
138. Marr AJ, Groves DM (2003) Ion mobility spectrometry of peroxide explosives TATP and HMTD. Int J Ion Mobility Spectrom 6(2):59–62
139. Matyas R (2013) Triacetonetriperoxide—a notorious explosive. Chem Listy 107(4):277–282
140. Matyas R, Chylkova J (2013) Study of TATP: method for determination of residual acids in TATP. Forensic Sci Int 228(1–3):170–173. doi:10.1016/j.forsciint.2013.01.007
141. Matyas R, Jirasko R, Lycka A, Pachman J (2011) Study of TATP: formation of new chloroderivates of triacetone triperoxide. Propellants Explos Pyrotech 36(3):219–224. doi:10.1002/prep.201000158
142. Matyas R, Pachman J (2007) Thermal stability of triacetone triperoxide. Sci Technol Energ Mater 68(4):111–116
143. Matyas R, Pachman J (2010) Study of TATP: influence of reaction conditions on product composition. Propellants Explos Pyrotech 35(1):31–37. doi:10.1002/prep.200800044
144. Matyas R, Pachman J, Ang H-G (2008) Study of TATP: spontaneous transformation of TATP to DADP. Propellants Explos Pyrotech 33(2):89–91. doi:10.1002/prep.200700247
145. Matyas R, Pachman J, Ang H-G (2009) Study of TATP: spontaneous transformation of TATP to DADP—Full Paper. Propellants Explos Pyrotech 34(6):484–488. doi:10.1002/prep.200800043
146. Matyas R, Selesovsky J (2009) Power of TATP based explosives. J Hazard Mater 165(1–3):95–99. doi:10.1016/j.jhazmat.2008.09.063
147. Matyas R, Selesovsky J, Musil T (2012) Study of TATP: mass loss and friction sensitivity during ageing. Cent Eur J Energ Mater 9(3):251–260
148. Matyas R, Selesovsky J, Musil T (2013) Decreasing the friction sensitivity of TATP, DADP and HMTD. Cent Eur J Energ Mater 10(2):263–275
149. Matyas R, Zeman S, Trzcinski W, Cudzilo S (2008) Detonation performance of TATP/AN-based explosives. Propellants Explos Pyrotech 33(4):296–300. doi:10.1002/prep.200700230
150. Mbah J, Knott D, Steward S (2014) Thermogravimetric study of vapor pressure of TATP synthesized without recrystallization. Talanta 129:586–593. doi:10.1016/j.talanta.2014.06.031
151. McGann WJ, Haigh P, Neves JL (2002) Expanding the capability of IMS explosive trace detection. Int J Ion Mobility Spectrom 5(3):119–122
152. Mills A, Grosshans P, Snadden E (2009) Hydrogen peroxide vapor indicator. Sens Actuators B 136(2):458–463. doi:10.1016/j.snb.2008.12.032
153. Mowlawi AA, Yazdani M (2009) Monte carlo simulation of soil moisture effects on anti-tank landmines detection by neutron backscattering technique. Int J Mod Phys B 23 (32):5907–5913. doi:10.1142/S0217979209049735

154. Mullen C, Huestis D, Coggiola M, Oser H (2006) Laser photoionization of triacetone triperoxide (TATP) by femtosecond and nanosecond laser pulses. Int J Mass Spectrom 252 (1):69–72. doi:10.1016/j.ijms.2006.01.018
155. Muller D, Levy A, Shelef R, Abramovich-Bar S, Sonenfeld D, Tamiri T (2004) Improved method for the detection of TATP after explosion. J Forensic Sci 49(5):935–938
156. Munoz RAA, Lu D, Cagan A, Wang J (2007) “One-step” simplified electrochemical sensing of TATP based on its acid treatment. Analyst 132(6):560–565
157. Odbadrakh K, Lewis JP, Nicholson DM (2010) Interaction of the explosive molecules RDX and TATP with IRMOF-8. J Phys Chem C 114(17):7535–7540. doi:10.1021/jp906192g
158. Oestmark H, Wallin S, Ang HG (2012) Vapor pressure of explosives: a critical review. Propellants Explos Pyrotech 37(1):12–23. doi:10.1002/prep.201100083
159. Oxley J et al (2008) Raman and infrared fingerprint spectroscopy of peroxide-based explosives. Appl Spectrosc 62(8):906–915. doi:10.1366/000370208785284420
160. Oxley J, Smith J, Luo W (2006) Peroxide explosives: detection and destruction. Proc NATAS Annu Conf Therm Anal Appl 34th:027.05.901/1-027.05.901/7
161. Oxley J, Smith JL, Brady J, Naik S (2010) Determination of urea nitrate and guanidine nitrate vapor pressures by isothermal thermogravimetry. Propellants Explos Pyrotech 35 (3):278–283. doi:10.1002/prep.200800013
162. Oxley JC (2014) Explosive detection: how we got here and where are we going? Int J Energ Mater Chem Propul 13(4):373–381. doi:10.1615/IntJEnergeticMaterialsChemProp.2014011493
163. Oxley JC, Brady J, Wilson SA, Smith JL (2012) The risk of mixing dilute hydrogen peroxide and acetone solutions. J Chem Health Saf 19(2):27–33. doi:10.1016/j.jchas.2011.07.010
164. Oxley JC et al (2012) Accumulation of explosives in hair—part 3: binding site study. J Forensic Sci 57(3):623–635. doi:10.1111/j.1556-4029.2011.02020.x
165. Oxley JC, Smith JL, Bowden PR, Rettinger RC (2013) Factors influencing triacetone triperoxide (TATP) and diacetone diperoxide (DADP) formation: part I. Propellants Explos Pyrotech 38(2):244–254. doi:10.1002/prep.201200116
166. Oxley JC, Smith JL, Bowden PR (2012) Rettinger RC Factors influencing triacetone triperoxide (TATP) and diacetone diperoxide (DADP) formation. In North american thermal analysis society, pp 65–77
167. Oxley JC, Smith JL, Brady JE, Steinkamp L (2014) Factors influencing destruction of triacetone triperoxide (TATP). Propellants Explos Pyrotech 39(2):289–298. doi:10.1002/prep.201300063
168. Oxley JC, Smith JL, Chen H (2002) Decomposition of a multi-peroxidic compound: triacetone triperoxide (TATP). Propellants Explos Pyrotech 27(4):209–216. doi:10.1002/1521-4087(200209)27:4<209:AID-PREP209>3.0.CO;2-J
169. Oxley JC, Smith JL, Huang J, Luo W (2009) Destruction of peroxide explosives. J Forensic Sci 54(5):1029–1033. doi:10.1111/j.1556-4029.2009.01130.x
170. Oxley JC, Smith JL, Kirschenbaum L, Marimganti S, Bernier E (2005) Transfer of explosives to hair. Proc NATAS Annu Conf Therm Anal Appl 33rd:094.36.892/1-094.36.892/9
171. Oxley JC, Smith JL, Kirschenbaum L, Shinde KP, Marimganti S (2004) New source of evidence: explosive traces in hair. Proc SPIE-Int Soc Opt Eng 5403:246–255 (Pt. 1, Sensors, and command, control communications, and intelligence (C31) technologies for homeland security and homeland defense III) doi:10.1117/12.548165
172. Oxley JC, Smith JL, Kirschenbaum LJ, Marimganti S (2007) Accumulation of explosives in hair–part II: factors affecting sorption. J Forensic Sci 52(6):1291–1296
173. Oxley JC, Smith JL, Kirschenbaum LJ, Marimganti S, Vadlamannati S (2008) Detection of explosives in hair using ion mobility spectrometry. J Forensic Sci 53(3):690–693. doi:10.1111/j.1556-4029.2008.00719.x
174. Oxley JC, Smith JL, Kirschenbaum LJ, Marimganti S, Vadlamannati S (2008) Detection of explosives in hair using ion mobility spectrometry. J Forensic Sci 53(3):690–693

175. Oxley JC, Smith JL, Kirschenbaum LJ, Shinde KP, Marimganti S (2005) Accumulation of explosives in hair. J Forensic Sci 50(4):826–831. doi:10.1520/JFS2004545
176. Oxley JC, Smith JL, Luo W, Brady J (2009) Determining the vapor pressures of diacetone diperoxide (DADP) and hexamethylene triperoxide diamine (HMTD). Propellants Explos Pyrotech 34(6):539–543. doi:10.1002/prep.200800073
177. Oxley JC, Smith JL, Marimaganti K (2010) Developing small-scale tests to predict explosivity. J Therm Anal Calorim 102(2):597–603. doi:10.1007/s10973-010-0983-6
178. Oxley JC, Smith JL, Resende E (2001) Determining explosivity part II: comparison of small-scale cartridge tests to actual pipe bombs. J Forensic Sci 46(5):1070–1075
179. Oxley JC, Smith JL, Resende E, Pearce E, Chamberlain T (2003) Trends in explosive contamination. J Forensic Sci 48(2):334–342
180. Oxley JC, Smith JL, Shinde K, Moran J (2005) Determination of the vapor density of triacetone triperoxide (TATP) using a gas chromatography headspace technique. Propellants Explos Pyrotech 30(2):127–130. doi:10.1002/prep.200400094
181. Oxley JC, Smith JL, Steinkamp L, Zhang G (2013) Factors influencing triacetone triperoxide (TATP) and diacetone diperoxide (DADP) formation: part 2. Propellants Explos Pyrotech 38 (6):841–851. doi:10.1002/prep.201200215
182. Pacheco-Londono LC, Primera-Pedrozo OM, Hernandez-Rivera SP (2004) Experimental and theoretical model of reactivity and vibrational detection modes of triacetone triperoxide (TATP) and homologues. Proc SPIE-Int Soc Opt Eng 5617:190–201. doi:10.1117/12.578603
183. Pachman J, Matyas R (2011) Study of TATP: stability of TATP solutions. Forensic Sci Int 207(1–3):212–214. doi:10.1016/j.forsciint.2010.10.010
184. Pal A, Clark CD, Sigman M, Killinger DK (2009) Differential absorption lidar CO_2 laser system for remote sensing of TATP related gases. Appl Opt 48(4):B145–B150. doi:10.1364/AO.48.00B145
185. Parajuli S, Miao W (2013) Sensitive Determination of Triacetone Triperoxide Explosives Using Electrogenerated Chemiluminescence. Anal Chem 85(16):8008–8015 (Washington DC, US) doi:10.1021/ac401962b
186. Partridge A, Walker S, Armitt D (2010) Detection of impurities in organic peroxide explosives from precursor chemicals. Aust J Chem 63(1):30–37. doi:10.1071/CH09481
187. Pena AJ, Pacheco-Londono L, Figueroa J, Rivera-Montalvo LA, Roman-Velazquez FR, Hernandez-Rivera SP (2005) Characterization and differentiation of high energy cyclic organic peroxides by GC/FT-IR, GC-MS, FT-IR, and Raman microscopy. Proc SPIE-Int Soc Opt Eng 5778:347–358 (Pt. 1, Sensors, and command, control, communications, and intelligence (C3I) technologies for homeland defense IV) doi:10.1117/12.604194
188. Pena-Quevedo AJ, Laramee JA, Durst HD, Hernandez-Rivera SP (2011) Cyclic organic peroxides characterization by mass spectrometry and Raman spectroscopy. IEEE Sens J 11 (4):1053–1060. doi:10.1109/JSEN.2010.2057730
189. Peterson GR, Bassett WP, Weeks BL, Hope-Weeks LJ (2013) Phase pure triacetone triperoxide: the influence of ionic strength, oxidant source, and acid catalyst. Cryst Growth Des 13(6):2307–2311. doi:10.1021/cg301795j
190. Petrova T, Michalkova A, Leszczynski J (2010) Adsorption of RDX and TATP on IRMOF-1: an ab initio study. Struct Chem 21(2):391–404. doi:10.1007/s11224-009-9542-9
191. Pettersson A, Johansson I, Wallin S, Nordberg M, Oestmark H (2009) Near real-time standoff detection of explosives in a realistic outdoor environment at 55 m distance. Propellants Explos Pyrotech 34(4):297–306. doi:10.1002/prep.200800055
192. Price MA, Ghee AH (2009) Modeling for detonation and energy release from peroxides and non-ideal improvised explosives. Cent Eur J Energ Mater 6(3–4):239–254
193. Primera-Pedrozo OM, Pacheco-Londono LC, De la Torre-Quintana LF, Hernandez-Rivera SP, Chamberlain RT, Lareau RT (2004) Use of fiber optic coupled FT-IR in detection of explosives on surfaces. Proc SPIE-Int Soc Opt Eng 5403:237–245 (Pt. 1, Sensors, and command, control communications, and intelligence (C31) technologies for homeland security and homeland defense III) doi:10.1117/12.542812

194. Ramirez ML, Felix-Rivera H, Sanchez-Cuprill RA, Hernandez-Rivera SP (2010) Thermal-spectroscopic characterization of acetone peroxide and acetone peroxide mixtures with nitrocompounds. J Therm Anal Calorim 102(2):549–555. doi:10.1007/s10973-010-0952-0
195. Rasanen R-M et al (2008) Determination of gas phase triacetone triperoxide with aspiration ion mobility spectrometry and gas chromatography-mass spectrometry. Anal Chim Acta 623 (1):59–65. doi:10.1016/j.aca.2008.05.076
196. Ray RS, Sarma B, Mohanty S, Misra M (2014) Theoretical and experimental study of sensing triacetone triperoxide (TATP) explosive through nanostructured TiO2 substrate. Talanta 118:304–311. doi:10.1016/j.talanta.2013.09.057
197. Reany O, Kapon M, Botoshansky M, Keinan E (2009) Rich polymorphism in triacetone-triperoxide. Cryst Growth Des 9(8):3661–3670. doi:10.1021/cg900390y
198. Romolo FS, Cassioli L, Grossi S, Cinelli G, Russo MV (2013) Surface-sampling and analysis of TATP by swabbing and gas chromatography/mass spectrometry. Forensic Sci Int 224(1–3):96–100. doi:10.1016/j.forsciint.2012.11.005
199. Rowell F, Seviour J, Lim AY, Elumbaring-Salazar CG, Loke J, Ma J (2012) Detection of nitro-organic and peroxide explosives in latent fingermarks by DART- and SALDI-TOF-mass spectrometry. Forensic Sci Int 221(1–3):84–91
200. Ryniec R, Piszczek M, Szustakowski M (2010) Multicriterial analysis of explosives in the THz range. Acta Phys Pol A 118(6):1235–1238
201. Salinas Y et al (2014) Chromo-fluorogenic detection of nitroaromatic explosives by using silica mesoporous supports gated with tetrathiafulvalene derivatives. Chem—Eur J 20 (3):855–866. doi:10.1002/chem.201302461
202. Salinas Y et al (2014) Chromo-fluorogenic detection of nitroaromatic explosives by using silica mesoporous supports gated with tetrathiafulvalene derivatives. Chemistry 20(3):855–866
203. Santos JP et al. (2014) Nanocrystalline tin oxide nanofibers deposited by a novel focused electrospinning method. Application to the detection of TATP precursors. Sensors 14 (12):24231–24243 doi:10.3390/s141224231
204. Schade W, Bohling C, Bauer C (2007) Laser optical sensors permit highly sensitive detection of explosives. Phys J 6(4):25–30
205. Schulte-Ladbeck R, Edelmann A, Quintas G, Lendl B, Karst U (2006) Determination of peroxide-based explosives using liquid chromatography with on-line infrared detection. Anal Chem 78(23):8150–8155. doi:10.1021/ac0609834
206. Schulte-Ladbeck R, Karst U (2003) Determination of triacetonetriperoxide in ambient air. Anal Chim Acta 482(2):183–188. doi:10.1016/S0003-2670(03)00212-5
207. Schulte-Ladbeck R, Kolla P, Karst U (2002) A field test for the detection of peroxide-based explosives. Analyst 127(9):1152–1154 (Cambridge, UK) doi:10.1039/b206673b
208. Schulte-Ladbeck R, Kolla P, Karst U (2003) Trace analysis of peroxide-based explosives. Anal Chem 75(4):731–735. doi:10.1021/ac020392n
209. Schulte-Ladbeck R, Vogel M, Karst U (2006) Recent methods for the determination of peroxide-based explosives. Anal Bioanal Chem 386(3):559–565. doi:10.1007/s00216-006-0579-y
210. Scott AM et al (2012) Molecular simulations of adsorption of RDX and TATP on IRMOF-1 (Be). J Mol Model 18(7):3363–3378. doi:10.1007/s00894-011-1338-3
211. Scott AM, Petrova T, Hill F, Leszczynski J (2012) Density functional theory study of interactions of cyclotrimethylene trinitramine (RDX) and triacetone triperoxide (TATP) with metal-organic framework (IRMOF-1(Be)). Struct Chem 23(4):1143–1154
212. Shaw A, Calhoun RL (2012) Electrogenerated chemiluminescence with ruthenium trisbipyridine and TATP. ECS Trans 41:49–56 (27, Physical and analytical electrochemistry (General session)–220th ECS meeting, 2011) doi:10.1149/1.3692523
213. Shen C, Li J, Han H, Wang H, Jiang H, Chu Y (2009) Triacetone triperoxide detection using low reduced-field proton transfer reaction mass spectrometer. Int J Mass Spectrom 285(1–2):100–103. doi:10.1016/j.ijms.2009.04.007

214. Sigman ME, Clark CD, Caiano T, Mullen R (2008) Analysis of triacetone triperoxide (TATP) and TATP synthetic intermediates by electrospray ionization mass spectrometry. Rapid Commun Mass Spectrom 22(2):84–90. doi:10.1002/rcm.3335
215. Sigman ME, Clark CD, Fidler R, Geiger CL, Clausen CA (2006) Analysis of triacetone triperoxide by gas chromatography/mass spectrometry and gas chromatography/tandem mass spectrometry by electron and chemical ionization. Rapid Commun Mass Spectrom 20 (19):2851–2857. doi:10.1002/rcm.2678
216. Sinditskii VP, Kolesov VI, Egorshev VY, Patrikeev DI, Dorofeeva OV (2014) Thermochemistry of cyclic acetone peroxides. Thermochim Acta 585:10–15. doi:10.1016/j.tca.2014.03.046
217. Song-im N, Benson S, Lennard C (2012) Establishing a universal swabbing and clean-up protocol for the combined recovery of organic and inorganic explosive residues. Forensic Sci Int 223(1–3):136–147. doi:10.1016/j.forsciint.2012.08.017
218. Song-im N, Benson S, Lennard C (2013) Stability of explosive residues in methanol/water extracts, on alcohol wipes and on a glass surface. Forensic Sci Int 226(1–3):244–253
219. Stambouli A, El BA, Bouayoun T, Bellimam MA (2004) Headspace-GC/MS detection of TATP traces in post-explosion debris. Forensic Sci Int 146(Suppl):S191–S194
220. Staples EJ (2004) Detecting chemical vapours from explosives using the zNose, an ultra-high speed gas chromatograph. NATO Sci Ser, II 159:235–248 (Electronic noses & sensors for the detection of explosives)
221. Tarvin M, McCord B, Mount K, Sherlach K, Miller ML (2010) Optimization of two methods for the analysis of hydrogen peroxide: high performance liquid chromatography with fluorescence detection and high performance liquid chromatography with electrochemical detection in direct current mode. J Chromatogr A 1217(48):7564–7572. doi:10.1016/j.chroma.2010.10.022
222. Todd MW et al (2002) Application of mid-infrared cavity-ringdown spectroscopy to trace explosives vapor detection using a broadly tunable (6–8 μm) optical parametric oscillator. Appl Phys B: Lasers Opt 75(2–3):367–376. doi:10.1007/s00340-002-0991-8
223. Tomlinson-Phillips J, Wooten A, Kozole J, Deline J, Beresford P, Stairs J (2014) Characterization of TATP gas phase product ion chemistry via isotope labeling experiments using ion mobility spectrometry interfaced with a triple quadrupole mass spectrometer. Talanta 127:152–162. doi:10.1016/j.talanta.2014.03.044
224. Tsaplev YB (2012) Decomposition of cyclic acetone peroxides in acid media. Kinet Catal 53 (5):521–524. doi:10.1134/S0023158412050163
225. van Duin A, Zybin S, Chenoweth K, Han S-P, Goddard WA, III (2005) Reactive force fields based on quantum mechanics for applications to materials at extreme conditions. Lect Ser Comput Comput Sci 4 B:1109–1113 (Advances in computational methods in sciences and engineering)
226. van Duin ACT, Zeiri Y, Dubnikova F, Kosloff R, Goddard WA III (2005) Atomistic-scale simulations of the initial chemical events in the thermal initiation of triacetonetriperoxide. J Am Chem Soc 127(31):11053–11062. doi:10.1021/ja052067y
227. Viswanath DS, Reinig M, Ghosh TK, Boddu VM (2010) Vapor pressure of nitro compounds. In vol Pt. 1. University of Pardubice, Institute of energetic materials, pp 306–309
228. Walter MA et al (2010) Triacetone triperoxide (TATP): hapten design and development of antibodies. Langmuir 26(19):15418–15423. doi:10.1021/la1018339
229. Walter MA, Panne U, Weller MG (2011) A novel immunoreagent for the specific and sensitive detection of the explosive triacetone triperoxide (TATP). Biosensors 1:93–106. doi:10.3390/bios1030093
230. Widmer L, Watson S, Schlatter K, Crowson A (2002) Development of an LC/MS method for the trace analysis of triacetone triperoxide (TATP). Analyst 127(12):1627–1632 (Cambridge, UK). doi:10.1039/b208350g
231. Wilkinson J, Konek CT, Moran JS, Witko EM, Korter TM (2009) Terahertz absorption spectrum of triacetone triperoxide (TATP). Chem Phys Lett 478(4–6):172–174. doi:10.1016/j.cplett.2009.07.079

232. Willer U, Schade W (2009) Photonic sensor devices for explosive detection. Anal Bioanal Chem 395(2):275–282. doi:10.1007/s00216-009-2934-2
233. Wu S-H et al (2012) Thermal hazard analysis of triacetone triperoxide (TATP) by DSC and GC/MS. J Loss Prev Process Ind 25(6):1069–1074
234. Wu S-H et al (2013) Effects of various fire-extinguishing reagents for thermal hazard of triacetone triperoxide (TATP) by DSC/TG. J Therm Anal Calorim 113(2):991–995. doi:10.1007/s10973-012-2788-2
235. Xie Y, Cheng IF (2010) Selective and rapid detection of triacetone triperoxide by double-step chronoamperometry. Microchem J 94(2):166–170. doi:10.1016/j.microc.2009.10.016
236. Xu M, Han J-M, Wang C, Yang X, Pei J, Zang L (2014) Fluorescence ratiometric sensor for trace vapor detection of hydrogen peroxide. ACS Appl Mater Interfaces 6(11):8708–8714. doi:10.1021/am501502v
237. Xu X, van dCAM, Kok EM, de BPCAM (2004) Trace analysis of peroxide explosives by high performance liquid chromatography-atmospheric pressure chemical ionization-tandem mass spectrometry (HPLC-APCI-MS/MS) for forensic applications. J Forensic Sci 49 (6):1230–1236
238. Yamaguchi S, Uchimura T, Imasaka T, Imasaka T (2009) Gas chromatography/time-of-flight mass spectrometry of triacetone triperoxide based on femtosecond laser ionization. Rapid Commun Mass Spectrom 23(19):3101–3106. doi:10.1002/rcm.4225
239. Zeman S, Bartei C (2008) Some properties of explosive mixtures containing peroxides. J Hazard Mater 154(1–3):199–203. doi:10.1016/j.jhazmat.2007.10.013
240. Zeman S, Bartei C (2008) Some properties of explosive mixtures containing peroxides part II. Relationships between detonation parameters and thermal reactivity of the mixtures with triacetone triperoxide. J Hazard Mater 154(1–3):199–203
241. Zhang G (2010) A device for testing thermal impact sensitivity of high explosives. Propellants Explos Pyrotech 35(5):440–445. doi:10.1002/prep.201000030
242. Zhang W-H, Zhang W-D, Chen L-Y (2010) Highly sensitive detection of explosive triacetone triperoxide by an In_2O_3 sensor. Nanotechnology 21(31):315502
243. Zhukov IS, Kozak GD, Tsvigunov AN, Moroz NS (2010) Transformation of aluminum at explosion of its mixtures with TATP and HMTD. In vol Pt. 2. University of Pardubice, Institute of energetic materials, pp 822–824
244. Zuck A et al (2008) Explosive detection by microthermal analysis. J Energ Mater 26(3): 163–180

Chapter 10
Triacetone Triperoxide (TATP)

Abstract Information on thermophysical properties of energetic materials is limited and scattered in the literature. Although peroxides have been known as energetic materials for a long time, triacetonetriperoxide has become prominent as a homemade explosive in the recent years. The properties of TATP are extremely important in its detection, and this chapter reviews the synthesis, properties, for-mulations, detonation, and detection of triacetonetriperoxide.

10.1 Introduction

Improvised explosive devices have proved very fatal as has been evident in the Iraq war, and the use of homemade explosives [HME] have proven to be more effective. The HMEs, mostly peroxides, have eluded detection because of the low sensitivity of the currently available sensors/detectors. Synthesis and characterization of new energetic materials are receiving considerable interest to find materials that are safe and show better performance. Among some of the common HMEs such as hexamethylene triperoxide, nitrourea, urea nitrate and others, TATP has become a prominent one. In spite of the precautions taken during the manufacture of explosives, there are always possibilities that accidental explosions can occur, more so with extremely energetic materials such as TATP.

Triacetone triperoxide, TATP, is a simple but a powerful explosive. It has three acetone molecules joined together by O–O linkages. It is a primary explosive, white crystalline powder with an acid smell. It can be made easily and therefore the choice explosive of terrorists including suicide bombers.

This substance was used in 2005 London bombings. TATP has an explosive force equivalent to 50–80% of that of TNT. As TATP does not contain nitrogen, it is likely to go through airport scanners without detection as most of the scanners are calibrated for nitrogen containing chemicals. Reid, the shoe bomber, used TATP along with a plastic explosive. He used TATP as a trigger by using a small thread of TATP through 100 g of PETN [1]. The seven suspects who were arrested in Vollsmose in Denmark in 2006 [2] and eight Al-Queda terrorists arrested in

D.S. Viswanath et al., *Emerging Energetic Materials: Synthesis, Physicochemical, and Detonation Properties*, https://doi.org/10.1007/978-94-024-1201-7_10

Copenhagen had access to homemade TATP. These two events happened in 2006 and 2007, respectively. In 2005 October, Hinrichs, a student at the Oklahoma University, died near the football stadium after a backpack containing two to three pounds of TATP exploded [3] due to his carelessness. Two contractors were recently arrested by the Swedish police on suspicion that they were suspected of sabotage of the Oskarshamn nuclear plant in southeastern Sweden. One of them was carrying a small amount of TATP. These and many more incidents show the explosive power of TATP, the relative ease with which it can be made, the availability of chemicals for the synthesis of TATP, and the extreme difficulty in detecting this compound as most of the detectors are calibrated for explosives containing nitrogen. YouTube graphically illustrates the synthesis of TATP. Although the civilian and military uses of TATP are limited, and the public knowledge of peroxide explosives was very limited until recently, TATP has shot into prominence for reasons mentioned earlier. Reports of the use of TATP by the Mexican Drug Cartel during the past two to three years have been surfacing, and TATP has been linked to the explosion of home-made bombs. The ease of preparation of TATP has emboldened home grown terrorists, like Chad Wells, who was arrested recently as reported in the Augusta Chronicle [4].

These events indicate the gravity of the situation, and the need to know as much as possible about this chemical. Safe handling and disposal of these HMEs like TATP require a good understanding and knowledge of the properties of these compounds. To design and build sensitive and robust detection systems, it is imperative to have accurate vapor pressure data besides other thermophysical properties of these chemicals. Thermophysical properties are essential to develop models to predict properties such as vapor pressure when experimental data are lacking.

TATP is a white crystalline substance with an acid odor. It sublimes readily at room temperature, and is extremely sensitive to impact, friction and electrostatic discharge. It is extremely dangerous because of the constrained nature of the molecule in a ring form in three dimensions. The problems of handling and extreme sensitivity make it difficult to use TATP in military and civilian applications although it is very easy to synthesize. It is reported that TATP in quantities less than 2 g burns but more than 2 g detonates when ignited. A TATP bomb can be made with \$100–\$200 worth of chemicals, and simple equipment.

Denekamp et al. [5] have identified two stable conformal structures for TATP based on experimental and theoretical evidence. Figure 10.1 shows the two conformal forms of TATP. These two forms are stable with energy of transition of 26.3 kcal/mole. The authors have carried out B3LYP/6-31G computations to arrive at the crystal parameters. They note that this type of behavior is rare in cyclic organic systems and attribute it to the overlap in the “flip-flop” transition state. It is known that TATP contains the dimer of acetone peroxide [6] and a tetramer is also observed [7].

The chemical name for TATP is 3,3,6,6,9,9-hexamethyl-1,2,4,5,7,8-Hexoxonane and is also known as peroxyacetone. Acetone peroxide most

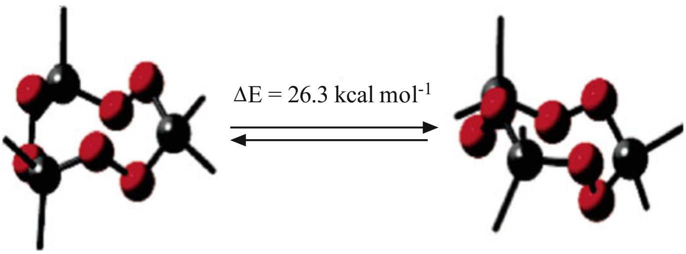

Fig. 10.1 Conformal Structures of TATP

commonly refers to the cyclic trimer TCAP (tri-cyclic acetone peroxide, or tri-cyclo). The CAS Number is 17088-37-8.

10.2 Synthesis

TATP is prepared starting with hydrogen peroxide and acetone. As early as 1895, Wolffenstein [8] discussed the effect of hydrogen peroxide concentration on acetone. He showed that 10% peroxide can be used to synthesize TATP. Acid catalyzed synthesis of TATP was first described in 1959 by Millas and Golubovic [9]. They added acetone (0.2 mol) at 273.15 K (0 °C) to a cold mixture of hydrogen peroxide (50%, 0.2 mol) and sulfuric acid, kept the mixture at 273.15 K (0 °C) for 3 h, and then extracted it with pentane. This procedure uses large quantities of sulfuric acid but is a fast and unsafe route to synthesize TATP. Dubnikova et al. [10] used the same method as Millas and Golubovic but used smaller amounts of sulfuric acid. This procedure improved the safety of the process. Mateo et al. [11] prepared TATP by treating acetone at 271.15 K (−2 °C) with concentrated hydrogen peroxide with sulfuric acid as the catalyst. They obtained 75% yield. Pacheco-Londono et al. [12] used different ratios of acetone and H_2O_2 with different inorganic acids as catalysts to make TATP. They used Density Functional Theory to elucidate the mechanism of the reaction, and used B3LYP functional with the 6-31G basis set to carry out calculations of the electronic structure of the intermediates and internal rotations and vibrations of TATP. A 1989 patent taken by Costantini [13] and assigned to Rhone-Poulenc gives details of TATP synthesis and destruction.

Jiang et al. [7] found $SnCl_4 \cdot 5H_2O$ and $SnCl_2 \cdot 2H_2O$ to be efficient catalysts for the oxidation of acetone with 30% hydrogen peroxide at room temperature. This method produced tetrameric acetone peroxide which was identified by molecular weight determination, elemental analysis, FTIR, NMR and MS. Jensen et al. [14] used Raman spectroscopy to study the synthesis of TATP. They studied the effect of temperature and pH, and observed spectral changes during the course of the reaction.

10.3 Structure

TATP crystalline is a monoclinic solid with a P21/c space group and a coordination number of 4. The lattice parameters are a = 13.925 Å, b = 10.790 Å, c = 7.970 Å, and β = 91.64° [15]. It exists in a twisted boat chair form with O–O distance = 1.483 Å, C–O bond length of 1.422 Å, and the C–O–O angle 107.4°. The C–O bond length is shorter than that found in other peroxides. Dubnikova et al. [10] compared experimental bond lengths with values based on B3lYP calculations, and their data are shown in Table 10.1. These values compare well with the values of Groth [15]. As a part of a forensic investigation, Evans et al. [16] provide chemical ionization and electron impact mass spectra, infrared spectrum, and some physical properties of TATP.

10.4 Detection

The synthesis of TATP mentioned above reveals that it can be made easily from readily available raw materials. This has made TATP a choice explosive for terrorist activities. In order to provide safety and protect human lives, it is essential to have extremely sensitive techniques to detect TATP. In recent years a great deal of attention has been paid to the detection of TATP. There was no reliable method to detect TATP until 2003 [17]. Since 2003, the number of papers published in the open literature on the detection of TATP has exceeded 100. The absence of nitro, amino, or aromatic groups makes it difficult to detect TATP. The explosive nature of TATP makes it difficult to even analyze the material, and therefore special care has to be taken to prepare a sample. Many national laboratories in the United States are involved in the detection of TATP [18].

Several methods including IR and Raman spectroscopy, ion mobility spectrometry, ^{1}H and ^{13}C NMR, HPLC, GC/MS, chemical ionization coupled to tandem mass spectrometry, and laser photo-acoustic and photoionization techniques have

Table 10.1 Comparison experimental and calculated bond lengths and bond angles [10]

Bond length/angle	Expt.	Calc.
O–C	1.419, 1.418, 1.417	1.422
O–C	1.422	1.421
O–O	1.466, 1.471, 1.473	1.458
C–C	1.512, 1.514, 1.516	1.528
C–C	1.505, 1.510	1.529
<O–C–O	112.2, 112.5, 112.8	112.9
<O–C–C	102.7, 103.2, 107.8	102.9
<O–C–C	112.1, 112.5, 112.8	112.3
<O–O–C	107.6, 112.8	108.6
<C–C–C	113.0, 114.2	113.6

been used to detect and analyze TATP. Utilizing the quantum cascade laser photoacoustic spectroscopy technique, Dunayevskiy et al. [19] were able to detect TATP to 18 ppb levels. However this level of sensitivity may not be enough to detect TATP from a distance of 5 to 10 m when someone is carrying this explosive. Because of the difficulties in handling TATP, Dunayevskiy et al. [19] describe a simple apparatus for preparation and collection of TATP for analysis. Mullen et al. [20] describe a laser ionization time-of-flight mass spectrometric technique to study its potential for detection of TATP. In addition to the laser ionization time-of-flight mass spectrum, the authors also present UV spectra of both TATP and H_2O_2 and compare with the available literature spectra.

Canines are commonly employed to detect various substances such as drugs and conventional explosives, however, canines are being trained to detect TATP as more incidents have taken place using TATP. It appears that trials reveal that canines can detect 200 lg of TATP [21] although the present method used for training canines is not too satisfactory. Muller et al. [22] report that they were able to detect 6.4 ng using a GC/MS system. They used Amberlite XAD7 as the adsorbent and acetonitrile as the eluent. They also report the presence of TATP in several post-explosion areas in and around Jerusalem, Israel.

Based on chemiluminescence principle, Scintrex Trace Systems [23] offers E3500 for TATP detection. This is a hand held unit but the sensitivity of this system is not mentioned. For portal detection of TATP, Synagen Guardian MS-ETD [24] has designed and built the personal screening portal based on a technology from Sandia National Laboratory. In this method, a puff of air dislodges trace amounts of chemicals such as TATP which are analyzed by an MS- electron transfer dissociation technique. Another hand-held unit has been developed by Acro [25], an Israeli small-scale company. It is a pen sized detector but its detection capability, cost, and sensitivity are not revealed. It is a colorimetric method and requires about 25–50 micrograms of TATP. Figure 10.2 shows the sensitivity of the instrument based on the information available on the company's website. This sensor uses the peroxidase enzyme method and is covered by a US Patent [26]. Nomadics [27] has several patents on the detection of peroxides. In general the peroxide such as TATP is decomposed and the released H_2O_2 is reacted further to finally yield CO_2 which is detected by light emission techniques.

A quantitative trace analysis of peroxide based explosives, hexamethylenetriperoxidediamine (HMTD) and triacetone triperoxide (TATP) has been developed by Ladbeck et al. [28] using fluorescence spectroscopy. The limit of detection was 2×10^{-6} mol l^{-1} for both TATP and HMTD. Sigman et al. [29] carried out the analysis of TATP and the other products by electronspray mass spectrometry, and were able to detect TATP at levels close to 60 ng. Compared to this level of detection, the GC-MS method developed by Roman et al. [30] appears to be more sensitive down to picogram levels. This method is claimed to be applicable to both TATP and DADP to 50 pg levels. Ion mobility spectroscopy coupled with a triple quadrupole mass spectrometer was used by Buttigieg [31] during the synthesis and analysis of TATP. Sella and Shabat [32] developed a molecular probe to detect TATP. This method is sensitive only at microgram levels, and may not be a practical tool.

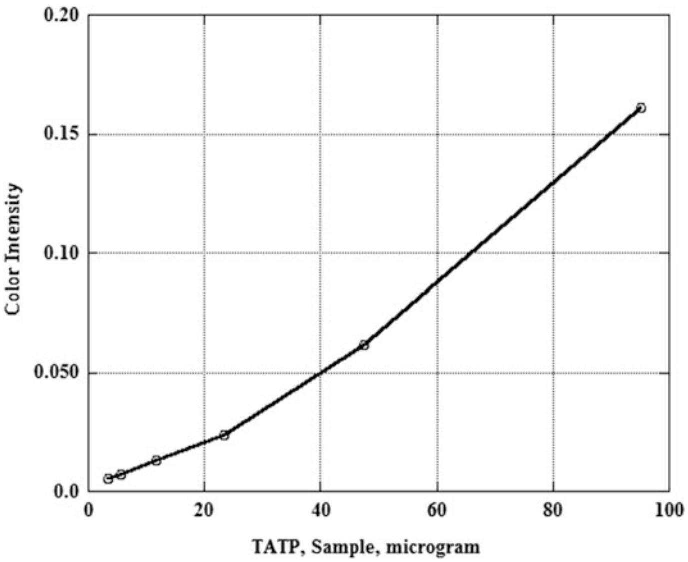

Fig. 10.2 Color sensitivity as a function of microgram TATP [25]

The detection systems described above have not been used as stand-off detection systems. Gaft and Nagli [33] describe a UV Raman spectroscopic method for standoff detection at distances close to 100 feet (30 m). The authors used a Schmidt–Cassegrain telescope fiber-coupled to an Oriel MS260i spectrometer with a gated ICCD detector along with a frequency- doubled Nd-YAG (532 nm, 20 mJ/pulse) pulsed (8 ns, 13 Hz) laser system. In addition to TATP, they report to have studied UN—urea–nitrate, TNT including by-products and mixtures, such as comp B (mixture with RDX), DNT, RDX and mixtures such as C4, A5, ANFO—ammonium-nitrate fuel-oil, PETN, HMX, and Semtex, a mixture of RDX and PETN. This appears to pave the way for commercialization of stand-off detection systems. They present typical Raman spectrum for each of these materials. Munoz et al. [34] report an electrochemical method for the detection of TATP. This method is carried out in liquid phase, and may not be useful as a practical detector. The sensitivity appears to be at nanogram levels. In their recent paper, Banerjee et al. [35] describe the use of titania nanotubes for the detection of TATP. The authors do not discuss the sensitivity but it appears to be at the ppm levels. One plus point of this research is that if the method could be made sensitive enough, it could be used in hand-held detectors. Apblett et al. [36] report the use of molybdenum hydrogen bronze nanoparticles for the detection of TATP and HMTD. As this is a calorimetric method, the sensitivity of the method may not get to pictogram levels. The authors discuss the possibility of this method as a method for in situ degradation of TATP. Cotte-Rodriguez et al. [37] used both desorption electrospray ionization and desorption atmospheric pressure chemical ionization in their work on the detection of TATP, HMTD, and other explosives. In this technique, the explosives were complexed with certain dopants for analysis. The method is claimed to be fast and reliable. Both TATP and HMTD were detected in the 1–5000 ng range.

10.5 Properties of TATP

The unstable nature of TATP and its explosive nature makes it difficult to determine accurately the thermochemical and thermophysical properties, and literature search revealed lack of data. Table 10.2 lists some of the common properties of TATP from different sources [4, 38, 39].

Oxley et al. [40] measured the vapor pressure of TATP and their data are tabulated in Table 10.3. Table 10.3 shows that the error between two measurements sometimes is between 10 to 20% and shows the need for better methods and accurate measurements.

The extremely unstable nature of the compound makes it difficult to measure accurate values. The authors represent the vapor pressure-temperature data by the relation.

$$\mathrm{Log}_{10} P(P\,\mathrm{on}\,Pa) = 19.791 - \frac{5708}{T\,(K)}$$

where P is in Pascal, and T in K.

Table 10.2 Common properties of TATP

Empirical formula	$C_9H_{18}O_6$	CAS No. 17088-37-8
Other names: 3,3,6,6,9,9-Hexamethyl-1,2,4,5,7,8-hexaoxacyclononane,		
Molecular mass, g/mole	222.24	
Crystal structure	Monoclilnic with cell parameters a = 13.788 Å, b = 10.664 Å, c = 7.894 Å, β = 91.77°, V = 1160.1 $Å^3$	[10]
Density, g/mL	1.004	[38]
Molar volume, cm^3mol^{-1}	221.1 ± 3.0	[38]
Boiling point, K	370.15-433.15; 458.05 ± 30 (97–160 °C; 184.9 ± 30 °C)	[38]
Melting point	367.15 (94 °C) 365.15-366.15 (92–93 °C)	[38] [12]
Flash point	51.5 ± 24.4	[38]
Enthalpy of vaporization, kJ/mol	40.39 ± 3.0 46.41 and 51.73	[38] [39]
Koc	325	[38]
Velocity of detonation, m/s	5300	
Aqueous solubility, g/L	3.1 at 298.15 K (25 °C)	[38]
Bioconcentration Factor	22.6	[38]

Table 10.3 Vapor pressure of TATP [40]

T, K	285	285	295	295	298	298	305	305
VP, Pa	0.95	1.13	1.85	1.44	6.95	6.86	16.8	18.9
T, K	315	315	325	325	331	331		
VP, Pa	46.1	51.2	98.4	101	720	596		

10.6 TATP Decomposition

TATP decomposes around 150–160 °C. It also undergoes spontaneous transformation to DADP under certain conditions [41]. This decomposition depends on the catalysts used, the ratio of reactants to catalyst, purity of chemicals used and reaction conditions. The spectra of pure TATP have been recorded by Oxley et al. [42] and their IR and Raman frequency assignments are shown in Table 10.4. In addition they also present a comparative study of the vibrational spectra of several peroxide compounds including HMTD, DADP, etc. Vibrational spectroscopy of TATP is the subject of a presentation by Pacheco-Londono et al. [43]. In their synthesis study, the authors used different acids as catalysts, and varied the ratio of acetone to hydrogen peroxide. A recent study of the vibrational spectroscopy of TATP was carried out by Brauer et al. [44]. They carried out experimental and theoretical studies to analyze the overtones and anharmonic interactions.

The products of decomposition of TATP depend on the rate of heating as noticed by Hiyoshi et al. [45]. Slow heating rates produced acetone whereas methane was the product at higher heating rates. This could be because of the type of O–O cleavage at different heating rates. Mullen et al. [46] in their study of laser ionization time-of-flight mass spectroscopy found TATP decomposition products, including acetyl ion $C_2H_3O^+$, acetone ion $C_3H_6O^+$, $C_3H_7O^+$, $C_3H_7O_2^+$, $C_3H_6O_4^+$, and $C_3H_6O_5^+$. Matyas and Pachman [47] have carried out DTA measurements of TATP in the presence of several inorganic acids. The decomposition rate was faster with sulfuric acid compared to hydrochloric, nitric, or perchloric acids. Armitt et al. [48] carried out a similar study to track the products of decomposition of TATP in the presence of inorganic acids. The products and the rates of decomposition were dependent on the type of acid. Part of this study is also reported elsewhere [49].

10.7 Formulations and Detonation Characteristics

The stability of TATP has prevented it to be used as a primary explosive although it can be made easily from chemicals that are readily available and cheap. Hanson [50] reports that TATP has 50–80% of the force of TNT, and creates a force of nearly 1.5 tons per square inch. To get a perspective of the damage that could be

Table 10.4 TATP calculated (at B3LYP/cc-pVDZ level of theory) harmonic frequencies (cm^{-1}), IR intensities (km/mole), Raman scattering activities (A4/AMU), and frequencies [42]

Frequency	IR intensity	Raman activity	Description	
n1	99.2	0.7	0.4	O–O–C–Methyl torsional tangent to ring
v2	100.1	0.6	0.4	O–O–C–Methyl torsional
v3	129.1	1.9	0.0	Collective O–O–C–Me torsional
v4	147.0	2.8	0.4	O–O–C–Methyl torsional and Methyl twist
v5	147.6	3.2	0.5	O–O–C–Methyl torsional and Methyl twist
Asynchronous				
v13	236.4	0.4	2.5	C–O–O–C shear
v14	237.3	0.4	2.5	C–O–O–C shear
v16	296.3	0.3	0.0	Collective bending
v21	393.7	0.0	5.4	Ring breathing
v22	429.1	0.6	0.4	O–C–Methyl scissoring
v23	430.1	0.7	0.4	O–C–Methyl scissoring
v25	547.2	10.6	4.2	O–C–Methyl scissoring and Methyl–C–
Methyl rocking				
v26	547.4	10.4	4.2	O–C–Methyl scissoring and Methyl–C–
Methyl rocking				
v27	557.1	0.0	22.8	Collective O–C–O scissoring
v28	572.9	13.0	0.0	Collective C–C–O scissoring
v29	623.8	6.6	2.5	O–C–O scissoring asynchronous
v30	624.1	6.6	2.5	O–C–O scissoring asynchronous
v31	792.1	28.6	0.3	O–C–O symmetrical stretching and Methyl
–C–Me sym stretching				
v32	792.6	28.6	0.3	O–C–O symmetrical stretching and Methyl–
C–Methyl symmetrical stretching				
v33	848.1	15.4	0.0	Collective O–C–O asymmetrical stretching
v34	855.5	0.0	7.4	Collective O–C–O and Methyl–C–Methyl
Symmetrical stretching				
v35	891.2	24.7	10.1	O–C–O and Methyl–C–Methyl asymmetric
Stretching Me–C–O symmetric stretching				
v36	891.8	24.7	10.1	O–C–O and Methyl–C–Methyl symmetric

(continued)

Table 10.4 (continued)

Frequency	IR intensity	Raman activity	Description	
Stretching Methyl–C–O asymmetric stretching				
v37	903.6	3.1	32.1	O–O stretching asynchronous and Methyl
Rocking asynchronous				
v38	904.6	3.0	32.8	O–O stretching asynchronous and Methyl
Rocking synchronous				
v39	906.6	0.1	19.9	O–O stretching synchronous Methyl–C–
Methyl symmetrical stretching and Methyl rocking				
synchronous				
v43	956.3	17.9	13.3	Methyl–C–Methyl stretching O–C–O
Symmetrical stretching				
v44	957.1	16.1	12.8	Methyl–C–Methyl and O–C–O symmetrical
Stretching				
v45	962.7	0.0	66.2	Collective O–O and C–O stretching
v48	1022.8	0.0	3.3	O–C–O symmetrical stretching
v49	1137.2	4.6	0.0	O–C–O asymmetric stretching
v50	1197.4	187.8	1.0	O–C–O and Methyl–C–Methyl asymmetric
Stretching Methyl–C–O symmetrical stretching				
v51	1197.6	192.6	1.0	O–C–O and Methyl–C–Methyl asymmetric
Stretching, Methyl–C–O symmetric stretching				
v52	1213.9	131.5	2.4	O–C–O and Methyl–C–Methyl
Symmetric stretching				
v53	1214.0	131.4	2.4	O–C–O and Methyl–C–Methyl symmetric stretching
v54	1220.9	0.0	9.8	Collective O–C–O and Methyl–C–Methyl
Symmetric stretching				

Table includes only the frequencies (all of them) that are concerned with O–O and C–O vibrations

done by such a force is to look at the force that support columns in buildings such as the Oklahoma City A.P. Murrah building. The columns were designed to withstand at least 3000 lb per square inch which is what TATP can create. In a

Truzl test, Dubnikova et al. [10] found TATP to be 80% as effective as TNT, but its volatility and unstable nature make it difficult to use for military and civilian purposes. Matyas and Selesovsky [51] have presented the detonation characteristics of various combinations of TATP, ammonium nitrate, water, uranium nitrate, fuel oil, etc.

Mayatas et al. [52] have studied TATP formulation with ammonium nitrate (AN) and water. They varied the mixture compositions from 21 to 31% TATP, 37 to 54% AN, and 19 to 32% water, and tested them for various properties including detonation velocity. The results were compared with those of 2,4,6-trinitrotoluene (TNT). The summary of their results are shown in Table 10.5. The compositions of the four mixtures are pretty close to one another. An interesting observation that the authors have made is the dependence of detonation velocity on charge diameter, and the criticality of the charge diameter. The results of Table 10.5 indicate larger charge diameters increase the detonation velocity and come closer to the detonation velocity of TNT. It is not clear how they prepared their explosion emulsion ammonium nitrate—ANE, but this low cost material has a detonation velocity closer to TNT. Another publication by the authors [53] provides more data on $TATP^+$ ammonium nitrate and $TATP^+$ urea nitrate.

Menning and Ostmark [54] measured the friction and impact sensitivity based on the up and down method. The results of their tests are shown in Table 10.6. The commercial samples used in these tests have been tested for purity by IR spectroscopy. The results of Table 10.6 are based on ten tests per sample. The authors determined friction sensitivity using a Julius Peters (BAM) apparatus, and performing the test by using an up-and-down method on both sides of the 50% probability level.

Table 10.5 Experimental results on various explosive mixtures [52]

Explosive composition			Internal charge diameter (mm)	Density (gcm^{-3})	Detonation velocity (ms^{-1})
TATP	AN	W			
27	54	19	28	1.19	4110
26	54	20	46	1.16	4400
26	54	20	12.3	1.29	2520
26	54	20	16.5	1.29	2880
26	54	20	105	1.28	4810
21	53	26	25	1.14	4800
31	37	32	25	1.14	4470
TNT—test 1			25	1.20	5480
TNT—test 2			25	1.20	5460
ANFO			25	0.75	2180
ANE			25	1.06	5460

Table 10.6 Friction and impact sensitivity of TATP based on up and down method [54]

Explosive	Form	Friction Sensitivity, BAM (kp/cm^2)	Impact Sensitivity, ERL (J)	Std dev (J)	Temp/RH (°C/%)
TATP (FOI)	Needle-like crystals	<1.0	<1.2	–	21/74
TATP (FOI)	Fine powder	<0.5	<2.0	–	18/27
TATP (FOI)	Fine powder	<0.5	1.9	0.9	19/26
TATP (FOI)	Crystals	<0.5	<1.2	–	17/25
TATP (FOI)	Fine powder	<0.5	2.3	0.3	19/28

10.8 Destruction

Several methods including oxidation-reduction, and catalytic, have been explored for the degradation and destruction of TATP. Fidler et al. [55] found 96% degradation using an alloy of MgPd. They observed acetone to be the product of decomposition. Bellamy [56] discusses a chemical reduction method for the safe disposal of TATP. The risks involved in handling this sensitive explosive are shown to be considerably reduced by dissolving it in toluene. Destruction of unwanted samples of TATP could in principal be achieved in three ways (a) burning, preferably of a TATP solution, (b) thermal degradation, and (c) chemical destruction.

References

1. Fresco A, O’Neill S, Tendler S (July 15, 2005) Jamaican-born bomber from the suburbs of Middle England. The Times, 15 July 2005, at www.timesonline.co.uk/article/0,22989–1694965,00.html
2. Perry M, Berg M, Krukones J (2010) Danish ‘homegrown’ vollsmose group on 5 September 2006. sources of European History: Since 1900
3. NBC NEWS (2005) Bomb blast at University of Oklahoma. Bomb blast outside of sooner football game. 2 Oct 2005
4. Sparks P (2009) Arrest warrant issued for man involving explosives. Augusta Chronicle, 20 Jan 2009
5. Denekamp C, Gottlieb L, Tamiri T, Tsoglin A, Shilav R, Kapon M (2005) Two separable conformers of tatp and analogues exist at room temperature. Org Lett 7(12):2461–2464
6. Bayer VV (1900) Ueber die einwirkung des caro’schen reagens auf ketone. Chem Ber 33:858–864
7. Jiang H, Chu G, Gong H, Qiao QD (1999) Tin chloride catalyzed oxidation of acetone with hydrogen peroxide to tetrameric acetone peroxide. J Chem Res 4:288–289
8. Wolffenstein (1895) Action of hydrogen peroxide on acetone and mesityl oxide. Berichte der Deutschen Chemischen Gesellschaft 28:2265–2269
9. Milas NA, Golubovic A (1959) Studies in organic peroxides XXVI organic peroxides derived from acetone and hydrogen peroxide. J Am Chem Soc 81:6461–6462
10. Dubnikova F, Kosloff R, Almog J, Zeiri Y, Boese R, Itzhaky H, Alt A, Keinan E (2005) Decomposition of triacetone triperoxide is an entropic explosion. J Am Chem Soc 127 (4):1146–1159

11. Mateo M, Eyler GN, Alvarez EE, Canizo AI (1998) New method for the synthesis of cyclic acetone triperoxide. Informacion Tecnologica 9(2):19–22
12. Pacheco-Londono LC PAJ, Primera-Pedrozo OM, Hernandez-Rivera SP, Mina N, Garcia R, Chamberlain RT, Lareau RT (2004) An experimental and theoretical study of the synthesis and vibrational spectroscopy of triacetone triperoxide (TATP). In: Proc SPIE-Int Soc Opt Eng 5403(Pt 1, Sensors, and Command, Control Communications, and Intelligence (C31) Technologies for Homeland Security and Homeland Defense III), pp 279–287
13. Costantini M (1989) Destruction of acetone peroxides. US Patent 5003109
14. Jensen L, Mortensen PM, Trane R, Harris P, Berg RW (2009) Reaction kinetics of acetone peroxide formation and structure investigations using Raman spectroscopy and X-ray diffraction. Appl Spectrosc 63(1):92–97
15. Groth P (1969) Crystal structure of 3,3,6,6,9,9-hexamethyl-1,2,4,5,7,8-hexaoxacyclononane (trimeric acetone peroxide). Acta Chem Scand 23(4):1311–1329
16. Evans HK, Tulleners FAJ, Sanchez BL, Rasmussen CA (1986) An unusual explosive, triacetonetriperoxide (TATP). J Forensic Sci 31(3):1119–1125
17. Ember L (2005) Biochemist arrested. Chem Eng News 83:20
18. Miller C (2007) Quality and contamination control in an explosives testing laboratory. In American Chemical Society p NW-009 Abstracts 62nd Northwest Regional Meeting of the American Chemical Society Boise ID United States
19. Dunayevskiy I, Tsekoun A, Prasanna M, Go R, Patel CKN (2007) High-sensitivity detection of triacetone triperoxide (TATP) and its precursor acetone. Appl Opt 46(25):6397–6404
20. Mullen C, Huestis D, Coggiola M, Oser H (2006) Laser photoionization of triacetone triperoxide (TATP) by femtosecond and nanosecond laser pulses. Int J Mass Spectrom 252 (1):69–72
21. Oxley JC, Smith JL, Moran J, Nelson K, Utley WE (2004) Training dogs to detect Triacetone Triperoxide (TATP). In: Proc SPIE-Int Soc Opt Eng 5403(Pt 1, Sensors, and Command, Control Communications, and Intelligence (C31) Technologies for Homeland Security and Homeland Defense III), pp 349–353
22. Muller D, Levy A, Shelef R, Abramovich-Bar S, Sonenfeld D, Tamiri T (2004) Improved method for the detection of TATP after explosion. J Forensic Sci 49(5):935–938
23. Scintrex Trace Systems. E3500 Trace Detector, Detects Explosives http://www.scintrextrace.com/brochures/current/e3500.pdf
24. Synagen Guardian MS-ETD, Syagen Technology Inc, Guardian Explosives Trace Detection (ETD), California, CA, USA. www.syagen.com/uploads/pdfs/news
25. ACRO Security Technologies. Detect & Protect with ACRO_PET. www.acrosec.com
26. Itzhaky H, Keinan E (2004) Method and kit for the detection of explosives. US Patent 6767717
27. Nomadics (2008) Detection of peroxides and explosives. (Inventors: Deans R, Rose A, Bardon KM, Hancock LF, Swager TM) PCT/US2007/019248
28. Ladbeck RS, Kolla P, Karst U (2003) Trace analysis of peroxide-based explosives. Anal Chem 75:731
29. Sigman ME, Clark CD, Caiano T, Mullen R (2008) Analysis of triacetone triperoxide (TATP) and TATP synthetic intermediates by electrospray ionization mass spectrometry. Rapid Commun Mass Spectrom 22(2):84–90
30. Roman FR, Pena-Quevedo AJ, Rivera LA (2005) Analytical method development for trace detection of energetic acetone peroxides by GC-MS. American Chemical Society p ANYL-097 230th ACS National Meeting Washington DC United States 28 Aug–1 Sept
31. Buttigieg GA, Knight AK, Denson S, Pommier C, Bonner DM (2003) Characterization of the explosive triacetone triperoxide and detection by ion mobility spectrometry. Forensic Sci Int 135(1):53–59
32. Sella DS (2008) Self-immolative dendritic probe for direct detection of triacetone triperoxide. Chem Commu 44:5701–5703
33. Gaft M, Nagli M (2008) UV gated Raman spectroscopy for standoff detection of explosives. Opt Mater 30:1739–1746

34. Munoz RAA, Lu D, Cagan A, Wang J (2007) “One-step” simplified electrochemical sensing of TATP based on its acid treatment. Analyst 132(6):560–565
35. Banerjee S, Mohapatra SK, Misra M, Mishra IB (2009) The detection of improvised nonmilitary peroxide based explosives using a titania nanotube array sensor. Nanotechnology 20(7):075502/1–075502/6
36. Apblett AW, Kiran BP, Malka S, Materer NF, Piquette A (2006) Nanotechnology for neutralization of terrorist explosives. Ceram Trans 172(Ceramic Nanomaterials and Nanotechnologies IV), pp 29–35
37. Cotte-Rodriguez I, Hernandez-Soto H, Chen H, Cooks RG (2008) In situ trace detection of peroxide explosives by desorption electrospray ionization and desorption atmospheric pressure. Chem Ionization Anal Chem (Washington, DC, US) 80(5):1512–1519
38. Calculated using Advanced Chemistry Development (ACD/Labs) Software V904 for Solaris (1994–2008 ACD/Labs)
39. Canizo GN, Eyler GP (2007) Barreto, determination of the enthalpies of vaporization of cyclic organic peroxides by correlation of changes in gas chromatographic retention times. Chromato graphia 65:31–34
40. Oxley JC, Smith JL, Shinde K, Moran J (2005) Determination of the vapor density of triacetone triperoxide (TATP) using a gas chromatography headspace technique. Propellants Explos Pyrotech 30(2):127–130
41. Matyas R, Pachman J, Ang H-G (2008) Study of TATP: spontaneous transformation of TATP to DADP. Propellants Explos Pyrotech 33:89–91
42. Oxley JC, Smith JL, Brady J, Dubnikova F, Kosloff R, Zeiri L, Zeiri Y (2008) Raman and infrared fingerprint spectroscopy of peroxide-based explosives. Appl Spectrosc 62(8):906–915
43. Pacheco-Londono L, Primera OM, Ramirez M, Ruiz O, Hernandez-Rivera S (2005) Review of the various analytical techniques and algorithms for detection and quantification of TATP. In: Proc SPIE-Int Soc Opt Eng 5778(Pt 1, Sensors, and Command, Control, Communications, and Intelligence (C3I) Technologies for Homeland Defense IV), pp 317–326
44. Brauer B, Dubnikova F, Zeiri Y, Kosloff R, Gerber RB (2008) Vibrational spectroscopy of triacetone triperoxide (TATP): anharmonic fundamentals, overtones and combination bands. Spectrochim Acta A Mol Biomol Spectrosc 71(4):1438–1445
45. Hiyoshi RI, Nakamura J, Brill TB (2007) Thermal decomposition of organic peroxides TATP and HMTD by T-jump/FTIR spectroscopy. Propellants Explos Pyrotech 32(2):127–134
46. Mullen C, Huestis D, Coggiola M, Oser H (2006) Laser photoionization of triacetone triperoxide (TATP) by femtosecond and nanosecond laser pulses Int J Mass Spectrom 252 (1):69–72. doi: 101016/jijms200601018
47. Matyas R, Pachman J (2007) Thermal stability of triacetone triperoxide. Sci Technol Energ Mater 68(4):111–116
48. Armitt D, Zimmermann P, Ellis-Steinborner S (2008) Gas chromatography/mass spectrometry analysis of triacetone triperoxide (TATP) degradation products rapid. Commun Mass Spectrom 22(7):950–958
49. Bilusich D, Fitzgerald M, Armitt D, Ellis-Steinborner S (2008) 19th Intl Symp On the Forensic Sci 6–9 October. Melbourne, Australia
50. Hanson D (2006) Officercom. 4 June 2006 updated 8 July 2008
51. Matyas R, Selesovsky J (2009) Power of TATP based explosives. J Hazard Mater 165(1–3):95–99
52. Matyas R, Zeman S, Trzcinski W, Cudzilo S (2008) Detonation performance of TATP/AN-based explosives. Propellants Explos Pyrotech 33(4):296–300
53. Zeman S, Trzcinski WA, Matyas R (2008) Some properties of explosive mixtures containing peroxides Part I Relative performance and detonation of mixtures with triacetone triperoxide. J Hazard Mater 154(1–3):192–198
54. Menning D, Ostmark H (2008) In: Schubert H, Kuznstov A (eds) Detection of Liquid Explosives and Flammable Agents in Connection with Terrorism. Springer, pp 55–70

55. Fidler R, Legron T, Carvalho-Knighton K, Geiger CL, Sigman ME, Clausen CA (2009) Degradation of TNT, RDX, and TATP using microscale mechanically alloyed bimetals. In: ACS Symp Ser 1027(Environmental Applications of Nanoscale and Microscale Reactive Metal Particles), pp 117–134
56. Bellamy AJ (1999) Triacetone triperoxide: its chemical destruction. J Forensic Sci 44 (3):603–608

Additional Scholarly Articles for Further Reading

57. Baconin J, Aveille J, Zoe J (1984) Experimental study of the spherical diverging detonation. In: Proc Symp Explos Pyrotech 12th, pp 1/71–1/76
58. Bailey A, Bellerby JM, Kinloch SA (1992) The identification of bonding agents for TATB/HTPB polymer bonded explosives. Philos Trans R Soc London, Ser A 339(1654):321–333
59. Belcher I, Drake RC, Fleming KA, Roberts RH (1991) Thermal modeling of confined explosive systems. Int Annu Conf ICT 22nd (Combust React Kinet), pp 9/1–9/11
60. Belmas R, Plotard JP (1995) Physical origin of hot spots in pressed explosive compositions. J Phys IV 5(C4, Approaches Microscopique et Macroscopique des Detonations), pp 61–87 doi: 10.1051/jp4:1995406
61. Benziger TM (1981) Manufacture of triaminotrinitrobenzene. Int Jahrestag—Fraunhofer-Inst Treib- Explosivst(Chem Mech Technol Treib-Explosivst), pp 491–503
62. Billon HH (1994) The rheology of a high-concentration triaminotrinitrobenzene/trinitrotoluene (TATB/TNT) suspension. Propellants Explos Pyrotech 19(5):245–248. doi:10.1002/prep.19940190506
63. Blais NC, Greiner NR, Fernandez WJ (1990) Detonation chemistry studies of energetic materials using laboratory scale samples. NATO ASI Ser, Ser C 309(Chem Phys Energ Mater), pp 477–509
64. Brasher CL (1981) TATB synthesis: processes, problems and progress. Tech Bull—Tex Eng Exp Stn 81–1:34–46
65. Breithaupt D, Kury J, McGuire R, Hallam J (1991) The extent of reaction of aluminum and ammonium perchlorate in TATB-containing explosives. Int Annu Conf ICT 22nd (Combust React Kinet), pp 6/1–6/7
66. Britt AD, Moniz WB, Chingas GC, Moore DW, Heller CA, Ko CL (1981) Free radicals of TATB (1,3,5-triamino-2,4,6-trinitrobenzene). Propellants Explos 6(4):94–95
67. Cady HH (1986) Microstructural differences in TATB that result from manufacturing techniques. Int Jahrestag—Fraunhofer-Inst Treib—Explosivst 17th (Anal Propellants Explos: Chem Phys Methods), pp 53/1–53/14
68. Catalano E, Rolon CE (1983) A study of the thermal decomposition of confined triaminotrinitrobenzene. The gaseous products and kinetics of evolution. Thermochim Acta 61(1–2):37–51. doi:10.1016/0040-6031(83)80302-5
69. Chaykovsky M, Adolph HG (1990) Synthesis and properties of some trisubstituted trinitrobenzenes. TATB analogs J Energ Mater 8(5):392–414. doi:10.1080/07370659008225431
70. Cherin H, Lemoine D, Gautier L (1996) Sensitivity to projectile impact of pre-heated explosive compositions. Int Annu Conf ICT 27th(Energetic Materials), pp 36.1–36.9
71. Cherin H, Lemoine D, Pauton M (1994) Sensitization by damage of explosive compositions. Int Annu Conf ICT 25th (Energetic Materials-Analysis, Characterization and Test Techniques), pp 101/1–101/9
72. Chisum ME (1991) Applications of negative ion analyses on the ELAN 250 ICP-MS. At Spectrosc 12(5):155–159
73. Cochran SG, Tarver CM (1984) Modeling particle size and initial temperature effects on shock initiation of TATB-based explosives. North-Holland, pp 593–596

74. Cortili G, Zerbi G (1967) Chain conformations of poly(vinylidene fluoride) as derived from its vibrational spectrum. Spectrochim Acta 23A(2):285–299
75. Delistraty J, Brandt H (1982) Detonation properties of 1,3,5-triamino-2,4,6-trinitrobenzene when impacted by hypervelocity projectiles. Propellants Explos Pyrotech 7(5):113–122. doi:10.1002/prep.19820070502
76. Dick JJ (1987) Short pulse initiation of plastic-bonded TATB explosive. J Energ Mater 5(3–4):267–285. doi:10.1080/07370658708012355
77. Dick JJ, Forest CA, Ramsay JB, Seitz WL (1988) The Hugoniot and shock sensitivity of a plastic-bonded TATB explosive PBX 9502. J Appl Phys 63(10):4881–4888. doi:10.1063/1.340428
78. Doherty RM, Short JM, Kamlet MJ (1989) Improved prediction of cylinder test energies. Combust Flame 76(3–4):297–306. doi:10.1016/0010-2180(89)90112-0
79. Doherty RM, Simpson RL (1997) A comparative evaluation of several insensitive high explosives. Int Annu Conf ICT 28th (Combustion and Detonation), pp 32.1–32.23
80. Duraes L, Campos J, Gois JC (1995) Deflagration and detonation predictions using a new equation of state. Int Annu Conf ICT 26th (Pyrotechnics), pp 67/1–67/13
81. Estes Z (1977) Summary of chlorine free synthesis of TATB. Process Development Endeavor No. 106. Mason and Hanger-Silas Mason Co., Inc., p 5
82. Firsich DW, Guse MP (1984) On the photochemical phenomenon in TATB. J Energ Mater 2 (3):205–214. doi:10.1080/07370658408012334
83. Foltz MF (1993) Pressure dependence of the reaction propagation rate of TATB at high pressure. Propellants Explos Pyrotech 18(4):210–216
84. Foltz MF, Ornellas DL, Pagoria PF, Mitchell AR (1996) Recrystallization and solubility of 1,3,5-triamino-2,4,6-trinitrobenzene in dimethyl sulfoxide. J Mater Sci 31(7):1893–1901. doi:10.1007/BF00372205
85. Fried LE, Ruggiero AJ (1994) Energy Transfer Rates in Primary, Secondary, and Insensitive Explosives. J Phys Chem 98(39):9786–9791. doi:10.1021/j100090a012
86. Fried LE, Souers PC (1996) BKWC: an empirical BKW parametrization based on cylinder test data. Propellants, Explos, Pyrotech 21(4):215–223. doi:10.1002/prep.19960210411
87. Fried LE, Tarver C (1996) Molecular dynamics simulation of shocks in porous TATB crystals. AIP Conf Proc 370 (Pt. 1, Shock Compression of Condensed Matter–1995), pp 179–182
88. Glazkova AP, Kazarova JA (1992) About self-inhibition in deflagration of 1,3,5-triamino-2,4,6-trinitrobenzene (TATB). Int Annu Conf ICT 23rd (Waste Manage. Energ. Mater. Polym.), pp 67/1–67/9
89. Greiner NR, Phillips DS, Johnson JD, Volk F (1988) Diamonds in detonation soot. Nature (London) 333(6172):440–442. doi:10.1038/333440a0
90. Gubin SA, Odintsov VV, Pepekin VI (1991) Thermodynamic calculations of detonation parameters. In: Proc Int Pyrotech Semin 16th, pp 325–335
91. Hadhoud MK, Shokry SA, El Morsi AK, Ragab S (1986) Study of kinetics and analysis of the amination of pentanitroaniline to produce TATB. Int Jahrestag—Fraunhofer-Inst Treib—Explosivst 17th (Anal Propellants Explos: Chem Phys Methods), pp 54/1–54/19
92. Harris BW (1985) TATB—strong basic reactions provide soluble derivatives for a simple, qualitative high explosive spot test. J Energ Mater 3(2):81–93. doi:10.1080/07370658508012336
93. Hertzberg M, Cashdollar KL, Zlochower IA, Green GM (1992) Explosives dust cloud combustion. Symp (Int) Combust, [Proc] 24th, pp 1837–43 doi: 10.1016/S0082-0784(06)80215-8
94. Hoffman DM, Matthews FM, Pruneda CO (1989) Dynamic mechanical and thermal analysis of crystallinity development in Kel-F 800 and TATB/Kel-F 800 plastic bonded explosives. Part I. Kel-F 800. Thermochim Acta 156(2):365–372. doi:10.1016/0040-6031(89)87203-X
95. Hua P (1995) Energy depression coefficients of TATB and other components. China Ordnance Society, pp 377–381

96. Hutchinson CD (1988) The initiation of TATB-based insensitive high explosives in diverging geometry. Int Annu Conf ICT 19th (Combust Detonation Phenom), pp 38/1–38/10
97. Kennedy DL (1995) The challenge of non-ideal detonation. J Phys IV 5 (C4, Approches Microscopique et Macroscopique des Detonations), pp 191–207 doi: 10.1051/jp4:1995417
98. Kolb JR, Rizzo HF (1979) Growth of 1,3,5-triamino-2,4,6-trinitrobenzene (TATB). I. Anisotropic thermal expansion Propellants Explos 4(1):10–16
99. Kunz AB (1996) Ab initio investigation of the structure and electronic properties of the energetic solids TATB and RDX. Phys Rev B: Condens Matter 53(15):9733–9738
100. Larson TE, Dimas P, Hannaford CE (1991) Electrostatic sensitivity testing of explosives at Los Alamos. Inst Phys Conf Ser 118 (Electrostatics 1991), pp 107–17
101. Loughran ED, Wewerka EM, Rogers RN, Berlin JK (1975) The influence of metals on the thermal decomposition of s-triaminotrinitrobenzene (TATB). Am. Def. Prep. Assoc., p I-E, 4 p
102. Loughran ED, Wewerka EM, Rogers RN, Berlin JK (1977) The influence of metals on the thermal decomposition of s-triaminotrinitrobenzene (TATB). Inst Chem Treib—Explos, pp 233–247
103. Mader C, Kershner JD (1992) Numerical modeling of the effect of temperature and particle size on shock initiation properties of HMX and TATB. J Energ Mater 10(2–3):69–95. doi:10.1080/07370659208018230
104. Mader CL (1996) Detonation performance. Nova Science Publishers, pp 165–249
105. Maienschein JL, Nichols AL III, Wardell JF (1995) Reactions of TATB-based explosive with molten metal. Propellants Explos Pyrotech 20(6):287–293. doi:10.1002/prep.19950200602
106. Makashir PS, Kurian EM (1996) Spectroscopic and thermal studies on the decomposition of 1,3,5-triamino-2,4,6-trinitrobenzene (TATB). J Therm Anal 46(1):225–236. doi:10.1007/BF01979963
107. Mal'kov IY, Titov VM (1995) The regimes of diamond formation under detonation. Elsevier, pp 666–669
108. Marcus Y (1987) The thermodynamics of solvation of ions. Part 2. The enthalpy of hydration at 298.15 K. J Chem Soc, Faraday Trans 1 83(2):339–349 doi: 10.1039/f19878300339
109. Marcus Y (1987) The thermodynamics of solvation of ions. Part 4. Application of the tetraphenylarsonium tetraphenylborate (TATB) extrathermodynamic assumption to the hydration of ions and to properties of hydrated ions. J Chem Soc, Faraday Trans 1 83(9):2985–2992 doi: 10.1039/f19878302985
110. Martz HE, Schneberk DJ, Roberson GP, Azevedo SG, Lynch SK (1991) Computerized tomography of high explosives. Plenum, pp 187–195
111. Miles MH, Gustaveson D, Devries KL (1983) Stress-induced radical generation in TATB. J Mater Sci 18(11):3243–3248. doi:10.1007/BF00544148
112. Mitchell AR, Pagoria PF, Schmidt RD (1996) A new synthesis of TATB using inexpensive starting materials and mild reaction conditions. Int Annu Conf ICT 27th (Energetic Materials), pp 29.1–29.11
113. Morozov VG, et al. (1994) Experimentally proved numerical modeling of detonation ignition and development in TATB-based HE in terms of desensitization by shock and detonation waves interaction. Proc Int Pyrotech Semin 20th, pp 701–717
114. Oestmark H (1996) Shock induced sub-detonation chemical reactions in 1,3,5-triamino-2,4,6-trinitrobenzene. AIP Conf Proc 370 (Pt. 2, Shock Compression of Condensed Matter–1995), pp 871–874
115. Oestmark H, Bergman H, Aaqvist G, Langlet A, Persson B (1991) Decomposition of NTO: some initial observations. Proc Int Pyrotech Semin 16th, pp 874–886
116. Oxley JC, Smith JL, Wang W (1994) Compatibility of Ammonium Nitrate with Monomolecular Explosives 1. J Phys Chem 98(14):3893–3900. doi:10.1021/j100065a053
117. Oxley JC, Smith JL, Wang W (1994) Compatibility of Ammonium Nitrate with Monomolecular Explosives. 2. Nitroarenes. J Phys Chem 98(14):3901–3907. doi:10.1021/j100065a054

118. Pertuis C, Marteau D, Gautier L, Cherin H, Paillard C, Dupre G (1997) Reactivity of a TATB-based explosive composition after mechanical damage. Int Annu Conf ICT 28th (Combustion and Detonation), pp 15.1–15.13
119. Piunti RL, Brower KR (1995) Thermolysis of various energetic substances by exposure to adiabatically compressed gas. J Energ Mater 13(1–2):107–139. doi:10.1080/07370659508019346
120. Plaksin IY, Gerasimenko VF, Shutov VI, Gerasimov VM (1996) On sensitivity of TATB-based shock wave damaged explosive. Int Annu Conf ICT 27th (Energetic Materials), pp 141.1–141.13
121. Plaksin IY, et al. (1996) Evolution of explosion in TATB HE in the process of its expansion into a free space followed by impact against hard barrier. AIP Conf Proc 370 (Pt. 2, Shock Compression of Condensed Matter–1995), pp 875–878
122. Pritchard RH (1976) Compatibility of TATB PBX with weapons materials. Am Def Prep Assoc, p III-A, 10 p
123. Pruneda CO, McGuire RR, Clements RE (1990) Development of a high-tensile-strain plastic-bonded TATB explosive. Int Annu Conf ICT 21st (Technol Polym Compd Energ Mater), pp 99/1–99/9
124. Ray SK, Sarkar S, Sinha S, Kundu KK (1994) Single-ion transfer energetics of some ions based on TATB assumption in aqueous mixtures of N, N-dimethylformamide. Indian J Chem Sect A: Inorg Bio-inorg Phys Theor Anal Chem 33A(9):805–815
125. Rigdon LP, Stephens FB, Harrar JE (1983) Precise assay of TATB by the determination of total amino and nitro functional groups. Propellants Explos Pyrotech 8(6):206–211. doi:10.1002/prep.830080607
126. Rivera T, Matuszak ML (1983) Surface properties of potential plastic-bonded explosives (PBX). J Colloid Interface Sci 93(1):105–108. doi:10.1016/0021-9797(83)90389-2
127. Rizzo HF, Humphrey JR, Kolb JR (1981) Growth of 1,3,5-triamino-2,4,6-trinitrobenzene (TATB). II. Control of growth by use of high Tg polymeric binders. Propellants Explos 6 (2):27–36
128. Rizzo HF, Humphrey JR, Kolb JR (1981) Growth of 1,3,5-triamino-2,4,6-trinitrobenzene (TATB). II. Control of growth by use of high-Tg polymeric binders. Propellants Explos 6 (3):57–62
129. Rosen JM, Dickinson C (1969) Vapor pressures and heats of sublimation of some high-melting organic explosives. J Chem Eng Data 14(1):120–124. doi:10.1021/je60040a044
130. Seitz WL (1984) Short-duration shock initiation of triaminotrinitrobenzene (TATB). North-Holland, pp 531–534
131. Sewell TD (1996) Monte Carlo simulations of crystalline TATB. Mater Res Soc Symp Proc 418 (Decomposition, Combustion, and Detonation Chemistry of Energetic Materials), pp 67–72
132. Sharma J, et al. (1984) Comparative study of molecular fragmentation in sub-initiated TATB caused by impact, UV, heat and electron beams. North-Holland, pp 543–546
133. Shlensky OF (1994) Vainshtein EF Prespinodal thermal decomposition of highly energetic materials, vol 2. Russian Section of the Combustion Institute, pp 466–468
134. Shokry SA, Shawki SM, Elmorsi AK (1990) TATB plastic-bonded compositions. Int Annu Conf ICT 21st (Technol Polym Compd Energ Mater), pp 100/1–100/16
135. Shorohov EV, Litvinov BV (1992) Shock compressibility of the TATB-based explosive composition in the pressure range from 0.1 to 40 GPa. Oxford & IBH, pp 866–868
136. Shorohov EV, Litvinov BV (1995) Hugoniot adiabate of plasticized TATB-based explosive compositions, vol 3, pp 295–298. Springer
137. Simpson RL, Pagoria PF, Mitchell AR, Coon CL (1994) Synthesis, properties and performance of the high explosive ANTA. Propellants Explos Pyrotech 19(4):174–179. doi:10.1002/prep.19940190405

138. Sinha S, Rudra S, Kundu KK (1993) Transfer energetics of some ions based on TATB assumption in some quasi-isodielectric ethylene carbonate + water mixtures. Indian J Chem Sect A: Inorg Bio-inorg Phys Theor Anal Chem 32A(1):1–11
139. Stolovy A, Jones EC Jr, Aviles JB Jr, Namenson AI, Fraser WA (1983) Exothermic reactions in TATB initiated by an electron beam. J Chem Phys 78(1):229–235. doi:10.1063/1.444545
140. Talukdar H, Kundu KK (1992) Transfer energetics of tetraalkylammonium ions in aquo-organic systems and the solvent effect on hydrophobic hydration. J Phys Chem 96 (2):970–975. doi:10.1021/j100181a078
141. Tarver CM (1990) Modeling shock initiation and detonation divergence tests on TATB-based explosives. Propellants Explos Pyrotech 15(4):132–142. doi:10.1002/prep.19900150404
142. Tarver CM (1992) The structure of detonation waves in solid explosives. North-Holland, pp 311–315
143. Tarver CM, Hoffman DM, Urtiew PA, Tao WC (1996) Shock initiation of TATB/FEFO formulations. J Energ Mater 14(3–4):217–256. doi:10.1080/07370659608216066
144. Tarver CM, Kury JW, Breithaupt RD (1997) Detonation waves in triaminotrinitrobenzene. J Appl Phys 82(8):3771–3782. doi:10.1063/1.365739
145. Trott WM, Renlund AM (1988) Single-pulse Raman scattering study of triaminotrinitrobenzene under shock compression. J Phys Chem 92(21):5921–5925. doi:10.1021/j100332a015
146. Trott WM, Renlund AM, Jungst RG (1985) Single-pulse Raman and photoacoustic spectroscopy studies of triaminotrinitrobenzene (TATB) and related compounds. Proc SPIE-Int Soc Opt Eng 540(Proc Southwest Conf Opt), pp 368–375 doi: 10.1117/12.976139
147. Upadhye RS, Watkins BE, Pruneda CO (1996) Recent advances in the molten salt technology for the destruction of energetic materials. Int Annu Conf ICT 27th (Energetic Materials), pp 110.1–110.13
148. Urbanski T, Vasudeva SK (1978) Heat resistant explosives. J Sci Ind Res 37(5):250–255
149. Urtiew PA, Tarver CM, Simpson RL (1996) Shock initiation of 2,4-dinitroimidazole (2,4-DNI). AIP Conf Proc 370 (Pt. 2, Shock Compression of Condensed Matter–1995), pp 887–890
150. Varghese AV, Kalidas C, Singh P, Hefter G (1995) Gibbs transfer energies and solvent transport numbers of some copper(II) salts in methanol-dimethylformamide mixtures. Aust J Chem 48(5):987–996. doi:10.1071/CH9950987
151. Volk F (1988) Detonation products of cast high explosives. Proc Int Pyrotech Semin 13th, pp 835–851
152. Von Holtz E, Scribner K, Moody G, McGuire R (1990) The search for high-energy low-vulnerability explosives. Int Annu Conf ICT 21st (Technol Polym Compd Energ Mater), pp 12/1–12/9
153. Walker FE (1994) A new kinetics and the simplicity of detonation. Propellants Explos Pyrotech 19(6):315–326. doi:10.1002/prep.19940190610
154. Wang Z, Chen Z (1991) Deflagration to detonation transition (DDT) study in mixed HMX bed. Int Annu Conf ICT 22nd (Combust React Kinet), pp 91/1–91/10
155. Ward RL, Felver T, Pyper JW (1984) Bound and free moisture in explosives and plastics. J Hazard Mater 9(1):69–76. doi:10.1016/0304-3894(84)80008-4
156. Zhang SQ, Wei YZ, Fang Q, Zhao F (1997) Detonation behavior of a TATB-based IHE. Int Annu Conf ICT 28th (Combustion and Detonation), pp 76.1–76.11

Chapter 11
1,3,3-Trinitroazetidine (TNAZ)

Abstract 1,3,3-Trinitroazetidine (Molecular Formula: $C_3H_4N_4O_6$, TNAZ) has been assessed as a potential high energy replacement for TNT. Australian industrial plant is a melt-castable explosive that has been proposed as a potential replacement for TNT. The structure of the compound has been confirmed by IR, NMR, mass, elemental analysis and by X-ray crystallography. HPLC technique has been employed to confirm the purity of TNAZ (>99%). The compound is further characterized by thermal techniques and is found to undergo limited decomposition at its melting point. Small scale sensitivity tests have also been carried out and the results show that TNAZ is significantly more sensitive to mechanical stimuli than TNT.

11.1 Introduction

The thermophysical properties of 1,3,3-trinitroazetidine, commonly known as TNAZ are included in this chapter. TNAZ is a four-membered ring high density explosive with several desirable properties compared to the conventional explosives RDX and HMX. It is a white crystalline melt-castable energetic material with performance similar to HMX. It was first synthesized by Archibald et al. [1]. It is 30% more energetic than TNT and 10% more than nitramines such as RDX and HMX [2]. The spectra of TNAZ and ideal gas thermodynamic properties have been evaluated [3].

11.2 Synthesis

As mentioned earlier, the first synthesis of TNAZ was accomplished by Archibald and Baum [1]. In spite of the fact that TNAZ is a simple molecule, its synthesis has not proved easy by any means. The first process is the Fluorochem Process which is described fully by Watt and Cliff [4]. A second process was developed at the University of Florida by Katritzky et al. [5]. The major disadvantage of these two processes in the use of epichlorohydrin was eliminated in the process developed by Marchand et al. [6]. At the same time, Los Alamos National Laboratory developed

D.S. Viswanath et al., *Emerging Energetic Materials: Synthesis, Physicochemical, and Detonation Properties*, https://doi.org/10.1007/978-94-024-1201-7_11

another process [7, 8]. Two of these processes have been scaled up to make close to 1000 lb batches of TNAZ. A pilot plant has been successfully demonstrated. Agrawal and Hogdson [9] summarize the Archibald et al., Marchand et al., and Axenrod et al. [10] processes for the synthesis of TNAZ. Jadhav et al. [11] describe a process involving cyclization of 1,3-dichloro-2,2-dinitropropane, and obtained yields of 30%. A recent review of the synthesis and properties is provided by Stepanova and Stepanova [12].

Table 11.1 lists the chemical names of TNAZ, and Table 11.2 lists physical properties.

Solubility in different solvents is provided by Watt and Cliff [4] and shown in Table 11.3. However the authors have not specified the temperature for these values.

11.3 Phase Diagrams

McKenney et al. [20] report TNAZ/TNT binary phase diagram calculated using enthalpy of fusion and melting points data. They used the simple relation

$$R\ln X = \Delta H_{fus}[(1/T)-(1/T_0)]$$

where T is the melting point [K] of the eutectic, ΔH_{fus}, T_0, and X are enthalpy of fusion, melting point, and mole fraction of either TNAZ or TNT, and R is the gas constant. Table 11.4 lists the composition and the corresponding temperatures of the eutectics of TNAZ/TNT.

Figure 11.1 shows data for two eutectics whose composition-temperature data and other details are provided in their report. Eutectics with other energetic materials, HMX, Tetryl, and TNT [14] are listed in Table 11.5.

Table 11.1 Chemical names of TNAZ

Properties	Literature values	References
Formula	$C_3H_4N_4O_6$	
CA index name	Azetidine, 1,3,3-trinitro-, TNAZ	
CAS number	97645-24-4	
Structural formula	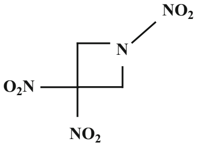	
Molecular mass	192	

Table 11.2 Physical properties of TNAZ

Melting point (K)	Amber-SRT: 390 Amber calculated: 462	[2]
Melting point (K)	373.74 ± 0.21 (100.59 ± 0.21 °C) Experimental. 374.74 (101 °C)	[13] [14]
Boiling point (K)	525.15 (252 °C)	[14]
Stable up to (K)	513.15 (240 °C)	[2]
Density (kg/m^3)	1860 (1.86 g/cm^3) 1840 (1.84 g/cm^3)	[2] [14]
Melting point (K)	374	[2]
Ionization potential (eV)	10.36 ± 0.1	[15]
Enthalpy of sublimation (kJ/mol)	95 63.22	[16] [14]
Enthalpy of vaporization (kJ/mol)	66	[14]
Enthalpy of formation (kcal/mol)	30.7 8.7 and 2.81 8.7 30.7	[15] [17] [16] [18]
Enthalpy of fusion (kcal/mol)	6.714 ± 0.115 6.7–7.2	[19] [15]
C-J pressure (GPa)	35.68	[18]
C-J energy (kJ/cc)	4.38	[18]
C-J temperature (K)	4659	[18]
C-J shock velocity (m/µs)	8.95	[18]
E total of detonation (kJ/cc)	11.06	[18]
Enthalpy of explosion (cal/g)	1731	[17]
Detonation velocity (m/s)	9597	[17]

Table 11.3 Solubility in different solvents

Solvent	Solubility (g/mL)
Ethyl acetate	0.436
Ethanol	0.055
Isopropanol	0.026
Acetone	0.442
Toluene	0.038
Iso-octane	0.014

11.4 Thermodynamic Properties

Ideal Gas Thermodynamic Properties at 1 bar [3] Made IR assignments and calculated equilibrium composition and compared some experimental data.

The quantities of Cp_o, S_o and ΔH_{To} were fitted in the following (NASA type) polynomials:

Table 11.4 Mol percent and calculated temperatures for the TNAZ/TNT system [20]

Mole % TNAZ	Temperature (K) (°C)
0.0	354.15 (81.0)
4.7	351.85 (78.7)
11.6	348.25 (75.1)
23.5	341.45 (68.3)
34.2	334.75 (61.6)
34.5	334.55 (61.4) (Eutectic point)
38.9	338.55 (65.4)
44.1	342.85 (69.7)
54.2	350.25 (77.1)
68.7	359.05 (85.9)
81.6	365.75 (92.6)
96.6	372.55 (99.4)
100.0	373.95 (100.8)

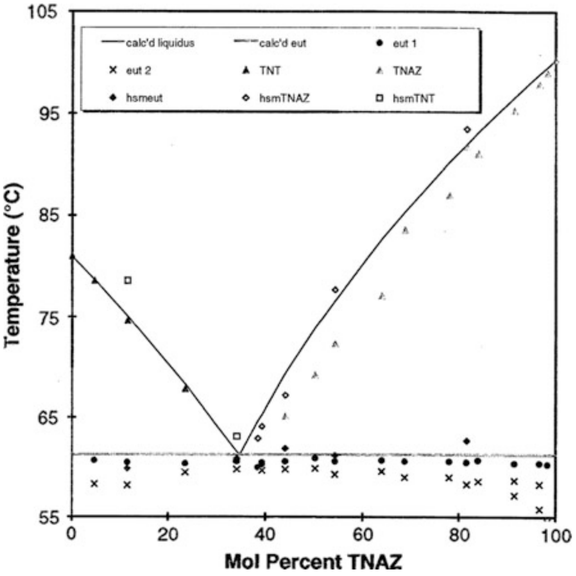

Fig. 11.1 Experimental and calculated phase diagram for TNAZ/TNT system [20] (hsm indicates Hot Stage Microscopy. Eu is eutectic.)

Table 11.5 Eutectic mixture composition and temperature

Additive	M.P of additive (K) (°C)	M.P. of eutectic (K) (°C)	TNAZ (mole %)
TNT	353.75 (80.6)	333.15 (60.0)	63.3–65.0
Tetryl	402.65 (129.5)	354.65–354.66 (81.5–81.6)	63.3–65.0
HMX	557.25 (284.1)	369.05 (95.9)	97.9

$$\frac{C_{po}}{R} = a1 + a2\,T + a3\,T^2 + a4\,T^3 + a5\,T^4$$

$$\frac{S_o}{R} = a1\,\ell n T + a2\,T + a3\,\frac{T^2}{2} + a4\,\frac{T^3}{3} + a5\,\frac{T^4}{4} + a7$$

$$\frac{\Delta H_{T_o}}{RT} = a1 + a2\,\frac{T}{2} + a3\,\frac{T^2}{3} + a4\,\frac{T^3}{4} + a5\,\frac{T^4}{5} + \frac{a6}{T}$$

where a1, *a2, a3, a4, a5, a6, a7* are the polynomial coefficients, *R* is universal gas constant and temperature in K.

Table 11.6 lists the ideal gas thermodynamic properties calculated by Yu et al. [3].

Table 11.7 summarizes the coefficients for the thermochemical relations shown above. Table 11.8 list ideal gas heat capacity and entropy calculated by Osmont et al. [21] using Ab initio quantum technique.

Table 11.6 Ideal gas thermodynamic properties for TNAZ at 1 bar [3]

T(K)	C°p J K^{-1} mol^{-1}	S°	$-(G^\circ - H^\circ_{298})/T$	$(H - H^\circ_{298})$ ($kJmol^{-1}$)	$\Delta_l H^0$	$\Delta_l G^0$	$\log_{10} k_f$
0	0.000	0.000	0.000	−20.954	170.971	170.911	00
100	47.963	273.233	442.763	−16.953	154.278	231.340	−120.83
200	83.151	315.355	368.737	−10.676	139.633	314.261	−82.075
298.15	134.990	358.096	358.096	0.000	128.449	402.491	−70.514
300	135.973	358.934	358.099	0.251	128.275	−404.193	−70.375
400	185.668	405.043	364.049	16.398	120.795	497.396	−64.952
500	226.313	451.018	376.865	37.076	116.592	592.092	−61.854
600	258.057	495.208	392.938	61.362	114.840	687.390	−59.842
700	282.708	536.918	410.558	88.452	114.883	782.833	−58.415
800	302.046	575.981	428.822	117.727	116.264	878.176	−57.338
900	317.431	612.479	447.224	148.730	118.641	973.275	−56.486
1000	329.844	646.588	465.474	181.115	121.784	1068.072	−55.789
1100	339.982	678.517	483.406	214.623	125.510	1162.527	55.203
1200	348.353	708.469	500.926	249.052	129.686	1256.619	54.698
1300	355.332	736.637	517.985	284.247	134.205	1350.351	54.257
1400	361.200	763.191	534.561	320.082	138.987	1443.727	53.865
1500	366.172	788.285	550.647	356.457	143.960	1536.747	53.513

Table 11.7 Coefficients of polynomials for ideal gas properties, specific heat, entropy and enthalpy

Temp. (K)	a_1	a_2	a_3	a_4	a_5	a_6	a_7
1000–5000	2.228e1	2.662e-2	−1.0795e-5	1.990e-9	−1.375e-13	4.792e3	−9.799e1
298–1000	−4.374	7.087e-2	1.773e-5	−8.906e-8	4.458e-11	1.360e4	4.6786e1

Table 11.8 Ideal gas heat capacity and entropy [22]

T (K)	300	400	500	600	800	1000	1500
Cp_o (cal mol^{-1} K^{-1})	42.4	52.1	60.0	66.3	75.1	80.8	88.4
T (K)	2000	2500	3000	3500	4000	4500	5000
Cp_o (cal mol^{-1} K^{-1})	91.9	93.7	94.8	95.4	95.9	96.2	96.4
T (K)	300	400	500	600	800	1000	1500
S_o,(cal mol^{-1} K^{-1})	109.8	123.4	135.9	147.5	167.8	185.3	219.7
T (K)	2000	2500	3000	3500	4000	4500	5000
S_o (cal mol^{-1} K^{-1})	245.6	266.4	283.6	298.2	311.0	322.3	332.4

11.5 Thermal Decomposition/Dissociation

Alavi et al. [18] made theoretical calculations on the thermal decomposition of TNAZ and, present pathways and rate of decomposition equations. A detailed description of the initial dissociation processes in TNAZ carried out by Photofrag-mentation Translational Spectroscopy can be found elsewhere [23]. Yu et al. [3] studied the thermal decomposition in a shock-tube at around 405 K and 500 torr pressure and determined the composition of the products of decomposition by spectroscopy. They provide spectra and equilibrium composition of the products of degradation.

To understand the environmental impact due to manufacture, storage, and use at different sites, it is essential to know the stability of TNAZ in soil. Jenkins et al. [22] carried out such stability studies of several energetic materials including TNAZ. Their work showed that the half-life in soil is less than 24 h for different soils. Table 11.9 some more properties evaluated by Advanced Chemistry Development (ACD/Labs) Software V8.14 for Solaris.

Table 11.9 Other properties calculated and not listed above [24]

Bioconcentration factor	1.0 pH 1 to pH 10	Temp, K: 298.15 (25 °C)
Flash point	543.65 ± 30.1 (270.5 ± 30.1 °C)	Freely rotatable bonds, 3
H acceptors	10	
H donors	0	
H donor/acceptor sum	10	
Koc	33.7	pH 1 and Temp, K: 298.15 (25 °C)
logP	0.277 ± 0.663	Temp, K: 298.15 (25 °C)
Mass intrinsic solubility 1.1 g/L	Slightly soluble	Temp, 25 K: 298.15 (25 °C)
Molar intrinsic solubility	5.8^{-3} (mol/L), Sparingly soluble	Temp, K: 298.15 (25 °C)
Molar volume	104.3 ± 5.0 (cm^3/mol)	Temp, 293.15 (20 °C), Press: 760 Torr
Molecular weight	192.09	
pKa	−15.72 ± 0.20	Most Basic, K: 298.15 (25 °C)
Polar surface area	141 A2	
Vapor pressure	4.64 × 10^{-11} Torr	Temp, K: 298.15 (25 °C)

References

1. Archibald TG, Gilardi R, Baum K, George C (1990) Synthesis and x-ray crystal structure of 1,3,3-trinitroazetidine. J Org Chem 55(9):2920–2924
2. Agrawal PM, Rice BM, Zheng L, Velardez GF, Thompson DL (2006) Molecular dynamics simulations of the melting of 1,3,3-Trinitroazetidine. J Phys Chem B 110(11):5721–5726
3. Yu C-L, Zhang Y-X, Bauer SH (1998) Estimation of the equilibrium distribution of products generated during high temperature pyrolyses of 1,3,3-trinitroazetidine; thermochemical parameters. J Mol Structure (Theochem) 432:63–68
4. Watt DS, Cliff MD (1998) TNAZ based melt-cast explosives: technology review and AMRL Research Directions, DSTO Aeronautical and Maritime Research Laboratory, AR-010-600, July 1998
5. Katritzky AR, Cundy DJ, Chen J (1994) Novel syntheses of 1,3,3-trinitroazetidine. J Heterocycl Chem 31(2):271–275
6. Marchand AP, Rajagopal D, Bott SG, Archibald TG (1995) A novel approach to the synthesis of 1,3,3-trinitroazetidine. J Org Chem 60(15):4943–4946
7. Coburn MD, Hiskey MA, Archibald TG (1998) Scale-up and waste-minimization of the Los Alamos process for 1,3,3-trinitroazetidine (TNAZ). Waste Manage (Oxford) 17(2/3):143–146
8. Nissan R, Ruppert W (2005) More than a decade of green energetics R&D research. Joint Services Environmental Management Conference Columbus, OH, US. Army RDECOM/ Hughes Assoc. INC
9. Axenrod T, Watnick C, Yazdekhasti H, Dave PR (1993) Synthesis of 1,3,3-trinitroazetidine. Tetrahedron Lett 34(42):6677–6680
10. Agrawal JP, Hogdson RD (2007) Organic chemistry of explosives. Wiley, New York, NY, pp 265–269
11. Jadhav HS, Talawar MB, Dhavale DD, Asthana SN, Krishnamurthy VN (2006) Alternate method for synthesis of 1,3,3-trinitroazetidine (TNAZ): next generation melt-castable high-energy material. Indian J Chem Technol 13(1):41–46
12. Stepanova EV, Stepanova AI (2015) Synthesis and properties of 1,3,3-trinitroazetidine, 58 (11):3–15
13. Sućeska M, Rajić M, Mateĉić-Muśyanić S, Zeman S, Jalovŷ Z (2003) Kinetics and heats of sublimation and evaporation of 1,3,3-trinitroazetidine (TNAZ). J Therm Anal Calorim 74 (3):853–866
14. Akhavan J (2004) Chemistry of explosives. 2nd edn. RSC Paperbacks, Cambridge, UK, p 47
15. Politzer P, Lane ME, Concha MC, Redfern PC (1995) Comparative computational analysis of some nitramine and difluoramine structures, dissociation energies and heats of formation. J Mol Struct (Theochem) 338(1–3):249–255
16. Garland NL, McElvany SW (1998) Ionization potentials of TNAZ and its decomposition products. Chem Phys Lett 297:147–153
17. Simpson RL, Garza RG, Foltz MF, Ornellas DL, Urtiew PA (1994) Characterisation of TNAZ. UCRL-ID-119672, Lawerence Livermore National Laboratory
18. Dewey MA, Blau RJ, Doll DW, Lee KE, Braithwaite PC (2003) ARDEC explosives development: melt/pour explosives containing TNAZ. Thiokol Corporation. In: Insensitive munitions & energetic materials technology symposium, March 10–13, 2003. Orlando, FL
19. Liu M-H, Chen C, Hong Y-S (2005) Theoretical study of the unimolecular decomposition mechanisms of energetic TNAD and TNAZ explosives. Int J Quantum Chem 102(4):398–408
20. McKenney RL, Floyd TG, Stevens WE (1997) Binary phase diagram series: 1,3,3-trinitroazetidine (TNAZ)/2,4,6-trinitrotoluene (TNT). Wright Laboratory, Armament Directorate Report, WL-TR-1997–7001, January 1997

21. Osmont L, Catoire I, Gökalp V, Yang V (2007) Ab initio quantum chemical predictions of enthalpies of formation, heat capacities, and entropies of gas-phase energetic compounds. Combust Flame 151(1–2):262–273
22. Jenkins TF, Bartolini C, Ranney TA (2003) Stability of CL-20, TNAZ, HMX, RDX, NG, and PETN in moist, unsaturated soil. ERDC/CRREL TR-03-7, April 2003
23. Liu Y, Liu Z-N, C-m Yin (2004) Phase diagram and eutectic of binary systems for 1,3,3-trinitroazetidine (TNAZ) with some energetic materials. Hanneng Cailiao 12(Suppl. 1):227–230
24. Annex DS, Allman JC, Lee YT (1991) Chemistry of energetic materials. In Olah GA, Squire DR (eds) Academic Press, New York, NY, pp 27–54

Additional Scholarly Articles for Further Reading

25. Agrawal PM, Rice BM, Zheng L, Velardez GF, Thompson DL (2006) Molecular dynamics simulations of the melting of 1,3,3-trinitroazetidine. J Phys Chem B 110(11):5721–5726. https://doi.org/10.1021/jp056690
26. Alavi S, Reilly LM, Thompson DL (2003) Theoretical predictions of the decomposition mechanism of 1,3,3-trinitroazetidine (TNAZ). J Chem Phys 119(16):8297–8304. https://doi.org/10.1063/1.1611471
27. Anderson K, Homsy J, Behrens R, Bulusu S (1997) Mechanistic and kinetic studies of the thermal decomposition of TNAZ and NDNAZ. CPIA Publ 657 (JANNAF Propulsion Systems Hazards Subcommittee Meeting, vol 1), pp 37–51
28. Anex DS, Allman JC, Lee YT (1991) Studies of initial dissociation processes in 1,3,3-trinitroazetidine by photofragmentation translational spectroscopy. Academic, pp 27–54
29. Archibald TG, Gilardi R, Baum K, George C (1990) Synthesis and x-ray crystal structure of 1,3,3-trinitroazetidine. J Org Chem 55(9):2920–2924. https://doi.org/10.1021/jo00296a066
30. Astrat'ev AA, Stepanov AI, Dashko DV (2013) Synthesis, energetic and some chemical properties of new explosive—3,4-bis(4'-nitrofurazan-3'-yl)furazan (BNTF). University of Pardubice, Institute of Energetic Materials, pp 482–496
31. Aubuchon CM, Rector KD, Holmes W, Fayer MD (1999) Nitro group asymmetric stretching mode lifetimes of molecules used in energetic materials. Chem Phys Lett 299(1):84–90. https://doi.org/10.1016/S0009-2614(98)01241-X
32. Axenrod T, Watnick C, Yazdekhasti H, Dave PR (1995) Synthesis of 1,3,3-trinitroazetidine via the Oxidative Nitrolysis of N-p-Tosyl-3-azetidinone Oxime. J Org Chem 60(7):1959–1964. https://doi.org/10.1021/jo00112a014
33. Bakhtiar R, Bulusu S (1995) Molecular complexes of cyclodextrins: application of ion-spray mass spectrometry to the study of complexes with selected nitramines. Rapid Commun Mass Spectrom 9(14):1391–1394. https://doi.org/10.1002/rcm.1290091413
34. Bartnik R, Cal D, Marchand AP, Alihodzic S, Devasagayaraj A (1998) New method for the generation and trapping of 1-azabicyclo [1.1.0] butane. Application to the synthesis of 1,3-dinitroazetidine. Synth Commun 28(21):3949–3954. https://doi.org/10.1080/00397919808004953
35. Bartnik R, Marchand AP (1997) Synthesis and chemistry of substituted 1-azabicyclo [1.1.0] butanes. Synlett (9):1029–1039. http://doi.org/10.1055/s-1997-1520
36. Bauer SH, Zhang Y-X (1999) Stability tests of TNAZ—thermal and shock impact. J Energ Mater 17(2 & 3):161–176. https://doi.org/10.1080/07370659908216101
37. Bottaro JC (1996) Recent advances in explosives and solid propellants. Chem Ind (London) (7):249–252

38. Braithwaite PC, Hatch RL, Lee K, Wardle RB (1998) Development of high performance CL-20 explosive formulations. In: International annual conference on ICT 29th (Energetic Materials), pp 4.1–4.7
39. Cahill S, Bulusu S (1993) Molecular complexes of explosives with cyclodextrins. I. Characterization of complexes with the nitramines RDX, HMX and TNAZ in solution by proton NMR spin-lattice relaxation time measurements. Magn Reson Chem 31(8):731–735. https://doi.org/10.1002/mrc.1260310808
40. Cahill S, Rinzler AG, Owens FJ, Bulusu S (1994) Molecular complexes of explosives with cyclodextrins. II. Preparation and characterization of a solid complex ofβ-cyclodextrin with the nitramine 1,3,3-trinitroazetidine (TNAZ). J Phys Chem 98(28):7095–7100. https://doi.org/10.1021/j100079a033
41. Calculated using Advanced Chemistry Development (ACD/Labs) Software V8.14 for Solaris (© 1994–2008 ACD/Labs)
42. Chakka S, Boddu VM, Maloney SW, Toghiani RK, Damavarapu R (2009) Vapor pressures and melting points of select munitions compounds. American Institute of Chemical Engineers, pp chakk1/1-chakk1/9
43. Chapman RD et al (1995) Phase behavior in TNAZ-based and other explosive formulations. American Defense Preparedness Association, pp 192–197
44. Coburn MD, Hiskey MA, Archibald TG (1998) Scale-up and waste-minimization of the Los Alamos process for 1,3,3-trinitroazetidine (TNAZ). Waste Manage (Oxford) 17(2/3):143–146. https://doi.org/10.1016/S0956-053X(97)10013-7
45. Coburn MD, Hiskey MA, Oxley JC, Smith JL, Zheng W, Rogers E (1998) Synthesis and spectra of some 2H-, 13C-, and 15 N-labeled isomers of 1,3,3-trinitroazetidine and 3,3-dinitroazetidinium nitrate. J Energ Mater 16(2 & 3):73–99. https://doi.org/10.1080/07370659808217506
46. Crowder GA, McKenney RL Jr (1999) Vibrational analysis of high-energy compounds: 1,3,3-trinitroazetidine and 1-acetyl-3,3-dinitroazetidine. J Energ Mater 17(1):49–68. https://doi.org/10.1080/07370659908216095
47. Dubovik AV, Kozak GD, Aleshkina EA (2007) Theoretical estimation of explosion hazard of NTO, FOX-7, TNAZ, and CL-20. University of Pardubice, pp 484–495
48. Dudek K, Marecek P, Jalovy Z (2002) Some properties of cast TNAZ mixtures. In: International annual conference on ICT 33rd (Energetic Materials), pp 53/1–53/7
49. Dudek K, Marecek P, Jalovy Z (2001) Synthesis and some properties of 1,3,3-trinitroazetidine (TNAZ). University of Pardubice, pp 75–80
50. Dudek K, Marecek P, Vavra P (2000) Laboratory testing of HNIW mixtures. In: International annual conference on ICT 31st (Energetic Materials), pp 110/1–110/6
51. Fan X, Li J, Zhang Y, Zhang W, Kang X (2005) Characteristics of the smokeless CMDB propellants with 1,3,3-trinitroazetidine. Huozhayao Xuebao 28(4):35–40
52. Florczak B, Lipinska K (2001) Thermochemical properties of composite propellants combustion products. University of Pardubice, pp 86–98
53. Fuchs B, Stec D, III (2007) Computational survey of representative energetic materials as propellants for microthruster applications. In: Proceedings of SPIE-international society optics engineering 6556 (Micro (MEMS) and Nanotechnologies for Defense and Security), pp 65561B/1–65561B/12. http://doi.org/10.1117/12.721756
54. Garland NL, McElvany SW (1998) Ionization potentials of TNAZ and its decomposition products. Chem Phys Lett 297(1,2):147–153. http://doi.org/10.1016/S0009-2614(98)01113-0
55. Garland NL, Nelson HH (1998) Laser-induced decomposition of TNAZ. J Phys Chem B 102 (15):2663–2667. https://doi.org/10.1021/JP980201D
56. Hayashi K, Kumagai T, Nagao Y (2000) Improved synthesis of an energetic material, 1,3,3-trinitroazetidine exploiting 1-azabicyclo [1.1.0] butane. Heterocycles 53(2):447–452

57. Hill LG, Seitz WL, Kramer JF, Murk DM, Medina RS (1996) Wedge test data for three new explosives: LAX112, 2,4-DNI, and TNAZ. In: AIP conference on proceedings 370 (Pt. 2, Shock Compression of Condensed Matter–1995), pp 803–806
58. Jadhav HS, Dhavale DD, Talawar MB, Asthana SN, Krishnamurthy VN (2003) 1-(3',5'-dinitrophenyl)-3,3-dinitroazetidine: a new energetic materials. University of Pardubice, pp 153–159
59. Jadhav HS, Talawar MB, Dhavale DD, Asthana SN, Krishnamurthy VN (2006) Alternate method for synthesis of 1,3,3-trinitroazetidine (TNAZ): next generation melt-castable high-energy material. Indian J Chem Technol 13(1):41–46
60. Jalovy Z, Zeman S, Suceska M, Vavra P, Dudek K, Rajic M (2001) 1,3,3-trinitroazetidine (TNAZ), Part I syntheses and properties. J Energ Mater 19(2 & 3):219–239. https://doi.org/10.1080/07370650108216127
61. Jizhen L, Xuezhong F, Xiping F, Fengqi Z, Rongzu H (2006) Compatibility study of 1,3,3-trinitroazetidine with some energetic components and inert materials. J Therm Anal Calorim 85(3):779–784. https://doi.org/10.1007/s10973-005-7370-8
62. Katorov DV, Rudakov GF, Ladonin AV, Zhilin VF, Veselova EV, Vyalova NA (2007) Preparation of low-melting explosive compositions based on 1,3,3-trinitroazetidine. Cent Eur J Energ Mater 4(1–2):125–133
63. Katritzky AR, Cundy DJ, Chen J (1994) Novel syntheses of 1,3,3-trinitroazetidine. J Heterocycl Chem 31(2):271–275. https://doi.org/10.1002/jhet.5570310202
64. Keshavarz MH (2007) Determining heats of detonation of non-aromatic energetic compounds without considering their heats of formation. J Hazard Mater 142(1–2):54–57. https://doi.org/10.1016/j.jhazmat.2006.07.057
65. Keshavarz MH, Moghadas MH, Tehrani MK (2009) Relationship between the electrostatic sensitivity of nitramines and their molecular structure. Propellants Explos Pyrotech 34 (2):136–141. https://doi.org/10.1002/prep.200700264
66. Keshavarz MH, Yousefi MH (2008) Heats of sublimation of nitramines based on simple parameters. J Hazard Mater 152(3):929–933. https://doi.org/10.1016/j.jhazmat.2007.07.067
67. Kim JS, Kim H, Kwon Y (2009) Synthesis of glycidyldinitroazetidine (GDNAZ) as an energetic monomers containing explosophoric group. In: International annual conference on ICT 40th (Energetic Materials), pp 53/1–53/11
68. Konrad S, Doris K (2000) Synthesis and properties of TNAZ. In: International annual conference on ICT 31st (Energetic Materials), pp 10/1–10/12
69. Lanzerotti MYD, Autera J, Sharma J (1996) Crystal growth of TNAZ during high acceleration. In: AIP conference proceedings 370 (Pt. 1, Shock Compression of Condensed Matter–1995), pp 243–246
70. Lanzerotti Y, Sharma J (2002) Mechanical behavior of energetic materials during high acceleration. In: AIP conference proceedings on 620 (Shock Compression of Condensed Matter, Pt. 2), pp 853–855
71. Lanzerotti Y, Sharma J (2003) Mechanical behavior of energetic materials during high acceleration. In: Materials research society symposium proceedings 759(Granular Material-Based Technologies), pp 155–159
72. Lanzerotti Y, Sharma J (2001) Mechanical behavior of energetic materials at high acceleration. Kluwer Academic/Plenum Publishers, pp 367–369
73. Li J, Zhang W, Wang B, Fan X, Liu Z (2005) Studies on the combustion characteristics and the thermal behavior of CMDB and NEPE propellants with 1,3,3-trinitroazetidine. Huozhayao Xuebao 28(2):16–20, 38
74. J-z Li, G-f Zhang, Fan X-z Hu, R-z Pan Q (2006) Thermal behavior of 1,3,3-trinitroazetidine. J Anal Appl Pyrolysis 76(1–2):1–5. https://doi.org/10.1016/j.jaap.2005.04.008

75. Liao L-Q et al (2012) Compatibility of PNIMMO with some energetic materials. J Therm Anal Calorim 109(3):1571–1576. https://doi.org/10.1007/s10973-011-1905-y
76. Liu M-H, Chen C, Hong Y-S (2004) Empirical methods for estimating the detonation properties of energetic TNAZ molecular derivatives. J Theor Comput Chem 3(3):379–389. https://doi.org/10.1142/S0219633604001100
77. Liu M-H, Chen C, Hong Y-S (2005) Theoretical study of the unimolecular decomposition mechanisms of energetic TNAD and TNAZ explosives. Int J Quantum Chem 102(4):398–408. https://doi.org/10.1002/qua.20284
78. Long GT, Wight CA (2002) Thermal decomposition of a melt-castable high explosive: isoconversional analysis of TNAZ. J Phys Chem B 106(10):2791–2795. https://doi.org/10.1021/jp012859o
79. Ma H-X et al (2010) Molecular structure, thermal behavior and adiabatic time-to-explosion of 3,3-dinitroazetidinium picrate. J Mol Struct 981(1–3):103–110. https://doi.org/10.1016/j.molstruc.2010.07.036
80. Makhova NN, Ovchinnikov IV (2008) New variant of 1,3,3-trinitroazetidine synthesis. vol Pt. 2. University of Pardubice, pp 639–641
81. Marchand AP, Rajagopal D, Bott SG, Archibald TG (1995) A novel approach to the synthesis of 1,3,3-trinitroazetidine. J Org Chem 60(15):4943–4946. https://doi.org/10.1021/jo00120a049
82. Marecek P, Dudek K (2002) Cast TNAZ mixtures. University of Pardubice, pp 164–168
83. Marecek P, Dudek K, Vavra P (2001) Laboratory testing of TNAZ mixtures. In: International annual conference on ICT 32nd (Energetic Materials), pp 90/1–90/8
84. McKenney RL Jr. et al (1998) Synthesis and thermal properties of 1,3-dinitro-3- (1’,3’-dinitroazetidin-3’-yl)azetidine (TNDAZ) and its admixtures with 1,3,3-trinitroazetidine (TNAZ). [Erratum to document cited in CA129:161458]. J Energ Mater 16(2 & 3):198–235
85. McKenney RL Jr et al (1998) Synthesis and thermal properties of 1,3-dinitro-3-(1,3-dinitro-3-azetidinyl) azetidine (TNDAZ) and its admixtures with 1,3,3-trinitroazetidine (TNAZ). J Energ Mater 16(1):1–22. https://doi.org/10.1080/07370659808216090
86. McKenney RL Jr, Stevens WE (2000) Binary phase diagram series: 1,3,3-trinitroazetidine (TNAZ)/1,3,5-trinitrobenzene (TNB). J Energ Mater 18(4):241–273. https://doi.org/10.1080/07370650008219112
87. McKenney RL Jr, Stevens WE, Floyd TG (1998) Binary phase diagram series: 1,3,3-trinitroazetidine (TNAZ)/2,4,6-trinitrotoluene (TNT). J Energ Mater 16(4):245–278. https://doi.org/10.1080/07370659808230234
88. McKenney RL Jr, Stevens WE, Floyd TG (1999) Binary phase diagram series: 1,3,3-trinitroazetidine (TNAZ)/N-Acetyl-3,3-dinitroazetidine (ADNAZ). J Energ Mater 17 (2 & 3):113–140. https://doi.org/10.1080/07370659908216099
89. Mondal T, Saritha B, Ghanta S, Roy TK, Mahapatra S, Durga Prasad M (2009) On some strategies to design new high energy density molecules. J Mol Struct Theochem 897(1–3):42–47. https://doi.org/10.1016/j.theochem.2008.11.013
90. Mostak P, Stancl M (2006) New trends in detection of explosives. University of Pardubice, pp 61–74
91. Nedel’ko VV et al (2009) Thermal decomposition of 1,3,3-trinitroazetidine in the gas phase, solution, and melt. Russ Chem Bull 58(10):2028–2034. https://doi.org/10.1007/s11172-009-0277-y
92. Nedelko VV, Korsounskii BL, Chukanov NV, Larikova TS, Makhova NN, Ovchinnikov IV (2006) Thermal decomposition of 1,3,3-trinitroazetidine in gas, solution and melt. In: International annual conference on ICT 37th (Energetic Materials), pp 154/1–154/12

93. Oehrle SA (1994) Analysis of CL-20 and TNAZ in the presence of other nitroaromatic and nitramine explosives using HPLC with photodiode array (PDA) detection. J Energ Mater 12 (4):211–222. https://doi.org/10.1080/07370659408018651
94. Oehrle SA (1996) Analysis of nitramine and nitroaromatic explosives by micellar electrokinetic capillary chromatography (MECC). J Energ Mater 14(1):47–56. https://doi.org/10.1080/07370659608216057
95. Oftadeh M, Khozani MH, Radhoosh M, Keshavarz MH (2011) DFT molecular orbital calculations of initial step in decomposition pathways of TNAZ and some of its derivatives with -F, -CN and -OCH3 groups. Comput Theor Chem 964(1–3):262–268. https://doi.org/10.1016/j.comptc.2011.01.007
96. Oftadeh M, Selahvarzi S, Keshavarz MH (2013) Intermolecular interactions between TNAZ and H_2O: a DFT study. Cent Eur J Energ Mater 10(2):289–300
97. Oxley J, Smith J, Zheng W, Rogers E, Coburn M (1997) Thermal Decomposition Pathways of 1,3,3-Trinitroazetidine (TNAZ), Related 3,3-Dinitroazetidium Salts, and 15 N, 13C, and 2H Isotopomers. J Phys Chem A 101(24):4375–4383. https://doi.org/10.1021/JP9700950
98. Oxley JC, Kooh AB, Szekeres R, Zheng W (1994) Mechanisms of nitramine thermolysis. J Phys Chem 98(28):7004–7008. https://doi.org/10.1021/j100079a019
99. Oyumi Y, Brill TB (1985) Thermal decomposition of energetic materials. 4. High-rate, in situ, thermolysis of the four, six, and eight membered, oxygen-rich, gem-dinitroalkyl cyclic nitramines, TNAZ, DNNC, and HNDZ. Combust Flame 62(3):225–231.https://doi.org/10.1016/0010-2180(85)90148-8
100. Parr TP, Hanson-Parr DM (1996) Solid propellant diffusion flame structure. In: Symposium (International) combust, [Proceedings] 26th (vol 2):1981–1987
101. Persson B, Ostmark H, Bergman H (1997) An HPLC method for analysis of HNIW and TNAZ in an explosive mixture. Propellants Explos Pyrotech 22(4):238–239. https://doi.org/10.1002/prep.19970220411
102. Pietrzyk S, Nowaczewski J, Bladek J (2007) Analysis of novel high energetic explosives: HNIW, TEX, TNAZ, DADNE. University of Pardubice, pp 853–858
103. Politzer P, Seminario JM (1993) Energy changes associated with some decomposition steps of 1,3,3-trinitroazetidine. A non-local density functional study. Chem Phys Lett 207(1):27–30. https://doi.org/10.1016/0009-2614(93)85006-A
104. Porollo AA, Pivina TS, Ivshin VP (1998) Theoretical technique for modeling of 1,3,3-trinitroazetidine (TNAZ) thermal decomposition. In: Proceedings on international pyrotech seminar 24th, pp 445–455
105. Rice VM et al (2001) Theoretical chemistry: applications in energetic materials research. Khim Fiz 20(10):9–13
106. Sarlauskas J et al (2014) Modern nitramines TNAZ and CL-20 (HNIW): their electron-accepting potency, enzymatic reactivity and cytotoxicity. vol 2. University of Pardubice, Institute of Energetic Materials, pp 987–1004
107. Shao Y-H, Ren X-N, Liu Z-R (2010) An investigation on eutectic binary phase diagram of volatilizable energetic materials by high pressure DSC. J Therm Anal Calorim 101(3):1135–1141. https://doi.org/10.1007/s10973-009-0620-4
108. Shao YH, Ren XN, Liu ZR, Zhang X (2011) Ternary phase diagrams of DNTF and TNAZ and their eutectics. J Therm Anal Calorim 103(2):617–623. https://doi.org/10.1007/s10973-010-0993-4
109. Sheffield SA, Gustavsen RL, Alcon RR (1996) Hugoniot and initiation measurements on TNAZ explosive. In: AIP conference on proceedings 370 (Pt. 2, Shock Compression of Condensed Matter–1995), pp 879–882
110. Shu Y, Li H, Huang Y, Liu S (2003) Synthesis of N-acetyl-3,3-dinitroazetidine. University of Pardubice, pp 543–546

111. Sikder N, Sikder AK, Bulakh NR, Gandhe BR (2004) 1,3,3-Trinitroazetidine (TNAZ), a melt-cast explosive: synthesis, characterization and thermal behaviour. J Hazard Mater 113 (1–3):35–43. https://doi.org/10.1016/j.jhazmat.2004.06.002
112. Sikder N, Sikder AK, Bulakh NR, Gandhe BR (2004) 1,3,3-Trinitroazetidine (TNAZ), a melt-cast explosive: synthesis, characterization and thermal behaviour. J Hazard Mater 113 (1–3):35–43
113. Sikder N, Sikder AK, Bulakh NR, Gandhe BR (2004) 1,3,3-Trinitroazetidine (TNAZ), a melt-cast explosive: synthesis, characterization and thermal behaviour. J Hazard Mater 113 (1–3):35–43. https://doi.org/10.1016/j.jhazmat.2004.06.002
114. Simpson RL, Urtiew PA, Tarver CM (1996) Shock initiation of 1,3,3-trinitroazetidine (TNAZ). In: AIP conference on proceedings 370 (Pt. 2, Shock Compression of Condensed Matter–1995), pp 883–886
115. Sinditskii VP, Egorshev VY, Berezin MV, Rudakov GF, Ladonin AV, Katorov DV (2005) Combustion behavior and flame structure of a melt-castable high explosive 1,3,3-trinitroazetidine (TNAZ). In: International annual conference on ICT 36th (Energetic Materials), pp 78/1–78/7
116. Singh A, Sikder N, Sikder AK (2005) Improved synthesis of an energetic material, 1,3,3-trinitroazetidine (TNAZ) exploiting 2-iodoxy benzoic acid (IBX) as an oxidising agent. Indian J Chem, Sect B: Org Chem Incl Med Chem 44B(12):2560–2563
117. Suceska M, Rajic M, Zeman S, Jalovy Z (2001) 1,3,3-trinitroazetidine (TNAZ). Study of thermal behaviour. Part II. J Energ Mater 19(2 & 3):241–254 http://doi.org/10.1080/07370650108216128
118. Suceska M, Zeman S, Rajic M, Jalovy Z (2001) Theoretical prediction of TNAZ detonation properties. University of Pardubice, pp 308–318
119. Suseska M, Rajis M, Matecis-Musanis S, Zeman S, Jalovy Z (2003) Kinetics and heats of sublimation and evaporation of 1,3,3-trinitroazetidine (TNAZ). J Therm Anal Calorim 74 (3):853–866. https://doi.org/10.1023/B:JTAN.0000011017.65451.96
120. Talawar MB et al (2006) Effect of organic additives on the mitigation of volatility of 1-nitro-3,3’-dinitroazetidine (TNAZ): next generation powerful melt castable high energy material. J Hazard Mater 134(1–3):8–18. https://doi.org/10.1016/j.jhazmat.2003.10.008
121. Thompson CA, Rice JK, Russell TP, Seminario JM, Politzer P (1997) Vibrational analysis of 1,3,3-trinitroazetidine using matrix isolation infrared spectroscopy and quantum chemical calculations. J Phys Chem A 101(42):7742–7748. https://doi.org/10.1021/JP971173M
122. Thompson CA, Russell TP, Concha MC, Politzer P (1997) Comparing quantum chemical calculations for azetidine strained ring compounds. American Chemical Society, pp COMP-125
123. Turker L (2013) Detonation velocity—a molecular aspect. Adv Chem Model 4:223–236
124. Turker L, Atalar T (2011) 1,3,3-Trinitroazetidine (TNAZ) and some of its constitutional isomers: a DFT study. vol 2. University of Pardubice, Institute of Energetic Materials, pp 982–993
125. Turker L, Varis S (2012) Desensitization of TNAZ via molecular structure modification and explosive properties—a DFT study. Acta Chim Slov 59(4):749–759
126. Veals JD, Thompson DL (2014) Thermal decomposition of 1,3,3-trinitroazetidine (TNAZ): A density functional theory and ab initio study. J Chem Phys 140(15):154306/1–154306/10 http://doi.org/10.1063/1.4870652
127. Wakeham GP, Chung DD, Nelson KA (2002) Femtosecond time-resolved spectroscopy of energetic materials. Thermochim Acta 384(1–2):7–21. https://doi.org/10.1016/S0040-6031(01)00774-2
128. Wilcox CF, Zhang YX, Bauer SH (2000) The thermochemistry of TNAZ (1,3,3-trinitroazetidine) and related species: models for calculating heats of formation. J Mol Struct: THEOCHEM 528:95–109. https://doi.org/10.1016/S0166-1280(99)00475-3

129. Wilcox CF, Zhang YX, Bauer SH (2001) The thermochemistry of TNAZ (1,3,3-trinitroazetidine) and related species: G3(MP2)//B3LYP heats of formation. J Mol Struct: THEOCHEM 538:67–72. https://doi.org/10.1016/S0166-1280(00)00646-1
130. Xue L, Zhao F-Q, Xing X-L, Gao H-X, Yi J-H, Hu R-Z (2009) Dissolution properties of 1,3,3-trinitroazetidine in ethyl acetate and N. N-dimethylformamide. Wuli Huaxue Xuebao 25(12):2413–2416
131. Yan B et al (2014) Thermodynamic properties, detonation characterization and free radical of N-2',4'-dinitrophenyl-3,3-dinitroazetidine. J Chem Thermodyn 69:152–156. https://doi.org/10.1016/j.jct.2013.10.014
132. Yan Q-L, Zeman S, Elbeih A (2012) Recent advances in thermal analysis and stability evaluation of insensitive plastic bonded explosives (PBXs). Thermochim Acta 537:1–12. https://doi.org/10.1016/j.tca.2012.03.009
133. Yu CL, Zhang YX, Bauer SH (1998) Estimation of the equilibrium distribution of products generated during high temperature pyrolyses of 1,3,3-trinitroazetidine; thermochemical parameters. J Mol Struct: THEOCHEM 432(1):63–68. https://doi.org/10.1016/S0166-1280(97)87495-7
134. Zeman S, Atalar T (2009) A new view of relationships of the N–N bond dissociation energies of cyclic nitramines. Part III. Relationship with detonation velocity. J Energ Mater 27(3):217–229. http://doi.org/10.1080/07370650802640374
135. Zhang J, Hu J-W, Wang J-L, Chen L-Z (2011) Solubility of 1,3,3-trinitroazetidine in ethanol + water systems from (293.15 K to 323.15 K). J Solution Chem 40(4):703–708. http://doi.org/10.1007/s10953-011-9673-7
136. Zhang J, Hu R, Zhu C, Feng G, Long Q (1997) Thermal behavior of 1,3,3-trinitroazetidine. Thermochim Acta 298(1–2):31–35. https://doi.org/10.1016/S0040-6031(97)00056-7
137. Zhang J, Hu R, Zhu C, Feng G, Long Q (1996) Thermal behavior of 1,3,3-trinitroazetidine. Beijing Institute of Technology Press, pp 133–138
138. Zhang M, Shi Z, Bai Y, Gao Y, Hu R, Zhao F (2006) Using molecular recognition of β-Cyclodextrin to determine molecular weights of low-molecular-weight explosives by MALDI-TOF mass spectrometry. J Am Soc Mass Spectrom 17(2):189–193. https://doi.org/10.1016/j.jasms.2005.10.005
139. Zhang X, Yang J, Wang T, Gong X, Wang G (2014) A theoretical study on the stability and detonation performance of 2,2,3,3-tetranitroaziridine (TNAD). J Phys Org Chem 27(6):532–539. https://doi.org/10.1002/poc.3297
140. Zhang Y-X, Bauer SH (1998) Gas-Phase Pyrolysis of 1,3,3-trinitroazetidine: shock tube kinetics. J Phys Chem A 102(29):5846–5856. https://doi.org/10.1021/JP980931L
141. Zhang Y-X, Bauer SH (1999) Gas-phase decomposition mechanisms of C-NO_2, N-NO_2 energetic materials: reevaluations. Int J Chem Kinet 31(9):655–673 http://doi.org/10.1002/(SICI)1097-4601(1999)31:9<655::AID-KIN7>3.0.CO;2-M
142. Zhang Y-X, Bauer SH (1999) Gas-phase decomposition mechanisms of C-NO_2, N-NO_2 energetic materials: reevaluations. Int J Chem Kinet 31(9):655–673. http://doi.org/10.1002/(SICI)1097-4601(1999)31:9<655::AID-KIN7>3.0.CO;2-M
143. Zhao Q, Zhang S, Li QS (2005) A direct ab initio dynamics study of the initial decomposition steps of gas phase 1,3,3-trinitroazetidine. Chem Phys Lett 412(4–6):317–321. https://doi.org/10.1016/j.cplett.2005.07.014
144. Zhao Q, Zhang S, Li QS (2005) The influence of ring strain and conjugation on the reaction energies of the NO_2 fission of nitramines: a DFT study. Chem Phys Lett 407(1–3):105–109. https://doi.org/10.1016/j.cplett.2005.03.059
145. Zheng W, Dong X, Rogers E, Oxley JC, Smith JL (1997) Improvements in the determination of decomposition gases from 1,3,3-trinitroazetidine and 5-nitro-2,4-dihydro-3H-1,2,4-traizol-3-one using capillary gas chromatography-mass spectrometry. J Chromatogr Sci 35(10):478–482. https://doi.org/10.1093/chromsci/35.10.478

146. Zheng W, Dong X, Rogers E, Oxley JC, Smith JL (1997) Improvements in the determination of decomposition gases from 1,3,3-trinitroazetidine and 5-nitro-2,4-dihydro-3H-1,2,4-traizol-3-one using capillary gas chromatography-mass spectrometry. J Chromatogr Sci 35 (10):478–482. https://doi.org/10.1093/chromsci/35.10.478
147. Zheng W, Rogers E, Coburn M, Oxley J, Smith J (1997) Mass spectral fragmentation pathways in 1,3,3-trinitroazetidine. J Mass Spectrom 32(5):525–532. https://doi.org/10.1002/(SICI)1096-9888(199705)32:5<525:AID-JMS505>3.0.CO;2-7

Appendix 1
Unit

Table A.1. Conversion Factors

Overview

The International System of Units (SI) is a modernized version of the metric system established by international agreement. The metric system of measurement was developed during the French Revolution and was first promoted in the U.S. by Thomas Jefferson. Its use was legalized in the U.S. in 1866. In 1902, proposed congressional legislation requiring the U.S. Government to use the metric system exclusively was defeated by a single vote.

SI provides a logical and interconnected framework for all measurements in science, industry, and commerce. The metric system is much simpler to use than the existing English system since all its units of measurement are divisible by 10.

Conversion Factors

The following list provides the conversion relationship between U.S. customary units and SI (International System) units. The proper conversion procedure is to multiply the specified value on the left (primarily U.S. customary values) by the conversion factor exactly as given below and then round to the appropriate number of significant digits desired. For example, to convert 11.4 ft to m: 11.4 × 0.3048 = 3.47472, which rounds to 3.47 m. Do not round either value before performing the multiplication, as accuracy would be reduced. A complete guide to the SI system and its use can be found in ASTM E 380, Metric Practice.

Select this link for an explanation of WSDOT's foot to meter conversion method (http://www.wsdot.wa.gov/Reference/metrics/foottometer.htm).

Note that Convert.exe (http://www.wsdot.wa.gov/NR/rdonlyres/4A1238B7-69FC-434E-8BF0-317AA149F5C0/0/convert.exe) uses the 1959 conversion factors for distance (http://www.wsdot.wa.gov/Reference/metrics/foottometer.htm) i.e. the 1959 definitions of inch and foot and their derived measurements, the ton to kilogram conversion factor differs from the conversion factor published on this page

D.S. Viswanath et al., *Emerging Energetic Materials: Synthesis, Physicochemical, and Detonation Properties*, https://doi.org/10.1007/978-94-024-1201-7

by 1 in the 7th digit, the Fahrenheit to Kelvin conversion factor differs by 0.017° K, the BTU/h to watt conversion differs by 3 in the 4th digit, and the ft/sec^2 to m/sec^2 conversion differs by 1 in the 6th digit.

Conversion Symbols

The prefixes and symbols listed below are commonly used to form names and symbols of the decimal multiples and sub multiples of the SI units.

SI Prefixes for decimal multiples

Number	Factor	Name	Symbol
1,000,000,000,000,000,000,000,000	10^{24}	yotta	Y
1,000,000,000,000,000,000,000	10^{21}	zetta	Z
1,000,000,000,000,000,000	10^{18}	exa	E
1,000,000,000,000,000	10^{15}	peta	P
1,000,000,000,000	10^{12}	tera	T
1,000,000,000	10^{9}	giga	G
1,000,000	10^{6}	mega	M
1000	10^{3}	kilo	k
100	10^{2}	hecto	h
10	10^{1}	deca	da
0.1	10^{-1}	deci	d
0.01	10^{-2}	centi	c
0.001	10^{-3}	milli	m
0.000001	10^{-6}	micro	µ
0.000000001	10^{-9}	nano	n
0.000000000001	10^{-12}	pico	p
0.000000000000001	10^{-15}	femto	f
0.000000000000000001	10^{-18}	atto	a
0.000000000000000000001	10^{-21}	zepto	z
0.000000000000000000000001	10^{-24}	yocto	y

Table A.2. Commercial standards

As used in the standard item table	Metric equivalent
Acre	Hectare (ha)
Cubic foot	Cubic meter (m^3)
Cubic yard	Cubic meter (m^3)
Gallon/Mgallon	Liter (l), Cubic meter (m^3)

(continued)

(continued)

As used in the standard item table	Metric equivalent
Hundred	Hundred for traffic buttons
Hundred weight	Kilogram (kg)
Linear foot	Meter (m)
Mboard feet	Cubic meter (m^3)
Mile	Kilometer (km)
Nautical mile	Nautical Mile
Pound	Kilogram (kg) for Mass newton (N) for Force
Square foot	Square meter (m^2)
Square yard	Square meter (m^2)
Ton	Tonne (t)

Units of measurement used in special provisions and general special provisions		Metric equivalent
Gage; Gauge	Metal thickness	gage (mm)
Fahrenheit	Temperature	kelvin (K) or degree Celsius (C)
Fathom	Water depth	Meter (m)
Foot/Lbs	Torque	Newton-meter (N-m)
Lbs/Sq. In	Pressures	Kilopascal (kPa) megapascal (MPa) (if very large number)
Lbs/Sq. Ft		Kilopascal (kPa)
Lbs/Sq Yd		Kilopascal (kPa)
Inch	Linear	Millimeter (mm)
Kips; Ksi	Tension	Kilopascal (kPa) or megapascal (MPa)
Lbs/Acre	Erosion control	Kilograms/hectare
Lbs/Cu. Ft.	Density	Kilogram per cubic meter (kg/m^3)
Mil	Thickness	Micrometer (um)
Ft. Lbs./Sec.	Horse power	Watt (W)

Units of measurements used on contract plans	Metric equivalent
Degrees/Bearings	No change for surveying
Stationing	1000 m = 1 Station
Mileposts	This one is still under review as mile posts are part of the signing issue. Use mileposts for now, but also state kilometerposts
Elevations	Meter (m)

Units of measurements used in commercial standards	Metric equivalent
Gals/Hr Or Min (Pumps)	Liters Per Second (l/s)
500 Gallon Tanks	Cubic Meter (m^3) But It Could Also Possi Bly Be In Liter (l)

(continued)

(continued)

Units of measurements used in commercial standards	Metric equivalent
55 Gallon Drums	Cubic meter (m^3) or Liter (l) For Liquid
94 Lbs/Sack (Cement)	Kilogram (kg)
Diameter of reinforcing steel	Millimeter (mm)
Lbs/Ft of reinforcing steel	Kilogram per meter kg/m)
Bushel	Cubic Meter (m^3)

Table A.3. Length Factors

Length Conversion Factors

Length		
To convert from	To	Multiply by
mile (US Statute)	kilometer (km)	1.609347
inch (in)	millimeter (mm)	25.4[a]
inch (in)	centimeter (cm)	2.54[a]
inch (in)	meter (m)	0.0254[a]
foot (ft)	meter (m)	0.3048[a]
yard (yd)	meter (m)	0.9144[a]

[a] Indicates that the factor given is exact

Area Conversion Factors

Area		
square foot (sq ft)	square meter (sq m)	0.09290304 E
square inch (sq in)	square meter (sq m)	0.00064516 E
square yard (sq yd)	square meter (sq m)	0.83612736 E
acre (ac)	hectare (ha)	0.4047

Volume Conversion Factors

Volume		
cubic inch (cu in)	cubic meter (cu m)	0.00001639
cubic foot (cu ft)	cubic meter (cu m)	0.02831685
cubic yard (cu yd)	cubic meter (cu m)	0.7645549
U.S. liquid[a]		
gallon (gal)	cubic meter (cu m)	0.00378541

(continued)

(continued)

Volume		
gallon (gal)	liter	3.785
fluid ounce (fl oz)	milliliters (ml)	29.57353
fluid ounce (fl oz)	cubic meter (cu m)	0.00002957

[a] One U.S. gallon equals 0.8327 Canadian gallon

Force Conversion Factors

Force		
kip (1000 lb)	kilogram (kg)	453.6
kip (1000 lb)	newton (N)	4448.222
pound (lb) avoirdupois	kilogram (kg)	0.4535924
pound (lb)	newton (N)	4.448222

Pressure or Stress Conversion Factors

Pressure or stress		
kip per square inch (ksi)	megapascal (MPa)	6.894757
pound per square foot (psf)	kilogram per square meter (kg/sq m)	4.8824
pound per square foot (psf)	pascal (Pa)	47.88
pound per square inch (psi)	pascal (Pa)	6894.757
pound per square inch (psi)	megapascal (MPa)	0.00689476

Mass conversion factors

Mass (weight)		
pound (lb) avoirdupois	kilogram (kg)	0.4535924
ton, 2000 lb	kilogram (kg)	907.1848
grain	kilogram (kg)	0.0000648
Mass (weight) per length		
kip per linear foot (klf)	kilogram per meter (kg/m)	0.001488
pound per linear foot (plf)	kilogram per meter (kg/m)	1.488
Mass per volume (density)		
pound per cubic foot (pcf)	kilogram per cubic meter (kg/cu m)	16.01846
pound per cubic yard (lb/cu yd)	kilogram per cubic meter (kg/cu m)	0.5933

Temperature conversion factors

Temperature		
degree Fahrenheit (°F)	degree Celsius (°C)	tc = (tF-32)/1.8

(continued)

(continued)

degree Fahrenheit (°F)	Kelvin (K)	tk = (tF + 459.7)/1.8
Kelvin (K)	degree Celsius (°C)	tc = tk-273.15
Energy and heat		
British thermal unit (Btu)	Joule (J)	1055.056
calorie (cal)	Joule (J)	4.1868E
Btu/degree	F × hr × ft^2 W/m^2—°K	5.678263
kilowatt-hour (kwh)	Joule (J)	3,600,000E
British thermal unit per pound (Btu/lb)	Calories per gram (cal/g)	0.55556
British thermal unit per hour (Btu/hr)	Watt (W)	0.2930711

Power conversion factors

Power		
horsepower (hp) (550 ft-lb/sec)	watt (W)	745.6999 E
Velocity		
mile per hour (mph)	kilometer per hour (km/hr)	1.60934
mile per hour (mph)	meter per second (m/s)	0.44704
Permeability		
darcy	centimeter per second (cm/sec)	0.000968
feet per day (ft/day)	centimeter per second (cm/sec)	0.000352

Note
t–A pascal equals 1000 N/m^2
One U.S. gallon of water weighs 8.34 pounds (U.S.) at 60° F
One cubic foot of water weighs 62.4 pounds (U.S.)
One milliliter of water has a mass of 1 g and has a volume of 1 M^3
One U.S. bag of cement weighs 94 lbs

More useful conversion factors

Quantity	From English units	To metric units	Multiply by[a]
Length			
	mile	km	1.609347
	yard	m	0.9144[b]
	foot	m	0.3048[b]
	inch	mm	25.40[b]
Area			
	square mile	km^2	2.590
	acre	m^2	4047
	acre	hectare	0.4047
	square yard	m^2	0.8361
	square foot	m^2	0.09290
	square inch	mm^2	645.2

(continued)

(continued)

Quantity	From English units	To metric units	Multiply by[a]
Volume			
	acre foot	m^3	1 233
	cubic yard	m^3	0.7646
	cubic foot	m^3	0.02832
	cubic foot	L (1000 cm^3)	28.32
	100 board feet	m^3	0.2360
	gallon	L (1000 cm^3)	3.785
Mass			
	lb	kg	0.4536
	kip (1000 lb)	Metric ton (1000 kg)	0.4536
Mass/unit length			
	plf	kg/m	1.488
Mass/unit area			
	psf	kg/m^2	4.882
Mass density			
	pcf	kg/m^3	16.02
Force			
	lb	N	4.448
	kip	kN	4.448
Force/unit length			
	plf	N/m	14.59
	klf	kN/m	14.59
Pressure, stress, modules of elasticity			
	psf	Pa	47.88
	ksf	kPa	47.88
	psi	kPa	6.895
	ksi	MPa	6.895
Bending moment, torque, moment of force			
	ft-lb	N·m	1.356
	ft-kip	kN·m	1.356

[a] 4 significant digits
[b] Denotes exact conversion

Quantity	From English units	To metric units	Multiply by[a]
Moment of mass			
	lb . ft	kg·m	0.1383
Moment of inertia			
	lb . ft^2	$kg·m^2$	0.04214

(continued)

(continued)

Quantity	From English units	To metric units	Multiply by[a]
Second moment of area			
	in^4	mm^4	416,200
Section modulus			
	in^3	mm^3	16,390
Power			
	ton (refrig)	kW	3.517
	Btu/s	kW	1.054
	hp (electric)	W	745.7
	Btu/h	W	0.2931
Volume rate of flow			
	ft^3/s	m^3/s	0.02832
	cfm	m^3/s	0.0004719
	cfm	L/s	0.4719
	mgd	m^3/s	0.0438
Velocity, speed			
	ft/s	m/s	0.3048[b]
Acceleration			
	f/s^2	m/s^2	0.3048
Momentum			
	lb . ft/sec	kg·m/s	0.1383
Angular momentum			
	lb . ft^2/s	kg·m ^{2}/s	0.04214
Plane Angle			
	degree	rad	0.01745
		mrad	17.45

[a] 4 significant digits
[b] Denotes exact conversion

Pavement Conversion Factors

Metric conversion—Pavements								
Roadway			Dimensions		Bridge Ht.		PCCP Thickness’	
							Resilient	Modulus
ft	m	ft	m		(inches)	(mm)	psi	MPa
Lane								
	12	3.6	14.5	4.4	9	225	3000	21
Shoulder								
	4	1.2	16.0	4.9	10	250	4000	28
	10	3.0			11	275	5000	34
					12	300	10,000	69

(continued)

(continued)

Metric conversion—Pavements								
Roadway			Dimensions		Bridge Ht.		PCCP Thickness’	
							Resilient	Modulus
ft	m	ft	m		(inches)	(mm)	psi	MPa
							12,000	83
							15,000	103
							20,000	138

Typical density values			Axle loads		Tire loads (per tire width)	
	pcf	kg/m^2	lbs	K N	lbs/inch	kg/mm
PCCP	150	2403	18,000	80	500	9
ACP	137/0.10’ depth	2439				

Pavement Marking Conversion Chart

Wet material thickness		Edge line coverage			Area coverage		
English mils (0.001″)	Metric mm (0.001 M)	English Ft/gal	Met./Eng. M/gal	Metric M/Liter	English SF/gal	Met./Eng. SM/gal	Metric SM/Lit
1.0	0.025	4832	1473	393.7	1611	150	39.37
10.0	0.254	483	147	39.4	161	15	3.94
15.0	0.381	322	98.2	26.2	107	10	2.62
19.7	0.500	245	74.8	20.0	82	7.6	2.00
20.0	0.508	242	73.6	19.7	81	7.5	1.97
25.0	0.635	193	58.9	15.7	64	6.0	1.57
30.0	0.762	161	49.1	13.1	54	5.0	1.31
35.0	0.889	138	42.1	11.2	46	4.3	1.12
39.4	1.000	123	37.4	10.0	41	3.8	1.00
40.0	1.016	121	36.8	9.8	40	3.7	0.98
45.0	1.143	107	32.7	8.7	36	3.3	0.87
49.2	1.250	98	29.9	8.0	33	3.0	0.80
50.0	1.270	97	29.5	7.9	32	3.0	0.79
59.1	1.500	82	24.9	6.7	27	2.5	0.67
60.0	1.524	81	24.5	6.6	27	2.5	0.66
78.7	2.000	61	18.7	5.0	20	1.9	0.50
88.6	2.250	55	16.6	4.4	18	1.7	0.44
90.0	2.286	54	16.4	4.4	18	1.7	0.44
98.4	2.500	49	15.0	4.0	16	1.5	0.40
100.0	2.540	48	14.7	3.9	16	1.5	0.39

(continued)

(continued)

Wet material thickness		Edge line coverage			Area coverage		
English mils (0.001″)	Metric mm (0.001 M)	English Ft/gal	Met./ Eng. M/gal	Metric M/Liter	English SF/gal	Met./ Eng. SM/gal	Metric SM/Lit
118.1	3.000	41	12.5	3.3	14	1.3	0.33
120.0	3.048	40	12.3	3.3	13	1.2	0.33
236.2	6.000	20	6.2	1.7	7	0.6	0.17
250.0	6.350	19	5.9	1.6	6	0.6	0.16
255.9	6.500	19	5.8	1.5	6	0.6	0.15
260.0	6.604	19	5.7	1.5	6	0.6	0.15

WDB 4.22.97

Table A.3. Length Factors

Sheet Metal Conversion Factors

Sheet Metal Most specification references use gage number followed by the decimal inch thickness. Example: 22 gage (0.034 inch) Metric specifications use the absolute mm thickness. It is not the intent of this guidance to change the thickness of currently used sheeting. The following chart may be used to specify sheet metal. The thickness under “Specify” is thinner than the actual gage thickness, since specifications give minimum thickness.

Gage	Inch	Exact (mm)	Specify (mm)	Percent thinner than “Exact” value
32	0.0134	0.3404	0.34	0.1
30	0.0157	0.3988	0.39	2.2
28	0.0187	0.4750	0.47	1.1
26	0.0217	0.5512	0.55	0.2
24	0.0276	0.7010	0.70	0.1
22	0.0336	0.8534	0.85	0.4
20	0.0396	1.0058	1.0	0.6
18	0.0516	1.3106	1.3	0.8
16	0.0635	1.6129	1.6	0.8
14	0.0785	1.9939	1.9	4.7
12	0.1084	2.7534	2.7	1.9
10	0.1382	3.5103	3.5	0.3
8	0.1681	4.2697	4.2	1.6

This schedule was developed since no existing material was found to clearly identify existing sheeting in metric units. Until a more efficient method is developed to address this issue, specifiers may wish to retain the gage number in specifications, and couple this with a rounded mm size in parenthesis.

Reinforcing Steel Conversion Factors

Reinforcing Steel

WSDOT Metric projects will continue to use U.S. Customary units on PS&E's.

The following table shows the current U.S. customary rebar sizes in relationship to the respective diameters and cross-sectional areas.

U.S. customary designation	Customary English system		Metric equivalent	
	Diameter (in.)	Area (in^2)	Diameter (mm)	Area (mm^2)
#3	0.375	0.11	9.5	71
#4	0.500	0.20	12.7	127
#5	0.625	0.31	15.9	198
#6	0.750	0.44	19.1	285
#7	0.875	0.60	22.2	388
#8	1.000	0.79	25.4	507
#9	1.125	1.00	28.6	641
#10	1.270	1.27	32.3	817
#11	1.410	1.56	35.8	1007
#14	1.693	2.25	43.0	1452
#18	2.257	4.00	57.3	2581

Table A.5. Wire

Wire Conversion Factors

Seven-Wire, Uncoated Strand for Prestressed Concrete Structures The prestressing industry again uses the soft conversion for all dimensional units of prestressing wire. This soft conversion is utilized worldwide and a copy of the equivalent physical properties for Grade 270 low-relaxation strand, as provided by Florida Wire and Cable Company, is provided:

270 Grade low-relaxation ASTM A-416					
Nominal strand diameter		Minimum strength		Area	
(mm)	(in.)	(kN)	(lb.)	(mm^2)	(in^2)
10	(3/8)	102.3	(23,000)	54.8	(0.085)
11	(7/16)	137.9	(31,000)	74.2	(0.115)
12	(15/32)	160.1	(36,000)	85.8	(0.133)
13	(1/2)	183.7	(41,300)	98.7	(0.153)
14	(9/16)	230.0	(51,700)	123.9	(0.192)
15	(0.600)	260.6	(58,600)	140.0	(0.217)

Table A.6. Sieves

Sieve Conversion Factors

Sieves

Sieve designation (W)						
Standard (mm)	Alternative (in.)	Nominal sieve opening (in.)	Permissible variation of average opening from the standard sieve designation (mm)	Intermediate tollerance (mm)	Maximum individual opening (mm)	Nominal wire diameter (mm)
			(y) + or	(x)	(x)	
125	5	5	3.70	130.0	130.9	8.00
106	4.24	4.24	3.20	110.2	111.1	6.40
100	4	4	3.00	104.0	104.8	6.30
90	3 1/2	3.5	2.70	93.6	94.4	6.08
75	3	3	2.20	78.1	78.7	5.80
63	2 1/2	2.5	1.90	65.6	66.2	5.50
53	2.12	2.12	1.60	55.2	55.7	5.15
50	2	2	1.50	52.1	52.6	5.05
45	1 3/4	1.75	1.40	46.9	47.4	4.85
37.5	1 1/2	1.5	1.10	39.1	39.5	4.59
31.5	1 1/4	1.25	1.00	32.9	33.2	4.23
26.5	1.06	1.06	0.80	27.7	28.0	3.90
25.0	1	1	0.80	26.1	26.4	3.80

(continued)

(continued)

Sieve designation (W)						
Standard (mm)	Alternative (in.)	Nominal sieve opening (in.)	Permissible variation of average opening from the standard sieve designation (mm)	Intermediate tollerance (mm)	Maximum individual opening (mm)	Nominal wire diameter (mm)
			(y) + or	(x)	(x)	
22.4		0.875	0.70	23.4	23.7	3.50
19.0	3/4	0.750	0.60	19.9	20.1	3.30
16.0		0.625	0.50	16.7	17.0	3.00
13.2	0.530	0.530	0.41	13.83	14.05	2.75
12.5	1/2	0.500	0.39	13.10	13.31	2.67
11.2	7/16	0.438	0.35	11.75	11.94	2.45
9.50		0.375	0.30	9.97	10.16	2.27
8.00	5/16	0.312	0.25	8.41	8.58	2.07
6.70	0.265	0.265	0.21	7.05	7.20	1.87
6.30	1/4	0.250	0.20	6.64	6.78	1.82
5.60	No. 3 1/2	0.223	0.18	5.90	6.04	1.68
4.75	No. 4	0.187	0.15	5.02	5.14	1.54
4.00	No. 5	0.157	0.13	4.23	4 35	1.37
3.35	No. 6	0.132	0.11	3.55	3.66	1.23
2.80	No. 7	0.11	0.095	2.975	3.070	1.10
2.36	No. 8	0.0937	0.080	2.515	2.600	1.00
2.00	No. 10	0.0787	0.070	2.135	2.215	0.900
1.70	No. 12	0.0661	0.060	1.820	1.890	0.810
1.40	No. 14	0.0555	0.050	1.505	1.565	0.725
1.18	No. 16	0.0469	0.045	1.270	1.330	0.650
1.00	No. 18	0.0394	0.040	1.080	1.135	0.580
0.850	No. 20	0.0331	0.035	0.925	0.970	0.510
0.710	No. 25	0.0278	0.030	0.775	0.815	0.450
0.600	No. 30	0.0234	0.025	0.660	0.695	0.390
0.500	No. 35	0.0197	0.020	0.550	0.585	0.340
0.425	No. 40	0.0165	0.019	0.471	0.502	0.290
0.355	No. 45	0.0139	0.016	0.396	0.425	0.247
0.300	No. 50	0.0117	0.014	0.337	0.363	0.215
0.250	No. 60	0.0098	0.012	0.283	0.306	0.180
0.212	No. 70	0.0083	0.010	0.242	0.263	0.152
0.180	No. 80	0.0070	0.009	0.207	0.227	0.131
0.150	No. 100	0.0059	0.008	0.174	0.192	0.110

(continued)

(continued)

Sieve designation (W)						
Standard (mm)	Alternative (in.)	Nominal sieve opening (in.)	Permissible variation of average opening from the standard sieve designation (mm)	Intermediate tollerance (mm)	Maximum individual opening (mm)	Nominal wire diameter (mm)
			(y) + or	(x)	(x)	
0.125	No. 120	0.0049	0.007	0.147	0.163	0.091
0.106	No. 140	0.0041	0.006	0.126	0.141	0.076
0.090	No. 170	0.0035	0.005	0.108	0.122	0.064
0.075	No. 200	0.0029	0.005	0.091	0.103	0.053
0.063	No. 230	0.0025	0.004	0.077	0.089	0.044
0.053	No. 270	0.0021	0.004	0.066	0.076	0.037
0.045	No. 325	0.0017	0.003	0.057	0.066	0.030
0.038	No. 400	0.0015	0.003	0.048	0.057	0.025
0.032	No. 450	0.0012	0.003	0.042	0.050	0.028
0.025	No. 500	0.0010	0.003	0.034	0.041	0.025
0.020	No. 635	0.0008	0.003	0.029	0.035	0.020

Table A.7. Hard Conversions

Hard conversions for construction materials

Hard conversion for construction materials			
Structural Steel (M270)			
Grade	Min. tensile strength (MPa)	Min. yield strength (MPa)	Min. yield strength (ksi)
36	400	250	36
50	450	345	50
50W	485	345	50
70W	620	480	70

Reinforcing Bars (M31M)				
Grade		Tensile and yield strengths		
Metric Value	English Value	Tensile strength (MPa)	Min. yield strength (MPa)	Min. yield strength (ksi)
300	40	500	300	40
400	60	600	400	60

Common concrete strengths (f'c)						
Metric (MPa)	20	28	35	43	48	55
English (psi)	3000	4000	5000	6000	7000	8000

Coefficient of thermal expansion		
	Metric value	English value
Steel	0.0000117/°C	0.0000065/°F
Concrete	0.0000108/°C	0.000006/°F

Unit Weights		
	Metric value	English value
Steel	7848.3 kg/m^3	490 pcf
Concrete	2402.5 kg/m^3	150 pcf

Table A.8. The Construction Trades

The Construction Trades

Here are the metric units that will be used by the construction trades. The term "length" includes all linear measurements–length, width, height, thickness, diameter, and circumference.

Quantity	Unit	Symbol
Surveying		
length	kilometer, meter	km, m
area	square kilometer	km^2
	hectare (10,000 m^2)	ha
	square meter	m^2

(continued)

(continued)

Quantity	Unit	Symbol
plane angle	degree (non metric)	°
	minute (non metric)	′
	second (non metric)	″
Excavating		
length	meter, millimeter	m
volume	cubic meter	m^3
Trucking		
distance	kilometer	km
volume	cubic meter	m^3
mass	metric ton (1000 kg)	t
Paving		
length	meter, millimeter	m, mm
area	square meter	m^2
Concrete		
length	meter, millimeter	m, mm
area	square meter	m^2
volume	cubic meter	m^3
temperature	degree Celsius	°C
water capacity	liter (1000 cm)	L
mass (weight)	kilogram, gram	kg, g
cross-sectional area	square millimeter	mm^2

Table A.9. Pipe

Pipe Conversion Factors

Pipe is one of the most ubiquitous products in construction. It is made of a wide variety of materials, including galvanized steel, black steel, copper, cast iron, concrete, and various plastics such as ABS, PVC, CPVC, polyethylene, and polybutylene, among others.

But like wood 2-by-4’s which are not really 2 inches by 4 inches, pipe is identified by “nominal” or “trade” names that are related only loosely to actual dimensions. For instance, a 2-inch galvanized steel pipe has n inside diameter of about 2-1/8 inches and an outside diameter of about 2-5/8 inches. It is called “2-inch pipe” only for the sake of convenience.

Since few, if any, pipe products have actual dimensions that are in even, round inch-pound numbers, there is no need to convert them to even, round metric numbers. Instead, only their names will change–from inch-pound to metric. Pipe cross sections will not change. Fittings, flanges, couplings, valves, and other piping components will be renamed in like manner as will pipe threads. Here are the inch-pound names for pipe products (called NPS or “nominal pipe size”) and their metric equivalents (called DN or “diameter nominal”). The metric names conform to International Standards Organization (ISO) usage and apply to all plumbing, natural gas, heating oil, drainage, and miscellaneous piping used in buildings and civil works projects.

NPS (″)	DN (mm)	NPS (″)	DN (mm)
1/8	6	8	200
3/16	7	10	250
1/4	8	12	300
3/8	10	14	350
1/2	15	16	400
5/8	18	18	450
3/4	20	20	500
1	25	24	600
1–1/4	32	28	700
1–1/2	40	30	750
2	50	32	800
2–1/2	65	36	900
3	80	40	1000
3–1/2	90	44	1100
4	100	48	1200
4–1/2	115	52	1300
5	125	56	1400
6	150	60	1500

For pipe over 60 inches, use 1 inch equals 25 mm

Proposed metric CSP diameter sizes	
Proposed metric (mm)	Current standard (inches)
150	6
200	8
250	10
300	12
375	15
450	18
525	21
600	24
675	27
750	30
825	33

(continued)

(continued)

Proposed metric CSP diameter sizes	
Proposed metric (mm)	Current standard (inches)
900	36
1050	42
1200	48
1350	54
1500	60
1650	66
1800	72
1950	78
2100	84
2250	90
2400	96
2550	102
2700	108
2850	114
3000	120
3150	126
3300	132
3450	138
3600	144

Current (inches)	Corrugation sizes proposed (mm)
2 2/3 × 1/2	68 × 13
3 × 1	76 × 25
5 × 1	125 × 25
3/4 × 3/4 × 7 1/2	19 × 19 × 191
3/4 × 1 × 11 1/2	19 × 25 × 292

Pipe wall thickness		
Current gage	Nominal thickness (inches)	Proposed nominal thickness (mm)
16	0.064	1.6
14	0.079	2.0
12	0.109	2.8
10	0.138	3.5
8	0.168	4.3

Pipe arch sizes			
Corrugations		Corrugations	
inches	(mm)	inches	(mm)
2 2/3 × 1/2	68 × 13	3 × 1 & 5 × 1	76 × 25 & 125 × 25
Span × Rise	Span × Rise	Span × Rise	Span × Rise
17 × 13	425 × 325	53 × 41	1325 × 1025
21 × 15	525 × 375	60 × 46	1500 × 1150
24 × 18	600 × 450	66 × 51	1650 × 1275
28 × 20	700 × 500	73 × 55	1825 × 1375
35 × 24	875 × 600	81 × 59	2025 × 1475
42 × 29	1050 × 725	87 × 63	2175 × 1575
49 × 33	1225 × 825	95 × 67	2375 × 1675
57 × 38	1425 × 950	103 × 71	2575 × 1775
64 × 43	1600 x 1075	112 × 75	2800 × 1875
71 × 47	1775 × 1175	117 × 79	2925 × 1975
77 × 52	1925 × 1300	128 × 83	3200 × 2075
83 × 57	2075 × 1425	137 × 87	3425 × 2175
142 × 91	3550 × 2275		

Note millimeters equal to inches ×25. Assumed pipe diameters will be ×25

Pipe arch sizes	
Corrugations (inches)	Corrugations (mm)
3/4 × 3/4 × 7 1/2	19 × 19 × 191
Span × Rise	Span × Rise
20 × 16	500 × 400
23 × 19	575 × 475
27 × 21	675 × 525
33 × 26	825 × 650
40 × 31	1000 × 775
46 × 36	1150 × 900
53 × 41	1325 × 1025
60 × 46	1500 × 1150
66 × 51	1650 × 1275
73 × 55	1825 × 1375
81 × 59	2025 × 1475
87 × 63	2175 × 1575
95 × 67	2375 × 1675

Note millimeters equal to inches ×25. Assumed pipe diameters will be ×25

Structural plate conversion factors

Structural plate dimensions			
6 × 2 Corrugation			
31 inch corner radius			
Span (ft-in.)	Rise (ft-in.)	R (ft.)	R (ft.)
13–3	9–4	6.68	16.05
14–11	10–2	7.48	18.98
16–6	11–0	8.29	21.93
18–1	11–10	9.09	24.98
19–8	12–8	9.90	28.04

Structural plate dimensions			
152 × 51 Corrugation			
787 mm corner radius (mm)			
Span	Rise	R	R
4039	2845	2036	4892
4547	3099	2280	5785
5029	3353	2527	6684
5512	3607	2771	7614
5994	3861	3018	8547

Structural plate thickness		
Current specification		Proposed
Gage	Inches	Millimeters
12	0.111	2.5
10	0.140	3.5
8	0.170	4.5
7	0.188	–
5	0.218	5.5
3	0.249	6.5
1	0.280	7.0
5/16	0.318	8.0
3/8	0.377	9.5

Appendix 2
Munitions and Dual-Use Items

Items, information, and software subject to US Export Control Laws and used in a university environment are generally categorized on the following two lists:

US Munitions List (USML)—(ITAR)

Published by the US State Department in its International Traffic in Arms Regulations (ITAR):

- Category I
  Firearms, Close Assault Weapons, and Combat Shotguns
- Category II
  Materials, Chemicals, Microorganisms, and Toxins
- Category III
  Ammunition/Ordnance
- Category IV
  Launch Vehicles, Guided Missiles, Ballistic Missiles, Rockets, Torpedoes, Bombs, and Mines
- Category V
  Explosives and Energetic Materials, Propellants, Incendiary Agents, and Their Constituents
- Category VI
  Vessels of War and Special Naval Equipment
- Category VII
  Tanks and Military Vehicles
- Category VIII
  Aircraft and Associated Equipment
- Category IX
  Military Training Equipment
- Category X
  Protective Personnel Equipment

D.S. Viswanath et al., *Emerging Energetic Materials: Synthesis, Physicochemical, and Detonation Properties*, https://doi.org/10.1007/978-94-024-1201-7

- Category XI
  Military Electronics
- Category XII
  Fire Control, Range Finder, Optical, Guidance, and Control Equipment
- Category XIII
  Auxiliary Military Equipment
- Category XIV
  Toxicological Agents, Including Chemical Agents, Biological Agents, and Associated Equipment
- Category XV
  Spacecraft Systems and Associated Equipment
- Category XVI
  Nuclear Weapons, Design, and Testing Related Items
- Category XVII
  Classified Articles, Technical Data, and Defense Services Not Otherwise Enumerated
- Category XVIII
  Directed Energy Weapons
- Category XX
  Submersible Vessels, Oceanographic, and Associated Equipment

Commerce Control List (CCL)—(EAR)

Published by the US Commerce Department in its Export Administration Regulations (EAR)

- Category 0
  Nuclear Materials, Facilities and Equipment (and Miscellaneous Items)
- Category 1
  Materials, Chemicals, Microorganisms, and Toxins
- Category 2
  Materials Processing
- Category 3
  Electronics Design, Development, and Production
- Category 4
  Computers
- Category 5
  Part 1: Telecommunications
  Part 2: Information Security
- Category 6
  Sensors and Lasers
- Category 7
  Navigation and Avionics

- Category 8
  Marine
- Category 9
  Propulsion Systems, Space Vehicles, and Related Equipment

Pathogens and Toxins

Department of Commerce dual-use export control-listed pathogens and toxins are listed below. These pathogens and toxins are found on the Commerce Control List (CCL) in Category 1 at ECCNs 1C351 through 1C360. Please note that export controls also apply to genetic elements and genetically modified organisms that contain DNA associated with the pathogenicity of these biological materials. Severe civil and/or criminal penalties apply to international shipments without an export license of ANY export controlled pathogen or genetic material containing the controlled DNA.

You will need to contact Stanford's Export Control Officer if your research requires an export controlled pathogen or genetic material containing the controlled DNA to be sent outside of the US so that an export license application can be prepared. Export licenses take 4–6 weeks for approval, so please plan in advance.

Also note that the International Traffic in Arms Regulations (ITAR) controls certain military-related toxins and pathogens at Category XIV of the US Munitions List (USML). The ITAR treats as a defense article any "biological agent or biologically derived substance specifically developed or modified to increase its capability to produce casualties in humans or livestock or to degrade equipment or damage crops." These ITAR export control-listed biological materials will also require an export license. Furthermore, foreign nationals may not access ITAR-controlled biological materials or their disclosure-restricted technologies in the US without government approval.

In the unlikely event that you need access to a disclosure-restricted ITAR controlled biological material or its technology at Stanford, you must first contact Steve Eisner as required by the RPH Chapter: Export Control before receipt.

A
African horse sickness virus
African swine fever virus
Andean potato latent virus (Potato Andean latent tymovirus)
Andes virus
Avian Influenza identified as having high pathogenicity

Toxins
Abrin
Aflatoxins

B
Bacillus anthracis
Blue Tongue virus
Brucella abortus
Brucella melitensis
Brucella suis
Burkholderia mallei (Pseudomonas mallei)
Burkholderia pseudomallei

Toxins
Botulinum toxins

C
Chapare virus
Chikungunya virus
Chlamydophilia psittaci (Chlamydia psittaci)
Choclo virus
Clavibacter michiganensis subspecies sepedonicus (Corynebacterium sepedonicum)
Clostridium Argentinense, botulinum neurotoxin producing strains (Clostricium botulinum Type G)
Clostridium baratii, botulinum neurotoxin producing strains
Clostridium botulinum
Clostridium butyricum
Clostridium perfringens (epsilon toxin producing type)
Coccidioides immitis
Coccidioides posadasii
Cochliobolus miyabeanus (Helminthosporium oryzae)
Colletotrichum kahawae (Colleototrichum coffeanum var. virulans)
Congo-Crimean haemorrhagic fever virus
Coxiella burnetii

Toxins
Cholera toxin
Clostridium perfringens toxin
Conotoxins

D
Dengue fever virus
Dobrava-Belgrade virus

Toxins
Diacetoxyscirpenol toxin

E
Eastern equine encephalitis virus
Ebola virus

F
Foot and Mouth Disease virus
Francisella tularensis

G
Goat Pox virus
Guanarito virus

H
Hantaan virus
Hendra virus

Toxins
HT-2 toxin

I
none listed

J
Japanese Encephalitis virus
Junin virus

K
Kyasanur Forest virus

L
Laguna Negra virus
Lassa fever virus
Louping Ill virus
Lujo virus
Lumpy Skin Disease virus
Lymphocytic choriomeningitis virus
Lyssa virus

M

Machupo virus
Magnaporthea grisea (Pyricularia oryzae)
Marburg virus
Microcyclus ulei (Dothidella ulei)
Monkeypox virus
Murray Valley encephalitis virus
Mycoplasma capricolum subspecies capripneumonaie (strain F38)
Mycoplasma mycoides subspecies mycoides small colony (contagious bovine pleuroneumo nia)

Toxins

Microcystin (Cyanginosin)
Modeccin toxin

N

Newcastle disease virus
Nipah virus

O

Omsk haemorrhagic fefer virus
Oropouche Virus

P

Peronosclerospora philippinensis (Peronosclerospora sacchari)
Peste des Petitis Ruminants virus
Phoma glycinicola (Pyrenochaeta glycines)
Porcine enterovirus type 9 (swine vesicular disease virus)
Porcine herpes virus (Aujeszky's disease)
Potato spindle tuber viroid
Powassan virus
Puccinia Graminis (Puccinia graminis f. sp. Tritici)
Puccinia striiformis (Puccinia glumarum)

Q

none listed

R
Ralstonia solanacearum Race 3, biovar 2
Rathayibacter toxicus
Reconstructed replication competent forms of the 1918 pandemic influenza virus containing any portion of the coding regions of all eight gene sement
Rickettsia prowazekii
Rift Valley fever virus
Rinderpest virus
Rocio virus

Toxins
Ricin

S
Sabia virus
Salmonella typhi
SARS-associated coronavirus (SARS-CoV)
Sclerophthora rayssiae var.zeae
Seoul virus
Sheep Pox virus
Shigella dysenteriae
Sin Nombre virus
St. Louis encephalitis
Swine Fever virus (Hog cholera virus)
Synchytrium endobioticum

Toxins
Saxitoxin
Shiga toxin
Shiga toxin producing Escherichia coli (STEC) of serogroups 026, 045, 0103, 0104, 0111, 0121, 0145, 0157, and other shiga toxin producing serogoups (EGEC or VTEC)
Staphylococcus aureus enterotoxins, hemolysin alpha toxin, and toxic shock syndrome toxin (Staphylococcus enterotoxin F)

T
Teschen Disease virus
Thecaphora solani
Tick-borne encephalitis virus (Far Eastern Subtype)
Tick-borne encephalitis virus (Siberian Subtype)
Tilletia indica

Toxins
T-2 toxin
Tetrodotoxin

U
None listed

V
Variola virus
Venezuelan Equine Encephalitis virus
Vesicular stomatitis virus
Vibrio cholerae

Toxins
Verotoxin and other Shiga-like ribosome inactivating proteins
Viscum Album Lectin 1 (Viscumin)
Volkensin toxin

W, X, Y, Z
Western Equine Encephalitis virus
Xanthmonas alibilineans
Xanthmonas axonopodis pv. Citri (Xanthomonas campestris pv. citri)
Xanthomonas oryzae pv. Oryzae (Pseudomonas campestris pv. Oryzae)
Yellow fever virus
Yersinia pestis

*AI viruses that have an intravenous pathogenicity index in 6-week-old chickens greater than 1.2; AI viruses that cause at least 75% mortality in 4–8 week old chickens infected intravenously; AI viruses of the H5 or H7 should be submitted to further testing.

Chemicals, Chemical Agent Precursors, Propellants, Explosives, and Energetic Materials

The ITAR controls certain military-related chemicals, chemical agent precursors, propellants, explosives and energetic materials at Category V and Category XIV of the US Munitions List (USML). In addition, under the provisions of the International Chemical Weapons Convention, the United States may require special declarations related to chemical shipments under either the ITAR or the EAR. For your convenience, we've created this reference list.

Appendix 3
Chemical Weapons Convention (CWC)

Chemical Weapons Convention (CWC) Schedule 2 and 3 chemicals and families of chemicals not controlled by ECCN 1C350 or by the Department of State under the ITAR.

a. **CWC Schedule 2 chemicals and mixtures containing Schedule 2 chemicals**:

  a.1. Toxic chemicals, as follows, and mixtures containing toxic chemicals:

    a.1.a. PFIB: 1,1,3,3,3-Pentafluoro-2-(trifluoromethyl)-1-propene (C.A.S. 382-21-8) and mixtures in which PFIB constitutes more than 1% of the weight of the mixture;
    a.1.b. [RESERVED].

  a.2. Precursor chemicals, as follows, and mixtures in which at least one of the following precursor chemicals constitutes more than 10% of the weight of the mixture:

    a.2.a. Chemicals, except for those listed in Schedule 1, containing a phosphorus atom to which is bonded one methyl, ethyl, or propyl (normal or iso) group but not further carbon atoms.

Note: 1C355.a.2.a does not control Fonofos: O-Ethyl S-phenyl ethylphosphonothiolothionate (C.A.S. 944-22-9).

  a.2.b. FAMILY: N,N-Dialkyl (Me, Et, n-Pr or i-Pr) phosphoramidic dihalides;
  a.2.c. FAMILY: Dialkyl (Me, Et, n-Pr or i-Pr) N,N-dialkyl (Me, Et, n-Pr, or i-Pr)-phosphoramidates;
  a.2.d. FAMILY: N,N-Dialkyl (Me, Et, n-Pr or i-Pr) aminoethyl-2-chlorides and corresponding protonated salts;
  a.2.e. FAMILY: N,N-Dialkyl (Me, Et, n-Pr or i-Pr) aminoethane-2-ols and corresponding protonated salts;

Note: 1C355.a.2.e. does not control N,N-Dimethylaminoethanol and corresponding protonated salts (C.A.S. 108-01-0) or N,N-Diethylaminoethanol and corresponding protonated salts (C.A.S. 100-37-8).

D.S. Viswanath et al., *Emerging Energetic Materials: Synthesis, Physicochemical, and Detonation Properties*, https://doi.org/10.1007/978-94-024-1201-7

a.2.f. FAMILY: N,N-Dialkyl (Me, Et, n-Pr or i-Pr) aminoethane-2-thiols and corresponding protonated salts.

b. **CWC Schedule 3 chemicals and mixtures containing Schedule 3 chemicals**:

b.1. Toxic chemicals, as follows, and mixtures in which at least one of th following toxic chemicals constitutes 30% or more of the weight of the mixture:

b.1.a. Phosgene: Carbonyl dichloride (C.A.S. 75-44-5);

b.1.b. Cyanogen chloride (C.A.S. 506-77-4);
b.1.c. Hydrogen cyanide (C.A.S. 74-90-8);
b.1.d. Chloropicrin: Trichloronitromethane (CAS 76-06-2).

b.2. Precursor chemicals, as follows, and mixtures in which at least one of the following precursor chemicals constitutes 30% or more of the weight of the mixture:

b.2.a. [RESERVED];
b.2.b. Methyldiethanolamine (C.A.S. 105-59-9).

Category V—Explosives and Energetic Materials, Propellants, Incendiary Agents and Their Constituents

*(a) Explosives, and mixtures thereof:

(1) ADNBF (aminodinitrobenzofuroxan or 7-Amino 4,6-dinitrobenzofurazane-1-oxide) (CAS 97096.–78.–1);
(2) BNCP (cis-bis (5-nitrotetrazolato) tetra amine-cobalt (III) perchlorate) (CAS 117412.–28.–9);
(3) CL.–14 (diamino dinitrobenzofuroxan or 5,7-diamino-4,6-dinitrobenzofurazane-1-oxide) (CAS 117907.–74.–1);
(4) CL.–20 (HNIW or Hexanitrohexaazaisowurtzitane); (CAS 135285.–90-4); chlathrates of CL.–20 (see paragraphs (g)(3) and (4) of this category);
(5) CP (2-(5-cyanotetrazolato) penta aminecobalt (III) perchlorate); (CAS 70247.–32.–4);
(6) DADE (1,1-diamino-2,2-dinitroethylene, FOX7);
(7) DDFP (1,4-dinitrodifurazanopiperazine);
(8) DDPO (2,6-diamino-3,5-dinitropyrazine-1-oxide, PZO); (CAS 194486.–77.–6);
(9) DIPAM (3,3′-Diamino-2,2′,4,4′,6,6′-hexanitrobiphenyl or dipicramide) (CAS 17215.–44.–0);
(10) DNGU (DINGU or dinitroglycoluril) (CAS 55510.–04.–8);

(11) Furazans, as follows:

  (i) DAAOF (diaminoazoxyfurazan);
  (ii) DAAzF (diaminoazofurazan) (CAS 78644.–90.–3);

(12) HMX and derivatives (see paragraph (g)(5) of this category):

  (i) HMX (Cyclotetramethylenetetranitramine; octahydro-1,3,5,7 tetranitro-1,3,5,7-tetrazine; 1,3,5,7-tetranitro-1,3,5,7-tetraza-cyclooctane; octogen, octogene) (CAS 2691.41.–0);
  (ii) Diflouroaminated analogs of HMX;
  (iii) K.–55 (2,4,6,8-tetranitro-2,4,6,8-tetraazabicyclo [3,3,0]-octanone-3, tetranitrosemiglycouril,or keto-bicyclic HMX) (CAS 130256-72.–3);

(13) HNAD (hexanitroadamantane) (CAS 143850.–71.–9);
(14) HNS (hexanitrostilbene) (CAS 20062.–22.–0);
(15) Imidazoles, as follows:

  (i) BNNII (Octohydro-2,5-bis(nitroimino) imidazo [4,5-d]Imidazole);
  (ii) DNI (2,4-dinitroimidazole) (CAS 5213.–49.–0);
  (iii) FDIA (1-fluoro-2,4-dinitroimidazole);
  (iv) NTDNIA (N-(2-nitrotriazolo)-2,4-dinitro-imidazole);
  (v) PTIA (1-picryl-2,4,5-trinitroimidazole);

(16) NTNMH (1-(2-nitrotriazolo)-2-dinitromethylene hydrazine);
(17) NTO (ONTA or 3-nitro-1,2,4-triazol-5-one) (CAS 932.–64.–9);
(18) Polynitrocubanes with more than four nitro groups;
(19) PYX (2,6-Bis(picrylamino)-3,5-dinitropyridine) (CAS 38082.–89.–2);
(20) RDX and derivatives:

  (i) RDX (cyclotrimethylenetrinitramine), cyclonite, T4, hexahydro-1,3,5-trinitro-1,3,5-triazine,1,3,5-trinitro-1,3,5-triaza-cyclohexane, hexogen, or hexogene) (CAS 121.–82.–4);
  (ii) Keto-RDX (K.–6 or 2,4,6-trinitro-2,4,6-triazacyclohexanone (CAS 115029.–35.–1);

(21) TAGN (Triaminoguanidinenitrate) (CAS 4000.–16.–2);
(22) TATB (Triaminotrinitrobenzene) (CAS 3058.–38.–6) (see paragraph (g)(7) of this category);
(23) TEDDZ (3,3,7,7-tetrabis(difluoroamine) octahydro-1,5-dinitro-1,5-diazocine;
(24) Tetrazoles, as follows:

  (i) NTAT (nitrotriazol aminotetrazole);
  (ii) NTNT (1-N-(2-nitrotriazolo)-4-nitrotetrazole);

(25) Tetryl (trinitrophenylmethylnitramine) (CAS 479.–45.–8);
(26) TNAD (1,4,5,8-tetranitro-1,4,5,8-tetraazadecalin) (CAS 135877-16.–6)(see paragraph (g)(6) of this category);

(27) TNAZ (1,1,3-trinitroazetidine) (CAS 97645.–24.–4) (see paragraph (g)(2) of this category);
(28) TNGU (SORGUYL or tetranitroglycoluril) (CAS 55510.–03.–7);
(29) TNP (1,4,5,8-tetranitro-pyridazino [4,5-d] pyridazine) (CAS 229176.–04.–9);
(30) Triazines, as follows:

  (i) DNAM (2-oxy-4,6-dinitroamino-s-triazine) (CAS 19899.–80.–0);
  (ii) NNHT (2-nitroimino-5-nitro-hexahydro-1,3,5 triazine) (CAS 130400.–13.–4);

(31) Triazoles, as follows:

  (i) 5-azido-2-nitrotriazole;
  (ii) ADHTDN (4-amino-3,5-dihydrazino-1,2,4-triazole dinitramide) (CAS 1614.–08.–0);
  (iii) ADNT (1-amino-3,5-dinitro-1,2,4-triazole);
  (iv) BDNTA ([Bis-dinitrotriazole]amine);
  (v) DBT (3,3☐-dinitro-5,5-bi-1,2,4-triazole) (CAS 30003.–46.–4);
  (vi) DNBT (dinitrobistriazole) (CAS 70890.–46.–9);
  (vii) NTDNA (2-nitrotriazole 5-dinitramide) (CAS 75393.–84.–9);
  (viii) NTDNT (1-N-(2-nitrotriazolo) 3,5-dinitro-triazole);
  (ix) PDNT (1-picryl-3,5-dinitrotriazole);
  (x) TACOT (tetranitrobenzotriazolobenzotriazole) (CAS 25243.–36.–1);

(32) Any explosive not listed elsewhere in paragraph (a) of this category with a detonation velocity exceeding 8700 m/s at maximum density or a detonation pressure exceeding 34 Gpa (340 kbar).
(33) Other organic explosives not listed elsewhere in paragraph (a) of this category yielding detonation pressures of 25 Gpa (250 kbar) or more that will remain stable at temperatures of 523 K (250 °C) or higher for periods of 5 min or longer;
(34) Diaminotrinitrobenzene (DATB) (CAS 1630.–08.–6);
(35) Any other explosive not elsewhere identified in this category specifically designed, modified, adapted, or configured (e.g., formulated) for military application.

***(b) Propellants**:

(1) Any United Nations (UN) Class 1.1 solid propellant with a theoretical specific impulse (under standard conditions) of more than 250 s for non-metallized, or 270 s for metalized compositions;
(2) Any UN Class 1.3 solid propellant with a theoretical specific impulse (under standard conditions) of more than 230 s for non-halogenized, or 250 s for non-metallized compositions;
(3) Propellants having a force constant of more than 1200 kJ/Kg;

(4) Propellants that can sustain a steady-state burning rate more than 38 mm/s under standard conditions (as measured in the form of an inhibited single strand) of 6.89 Mpa (68.9 bar) pressure and 294 K (21 °C);
(5) Elastomer modified cast double based propellants with extensibility at maximum stress greater than 5% at 233 K (40 C);
(6) Any propellant containing substances listed in Category V;
(7) Any other propellant not elsewhere identified in this category specifically designed, modified, adapted, or configured (e.g., formulated) for military application.

(c) **Pyrotechnics, fuels and related substances, and mixtures thereof**:

(1) Alane (aluminum hydride)(CAS 7784.–21.–6);
(2) Carboranes; decaborane (CAS 17702.–41.–9); pentaborane and derivatives thereof;
(3) Hydrazine and derivatives:

    (i) Hydrazine (CAS 302.–01.–2) in concentrations of 70% or more (not hydrazine mixtures specially formulated for corrosion control);
    (ii) Monomethyl hydrazine (CAS 60.–34.–4);
    (iii) Symmetrical dimethyl hydrazine (CAS 540.–73.–8);
    (iv) Unsymmetrical dimethyl hydrazine (CAS 57.–14.–7);

(4) Liquid fuels specifically formulated for use by articles covered by Categories IV, VI, and VIII;
(5) Spherical aluminum powder (CAS 7429.–90.–5) in particle sizes of 60 micrometers or less manufactured from material with an aluminum content of 99% or more;
(6) Metal fuels in particle form whether spherical, atomized, spheroidal, flaked or ground, manufactured from material consisting of 99% or more of any of the following:

    (i) Metals and mixtures thereof:

        (a) Beryllium (CAS 7440.–41.–7) in particle sizes of less than 60 micrometers;
        (b) Iron powder (CAS 7439.–89.–6) with particle size of 3 m crome ters or less produced by reduction of iron oxide with hydrogen;

    (ii) Mixtures, which contain any of the following:

        (a) Boron (CAS 7440.–42.–8) or boron carbide (CAS 12069.–32.–8) fuels of 85% purity or higher and particle sizes of less than 60 micrometers;
        (b) Zirconium (CAS 7440.–67.–7), magnesium (CAS 7439.–95.–4 or alloys of these in particle sizes of less than 60 micrometers;

    (iii) Explosives and fuels containing the metals or alloys listed in paragraphs (c)(6)(i) and(c)(6)(ii) of this category whether or not the metals or alloys are encapsulated in aluminum, magnesium, zirconium, or beryllium;

(7) Pyrotechnics and pyrophoric materials specifically formulated for military purposes to enhance or control the production of radiated energy in any part of the IR spectrum.
(8) Titanium subhydride (TiHn) of stoichiometry equivalent to n = 0.65.–1.68;
(9) Military materials containing thickeners for hydrocarbon fuels specially formulated for use in flame throwers or incendiary munitions; metal stearates or palmates (also known as octol); and M1, M2 and M3 thickeners;
(10) Any other pyrotechnic, fuel and related substance and mixture thereof not elsewhere identified in this category specifically designed, modified, adapted, or configured (e.g., formulated) for military application.

(d) **Oxidizers, to include**:
(1) ADN (ammonium dinitramide or SR.–12) (CAS 140456.–78.–6);
(2) AP (ammonium perchlorate) (CAS 7790.–98.–9);
(3) BDNPN (bis,2,2-dinitropropylnitrate) (CAS 28464.–24.–6);
(4) DNAD (1,3-dinitro-1,3-diazetidine) (CAS 78246.–06.–7);
(5) HAN (Hydroxylammonium nitrate) (CAS 13465.–08.–2);
(6) HAP (hydroxylammonium perchlorate) (CAS 15588.–62.–2);
(7) HNF (Hydrazinium nitroformate) (CAS 20773.–28.–8);
(8) Hydrazine nitrate (CAS 37836.–27.–4);
(9) Hydrazine perchlorate (CAS 27978.–54.–7);
(10) Liquid oxidizers comprised of or containing inhibited red fuming nitric acid (IRFNA) (CAS 8007.–58.–7) or oxygen diflouride;
(11) Perchlorates, chlorates, and chromates composited with powdered metal or other high energy fuel components controlled by this category;
(12) Any other oxidizer not elsewhere identified in this category specifically designed, modified, adapted, or configured (e.g., formulated) for military application.

***(e) Binders, and mixtures thereof**:

(1) AMMO (azidomethylmethyloxetane and its polymers) (CAS 90683.–29.–7) (see paragraph (g)(1) of this category);
(2) BAMO (bisazidomethyloxetane and its polymers) (CAS 17607.–20.–4) (see paragraph (g)(1)of this category);
(3) BTTN (butanetrioltrinitrate) (CAS 6659.–60.–5) (see paragraph (g)(8) of this category);

(4) FAMAO (3-difluoroaminomethyl-3-azidomethyl oxetane) and its polymers;
(5) FEFO (bis-(2-fluoro-2,2-dinitroethyl)formal) (CAS 17003.–79.–1);
(6) GAP (glycidylazide polymer) (CAS 143178.–24.–9) and its derivatives;
(7) HTPB (hydroxyl terminated polybutadiene) with a hydroxyl functionality equal to or greater than 2.2 and less than or equal to 2.4, a hydroxyl value of less than 0.77 meq/g, and a viscosity at 30 °C of less than 47 poise (CAS 69102.–90.–5);
(8) NENAS (nitratoethylnitramine compounds) (CAS 17096.–47.–8, 85068-73.–1 and 82486.–82.–6);
(9) Poly-NIMMO (poly nitratomethylmethyoxetane, poly-NMMO, (poly [3-nitratomethyl-3-methyl oxetane]) (CAS 84051.–81.–0);
(10) Energetic monomers, plasticizers and polymers containing nitro, azido nitrate, nitraza or difluoromaino groups specially formulated for military use;
(11) TVOPA 1,2,3-Tris [1,2-bis(difluoroamino) ethoxy]propane; tris vinoxy propane adduct; (CAS 53159.–39.–0);
(12) Polynitrorthocarbonates;
(13) FPF.–1 (poly-2,2,3,3,4,4-hexafluoro pentane-1,5-diolformal) (CAS 376.–90.–9);
(14) FPF.–3 (poly-2,4,4,5,5,6,6-heptafluoro-2-trifluoromethyl-3-oxaheptane-1,7-diolformal);
(15) PGN (Polyglycidylnitrate or poly(nitratomethyl oxirane); poly-GLYN); (CAS 27814.–48.–8);
(16) N-methyl-p-nitroaniline;
(17) Low (less than 10,000) molecular weight, alcohol-functionalized, poly (epichlorohydrin); poly(epichlorohydrindiol); and triol;
(18) Bis(2,2-dinitropropyl) formal and acetal;
(19) Any other binder and mixture thereof not elsewhere identified in this category specifically designed, modified, adapted, or configured (e.g., formulated) for military application.

(f) **Additives**:
(1) Basic copper salicylate (CAS 62320.–94.–9);
(2) BHEGA (Bis-(2-hydroxyethyl)glycolamide) (CAS 17409.–41.–5);
(3) Ferrocene Derivatives:

  (i) Butacene (CAS 125856.–62.–4);
  (ii) Catocene (2,2-Bis-ethylferrocenyl propane) (CAS 37206.–42.–1);
  (iii) Ferrocene carboxylic acids;
  (iv) n-butyl-ferrocene (CAS 31904.–29.–7);

(4) Lead beta-resorcylate (CAS 20936.–32.–7);
(5) Lead citrate (CAS 14450.–60.–3);
(6) Lead-copper chelates of beta-resorcylate or salicylates (CAS 68411.–07.–4);
(7) Lead maleate (CAS 19136.–34.–6);
(8) Lead salicylate (CAS 15748.–73.–9);

(9) Lead stannate (CAS 12036.–31.–6);

(10) MAPO (tris-1-(2-methyl)aziridinyl phosphine oxide) (CAS 57.–39.–6); BOBBA.–8 (bis(2-methyl aziridinyl) 2-(2-hydroxypropanoxy) propylamino phosphine oxide); and other MAPO derivatives;

(11) Methyl BAPO (Bis(2-methyl aziridinyl) methylamino phosphine oxide) (CAS 85068.–72.–0);

(12) (12) 3-Nitraza-1,5 pentane diisocyanate (CAS 7406.–61.–9);

(13) Organo-metallic coupling agents, specifically:

  (i) Neopentyl[diallyl]oxy, tri [dioctyl] phosphatotitanate (CAS 103850.–22.–2); also known as titanium IV, 2,2[bis 2-propenolato-methyl, butanolato, tris (dioctyl) phosphato] (CAS 110438.– 25.–0), or LICA 12 (CAS 103850.–22.–2);

  (ii) Titanium IV, [(2-propenolato-1) methyl, n-propanolatomethyl] butanolato-1, tris(dioctyl)pyrophosphate, or KR3538;

  (iii) Titanium IV, [2-propenolato-1)methyl, propanolatomethyl] butanolato-1, tris(dioctyl) phosphate;

(14) Polyfunctional aziridine amides with isophthalic, trimesic (BITA or butylene imine trimesamide), isocyanuric, or trimethyladipic backbone structures and 2-methyl or 2-ethyl substitutions on the aziridine ring and its polymers;

(15) Superfine iron oxide (Fe_2O_3 hematite) with a specific surface area more than 250 m^2/g and an average particle size of 0.003 [micro]m or less (CAS 1309.–37.–1);

(16) TEPAN (tetraethylenepentaamineacrylonitrile) (CAS 68412.–45.–3); cyanoethylated polyamines and their salts;

(17) TEPANOL (Tetraethylenepentaamineacrylo-nitrileglycidol) (CAS 110445.–33.–5); cyanoethylated polyamines adducted with glycidol and their salts;

(18) TPB (triphenyl bismuth) (CAS 603.–33.–8);

(19) PCDE (Polycyanodifluoroaminoethyleneoxide);

(20) BNO (Butadienenitrileoxide);

(21) Any other additive not elsewhere identified in this category specifically designed, modified, adapted, or configured (e.g., formulated) for military application.

(g) **Precursors, as follows**:

(1) BCMO (bischloromethyloxetane) (CAS 142173.–26.–0) (see paragraphs (e)(1) and (2) of this category);

(2) Dinitroazetidine-t-butyl salt (CAS 125735.–38.–8) (see paragraph (a)(27) of this category);

(3) HBIW (hexabenzylhexaazaisowurtzitane) (CAS 124782.–15.–6) (see paragraph (a)(4) of this category);

(4) TAIW (tetraacetyldibenzylhexa-azaisowurtzitane) (see paragraph (a)(4) of this category);

(5) TAT (1, 3, 5, 7-tetraacetyl-1, 3, 5, 7-tetraaza-cyclooctane) (CAS 41378.–98.–7) (see paragraph (a)(12) of this category);
(6) Tetraazadecalin (CAS 5409.–42.–7) (see paragraph (a)(26) of this category);
(7) 1,3,5-trichorobenzene (CAS 108.–70.–3) (see paragraph (a)(22) of this category);
(8) 1,2,4-trihydroxybutane (1,2,4-butanetriol) (CAS 3068.–00.–6) (see paragraph (e)(3) of this category);

(i) The following interpretations explain and amplify the terms used in this category and elsewhere in this subchapter.

(1) Category V contains explosives, energetic materials, propellants and pyrotechnics and specially formulated fuels for aircraft, missile and naval applications. Explosives are solid, liquid or gaseous substances or mixtures of substances, which, in their primary, booster or main charges in warheads, demolition or other military applications, are required to detonate.
(2) Paragraph (c)(6)(ii)(A) of this category does not control boron and boron carbide enriched with boron-10 (20% or more of total boron-10 content.
(3) The resulting product of the combination of any controlled or non-controlled substance compounded or mixed with any item controlled by this subchapter is also subject to the controls of this category.

Note 1: To assist the exporter, an item has been categorized by the most common use. Also, a reference has been provided to the related controlled precursors (e.g., see paragraph (a)(12) of this category). Regardless of where the item has been placed in the category, all exports are subject to the controls of this subchapter.
Note 2: Chemical Abstract Service (CAS) registry numbers do not cover all the substances and mixtures controlled by this category. The numbers are provided as examples to assist the government agencies in the license review process and the exporter when completing their

ECCN 1C350 Chemicals that may be used as precursors for toxic chemical agents.

b. Australia Group-controlled precursor chemicals also identified as Schedule 2 chemicals under the CWC, as follows, and mixtures in which at least one of the following chemicals constitutes 30% or more of the weight of the mixture:

b.1. (C.A.S. #7784-34-1) Arsenic trichloride;
b.2. (C.A.S. #76-93-7) Benzilic acid;
b.3. (C.A.S. #78-38-6) Diethyl ethylphosphonate;
b.4. (C.A.S. #15715-41-0) Diethyl methylphosphonite;
b.5. (C.A.S.#2404-03-7) Diethyl-N,N-dimethylphosphoroamidate;
b.6. (C.A.S. #5842-07-9) N,N-Diisopropyl-beta-aminoethane thiol;

b.7. (C.A.S. #4261-68-1) N,N-Diisopropyl-beta-aminoethyl chloride hydrochloride;
b.8. (C.A.S. #96-80-0) N,N-Diisopropyl-beta-aminoethanol;
b.9. (C.A.S. #96-79-7), N,N-Diisopropyl-beta-aminoethyl chloride;
b.10. (C.A.S. #6163-75-3) Dimethyl ethylphosphonate;
b.11. (C.A.S. #756-79-6) Dimethyl methylphosphonate;
b.12. (C.A.S. #1498-40-4) Ethyl phosphonous dichloride [Ethyl phosphinyl di chloride;
b.13. (C.A.S. #430-78-4) Ethyl phosphonus difluoride [Ethyl phosphinyl difluoride];
b.14. (C.A.S. #1066-50-8) Ethyl phosphonyl dichloride;
b.15. [RESERVED]
b.16. [RESERVED]
b.17. [RESERVED]
b.18. (C.A.S. #464-07-3) Pinacolyl alcohol;
b.19. (C.A.S. #1619-34-7) 3-Quinuclidinol;
b.20. (C.A.S. #111-48-8) Thiodiglycol;
b.21. (C.A.S. #993-13-5) Methylphosphonic acid;
b.22. (C.A.S. #683-08-9) Diethyl methylphosphonate;
24. b.23. (C.A.S. #677-43-0) N,N-dimethylamino-phosphoryl dichloride;
b.24. (C.A.S. #676-98-2) Methylphosphonothioic dichloride.

c. Australia Group-controlled precursor chemicals also identified as Schedule 3 chemicals under the CWC, as follows, and mixtures in which at least one of the following chemicals constitutes 30% or more of the weight of the mixture:
c.1. (C.A.S. #762-04-9) Diethyl phosphite;
c.2. (C.A.S. #868-85-9) Dimethyl phosphate (dimethyl hydrogen phosphite);
c.3. (C.A.S. #10025-87-3) Phosphorus oxychloride;
c.4. (C.A.S. #10026-13-8) Phosphorus pentachloride;
c.5. (C.A.S. #7719-12-2) Phosphorus trichloride;
c.6. (C.A.S. #10025-67-9) Sulfur monochloride;
c.7. (C.A.S. #10545-99-0) Sulfur dichloride;
c.8. (C.A.S. #7719-09-7) Thionyl chloride;
c.9. (C.A.S. #102-71-6) Triethanolamine;
c.10. (C.A.S. #122-52-1) Triethyl phosphite;
c.11. (C.A.S. #121-45-9) Trimethyl phosphite
c.12. (C.A.S. #139-87-7) Ethyldiethanolamine.

d. Other Australia Group-controlled precursor chemicals not also identified as Schedule 1, 2, or 3 chemicals under the CWC, as follows, and mixtures in which at least one of the following chemicals constitutes 30% or more of the weight of the mixture:

d.1. (C.A.S. #1341-49-7) Ammonium hydrogen fluoride;
d.2. (C.A.S. #107-07-3) 2-Chloroethanol;
d.3. (C.A.S. #100-37-8) N,N-Diethylaminoethanol;
d.4. (C.A.S. #108-18-9) Di-isopropylamine;
d.5. (C.A.S. #124-40-3) Dimethylamine;
d.6. (C.A.S. #506-59-2) Dimethylamine hydrochloride;
d.7. (C.A.S. #7664-39-3) Hydrogen fluoride;
d.8. (C.A.S. #3554-74-3) 3-Hydroxyl-1-methylpiperidine;
d.9. (C.A.S. #76-89-1) Methyl benzilate;
d.10. (C.A.S. #1314-80-3) Phosphorus pentasulfide;
d.11. (C.A.S. #75-97-8) Pinacolone;
d.12. (C.A.S. #151-50-8) Potassium cyanide;
d.13. (C.A.S. #7789-23-3) Potassium fluoride;
d.14. (C.A.S. #7789-29-9) Potassium bifluoride;
d.15. (C.A.S. #3731-38-2) 3-Quinuclidone;
d.16. (C.A.S. #1333-83-1) Sodium bifluoride;
d.17. (C.A.S. #143-33-9) Sodium cyanide;
d.18. (C.A.S. #7681-49-4) Sodium fluoride;
d.19. (C.A.S. #1313-82-2) Sodium sulfide;
d.20. (C.A.S. #637-39-8) Triethanolamine hydrochloride;
d.21. (C.A.S. #116-17-6) Tri-isopropyl phosphite;
d.22. (C.A.S. #2465-65-8) O,O-diethyl phosphorothioate;
d.23. (C.A.S. #298-06-6) O,O-diethyl phosphorodithioate;
d.24. (C.A.S. #16893-85-9) Sodium hexafluorosilicate.

Appendix 4
Chemical Weapons Convention Bulletin

News, Background and Comment on Chemical and Biological Warfare Issues ISSUE NO. 21 SEPTEMBER 1993 Quarterly Journal of the Harvard Sussex Program on CBW Armament and Arms Limitation

Guest Article by Dr. RJ Mathews 1–3

CWC Non-Signatory States 3

Progress in The Hague: Quarterly Review 4–9 Editorial comment: The AG and the CWC 5 Forthcoming events 9.

News Chronology: May–August 1993 10–27 New Board Member 17 Obituary: Charles Flowerree 22 Recent Publications 27–28 Particular chemicals or families of chemicals have been placed on one of the three CWC schedules based on a number of factors, including the risk that the particular chemical poses to the objectives of the CWC, and, in the case of commercially produced chemicals, on the practicality of subjecting the chemical to a particular monitoring regime. A major factor in the development of these schedules has been the recognition that it would be impractical, and in many cases unnecessary, to have a monitoring system that will guarantee the non-diversion of every relevant chemical from industrial applications to CW use. Instead, the system will focus on monitoring an appropriate range of key chemicals, which will sustain confidence in the overall CWC regime.

Each Schedule is subdivided into Part A—Toxic Chemicals, and Part B—Precursor Chemicals.

Schedule 1 contains chemicals that are deemed to pose a high risk to the purposes of the CWC, but which have very limited, if any, commercial applications. Part A includes nerve agents (including tabun, sarin and VX, and their homologues or "family" members), blister agents (including sulphur mustard) and certain toxins. Part B includes nerve agent precursors for binary chemical weapons. Each stat party to the CWC will be permitted to produce and use Schedule 1 chemicals for research, medical, pharmaceutical or protective purposes (for example, testing gas masks) provided the types and quantities of the Schedule

D.S. Viswanath et al., *Emerging Energetic Materials: Synthesis, Physicochemical, and Detonation Properties*, https://doi.org/10.1007/978-94-024-1201-7

1 chemicals are strictly limited to those which can be justified for such purposes. In addition, the aggregate amount of such chemicals that a State Party may acquire annually, or possess at any given time, must not exceed one tonne. The types of facilities that are permitted to produce these chemicals are clearly defined in the CWC text. These facilities will be required to make annual declarations of relevant activities, and will be subject to international monitoring. Schedule 2 contains chemicals that are deemed to pose a significant risk to the purposes of the CWC. Part A contains toxic chemicals that could be used as chemical warfare agents (for example, amiton, which was developed as a pesticide in the 1950s but found to be too toxic for that purpose). Part B contains key precursors to chemicals in Schedule 1 or Schedule 2 Part A. Some of these chemicals have limited commercial applications. For example, thiodiglycol is used in the printing industry but is also a key precursor which is readily converted into sulphur mustard. It has been agreed that there will be no restrictions on the quantities of chemicals in Schedule 2 that a State Party can produce, process or consume. However, facilities that produce, process or consume chemicals in Schedule 2 in quantities above agreed thresholds will be required to make annual declarations, and will be subject to international onsite annual declarations, and will be subject to international onsite inspections.

Schedule 3 contains other chemicals that are considered to pose a risk to the purposes of the CWC. Part A includes "dual purpose" toxic chemicals such as phosgene (which was used as chemical weapon in World War 1, but which currently has large commercial applications in the production of a range of products including plastics and pesticides). Part B includes other precursors for chemical warfare agents, for example, trimethyl phosphite, which is a precursor for insecticides and flame retardants, and also a precursor for nerve agents. It has been agreed that there will be no restrictions on the quantities of chemicals in Schedule 3 that a State Party can produce, process or consume. However, facilities that produce chemicals in Schedule 3 in quantities above agreed thresholds will be required to make annual declarations, and will be subject to international on-site inspections. Comparison of the Lists

From the above discussion it can be appreciated that while the major focus of concern of both the Australia Group and the CWC are the same CW agents, the objectives are rather different. In particular, the objective of the AGL is to stop the inadvertent supply of CW precursors to a small number of nations that have chosen to produce chemical weapons. Thus, the AGL contains CW precursors but not CW agents. On the other hand, the objective of the verification measures under the CWC is to provide assurance to each State Party to the CWC that the other States Parties to the CWC are complying with their obligations under the CWC, including not to produce chemical weapons. Therefore, the CWC

Schedules include CW agents and their precursors. It is not surprising that many of the individual precursor chemicals on the AGL are also covered under the CWC schedules, either as an individually listed chemical or as a member of a family of chemicals. However, because of the more limited and highly focussed nature of the objectives of the AGL, some of the precursor chemicals which are early in the production process and/or are widely produced in industry (and hence not considered suitable for effective monitoring under the CWC) have been included on the AGL, because they are either known or suspected to have been sought for CW purposes. Such precursors include:

- The fluoride chemicals (chemicals 14, 24, 41, 42, 43 and 44) for the pr duction of sarin-family nerve agents;
- Early precursors for a number of CW agents, including sulphur mustard (chemicals 15 and 50), tabun (chemicals 16, 20, 40 and 45), soman (chemical 39), VX (chemical 48), amiton (chemical 47) and certain psychochemical agents (chemical 37).

The cyanide salts (chemicals 40 and 45) may also be used for the production of hydrogen cyanide and cyanogen chloride, which were used as CW agents in WW1 and are covered by Schedule 3 of the CWC. It is interesting to note that two sulphur mustard precursors (sulphur monochloride and sulphur dichloride) which were listed in Schedule 3 of the CWC in 1986 were not CWCB 21 Page 2 September 1993 added to the AGL until June 1992. These chemicals were initially considered for inclusion to the AGL in 1986. However, the information available to the AG at that time was that CW proliferators were choosing to produce sulphur mustard by the thiodiglycol process rather than the sulphur chloride/ethylene process. This issue has been regularly reviewed by the AG, and the decision to add the two chemicals to the AGL (chemicals 51 and 52) was made after information became available indicating that the chemicals have recently been sought for CW purposes (and openly advertised for that purpose by one company within a non-participating country). It is also interesting to note that thionyl chloride (chemical 9), which was on the original AGL of 40 chemicals 1986, was included Schedule 3 of the CWC for the firs time in 1989. Thus the addition of chemicals to both the AGL and the schedules of the CWC should be seen as

A dynamic process.

Australia Group Export Control List: Chemical Weapons Precursors Chemical name and CAS number CWC schedule

1. thiodiglycol [111-48-8] 2B
2. phosphoryl chloride [10025-87-3] 3B
3. dimethyl methylphosphonate [756-79-6] 2B
4. methylphosphonyl difluoride (DF) [676-99-3] 1B
5. methylphosphonyl dichloride (DC) [676-97-1] 2B
6. dimethyl phosphite (DMP) [868-85-9] 3B
7. phosphorus trichloride [7719-12-2] 3B
8. trimethyl phosphite (TMP) [121-45-9] 3B
9. thionyl chloride [7719-09-7] 3B
10. 3-hydroxy-1-methylpiperidine [3554-74-3] –

11. 2-N,N-diisopropylaminoethyl chloride [96-79-7] 2B
12. 2-N,N-diisopropylaminoethyl mercaptan [5842-07-9] 2B
13. 3-quinuclidinol [1619-34-7] 2B
14. potassium fluoride [7789-23-3] –
15. 2-chloroethanol [107-07-3] –
16. dimethylamine [124-40-3] –
17. diethyl ethylphosphonate [78-38-6] 2B
18. diethyl N,N-dimethylphosphoramidate [2404-03-7] 2B
19. diethyl phosphite [762-04-9] 3B
20. dimethylamine hydrochloride [506-59-2] –
21. ethylphosphonous dichloride [1498-40-4] 2B
22. ethylphosphonyl dichloride [1066-50-8] 2B
23. ethylphosphonyl difluoride [753-98-0] 1B
24. hydrogen fluoride [7664-39-3] –
25. methyl benzilate [76-89-1] –
26. methylphosphonous dichloride [676-83-5] 2B
27. 2-N,N-diisopropylaminoethyl alcohol [96-80-0] 2B
28. 28 pinacolyl alcohol [464-07-3] 2B
29. ethyl 2-diisopropylaminoethyl methylphosphonite (QL) [57856-11-8] 1B
30. triethyl phosphite [122-52-1] 3B
31. arsenic trichloride [7784-34-1] 2B
32. benzilic acid [76-93-7] 2B
33. diethyl methylphosphonite [15715-41-0] 2B
34. dimethyl ethylphosphonate [6163-75-3] 2B
35. ethylphosphonous difluoride [430-78-4] 2B
36. methylphosphonous difluoride [753-59-3] 2B
37. 3-quinuclidone [3731-38-2] –
38. phosphorus pentachloride [10026-13-8] 3B
39. pinacolone [75-97-8] –
40. potassium cyanide [151-50-8] –
41. potassium bifluoride [7789-29-9] –
42. ammonium bifluoride [1341-49-7] –
43. sodium bifluoride [1333-83-1] –
44. sodium fluoride [7681-49-4] –
45. sodium cyanide [143-33-9] –
46. tris-ethanolamine [102-71-6] 3B
47. phosphorus pentasulphide [1314-80-3] –
48. diisopropylamine [108-18-9] –
49. 2-diethylaminoethanol [100-37-8] –
50. sodium sulphide [1313-82-2] –
51. sulphur monochloride [10025-67-9] 3B
52. sulphur dichloride [100545-99-0] 3B
53. tris-ethanolamine hydrochloride [637-39-8] –
54. 2-N,N-diisopropylaminoethyl chloride hydrochloride [4261-68-1] 2B

CWC Non-Signatory State (as of 1 September 1993)

- Angola
- Botswana
- Chad
- Djibouti
- Egypt
- Lesotho
- Libya
- Mozambique
- Sao Tome & Principe
- Somalia
- Sudan
- Swaziland
- Tanzania
- Bhutan
- Iraq
- Jordan
- Korea, North
- Lebanon
- Maldives
- Solomon Islands
- Syria
- Taiwan
- Vanuatu
- Bosnia-Hercegovina
- Macedonia, FYR of
- Turkmenistan
- Uzbekistan
- Yugoslavia
- Antigua & Barbuda
- Bahamas
- Barbados
- Belize
- Grenada
- Guyana
- Jamaica
- St Christopher & Nevis
- St Vincent & Grenadines
- Suriname
- Trinidad & Tobago
- Andorra
- Monaco

September 1993 Page 3 CWCB 21

- **UN Storage Compatibility Groupings**
  Under the UNO system, there are 13 storage compatibility groupings, which further categorize Class 1 explosives by their form or composition, ease of ignition, and sensitivity to detonation.
- **SCG A**–Bulk-initiating explosives that have the necessary sensitivity to friction, heat, or percussion (shock) to make them suitable for use as initiating elements in an explosive train. A distinction is made between primary initiating explosives and nonprimary initiating explosives. Examples of primary initiating explosives are lead azide, lead styphnate, mercury fulminate, and tetracene. Examples of nonprimary initiating explosives are dry forms of cyclotetramethylene tetranitramine (HMX), cyclotrimethylene trinitramine (RDX), and pentaerythritol tetranitrate (PETN).
- **SCG B**–Detonators and similar initiating devices that do not contain two or more independent safety features. This group also consists of items that contain initiating explosives designed to initiate or continue the functioning of an explosives train. Examples are blasting caps, small arms primers, fuzes, and detonators of all types.
- **SCG C**–Bulk propellants, propelling charges, and devices containing propellant with or without their own means of initiation. Upon initiation, these items will deflagrate, explode, or detonate. Examples are single-, double-, and triple-base propellants; composite propellants; rocket motors (solid propellant); and ammunition with inert projectiles.
- **SCG D**–High explosives (HE) and devices containing HE without their own means of initiation and without a propelling charge. This group includes explosives and ammunition that can be expected to explode or detonate when any given item or component thereof is initiated. This group does not include devices containing initiating explosives with independent safety features. Examples are wet HMX, plastic-bonded explosives (explosives formulated with a desensitizing plastic binder), trinitrotoluene (TNT), and black powder.
- **SCG E**–Explosives devices that lack their own means of initiation but contain or have a propelling charge (other than one containing a flammable or hypergolic liquid). Examples are artillery ammunition, rockets, and guided missiles.
- **SCG F**–Explosives devices that have their own means of initiation and with or without propelling charge. Examples are grenades, sounding devices, and similar items with an in-line explosive train in the initiator.
- **SCG G**–Pyrotechnic materials and devices containing pyrotechnic materials. Examples are devices that, when functioning, result in illumination, smoke, or an incendiary, lachrymatory, or sound effect.
- **SCG H**–Ammunition containing both explosives and white phosphorus (WP) or other pyrophoric material. Ammunition in this group contains fillers that are spontaneously flammable when exposed to the atmosphere. Examples are WP, plasticized white phosphorus (PWP), or other ammunition containing pyrophoric material.

- **SCG J**–Ammunition containing both explosives and flammable liquids or gels. Ammunition in this group contains flammable liquids or gels other than those that are spontaneously flammable when exposed to water or the atmosphere. Examples are liquid- or gel-filled incendiary ammunition, fuel-air explosive (FAE) devices, flammable liquid-fueled missiles, and torpedoes.
- **SCG K**–Ammunition containing both explosives and toxic chemical agents. Ammunition in this group contains chemicals specifically designed for incapacitating effects more severe than lachrymation. Examples are artillery or mortar ammunition (fuzed or unfuzed), grenades, and rockets or bombs filled with a lethal or incapacitating chemical agent.
- **SCG L**–Explosives or ammunition not included in other SC/HC groups. This group includes explosives or ammunition with characteristics that do not permit storage with other similar or dissimilar materials. Examples are damaged or suspect explosives devices or containers, explosives that have undergone severe testing, fuel-air explosive devices, and water-activated devices. Also included are experimental explosives, explosives of temporary interest, newly synthesized compounds, new mixtures, and salvaged explosives, unless established as being compatible with the original materials. Types of explosives in this group presenting similar hazards may be stored together.
- **SCG N**–Hazard Division 1.6 ammunition containing only extremely insensitive detonating substances (IEDS). Examples are bombs and warheads. If dissimilar Group N munitions, such as MK 82 and MK 84 bombs, are mixed together and have not been tested to assure nonpropagation, the mixed munitions are considered to be Hazard Division 1.2, Storage and Compatibility Group D, for purposes of transportation and storage.
- **SCG S**–Explosives, explosives devices, or ammunition presenting no significant hazard. Explosives ammunition, so designated or packed that, when in storage, all hazardous explosives effects are confined and self-contained within the item or package. Materials in this group are such that an incident that destroys all items in a single pack will not be communicated to other packs. Examples are thermal batteries, cable cutters, explosive actuators, and other ammunition items packaged to meet the criteria of this group.

Group A–Initiating explosives (* indicates primary initiating explosives)

CL-20 (Hexanitrohexaazaisowurtzitane; dry)
CP (5-Cyanotetrazolpentaamine Cobalt III perchlorate)
HMX (Cyclotetramethylene tetranitramine; dry)
*Lead azide
*Lead styphnate
*Mercury fulminate
*Nitrocellulose (dry)
PETN (Pentaerythritol tetranitrate; dry)
RDX (Cyclotrimethylene trinitramine; dry)

*TATNB (Triazidotrinitrobenzene)
*Tetracene

Group B–Detonators and similar initiating devices

Blasting caps
Detonators (excluding EBW and slapper)
Explosive bolts
Fragmenting actuators
Ignitors
Low-energy initiators (LEIs)
MDF (mild detonating fuze) detonator assemblies
Pressure cartridges
Primers
Squibs

Group C–Bulk propellant, propellant charges, and devices containing propellants with or without their own means of initiation

Smokeless powder
Pistol and rifle powder
Rocket-motor solid propellants

Group D–High explosives and devices containing explosives without their own means of initiation (* indicates that classification may change depending on nitrogen and moisture content. Contact Hazards Control Department explosives safety personnel for additional guidance.)

Ammonium picrate
Baratol
Black Powder
Boracitol
Chemical lenses
CL-20 (Hexanitrohexaazaisowurtzitane; wet)
Compositions A, B, and C (all types)
Cyclotols (<85% RDX)
DATB (Diaminotrinitrobenzene)
Detasheet
Detonating cord (primacord or mild detonating fuze)
bis-Dinitropropyl adipate
bis-Dinitropropyl glutarate
bis-Dinitropropyl maleate
Dinitropropane
Dinitropropanol
Dinitropropyl acrylate monomer (DNPA)
Dinitroproply acrylate polymer (PDNPA)
EBW and slapper detonators
Elastomeric plastic bonded explosives

Explosive D
GAP (Glyceryl azide polymer)
HMX (Cyclotetramethylene tetranitramine; wet)
HMX/wax (formulated with at least 1% wax)
HNS (Hexanitrostilbene; wet or dry)
Linear-shaped charge
Methyl dinitropentanoate
Mild detonating fuze (MDF)
NG/TA (Nitroglycerine-triacetine)
*Nitrocellulose (wet)
Nitroguanidine (NQ)
Octol (<75% HMX)
Pentolite
PETN (Pentaerythritol tetranitrate; wet)
PETN/extrudable binder
PGN (Polyglycidyl nitrate)
Plane wave lenses (composed of SC/HC Group D explosives)
Plastic-bonded explosive, PBX (a SC/HC Group D formulated with a desensitizing binder)
Potassium picrate
Primacord
RDX (Cyclotrimethylene trinitramine; wet)
Shaped charges (composed of SC/HC Group D explosives)
TATB (Triamino trinitrobenzene)
TATB/DATB mixtures
TEGDN (Triethylene glycol dinitrate)
Tetryl
TMETN (Trimethylolethane trinitrate)
TNAZ (Trinitoazetidine)
TNT (Trinitrotoluene)

Group E–Explosives devices without their own means of initiation and with propelling charge

Artillery ammunition
Rockets (e.g., M66 LAW)

Group F–Explosives devices with detonators and detonating trains assembled to the devices and with propelling charge

Grenades
Sounding devices

Group G–Pyrotechnic material and devices that produce an incendiary, illumination, lachrymatory, smoke, or sound effect

Smoke pots/grenades
Flares
Incendiary ammunition

Group H–Ammunition containing both explosives and white phosphorus (WP) or other pyrophoric material

White phosphorus
Plasticized white phosphorus

Group J–Ammunition containing both explosives and flammable liquids or gels.

Liquid- or gel-filled incendiary ammunition
Fuel-air explosive (FAE) devices
Flammable liquid-fueled missiles
Torpedoes

Group K–Ammunition containing both explosives and toxic chemicals

Artillery or mortar ammunition (fuzed or unfuzed), grenades, rockets, or bombs filled with a lethal or incapacitating agent

Group L–Explosives or other ammunition not included in other storage compatibility groups

Damaged or suspect explosives devices or containers
Explosives that have undergone severe testing
Experimental explosives, explosives of temporary interest, newly synthesized compounds, new mixtures, and some salvaged explosives

Group N–Hazard Class/Division 1.6 ammunition containing only extremely insensitive detonating substances (EIDS)

Bombs
Warheads

Group S–Explosives, explosives devices, or ammunition presenting no significant hazard

Propellant cartridge-actuated devices (which yield a nonfragmenting, nonflame-producing controlled reaction). Examples include cable cutters, cartridge-actuated valves, and linear actuators (e.g., dimple, piston, or bellows motors)
Safety fuse
Most small arms ammunition below 50 caliber
Thermal batteries

Appendix 5
CAS RN Reportable Chemicals

ID	Chemical Name	CAS	DHS	EPCRA	SARA	HAPS	P H C	OSHA
1	(1,2-Phenylenebis (iminocarbonothioyl)) biscarbamic acid diethyl ester	23564-06-9	☐	☐	☑	☐	☐	☑
2	(4-Chloro-2-methylphenoxy) acetate sodium salt	3653-48-3	☐	☑	☑	☐	☐	☑
3	(4-Chloro-2-methylphenoxy) acetic acid	94-74-6	☐	☑	☑	☐	☐	☑
4	apha.-(2-Chlorophenyl)-.alpha.-4-chlorophenyl)-5-pyrimidinemethanol	60168-88-9	☐	☑	☑	☐	☐	☑
5	alpha.-Butyl-.alpha.-(4-chlorophenyl)-1H-1,2,4-triazole-1-propanenitrile	88671-89-0	☐	☑	☑	☐	☐	☑
6	1-METHYL 1H-TETRAZOLE	16681-77-9	☑	☐	☐	☐	☐	☑
7	1-(2-(2,4-Dichlorophenyl)-2-(2-propenyloxy)ethyl)-1H-imidazole	35554-44-0	☐	☑	☑	☐	☐	☑
8	1-(2-(2,4-Dichlorophenyl)-4-propyl-1,3-dioxolan-2-yl)-methyl-1H-1,2,4,-triazol	60207-90-1	☐	☑	☑	☐	☐	☑
9	1-(3-Chloroallyl)-3,5,7-triaza-1-azoniaadamantane chloride	4080-31-3	☐	☑	☑	☐	☐	☑
10	1-(4-Chlorophenoxy)-3,3-dimethyl-1-(1H-1,2,4-triazol-1-yl)-2-butanone	43121-43-3	☐	☑	☑	☐	☐	☑
11	1,1,2,2-Tetrachloroethane	79-34-5	☐	☑	☑	☑	☑	☑
12	1,1,2-Trichloroethane	79-00-5	☐	☑	☑	☑	☑	☑
13	1,1-Dichloro-1,2,2,3,3-pentafluoropropane	13474-88-9	☐	☑	☑	☐	☑	☑
14	1,1-Dichloro-1,2,2-trifluoroethane	812-04-4	☐	☑	☑	☐	☑	☑
15	1,1-Dichloro-1,2,3,3,3-pentafluoropropane	111512-56-2	☐	☑	☑	☐	☑	☑
16	1,1-Dichloro-1-fluoroethane	1717-00-6	☐	☑	☑	☐	☑	☑
17	1,1-Dichloroethylene	75-35-4	☑	☑	☑	☑	☐	☑
18	1,1-Dichloropropane	78-99-9	☐	☑	☑	☐	☐	☑
19	1,1-Difluoroethane	75-37-6	☑	☑	☑	☐	☐	☑
20	1,1-Difluoroethylene	75-38-7	☑	☑	☑	☐	☐	☑
21	1,2,3,4,6,7,8,9-octachlorodibenzofuran	39001-02-0	☐	☑	☑	☐	☐	☑
22	1,2,3,4,6,7,8,9-octachlorodibenzo-p-dioxin	3268-87-9	☐	☑	☑	☐	☐	☑

(continued)

D.S. Viswanath et al., *Emerging Energetic Materials: Synthesis, Physicochemical, and Detonation Properties*, https://doi.org/10.1007/978-94-024-1201-7

(continued)

ID	Chemical Name	CAS	DHS	EPCRA	SARA	HAPS	P H C	OSHA
23	1,2,3,4,6,7,8-heptachlorodibenzofuran	67562-39-4	☐	☑	☑	☐	☐	☑
24	1,2,3,4,6,7,8-heptachlorodibenzo-p-dioxin	35822-46-9	☐	☑	☑	☐	☐	☑
25	1,2,3,4,7,8,9-heptachlorodibenzofuran	55673-89-7	☐	☑	☑	☐	☐	☑
26	1,2,3,4,7,8-hexachlorodibenzofuran	70648-26-9	☐	☑	☑	☐	☐	☑
27	1,2,3,4,7,8-hexachlorodibenzo-p-dioxin	39227-28-6	☐	☑	☑	☐	☐	☑
28	1,2,3,6,7,8-hexachlorodibenzofuran	57117-44-9	☐	☑	☑	☐	☐	☑
29	1,2,3,6,7,8-hexachlorodibenzo-p-dioxin	57653-85-7	☐	☑	☑	☐	☐	☑
30	1,2,3,7,8,9-hexachlorodibenzofuran	72918-21-9	☐	☑	☑	☐	☐	☑
31	1,2,3,7,8,9-hexachlorodibenzo-p-dioxin	19408-74-3	☐	☑	☑	☐	☐	☑
32	1,2,3,7,8-pentachlorodibenzofuran	57117-41-6	☐	☑	☑	☐	☐	☑
33	1,2,3,7,8-pentachlorodibenzo-p-dioxin	40321-76-4	☐	☑	☑	☐	☐	☑
34	1,2,3-Trichloropropane	96-18-4	☐	☑	☑	☐	☐	☑
35	1,2,4,5-Tetrachlorobenzene	95-94-3	☐	☑	☑	☐	☐	☑
36	1,2,4-Trichlorobenzene	120-82-1	☐	☑	☑	☑	☐	☑
37	1,2,4-Trimethylbenzene	95-63-6	☐	☑	☑	☐	☐	☑
38	1,2-Bis(2-chloroethylthio)ethane	3563-36-8	☑	☐	☐	☐	☐	☑
39	1,2-Dibromo-3-chloropropane	96-12-8	☐	☑	☑	☑	☑	☑
40	1,2-Dichloro-1,1,2,3,3-pentafluoropropane	422-44-6	☐	☑	☑	☐	☐	☑
41	1,2-Dichloro-1,1,2-trifluoroethane	354-23-4	☐	☑	☑	☐	☐	☑
42	1,2-Dichloro-1,1,3,3,3-pentafluoropropane	431-86-7	☐	☑	☑	☐	☐	☑
43	1,2-Dichloro-1,1-difluoroethane	1649-08-7	☐	☑	☑	☐	☐	☑
44	1,2-Dichloroethylene	156-60-5	☐	☑	☑	☐	☐	☑
45	1,2-Dichloroethylene	540-59-0	☐	☑	☑	☐	☐	☑
46	1,2-Diphenylhydrazine	122-66-7	☐	☑	☑	☑	☐	☑
47	1,2-Epoxybutane	106-88-7	☐	☑	☑	☑	☐	☑
48	1,2-Ethylenediamine	107-15-3	☑	☑	☑	☐	☑	☑
49	1,2-Phenylenediamine	95-54-5	☐	☑	☑	☐	☐	☑
50	1,2-Phenylenediamine dihydrochloride	615-28-1	☐	☑	☑	☐	☐	☑
51	1,3,5-Trinitrobenzene	99-35-4	☑	☑	☑	☐	☐	☑
52	1,3,5-Trinitrohexahydro-s-triazine	121-82-4	☑	☐	☐	☐	☐	☑
53	1,3-Benzenedicarbonitrile, 2,4,5,6-tetrachloro-	1897-45-6	☐	☑	☑	☐	☐	☑
54	1,3-Bis(2-chloroethylthio)propane	63905-10-2	☑	☑	☑	☐	☐	☑
55	1,3-Bis(methylisocyanate)cyclohexane	38661-72-2	☐	☑	☑	☐	☐	☑
56	1,3-Butadiene	106-99-0	☑	☑	☑	☑	☑	☑
57	1,3-Dichloro-1,1,2,2,3-pentafluoropropane	507-55-1	☐	☑	☑	☐	☐	☑
58	1,3-Dichloro-1,1,2,3,3-pentafluoropropane	136013-79-1	☐	☑	☑	☐	☐	☑
59	1,3-Dichlorobenzene	541-73-1	☐	☑	☑	☐	☐	☑
60	1,3-Dichloropropane	142-28-9	☐	☑	☑	☐	☐	☑
61	1,3-Dichloropropene	542-75-6	☐	☑	☑	☑	☑	☑
62	1,3-Pentadiene, mixture of cis and trans	504-60-9	☑	☑	☑	☐	☐	☑
63	1,3-Phenylene diisocyanate	123-61-5	☐	☑	☑	☐	☐	☑

(continued)

(continued)

ID	Chemical Name	CAS	DHS	EPCRA	SARA	HAPS	P H C	OSHA
64	1,3-Phenylenediamine	108-45-2	☐	☑	☑	☐	☐	☑
65	1,3-Propane sultone	1120-71-4	☐	☑	☑	☑	☐	☑
66	1,4-Bis(2-chloroethylthio)butane	142868-93-7	☑	☐	☐	☐	☐	☑
67	1,4-Bis(methylisocyanate)cyclohexane	10347-54-3	☐	☑	☑	☐	☐	☑
68	1,4-Cyclohexane diisocyanate	2556-36-7	☐	☑	☑	☐	☐	☑
69	1,4-Dichlorobenzene(p)	106-46-7	☐	☑	☑	☑	☐	☑
70	1,4-Dioxane (1,4-Diethyleneoxide)	123-91-1	☐	☑	☑	☑	☑	☑
71	1,4-Naphthoquinone	130-15-4	☐	☑	☑	☐	☐	☑
72	1,4-Phenylene diisocyanate	104-49-4	☐	☑	☑	☐	☐	☑
73	1,4-Phenylenediamine dihydrochloride	624-18-0	☐	☑	☑	☐	☐	☑
74	1,5-bis[(2-chloroethyl)thio]-n-pentane	142868-94-8	☑	☐	☐	☐	☐	☑
75	1,5-Naphthalene diisocyanate	3173-72-6	☐	☑	☑	☐	☐	☑
76	1-Acetyl-2-thiourea	591-08-2	☐	☑	☑	☐	☐	☑
77	1-Amino-2-methylanthraquinone	82-28-0	☐	☑	☑	☐	☐	☑
78	1-Bromo-1-(bromomethyl)-1,3-propanedicarbonitrile	35691-65-7	☐	☑	☑	☐	☐	☑
79	1-Butene	106-98-9	☑	☑	☑	☐	☐	☑
80	1-Butene	25167-67-3	☑	☑	☑	☐	☐	☑
81	1-Butyne	107-00-6	☑	☑	☑	☐	☐	☑
82	1-Chloro-1,1,2,2-tetrafluoroethane	354-25-6	☐	☑	☑	☐	☐	☑
83	1-Chloro-1,1-difluoroethane	75-68-3	☐	☑	☑	☐	☐	☑
84	1H-Azepine-1 carbothioic acid, hexahydro-S-ethyl ester	2212-67-1	☐	☑	☑	☐	☐	☑
85	1H-TETRAZOLE	288-94-8	☑	☐	☐	☐	☐	☑
86	1H-Tetrazole-1-acetic acid	21732-17-2	☑	☐	☐	☐	☐	☑
87	1-Pentene	109-67-1	☑	☑	☑	☐	☐	☑
88	2-((Ethoxyl((1-methylethyl)amino] phosphinothioyl]oxy) benzoic acid 1-methy	25311-71-1	☐	☑	☑	☐	☐	☑
89	2-(1-(Ethoxyimino) butyl)-5-(2-(ethylthio)propyl)-3-hydroxyl-2-cyclohexen-1-	74051-80-2	☐	☑	☑	☐	☐	☑
90	2-(3,4-Dichlorophenyl)-4-methyl-1,2,4-oxadiazolidine-3,5-dione	20354-26-1	☐	☑	☑	☐	☐	☑
91	2-(4-((6-Chloro-2-benzoxazolylen)oxy) phenoxy)propanoic acid, ethyl ester	66441-23-4	☐	☑	☑	☐	☐	☑
92	2-(4-((6-Chloro-2-quinoxalinyl)oxy] phenoxy) propanoic acid ethyl ester	76578-14-8	☐	☑	☑	☐	☐	☑
93	2-(4-(2,4-Dichlorophenoxy)phenoxy) propanoic acid, methyl ester	51338-27-3	☐	☑	☑	☐	☐	☑
94	2-(4-Methoxy-6-methyl-1,3,5-triazin-2-yl)-methylamino)carbonyl)amino)sulfo	101200-48-0	☐	☑	☑	☐	☐	☑
95	2-(Diisopropylamino)ethanol	96-80-0	☑	☐	☐	☐	☐	☑
96	2-(Diisopropylamino)ethyl chloride hydrochloride	4261-68-1	☑	☐	☐	☐	☐	☑
97	2,2,4-Trimethylhexamethylene diisocyanate	16938-22-0	☐	☑	☑	☐	☐	☑
98	2,2,4-Trimethylpentane	540-84-1	☐	☑	☑	☑	☐	☑
99	2,2'-Bioxirane	1464-53-5	☐	☑	☑	☐	☐	☑

(continued)

(continued)

ID	Chemical Name	CAS	DHS	EPCRA	SARA	HAPS	P H C	OSHA
100	2,2-Dibromo-3-nitrilopropionamide	10222-01-2	☐	☑	☑	☐	☐	☑
101	2,2-Dichloro-1,1,1,3,3-pentafluoropropane	128903-21-9	☐	☑	☑	☐	☐	☑
102	2,2-Dichloro-1,1,1-trifluoroethane	306-83-2	☐	☑	☑	☐	☐	☑
103	2,2'-Dichloro-N-methyldiethylamine	51-75-2	☑	☑	☑	☐	☐	☑
104	2,2-Dichloropropionic acid	75-99-0	☐	☑	☑	☐	☐	☑
105	2,2-Dimethyl-3-(2-methyl-1-propenyl)cyclopropanecarboxylic acid (1,3,4,5,6,	7696-12-0	☐	☑	☑	☐	☐	☑
106	2,2-Dimethyl-3-(2-methyl-1-propenyl)cyclopropanecarboxylic acid (3-phenox	26002-80-2	☐	☑	☑	☐	☐	☑
107	2,2-Dimethylpropane	463-82-1	☑	☑	☑	☐	☐	☑
108	2,2'-Thiodiethanol	111-48-8	☑	☐	☐	☐	☐	☑
109	2,3,4,6,7,8-hexachlorodibenzofuran	60851-34-5	☐	☑	☑	☐	☐	☑
110	2,3,4,6-Tetrachlorophenol	58-90-2	☐	☑	☑	☐	☐	☑
111	2,3,4,7,8-pentachlorodibenzofuran	57117-31-4	☐	☑	☑	☐	☐	☑
112	2,3,4-Trichlorophenol	15950-66-0	☐	☑	☑	☐	☐	☑
113	2,3,5-Trichlorophenol	933-78-8	☐	☑	☑	☐	☐	☑
114	2,3,5-Trimethylphenyl methylcarbamate	2655-15-4	☐	☑	☑	☐	☐	☑
115	2,3,6-Trichlorophenol	933-75-5	☐	☑	☑	☐	☐	☑
116	2,3,7,8-tetrachlorodibenzofuran	51207-31-9	☐	☑	☑	☐	☐	☑
117	2,3,7,8-Tetrachlorodibenzo-p-dioxin	1746-01-6	☐	☑	☑	☑	☑	☑
118	2,3,-Dihydro-5,6-dimethyl-1,4-dithiin 1,1,4,4-tetraoxide	55290-64-7	☐	☑	☑	☐	☐	☑
119	2,3-Dichloro-1,1,1,2,3-pentafluoropropane	422-48-0	☐	☑	☑	☐	☐	☑
120	2,3-Dichloropropene	78-88-6	☐	☑	☑	☐	☐	☑
121	2,4,4-Trimethylhexamethylene diisocyanate	15646-96-5	☐	☑	☑	☐	☐	☑
122	2,4,5-T acid	93-76-5	☐	☑	☑	☐	☐	☑
123	2,4,5-T amines	6369-97-7	☐	☑	☑	☐	☐	☑
124	2,4,5-T amines	3813-14-7	☐	☑	☑	☐	☐	☑
125	2,4,5-T amines	2008-46-0	☐	☑	☑	☐	☐	☑
126	2,4,5-T amines	1319-72-8	☐	☑	☑	☐	☐	☑
127	2,4,5-T amines	6369-96-6	☐	☑	☑	☐	☐	☑
128	2,4,5-T esters	2545-59-7	☐	☑	☑	☐	☐	☑
129	2,4,5-T esters	25168-15-4	☐	☑	☑	☐	☐	☑
130	2,4,5-T esters	1928-47-8	☐	☑	☑	☐	☐	☑
131	2,4,5-T esters	61792-07-2	☐	☑	☑	☐	☐	☑
132	2,4,5-T esters	93-79-8	☐	☑	☑	☐	☐	☑
133	2,4,5-T salts	13560-99-1	☐	☑	☑	☐	☐	☑
134	2,4,5-TP esters	32534-95-5	☐	☑	☑	☐	☐	☑
135	2,4,5-Trichlorophenol	95-95-4	☐	☑	☑	☑	☐	☑
136	2,4,6-Trichlorophenol	88-06-2	☐	☑	☑	☑	☐	☑
137	2,4,6-Trinitroaniline	26952-42-1	☑	☑	☑	☐	☐	☑
138	2,4,6-Trinitroaniline	489-98-5	☑	☑	☑	☐	☐	☑

(continued)

(continued)

ID	Chemical Name	CAS	DHS	EPCRA	SARA	HAPS	P H C	OSHA
139	2,4,6-Trinitroanisole	606-35-9	☑	☑	☑	☐	☐	☑
140	2,4,6-Trinitrobenzenesulfonic acid dihydrate	7432-77-1	☑	☑	☑	☐	☐	☑
141	2,4,6-Trinitrobenzenesulfonic acid dihydrate	37006-19-2	☑	☑	☑	☐	☐	☑
142	2,4,6-Trinitrobenzenesulfonic acid dry	2508-19-2	☑	☑	☑	☐	☐	☑
143	2,4,6-Trinitrobenzoic acid	129-66-8	☑	☑	☑	☐	☐	☑
144	2,4,6-Trinitro-m-cresol	602-99-3	☑	☑	☑	☐	☐	☑
145	2,4,6-Trinitrophenetole	4732-14-3	☑	☑	☑	☐	☐	☑
146	2,4,6-Trinitrotoluene	118-96-7	☑	☑	☑	☐	☐	☑
147	2,4,7-Trinitro-9-fluorenone	129-79-3	☑	☑	☑	☐	☐	☑
148	2,4-D 2-ethyl-4-methylpentyl ester	53404-37-8	☐	☑	☑	☐	☐	☑
149	2,4-D 2-ethylhexyl ester	1928-43-4	☐	☑	☑	☐	☐	☑
150	2,4-D butoxyethyl ester	1929-73-3	☐	☑	☑	☐	☐	☑
151	2,4-D butyl ester	94-80-4	☐	☑	☑	☐	☐	☑
152	2,4-D chlorocrotyl ester	2971-38-2	☐	☑	☑	☐	☐	☑
153	2,4-D Esters	94-79-1	☐	☑	☑	☐	☐	☑
154	2,4-D Esters	53467-11-1	☐	☑	☑	☐	☐	☑
155	2,4-D Esters	25168-26-7	☐	☑	☑	☐	☐	☑
156	2,4-D Esters	94-11-1	☐	☑	☑	☐	☐	☑
157	2,4-D Esters	1928-38-7	☐	☑	☑	☐	☐	☑
158	2,4-D Esters	1928-61-6	☐	☑	☑	☐	☐	☑
159	2,4-D Esters	1320-18-9	☐	☑	☑	☐	☐	☑
160	2,4-D sodium salt	2702-72-9	☐	☑	☑	☐	☐	☑
161	2,4-D, salts and esters	94-75-7	☐	☑	☑	☑	☐	☑
162	2,4-DB	94-82-6	☐	☑	☑	☐	☐	☑
163	2,4-Diaminoanisole	615-05-4	☐	☑	☑	☐	☐	☑
164	2,4-Diaminoanisole sulfate	39156-41-7	☐	☑	☑	☐	☐	☑
165	2,4-Dichlorophenol	120-83-2	☐	☑	☑	☐	☐	☑
166	2,4'-Diisocyanatodiphenyl sulfide	75790-87-3	☐	☑	☑	☐	☐	☑
167	2,4-Dimethylphenol	105-67-9	☐	☑	☑	☐	☐	☑
168	2,4-Dinitrophenol	51-28-5	☐	☑	☑	☑	☐	☑
169	2,4-Dinitrotoluene	121-14-2	☐	☑	☑	☑	☐	☑
170	2,4-DP	120-36-5	☐	☑	☑	☐	☐	☑
171	2,4-Toluene diamine	95-80-7	☐	☑	☑	☑	☑	☑
172	2,5-Cyclohexadiene-1,4-dione, 2,3,5-tris(1-aziridinyl)-	68-76-8	☐	☑	☑	☐	☐	☑
173	2,5-Dinitrophenol	329-71-5	☐	☑	☑	☐	☐	☑
174	2,6-Dichlorophenol	87-65-0	☐	☑	☑	☐	☐	☑
175	2,6-Dinitrophenol	573-56-8	☐	☑	☑	☐	☐	☑
176	2,6-Dinitrotoluene	606-20-2	☐	☑	☑	☐	☐	☑
177	2-Acetylaminofluorene	53-96-3	☐	☑	☑	☑	☑	☑
178	2-Aminoanthraquinone	117-79-3	☐	☑	☑	☐	☐	☑
179	2-Butene	107-01-7	☑	☑	☑	☐	☐	☑
180	2-Butene, 1,4-dichloro-	764-41-0	☐	☑	☑	☐	☐	☑
181	2-Chloro-1,1,1,2-tetrafluoroethane	2837-89-0	☐	☑	☑	☐	☐	☑

(continued)

(continued)

ID	Chemical Name	CAS	DHS	EPCRA	SARA	HAPS	P H C	OSHA
182	2-Chloro-1,1,1-trifluoroethane	75-88-7	☐	☑	☑	☐	☐	☑
183	2-Chloro-1,3,5-trinitrobenzene	88-88-0	☑	☐	☐	☐	☐	☑
184	2-Chloro-1-propene	557-98-2	☑	☑	☑	☐	☐	☑
185	2-Chloro-6-(trichloromethyl)pyridine	1929-82-4	☐	☑	☑	☐	☐	☑
186	2-Chloroacetophenone	532-27-4	☐	☑	☑	☑	☐	☑
187	2-Chloroethyl vinyl ether	110-75-8	☐	☑	☑	☐	☐	☑
188	2-Chloroethylchloromethylsulfide	2625-76-5	☑	☐	☐	☐	☐	☑
189	2-Chloro-N-(((4-methoxy-6-methyl-1,3,5-triazin-2-yl)amino]carbonyl) benzene	64902-72-3	☐	☑	☑	☐	☐	☑
190	2-Chloro-N-(1-methylethyl)-N-phenylacetamide	1918-16-7	☐	☑	☑	☐	☐	☑
191	2-Chloronaphthalene	91-58-7	☐	☑	☑	☐	☐	☑
192	2-Chlorophenol	95-57-8	☐	☑	☑	☐	☐	☑
193	2-Cyclohexyl-4,6-dinitrophenol	131-89-5	☐	☑	☑	☐	☐	☑
194	2-Methoxyethanol	109-86-4	☐	☑	☑	☐	☐	☑
195	2-Methyl-1-butene	563-46-2	☑	☑	☑	☐	☐	☑
196	2-Methylaziridine	75-55-8	☑	☑	☑	☑	☐	☑
197	2-Methylpropane	75-28-5	☑	☑	☑	☐	☐	☑
198	2-Methylpropene	115-11-7	☑	☑	☑	☐	☐	☑
199	2-Methylpyridine	109-06-8	☐	☑	☑	☐	☐	☑
200	2-Nitrophenol	88-75-5	☐	☑	☑	☐	☐	☑
201	2-Nitropropane	79-46-9	☐	☑	☑	☑	☑	☑
202	2-PENTENE,(E)-	646-04-8	☑	☑	☑	☐	☐	☑
203	2-PENTENE,(Z)-	627-20-3	☑	☑	☑	☐	☐	☑
204	2-Propyl methylphosphonochloridate	1445-76-7	☑	☐	☐	☐	☐	☑
205	3-((Ethylamino) methoxyphosphinothioyl)oxy)-2-butenoic acid, 1-methylethyl	31218-83-4	☐	☑	☑	☐	☐	☑
206	3-(2,2-Dichloroethenyl)-2,2-dimethylcyclopropane carboxylic acid (3-phenox	52645-53-1	☐	☑	☑	☐	☐	☑
207	3-(2,4-Dichloro-5-(1-methylethoxy) phenyl)-5-(1,1-dimethylethyl)-1,3,4-oxadi	19666-30-9	☐	☑	☑	☐	☐	☑
208	3-(2-Chloro-3,3,3-trifluoro-1-propenyl)-2,2-dimethylcyclopropanecarboxylic a	68085-85-8	☐	☑	☑	☐	☐	☑
209	3-(3,5-Dichlorophenyl)-5-ethenyl-5-methyl-2,4-oxazolidinedione	50471-44-8	☐	☑	☑	☐	☐	☑
210	3,3-Dichloro-1,1,1,2,2-pentafluoropropane	422-56-0	☐	☑	☑	☐	☐	☑
211	3,3-Dichlorobenzidene	91-94-1	☐	☑	☑	☑	☑	☑
212	3,3'-Dichlorobenzidine dihydrochloride	612-83-9	☐	☑	☑	☐	☐	☑
213	3,3'-Dichlorobenzidine sulfate	64969-34-2	☐	☑	☑	☐	☐	☑
214	3,3-Dimethoxybenzidine	119-90-4	☐	☑	☑	☑	☐	☑
215	3,3'-Dimethoxybenzidine-4,4'-diisocyanate	91-93-0	☐	☑	☑	☐	☐	☑
216	3,3'-Dimethyl benzidine	119-93-7	☐	☑	☑	☑	☐	☑

(continued)

(continued)

ID	Chemical Name	CAS	DHS	EPCRA	SARA	HAPS	P H C	OSHA
217	3,3-Dimethyl-2-butanol	464-07-3	☑	☐	☐	☐	☐	☑
218	3,3'-Dimethyl-4,4'-diphenylene diisocyanate	91-97-4	☐	☑	☑	☐	☐	☑
219	3,3'-Dimethylbenzidine dihydrochloride	612-82-8	☐	☑	☑	☐	☐	☑
220	3,3'-Dimethylbenzidine dihydrofluoride	41766-75-0	☐	☑	☑	☐	☐	☑
221	3,3'-Dimethyldiphenylmethane-4,4'-diisocyanate	139-25-3	☐	☑	☑	☐	☐	☑
222	3,4,5-Trichlorophenol	609-19-8	☐	☑	☑	☐	☐	☑
223	3,4-Dinitrotoluene	610-39-9	☐	☑	☑	☐	☐	☑
224	3,6-Dichloro-2-methoxybenzoic acid, sodium salt	1982-69-0	☐	☑	☑	☐	☐	☑
225	3-Chloro-1,1,1-trifluoropropane	460-35-5	☐	☑	☑	☐	☐	☑
226	3-Chloropropionitrile	542-76-7	☐	☑	☑	☐	☐	☑
227	3-Iodo-2-propynyl butylcarbamate	55406-53-6	☐	☑	☑	☐	☐	☑
228	3-Methyl-1-butene	563-45-1	☑	☑	☑	☐	☐	☑
229	3-Methylcholanthrene	56-49-5	☐	☑	☑	☐	☐	☑
230	3-Quinuclidinol	1619-34-7	☑	☐	☐	☐	☐	☑
231	4-(Dipropylamino)-3,5-dinitrobenzenesulfonamide	19044-88-3	☐	☑	☑	☐	☐	☑
232	4,4¬-Methylenedianiline	101-77-9	☐	☑	☑	☑	☐	☑
233	4,4'-Diisocyanatodiphenyl ether	4128-73-8	☐	☑	☑	☐	☐	☑
234	4,4-Methylene bis(2-chloroaniline)	101-14-4	☐	☑	☑	☑	☐	☑
235	4,4'-Methylenebis(N,N-dimethyl) benzenamine	101-61-1	☐	☑	☑	☐	☐	☑
236	4,6-Dinitro-o-cresol, and salts	534-52-1	☐	☑	☑	☑	☐	☑
237	4-Aminoazobenzene	60-09-3	☐	☑	☑	☐	☐	☑
238	4-Aminobiphenyl	92-67-1	☐	☑	☑	☑	☑	☑
239	4-Aminopyridine	504-24-5	☐	☑	☑	☐	☐	☑
240	4-Bromophenyl phenyl ether	101-55-3	☐	☑	☑	☐	☐	☑
241	4-Chloro-5-(methylamino)-2-[3-(trifluoromethyl)phenyl]-3(2H)-pyridazinone	27314-13-2	☐	☑	☑	☐	☐	☑
242	4-Chloro-alpha-(1-methylethyl) benzeneacetic acid cyano(3-phenoxyphenyl)m	51630-58-1	☐	☑	☑	☐	☐	☑
243	4-Chloro-o-toluidine, hydrochloride	3165-93-3	☐	☑	☑	☐	☐	☑
244	4-Chlorophenyl phenyl ether	7005-72-3	☐	☑	☑	☐	☐	☑
245	4-Methyldiphenylmethane-3,4-diisocyanate	75790-84-0	☐	☑	☑	☐	☐	☑
246	4-Nitrobiphenyl	92-93-3	☐	☑	☑	☐	☐	☑
247	4-Nitrophenol	100-02-7	☐	☑	☑	☑	☑	☑
248	5-(2-Chloro-4-(trifluoromethyl) phenoxy)-N-methylsulfonyl)-2-nitrobenzamide	72178-02-0	☐	☑	☑	☑	☐	☑
249	5-(Aminomethyl)-3-isoxazolol	2763-96-4	☐	☑	☑	☐	☐	☑
250	5-(Phenylmethyl)-3-furanyl)methyl—2,2-dimethyl-3-(2-methyl-1-propenyl)cycl	10453-86-8	☐	☑	☑	☐	☐	☑
251	5,7-Dinitro-1,2,3-benzoxadiazole	87-31-0	☑	☐	☐	☐	☐	☑

(continued)

(continued)

ID	Chemical Name	CAS	DHS	EPCRA	SARA	HAPS	P H C	OSHA
252	5-Chloro-3-(1,1-dimethylethyl)-6-methyl-2,4(1H,3H)-pyrimidinedione	5902-51-2	☐	☑	☑	☐	☐	☑
253	5-Nitrobenzotriazole	2338-12-7	☑	☐	☐	☐	☐	☑
254	5-Nitro-o-anisidine	99-59-2	☐	☑	☑	☐	☐	☑
255	7,12-Dimethylbenz[a]anthracene	57-97-6	☐	☑	☑	☐	☐	☑
256	7H-Dibenzo(c,g)carbazole	194-59-2	☐	☑	☑	☐	☐	☑
257	Abamectin	71751-41-2	☐	☑	☑	☐	☐	☑
258	Acenaphthene	83-32-9	☐	☑	☑	☐	☐	☑
259	ACENAPHTHENE, 5-NITRO-	602-87-9	☐	☐	☐	☐	☑	☑
260	Acenaphthylene	208-96-8	☐	☑	☑	☐	☐	☑
261	Acephate	30560-19-1	☐	☑	☑	☐	☐	☑
262	Acetaldehyde	75-07-0	☑	☑	☑	☑	☐	☑
263	Acetaldehyde, trichloro-	75-87-6	☐	☑	☑	☐	☐	☑
264	Acetamide	60-35-5	☐	☑	☑	☑	☐	☑
265	ACETAMIDE, N-(4-(5-NITRO-2-FURYL)-2-THIAZOLYL)-	531-82-8	☐	☐	☐	☐	☑	☑
266	ACETAMIDE, THIO-	62-55-5	☐	☑	☑	☐	☑	☑
267	Acetic acid	64-19-7	☐	☑	☑	☐	☐	☑
268	ACETIC ACID, METHOXY((l-OXO-2-PROPENYL)AMINO)-, METHYL ESTER	77402-03-0	☐	☐	☐	☐	☑	☑
269	ACETIC ACID, NITRILOTRI-	139-13-9	☐	☑	☑	☐	☑	☑
270	Acetic anhydride	108-24-7	☐	☑	☑	☐	☐	☑
271	Acetone	67-64-1	☑	☑	☑	☐	☐	☑
272	Acetone thiosemicarbazide	1752-30-3	☐	☑	☑	☐	☐	☑
273	Acetonitrile	75-05-8	☐	☑	☑	☑	☐	☑
274	ACETONITRILE, HYDROXY-	107-16-4	☐	☑	☑	☐	☑	☑
275	ACETONITRILE, PHENYL-	140-29-4	☐	☑	☑	☐	☑	☑
276	ACETOPHENETIDIDE, p-	62-44-2	☐	☑	☑	☐	☑	☑
277	Acetophenone	98-86-2	☐	☑	☑	☑	☐	☑
278	Acetyl bromide	506-96-7	☑	☑	☑	☐	☐	☑
279	Acetyl chloride	75-36-5	☑	☑	☑	☐	☐	☑
280	Acetyl iodide	507-02-8	☑	☐	☐	☐	☐	☑
281	Acetylene	74-86-2	☑	☑	☑	☐	☐	☑
282	Ac ifluorfen,sodium salt	62476-59-9	☐	☑	☑	☐	☐	☑
283	Acrolein	107-02-8	☑	☑	☑	☑	☑	☑
284	Acrylamide	79-06-1	☐	☑	☑	☑	☑	☑
285	Acrylic acid	79-10-7	☐	☑	☑	☑	☐	☑
286	ACRYLIC ACID, 2-(DIMETHYLAMINO)ETHYL ESTER	2439-35-2	☐	☐	☐	☐	☑	☑
287	Acrylonitrile	107-13-1	☑	☑	☑	☑	☑	☑
288	Acryloyl chloride	814-68-6	☑	☑	☑	☐	☐	☑
289	Adipic acid	124-04-9	☐	☑	☑	☐	☐	☑
290	Adiponitrile	111-69-3	☐	☑	☑	☐	☐	☑
291	a-Hydroxyisobutyronitrile	75-86-5	☑	☑	☑	☐	☑	☑
292	Alachlor	814-68-6	☐	☑	☑	☐	☐	☑
293	Aldicarb	116-06-3	☐	☑	☑	☐	☐	☑

(continued)

(continued)

ID	Chemical Name	CAS	DHS	EPCRA	SARA	HAPS	P H C	OSHA
294	Aldicarb sulfone	1646-88-4	☐	☑	☑	☐	☐	☑
295	Aldrin	309-00-2	☐	☑	☑	☐	☐	☑
296	Allene	463-49-0	☑	☑	☑	☐	☐	☑
297	Allyl alcohol	107-18-6	☑	☑	☑	☐	☐	☑
298	Allyl chloride	107-05-1	☐	☑	☑	☑	☐	☑
299	Allylamine	107-11-9	☑	☑	☑	☐	☑	☑
300	ALLYLTRICHLOROSILANE	107-37-9	☑	☐	☐	☐	☐	☑
301	alpha-Endosulfan	959-98-8	☐	☑	☑	☐	☐	☑
302	alpha-BHC	319-84-6	☐	☑	☑	☐	☐	☑
303	Aluminum (fume or dust)	3012-65-5	☐	☑	☑	☐	☐	☑
304	Aluminum bromide	7727-15-3	☑	☐	☐	☐	☐	☑
305	Aluminumchloride	7446-70-0	☑	☐	☐	☐	☐	☑
306	Aluminum oxide(fibrous forms)	3012-65-5	☐	☑	☑	☐	☐	☑
307	Aluminum phosphide	20859-73-8	☑	☑	☑	☐	☐	☑
308	Aluminum sulfate	10043-01-3	☐	☑	☑	☐	☐	☑
309	ALUMINUM, CHLORODIISOBUTYL-	1779-25-5	☐	☐	☐	☐	☑	☑
310	Ametryn	834-12-8	☐	☑	☑	☐	☐	☑
311	Aminopterin	54-62-6	☐	☑	☑	☐	☐	☑
312	Amiton	78-53-5	☑	☑	☑	☐	☐	☑
313	Amiton oxalate	3734-97-2	☐	☑	☑	☐	☐	☑
314	Amitraz	33089-61-1	☐	☑	☑	☐	☐	☑
315	Ammonia gas	7664-41-7	☑	☑	☑	☐	☐	☑
316	Ammonium acetate	631-61-8	☐	☑	☑	☐	☐	☑
317	Ammonium benzoate	1863-63-4	☐	☑	☑	☐	☐	☑
318	Ammonium bicarbonate	1066-33-7	☐	☑	☑	☐	☐	☑
319	Ammonium bichromate	7789-09-5	☐	☑	☑	☐	☐	☑
320	Ammonium bifluoride	1341-49-7	☐	☑	☑	☐	☐	☑
321	Ammonium bisulfite	10192-30-0	☐	☑	☑	☐	☐	☑
322	Ammonium carbamate	1111-78-0	☐	☑	☑	☐	☐	☑
323	Ammonium carbonate	506-87-6	☐	☑	☑	☐	☐	☑
324	Ammonium chloride	12125-02-9	☐	☑	☑	☐	☐	☑
325	Ammonium chromate	7788-98-9	☐	☑	☑	☐	☐	☑
326	Ammonium citrate, dibasic	3012-65-5	☐	☑	☑	☐	☐	☑
327	Ammonium fluoborate	13826-83-0	☐	☑	☑	☐	☐	☑
328	Ammonium fluoride	12125-01-8	☐	☑	☑	☐	☐	☑
329	Ammonium hydroxide	1336-21-6	☐	☑	☑	☐	☐	☑
330	Ammonium nitrate	6484-52-2	☑	☐	☐	☐	☐	☑
331	Ammonium oxalate	6009-70-7	☐	☑	☑	☐	☐	☑
332	Ammonium oxalate	14258-49-2	☐	☑	☑	☐	☐	☑
333	Ammonium oxalate	5972-73-6	☐	☑	☑	☐	☐	☑
334	Ammonium perchlorate	7790-98-9	☑	☐	☐	☐	☐	☑
335	Ammonium picrate, <10% water	131-74-8	☑	☑	☑	☐	☐	☑
336	Ammonium silicofluoride	16919-19-0	☐	☑	☑	☐	☐	☑
337	Ammonium sulfamate	7773-06-0	☐	☑	☑	☐	☐	☑
338	AMMONIUM SULFATE	7783-20-2	☐	☐	☐	☐	☑	☑

(continued)

(continued)

ID	Chemical Name	CAS	DHS	EPCRA	SARA	HAPS	P H C	OSHA
339	Ammonium sulfide	12135-76-1	☐	☑	☑	☐	☐	☑
340	Ammonium sulfite	10196-04-0	☐	☑	☑	☐	☐	☑
341	Ammonium tartrate	14307-43-8	☐	☑	☑	☐	☐	☑
342	Ammonium tartrate	3164-29-2	☐	☑	☑	☐	☐	☑
343	Ammonium thiocyanate	1762-95-4	☐	☑	☑	☐	☐	☑
344	Ammonium vanadate	7803-55-6	☐	☑	☑	☐	☐	☑
345	Amphetamine	300-62-9	☐	☑	☑	☐	☐	☑
346	Amyl acetate	628-63-7	☐	☑	☑	☐	☐	☑
347	Amyltrichlorosilane	107-72-2	☑	☐	☐	☐	☐	☑
348	ANALINE,((5-CHLORO-8-HYDROXY-3-METHYL- l-OXO-7-ISOCHROMANYL) CAR	303-47-9	☐	☐	☐	☐	☑	☑
349	Anilazine	101-05-3	☐	☑	☑	☐	☐	☑
350	Aniline	62-53-3	☐	☑	☑	☑	☐	☑
351	Aniline, 2,4,6-trimethyl-	88-05-1	☐	☑	☑	☐	☐	☑
352	ANILINE, 4,4'-OXYDI-	101-80-4	☐	☑	☑	☐	☑	☑
353	ANILINE, 4,4'-THIODI-	139-65-1	☐	☑	☑	☐	☑	☑
354	ANILINE, P-CHLORO	106-47-8	☐	☑	☑	☐	☑	☑
355	ANISIDINE, 5-METHYL-,o-	120-71-8	☐	☑	☑	☐	☑	☑
356	Anthracene	120-12-7	☐	☑	☑	☐	☐	☑
357	ANTHRACENEDIONE, 1,4,5,8-TETRAAMINO-,	2475-45-8	☐	☐	☑	☐	☑	☑
358	ANTHRAQUINONE, 1,8-DIHYDROXY-	117-10-2	☐	☐	☑	☐	☑	☑
359	ANTHRAQUINONE, 2-METHYL-1-NITRO-	129-15-7	☐	☐	☑	☐	☑	☑
360	Antimony	7440-36-0	☐	☑	☑	☐	☐	☑
361	Antimony hydride	7803-52-3	☑	☐	☐	☐	☐	☑
362	ANTIMONY OXIDE	1309-64-4	☐	☑	☑	☐	☑	☑
363	Antimony pentachloride	7647-18-9	☐	☑	☑	☐	☐	☑
364	Antimony potassium	28300-74-5	☐	☑	☑	☐	☐	☑
365	Antimony tribromide	7789-61-9	☐	☑	☑	☐	☐	☑
366	Antimony trichloride	10025-91-9	☐	☑	☑	☐	☐	☑
367	Antimony trifluoride	7783-56-4	☐	☑	☑	☐	☐	☑
368	Antimony(V) fluoride	7783-70-2	☑	☑	☑	☐	☐	☑
369	Antimycin A	1397-94-0	☐	☑	☑	☐	☐	☑
370	ANTU	86-88-4	☐	☑	☑	☐	☐	☑
371	Aroclor 1016	12674-11-2	☐	☑	☑	☐	☐	☑
372	Aroclor 1221	11104-28-2	☐	☑	☑	☐	☐	☑
373	Aroclor 1232	11141-16-5	☐	☑	☑	☐	☐	☑
374	Aroclor 1242	53469-21-9	☐	☑	☑	☐	☐	☑
375	Aroclor 1248	12672-29-6	☐	☑	☑	☐	☐	☑
376	Aroclor 1254	11097-69-1	☐	☑	☑	☐	☐	☑
377	Aroclor 1260	11096-82-5	☐	☑	☑	☐	☐	☑
378	ARSENIC	7440-38-2	☐	☑	☑	☐	☑	☑
379	Arsenic acid	1327-52-2	☐	☑	☑	☐	☐	☑
380	Arsenic acid	7778-39-4	☐	☑	☑	☐	☐	☑

(continued)

(continued)

ID	Chemical Name	CAS	DHS	EPCRA	SARA	HAPS	P H C	OSHA
381	Arsenic disulfide	1303-32-8	☐	☑	☑	☐	☐	☑
382	Arsenic pentoxide	1303-28-2	☐	☑	☑	☐	☐	☑
383	Arsenic trioxide	1327-53-3	☐	☑	☑	☐	☐	☑
384	Arsenic trisulfide	1303-33-9	☐	☑	☑	☐	☐	☑
385	Arsenic (III) chloride	7784-34-1	☑	☑	☑	☐	☐	☑
386	Arsine	7784-42-1	☑	☑	☑	☐	☐	☑
387	Asbestos	1332-21-4	☐	☑	☑	☑	☐	☑
388	Auramine	492-80-8	☐	☑	☑	☐	☐	☑
389	AZEPIN-2-ONE, HEXAHYDRO-, 2H-	105-60-2	☐	☐	☐	☐	☑	☑
390	Azinphos-ethyl	2642-71-9	☐	☑	☑	☐	☐	☑
391	Azinphos-methyl	86-50-0	☐	☑	☑	☐	☐	☑
392	AZIRINO(2',3'3,4)PYRROLO(1,2-a) INDOLE-4,7-DIONE,CARBAMATE (ESTER)	50-07-7	☐	☑	☑	☐	☑	☑
393	AZOBENZENE	1103-33-3	☐	☐	☐	☐	☑	☑
394	Barban	101-27-9	☐	☑	☑	☐	☐	☑
395	Barium	7440-39-3	☐	☑	☑	☐	☐	☑
396	BARIUM AZIDE (wet)	18810-58-7	☑	☐	☐	☐	☐	☑
397	Barium cyanide	542-62-1	☐	☑	☑	☐	☐	☑
398	Bendiocarb	22781-23-3	☐	☑	☑	☐	☐	☑
399	Bendiocarb phenol	22961-82-6	☐	☑	☑	☐	☐	☑
400	Benfluralin	1861-40-1	☐	☑	☑	☐	☐	☑
401	Benomyl	17804-35-2	☐	☑	☑	☐	☐	☑
402	BENZ(A)ANTHRACENE	56-55-3	☐	☑	☑	☐	☑	☑
403	Benz[c]acridine	225-51-4	☐	☑	☑	☐	☐	☑
404	Benzamide	55-21-0	☐	☑	☑	☐	☐	☑
405	Benzamide, 3,5-dichloro-N-(1,1-dimethyl-2-propynyl	23950-58-5	☐	☑	☑	☐	☐	☑
406	Benzenamine, 3-(trifluoromethyl)-	98-16-8	☐	☑	☑	☐	☐	☑
407	BENZENAMINE, 4-((4-AMINOPHENYL) (4-IMINO-2,5-CYCLOHEXADIEN- 1- YLIDE	569-61-9	☐	☐	☐	☐	☑	☑
408	Benzenamine, N-phenyl-, hexanitro derivative	35860-31-2	☑	☐	☐	☐	☐	☑
409	Benzene (including benzene from gasoline)	71-43-2	☐	☑	☑	☑	☑	☑
410	BENZENE, (DICHLOROMETHYL)-	98-87-3	☐	☑	☑	☐	☑	☑
411	Benzene, 1-(chloromethyl)-4-nitro-	100-14-1	☐	☑	☑	☐	☐	☑
412	Benzene, 1,1'-(1,2-Ethenediyl)-Bis 2,4,6-Trinitro-	20062-22-0	☑	☐	☐	☐	☐	☑
413	BENZENE, 1,3-BIS(l-METHYLETHYL)-2-ISOCYANATO	28178-42-9	☐	☐	☐	☐	☑	☑
414	Benzene, 2,4-dichloro-1-(4-nitrophenoxy)-	1836-75-5	☐	☑	☑	☐	☐	☑
415	BENZENE, 4-ALLYL-1,2-(METHYLENEDIOXY)-	94-59-7	☐	☑	☑	☐	☑	☑
416	Benzeneamine, N-hydroxy-N-nitroso, ammonium salt	135-20-6	☐	☑	☑	☐	☐	☑

(continued)

(continued)

ID	Chemical Name	CAS	DHS	EPCRA	SARA	HAPS	P H C	OSHA
417	Benzenearsonic acid	98-05-5	☐	☑	☑	☐	☐	☑
418	Benzeneethanamine, alpha,alpha-dimethyl-	122-09-8	☐	☑	☑	☐	☐	☑
419	Benzenemethanol, 4-chloro-.alpha.-4-chlorophenyl)-.alpha.-(trichloromethyl)	115-32-2	☐	☑	☑	☐	☐	☑
420	Benzenesulfonyl chloride	98-09-9	☐	☑	☑	☐	☐	☑
421	BENZENETHIOL	108-98-5	☐	☑	☑	☐	☑	☑
422	Benzidine	92-87-5	☐	☑	☑	☑	☑	☑
423	BENZIDINE, 3,3'-DIMETHOXY-, DIHYDROCHLORIDE	20325-40-0	☐	☑	☑	☐	☑	☑
424	Benzilic acid	76-93-7	☑	☐	☐	☐	☐	☑
425	Benzimidazole, 4,5-dichloro-2-(trifluoromethyl)-	3615-21-2	☐	☑	☑	☐	☐	☑
426	Benzo(a)phenanthrene	218-01-9	☐	☑	☑	☐	☐	☑
427	Benzo(j)fluoranthene	205-82-3	☐	☑	☑	☐	☐	☑
428	Benzo(k)fluoranthene	207-08-9	☐	☑	☑	☐	☐	☑
429	Benzo(rst)pentaphene	189-55-9	☐	☑	☑	☐	☐	☑
430	Benzo[a]pyrene	50-32-8	☐	☑	☑	☐	☐	☑
431	Benzo[b]fluoranthene	205-99-2	☐	☑	☑	☐	☐	☑
432	Benzo[g,h,i]perylene	191-24-2	☐	☑	☑	☐	☐	☑
433	Benzoic acid	65-85-0	☐	☑	☑	☐	☐	☑
434	Benzoic acid , 5-(2-chloro-4-(trifluoromethyl)phenoxy)-2-nitro-, 2-ethoxy-1-m	77501-63-4	☐	☑	☑	☐	☐	☑
435	Benzonitrile	100-47-0	☐	☑	☑	☐	☐	☑
436	Benzotrichloride	98-07-7	☐	☑	☑	☑	☑	☑
437	Benzoyl chloride	98-88-4	☐	☑	☑	☐	☐	☑
438	Benzoyl peroxide	94-36-0	☐	☑	☑	☐	☐	☑
439	Benzyl chloride	100-44-7	☐	☑	☑	☑	☑	☑
440	Beryllium	7440-41-7	☐	☑	☑	☐	☐	☑
441	Beryllium chloride	7787-47-5	☐	☑	☑	☐	☐	☑
442	Beryllium fluoride	7787-49-7	☐	☑	☑	☐	☐	☑
443	Beryllium nitrate	13597-99-4	☐	☑	☑	☐	☐	☑
444	Beryllium nitrate	7787-55-5	☐	☑	☑	☐	☐	☑
445	BERYLLIUM SULFATE, TETRAHYDRATE (114)	7787-56-6	☐	☐	☐	☐	☑	☑
446	beta-Endosulfan	33213-65-9	☐	☑	☑	☐	☐	☑
447	beta-BHC	319-85-7	☐	☑	☑	☐	☐	☑
448	beta-Propiolactone	57-57-8	☐	☑	☑	☑	☑	☑
449	Bicyclo[2.2.1]heptane-2-carbonitrile, 5-chloro-6-((((methylamino)carbonyl)ox	15271-41-7	☐	☑	☑	☐	☐	☑
450	Bifenthrin	82657-04-3	☐	☑	☑	☐	☐	☑
451	Biphenyl	92-52-4	☐	☑	☑	☑	☐	☑
452	BIPHENYLOL, 2-	90-43-7	☐	☑	☑	☐	☑	☑
453	Bis(2-chloro-1-methylethyl)ether	108-60-1	☐	☑	☑	☐	☐	☑
454	Bis(2-chloroethoxy) methane	111-91-1	☐	☑	☑	☐	☐	☑
455	Bis(2-Chloroethyl)sulfide	505-60-2	☑	☑	☑	☐	☐	☑

(continued)

(continued)

ID	Chemical Name	CAS	DHS	EPCRA	SARA	HAPS	P H C	OSHA
456	Bis(2-chloroethylthio)methane	63869-13-6	☑	☐	☐	☐	☐	☑
457	Bis(2-chloroethylthioethyl) ether	63918-89-8	☑	☐	☐	☐	☐	☑
458	Bis(2-chloroethylthiomethyl)ether	63918-90-1	☑	☐	☐	☐	☐	☑
459	Bis(2-chlorovinyl)chloroarsine	40334-69-8	☑	☐	☐	☐	☐	☑
460	Bis(2-ethylhexyl)phthalate (DEHP)	117-81-7	☐	☑	☑	☑	☐	☑
461	Bis(chloromethyl)ether	542-88-1	☑	☑	☑	☑	☐	☑
462	Bis(tributyltin) oxide	56-35-9	☐	☑	☑	☐	☐	☑
463	Bitoscanate	4044-65-9	☐	☑	☑	☐	☐	☑
464	BLEOMYCIN	11116-32-8	☐	☐	☐	☐	☑	☑
465	BLEOMYCIN, SULFATE	9041-93-4	☐	☐	☐	☐	☑	☑
466	BORON	7440-42-8	☐	☐	☐	☐	☑	☑
467	Boron tribromide	10294-33-4	☑	☐	☐	☐	☐	☑
468	Boron trichloride	10294-34-5	☑	☑	☑	☐	☑	☑
469	Boron trifluoride methyl etherate	353-42-4	☑	☑	☑	☐	☐	☑
470	Boron trifluoride, gas	7637-07-2	☑	☑	☑	☐	☐	☑
471	Bromacil	314-40-9	☐	☑	☑	☐	☐	☑
472	Bromacil, lithium salt	53404-19-6	☐	☑	☑	☐	☐	☑
473	Bromadiolone	28772-56-7	☐	☑	☑	☐	☐	☑
474	BROMIC acid , POTASSIUM SALT	7758-01-2	☐	☑	☑	☐	☑	☑
475	Bromine	7726-95-6	☑	☑	☑	☐	☑	☑
476	Bromine chloride	13863-41-7	☑	☐	☐	☐	☐	☑
477	Bromine pentafluoride	7789-30-2	☑	☐	☐	☐	☐	☑
478	Bromine trifluoride	7787-71-5	☑	☐	☐	☐	☐	☑
479	Bromoacetone	598-31-2	☐	☑	☑	☐	☐	☑
480	Bromochlorodifluoromethane	353-59-3	☐	☑	☑	☐	☐	☑
481	Bromoform	75-25-2	☐	☑	☑	☑	☑	☑
482	Bromomethane	74-83-9	☑	☑	☑	☑	☑	☑
483	Bromotrifluoroethylene	598-73-2	☑	☑	☑	☐	☐	☑
484	Bromotrifluoromethane	75-63-8	☐	☑	☑	☐	☐	☑
485	Bromoxynil	1689-84-5	☐	☑	☑	☐	☐	☑
486	Bromoxynil octanoate	1689-99-2	☐	☑	☑	☐	☐	☑
487	Brucine	357-57-3	☐	☑	☑	☐	☐	☑
488	Butane	106-97-8	☑	☑	☑	☐	☐	☑
489	BUTANE, (+-)-1,2,3,4-DIEPOXY-	298-18-0	☐	☐	☐	☐	☑	☑
490	BUTANE, 1,2-EPOXY-		☐	☑	☑	☐	☑	☑
491	BUTANEDIOL, DIMETHANESULFONATE, 1,4-	55-98-1	☐	☐	☐	☐	☑	☑
492	BUTEN-2-ONE 3-	78-94-4	☐	☑	☑	☐	☑	☑
493	BUTENE, 1,4-DICHLORO-,(E)-,2-	110-57-6	☐	☑	☑	☐	☑	☑
494	BUTENE, 2,3-DICHLOROHEXAFLUORO-,2-	303-04-8	☐	☐	☐	☐	☑	☑
495	Butyl acetate	123-86-4	☐	☑	☑	☐	☐	☑
496	Butyl acrylate	141-32-2	☐	☑	☑	☐	☐	☑
497	Butylamine	109-73-9	☐	☑	☑	☐	☐	☑
498	Butylethylcarbamothioic acid S-propyl ester	1114-71-2	☐	☑	☑	☐	☐	☑

(continued)

(continued)

ID	Chemical Name	CAS	DHS	EPCRA	SARA	HAPS	P H C	OSHA
499	BUTYL-N-NITROSO-1-BUTAMINE, N-	924-16-3	☐	☑	☑	☐	☑	☑
500	Butyltrichlorosilane	7521-80-4	☑	☐	☐	☐	☐	☑
501	Butyraldehyde	123-72-8	☐	☑	☑	☐	☐	☑
502	Butyric acid	107-92-6	☐	☑	☑	☐	☐	☑
503	BUTYRIC acid	305-03-3	☐	☑	☑	☐	☑	☑
504	C.I. acid Green 338	4680-78-8	☐	☑	☑	☐	☐	☑
505	C.I. Basic Green 4218	569-64-2	☐	☑	☑	☐	☐	☑
506	C.I. Basic Red 1	989-38-8	☐	☑	☑	☐	☐	☑
507	C.I. Direct Black	1937-37-7	☐	☑	☑	☐	☐	☑
508	C.I. Direct Blue	28407-37-6	☐	☑	☑	☐	☐	☑
509	C.I. Direct Blue 6	2602-46-2	☐	☑	☑	☐	☐	☑
510	C.I. Direct Brown 95	16071-86-6	☐	☑	☑	☐	☐	☑
511	C.I. Disperse Yellow 3	2832-40-8	☐	☑	☑	☐	☐	☑
512	C.I. Food Red 15	81-88-9	☐	☑	☑	☐	☐	☑
513	C.I. Vat Yellow 4	128-66-5	☐	☑	☑	☐	☐	☑
514	Cacodylic acid	75-60-5	☐	☑	☑	☐	☐	☑
515	CADMIUM	7440-43-9	☐	☑	☑	☐	☑	☑
516	Cadmium acetate	543-90-8	☐	☑	☑	☐	☐	☑
517	Cadmium bromide	7789-42-6	☐	☑	☑	☐	☐	☑
518	CADMIUM CHLORIDE	10108-64-2	☐	☑	☑	☐	☑	☑
519	CADMIUM OXIDE	1306-19-0	☐	☑	☑	☐	☑	☑
520	Cadmium stearate	2223-93-0	☐	☑	☑	☐	☐	☑
521	Calcium arsenate	7778-44-1	☐	☑	☑	☐	☐	☑
522	Calcium arsenite	52740-16-6	☐	☑	☑	☐	☐	☑
523	Calcium carbide	75-20-7	☐	☑	☑	☐	☐	☑
524	Calcium chromate	13765-19-0	☐	☑	☑	☐	☐	☑
525	Calcium cyanamide	156-62-7	☐	☑	☑	☑	☐	☑
526	Calcium cyanide	592-01-8	☐	☑	☑	☐	☐	☑
527	Calcium dithionite	15512-36-4	☑	☐	☐	☐	☐	☑
528	Calcium dodecylbenz enesulfonate	26264-06-2	☐	☑	☑	☐	☐	☑
529	Calcium hypochlorite	7778-54-3	☐	☑	☑	☐	☐	☑
530	Calcium phosphide	1305-99-3	☑	☑	☑	☐	☐	☑
531	Cantharidin	56-25-7	☐	☑	☑	☐	☐	☑
532	Captan	133-06-2	☐	☑	☑	☑	☐	☑
533	Carbachol chloride	51-83-2	☐	☑	☑	☐	☐	☑
534	Carbamic acid , diethylthio-, S-(p-chlorobenzyl)	28249-77-6	☐	☑	☑	☐	☐	☑
535	Carbamic acid , methyl-, O-(((2,4-dimethyl-1,3-dithiolan-2-yl)methylene) amin	26419-73-8	☐	☑	☑	☐	☐	☑
536	CARBAMIC acid , METHYL-,2,3-DIHYDRO-2,2-DIMETHYL-7-BENZOFURANYLES	1563-66-2	☐	☑	☑	☐	☑	☑
537	Carbamodithioic acid , 1,2-ethanediylbis-, zinc complex	12122-67-7	☐	☑	☑	☐	☐	☑

(continued)

(continued)

ID	Chemical Name	CAS	DHS	EPCRA	SARA	HAPS	P H C	OSHA
538	Carbamothioic acid , bis(1-methylethyl)-S-(2,3-dichloro-2-propenyl)ester	2303-16-4	☐	☑	☑	☐	☐	☑
539	Carbamothioic acid , dipropyl-, S-(phenylmethyl) ester	52888-80-9	☐	☑	☑	☐	☐	☑
540	Carbaryl	63-25-2	☐	☑	☑	☑	☐	☑
541	Carbendazim	10605-21-7	☐	☑	☑	☐	☐	☑
542	Carbofuran phenol	1563-38-8	☐	☑	☑	☐	☐	☑
543	Carbon disulfide	75-15-0	☑	☑	☑	☑	☐	☑
544	Carbon monoxide gas	630-08-0	☑	☐	☐	☐	☐	☑
545	Carbon tetrachloride	56-23-5	☐	☑	☑	☑	☑	☑
546	Carbonyl fluoride	353-50-4	☑	☑	☑	☐	☐	☑
547	Carbonyl sulfide	463-58-1	☑	☑	☑	☑	☐	☑
548	Carbophenothion	786-19-6	☐	☑	☑	☐	☐	☑
549	Carbosulfan	55285-14-8	☐	☑	☑	☐	☐	☑
550	Carboxin	5234-68-4	☐	☑	☑	☐	☐	☑
551	CARBOXYLIC acid ,3-beta,20-alpha-YOHIMBAN-16-beta-	50-55-5	☐	☑	☑	☐	☑	☑
552	CARRAGEENAN,DEGRADED	9000-07-1	☐	☑	☑	☐	☑	☑
553	Catechol	120-80-9	☐	☑	☑	☑	☑	☑
554	CFC-11	75-69-4	☐	☐	☐	☐	☐	☑
555	CFC-114	76-14-2	☐	☑	☑	☐	☐	☑
556	CFC-115	76-15-3	☐	☑	☑	☐	☐	☑
557	CFC-12	75-71-8	☐	☑	☑	☐	☐	☑
558	CFC-13	75-72-9	☐	☑	☑	☐	☐	☑
559	Chinomethionat	2439-01-2	☐	☑	☑	☐	☐	☑
560	Chloramben	133-90-4	☐	☑	☑	☑	☐	☑
561	Chlordane	57-74-9	☐	☑	☑	☑	☑	☑
562	Chlorfenvinfos	470-90-6	☐	☑	☑	☐	☐	☑
563	Chlorimuron ethyl	90982-32-4	☐	☑	☑	☐	☐	☑
564	Chlorine dioxide, gas	10049-04-4	☑	☑	☑	☐	☐	☑
565	Chlorine monoxide	7791-21-1	☑	☑	☑	☐	☐	☑
566	Chlorine pentafluoride	13637-63-3	☑	☐	☐	☐	☐	☑
567	Chlorine trifluoride	7790-91-2	☑	☐	☐	☐	☐	☑
568	Chlorine, gas	7782-50-5	☑	☑	☑	☑	☐	☑
569	Chlormephos	24934-91-6	☐	☑	☑	☐	☐	☑
570	Chlormequat chloride	999-81-5	☐	☑	☑	☐	☐	☑
571	Chlornaphazine	494-03-1	☐	☑	☑	☐	☐	☑
572	Chloroacetaldehyde	107-20-0	☐	☑	☑	☐	☐	☑
573	Chloroacetic acid	79-11-8	☐	☑	☑	☑	☑	☑
574	Chloroacetyl chloride	79-04-9	☑	☐	☐	☐	☐	☑
575	Chlorobenzene	108-90-7	☐	☑	☑	☑	☐	☑
576	Chlorobenzilate	510-15-6	☐	☑	☑	☑	☐	☑
577	Chlorodifluoromethane	75-45-6	☐	☑	☑	☐	☐	☑
578	Chloroethyl chloroformate	627-11-2	☐	☑	☑	☐	☐	☑
579	Chloroform	67-66-3	☑	☑	☑	☑	☑	☑
580	Chloromethane	74-87-3	☑	☑	☑	☑	☐	☑

(continued)

(continued)

ID	Chemical Name	CAS	DHS	EPCRA	SARA	HAPS	P H C	OSHA
581	Chloromethyl methyl ether	107-30-2	☑	☑	☑	☑	☑	☑
582	Chlorophacinone	3691-35-8	☐	☑	☑	☐	☐	☑
583	Chloropicrin	76-06-2	☑	☑	☑	☐	☑	☑
584	Chloroprene	126-99-8	☐	☑	☑	☑	☑	☑
585	Chlorosulfonic acid	7790-94-5	☑	☑	☑	☐	☐	☑
586	Chlorotetrafluoroethane	63938-10-3	☐	☑	☑	☐	☐	☑
587	Chlorotrifluoroethylene	79-38-9	☑	☑	☑	☐	☐	☑
588	Chlorotrimethylsilane	75-77-4	☑	☑	☑	☐	☐	☑
589	Chloroxuron	1982-47-4	☐	☑	☑	☐	☐	☑
590	Chlorpyrifos	2921-88-2	☐	☑	☑	☐	☐	☑
591	Chlorpyrifos methyl	5598-13-0	☐	☑	☑	☐	☐	☑
592	Chlorthiophos	21923-23-9	☐	☑	☑	☐	☐	☑
593	Chromic acetate	1066-30-4	☐	☑	☑	☐	☐	☑
594	Chromic acid	7738-94-5	☐	☑	☑	☐	☐	☑
595	Chromic acid	11115-74-5	☐	☑	☑	☐	☐	☑
596	CHROMIC acid , DIPOTASSIUM SALT	7789-00-6	☐	☑	☑	☐	☑	☑
597	Chromic chloride	10025-73-7	☐	☑	☑	☐	☐	☑
598	CHROMIC SULFATE	10101-53-8	☐	☑	☑	☐	☑	☑
599	Chromium	7440-47-3	☐	☑	☑	☐	☐	☑
600	Chromium oxychloride (CrCl2O2)	14977-61-8	☑	☐	☐	☐	☐	☑
601	CHROMIUM(VI) OXIDE (13)	1333-82-0	☐	☐	☐	☐	☑	☑
602	Chromous chloride	10049-05-5	☐	☑	☑	☐	☐	☑
603	CHRYSENE, 5-METHYL-	3697-24-3	☐	☑	☑	☐	☑	☑
604	CHRYSENE, 6-NITRO-	7496-02-8	☐	☐	☐	☐	☑	☑
605	CINNAMIC acid , 3,4-DIHYDROXY-	331-39-5	☐	☐	☐	☐	☑	☑
606	cis-2-Butene	590-18-1	☑	☑	☑	☐	☐	☑
607	Cobalt	7440-48-4	☐	☑	☑	☐	☐	☑
608	COBALT(2+) OXIDE	1307-96-6	☐	☐	☐	☐	☑	☑
609	COBALT(II) CHLORIDE	7646-79-9	☐	☐	☑	☐	☑	☑
610	Cobalt, ((2,2'-(1,2-ethanediylbis (nitrilomethylidyne))bis(6-fluorophenylato))(2	62207-76-5	☐	☑	☑	☐	☐	☑
611	COBALT, DI-mu-CARBONYLHEXACARBONYLDI-, (Co-Co)	10210-68-1	☐	☑	☑	☐	☑	☑
612	Cobaltous bromide	7789-43-7	☐	☑	☑	☐	☐	☑
613	Cobaltous formate	544-18-3	☐	☑	☑	☐	☐	☑
614	Cobaltous sulfamate	14017-41-5	☐	☑	☑	☐	☐	☑
615	Colchicine	64-86-8	☐	☑	☑	☐	☐	☑
616	Copper	7440-50-8	☐	☑	☑	☐	☐	☑
617	Copper cyanide	544-92-3	☐	☑	☑	☐	☐	☑
618	Coumaphos	56-72-4	☐	☑	☑	☐	☐	☑
619	COUMARIN, 3-(alpha-ACETONYLBENZYL)-4-HYDROXY-	81-81-2	☐	☑	☑	☐	☑	☑
620	Coumatetralyl	5836-29-3	☐	☑	☑	☐	☐	☑

(continued)

(continued)

ID	Chemical Name	CAS	DHS	EPCRA	SARA	HAPS	P H C	OSHA
621	Creosote	8001-58-9	☐	☑	☑	☐	☐	☑
622	Cresols/Cresylic acid (isomers and mixture)	1319-77-3	☐	☑	☑	☑	☐	☑
623	Crimidine	535-89-7	☐	☑	☑	☐	☐	☑
624	Crotonaldehyde (cis and trans)	4170-30-3	☑	☑	☑	☐	☐	☑
625	Crotonaldehyde, trans-	123-73-9	☑	☑	☑	☐	☐	☑
626	Cumene	98-82-8	☐	☑	☑	☑	☐	☑
627	Cumene hydroperoxide	80-15-9	☐	☑	☑	☐	☐	☑
628	Cupric acetate	142-71-2	☐	☑	☑	☐	☐	☑
629	Cupric acetoarsenite	12002-03-8	☐	☑	☑	☐	☐	☑
630	Cupric chloride	7447-39-4	☐	☑	☑	☐	☐	☑
631	Cupric nitrate	3251-23-8	☐	☑	☑	☐	☐	☑
632	Cupric oxalate	5893-66-3	☐	☑	☑	☐	☐	☑
633	Cupric sulfate	7758-98-7	☐	☑	☑	☐	☐	☑
634	Cupric sulfate, ammoniated	10380-29-7	☐	☑	☑	☐	☐	☑
635	Cupric tartrate	815-82-7	☐	☑	☑	☐	☐	☑
636	Cyanazine	21725-46-2	☐	☑	☑	☐	☐	☑
637	Cyanides (soluble salts and complexes)	57-12-5	☐	☑	☑	☐	☐	☑
638	Cyanogen	460-19-5	☑	☑	☑	☐	☐	☑
639	CYANOGEN BROMIDE	506-68-3	☐	☑	☑	☐	☑	☑
640	Cyanogen chloride	506-77-4	☑	☑	☑	☐	☐	☑
641	Cyanogen iodide	506-78-5	☐	☑	☑	☐	☐	☑
642	Cyanophos	2636-26-2	☐	☑	☑	☐	☐	☑
643	Cycloate	1134-23-2	☐	☑	☑	☐	☐	☑
644	Cyclohexane	110-82-7	☐	☑	☑	☐	☐	☑
645	CYCLOHEXANE, NITRO-	1122-60-7	☐	☑	☑	☐	☑	☑
646	Cyclohexanol	108-93-0	☐	☑	☑	☐	☐	☑
647	Cyclohexanone	108-94-1	☐	☑	☑	☐	☐	☑
648	CYCLOHEXENE, 4-VINYL-1-	100-40-3	☐	☑	☑	☐	☑	☑
649	Cycloheximide	66-81-9	☐	☑	☑	☐	☐	☑
650	Cyclohexylamine	108-91-8	☑	☑	☑	☐	☐	☑
651	CYCLOPENTA(c)FURO(3',2'4,5) FURO(2,3-h) (l)BENZOPYRAN-1,11-DIONE	1162-65-8	☐	☐	☐	☐	☑	☑
652	Cyclophosphamide	50-18-0	☐	☑	☑	☐	☐	☑
653	Cyclopropane	75-19-4	☑	☑	☑	☐	☐	☑
654	CYCLOSPORIN A	59865-13-3	☐	☐	☐	☐	☑	☑
655	Cyclotetramethylene tetranitramine (dry or not stabilized)	2691-41-0	☑	☐	☐	☐	☐	☑
656	Cyfluthrin	68359-37-5	☐	☑	☑	☐	☐	☑
657	Daunomycin	20830-81-3	☐	☑	☑	☐	☐	☑
658	Dazomet	533-74-4	☐	☑	☑	☐	☐	☑
659	Dazomet, sodium salt	53404-60-7	☐	☑	☑	☐	☐	☑
660	DDD	72-54-8	☐	☑	☑	☐	☐	☑
661	DDE	3547-04-4	☐	☑	☑	☑	☐	☑
662	DECABORANE(14)	17702-41-9	☐	☑	☑	☐	☑	☑
663	Decabromodiphenyl oxide	1163-19-5	☐	☑	☑	☐	☐	☑

(continued)

(continued)

ID	Chemical Name	CAS	DHS	EPCRA	SARA	HAPS	P H C	OSHA
664	DECYL ALCOHOL	112-30-1	☐	☐	☐	☐	☑	☑
665	DEF	78-48-8	☐	☑	☑	☐	☐	☑
666	delta-BHC	319-86-8	☐	☑	☑	☐	☐	☑
667	Demeton	8065-48-3	☐	☑	☑	☐	☐	☑
668	Demeton-S-methyl	919-86-8	☐	☑	☑	☐	☐	☑
669	Desmedipham	13684-56-5	☐	☑	☑	☐	☐	☑
670	Deuterium bromide, gas	13536-59-9	☑	☐	☐	☐	☐	☑
671	Deuterium chloride, gas	7698-05-7	☑	☐	☐	☐	☐	☑
672	Dialifor	10311-84-9	☐	☑	☑	☐	☐	☑
673	Diaminotoluene	496-72-0	☐	☑	☑	☐	☐	☑
674	Diaminotoluene	823-40-5	☐	☑	☑	☐	☐	☑
675	Diaminotoluene (mixed isomers)	25376-45-8	☐	☑	☑	☐	☐	☑
676	Diazinon	333-41-5	☐	☑	☑	☐	☐	☑
677	Diazodinitrophenol, wetted with not less than 40% water	4682-03-5	☑	☐	☐	☐	☐	☑
678	Diazomethane	334-88-3	☐	☑	☑	☑	☐	☑
679	Dibenz(a,h)acridine	226-36-8	☐	☑	☑	☐	☐	☑
680	DIBENZ(a,h)ANTHRACENE	53-70-3	☐	☑	☑	☐	☑	☑
681	Dibenz(a,j)acridine	224-42-0	☐	☑	☑	☐	☐	☑
682	Dibenzo(a,e)fluoranthene	5385-75-1	☐	☑	☑	☐	☐	☑
683	Dibenzo(a,e)pyrene	192-65-4	☐	☑	☑	☐	☐	☑
684	Dibenzo(a,h)pyrene	189-64-0	☐	☑	☑	☐	☐	☑
685	Dibenzo(a,l)pyrene	191-30-0	☐	☑	☑	☐	☐	☑
686	Dibenzofurans	132-64-9	☐	☑	☑	☑	☐	☑
687	Diborane	19287-45-7	☑	☑	☑	☐	☐	☑
688	Dibromotetrafluoroethane	124-73-2	☐	☑	☑	☐	☐	☑
689	Dibutylphthalate	84-74-2	☐	☑	☑	☑	☐	☑
690	Dicamba	1918-00-9	☐	☑	☑	☐	☐	☑
691	Dichlobenil	1194-65-6	☐	☑	☑	☐	☐	☑
692	Dichlone	117-80-6	☐	☑	☑	☐	☐	☑
693	Dichloran	99-30-9	☐	☑	☑	☐	☐	☑
694	Dichloro(methyl)phenylsilane	149-74-6	☑	☑	☑	☐	☐	☑
695	Dichloro-1,1,2-trifluoroethane	90454-18-5	☐	☑	☑	☐	☐	☑
696	Dichlorobenzene	25321-22-6	☐	☑	☑	☐	☐	☑
697	Dichlorodiethylsilane	1719-53-5	☑	☐	☐	☐	☐	☑
698	Dichlorodiphenylsilane	80-10-4	☑	☐	☐	☐	☐	☑
699	Dichloroethyl ether (Bis(2-chloroethyl) ether)	111-44-4	☐	☑	☑	☑	☑	☑
700	Dichlorofluoromethane	75-43-4	☐	☑	☑	☐	☐	☑
701	Dichloromethylsilane	75-54-7	☑	☐	☐	☐	☐	☑
702	Dichloropentafluoropropane	127564-92-5	☐	☑	☑	☐	☐	☑
703	Dichlorophene	97-23-4	☐	☑	☑	☐	☐	☑
704	Dichlorophenylarsine	696-28-6	☐	☑	☑	☐	☐	☑
705	Dichloropropane	26638-19-7	☐	☑	☑	☐	☐	☑
706	Dichloropropane Dichloropropene (mixture)	8003-19-8	☐	☑	☑	☐	☐	☑

(continued)

(continued)

ID	Chemical Name	CAS	DHS	EPCRA	SARA	HAPS	P H C	OSHA
707	Dichloropropene	26952-23-8	☐	☑	☑	☐	☐	☑
708	Dichlorosilane	4109-96-0	☑	☑	☑	☐	☐	☑
709	Dichlorotrifluoroethane	34077-87-7	☐	☑	☑	☐	☐	☑
710	Dichlorvos	62-73-7	☐	☑	☑	☑	☐	☑
711	Dicrotophos	141-66-2	☐	☑	☑	☐	☐	☑
712	Dicyclopentadiene	77-73-6	☐	☑	☑	☐	☐	☑
713	Dieldrin	60-57-1	☐	☑	☑	☐	☐	☑
714	Diethanolamine	111-42-2	☐	☑	☑	☑	☐	☑
715	Diethatyl ethyl	38727-55-8	☐	☑	☑	☐	☐	☑
716	Diethyl ethylphosphonate	78-38-6	☑	☐	☐	☐	☐	☑
717	Diethyl phosphite	762-04-9	☑	☐	☐	☐	☐	☑
718	Diethyl phthalate	84-66-2	☐	☑	☑	☐	☐	☑
719	Diethyl sulfate	64-67-5	☐	☑	☑	☑	☑	☑
720	Diethylamine	109-89-7	☐	☑	☑	☐	☐	☑
721	DIETHYLAMINE, HYDROCHLORIDE	55-86-7	☐	☐	☐	☐	☑	☑
722	Diethylarsine	692-42-2	☐	☑	☑	☐	☐	☑
723	Diethyldiisocyanatobenzene	134190-37-7	☐	☑	☑	☐	☐	☑
724	Diethyleneglycol dinitrate	693-21-0	☑	☐	☐	☐	☐	☑
725	Diethyl-N,N-dimethylphosphoroamidate	2404-03-7	☑	☐	☐	☐	☐	☑
726	Diethyl-p-nitrophenyl phosphate	311-45-5	☐	☑	☑	☐	☐	☑
727	Diflubenzuron	35367-38-5	☐	☑	☑	☐	☐	☑
728	Digitoxin	71-63-6	☐	☑	☑	☐	☐	☑
729	Diglycidyl ether	2238-07-5	☐	☑	☑	☐	☐	☑
730	Digoxin	20830-75-5	☐	☑	☑	☐	☐	☑
731	Dihydrosafrole	94-58-6	☐	☑	☑	☐	☐	☑
732	Dimefox	115-26-4	☐	☑	☑	☐	☐	☑
733	Dimethoate	60-51-5	☐	☑	☑	☐	☐	☑
734	Dimethyl aminoazobenzene	60-11-7	☐	☑	☑	☑	☑	☑
735	Dimethyl carbamoyl chloride	79-44-7	☐	☑	☑	☑	☑	☑
736	Dimethyl chlorothiophosphate	2524-03-0	☐	☑	☑	☐	☐	☑
737	Dimethyl ether	115-10-6	☑	☑	☑	☐	☐	☑
738	Dimethyl ethylphosphonate	6163-75-3	☑	☐	☐	☐	☐	☑
739	Dimethyl formamide	68-12-2	☐	☑	☑	☑	☐	☑
740	Dimethyl phosphite	868-85-9	☑	☐	☐	☐	☑	☑
741	Dimethyl phthalate	131-11-3	☐	☑	☑	☑	☐	☑
742	Dimethyl sulfate	77-78-1	☐	☑	☑	☑	☑	☑
743	Dimethylamine	124-40-3	☑	☑	☑	☐	☐	☑
744	Dimethylamine dicamba	2300-66-5	☐	☑	☑	☐	☐	☑
745	Dimethyldichlorosilane	75-78-5	☑	☑	☑	☐	☐	☑
746	Dimethylmethylphosphonate	756-79-6	☑	☐	☐	☐	☐	☑
747	Dimethyl-p-phenylenediamine	99-98-9	☐	☑	☑	☐	☐	☑
748	Dimetilan	644-64-4	☐	☑	☑	☐	☐	☑
749	Dinitrobenzene(mixed isomers)	25154-54-5	☐	☑	☑	☐	☐	☑

(continued)

(continued)

ID	Chemical Name	CAS	DHS	EPCRA	SARA	HAPS	P H C	OSHA
750	Dinitrobutyl phenol	88-85-7	☐	☑	☑	☐	☐	☑
751	Dinitroglycoluril	55510-04-8	☑	☐	☐	☐	☐	☑
752	Dinitrophenol	25550-58-7	☑	☑	☑	☐	☐	☑
753	Dinitr oresorcinol, wetted with not less than15% water by mass	35860-51-6	☑	☐	☐	☐	☐	☑
754	Din itrosobenzene	25550-55-4	☑	☐	☐	☐	☐	☑
755	Dinitrotoluene (mixed isomers)	25321-14-6	☐	☑	☑	☐	☐	☑
756	Dinocap	39300-45-3	☐	☑	☑	☐	☐	☑
757	Di-n-octyl phthalate	117-84-0	☐	☑	☑	☐	☐	☑
758	Dinoterb	1420-07-1	☐	☑	☑	☐	☐	☑
759	Dioxathion	78-34-2	☐	☑	☑	☐	☐	☑
760	Diphacinone	82-66-6	☐	☑	☑	☐	☐	☑
761	Diphenamid	957-51-7	☐	☑	☑	☐	☐	☑
762	Diphenylamine	122-39-4	☐	☑	☑	☐	☐	☑
763	Diphosphoramide, octamethyl-	152-16-9	☐	☑	☑	☐	☐	☑
764	Dipicryl sulfide, dry	2217-06-3	☑	☐	☐	☐	☐	☑
765	Dipotassium endothall	2164-07-0	☐	☑	☑	☐	☐	☑
766	DIPROPIONATE, 9-'CHLORO-1 6-beta-METHYL-11 -beta, 17,21-TRIHYDROXY-,	5534-09-8	☐	☐	☐	☐	☑	☑
767	Dipropyl isocinchomeronate	136-45-8	☐	☑	☑	☐	☐	☑
768	Dipropylamine	142-84-7	☐	☑	☑	☐	☐	☑
769	DIPROPYLAMINE, N-NITROSO-	621-64-7	☐	☑	☑	☐	☑	☑
770	Diquat	2764-72-9	☐	☑	☑	☐	☐	☑
771	Diquat	85-00-7	☐	☑	☑	☐	☐	☑
772	Disodium cyanodithioimidocarbonate	138-93-2	☐	☑	☑	☐	☐	☑
773	DISULFIDE, DIMETHYL	624-92-0	☐	☑	☑	☐	☑	☑
774	Disulfoton	298-04-4	☐	☑	☑	☐	☐	☑
775	Dithiazanine iodide	514-73-8	☐	☑	☑	☐	☐	☑
776	Dithiobiuret	541-53-7	☐	☑	☑	☐	☐	☑
777	Diuron	330-54-1	☐	☑	☑	☐	☐	☑
778	Dodecylbenzenesulfonic acid	27176-87-0	☐	☑	☑	☐	☐	☑
779	Dodecylguanidine monoacetate	2439-10-3	☐	☑	☑	☐	☐	☑
780	Dodecyltrichlorosilane	4484-72-4	☑	☐	☐	☐	☐	☑
781	d-trans-Allethrin	28057-48-9	☐	☑	☑	☐	☐	☑
782	Emetine, dihydrochloride	316-42-7	☐	☑	☑	☐	☐	☑
783	Endosulfan	115-29-7	☐	☑	☑	☐	☐	☑
784	Endosulfan sulfate	1031-07-8	☐	☑	☑	☐	☐	☑
785	Endothall	145-73-3	☐	☑	☑	☐	☐	☑
786	Endothion	2778-04-3	☐	☑	☑	☐	☐	☑
787	Endrin	72-20-8	☐	☑	☑	☐	☐	☑
788	Endrin aldehyde	7421-93-4	☐	☑	☑	☐	☐	☑
789	Epichlorohydrin	106-89-8	☑	☑	☑	☑	☑	☑
790	Epinephrine	51-43-4	☐	☑	☑	☐	☐	☑
791	EPN	2104-64-5	☐	☑	☑	☐	☐	☑
792	EPTC	759-94-4	☐	☑	☑	☐	☐	☑

(continued)

(continued)

ID	Chemical Name	CAS	DHS	EPCRA	SARA	HAPS	P H C	OSHA
793	Ergocalciferol	50-14-6	☐	☑	☑	☐	☐	☑
794	Ergotamine tartrate	379-79-3	☐	☑	☑	☐	☐	☑
795	Ethanamine	75-04-7	☐	☑	☑	☐	☐	☑
796	Ethane	74-84-0	☑	☑	☑	☐	☑	☑
797	Ethane, 1,1,1,2-tetrachloro-	630-20-6	☐	☑	☑	☐	☐	☑
798	ETHANE, 1,1,1-TRICHLORO-2,2-BIS (p-CHLOROPHENYL)-	50-29-3	☐	☑	☑	☐	☑	☑
799	Ethane, 1,1,2-trichloro-1,2,2,-trifluoro-	76-13-1	☐	☑	☑	☐	☐	☑
800	ETHANE, IODO-	75-03-6	☐	☐	☐	☐	☐	☑
801	Ethanesulfonyl chloride, 2-chloro-	1622-32-8	☐	☑	☑	☐	☐	☑
802	Ethanethiol	75-08-1	☑	☑	☑	☐	☐	☑
803	Ethanimidothioic acid , 2-(dimethylamino)-N-hydroxy-2-oxo-, methyl ester	30558-43-1	☐	☑	☑	☐	☐	☑
804	Ethanimidothioic acid , N-[[methylamino)carbonyl]	16752-77-5	☐	☑	☑	☐	☐	☑
805	Ethanol, 1,2-dichloro-, acetate	10140-87-1	☐	☑	☑	☐	☐	☑
806	Ethanol 2,2'-oxybis-, dicarbamate	5952-26-1	☐	☑	☑	☐	☐	☑
807	ETHANOL, -CHLORO-	107-07-3	☐	☑	☑	☐	☑	☑
808	Ethanol, 2-ethoxy-	110-80-5	☐	☑	☑	☐	☐	☑
809	ETHANOL, 2-FLUORO-	371-62-0	☐	☑	☑	☐	☑	☑
810	ETHANOL, N-NITROSOIMINODI-	1116-54-7	☐	☑	☑	☐	☑	☑
811	Ethion	563-12-2	☐	☑	☑	☐	☐	☑
812	Ethoprop	13194-48-4	☐	☑	☑	☐	☐	☑
813	Ethyl acetate	141-78-6	☐	☑	☑	☐	☐	☑
814	Ethyl acrylate	140-88-5	☐	☑	☑	☑	☑	☑
815	Ethyl benzene	100-41-4	☐	☑	☑	☑	☐	☑
816	Ethyl bis(2-chloroethyl)amine	538-07-8	☑	☑	☑	☐	☐	☑
817	Ethyl carbamate (Urethane)	51-79-6	☐	☑	☑	☐	☐	☑
818	Ethyl chloride	75-00-3	☑	☑	☑	☑	☐	☑
819	Ethyl ether	60-29-7	☑	☑	☑	☑	☐	☑
820	ETHYL ISOCYANATE	109-90-0	☐	☐	☐	☐	☑	☑
821	Ethyl methacrylate	97-63-2	☐	☑	☑	☐	☐	☑
822	Ethyl nitrite	109-95-5	☑	☑	☑	☐	☐	☑
823	Ethyl vinyl ether	109-92-2	☑	☑	☑	☐	☐	☑
824	ETHYLAMINE,N-METHYL-N-NITROSO-	10595-95-6	☐	☐	☐	☐	☑	☑
825	Ethylene	74-85-1	☑	☑	☑	☐	☐	☑
826	Ethylene dibromide (Dibromoethane)	106-93-4	☐	☑	☑	☑	☑	☑
827	Ethylene dichloride (1,2-Dichloroethane)	107-06-2	☐	☑	☑	☑	☑	☑
828	Ethylene glycol	107-21-1	☐	☑	☑	☑	☐	☑
829	Ethylene oxide	75-21-8	☑	☑	☑	☑	☑	☑
830	Ethylene thiourea	96-45-7	☐	☑	☑	☑	☑	☑
831	ETHYLENE, 1,1-DICHLORO-2,2-BIS (p-CHLOROPHENYL)-	72-55-9	☐	☑	☑	☐	☑	☑

(continued)

(continued)

ID	Chemical Name	CAS	DHS	EPCRA	SARA	HAPS	P H C	OSHA
832	Ethylenebisdithiocarbamic acid , salts & esters	111-54-6	☐	☑	☑	☐	☐	☑
833	Ethylenediamine-tetraacetic acid (EDTA)	60-00-4	☐	☑	☑	☐	☐	☑
834	Ethyleneimine	151-56-4	☑	☑	☑	☑	☑	☑
835	Ethylidene dichloride (1,1-Dichloroethane)	75-34-3	☐	☑	☑	☑	☐	☑
836	Ethylphosphonic dichloride	1066-50-8	☑	☐	☐	☐	☐	☑
837	Ethylphosphonyl difluoride	753-98-0	☑	☐	☐	☐	☐	☑
838	Ethylthiocyanate	542-90-5	☐	☑	☑	☐	☐	☑
839	Famphur	52-85-7	☐	☑	☑	☐	☐	☑
840	Fenamiphos	22224-92-6	☐	☑	☑	☐	☐	☑
841	Fenbutatin oxide	13356-08-6	☐	☑	☑	☐	☐	☑
842	Fenoxycarb	72490-01-8	☐	☑	☑	☐	☐	☑
843	Fenpropathrin	39515-41-8	☐	☑	☑	☐	☐	☑
844	Fensulfothion	115-90-2	☐	☑	☑	☐	☐	☑
845	Ferbam	14484-64-1	☐	☑	☑	☐	☐	☑
846	Ferric ammonium citrate	1185-57-5	☐	☑	☑	☐	☐	☑
847	Ferric ammonium oxalate	2944-67-4	☐	☑	☑	☐	☐	☑
848	Ferric ammonium oxalate	55488-87-4	☐	☑	☑	☐	☐	☑
849	Ferric chloride	7705-08-0	☐	☑	☑	☐	☐	☑
850	Ferric fluoride	7783-50-8	☐	☑	☑	☐	☐	☑
851	Ferric nitrate	10421-48-4	☐	☑	☑	☐	☐	☑
852	Ferric sulfate	10028-22-5	☐	☑	☑	☐	☐	☑
853	Ferrous ammonium sulfate	10045-89-3	☐	☑	☑	☐	☐	☑
854	Ferrous chloride	7758-94-3	☐	☑	☑	☐	☐	☑
855	Ferrous sulfate	7782-63-0	☐	☑	☑	☐	☐	☑
856	Ferrous sulfate	7720-78-7	☐	☑	☑	☐	☐	☑
857	Fluazifop butyl	69806-50-4	☐	☑	☑	☐	☐	☑
858	Fluenetil	4301-50-2	☐	☑	☑	☐	☐	☑
859	Fluoranthene	206-44-0	☐	☑	☑	☐	☐	☑
860	FLUORANTHENE, 3-NITRO-	892-21-7	☐	☐	☐	☐	☑	☑
861	Fluorene	86-73-7	☐	☑	☑	☐	☐	☑
862	Fluorine	7782-41-4	☑	☑	☑	☐	☐	☑
863	Fluoroacetamide	640-19-7	☐	☑	☑	☐	☐	☑
864	Fluoroacetic acid	144-49-0	☐	☑	☑	☐	☐	☑
865	Fluoroacetic acid , sodium salt	62-74-8	☐	☑	☑	☐	☐	☑
866	Fluoroacetyl chloride	359-06-8	☐	☑	☑	☐	☐	☑
867	Fluorosulfonic acid	7789-21-1	☑	☐	☐	☐	☐	☑
868	Folpet	133-07-3	☐	☑	☑	☐	☐	☑
869	Fonofos	944-22-9	☐	☑	☑	☐	☐	☑
870	Formaldehyde, 37% solution with	10-15%	☑	☑	☑	☑	☑	☑
871	Formetanate hydrochloride	23422-53-9	☐	☑	☑	☐	☐	☑
872	Formic acid	64-18-6	☐	☑	☑	☐	☐	☑
873	FORMIC acid , CHLORO-, ALLYL ESTER	2937-50-0	☐	☐	☐	☑	☐	☑

(continued)

(continued)

ID	Chemical Name	CAS	DHS	EPCRA	SARA	HAPS	P H C	OSHA
874	FORMIC acid , CHLORO-, ETHYL ESTER	541-41-3	☐	☑	☑	☑	☐	☑
875	Formothion	2540-82-1	☐	☑	☑	☐	☐	☑
876	Formparanate	17702-57-7	☐	☑	☑	☐	☐	☑
877	Fosthietan	21548-32-3	☐	☑	☑	☐	☐	☑
878	Fuberidazole	3878-19-1	☐	☑	☑	☐	☐	☑
879	Fumaric acid	110-17-8	☐	☑	☑	☐	☐	☑
880	FURALDEHYDE, 5-NITRO-, SEMICARBAZONE, 2-	59-87-0	☐	☐	☐	☐	☑	☑
881	Furan	110-00-9	☑	☑	☑	☐	☐	☑
882	Furan, tetrahydro-	109-99-9	☐	☑	☑	☐	☐	☑
883	Furfural	98-01-1	☐	☑	☑	☐	☐	☑
884	Gallium trichloride	13450-90-3	☐	☑	☑	☐	☐	☑
885	Germane	7782-65-2	☑	☐	☐	☐	☐	☑
886	Germanium(IV) fluoride	7783-58-6	☑	☐	☐	☐	☐	☑
887	GLUCOPYRANOSE, 2-DEOXY-2-(3-METHYL-3-NITROSOUREIDO)-, D-	18883-66-4	☐	☑	☑	☐	☑	☑
888	GLUCOPYRANOSIDE, (METHYL-ONN-AZOXY)METHYL-, beta-D-	14901-08-7	☐	☐	☐	☐	☑	☑
889	GLUTAMIC acid	59-05-2	☐	☐	☐	☐	☑	☑
890	Glycidylaldehyde	765-34-4	☐	☑	☑	☐	☐	☑
891	GOLD (1-THIO-D-GLUCOPYRANOSATO)-	12192-57-3	☐	☐	☐	☐	☑	☑
892	GUANIDINE, 1-METHYL-3-NITRO-1-NITROSO-	70-25-7	☐	☑	☑	☐	☑	☑
893	Guanyl nitrosaminoguanyltetrazene	109-27-3	☑	☐	☐	☐	☐	☑
894	HCFC-121	354-14-3	☐	☑	☑	☐	☐	☑
895	HCFC-121a	354-11-0	☐	☑	☑	☐	☐	☑
896	Heptachlor	76-44-8	☐	☑	☑	☑	☐	☑
897	Heptachlor epoxide	1024-57-3	☐	☑	☑	☐	☐	☑
898	Hexachlorobenzene	118-74-1	☐	☑	☑	☑	☑	☑
899	Hexachlorobutadiene	87-68-3	☐	☑	☑	☑	☐	☑
900	Hexachlorocyclohexane (all isomers)	608-73-1	☐	☑	☑	☐	☐	☑
901	Hexachlorocyclopentadiene	77-47-4	☐	☑	☑	☑	☑	☑
902	Hexachloroethane	67-72-1	☐	☑	☑	☑	☑	☑
903	Hexachloronaphthalene	1335-87-1	☐	☑	☑	☐	☐	☑
904	Hexachloropropene	1888-71-7	☐	☑	☑	☐	☐	☑
905	Hexafluoroacetone	684-16-2	☑	☐	☐	☐	☐	☑
906	Hexamethylene-1,6-diisocyanate	822-06-0	☐	☑	☑	☑	☐	☑
907	Hexamethylenediamine, N,N'-dibutyl-	4835-11-4	☐	☑	☑	☐	☐	☑
908	Hexamethylphosphoramide	680-31-9	☐	☑	☑	☑	☑	☑
909	Hexane	110-54-3	☐	☑	☑	☑	☐	☑
910	Hexazinone	51235-04-2	☐	☐	☐	☐	☐	☑
911	Hexotonal	67713-16-0	☑	☐	☐	☐	☐	☑
912	Hexyltrichlorosilane	928-65-4	☑	☐	☐	☐	☐	☑
913	HYDANTOIN, 1-((5-NITROFURFURYLIDENE)AMINO)-	67-20-9	☐	☑	☑	☐	☑	☑

(continued)

(continued)

ID	Chemical Name	CAS	DHS	EPCRA	SARA	HAPS	P H C	OSHA
914	HYDANTOIN, 5,5-DIPHENYL-	57-41-0	☐	☑	☑	☐	☑	☑
915	Hydramethylnon	67485-29-4	☐	☑	☑	☐	☐	☑
916	Hydrazine sulfate	10034-93-2	☐	☑	☑	☐	☐	☑
917	Hydrazine, 1,2-diethyl-	1615-80-1	☐	☑	☑	☐	☐	☑
918	Hydrazine 1,2-dimethyl-	540-73-8	☐	☑	☑	☐	☐	☑
919	Hydrazine anhydrous	302-01-2	☑	☑	☑	☑	☑	☑
920	Hydrogen bromide, gas	10035-10-6	☑	☐	☐	☐	☐	☑
921	Hydrogen chloride, gas	7647-01-0	☑	☑	☑	☑	☐	☑
922	Hydrogen cyanide aqueous solution	74-90-8	☑	☑	☑	☐	☐	☑
923	Hydrogen fluoride gas	7664-39-3	☑	☑	☑	☑	☐	☑
924	Hydrogen gas	1333-74-0	☑	☑	☑	☐	☐	☑
925	Hydrogen iodide, anhydrous	10034-85-2	☑	☐	☐	☐	☐	☑
926	Hydrogen peroxide, 30-60 % aqueous solution	7722-84-1	☑	☑	☑	☐	☑	☑
927	Hydrogen selenide gas	7783-07-5	☑	☑	☑	☐	☐	☑
928	Hydrogen sulfide	7783-06-4	☑	☑	☑	☐	☐	☑
929	Hydroquinone	123-31-9	☐	☑	☑	☑	☑	☑
930	IMFERON	9004-66-4	☐	☐	☐	☐	☑	☑
931	IMIDAZOLE-4-CARBOXAMIDE, 5-(3,3-DIMETHYL-1-TRIAZENO)-	4342-03-4	☐	☐	☐	☐	☑	☑
932	IMIDAZOLIDINONE, 1-((5-NITROFURFURYLIDENE)AMINO)-, 2-	555-84-0	☐	☐	☐	☐	☑	☑
933	Indeno(1,2,3-cd)pyrene	193-39-5	☐	☑	☑	☐	☐	☑
934	Iodine pentafluoride	7783-66-6	☑	☑	☑	☐	☐	☑
935	IOSYANATE, T-BUTYL	7188-38-7	☐	☐	☐	☐	☑	☑
936	Iron(0)pentacarbonyl	13463-40-6	☑	☑	☑	☐	☑	☑
937	iso-Amyl acetate	123-92-2	☐	☑	☑	☐	☐	☑
938	Isobenzan	297-78-9	☐	☑	☑	☐	☐	☑
939	iso-Butyl acetate	110-19-0	☐	☑	☑	☐	☐	☑
940	Isobutyl alcohol	78-83-1	☐	☑	☑	☐	☐	☑
941	iso-Butylamine	78-81-9	☐	☑	☑	☐	☐	☑
942	Isobutyraldehyde	78-84-2	☐	☑	☑	☐	☐	☑
943	iso-Butyric acid	79-31-2	☐	☑	☑	☐	☐	☑
944	Isobutyronitrile	78-82-0	☑	☑	☑	☐	☐	☑
945	ISOCYANATE, N-BUTYL	111-36-4	☐	☐	☐	☐	☑	☑
946	ISOCYANIC acid , ,4-DICHLOROPHENYL ESTER	102-36-3	☐	☑	☑	☐	☑	☑
947	ISOCYANIC acid , METHYLENE (3,5,5-TRIMETHYL-3,1-CYCLOHEXYLENE)ESTER	4098-71-9	☐	☑	☑	☐	☑	☑
948	ISOCYANIC acid , METHYLENEDI-4,1-CYCLOHEXYLENE ESTER	5124-30-1	☐	☑	☑	☐	☑	☑
949	Isodrin	465-73-6	☐	☑	☑	☐	☐	☑
950	ISONICOTINIC acid HYDRAZIDE	54-85-3	☐	☐	☐	☐	☑	☑
951	Isopentane	78-78-4	☑	☑	☑	☐	☐	☑
952	Isophorone	78-59-1	☐	☑	☑	☑	☐	☑

(continued)

(continued)

ID	Chemical Name	CAS	DHS	EPCRA	SARA	HAPS	P H C	OSHA
953	Isoprene	78-79-5	☑	☑	☑	☐	☐	☑
954	Isopropanolamine dodecylbenzene sulfonate	42504-46-1	☐	☑	☑	☐	☐	☑
955	Isopropyl alcohol (mfg-strong acid process)	67-63-0	☐	☑	☑	☐	☐	☑
956	Isopropyl chloride	75-29-6	☑	☑	☑	☐	☐	☑
957	Isopropyl chloroformate	108-23-6	☑	☑	☑	☐	☐	☑
958	ISOPROPYL ETHANE FLUOROPHOSPHONATE	1943-83-5	☐	☐	☐	☐	☑	☑
959	Isopropylamine	75-31-0	☑	☑	☑	☐	☐	☑
960	Isopropylmethylpyrazolyl dimethylcarbamate	119-38-0	☐	☑	☑	☐	☐	☑
961	Isosafrole	120-58-1	☐	☑	☑	☐	☐	☑
962	Kepone	143-50-0	☐	☑	☑	☐	☐	☑
963	LACTONITRILE	78-97-7	☐	☑	☑	☐	☑	☑
964	Lasiocarpine	303-34-4	☐	☑	☑	☐	☐	☑
965	LEAD	7439-92-1	☐	☑	☑	☐	☑	☑
966	Lead acetate	301-04-2	☐	☑	☑	☐	☐	☑
967	Lead arsenate	7784-40-9	☐	☑	☑	☐	☐	☑
968	Lead arsenate	10102-48-4	☐	☑	☑	☐	☐	☑
969	Lead arsenate	7645-25-2	☐	☑	☑	☐	☐	☑
970	Lead azide	13424-46-9	☑	☐	☐	☐	☐	☑
971	Lead chloride	7758-95-4	☐	☑	☑	☐	☐	☑
972	Lead fluoborate	13814-96-5	☐	☑	☑	☐	☐	☑
973	Lead fluoride	7783-46-2	☐	☑	☑	☐	☐	☑
974	Lead iodide	10101-63-0	☐	☑	☑	☐	☐	☑
975	Lead nitrate	10099-74-8	☐	☑	☑	☐	☐	☑
976	Lead phosphate	7446-27-7	☐	☑	☑	☐	☐	☑
977	Lead stearate	56189-09-4	☐	☑	☑	☐	☐	☑
978	Lead stearate	7428-48-0	☐	☑	☑	☐	☐	☑
979	Lead stearate	1072-35-1	☐	☑	☑	☐	☐	☑
980	Lead stearate	52652-59-2	☐	☑	☑	☐	☐	☑
981	Lead styphnate, wetted with not less than 20% water, or mixture of alcohol	15245-44-0	☑	☐	☐	☐	☐	☑
982	Lead subacetate	1335-32-6	☐	☑	☑	☐	☐	☑
983	Lead sulfate	15739-80-7	☐	☑	☑	☐	☐	☑
984	Lead sulfate	7446-14-2	☐	☑	☑	☐	☐	☑
985	Lead sulfide	1314-87-0	☐	☑	☑	☐	☐	☑
986	Lead thiocyanate	592-87-0	☐	☑	☑	☐	☐	☑
987	Leptophos	21609-90-5	☐	☑	☑	☐	☐	☑
988	Lewisite	541-25-3	☑	☑	☑	☐	☐	☑
989	Lindane (all isomers)	58-89-9	☐	☑	☑	☑	☑	☑
990	Linuron	330-55-2	☐	☑	☑	☐	☐	☑
991	Lithium amide	7782-89-0	☑	☐	☐	☐	☐	☑
992	Lithium carbonate	554-13-2	☐	☑	☑	☐	☐	☑
993	Lithium chromate	14307-35-8	☐	☑	☑	☐	☐	☑
994	Lithium hydride	7580-67-8	☐	☑	☑	☐	☐	☑

(continued)

(continued)

ID	Chemical Name	CAS	DHS	EPCRA	SARA	HAPS	P H C	OSHA
995	Lithium nitride	26134-62-3	☑	☐	☐	☐	☐	☑
996	Magnesium aluminum phosphide	864738-69-2	☑	☐	☐	☐	☐	☑
997	Magnesium aluminum phosphide	134884-20-1	☑	☐	☐	☐	☐	☑
998	Magnesium aluminum phosphide	864738-68-1	☑	☐	☐	☐	☐	☑
999	Magnesium amide	7803-54-5	☑	☐	☐	☐	☐	☑
1000	Magnesium phosphide	12057-74-8	☑	☐	☐	☐	☐	☑
1001	Malathion	121-75-5	☐	☑	☑	☐	☐	☑
1002	Maleic acid	110-16-7	☐	☑	☑	☐	☐	☑
1003	Maleic anhydride	108-31-6	☐	☑	☑	☑	☐	☑
1004	Maleic hydrazide	123-33-1	☐	☑	☑	☐	☐	☑
1005	MALEIMIDE, N,N'-(m-PHENYLENE)DI-	3006-93-7	☐	☐	☐	☐	☑	☑
1006	Malononitrile	109-77-3	☐	☑	☑	☐	☐	☑
1007	MANGANESE	7439-96-5	☐	☑	☑	☐	☐	☑
1008	MANGANESE, (ETHYLENEBIS (DITHIOCARBAMATO))-	12427-38-2	☐	☑	☑	☐	☑	☑
1009	Manganese, bis (dimethylcarbamodithioato-S,S')-	15339-36-3	☐	☑	☑	☐	☑	☑
1010	MANGANESE, TRICARBONYL METHYLCYCLOPENTADIENYL	12108-13-3	☐	☑	☑	☐	☐	☑
1011	Mannitol hexanitrate	15825-70-4	☑	☐	☐	☐	☑	☑
1012	MBT	149-30-4	☐	☑	☑	☐	☐	☑
1013	m-Cresol	108-39-4	☐	☑	☑	☑	☐	☑
1014	m-Dinitrobenzene	99-65-0	☐	☑	☑	☐	☐	☑
1015	Mecoprop	93-65-2	☐	☑	☑	☐	☐	☑
1016	MELAMINE	108-78-1	☐	☐	☐	☐	☑	☑
1017	Melphalan	148-82-3	☐	☑	☑	☐	☐	☑
1018	MENTHA-6,8-DIEN-2-ONE, (S)-(+)-, p-	2244-16-8	☐	☐	☐	☐	☑	☑
1019	Mephosfolan	950-10-7	☐	☑	☑	☐	☐	☑
1020	Mercaptodimethur	2032-65-7	☐	☑	☑	☐	☐	☑
1021	Mercuric acetate	1600-27-7	☐	☑	☑	☐	☐	☑
1022	Mercuric chloride	7487-94-7	☐	☑	☑	☐	☐	☑
1023	Mercuric cyanide	592-04-1	☐	☑	☑	☐	☐	☑
1024	Mercuric nitrate	10045-94-0	☐	☑	☑	☐	☐	☑
1025	Mercuric oxide	21908-53-2	☐	☑	☑	☐	☐	☑
1026	Mercuric sulfate	7783-35-9	☐	☑	☑	☐	☐	☑
1027	Mercuric thiocyanate	592-85-8	☐	☑	☑	☐	☐	☑
1028	Mercurous nitrate	7782-86-7	☐	☑	☑	☐	☐	☑
1029	Mercurous nitrate	10415-75-5	☐	☑	☑	☐	☐	☑
1030	MERCURY	7439-97-6	☐	☑	☑	☐	☑	☑
1031	Mercury fulminate	628-86-4	☑	☑	☑	☐	☐	☑
1032	MERCURY, CHLOROMETHYL-	115-09-3	☐	☐	☐	☐	☑	☑
1033	Merphos	150-50-5	☐	☑	☑	☐	☑	☑
1034	Methacrylic anhydride	760-93-0	☐	☑	☑	☐	☐	☑
1035	Methacryloyl chloride	920-46-7	☐	☑	☑	☐	☐	☑
1036	MethacryloyloxyEthyl isocyanate	30674-80-7	☐	☑	☑	☐	☐	☑

(continued)

(continued)

ID	Chemical Name	CAS	DHS	EPCRA	SARA	HAPS	P H C	OSHA
1037	Metham sodium	137-42-8	☐	☑	☑	☐	☐	☑
1038	Methamidophos	10265-92-6	☐	☑	☑	☐	☐	☑
1039	Methane	74-82-8	☑	☑	☑	☐	☐	☑
1040	METHANE, BROMODICHLORO-	75-27-4	☐	☑	☑	☐	☑	☑
1041	METHANE, CHLORODIBROMO-	124-48-1	☐	☑	☑	☐	☑	☑
1042	METHANE,CHLOROFLUORO-	593-70-4	☐	☐	☐	☐	☑	☑
1043	METHANESULFONIC acid , ETHYL ESTER	62-50-0	☐	☑	☑	☐	☑	☑
1044	METHANESULFONIC acid , METHYL ESTER	66-27-3	☐	☐	☐	☐	☑	☑
1045	Methanesulfonyl fluoride	558-25-8	☐	☑	☑	☐	☐	☑
1046	Methanethiol	74-93-1	☑	☑	☑	☐	☐	☑
1047	Methanol	67-56-1	☐	☑	☑	☑	☐	☑
1048	METHANOL, (METHYL-ONN-AZOXY)-, ACETATE (ester)	592-62-1	☐	☐	☐	☐	☑	☑
1049	Methapyrilene	91-80-5	☐	☑	☑	☐	☐	☑
1050	Methidathion	950-37-8	☐	☑	☑	☑	☐	☑
1051	Methoxychlor	72-43-5	☐	☑	☑	☐	☑	☑
1052	Methoxyethylmercuric acetate	151-38-2	☐	☑	☑	☐	☐	☑
1053	Methyl 2-chloroacrylate	80-63-7	☐	☑	☑	☐	☐	☑
1054	Methyl acrylate	96-33-3	☐	☑	☑	☑	☐	☑
1055	Methyl chloroform (1,1,1-Trichloroethane)	71-55-6	☐	☑	☑	☐	☐	☑
1056	Methyl chloroformate	79-22-1	☑	☑	☑	☐	☑	☑
1057	Methyl ethyl ketone	78-93-3	☐	☑	☑	☐	☐	☑
1058	Methyl ethyl ketone peroxide	1338-23-4	☐	☑	☑	☐	☐	☑
1059	Methyl formate	107-31-3	☑	☑	☑	☑	☐	☑
1060	Methyl iodide (Iodomethane)	74-88-4	☐	☑	☑	☑	☐	☑
1061	Methyl isobutyl ketone (Hexone)	108-10-1	☐	☑	☑	☑	☑	☑
1062	Methyl isocyanate	624-83-9	☑	☑	☑	☐	☑	☑
1063	METHYL ISOTHIOCYANATE	556-61-6	☐	☑	☑	☑	☐	☑
1064	Methyl methacrylate	80-62-6	☐	☑	☑	☐	☐	☑
1065	Methyl parathion	298-00-0	☐	☑	☑	☐	☐	☑
1066	Methyl phenkapton	3735-23-7	☐	☑	☑	☐	☐	☑
1067	Methyl phosphonyl difluoride	676-99-3	☑	☐	☐	☐	☑	☑
1068	METHYL SULFIDE	75-18-3	☐	☐	☐	☑	☐	☑
1069	Methyl tert butyl ether	1634-04-4	☐	☑	☑	☐	☐	☑
1070	Methyl thiocyanate	556-64-9	☑	☑	☑	☐	☐	☑
1071	Methyl vinyl ether	107-25-5	☑	☑	☑	☐	☐	☑
1072	Methylacrylonitrile	126-98-7	☑	☑	☑	☐	☐	☑
1073	Methylamine, anhydrous	74-89-5	☑	☑	☑	☐	☐	☑
1074	Methylchlorosilane	993-00-0	☑	☐	☐	☐	☐	☑
1075	Methylene bromide	74-95-3	☐	☑	☑	☐	☐	☑
1076	Methylene chloride (Dichloromethane)	75-09-2	☐	☑	☑	☑	☑	☑
1077	Methylene diphenyl diisocyanate (MDI)	101-68-8	☐	☑	☑	☑	☑	☑

(continued)

(continued)

ID	Chemical Name	CAS	DHS	EPCRA	SARA	HAPS	P H C	OSHA
1078	Methylhydrazine	60-34-4	☑	☑	☑	☑	☑	☑
1079	Methylmercuric dicyanamide	502-39-6	☐	☑	☑	☐	☐	☑
1080	Methylphosphonic dichloride	676-97-1	☑	☑	☑	☐	☑	☑
1081	Methylthiouracil	56-04-2	☐	☑	☑	☐	☐	☑
1082	Methyltrichlorosilane	75-79-6	☑	☑	☑	☐	☐	☑
1083	Metiram	9006-42-2	☐	☑	☑	☐	☐	☑
1084	Metolcarb	1129-41-5	☐	☑	☑	☐	☐	☑
1085	Metribuzin	21087-64-9	☐	☑	☑	☐	☐	☑
1086	Mevinphos	7786-34-7	☐	☑	☑	☐	☐	☑
1087	Mexacarbate	315-18-4	☐	☑	☑	☐	☐	☑
1088	Michler's ketone	90-94-8	☐	☑	☑	☐	☐	☑
1089	m-Nitrophenol	554-84-7	☐	☑	☑	☐	☐	☑
1090	m-Nitrotoluene	99-08-1	☐	☑	☑	☐	☐	☑
1091	Molybdenum trioxide	1313-27-5	☐	☑	☑	☐	☐	☑
1092	MONOCROTALINE	315-22-0	☐	☐	☐	☐	☑	☑
1093	Monocrotophos	6923-22-4	☐	☑	☑	☐	☐	☑
1094	MORPHOLINE	110-91-8	☐	☐	☐	☐	☑	☑
1095	m-Xylenes	108-38-3	☐	☑	☑	☑	☐	☑
1096	N-(1-Ethylpropyl)-3,4-dimethyl-2,6-dinitrobenzenamine	40487-42-1	☐	☑	☑	☐	☐	☑
1097	N-(2-Chloro-4-(trifluoromethyl) phenyl)-DL-valine(+)-cyano(3-phenoxyphenyl)	69409-94-5	☐	☑	☑	☐	☐	☑
1098	N-(2-Chloroethyl)diisopropylamine	96-79-7	☑	☐	☐	☐	☐	☑
1099	N-(3,4-Dichlorophenyl)propanamide	709-98-8	☐	☑	☑	☐	☐	☑
1100	N-(5-(1,1-Dimethylethyl)-1,3,4-thiadiazol-2-yl)-N,N'-dimethylurea	34014-18-1	☐	☑	☑	☐	☐	☑
1101	N,N'-(1,4-Piperazinediylbis(2,2,2-trichloroethylidene)) bisformamide	26644-46-2	☐	☑	☑	☐	☐	☑
1102	N,N'-Bis(1-methylethyl)-6-methylthio-1,3,5-triazine-2,4-diamine	7287-19-6	☐	☑	☑	☐	☐	☑
1103	N,N-Diethylaniline	91-66-7	☐	☑	☑	☐	☐	☑
1104	N,N-Dimethylaniline	121-69-7	☐	☑	☑	☑	☐	☑
1105	N,N-Dimethylhydrazine	57-14-7	☑	☑	☑	☑	☑	☑
1106	N,N-Dimethylphosphoramidodichloridate	677-43-0	☑	☐	☐	☐	☐	☑
1107	Nabam	142-59-6	☐	☑	☑	☐	☐	☑
1108	Naled	300-76-5	☐	☑	☑	☐	☐	☑
1109	Naphthalene	91-20-3	☐	☑	☑	☑	☐	☑
1110	NAPHTHALENE DISULFONIC acid , 1,3-	6459-94-5	☐	☑	☑	☐	☑	☑
1111	NAPHTHALENE DISULFONIC acid , 2,7-	2429-74-5	☐	☐	☐	☐	☑	☑
1112	NAPHTHALENE DISULFONIC acid , 3-HYDROXY-4-((4-SULFO-1-NAPHTHYL)AZO	915-67-3	☐	☐	☐	☐	☑	☑
1113	NAPHTHALENE DISULFONIC acid , 3-HYDROXY-4-(2,4-XYLYLAZO)-DISODIUM S	3761-53-3	☐	☑	☑	☐	☑	☑

(continued)

(continued)

ID	Chemical Name	CAS	DHS	EPCRA	SARA	HAPS	P H C	OSHA
1114	NAPHTHALENEDIAMINE, 1,5-	2243-62-1	☐	☐	☐	☐	☑	☑
1115	Naphthenic acid	1338-24-5	☐	☑	☑	☐	☐	☑
1116	NAPHTHOL, 1-(2,4-XYLYLAZO)-, 2-	3118-97-6	☐	☑	☑	☐	☑	☑
1117	NAPHTHOL, 1-(o-TOLYLAZO)-, 2-	2646-17-5	☐	☐	☐	☐	☑	☑
1118	NAPHTHOL, 1-(PHENYLAZO)-, 2-	842-07-9	☐	☑	☑	☐	☑	☑
1119	NAPHTHYLAMINE,2-	91-59-8	☐	☑	☑	☐	☑	☑
1120	NAPHTHYLAMINE, alpha-	134-32-7	☐	☐	☐	☐	☑	☑
1121	NAPHTHYLAMINE, N-PHENYL-, 2-	135-88-6	☐	☑	☑	☐	☑	☑
1122	n-Butyl alcohol	71-36-3	☐	☐	☐	☐	☐	☑
1123	N-Ethyldiethanolamine	139-87-7	☑	☑	☑	☐	☐	☑
1124	NICKEL	7440-02-0	☐	☑	☑	☐	☑	☑
1125	Nickel ammonium sulfate	15699-18-0	☐	☑	☑	☐	☐	☑
1126	Nickel carbonyl	13463-39-3	☑	☑	☑	☐	☐	☑
1127	Nickel chloride	37211-05-5	☐	☑	☑	☐	☐	☑
1128	Nickel chloride	7718-54-9	☐	☑	☑	☐	☐	☑
1129	Nickel cyanide	557-19-7	☐	☑	☑	☐	☐	☑
1130	Nickel hydroxide	12054-48-7	☐	☑	☑	☐	☐	☑
1131	Nickel nitrate	14216-75-2	☐	☑	☑	☐	☐	☑
1132	Nickel sulfate	7786-81-4	☐	☑	☑	☐	☐	☑
1133	NICOTINE	54-11-5	☐	☑	☑	☐	☑	☑
1134	NICOTINE, SULFATE (21)	65-30-5	☐	☑	☑	☐	☑	☑
1135	Nitric acid , with less than70% Nitric acid	7697-37-2	☑	☑	☑	☐	☑	☑
1136	Nitrobenzene	98-95-3	☐	☑	☑	☑	☐	☑
1137	Nitrocellulose, dry or wet with less than 25% water or alcohol	9004-70-0	☑	☐	☐	☐	☐	☑
1138	NITROGEN DIOXIDE	10102-44-0	☐	☑	☑	☐	☑	☑
1139	Nitrogen monoxide	10102-43-9	☑	☑	☑	☐	☑	☑
1140	Nitrogen tetroxide, gas	10544-72-6	☑	☑	☑	☐	☑	☑
1141	Nitrogen trioxide	10544-73-7	☑	☐	☐	☐	☐	☑
1142	Nitroglycerin	55-63-0	☑	☑	☑	☐	☐	☑
1143	Nitroguanidine, dry or wetted with <20% water by mass	556-88-7	☑	☐	☐	☐	☐	☑
1144	Nitromethane	75-52-5	☑	☐	☐	☐	☐	☑
1145	Nitrophenol (mixed isomers)	25154-55-6	☐	☑	☑	☐	☐	☑
1146	Nitrostarch	9056-38-6	☑	☐	☐	☐	☐	☑
1147	Nitrosyl chloride	2696-92-6	☑	☐	☐	☐	☐	☑
1148	Nitrotoluene	1321-12-6	☐	☑	☑	☐	☐	☑
1149	Nitrotriazolone	932-64-9	☑	☐	☐	☐	☐	☑
1150	Nitrourea	556-89-8	☑	☐	☐	☐	☐	☑
1151	NITROUS acid , SODIUM SALT	7632-00-0	☐	☑	☑	☐	☑	☑
1152	N-Methyl-2-pyrrolidone	872-50-4	☐	☑	☑	☐	☐	☑
1153	N-Methyldiethanolamine	105-59-9	☑	☐	☐	☐	☐	☑
1154	N-Methylolacrylamide	924-42-5	☐	☑	☑	☐	☐	☑
1155	N-Nitrosodiethylamine	55-18-5	☐	☑	☑	☐	☐	☑
1156	N-Nitrosodimethylamine	62-75-9	☐	☑	☑	☑	☑	☑

(continued)

(continued)

ID	Chemical Name	CAS	DHS	EPCRA	SARA	HAPS	P H C	OSHA
1157	N-Nitrosodiphenylamine	86-30-6	☐	☑	☑	☐	☐	☑
1158	N-Nitrosomethylvinylamine	4549-40-0	☐	☑	☑	☐	☐	☑
1159	N-Nitrosomorpholine	59-89-2	☐	☑	☑	☑	☑	☑
1160	N-Nitroso-N-methylurea	684-93-5	☐	☑	☑	☑	☑	☑
1161	N-Nitroso-N-methylurethane	615-53-2	☐	☑	☑	☐	☐	☑
1162	N-Nitrosonornicotine	16543-55-8	☐	☑	☑	☐	☐	☑
1163	Nonyltrichlorosilane	5283-67-0	☑	☐	☐	☐	☐	☑
1164	Norbormide	991-42-4	☐	☑	☑	☐	☑	☑
1165	NORBORNENE-2,3-DICARBOXYLIC acid , 1,4,5,6,7,7-HEXACHLORO-,5-	115-28-6	☐	☑	☑	☐	☐	☑
1166	N-Pentane	109-66-0	☑	☑	☑	☐	☐	☑
1167	N-PROPYL ISOCYANATE	110-78-1	☐	☐	☐	☐	☑	☑
1168	n-Propylamine	107-10-8	☐	☑	☑	☐	☐	☑
1169	O-(2-(Diethylamino)-6-methyl-4-pyrimidinyl)-O,O-Dimethyl phosphorothioate	29232-93-7	☐	☑	☑	☐	☐	☑
1170	O-(4-Bromo-2-chlorophenyl)-O-ethyl-S-propylphosphorothioate	41198-08-7	☐	☑	☑	☐	☐	☑
1171	O,O-Diethyl O-pyrazinyl phosphorothioate	297-97-2	☐	☑	☑	☐	☐	☑
1172	O,O-Diethyl S-Methyl dithiophosphate	3288-58-2	☐	☑	☑	☐	☐	☑
1173	O,O-Dimethyl O-(3-methyl-4-(methylthio) phenyl) ester, phosphorothioic aci	55-38-9	☐	☑	☑	☐	☐	☑
1174	o-Anisidine	90-04-0	☐	☑	☑	☑	☐	☑
1175	o-Anisidine hydrochloride	134-29-2	☐	☑	☑	☐	☐	☑
1176	o-Cresol	95-48-7	☐	☑	☑	☑	☐	☑
1177	Octachloronaphthalene	2234-13-1	☐	☑	☑	☐	☐	☑
1178	Octachlorostyrene	29082-74-4	☐	☑	☑	☐	☐	☑
1179	Octolite	57607-37-1	☑	☐	☐	☐	☐	☑
1180	Octonal	78413-87-3	☑	☐	☐	☐	☐	☑
1181	Octyltrichlorosilane	5283-66-9	☑	☐	☐	☐	☐	☑
1182	o-Dianisidine hydrochloride	111984-09-9	☐	☑	☑	☐	☐	☑
1183	o-Dichlorobenzene	95-50-1	☐	☑	☑	☐	☐	☑
1184	o-Dinitrobenzene	528-29-0	☐	☑	☑	☐	☐	☑
1185	O-Ethyl O-(4-(methylthio)phenyl) phosphorodithioic acid S-propyl ester	35400-43-2	☐	☑	☑	☐	☐	☑
1186	6O-Ethyl S-2-diisopropylaminoethyl methylphosphonothiote	50782-69-9	☑	☑	☑	☐	☐	☑
1187	o-Ethyl-2-diisopropylaminoethyl Methyl phosphonite	57856-11-8	☑	☐	☐	☐	☐	☑
1188	o-Nitrotoluene	88-72-2	☐	☑	☑	☐	☐	☑
1189	O-Pinacolyl methylphosphonochloridate	7040-57-5	☑	☐	☐	☐	☐	☑
1190	o-Pinacolyl methylphosphonofluoridate	96-64-0	☑	☐	☐	☐	☐	☑
1191	Osmium oxide OsO4 (T-4)-	20816-12-0	☐	☑	☑	☐	☐	☑
1192	o-Toluidine	95-53-4	☐	☑	☑	☑	☐	☑

(continued)

(continued)

ID	Chemical Name	CAS	DHS	EPCRA	SARA	HAPS	P H C	OSHA
1193	o-Toluidine hydrochloride	636-21-5	☐	☑	☑	☐	☐	☑
1194	Ouabain	630-60-4	☐	☑	☑	☐	☐	☑
1195	OXABICYCLO(4.1.0)HEPTANE 3-(EPOXYETHYL)-, 7-	106-87-6	☐	☐	☐	☐	☑	☑
1196	Oxamyl	23135-22-0	☐	☑	☑	☐	☐	☑
1197	Oxetane, 3,3-bis(chloromethyl)-	78-71-7	☐	☑	☑	☐	☐	☑
1198	Oxydisulfoton	2497-07-6	☐	☑	☑	☐	☐	☑
1199	Oxyfluorfen	42874-03-3	☐	☑	☑	☐	☐	☑
1200	Oxygen difluoride	7783-41-7	☑	☐	☐	☐	☐	☑
1201	o-Xylenes	95-47-6	☐	☑	☑	☑	☐	☑
1202	Ozone	10028-15-6	☐	☑	☑	☐	☐	☑
1203	p-Anisidine	104-94-9	☐	☑	☑	☐	☐	☑
1204	Paraformaldehyde	30525-89-4	☐	☑	☑	☐	☐	☑
1205	Paraldehyde	123-63-7	☐	☑	☑	☐	☐	☑
1206	Paraquat dichloride	1910-42-5	☐	☑	☑	☐	☐	☑
1207	Paraquat methosulfate	2074-50-2	☐	☑	☑	☐	☐	☑
1208	Parathion	56-38-2	☐	☑	☑	☑	☐	☑
1209	p-Chloro-m-cresol	59-50-7	☐	☑	☑	☐	☐	☑
1210	p-Chloro-o-toluidine	95-69-2	☐	☑	☑	☐	☐	☑
1211	p-Chlorophenyl isocyanate	104-12-1	☐	☑	☑	☐	☐	☑
1212	p-Cresol	106-44-5	☐	☑	☑	☑	☐	☑
1213	p-Dinitrobenzene	100-25-4	☐	☑	☑	☐	☐	☑
1214	Pentaborane	19624-22-7	☐	☑	☑	☐	☐	☑
1215	Pentachlorobenzene	608-93-5	☐	☑	☑	☐	☐	☑
1216	Pentachloroethane	76-01-7	☐	☑	☑	☐	☐	☑
1217	Pentachloronitrobenzene (Quintobenzene)	82-68-8	☐	☑	☑	☑	☐	☑
1218	Pentachlorophenol	87-86-5	☐	☑	☑	☑	☑	☑
1219	Pentadecylamine	2570-26-5	☐	☑	☑	☐	☐	☑
1220	Pentaerythritol, tetranitrate	78-11-5	☑	☐	☐	☐	☐	☑
1221	Pentobarbital sodium	57-33-0	☐	☑	☑	☐	☐	☑
1222	Pentolite, dry or wetted with <15% water, by mass	8066-33-9	☑	☐	☐	☐	☐	☑
1223	Peracetic acid	79-21-0	☑	☑	☑	☐	☑	☑
1224	Perchloryl fluoride	7616-94-6	☑	☐	☐	☐	☐	☑
1225	Perfluoroisobutylene	382-21-8	☑	☐	☐	☐	☐	☑
1226	Phenanthrene	85-01-8	☐	☑	☑	☐	☐	☑
1227	Phenol	108-95-2	☐	☑	☑	☑	☑	☑
1228	PHENOL, (1,1-DIMETHYLETHYL)-4-METHOXY-	25013-16-5	☐	☐	☐	☐	☑	☑
1229	PHENOL, 2,2'-METHYLENEBIS (3,4,6-TRICHLORO-	70-30-4	☐	☑	☑	☐	☑	☑
1230	Phenol 2,2'-thiobis[4-chloro-6-methyl-	4418-66-0	☐	☑	☑	☐	☐	☑
1231	Phenol, 3-(1-methylethyl)-, methylcarbamate	64-00-6	☐	☑	☑	☐	☐	☑
1232	PHENOL, 4,4'-ISOPROPYLIDENEDI-	80-05-7	☐	☑	☑	☐	☑	☑
1233	PHENOL, 4-AMINO-2-NITRO-	119-34-6	☐	☐	☐	☐	☑	☑

(continued)

(continued)

ID	Chemical Name	CAS	DHS	EPCRA	SARA	HAPS	P H C	OSHA
1234	PHENOL, P-CHLORO-	106-48-9	☐	☐	☐	☐	☑	☑
1235	PHENOTHIAZINE, 2-CHLORO-10-(3-(DIMETHYLAMINO)PROPYL)-, MONOHYDR	69-09-0	☐	☐	☐	☐	☑	☑
1236	Phenoxarsine, 10,10'-oxydi-	58-36-6	☐	☑	☑	☐	☐	☑
1237	PHENYLENEDIAMINE, 4-CHLORO-, m	5131-60-2	☐	☐	☐	☐	☐	☑
1238	PHENYLENEDIAMINE, 4-CHLORO-,o-	95-83-0	☐	☐	☐	☐	☑	☑
1239	Phenylhydrazine hydrochloride	59-88-1	☐	☑	☑	☐	☑	☑
1240	Phenylmercuric acetate	62-38-4	☐	☑	☑	☐	☐	☑
1241	Phenylsilatrane	2097-19-0	☐	☑	☑	☐	☐	☑
1242	Phenylthiourea	103-85-5	☐	☑	☑	☐	☐	☑
1243	Phenyltrichlorosilane	98-13-5	☑	☑	☑	☐	☐	☑
1244	Phorate	298-02-2	☐	☑	☑	☐	☐	☑
1245	Phosacetim	4104-14-7	☐	☑	☑	☐	☐	☑
1246	Phosfolan	947-02-4	☐	☑	☑	☐	☐	☑
1247	Phosgene, gas	75-44-5	☑	☑	☑	☑	☐	☑
1248	Phosphamidon	13171-21-6	☐	☑	☑	☐	☐	☑
1249	Phosphine	7803-51-2	☑	☑	☑	☑	☐	☑
1250	PHOSPHINE, PHENYL-	638-21-1	☐	☐	☐	☐	☑	☑
1251	PHOSPHONIC acid , (2,2,2-TRICHLORO-1-HYDROXYETHYL)-DIMETHYL ESTER	52-68-6	☐	☑	☑	☐	☑	☑
1252	PHOSPHONIC acid , (2-CHLOROETHYL)-	16672-87-0	☐	☐	☐	☐	☑	☑
1253	PHOSPHONIUM, TETRABUTYL-, BROMIDE	3115-68-2	☐	☐	☐	☐	☑	☑
1254	PHOSPHONIUM, TETRABUTYL-, CHLORIDE	2304-30-5	☐	☐	☐	☐	☑	☑
1255	Phosphonothioic acid , methyl-, O-(4-nitrophenyl) O-phenyl ester	2665-30-7	☐	☑	☑	☐	☐	☑
1256	Phosphonothioic acid , methyl-, O-ethyl O-(4-(methylthio)phenyl) ester	2703-13-1	☐	☑	☑	☐	☐	☑
1257	PHOSPHORIC acid	7664-38-2	☐	☑	☑	☐	☑	☑
1258	Phosphoric acid , 2-chloro-1-(2,3,5-trichlorophenyl) ethenyl Dimethyl ester	961-11-5	☐	☑	☑	☐	☐	☑
1259	Phosphoric acid , Dimethyl 4-(methylthio) phenyl ester	3254-63-5	☐	☑	☑	☐	☐	☑
1260	PHOSPHOROCHLORIDIC acid , DIETHYL ESTER	814-49-3	☐	☑	☑	☐	☑	☑
1261	PHOSPHOROCHLORIDOTHIOIC acid , O,O-DIETHYL ESTER	2524-04-1	☐	☐	☐	☐	☑	☑
1262	PHOSPHORODICHLORIDOTHIOIC acid , O-ETHYL ESTER	1498-64-2	☐	☐	☐	☐	☑	☑
1263	PHOSPHOROFLUORIDIC acid , BIS (l-METHYLETHYL) ESTER	55-91-4	☐	☑	☑	☐	☑	☑
1264	Phosphorothioic acid , O,O-dimethyl-5-(2-(methylthio)ethyl)ester	2587-90-8	☐	☑	☑	☐	☐	☑
1265	Phosphorous trichloride	7719-12-2	☑	☑	☑	☐	☐	☑

(continued)

(continued)

ID	Chemical Name	CAS	DHS	EPCRA	SARA	HAPS	P H C	OSHA
1266	PHOSPHORUS OXIDE	1314-56-3	☐	☐	☐	☐	☑	☑
1267	Phosphorus oxychloride	10025-87-3	☑	☑	☑	☐	☑	☑
1268	Phosphorus pentachloride	10026-13-8	☑	☑	☑	☐	☑	☑
1269	Phosphorus pentasulfide	1314-80-3	☑	☑	☑	☐	☐	☑
1270	Phosphorus, red	7723-14-0	☑	☑	☑	☑	☐	☑
1271	PHTHALIC acid , BENZYL BUTYL ESTER	85-68-7	☐	☑	☑	☐	☑	☑
1272	Phthalic anhydride	85-44-9	☐	☑	☑	☑	☐	☑
1273	Physostigmine	57-47-6	☐	☑	☑	☐	☐	☑
1274	Physostigmine, salicylate(1:1)	57-64-7	☐	☑	☑	☐	☐	☑
1275	PICOLINIC acid , 4-AMINO-3,5,6-TRICHLORO-	1918-02-1	☐	☑	☑	☐	☑	☑
1276	Picric acid , moist (10 to 40% water)	88-89-1	☑	☑	☑	☐	☐	☑
1277	Picrotoxin	124-87-8	☐	☑	☑	☐	☐	☑
1278	Piperidine	110-89-4	☑	☑	☑	☐	☐	☑
1279	PIPERIDINE, 1-NITROSO-	100-75-4	☐	☑	☑	☐	☑	☑
1280	Piperonyl butoxide	51-03-6	☐	☑	☑	☐	☐	☑
1281	Pirimifos-ethyl	23505-41-1	☐	☑	☑	☐	☐	☑
1282	PLATINUM(II), DIAMMINEDICHLORO-, cis-	15663-27-1	☐	☐	☐	☑	☐	☑
1283	PLUMBANE, TETRAETHYL-	78-00-2	☐	☑	☑	☑	☐	☑
1284	p-Nitroaniline	100-01-6	☐	☑	☑	☐	☐	☑
1285	p-Nitrosodiphenylamine	156-10-5	☐	☑	☑	☐	☐	☑
1286	p-Nitrotoluene	99-99-0	☐	☑	☑	☐	☐	☑
1287	Polychlorinated biphenyls(Aroclors)	1336-36-3	☐	☑	☑	☑	☑	☑
1288	Polymeric diphenylmethane diisocyanate	9016-87-9	☐	☑	☑	☐	☐	☑
1289	POLYVINYL ALCOHOL	9002-89-5	☐	☐	☐	☐	☑	☑
1290	Potassium arsenate	7784-41-0	☐	☑	☑	☐	☐	☑
1291	Potassium arsenite	10124-50-2	☐	☑	☑	☐	☐	☑
1292	Potassium bichromate	7778-50-9	☐	☑	☑	☐	☐	☑
1293	Potassium chlorate	3811-04-9	☑	☐	☐	☐	☐	☑
1294	Potassium cyanide	151-50-8	☑	☑	☑	☐	☐	☑
1295	Potassium dimethyldithiocarbamate	128-03-0	☐	☑	☑	☐	☐	☑
1296	Potassium hydroxide	1310-58-3	☐	☑	☑	☐	☐	☑
1297	Potassium nitrate	7757-79-1	☑	☐	☐	☐	☐	☑
1298	Potassium N-methyldithiocarbamate	137-41-7	☐	☑	☑	☐	☐	☑
1299	Potassium perchlorate	7778-74-7	☑	☐	☐	☐	☐	☑
1300	Potassium permanganate	7722-64-7	☐	☑	☑	☐	☐	☑
1301	Potassium phosphide	20770-41-6	☑	☐	☐	☐	☐	☑
1302	Potassium silver cyanide	506-61-6	☐	☑	☑	☐	☐	☑
1303	p-Phenylenediamine	106-50-3	☐	☑	☑	☐	☐	☑
1304	Promecarb	2631-37-0	☐	☑	☑	☐	☑	☑
1305	Propane	74-98-6	☑	☑	☑	☐	☐	☑
1306	PROPANE, 1,2-EPOXY-3-PHENOXY-	122-60-1	☐	☐	☐	☐	☑	☑
1307	Propanenitrile	107-12-0	☑	☑	☑	☐	☑	☑

(continued)

(continued)

ID	Chemical Name	CAS	DHS	EPCRA	SARA	HAPS	P H C	OSHA
1308	PROPANOL, 2,3-EPOXY-1-	556-52-5	☐	☐	☐	☐	☑	☑
1309	PROPANONE, 1,1,3-TRICHLORO-, 2-	921-03-9	☐	☐	☐	☐	☑	☑
1310	PROPANONE, 1,3-DICHLORO-, 2-	534-07-6	☐	☑	☑	☐	☐	☑
1311	PROPANONE, 1-CHLORO-, 2-	78-95-5	☐	☐	☐	☐	☐	☑
1312	Propargite	2312-35-8	☐	☑	☑	☐	☐	☑
1313	Propargyl bromide	106-96-7	☐	☑	☑	☐	☑	☑
1314	Propene	115-07-1	☑	☑	☑	☐	☑	☑
1315	PROPENE, 1-CHLORO-2-METHYL-	513-37-1	☐	☐	☐	☐	☑	☑
1316	PROPENE, 3-CHLORO-2-METHYL-	563-47-3	☐	☑	☑	☐	☐	☑
1317	PROPENE-1,1-DIOL, 2-METHYL-, DIACETATE, 2-	10476-95-6	☐	☑	☑	☐	☐	☑
1318	PROPENYL CHLORIDE	590-21-6	☑	☑	☑	☐	☐	☑
1319	Propham	122-42-9	☐	☑	☑	☐	☐	☑
1320	Propionaldehyde	123-38-6	☐	☑	☑	☑	☐	☑
1321	Propionic acid	79-09-4	☐	☑	☑	☐	☐	☑
1322	Propionic anhydride	123-62-6	☐	☑	☑	☐	☐	☑
1323	Propiophenone, 4'-amino	70-69-9	☐	☑	☑	☐	☐	☑
1324	Propoxur (Baygon)	114-26-1	☐	☑	☑	☑	☐	☑
1325	Propyl chloroformate	109-61-5	☑	☑	☑	☐	☐	☑
1326	Propylene dichloride (1,2-Dichloropropane)	78-87-5	☐	☑	☑	☑	☑	☑
1327	Propylene oxide	75-56-9	☑	☑	☑	☑	☑	☑
1328	PROPYN-1-OL, 2	107-19-7	☐	☑	☑	☐	☑	☑
1329	Propyne	74-99-7	☑	☑	☑	☐	☐	☑
1330	Prothoate	2275-18-5	☐	☑	☑	☐	☐	☑
1331	p-Toluidine	106-49-0	☐	☑	☑	☐	☐	☑
1332	PURINE, 6-((l-METHYL-4-NITROIMIDAZOL-5-YL)THIO)-	446-86-6	☐	☐	☐	☐	☑	☑
1333	p-Xylenes	106-42-3	☐	☑	☑	☑	☑	☑
1334	PYRAZ0LIDINEDIONE, 4-BUTYL-1,2-DIPHENYL-, 3,5-	50-33-9	☐	☐	☐	☐	☑	☑
1335	PYRENE	129-00-0	☐	☑	☑	☐	☑	☑
1336	PYRENE, 1,3-DINITRO-	75321-20-9	☐	☐	☐	☐	☑	☑
1337	PYRENE, 1,6-DINITRO-	42397-64-8	☐	☐	☐	☐	☐	☑
1338	PYRENE, 1-NITRO-	5522-43-0	☐	☑	☑	☐	☐	☑
1339	Pyrethrins	121-29-9	☐	☑	☑	☐	☐	☑
1340	Pyrethrins	121-21-1	☐	☑	☑	☐	☐	☑
1341	Pyrethrins	8003-34-7	☐	☑	☑	☐	☐	☑
1342	Pyridine	110-86-1	☐	☑	☑	☐	☐	☑
1343	PYRIDINE, 2,6-DIAMINO-3-(PHENYLAZO)-, MONOHYDROCHLORIDE	136-40-3	☐	☐	☐	☐	☑	☑
1344	Pyridine, 2-methyl-5-vinyl-	140-76-1	☐	☑	☑	☐	☐	☑
1345	Pyridine, 4-nitro-, 1-oxide	1124-33-0	☐	☑	☑	☐	☐	☑

(continued)

(continued)

ID	Chemical Name	CAS	DHS	EPCRA	SARA	HAPS	P H C	OSHA
1346	Pyriminil	53558-25-1	☐	☑	☑	☐	☐	☑
1347	PYRROLE-2,5-DIONE, 1,1'-(4-METHYL-1,3-PHENYLENE)BIS-, 1H-	6422-83-9	☐	☐	☐	☐	☑	☑
1348	PYRROLIDINE, 1-NITROSO-	930-55-2	☐	☑	☑	☐	☑	☑
1349	PYRROLIDINONE, 1-CYCLOHEXYL-, 2-	6837-24-7	☐	☑	☑	☐	☑	☑
1350	Quinoline	91-22-5	☐	☑	☑	☑	☐	☑
1351	QUINOLINE, 2-AMINO-3-METHYL-3H-IMIDAZO(4,5-f)	76180-96-6	☐	☐	☐	☐	☑	☑
1352	QUINOLINOL, 8-	148-24-3	☐	☐	☐	☐	☑	☑
1353	Quinone	106-51-4	☐	☑	☑	☑	☐	☑
1354	R-(-)-3-Quinuclidinyl benzilate	62869-69-6	☑	☐	☐	☐	☐	☑
1355	Resorcinol	108-46-3	☐	☑	☑	☐	☐	☑
1356	Resorcinol, 2,4,6-trinitro-	82-71-3	☑	☐	☐	☐	☐	☑
1357	RESORCINOL, DIGLYCIDYL-	101-90-6	☐	☑	☑	☐	☑	☑
1358	S-(2-(Ethylsulfinyl)ethyl) O,O-Dimethyl ester phosphorothioic acid	301-12-2	☐	☑	☑	☐	☐	☑
1359	Saccharin (manufacturing)	81-07-2	☐	☑	☑	☐	☐	☑
1360	Salcomine	14167-18-1	☐	☑	☑	☐	☐	☑
1361	Sarin	107-44-8	☑	☑	☑	☐	☐	☑
1362	sec-Amyl acetate	626-38-0	☐	☑	☑	☐	☐	☑
1363	sec-Butyl acetate	105-46-4	☐	☑	☑	☐	☐	☑
1364	sec-Butyl alcohol	78-92-2	☐	☑	☑	☐	☐	☑
1365	sec-Butylamine	513-49-5	☐	☑	☑	☐	☐	☑
1366	sec-Butylamine	13952-84-6	☐	☑	☑	☐	☐	☑
1367	SELENIC acid , DISODIUM SALT	13410-01-0	☐	☑	☑	☐	☑	☑
1368	Selenious acid	7783-00-8	☐	☑	☑	☐	☐	☑
1369	Selenious acid , dithallium(1+) salt	12039-52-0	☐	☑	☑	☐	☐	☑
1370	Selenium	7782-49-2	☐	☑	☑	☐	☐	☑
1371	Selenium dioxide	7446-08-4	☐	☑	☑	☐	☐	☑
1372	Selenium hexafluoride	7783-79-1	☑	☐	☐	☐	☐	☑
1373	Selenium oxychloride	7791-23-3	☐	☑	☑	☐	☐	☑
1374	Selenium sulfide	7488-56-4	☐	☑	☑	☐	☐	☑
1375	Selenourea	630-10-4	☐	☑	☑	☐	☐	☑
1376	Semicarbazide hydrochloride	563-41-7	☐	☑	☑	☐	☐	☑
1377	SERINE, DIAZOACETATE (ESTER)	115-02-6	☐	☑	☑	☐	☑	☑
1378	Silane, (4-aminobutyl)diethoxymethyl-	3037-72-7	☐	☑	☑	☐	☐	☑
1379	Silane, gas	7803-62-5	☑	☑	☑	☐	☐	☑
1380	SILANETRIAMINE, N,N,N',N',N``,N''-HEXAMETHYL-	15112-89-7	☐	☐	☐	☐	☑	☑
1381	SILICA, AMORPHOUS FUMED	112945-52-5	☐	☐	☐	☐	☑	☑
1382	SILICA, CRYSTALLINE QUARTZ	14808-60-7	☐	☐	☐	☐	☑	☑
1383	Silicon tetrafluoride	7783-61-1	☑	☐	☐	☐	☐	☑
1384	Silver	7440-22-4	☐	☑	☑	☐	☐	☑
1385	Silver cyanide	506-64-9	☐	☑	☑	☐	☐	☑
1386	Silver nitrate	7761-88-8	☐	☑	☑	☐	☐	☑

(continued)

(continued)

ID	Chemical Name	CAS	DHS	EPCRA	SARA	HAPS	P H C	OSHA
1387	Silvex (2,4,5-TP)	93-72-1	☐	☑	☑	☐	☐	☑
1388	Simazine	122-34-9	☐	☑	☑	☐	☐	☑
1389	Sodium	7440-23-5	☐	☑	☑	☐	☐	☑
1390	Sodium arsenate	7631-89-2	☐	☑	☑	☐	☐	☑
1391	Sodium arsenite	7784-46-5	☐	☑	☑	☐	☐	☑
1392	SODIUM AZIDE	26628-22-8	☐	☑	☑	☐	☑	☑
1393	Sodium bichromate	10588-01-9	☐	☑	☑	☐	☐	☑
1394	Sodium bifluoride	1333-83-1	☐	☑	☑	☐	☐	☑
1395	Sodium bisulfite	7631-90-5	☐	☑	☑	☐	☐	☑
1396	Sodium cacodylate	124-65-2	☐	☑	☑	☐	☐	☑
1397	Sodium chlorate	7775-09-9	☑	☐	☐	☐	☐	☑
1398	SODIUM CHLORITE	7758-19-2	☐	☐	☐	☐	☑	☑
1399	Sodium chromate	7775-11-3	☐	☑	☑	☐	☐	☑
1400	Sodium cyanide	143-33-9	☑	☑	☑	☐	☐	☑
1401	Sodium dimethyldithiocarbamate	128-04-1	☐	☑	☑	☐	☐	☑
1402	Sodium dinitro-o-cresylate, dry	25641-53-6	☑	☐	☐	☐	☐	☑
1403	Sodium dithionite	7775-14-6	☑	☐	☐	☐	☐	☑
1404	Sodium dodecylbenzenesulfonate	25155-30-0	☐	☑	☑	☐	☐	☑
1405	Sodium fluoride	7681-49-4	☐	☑	☑	☐	☐	☑
1406	Sodium hydrosulfide	16721-80-5	☐	☑	☑	☐	☐	☑
1407	Sodium hydroxide	1310-73-2	☐	☑	☑	☐	☐	☑
1408	Sodium hypochlorite	7681-52-9	☐	☑	☑	☐	☐	☑
1409	Sodium hypochlorite	10022-70-5	☐	☑	☑	☐	☐	☑
1410	Sodium methylate	124-41-4	☐	☑	☑	☐	☐	☑
1411	Sodium nitrate	7631-99-4	☑	☐	☐	☐	☐	☑
1412	Sodium o-phenylphenoxide	132-27-4	☐	☑	☑	☐	☐	☑
1413	Sodium pentachlorophenate	131-52-2	☐	☑	☑	☐	☐	☑
1414	Sodium phosphate, dibasic	10039-32-4	☐	☑	☑	☐	☐	☑
1415	Sodium phosphate, dibasic	10140-65-5	☐	☑	☑	☐	☐	☑
1416	Sodium phosphate, dibasic	7558-79-4	☐	☑	☑	☐	☐	☑
1417	Sodium phosphate, tribasic	10124-56-8	☐	☑	☑	☐	☐	☑
1418	Sodium phosphate, tribasic	7785-84-4	☐	☑	☑	☐	☐	☑
1419	Sodium phosphate, tribasic	10361-89-4	☐	☑	☑	☐	☐	☑
1420	Sodium phosphate, tribasic	7601-54-9	☐	☑	☑	☐	☐	☑
1421	Sodium phosphate, tribasic	10101-89-0	☐	☑	☑	☐	☐	☑
1422	Sodium phosphate, tribasic	7758-29-4	☐	☑	☑	☐	☐	☑
1423	Sodium phosphide (Na(H2P))	24167-76-8	☑	☐	☐	☐	☐	☑
1424	Sodium phosphide (Na3P)	12058-85-4	☑	☐	☐	☐	☐	☑
1425	Sodium picramate, (Wet >20 water)	831-52-7	☑	☐	☐	☐	☐	☑
1426	Sodium selenite	10102-18-8	☐	☑	☑	☐	☐	☑
1427	Sodium selenite	7782-82-3	☐	☑	☑	☐	☐	☑
1428	Sodium tellurite	10102-20-2	☐	☑	☑	☐	☐	☑
1429	Stannane, acetoxytriphenyl-	900-95-8	☐	☑	☑	☐	☐	☑
1430	STILBENEDIOL, alpha,alpha'-DIETHYL-, 4 ,4-	56-53-1	☐	☑	☑	☐	☑	☑
1431	Strontium chromate	7789-06-2	☐	☑	☑	☐	☐	☑

(continued)

(continued)

ID	Chemical Name	CAS	DHS	EPCRA	SARA	HAPS	P H C	OSHA
1432	STRONTIUM PHOSPHIDE	12504-13-1	☑	☐	☐	☐	☐	☑
1433	Strychnine	57-24-9	☐	☑	☑	☐	☐	☑
1434	Strychnine, sulfate	60-41-3	☐	☑	☑	☐	☐	☑
1435	Styrene	100-42-5	☐	☑	☑	☑	☑	☑
1436	Styrene oxide	96-09-3	☐	☑	☑	☑	☐	☑
1437	SULFONE, METHYL VINYL	3680-02-2	☐	☐	☐	☐	☑	☑
1438	Sulfoxide, 3-chloropropyl octyl	3569-57-1	☐	☑	☑	☐	☐	☑
1439	Sulfur dichloride	10545-99-0	☑	☐	☐	☐	☐	☑
1440	Sulfur dioxide	7446-09-5	☑	☑	☑	☐	☐	☑
1441	Sulfur monochloride	10025-67-9	☑	☐	☐	☐	☐	☑
1442	Sulfur monochloride	12771-08-3	☐	☑	☑	☐	☐	☑
1443	Sulfur tetrafluoride	7783-60-0	☑	☑	☑	☐	☐	☑
1444	Sulfur trioxide	7446-11-9	☑	☑	☑	☐	☐	☑
1445	Sulfuric acid	7664-93-9	☐	☑	☑	☐	☐	☑
1446	Sulfuric acid, fuming	8014-95-7	☑	☑	☑	☐	☐	☑
1447	Sulfuric acid, fumin g	7783-05-3	☑	☐	☐	☐	☐	☑
1448	Sulfuryl chloride	7791-25-5	☑	☐	☐	☐	☑	☑
1449	Sulfuryl fluoride	2699-79-8	☑	☑	☑	☐	☐	☑
1450	Tabun	77-81-6	☑	☑	☑	☐	☐	☑
1451	TANNIC ACID	1401-55-4	☐	☐	☐	☐	☑	☑
1452	TECRAETHYL DITHIOPYROPHOSPHATE	3689-24-5	☐	☑	☑	☐	☑	☑
1453	Tellurium hexafluoride	7783-80-4	☑	☑	☑	☐	☐	☑
1454	Temephos	3383-96-8	☐	☑	☑	☐	☐	☑
1455	Terbufos	13071-79-9	☐	☑	☑	☐	☐	☑
1456	tert-Amyl acetate	625-16-1	☐	☑	☑	☐	☐	☑
1457	tert-Butyl acetate	540-88-5	☐	☑	☑	☐	☐	☑
1458	tert-Butyl alcohol	75-65-0	☐	☑	☑	☐	☐	☑
1459	tert-Butylamine	75-64-9	☐	☑	☑	☐	☐	☑
1460	Tetrabromobisphenol A	79-94-7	☐	☑	☑	☐	☐	☑
1461	Tetrachloroethylene (Perchloroethylene)	127-18-4	☐	☑	☑	☑	☑	☑
1462	Tetrachlorosilane	10026-04-7	☑	☐	☐	☐	☐	☑
1463	Tetracycline hydrochloride	64-75-5	☐	☑	☑	☐	☐	☑
1464	Tetraethyltin	597-64-8	☐	☑	☑	☐	☐	☑
1465	Tetrafluoroethylene	116-14-3	☑	☑	☑	☐	☐	☑
1466	Tetramethyllead	75-74-1	☑	☑	☑	☐	☐	☑
1467	Tetramethylsilane	75-76-3	☑	☑	☑	☐	☐	☑
1468	Tetranitroaniline	53014-37-2	☑	☐	☐	☐	☐	☑
1469	Tetranitromethane	509-14-8	☑	☑	☑	☐	☑	☑
1470	Tetraphosphoric acid, hexaethyl	757-58-4	☑	☑	☑	☐	☐	☑
1471	TETRETHYL PYROPHOSPHATE	107-49-3	☐	☑	☑	☐	☑	☑
1472	Thallic oxide	1314-32-5	☐	☑	☑	☐	☐	☑
1473	Thallium	7440-28-0	☐	☑	☑	☐	☐	☑
1474	Thallium chloride TlCl	7791-12-0	☐	☑	☑	☐	☐	☑
1475	Thallium sulfate	10031-59-1	☐	☑	☑	☐	☐	☑

(continued)

(continued)

ID	Chemical Name	CAS	DHS	EPCRA	SARA	HAPS	P H C	OSHA
1476	Thallium(I) acetate	563-68-8	☐	☑	☑	☐	☐	☑
1477	Thallium(I) carbonate	6533-73-9	☐	☑	☑	☐	☐	☑
1478	Thallium(I) nitrate	10102-45-1	☐	☑	☑	☐	☐	☑
1479	Thallium(I) sulfate	7446-18-6	☐	☑	☑	☐	☐	☑
1480	Thallous malonate	2757-18-8	☐	☑	☑	☐	☐	☑
1481	Thiabendazole	148-79-8	☐	☑	☑	☐	☐	☑
1482	THIAZOLE, 2-AMINO-5-NITRO-	121-66-4	☐	☐	☐	☐	☑	☑
1483	Thiocarbazide	2231-57-4	☐	☑	☑	☐	☐	☑
1484	Thiodicarb	59669-26-0	☐	☑	☑	☐	☐	☑
1485	Thiofanox	39196-18-4	☐	☑	☑	☐	☐	☑
1486	Thionyl chloride	7719-09-7	☑	☐	☐	☐	☐	☑
1487	Thiophanate-methyl	23564-05-8	☐	☐	☐	☐	☐	☑
1488	THIOPHENE, 2,3,4,5-TETRACHLORO-	6012-97-1	☐	☑	☑	☐	☑	☑
1489	THIOPHOSPHORYL CHLORIDE	3982-91-0	☐	☑	☑	☐	☑	☑
1490	Thiosemicarbazide	79-19-6	☐	☑	☑	☐	☐	☑
1491	Thiourea, (2-chlorophenyl)-	5344-82-1	☐	☑	☑	☐	☐	☑
1492	Thiourea, (2-methylphenyl)-	614-78-8	☐	☑	☑	☐	☐	☑
1493	Thiram	137-26-8	☐	☑	☑	☐	☐	☑
1494	Thorium dioxide	1314-20-1	☐	☑	☑	☐	☐	☑
1495	Titanium(IV) chloride	7550-45-0	☑	☑	☑	☑	☑	☑
1496	Toluene	108-88-3	☐	☑	☑	☑	☐	☑
1497	Toluene 2,6-diisocyanate	91-08-7	☑	☑	☑	☐	☐	☑
1498	Toluene diisocyanate	26471-62-5	☑	☑	☑	☐	☐	☑
1499	Toluene-2,4-diisocyanate	584-84-9	☑	☑	☑	☑	☑	☑
1500	TOLUIDINE, 4-(o-TOLYLAZO)-, o-	97-56-3	☐	☑	☑	☐	☑	☑
1501	TOLUIDINE, 5-NITRO-, o-	99-55-8	☐	☑	☑	☐	☑	☑
1502	Toxaphene (chlorinated camphene)	8001-35-2	☐	☑	☑	☑	☑	☑
1503	trans-1,3-Dichloropropene	10061-02-6	☐	☑	☑	☐	☐	☑
1504	trans-2-Butene	624-64-6	☑	☑	☑	☐	☐	☑
1505	Triallate	2303-17-5	☐	☑	☑	☐	☐	☑
1506	Triamiphos	1031-47-6	☐	☑	☑	☐	☐	☑
1507	TRIAZIN-2(lH)-ONE, 4-AMINO-1-beta-D-RIBOFURANOSYL-, s-	320-67-2	☐	☐	☐	☐	☑	☑
1508	TRIAZINE, 2,4,6-TRIFLUORO-,s-	675-14-9	☐	☑	☑	☐	☑	☑
1509	TRIAZINE, 2,4,6-TRIS (ALLYLOXY)-, s-	101-37-1	☐	☐	☐	☐	☑	☑
1510	TRIAZINE, 2-CHLORO-4-ETHYLAMINO-6-ISOPROPYLAMINO-, s-	1912-24-9	☐	☑	☑	☐	☑	☑
1511	Triazofos	24017-47-8	☐	☑	☑	☐	☐	☑
1512	TRIAZOLE, 3-AMINO-, s-	61-82-5	☐	☑	☑	☐	☑	☑
1513	Tributyltin fluoride	1983-10-4	☐	☑	☑	☐	☐	☑
1514	Tributyltin methacrylate	2155-70-6	☐	☑	☑	☐	☐	☑
1515	Trichloro(chloromethyl)silane	1558-25-4	☐	☑	☑	☐	☐	☑
1516	Trichloro(cyclohexyl)silane	98-12-4	☑	☐	☐	☐	☐	☑
1517	Trichloro(dichlorophenyl)silane	27137-85-5	☐	☑	☑	☐	☐	☑

(continued)

(continued)

ID	Chemical Name	CAS	DHS	EPCRA	SARA	HAPS	P H C	OSHA
1518	Trichloro(octadecyl)silane	112-04-9	☑	☐	☐	☐	☐	☑
1519	Trichloro(propyl)silane	141-57-1	☑	☐	☐	☐	☐	☑
1520	TRICHLOROACETYL CHLORIDE	76-02-8	☐	☑	☑	☐	☑	☑
1521	Trichloroethylene	79-01-6	☐	☑	☑	☑	☑	☑
1522	Trichloroethylsilane	115-21-9	☑	☑	☑	☐	☐	☑
1523	Trichloromethanesulfenyl chloride	594-42-3	☑	☑	☑	☐	☑	☑
1524	Trichloronate	327-98-0	☐	☑	☑	☐	☐	☑
1525	Trichlorophenol	25167-82-2	☐	☑	☑	☐	☐	☑
1526	Trichlorosilane	10025-78-2	☑	☑	☑	☐	☐	☑
1527	Trichlorovinylsilane	75-94-5	☑	☐	☐	☐	☐	☑
1528	TRICHOTHEC-9-ENE-3-alpha,4-beta,8-alpha, 15-TETROL,12,13-EPOXY-	21259-20-1	☐	☐	☐	☐	☑	☑
1529	Triclopyr triethylammonium salt	57213-69-1	☐	☑	☑	☐	☐	☑
1530	Triethanolamine	102-71-6	☑	☐	☐	☐	☐	☑
1531	Triethanolamine dodecylbenzene sulfonate	27323-41-7	☐	☑	☑	☐	☐	☑
1532	Triethanolamine hydrochloride	637-39-8	☑	☐	☐	☐	☐	☑
1533	Triethoxysilane	998-30-1	☐	☑	☑	☐	☐	☑
1534	Triethyl phosphite	122-52-1	☑	☐	☐	☐	☐	☑
1535	Triethylamine	121-44-8	☐	☑	☑	☑	☐	☑
1536	TRIETHYLAMINE, 2,2',2``-TRICHLORO-, HYDROCHLORIDE	817-09-4	☐	☐	☐	☐	☑	☑
1537	Trifluoroacetyl chloride	354-32-5	☑	☐	☐	☐	☐	☑
1538	Trifluralin	1582-09-8	☐	☑	☑	☑	☐	☑
1539	Trimethyl phosphite	121-45-9	☑	☐	☐	☐	☐	☑
1540	Trimethylamine	75-50-3	☑	☑	☑	☐	☐	☑
1541	Trimethylolpropane phosphite	824-11-3	☐	☑	☑	☐	☐	☑
1542	Trimethyltin chloride	1066-45-1	☐	☑	☑	☐	☐	☑
1543	Trinitronaphthalene	55810-17-8	☑	☐	☐	☐	☐	☑
1544	Triphenyltin chloride	639-58-7	☐	☑	☑	☐	☐	☑
1545	Triphenyltin hydroxide	76-87-9	☐	☑	☑	☐	☐	☑
1546	Tris(2,3-dibromopropyl) phosphate	126-72-7	☐	☑	☑	☐	☐	☑
1547	Tris(2-chloroethyl)amine	555-77-1	☑	☑	☑	☐	☐	☑
1548	Tris(2-chlorovinyl)arsine	40334-70-1	☑	☐	☐	☐	☐	☑
1549	Tritonal	54413-15-9	☑	☐	☐	☐	☐	☑
1550	Trypan blue	72-57-1	☐	☑	☑	☐	☐	☑
1551	Tungsten hexafluoride	7783-82-6	☑	☐	☐	☐	☐	☑
1552	UCON 50-HB-5100	9038-95-3	☐	☐	☐	☐	☑	☑
1553	UNDECANOIC acid , 11-AMINO	2432-99-7	☐	☐	☐	☐	☑	☑
1554	URACIL, 5-(BIS(2-CHLOROETHYL) AMINO)-	66-75-1	☐	☑	☑	☐	☑	☑
1555	URACIL, 5-FLUORO-	51-21-8	☐	☑	☑	☐	☑	☑
1556	URACIL, 6-PROPYL-2-THIO-	51-52-5	☐	☐	☐	☐	☑	☑
1557	Uranium hexafluoride	7783-81-5	☑	☐	☐	☐	☐	☑
1558	Uranyl acetate	541-09-3	☐	☑	☑	☐	☐	☑
1559	Uranyl nitrate	10102-06-4	☐	☑	☑	☐	☐	☑

(continued)

(continued)

ID	Chemical Name	CAS	DHS	EPCRA	SARA	HAPS	P H C	OSHA
1560	Uranyl nitrate	36478-76-9	☐	☑	☑	☐	☐	☑
1561	Urea	57-13-6	☑	☐	☐	☐	☐	☑
1562	Urea nitrate, wetted	124-47-0	☑	☐	☐	☐	☐	☑
1563	UREA 1-(2-CHLOROETHYL)-3 (4-METHYLCYCLOHEXYL)-l-NITROSO-	13909-09-6	☐	☐	☐	☐	☑	☑
1564	UREA, 1-(2-CHLOROETHYL)-3-CYCLOHEXYL-1-NITROSO-	13010-47-4	☐	☐	☐	☐	☑	☑
1565	UREA, 2-THIO-	62-56-6	☐	☑	☑	☐	☑	☑
1566	UREA, 3-(p-CHLOROPHENYL)-1,1-DIMETHYL-	150-68-5	☐	☑	☑	☐	☑	☑
1567	UREA, l-ETHYL-1-NITROSO-	759-73-9	☐	☑	☑	☐	☑	☑
1568	UREA,1,1-DIMETHYL-3- (alpha, alpha,alpha-TRIFLUORO-m-TOLYL)-	2164-17-2	☐	☑	☑	☐	☑	☑
1569	VALINOMYCIN	2001-95-8	☐	☑	☑	☐	☑	☑
1570	Vanadium pentoxide	1314-62-1	☐	☑	☑	☐	☐	☑
1571	Vanadyl sulfate	27774-13-6	☐	☑	☑	☐	☐	☑
1572	Vandium (except when contained in an alloy)	7440-62-2	☐	☑	☑	☐	☐	☑
1573	Vinyl acetate	108-05-4	☑	☑	☑	☑	☐	☑
1574	Vinyl acetylene	689-97-4	☑	☑	☑	☐	☐	☑
1575	Vinyl bromide	593-60-2	☐	☑	☑	☑	☑	☑
1576	Vinyl chloride	75-01-4	☑	☑	☑	☑	☑	☑
1577	Vinyl fluoride	75-02-5	☑	☑	☑	☐	☐	☑
1578	Warfarin sodium	129-06-6	☐	☑	☑	☐	☐	☑
1579	XANTHEN-7-ONE, 7H-FURO (3',2'4,5)FURO(2,3-c)	10048-13-2	☐	☐	☐	☐	☑	☑
1580	Xylenes (isomers and mixture)	1330-20-7	☐	☑	☑	☑	☐	☑
1581	Xylenol	1300-71-6	☐	☑	☑	☐	☐	☑
1582	XYLIDINE, 2,6	87-62-7	☐	☑	☑	☐	☑	☑
1583	Xylylene dichloride	28347-13-9	☐	☑	☑	☐	☐	☑
1584	Zinc	7440-66-6	☐	☑	☑	☐	☐	☑
1585	Zinc acetate	557-34-6	☐	☑	☑	☐	☐	☑
1586	Zinc ammonium chloride	52628-25-8	☐	☑	☑	☐	☐	☑
1587	Zinc ammonium chloride	14639-97-5	☐	☑	☑	☐	☐	☑
1588	Zinc ammonium chloride	14639-98-6	☐	☑	☑	☐	☐	☑
1589	Zinc borate	1332-07-6	☐	☑	☑	☐	☐	☑
1590	Zinc bromide	7699-45-8	☐	☑	☑	☐	☐	☑
1591	Zinc carbonate	3486-35-9	☐	☑	☑	☐	☐	☑
1592	Zinc chloride	7646-85-7	☐	☑	☑	☐	☐	☑
1593	Zinc cyanide	557-21-1	☐	☑	☑	☐	☐	☑
1594	Zinc dithionite	7779-86-4	☑	☑	☑	☐	☐	☑
1595	Zinc fluoride	7783-49-5	☐	☑	☑	☐	☐	☑
1596	Zinc formate	557-41-5	☐	☑	☑	☐	☐	☑
1597	Zinc nitrate	7779-88-6	☐	☑	☑	☐	☐	☑
1598	Zinc phenolsulfonate	127-82-2	☐	☑	☑	☐	☐	☑
1599	Zinc phosphide	1314-84-7	☐	☑	☑	☐	☐	☑

(continued)

(continued)

ID	Chemical Name	CAS	DHS	EPCRA	SARA	HAPS	P H C	OSHA
1600	Zinc silicofluoride	16871-71-9	☐	☑	☑	☐	☐	☑
1601	Zinc sulfate	7733-02-0	☐	☑	☑	☐	☐	☑
1602	ZINC, BIS (DIMETHYLDITHIOCARBAMATO)-	137-30-4	☐	☑	☑	☐	☑	☑
1603	Zinc, dichloro(4,4-dimethyl-5 ((((methylamino)carbonyl)oxy)imino) pentanenit	58270-08-9	☐	☑	☑	☐	☐	☑
1604	Zirconium nitrate	13746-89-9	☐	☑	☑	☐	☐	☑
1605	Zirconium picramate	63868-82-6	☑	☐	☐	☐	☐	☑
1606	Zirconium Potassium fluoride	16923-95-8	☐	☑	☑	☐	☐	☑
1607	Zirconium sulfate	14644-61-2	☐	☑	☑	☐	☐	☑
1608	Zirconium tetrachloride	10026-11-6	☐	☑	☑	☐	☐	☑

Appendix 6
Material Safety Data

MSD 6.1. Safety Data Sheets (SDS)

Related Links

MSDSonline
Advantor (Mallinckrodt Baker)
Fisher Scientific
Sigma Aldrich
VWR Scientific Prod.
Vermont SIRI
SDS Guide (PDF)

Safety Data Sheets (SDS) and hazard communication labels are the first place to look for information concerning hazardous properties of chemical products. The OSHA Hazard Communication Standard requires that all chemical manufacturers and importers supply an appropriate SDS to their customers. Chemical manufactures typically develop their own SDS. All users should be able to access an SDS for all hazardous chemicals used.

SDS Management at MU

The University of Missouri is taking a two-pronged approach to SDS Management. Colleges, Departments and Units can choose to manage SDSs electronically (either on their own or through the MU-Sponsored method) or with physical paper copies. The MU-Sponsored Method is a commercial product which has been purchased called MSDSonline. Complete information about this program is available on the MSDSonline portal page

Users that wish to create their own solution should probably include links to the common manufacturers found in their workspace such as Fisher Scientific, Sigma-Aldrich, & Mallinckrodt/ Baker. These sites, plus other useful links, can be found in the "Related Links" box on this page.

D.S. Viswanath et al., *Emerging Energetic Materials: Synthesis, Physicochemical, and Detonation Properties*, https://doi.org/10.1007/978-94-024-1201-7

User that prefer to manage paper copies (aka “hard copies”) of SDSs may continue to do so. However, keep in mind that the more chemicals you are managing, the more difficult it becomes to keep your hard copies current. You may decide to only keep the most frequently used or most hazardous chemicals used in hard copies, while also participating in one of the electronic solutions described above.

What does an SDS Contain?

Most modern SDS contain 16 sections. In the “Related Links” box, you can access the SDS Guide, a PDF that describes SDSs in detail. If you need this information in another format, please don't hesitate to contact EHS by phone at (573) 882-7018 or by e-mail atehs@missouri.edu.

https://www.osha.gov/Publications/OSHA3514.html
https://www.osha.gov/Publications/HazComm_QuickCard_SafetyData.html
https://www.osha.gov/dsg/hazcom/
https://www.osha.gov/pls/oshaweb/owadisp.show_document?p_table=standards&p_id=10103
https://www.msdsonline.com/resources/ghs-answer-center/ghs-101-safety-data-sheets-sds

NIOSH—On-line chemical safety information: www.cdc.gov/niosh/npg/

CDC—NIOSH Pocket Guide to Chemical Hazards (NPG): www.cdc.gov/niosh/npg/

SDS Requirements

Johns Hopkins staff, including Supervisors, Principal Investigators and Laboratory Managers, are responsible for ensuring their employees have access to Safety Data Sheets for all hazardous chemicals used in the workplace or laboratory. The information in the Safety Data Sheets information must be accessible for employees during all shifts, including laboratory personnel. Access to SDSs can mean access to paper copies or electronic access via the Internet.

HSE strongly recommends paper copies be kept in the workplace or laboratory; however, having SDS websites bookmarked is acceptable as long as all employees in the workplace know where to find the SDS information online.

Keep in mind that any accidents involving a chemical will require an SDS being provided to emergency personnel and to the attending physician so proper treatment can be administered.

- Emergency contact information is available at: http://www.hopkinsmedicine.org/hse/emergency/
- For more information about our chemical and safety policies, see: http://www.hopkinsmedicine.org/hse/policies/index.html

How to Obtain an SDS

Our recommended guidelines for obtaining an SDS are as follows:

1. Keep and use the SDS which is shipped to you with a chemical, or use the SDS which is forwarded to you or your department from HSE.
2. Use the Internet access to find an SDS for a chemical or product.
3. If you still can't locate an SDS, you may request one from our office or by using the “Right-to-Know Chemical Information Request Form.”

GHS 101 Safety Data Sheets (SDS)

Role of Safety Data Sheets in the Harmonized System

Safety Data Sheets are an essential component of the GHS and are intended to provide comprehensive information about a substance or mixture for use in workplace chemical management.

In the GHS, they serve the same function that the Material Safety Data Sheet or MSDS does in OSHA's HazCom Standard.

They are used as a source of info about hazards, including environmental hazards, and to obtain advice on safety precautions.

The SDS is normally product related and not specific to workplace; nevertheless, the information on an SDS enables the employer to:

1. Develop an active program of worker protection measures, including training, which is specific to the workplace.
2. Consider measures necessary to protect the environment.

Criteria for Determining Whether an SDS Should be Produced

An SDS should be produced for substances and mixtures which meet the harmonized criteria for physical, health, or environmental hazards under the GHS and for all mixtures which contain ingredients that meet the criteria for carcinogenic, toxic to reproduction or specific target organ toxicity in concentrations exceeding the cut-off limits for SDS specified by the criteria for mixtures.

Competent authorities may also requires SDSs for mixtures not meeting the criteria for classification but containing hazardous ingredients in certain concentrations.

SDS Format

Information in the SDS should be presented using the following 16 headings in the order given below

1. Identification
2. Hazard(s) identification
3. Composition/information on ingredients
4. First-aid measures
5. Fire-fighting measures
6. Accidental release measures
7. Handling and Storage
8. Exposure controls/personal protection
9. Physical and chemical properties
10. Stability and reactivity
11. Toxicological information
12. Ecological information
13. Disposal considerations
14. Transport information
15. Regulatory information
16. Other information

Brief

Hazard Communication Standard: Safety Data Sheets

The Hazard Communication Standard (HCS) (29 CFR 1910.1200(g)), revised in 2012, requires that the chemical manufacturer, distributor, or importer provide Safety Data Sheets (SDSs) (formerly MSDSs or Material Safety Data Sheets) for each hazardous chemical to downstream users to communicate information on these hazards. The information contained in the SDS is largely the same as the MSDS, except now the SDSs are required to be presented in a consistent user-friendly, 16-section format. This brief provides guidance to help workers who handle hazardous chemicals to become familiar with the format and understand the contents of the SDSs.

The SDS includes information such as the properties of each chemical; the physical, health, and environmental health hazards; protective measures; and safety precautions for handling, storing, and transporting the chemical. The information contained in the SDS must be in English (although it may be in other languages as well). In addition, OSHA requires that SDS preparers provide specific minimum information as detailed in Appendix D of 29 CFR 1910.1200. The SDS preparers may also include additional information in various section(s).

Sections 1 through 8 contain general information about the chemical, identification, hazards, composition, safe handling practices, and emergency control measures (e.g., fire fighting). This information should be helpful to those that need to get the information quickly. Sections 9 through 11 and 16 contain other technical and scientific information, such as physical and chemical properties, stability and reactivity information, toxicological information, exposure control information, and other information including the date of preparation or last revision. The SDS must also state that no applicable information was found when the preparer does not find relevant information for any required element.

The SDS must also contain Sections 12 through 15, to be consistent with the UN Globally Harmonized System of Classification and Labeling of Chemicals (GHS), but OSHA will not enforce the content of these sections because they concern matters handled by other agencies.

A description of all 16 sections of the SDS, along with their contents, is presented below:

Section 1: Identification

This section identifies the chemical on the SDS as well as the recommended uses. It also provides the essential contact information of the supplier. The required information consists of:

- Product identifier used on the label and any other common names or syn nyms by which the substance is known.
- Name, address, phone number of the manufacturer, importer, or other responsible party, and emergency phone number.
- Recommended use of the chemical (e.g., a brief description of what it actually does, such as flame retardant) and any restrictions on use (including recommendations given by the supplier). [1]

Section 2: Hazard(s) Identification

This section identifies the hazards of the chemical presented on the SDS and the appropriate warning information associated with those hazards. The required information consists of:

- The hazard classification of the chemical (e.g., flammable liquid, category^1).
- Signal word.
- Hazard statement(s).
- Pictograms (the pictograms or hazard symbols may be presented as graphical reproductions of the symbols in black and white or be a description of the name of the symbol (e.g., skull and crossbones, flame).
- Precautionary statement(s).
- Description of any hazards not otherwise classified.
- For a mixture that contains an ingredient(s) with unknown toxicity, a statement describing how much (percentage) of the mixture consists of ingredient(s) with unknown acute toxicity. Please note that this is a total percentage of the mixture and not tied to the individual ingredient(s).

Section 3: Composition/Information on Ingredients

This section identifies the ingredient(s) contained in the product indicated on the SDS, including impurities and stabilizing additives. This section includes information on substances, mixtures, and all chemicals where a trade secret is claimed. The required information consists of:

Substances

- Chemical name.
- Common name and synonyms.
- Chemical Abstracts Service (CAS) number and other unique identifiers.
- Impurities and stabilizing additives, which are themselves classified and which contribute to the classification of the chemical.

Mixtures

- Same information required for substances.
- The chemical name and concentration (i.e., exact percentage) of all ingredients which are classified as health hazards and are:
- Present above their cut-off/concentration limits or
- Present a health risk below the cut-off/concentration limits.
- The concentration (exact percentages) of each ingredient must be specified except concentration ranges may be used in the following situations:
- A trade secret claim is made,
- There is batch-to-batch variation, or
- The SDS is used for a group of substantially similar mixtures.

Chemicals where a trade secret is claimed

- A statement that the specific chemical identity and/or exact percentage (concentration) of composition has been withheld as a trade secret is required.

Section 4: First-Aid Measures

This section describes the initial care that should be given by untrained responders to an individual who has been exposed to the chemical. The required information consists of:

- Necessary first-aid instructions by relevant routes of exposure (inhalation, skin and eye contact, and ingestion).
- Description of the most important symptoms or effects, and any symptoms that are acute or delayed.
- Recommendations for immediate medical care and special treatment needed, when necessary.

Section 5: Fire-Fighting Measures

This section provides recommendations for fighting a fire caused by the chemical. The required information consists of:

- Recommendations of suitable extinguishing equipment, and information about extinguishing equipment that is not appropriate for a particular situation.
- Advice on specific hazards that develop from the chemical during the fire, such as any hazardous combustion products created when the chemical burns.
- Recommendations on special protective equipment or precautions for firefighters.

Section 6: Accidental Release Measures

This section provides recommendations on the appropriate response to spills, leaks, or releases, including containment and cleanup practices to prevent or minimize exposure to people, properties, or the environment. It may also include recommendations distinguishing between responses for large and small spills where the spill volume has a significant impact on the hazard. The required information may consist of recommendations for:

- Use of personal precautions (such as removal of ignition sources or providing sufficient ventilation) and protective equipment to prevent the contamination of skin, eyes, and clothing.
- Emergency procedures, including instructions for evacuations, consulting experts when needed, and appropriate protective clothing.
- Methods and materials used for containment (e.g., covering the drains and capping procedures).
- Cleanup procedures (e.g., appropriate techniques for neutralization, decontamination, cleaning or vacuuming; adsorbent materials; and/or equipment required for containment/clean up)

Section 7: Handling and Storage

This section provides guidance on the safe handling practices and conditions for safe storage of chemicals. The required information consists of:

- Precautions for safe handling, including recommendations for handling incompatible chemicals, minimizing the release of the chemical into the environment, and providing advice on general hygiene practices (e.g., eating, drinking, and smoking in work areas is prohibited).

- Recommendations on the conditions for safe storage, including any incompatibilities. Provide advice on specific storage requirements (e.g., ventilation requirements)

Section 8: Exposure Controls/Personal Protection

This section indicates the exposure limits, engineering controls, and personal protective measures that can be used to minimize worker exposure. The required information consists of:

- OSHA Permissible Exposure Limits (PELs), American Conference of Governmental Industrial Hygienists (ACGIH) Threshold Limit Values (TLVs), and any other exposure limit used or recommended by the chemical manufacturer, importer, or employer preparing the safety data sheet, where available.
- Appropriate engineering controls (e.g., use local exhaust ventilation, or use only in an enclosed system).
- Recommendations for personal protective measures to prevent illness or injury from exposure to chemicals, such as personal protective equipment (PPE) (e.g., appropriate types of eye, face, skin or respiratory protection needed based on hazards and potential exposure).
- Any special requirements for PPE, protective clothing or respirators (e.g., type of glove material, such as PVC or nitrile rubber gloves; and breakthrough time of the glove material).

Section 9: Physical and Chemical Properties This section identifies physical and chemical properties associated with the substance or mixture. The minimum required information consists of:

- Appearance (physical state, color, etc.);
- Upper/lower flammability or explosive limits;
- Odor;
- Vapor pressure;
- Odor threshold;
- Vapor density;
- pH;
- Relative density;
- Melting point/freezing point;
- Solubility(ies);
- Initial boiling point and boiling range;
- Flash point;
- Evaporation rate;
- Flammability (solid, gas);
- Partition coefficient: n-octanol/water;
- Auto-ignition temperature;
- Decomposition temperature; and
- Viscosity.

The SDS may not contain every item on the above list because information may not be relevant or is not available. When this occurs, a notation to that effect must be made for that chemical property. Manufacturers may also add other relevant properties, such as the dust deflagration index (Kst) for combustible dust, used to evaluate a dust's explosive potential

Section 10: Stability and Reactivity

This section describes the reactivity hazards of the chemical and the chemical stability information. This section is broken into three parts: reactivity, chemical stability, and other. The required information consists of:

Reactivity

- Description of the specific test data for the chemical(s). This data can be for a class or family of the chemical if such data adequately represent the anticipated hazard of the chemical(s), where available.

Chemical stability

- Indication of whether the chemical is stable or unstable under normal ambient temperature and conditions while in storage and being handled.
- Description of any stabilizers that may be needed to maintain chemical stability.
- Indication of any safety issues that may arise should the product change in physical appearance.

Other

- Indication of the possibility of hazardous reactions, including a statement whether the chemical will react or polymerize, which could release excess pressure or heat, or create other hazardous conditions. Also, a description of the conditions under which hazardous reactions may occur.
- List of all conditions that should be avoided (e.g., static discharge, shock, vibrations, or environmental conditions that may lead to hazardous conditions).
- List of all classes of incompatible materials (e.g., classes of chemicals or specific substances) with which the chemical could react to produce a hazardous situation.
- List of any known or anticipated hazardous decomposition products that could be produced because of use, storage, or heating. (Hazardous combustion products should also be included in Section 5 (Fire-Fighting Measures) of the SDS.)

Section 11: Toxicological Information

This section identifies toxicological and health effects information or indicates that such data are not available. The required information consists of:

- Information on the likely routes of exposure (inhalation, ingestion, skin and eye contact). The SDS should indicate if the information is unknown.
- Description of the delayed, immediate, or chronic effects from short- and long-term exposure.

- The numerical measures of toxicity (e.g., acute toxicity estimates such as the LD50 (median lethal dose))—the estimated amount [of a substance] expected to kill 50% of test animals in a single dose.
- Description of the symptoms. This description includes the symptoms associated with exposure to the chemical including symptoms from the lowest to the most severe exposure.
- Indication of whether the chemical is listed in the National Toxicology Program (NTP) Report on Carcinogens (latest edition) or has been found to be a potential carcinogen in the International Agency for Research on Cancer (IARC) Monographs (latest editions) or found to be a potential carcinogen by OSHA

Section 12: Ecological Information (non-mandatory)

This section provides information to evaluate the environmental impact of the chemical(s) if it were released to the environment. The information may include:

- Data from toxicity tests performed on aquatic and/or terrestrial organisms, where available (e.g., acute or chronic aquatic toxicity data for fish, algae, crustaceans, and other plants; toxicity data on birds, bees, plants).
- Whether there is a potential for the chemical to persist and degrade in the environment either through biodegradation or other processes, such as oxidation or hydrolysis.
- Results of tests of bioaccumulation potential, making reference to the octanol-water partition coefficient (Kow) and the bioconcentration factor (BCF), where available.
- The potential for a substance to move from the soil to the groundwater (indicate results from adsorption studies or leaching studies).
- Other adverse effects (e.g., environmental fate, ozone layer depletion potential, photochemical ozone creation potential, endocrine disrupting potential, and/or global warming potential).

Section 13: Disposal Considerations (non-mandatory)

This section provides guidance on proper disposal practices, recycling or reclamation of the chemical(s) or its container, and safe handling practices. To minimize exposure, this section should also refer the reader to Section 8 (Exposure Controls/Personal Protection) of the SDS. The information may include:

- Description of appropriate disposal containers to use.
- Recommendations of appropriate disposal methods to employ.
- Description of the physical and chemical properties that may affect disposal activities.
- Language discouraging sewage disposal.
- Any special precautions for landfills or incineration activities

Section 14: Transport Information (non-mandatory)

This section provides guidance on classification information for shipping and transporting of hazardous chemical(s) by road, air, rail, or sea. The information may include:

- UN number (i.e., four-figure identification number of the substance)[1].
- UN proper shipping name[1].
- Transport hazard class(es)[1].
- Packing group number, if applicable, based on the degree of hazard[2].
- Environmental hazards (e.g., identify if it is a marine pollutant according to the International Maritime Dangerous Goods Code (IMDG Code)).
- Guidance on transport in bulk (according to Annex II of MARPOL 73/78[3] and the International Code for the Construction and Equipment of Ships Carrying Dangerous Chemicals in Bulk (International Bulk Chemical Code (IBC Code)).
- Any special precautions which an employee should be aware of or needs to comply with, in connection with transport or conveyance either within or outside their premises (indicate when information is not available).

Section 15: Regulatory Information (non-mandatory)

This section identifies the safety, health, and environmental regulations specific for the product that is not indicated anywhere else on the SDS. The information may include:

- Any national and/or regional regulatory information of the chemical or mixtures (including any OSHA, Department of Transportation, Environmental Protection Agency, or Consumer Product Safety Commission regulations)

Section 16: Other Information

This section indicates when the SDS was prepared or when the last known revision was made. The SDS may also state where the changes have been made to the previous version. You may wish to contact the supplier for an explanation of the changes. Other useful information also may be included here.

Employer Responsibilities

Employers must ensure that the SDSs are readily accessible to employees for all hazardous chemicals in their workplace. This may be done in many ways. For example, employers may keep the SDSs in a binder or on computers as long as the employees have immediate access to the information without leaving their work area when needed and a back-up is available for rapid access to the SDS in the case of a power outage or other emergency. Furthermore, employers may want to designate a person(s) responsible for obtaining and maintaining the SDSs. If the employer does not have an SDS, the employer or designated person(s) should contact the manufacturer to obtain one.

---

[1] Chemical, as defined in the HCS, is any substance, or mixture of substances.

[2] Found in the most recent edition of the United Nations Recommendations on the Transport of Dangerous Goods.

[3] MARPOL 73/78 means the International Convention for the Prevention of Pollution from Ships, 1973, as modified by the Protocol of 1978 relating thereto, as amended

References

OSHA, 29 CFR 1910.1200(g) and Appendix D. United Nations Globally Harmonized System of Classification and Labelling of Chemicals (GHS), third revised edition, United Nations, 2009. These references and other information related to the revised Hazard Communication Standard can be found on OSHA's Hazard Communication Safety and Health Topics page, located at:http://www.osha.gov/dsg/hazcom/index.html.

Disclaimer: This brief provides a general overview of the safety data sheet requirements in the Hazard Communication Standard (see 29 CFR 1910.1200 (g) and Appendix D of 29 CFR 1910.1200). It does not alter or determine compliance responsibilities in the standard or the Occupational Safety and Health Act of 1970. Since interpretations and enforcement policy may change over time, the reader should consult current OSHA interpretations and decisions by the Occupational Safety and Health Review Commission and the courts for additional guidance on OSHA compliance requirements. Please note that states with OSHA-approved state plans may have additional requirements for chemical safety data sheets, outside of those outlined above. For more information on those standards, please visit: http://www.osha.gov/dcsp/osp/statestandards.html.

This is one in a series of informational briefs highlighting OSHA programs, policies or standards. It does not impose any new compliance requirements. For a comprehensive list of compliance requirements of OSHA standards or regulations, refer to Title 29 of the Code of Federal Regulations. This information will be made available to sensory-impaired individuals upon request. The voice phone is (202) 693-1999; teletypewriter (TTY) number: (877) 889-5627.

For assistance, contact us. We can help. It's confidential

OSHA®
Occupational
Safety and Health
Administration

U.S. Department of Labor
www.osha.gov (800) 321 OSHA (6742)
DSG BR-3514 2/2012

MSD 6.2. Hexanitrohexaazaisowurtzitane (HNIW, CL-20)

MSDs D0211

Revision 5

Latest Revision: 4 August 1998; Superseding 17 June 1997

Thiokol Corporation Emergency	Phone No. (801) 863-8545
P.O. Box 707	Product Information (801) 863-33251
Brigham City, UT 84302-0707	

Section 1. CHEMICAL PRODUCT IDENTIFICATION

NAME: Trade Name: CL-20

Synonyms: CL-20 Explosive, Alpha CL-20,

Epsilon CL-20,

Epsilon CL-20 Energetic Filler

For R&D Use Only

Section 2. COMPOSITION AND INFRMATION ON INGREDIENTS

Ingredients	Percent	PEL (TWA)	STEL	TLV
CL-201 CAS NO, 135285-90-4	*	NE	NE	NE

NE: Not established

*: The safety data provided should be sufficient for most handling and exposure situations. Additional data may only be provided if appropriate DOD approval is granted.I

Chemical Names:

A 5,2,6-(Imrinomethenimino) -1H-imidazo[4,5-b]pyrazine, octahydro 1,3,4,7,8,10-hexanitro

B 2,4,6,8,10,12-He-xanitro-2,4,6,8,10,12-hexaazatetracyclo [5.5.0.05,9.03.11]-dodecane

C Hexanitrohexaazaisowurtzitane

Section 3. Hazards Identification

Exposure Limits: Not applicable.

Effects of Exposure: .

Inhalation: Not known. Explosives similar to CL-20 may sensitizesusceptible individuals, causing asthma-like allergic reactions.

Eyes: Not known.

Skin: Not known.

Ingestion: Not known. May be highly toxic if ingested.

Existing conditions which may be aggravated: .

Section 4. First AI Measures

Inhalation: Contact physician, Give oxygen or artificial respiration if needed. For thermal burns contact physician.

Eyes: Flush immediately with water for least 15 min. Contact physician.

Skin: Wash with soap and water. Contact physician.

Ingestion: Contact physician

Section 5. Fire-Fighting Measures

Extinguishing Media: Do not attempt to fight CL-20 explosive fires.

Special Fire Fighting Procedures: Do not fight fires involving this CL-20 explosive. If ignited, this explosive may detonate. Thrust and overpressure created while burning may give this CL-20 explosive uncontrollable ballistic properties. Fire fighting should be limited to evacuating an area proportional to the amount of CL-20 explosive which may detonate or bum, and preventing the spread of fire beyond the isolated area.

Unusual Fire and Explosions Hazards: Static discharge, impact, friction and pinch points between hard surfaces may initiate a conflagration or detonation. Overpressures associated with rapidly burning CL-20 explosive can be explosive-like, creating fireballs and shock waves.

Section 6. Accidental Release Measures

Precautions if Container is Damaged or Material Spilled: CL-20 explosive must be protected from sources of ignition (see Section 7). If ignited accidentally, a detonation should be anticipated, causing a shock wave, spreading burning material over a wide area, and producing toxic decomposition fumes. Contact appropriate authorities.

Section 7. Handling and Storage

Buildings and transporting equipment must be protected from lightning and other forms of static discharge. Protect CL-20 explosive from ignition sources, static charge buildup, mechanical shock, friction. Burning characteristics may only be predicted when the environmental history is known, and aging and temperature limits set by design and aging studies have not been exceeded. CL-20 should be shipped wet-packed to minimize sensitivity.

Other Precautions: CL-20 explosive is federally controlled, CL-20 explosive should be controlled and handled only by personnel properly trained and authorized to handle explosive materials.

Section 8. Exposure Controls—Personal Protection

Ventilation: Provide sufficient mechanical (general and/or exhaust ventilation to limit vapor inhalation.

Respiratory Protection: A NIOSH/MSHA approve air supplied respirator is advised in the absence of proper environmental control. Engineering and/or administrative controls may be implemented to reduce exposure.

Protective Gloves: Wear nonporous gloves such as natural rubber or neoprene for handling.

Eye Protection: Protect from exposure to dust. Chemical monogoggles should be worn for most applications, Workers who risk exposure should have access to an eye fountain and safety shower.

Other Protective Equipment: Clothing combinations which may create static discharges must be avoided. Workers handling this explosive should be grounded, wearing conductive shoes or equivalent on a clean conductive floor. Flame resistant clothing is advised. CL-20 explosive should be contained in conductive containers, Glassware, metal tools, and grainy or gritty surfaces should be avoided.

Section 9. Physical and Chemical Properties

Vapor Density:	N/A
Specific Gravity:	>1.8 g/cc
Solubility in Water:	NIL
Vapor Pressure:	N/A
Evaporation Rate:	N/A
Melting Point:	Decomposes.

Bouing Point:	Decomposes.
Appearance and Color:	White crystalline solid.
Detection Methods:	N/A
pH:	N/A
Flashpoint:	Not applicable

Section 10. Stability and Reactivity

Stability: Unstable, if heated.
Conditions to Avoid: Shock, impact, friction, and static charge buildup and high temperatures.
Incompatibility (Materials to Avoid): Not known.
Hazardous Decomposition Products:
Hazardous Polymerization: Will not occur.
Other Hazards:

Section 11. Tomocological Information

Acute Effects: See Section 3.
Chronic Effects: May sensitize susceptible individuals causing asthma-like allergic reactions.
Target Organ(s): Unknown.

Section 12. Ecological Information

No data available.

Section 13. Disposal Considerations

Dispose of in accordance with federal, state, and local regulations. This material is an explosive and may detonate,

Section 14. Transportation Information

Transport in accordance with federal, state, and local regulations. See 49 CPR—Rules governing transportation.

CL-20 Dry

Proper Shipping Names: Substances, explosive, n.o.s., (Hexanitro hexaazaisowurtzitane)
Hazard Class: 1.1D
I.D. Number: UN0475
Packing Group: II
Label: Explosive 1.1 D
Packing Method: E-5 49 CFR 173.62(C)
EX-Number: EX-9410242

CL-2O.Wetted with 15% Water

Proper Shipping Names: Substances, explosive, n.o.s., (Hexanitr hexaazaisowurtzitane)
Hazard Class: 1.ID
Number: UN0475
Packing Group: Hl
Label: Explosive 1.1 D
Packing Method: (E-6 (a)(i)), (E-6(a)(ii)) 49 CFR 173.62(C)
EX-Number: EX-9405294

Section 15. Regulatory Information

Toxic Substances Control Act (TSCA)

NOTICE: CL-20 is not registered on the TSCA Inventory and therefore this chemical material is for Research and Development Use Only under the supervision of a technically qualified individual.

Section 16 Other Information

For R&D use only. To the best of our knowledge the information contained herein is correct. All chemicals may present unknown health hazards and must be used with caution. Although certain hazards are described herein, we cannot guarantee that these are the only hazards which exist. Final determination of the suitability of the chemical is the sole responsibility of the user. Users of any chemical should satisfy themselves that the conditions and methods of use assure that the chemical is used safely.

NO REPRESENTATIONS OR WARRANTIES, EITHER EXPRESS OR IMPLIED, TO INCLUDE WARRANTIES OF MERCHANTABILITY, FITNESS FOR A PARTICULAR PURPOSE OR ANY OTHER NATURE ARE MADE HEREUNDER WITH RESPECT TO THE INFORMATION CONTAINED HEREIN OR THE CHEMICAL TO WHICH THE INFORMATION REFERS.

MSD 6.3. 1,1-diamino-2,2-dinitroethylene (DADN; FOX-7)

DADNE (FOX-7)

For more than 10 years, our R&D teams perform research and development of new energetic substances to satisfy the future requirements of our customers. Leading worldwide specialist in the field of high explosives, EURENCO offers further new energetic molecules such as DADNE (FOX-7), developed in cooperation with FOI (the Swedish Defence Research Agency) and manufactured thanks to its modern multipurpose units.

PRODUCT

- Trade name: DADNE (or FOX-7)
- Chemical name: 1,1-diamino 2,2-dinitro ethylene
- Chemical formula: $C_2(NH_2)_2(NO_2)_2$
- Compatibility with binders such as estane, CAB, HTPB, viton, isocyanate, K-10, butyl-nena, etc.
- EURENCO offers 4 different classes of DADNE (FOX-7) with different crystal sizes:
    - Class 1: 20 – 40 µm
    - Class 2: 50 – 100 µm
    - Class 3: 100 – 200 µm
    - Class 4: 250 – 300 µm

CHARACTERISTICS

- Density: 1.885 g/cm^3
- Heat of formation: -8 kJ/mole
- Friction sensitivity (ISF): > 350 N (RDX: 120 N)
- Impact sensitivity (ISI): 20 – 40 J (RDX: 4 – 5 J)
- Sensitivity ESD (Bofors): > 8 J
- Auto-ignition temperature: 215 °C
- Detonation pressure: 34 GPa (RDX: 35 GPa)
- Detonation velocity: 8800 m/s (RDX: 8930 m/s)

USES

Characterized by an inherent lower sensitivity than usual military explosives, DADNE (FOX-7) is drastically more resistant towards all forms of impact and friction and provides safe handling of ammunition. With same performance as RDX, DADNE (FOX-7) can thus be used for insensitive warhead fillings.

Increasing the burning rate in propellants more than RDX does, DADNE (FOX-7) can also be used as a main ingredient of high performance propellants for tank ammunition.

RESULTS

Small-Scale Slow Cook-Off Test(1)

A formulation was tested in Small-Scale Slow Cook-Off Test, based on DADNE (FOX-7) with PolyGlyn as binder and Bu-NENA as plasticizer. The bomb was heated at the rate of 3.3°C/h. The formulation started to burn non-violently at 150°C without fragmentation of the bomb (type V)(2).

As a reference, another test was conducted on Composition B; it reacted violently with extensively fragmentation (Type I) at 207°C.

(1) *B. Janzon, H. Bergman, C. Eldsäter, C. Lamnevik and H. Östmark, 20th International Symposium on Ballistics Orlando, FL. 23-27 September, 2002.*
(2) *The results were classified according to the Stanag 4382 Ed. 1.*

EURENCO
Explosive Charges & Additives Business Unit
12 quai Henri IV - 75004 Paris – France
Tel.: +33 (0) 1 49 96 74 00 - Fax: +33 (0) 1 49 96 74 03
E-mail: eca.bu@eurenco.com - www.eurenco.com

MSD 6.4. 2,4-Dinitroanisole (DNAN)

SIGMA-ALDRICH

Material Safety Data Sheet
Version 3.0
Revision Date 12/28/2008
Print Date 02/13/2011

---

1. PRODUCT AND COMPANY IDENTIFICATION

Product name :	2,4-Dinitroanisole
Product Number :	S627631
Brand :	Aldrich
Company :	Sigma-Aldrich 3050 Spruce Street SAINT LOUIS MO 63103 USA
Telephone :	+18003255832
Fax :	+18003255052
Emergency Phone # :	(314) 776-6555

---

2. COMPOSITION/INFORMATION ON INGREDIENTS2.

Formula : $C_7H_6N_2O_5$
Molecular Weight : 198.14 g/mol

CAS No.	EC No.	Index No.	Concentration
2,4-Dinitroanisole			
119-27-7	204-310-9		

---

3. HAZARDS IDENTIFICATION

Emergency Overview

OSHA Hazards
Target Organ Effect, Harmful by ingestion.

Target Organs
Blood

HMIS Classification

Health Hazard:	**1**
Chronic Health Hazard:	*****
Flammability:	**0**
Physical hazards:	**0**

NFPA Rating

Health Hazard:	**1**
Fire:	**0**
Reactivity Hazard:	**0**

Potential Health Effects

Inhalation	**May be harmful if inhaled. May cause respiratory tract irritation.**
Skin	**May be harmful if absorbed through skin. May cause skin irritation.**
Eyes	May cause eye irritation.
Ingestion	Harmful if swallowed.

---

4. FIRST AID MEASURES

General advice

Consult a physician. Show this safety data sheet to the doctor in attendance.

If inhaled

If breathed in, move person into fresh air. If not breathing give artificial respiration Consult a physician.

In case of skin contact

Wash off with soap and plenty of water. Consult a physician.

In case of eye contact

Rinse thoroughly with plenty of water for at least 15 minutes and consult a physician.

If swallowed

Never give anything by mouth to an unconscious person. Rinse mouth with water. Consult a physician.

---

5. FIRE-FIGHTING MEASURES

Flammable properties

Flash point no data available

Ignition temperature no data available

Suitable extinguishing media

Use water spray, alcohol-resistant foam, dry chemical or carbon dioxide.

Special protective equipment for fire-fighters
Wear self contained breathing apparatus for fire fighting if necessary.

---

6. ACCIDENTAL RELEASE MEASURES

Personal precautions

Use personal protective equipment. Avoid dust formation. Avoid breathing dust. Ensure adequate ventilation.

Environmental precautions
Do not let product enter drains.

Methods for cleaning up

Pick up and arrange disposal without creating dust. Keep in suitable, closed containers for disposal.

---

7. HANDLING AND STORAGE

Handling
Avoid formation of dust and aerosols.

Provide appropriate exhaust ventilation at places where dust is formed. Normal measures for preventive fire protection.

Storage
Keep container tightly closed in a dry and well-ventilated place.

Keep in a dry place.

---

8. EXPOSURE CONTROLS/PERSONAL PROTECTION

Contains no substances with occupational exposure limit values.

Personal protective equipment
Respiratory protection

Where risk assessment shows air-purifying respirators are appropriate use a dust mask type N95 (US) or type P1 (EN 143) respirator. Use respirators and components tested and approved under appropriate government standards such as NIOSH (US) or CEN (EU).

Hand protection

Handle with gloves. For prolonged or repeated contact use protective gloves.

Eye protection

Safety glasses

Skin and body protection

Choose body protection according to the amount and concentration of the dangerous substance at the work place.

Hygiene measures

Handle in accordance with good industrial hygiene and safety practice. Wash hands before breaks and at the end of workday.

9. PHYSICAL AND CHEMICAL PROPERTIES

Appearance

Form	powder
Colour	tan

Safety data

pH	no data available
Melting point	94 - 96 °C (201 - 205 °F)
Boiling point	no data available
Flash point	no data available
Ignition temperature	no data available
Lower explosion limit	no data available
Upper explosion limit	no data available
Density	1.340 g/cm3
Water solubility	no data available

10. STABILITY AND REACTIVITY

Storage stability

Stable under recommended storage conditions.

Materials to avoid

Strong oxidizing agents, Strong bases

Hazardous decomposition products

Hazardous decomposition products formed under fire conditions. - Carbon oxides, nitrogen oxides (NOx)

11. TOXICOLOGICAL INFORMATION

Acute toxicity

no data available

Irritation and corrosion

no data available

Sensitisation

no data available

Chronic exposure

IARC:	No component of this product present at levels greater than or equal to 0.1% is identified as probable, possible or confirmed human carcinogen by IARC.
ACGIH:	No component of this product present at levels greater than or equal to 0.1% is identified as a carcinogen or potential carcinogen by ACGIH.
NTP:	No component of this product present at levels greater than or equal to 0.1% is identified as a known or anticipated carcinogen by NTP.
OSHA:	No component of this product present at levels greater than or equal to 0.1% is identified as a carcinogen or potential carcinogen by OSHA.

Genotoxicity in vitro - Histidine reversion (Ames)

Signs and Symptoms of Exposure

Absorption into the body leads to the formation of methemoglobin which in sufficient concentration causes cyanosis. Onset may be delayed 2 to 4 hours or longer., To the best of our knowledge, the chemical, physical, and toxicological properties have not been thoroughly investigated.

Potential Health Effects

Inhalation	May be harmful if inhaled. May cause respiratory tract irritation.
Skin	May be harmful if absorbed through skin. May cause skin irritation.
Eyes	May cause eye irritation.
Ingestion	Harmful if swallowed.
Target Organs	Blood,

Additional Information

RTECS: DA5250000

---

12. ECOLOGICAL INFORMATION

Elimination information (persistence and degradability)

no data available

Ecotoxicity effects

no data available

Further information on ecology

no data available

---

13. DISPOSAL CONSIDERATIONS

Product

Observe all federal, state, and local environmental regulations.

Contaminated packaging

Dispose of as unused product.

---

14. TRANSPORT INFORMATION

DOT (US)

Not dangerous goods

IMDG

Not dangerous goods

IATA

Not dangerous goods

---

15. REGULATORY INFORMATION

OSHA Hazards

Target Organ Effect, Harmful by ingestion.

DSL Status

This product contains the following components listed on the Canadian NDSL list. All other components are on the Canadian DSL list.

	CAS-No
2,4-Dinitroanisole	119-27-7

SARA 302 Components

SARA 302: No chemicals in this material are subject to the reporting requirements of SARA Title III, Section 302.

SARA 313 Components

SARA 313: This material does not contain any chemical components with known CAS numbers that exceed the

threshold (De Minimis) reporting levels established by SARA Title III, Section 313.

SARA 311/312 Hazards

Acute Health Hazard, Chronic Health Hazard

Massachusetts Right To Know Components

No components are subject to the Massachusetts Right to Know Act.

Pennsylvania Right To Know Components

	CAS-No.	
2,4-Dinitroanisole	119-27-7	Revision Date

New Jersey Right To Know Components

	CAS-No.	
2,4-Dinitroanisole	119-27-7	Revision Date

California Prop. 65 Components

This product does not contain any chemicals known to State of California to cause cancer, birth, or any other reproductive defects.

16. OTHER INFORMATION

Further information

Copyright 2008 Sigma-Aldrich Co. License granted to make unlimited paper copies for internal use only. The above information is believed to be correct but does not purport to be all inclusive and shall be used only as a guide. The information in this document is based on the present state of our knowledge and is applicable to the product with regard to appropriate safety precautions. It does not represent any guarantee of the properties of the product. Sigma-Aldrich Co., shall not be held liable for any damage resulting from handling or from contact with the above product. See reverse side of invoice or packing slip for additional terms and conditions of sale.

MSD 6.5. 5-Nitro-2,4-Dihydro-3H-1,2,4-Triazole-3-One (NTO)

Product: Dinitrogen Tetroxide P-4633-E Date: December 2007

Praxair Material Safety Data Sheet

1. Chemical Product and Company Identification

Product Name: Dinitrogen tetroxide (MSDS No. P-4633-E)	Trade Names: Nitrogen Dioxide
Chemical Name: Nitrogen dioxide and dinitrogen tetroxide in equilibrium	Synonyms: Dinitrogen tetroxide, nitrito, nitrogen oxide, nitrogen peroxide, nitrogen tetroxide, NTO, red oxide of nitrogen
Chemical Family: Nitrogen oxides (NOx)	Product Grades: 2.5

Telephone: Emergencies: 1-800-645-4633* Company Name: Praxair, Inc.
CHEMTREC: 1-800-424-9300* 39 Old Ridgebury Road
Routine: 1-800-PRAXAIR Danbury, CT 06810-5113

* Call emergency numbers 24 hours a day only for spills, leaks, fire, exposure, or accidentsinvolving this product. For routine information, contact your supplier, Praxair sales representative, or call 1-800-PRAXAIR (1-800-772-9247).

2. Hazards Identification

EMERGENCY OVERVIEW
DANGER! Poisonous, corrosive, oxidizing liquid and gas under pressure.
May be fatal if inhaled.
Can cause severe lung damage.
Can cause eye and skin burns.
Symptoms may be delayed.
Vigorously accelerates combustion.
Self-contained breathing and protective clothing must be worn by rescue workers.

Under ambient conditions, this is a reddish-brown gas with an irritating odor.

OSHA REGULATORY STATUS: This material is considered hazardous by the OSHA Hazard
Communications Standard (29 CFR 1910.1200).

Potential Health Effects:

Effects of a Single (Acute) Overexposure

Inhalation. Overexposure may irritate the mucous membranes, sinuses, pharynx, and bronchia, with pain, headache, cyanosis, irregular respiration, choking, dizziness, and possibly pulmonary edema. Pulmonary symptoms may be delayed from 5 to 72 h. High concentrations of vapor may cause pain, choking, bronchoconstriction, reflex slowing of the heart, and possibly asphyxiation. Lack of oxygen can kill.

Skin Contact. Severe irritant; may cause burns. Prolonged or widespread skin contact may result in absorption of harmful amounts of nitrogen dioxide.

Swallowing. A highly unlikely route of exposure; this product is a gas at normal temperature and pressure. May cause burns of the mouth, esophagus, and stomach.

Eye Contact. May cause severe conjunctivitis, seen as marked excess redness and

swelling of the conjunctiva, and corneal injury with opacification.

Effects of Repeated (Chronic) Overexposure. Repeated inhalation may cause bronchitis or emphysema; repeated skin contact may cause dermatitis.

Other Effects of Overexposure. None known.

Medical Conditions Aggravated by Overexposure. Inhalation may aggravate asthma and inflammatory or fibrotic pulmonary disease. Skin irritating properties may aggravate dermatitis.

Carcinogenicity: Nitrogen dioxide is not listed by NTP, OSHA, or IARC.

Potential Environmental Effects: None known. For further information, see section 12, Ecological Information.

3. Composition/Information on Ingredients

See section 16 for important information about mixtures

Component	**CAS number**	**Concentration**
Nitrogen Dioxide	10102-44-0	>99%[a]
Dinitrogen Tetroxide	10544-72-6	Trace

[a] The symbol > means "greater than"

4. First Aid Measures

Inhalation: Remove to fresh air. If not breathing, give artificial respiration. WARNING:

Rescuer could receive chemical burns from giving mouth-to-mouth. Rescuer should avoid breathing air exhaled by victim. If breathing is difficult, qualified personnel may give oxygen. Keep patient warm. Call a physician immediately. Keep under medical observation. Symptoms may be delayed.

Skin Contact: Immediately flush skin with plenty of water for at least 15 min whileremoving contaminated clothing and shoes. Discard clothing and shoes. Call a physician.

Swallowing: An unlikely route of exposure. This product is a gas at normal temperature and pressure.

Eye Contact: Immediately flush eyes thoroughly with water for at least 15 min. Hold the eyelids open and away from the eyeballs to ensure that all surfaces are flushed thoroughly. See a physician, preferably an ophthalmologist, immediately.

Notes to Physician: In case of overexposure, keep patient under medical observation for at least 72 h to observe for pulmonary edema. Patient may have a second acute pulmonary reaction 2–6 weeks after the first. The hazards of this material are due chiefly to its severe irritant and corrosive properties on the skin and mucosal surfaces. There is no specific antidote. Treatment of overexposure should be directed at the control of symptoms and the clinical condition of the patient.

Contact the Poison Control Center in your area for additional information on patientmanagement and follow-up.

5. Fire Fighting Measures

Flammable Properties: Oxidizing agent; may accelerate combustion. Contact with flammable materials may cause fire or explosion.

Suitable Extinguishing Media: Oxidizing agent; may accelerate combustion. Use media appropriate for surrounding fire.

Products of Combustion: Not applicable. Decomposition due to heating may produce toxic fumes. (See section 10.)

Protection of Firefighters: Danger! Poisonous, corrosive, oxidizing liquid and gas under pressure. Evacuate all personnel from danger area. Do not approach area without self-contained breathing apparatus and protective clothing. Immediately spray cylinders with water from maximum distance until cool; then move them away from fire area if without risk. Remove ignition sources if without risk. If cylinders are leaking, reduce vapors with water spray or fog. Do not spray water directly onto leak; this may only increase the leak. Reverse flow into cylinder may cause it to rupture. Shut off leak if without risk. On-site fire brigades must comply with OSHA 29 CFR 1910.156.

Specific Physical and Chemical Hazards. Heat of fire can build pressure in cylinder and cause it to rupture. To provide maximum containment up to cylinder burst pressure, nitrogen dioxide cylinders are not equipped with a pressure-relief device. No part of a cylinder should be subjected to a temperature higher than 125 ° F (52 °C). Vapors are irritating; contact may cause skin and eye burns.

Protective Equipment and Precautions for Firefighters. Firefighters should wear selfcontained breathing apparatus and full fire-fighting turnout gear.

6. Accidental Release Measures

Steps to be taken if Material is Released or Spilled:

Danger! Poisonous, corrosive, oxidizing liquid and gas under pressure.

Personal Precautions. Immediately evacuate all personnel from danger area. Use selfcontained breathing apparatus and protective clothing where needed. Reduce vapors with fog or fine water spray. Reverse flow into cylinder may cause it to rupture. Shut off flow if without risk. Ventilate area or move leaking cylinder to well-ventilated area. Toxic, corrosive vapors may spread from spill. Before entering area, especially confined areas, check atmosphere with an appropriate device.

Environmental Precautions. Prevent waste from contaminating the surrounding environment. Keep personnel away. Discard any product, residue, disposable container, or liner in an environmentally acceptable manner, in full compliance with federal, state, and local regulations. If necessary, call your local supplier for assistance.

7. Handling and Storage

Precautions to be taken in Handling: May be fatal if inhaled. Do not breathe gas. Do not get vapors or liquid in eyes, on skin, or on clothing. Keep away from oxidizing agents and from other flammables. Have safety showers and eyewash fountains immediately available. Protect cylinders from damage. Use a suitable hand truck to move cylinders; do not drag, roll, slide, or drop. All piped systems and associated equipment must be grounded. Electrical equipment must be non-sparking or explosion-proof. Leak check with soapy water; never use a flame. Never attempt to lift a cylinder by its cap; the cap is intended solely to protect the valve. Never insert an object (e.g., wrench, screwdriver, pry bar) into cap openings; doing so may damage the valve and cause a leak. Use an adjustable strap wrench to remove over-tight or rusted caps. Open valve slowly. Close valve after each use; keep closed even when empty. If valve is hard to open, discontinue use and contact your supplier. For other precautions in using nitrogen dioxide, see section 16.

Precautions to be taken in Storage: Store and use with adequate ventilation, away from oil, grease, and combustibles. Firmly secure cylinders upright to keep them from falling or being knocked over. Nitrogen dioxide cylinders designed to accept a valve protection cap must be provided with a cap. Screw cap firmly in place by hand. Store only where temperature will not exceed 125°F (52°C). Store full and empty cylinders separately. Use a first-in, first-out inventory system to prevent storing full cylinders for long periods.

Recommended Publications: For further information on storage, handling, and use, see Praxair publication P-14-153, Guidelines for Handling Gas Cylinders and Containers. Obtain from your local supplier.

8. Exposure Controls/Personal Protection

Component	OSHA PEL	ACGIH TLV-TWA (2007)
Nitrogen Dioxide Dinitrogen Tetroxide	5 ppm (c)[a]	3 ppm; 5 ppm, 15 min STEL

Values above are for equilibrium mixture

[a] (c)—ceiling. Ceiling values are not Time-Weighted-Average (TWA)

TLV-TWAs should be used as a guide in the control of health hazards and not as fine lines between safe and dangerous concentrations.

IDLH = 20 ppm

Engineering Controls:

Local Exhaust. Use a corrosion-resistant local exhaust system.

Mechanical (General). Inadequate. See SPECIAL.

Special. Use only in a closed system. A corrosion-resistant, forced-draft fume hood preferred.

Other. None

Personal Protective Equipment:

Skin Protection. Wear work gloves when handling cylinders; neoprene gloves where contact with product may occur. Metatarsal shoes for cylinder handling, protective clothing where needed. Select in accordance with OSHA 29 CFR 1910.132 and 1910.133. Regardless of protective equipment, never touch live electrical parts.

Eye/Face Protection. Select in accordance with OSHA 29 CFR 1910.133

Respiratory Protection. Use an air-supplied respirator or a full-face, positive-breathing apparatus. Respiratory protection must conform to OSHA 29 CFR 1910.134. Select per OSHA 29 CFR 1910.134 and ANSI Z88.2.

9. Physical and Chemical Properties

Appearance:	Reddish-brown gas
Odor:	Irritating
Odor Threshold:	Not available.
Physical State:	Gas at normal temperature and pressure

pH:	Acid when dissolved in H_2O.
Melting Point at 1 atm:	11.8 °F (−11.2 °C)
Boiling Point at 1 atm:	70.16 °F (21.20 °C)
Flash Point (test method):	Not applicable.
Evaporation Rate (Butyl Acetate = 1):	High
Flammability:	Nonflammable.
Flammable Limits in Air, % by volume:	Lower: Not applicable. Upper: Not applicable.
Vapor Pressure at 70 °F (21.1 °C):	14.7 psia (101.4 kPa abs)
Vapor Density at 70 °F (21.1 °C) and 1 atm:	Not available.
Specific Gravity (H_2O = 1) at 68°/39.9 °F (20°/4 °C):	. 1.448
Specific Gravity (Air = 1) at 70 °F (21.1 °C) and 1 atm:	. 2.62
Solubility in Water:	Reacts; forms nitric and nitrous acids.
Partition Coefficient:	n-octanol/water: Not available.
Autoignition Temperature:	Not applicable.
Decomposition Temperature:	>320 °F (160 °C)
Percent Volatiles by Volume:	100
Molecular Weight:	NO_2 = 46.0055, N_2O_4 = 92.0011
Molecular Formula:	NO_2 & N_2O_4 in equilibrium

10. Stability and Reactivity

Chemical Stability: ☐ Unstable ☒ Stable

Conditions to Avoid: None known.

Incompatible Materials: Water, bases, flammable and combustible materials, copper, aluminum. Very corrosive to metals when wet. Explosions may occur on contact with ammonia, boron trichloride, carbon disulfide, cyclohexane, fluorine, formaldehyde, nitrobenzene, toluene, incompletely halogenated hydrocarbons, propylene, alcohols, and ozone.

Hazardous Decomposition Products: Above 320 °F (160 °C), nitrogen dioxide decomposes to form nitric oxide and oxygen. Nitrogen dioxide reacts with water to form nitric acid and nitric oxide.

Possibility of Hazardous Reactions: ☒ May Occur ☐ Will Not Occur

Explosions may occur on contact with ammonia, boron trichloride, carbon disulfide, cyclohexane, fluorine, formaldehyde, nitrobenzene, toluene, incompletely halogenated hydrocarbons, propylene, alcohols, and ozone. Nitrogen dioxide reacts with water to form nitric acid and nitric oxide.

11. Toxicological Information

Acute Dose Effects: LC50, 1 hr, rat = 115 ppm
Study Results: Nitrogen dioxide has been shown to cause mutations in bacteria and to cause mutations, sister-chromatid exchanges, and chromasomal aberrations in mammalian cells.

12. Ecological Information

Ecotoxicity: No known effects.
Other Adverse Effects: Nitrogen dioxide does not contain any Class I or Class II ozonedepleting chemicals.

13. Disposal Considerations

Waste Disposal Method: Do not attempt to dispose of residual or unused quantities. Return cylinder to supplier.

14. Transport Information

DOT/IMO Shipping Name: Dinitrogen tetroxide

Hazard Class: 2.3	Packing Group/Zone: NA*/A	Identification number: UN1067	Product RQ: 10 lb (4.54 kg)

SHIPPING LABEL(s): POISON GAS, OXIDIZER, CORROSIVE**
PLACARD (when required): POISON GAS, OXIDIZER, CORROSIVE**
*NA = Not available
**The words in the POISON GAS diamond are INHALATION HAZARD
Special Shipping Information: Cylinders should be transported in a secure posi tion, in a well-ventilated vehicle. Cylinders transported in an enclosed, nonventilated compartment of a vehicle can present serious safety hazards
Additional Marking Requirement: Inhalation Hazard
Shipment of compressed gas cylinders that have been filled without the owner's consent is a violation of federal law [49 CFR 173.301(b)]
Marine Pollutants: Nitrogen dioxide is not listed as a marine pollutant by DOT

15. Regulatory Information

The following selected regulatory requirements may apply to this product. Not all such requirements are identified. Users of this product are solely responsible for compliance with all applicable federal, state, and local regulations.

U.S. FEDERAL REGULATIONS:
EPA (ENVIRONMENTAL PROTECTION AGENCY)
CERCLA: COMPREHENSIVE ENVIRONMENTAL RESPONSE, COMPENSATION, AND LIABILITY ACT OF 1980 (40 CFR Parts 117 and 302):
Reportable Quantity (RQ): 10 lb (4.54 kg)
SARA: SUPERFUND AMENDMENT AND REAUTHORIZATION ACT:
SECTIONS 302/304: Require emergency planning based on Threshold Planning Quantity (TPQ) and release reporting based on Reportable Quantities (RQ) of Extremely Hazardous Substances (EHS) (40 CFR Part 355):
TPQ: 100 lb (45.4 kg)
EHS RQ (40 C R 355): 10 lb (4.54 kg)
SECTIONS 311/312: Require submission of MSDSs and reporting of chemical inventories with identification of EPA hazard categories. The hazard categories for this product are as follows:

IMMEDIATE: Yes	PRESSURE: No
DELAYED: Yes	REACTIVITY: No
	FIRE: Yes

SECTION 313: Requires submission of annual reports of release of toxic chemicals that appear in 40 CFR Part 372.
Nitrogen dioxide is not subject to reporting under Section 313.

40 CFR 68: Risk Management Program for Chemical Accidental Release Prevention: Requires development and implementation of risk management programs at facilities that manufacture, use, store, or otherwise handle regulated substances in quantities that exceed specified thresholds.

Nitrogen dioxide is not listed as a regulated substance.

TSCA: Toxic Substances Control Act: Nitrogen dioxide is listed on the TSCA inventory.

OSHA: Occupational Safety and Health Administration:

29 CFR 1910.119: Process Safety Management of Highly Hazardous Chemicals: Requires facilities to develop a process safety management program based on Threshold Quantities (TQ) of highly hazardous chemicals.

Nitrogen dioxide is listed in Appendix A as a highly hazardous chemical in quantities of 250 lb (113.5 kg) or greater.

State Regulations:

California: Nitrogen dioxide is not listed by California under the SAFE DRINKING

Water and Toxic Enforcement Act of 1986 (Proposition 65).

Pennsylvania: Nitrogen dioxide is subject to the Pennsylvania Worker and Community Right-to-Know act (35 P.S. Sections 7301–7320).

16. Other Information

Be sure to read and understand all labels and instructions supplied with all containers of this product.

Other Hazardous Conditions of Handling, Storage, and Use: **Poisonous, corrosive, oxidizing liquid and gas under pressure. Store and use with adequate ventilation at all times**. Use only in a closed system constructed only of corrosion-resistant materials. Use with equipment cleaned for oxygen service. Use piping and equipment adequately designed to withstand pressures to be encountered. **Prevent reverse flow**. Reverse flow into cylinder may cause rupture. Use a check valve or other protective device in any line or piping from the cylinder. **Never work on a pressurized system**. If there is a leak, close the cylinder valve. Blow the system down in an environmentally safe manner in compliance with all federal, state, and local laws; then repair the leak. **When returning cylinder to supplier**, be sure valve is closed; then install valve outlet cap or plug leak-tight. **Never place a compressed gas cylinder where it may become part of an electrical circuit**.

Note: Prior to using any plastics, confirm their compatibility with nitrogen dioxide.

Mixtures. When you mix two or more gases or liquefied gases, you can create additional, unexpected hazards. Obtain and evaluate the safety information for each component before you produce the mixture. Consult an industrial hygienist or other trained person when you evaluate the end product. Remember, gases and liquids have properties that can cause serious injury or death.

Recommended Equipment: In semiconductor process gas and other suitable applications, Praxair recommends the use of engineering controls such as gas cabinet enclosures, automatic gas panels (used to purge systems on cylinder changeout), excess-flow valves throughout the gas distribution system, double containment for the distribution system, and continuous gas monitors.

Hazard rating systems	
NFPA ratings:	HMIS ratings:
Health = 3	Health = 3
Flammability = 0	Flammability = 0
Instability = 0	Physical hazard = 1
Special = OX	

Standard Valve Connections for U.S. and Canada:

Threaded:	CGA-660
Pin-Indexed Yoke:	Not applicable.
Ultra-High-Integrity Connection:	Not applicable

Use the proper CGA connections. Do Not Use Adapters. Additional limited-standard connections may apply. See CGA pamphlet V-1 listed below.

Ask your supplier about free Praxair safety literature as referred to in this MSDS and on the label for this product. Further information can be found in the following materials published by the Compressed Gas Association, Inc. (CGA), 4221 Walney Road, 5th Floor, Chantilly, VA 20151-2923, Telephone (703) 788–2700, http://www.cganet.com/Publication.asp.

AV-1	Safe Handling and Storage of Compressed Gases
P-1	Safe Handling of Compressed Gases in Containers
P-39	Oxygen-Rich Atmospheres
SB-2	Oxygen-Deficient Atmospheres
V-1	Compressed Gas Cylinder Valve Inlet and Outlet Connections
—	Handbook of Compressed Gases, Fourth Edition

Praxair asks users of this product to study this MSDS and become aware of product hazards and safety information. To promote safe use of this product, a user should (1) notify employees, agents, and contractors of the information in this MSDS and of any other known product hazards and safety information, (2) furnish this information to each purchaser of the product, and (3) ask each purchaser to notify its employees and customers of the product hazards and safety information.

The opinions expressed herein are those of qualified experts within Praxair, Inc. We believe that the information contained herein is current as of the date of this Material Safety Data Sheet. Since the use of this information and the conditions of use of the product are not within the control of Praxair, Inc., it is the user's obligation to determine the conditions of safe use of the product.

Praxair MSDSs are furnished on sale or delivery by Praxair or the independent distributors and suppliers who package and sell our products. To obtain current MSDSs for these products, contact your Praxair sales representative or local distributor or supplier, or download from www.praxair.com. If you have questions regarding Praxair MSDSs, would like the form number and date of the latest MSDS, or would like the names of the Praxair suppliers in your area, phone or write the Praxair Call Center (Phone: 1- 800-PRAXAIR; Address: Praxair Call Center, Praxair, Inc., PO Box 44, Tonawanda, NY 14151-0044).

Praxair and the Flowing Airstream design are trademarks or registered trademarks of Praxair Technology, Inc. in the United States and/or other countries.

Praxair, Inc.
39 Old Ridgebury Road, Danbury, CT 06810-5113

MSD 6.6. Hexanitrostilbene (HNS)

Central Pollution Control Board

Ministry of Environment & Forests, Govt of India, Parivesh Bhawan, East Arjun Nagar, Delhi - 110032

307 **Hexanitrostilbene 2,2,4,4,6,6**

1. CHEMICAL IDENTITY

Chemical Name : Hexanitrostilbene 2,2,4,4,6,6
Chemical Classification: Explosive **Trade Name :**
Synonyms: 2,2',4,4',6,6'-Hexanitrostilbene, Benzene,1,1'-(1,2-ethenediyl)bis[2,4,6 trinitro, HNS; 1,2-bis(2,4,6-trinitrophenyl) ethylene

Formula : C14H6N6O12 **CAS No:** 20062-22-0 **UN No:** 0392

Regulated Identification

Shipping Name : Hexanitrostilbene	**Hazchem Code :**
Codes / Label : Class 1.1D, Explosive	**Hazardous Waste ID No : 5**

Explosive
1. CHEMICAL IDENTITY
Chemical Classification: Trade Name :

	HAZARDOUS INGREDIENTS	C.A.S. No.		HAZARDOUS INGREDIENTS	C.A.S. No.
1	Hexanitrostilbene 2,2,4,4,6,6	20062-22-0	3		
2			4		

2. PHYSICAL / CHEMICAL DATA

Boiling Pt. °C:		**Physical State:**	Solid	**Appearance:**	Forms yellow crystals.
Melting Pt °C:	316	**Vapour Pressure @ 35°C mmHg:**		Odour:	
Vapour Density(Air =1):		**Solubility in water at 30°C g/100ml:**	Insoluble	**Others:**	

Specific Gravity (Water =1): 1.74 g/cm3 **pH :**

3. FIRE / EXPLOSION HAZARD DATA

Flammability :	**LEL:**	**Flash Point °C in OC:**
TDG Flammability:	**UEL:**	**Flash Point °C in CC:**

Autoignition Temperature °C : 331
Explosion sensitivity to impact:
Explosion sensitivity to static Electricity:
Hazardous Combustion Products :
Hazardous Polymerization :

Combustible Liquid:	**Explosive Material:** Yes	**Corrosive Material**
Flammable Material:	**Oxidiser :**	**Others:**
Pyrophoric Material:	**Organic Peroxide :**	

4. REACTIVITY DATA

Chemical Stability :	
Incompatibility with : other material	
Reactivity :	If mixed with reducing agents, including hydrides, sulfides and n trides, may begin a vigorous reaction that culminates in a detonation.
Hazardous : Reaction Products	

5. HEALTH HAZARD DATA

Routes of entry: Inhalation, Ingestion, Skin and Eyes
Effects of Exposure / Symptoms:
Inhalation may cause nervous system irregularities including headaches and dizziness.
Emergency Treatment:

Inhalation:	If symptoms develop, move individual away from exposure and into fresh air. If symptoms persist, seek medical attention. If breathing is difficult, administer oxygen. Keep person warm and quiet; seek immediate medical attention.
Skin:	Remove contaminated clothing. Wash exposed area with soap and water. If symptoms persist, seek medical attention. Launder clothing before reuse.
Eyes:	If symptoms develop, immediately move individual away from exposure and into fresh air. Flush eyes gently with water for at least 15 minutes while holding eyelids apart; seek immediate medical attention.
Ingestion:	Seek medical attention. If individual is drowsy or unconscious, do not give anything by mouth; place individual on the left side with the head down. Contact a physician

LD50 (oral-rat) mg/kg:	**STEL:**
LC50 (rat) mg/kg:	**Odour Threshold:**
Permissible Exposure Limit:	**TLV (ACGIH) :**

NFPA Hazard Signals	**Health**	**Flammability**	**Reactivity**	**Special**
		1	3	

6. PREVENTIVE MEASURES

Personal Protective : Equipment	Chemical splash goggles in compliance with OSHA regulations are advised; however, OSHA regulations also permit other type safety glasses. Whre chemical resistant gloves. To prevent repeated or prolonged skin contact, wear impervious clothing and boots.

Handling : All chemicals should be considered hazardous. Avoid direct physica contact. Use appropriate, approved safety equipment. Untrained individuals should not handle this chemical or its container. Handling should occur in a chemical fume hood.

Storage : Keep in a cool, dry, dark location in a tightly sealed container or cylinder. Keep away from incompatible materials, ignition sources and untrained individuals. Secure and label area. Protect containers/cylinders from physical damage.

Precautions :

---

7. EMERGENCY / FIRST AID MEASURES

FIRE:
Fire Extinguishing Media :
Special Procedure :
Unusual Hazards :

EXPOSURE: First Aid Measures:

Inhalation: If symptoms develop, move individual away from exposure and into fresh air. If symptoms persist, seek medical attention. If breathing is difficult, administer oxygen. Keep person warm and quiet; seek immediate medical attention.

Skin: Remove contaminated clothing. Wash exposed area with soap and water. If symptoms persist, seek medical attention. Launder clothing before reuse.

Eyes: If symptoms develop, immediately move individual away from exposure and into fresh air. Flush eyes gently with water for at least 15 minutes while holding eyelids apart; seek immediate medical attention.

Ingestion: Seek medical attention. If individual is drowsy or unconscious, do not give anything by mouth; place individual on the left side with the head down. Contact a physician

Antidotes / Dosages:

SPILLS :

Steps To Be Taken Keep sparks, flames, and other sources of ignition away. Keep material wet. Wet spilled material before picking it up. Do not attempt to sweep up dry material.

Waste Disposal Method:

8. ADDITIONAL INFORMATION / REFERENCES

9. MANUFACTURERS / SUPPLIERS DATA

NAME OF FIRM :
MAILING ADDRESS :
TELEPHONE / TELEX NOS :
TELEGRAPHIC ADDRESS:

Contact person in Emergency :
Local Bodies involved :
Standard Packing :

OTHERS : **Trem Card Details / Ref :**

10. DISCLAIMER

Information contained in this material data sheet is believed to be reliable but no representation, guarantee or warranties of any kind are made as to its accuracy, suitability for a particular application or results to be obtained from them. It is up to the manufacturer/ seller to ensure that the information contained in the material safety data sheet is relevant to the product manufactured / handled or sold by him as the case may be. The Government makes no warranties expressed or implied in the respect of the adequacy of this document for any particular purpose.

End of document

MSD 6.6. Hexanitrostilbene (HNS)

HEXANITROSTILBENE (HNS)

Leading worldwide specialist in the field of high explosives, EURENCO offers its customers a complete range of high explosives and compositions like HNS, owing to high-tech manufacturing capabilities.

PRODUCT

- Chemical names: HNS, 1,1'-(1,2-ethenediyl)bis(2,4,6-trinitrobenzene)
- CAS number: 20062-22-0
- Chemical formula: $C_{14}H_6N_6O_{12}$
- Melting point: 316 – 318 °C
- Heat of combustion: -6 434.2 ± 5.0 kJ/mol solid phase
- Density: 1.74 g/cm^3
- Detonation velocity: 7 000 to 7 100 m/s
- Volume of detonation gases: 700 l/kg
- Impact sensitivity: 5 J
- Friction sensitivity: 240 N

EURENCO manufactures all different types of HNS from type I to type IV:

- HNS Type I for initiation (WS 5003F specification): more stable than stipulated in the MIL-specification thanks to a special purification process.
- HNS Type II for oil and gas drilling: A special quality of HNS, coated with a high temperature resistant polymer, is produced according to WS 5003F specification.
- HNS Type III for nucleation of TNT: produced under German and US specifications.
- HNS type IV for slapper detonators: characterized by a high sensitivity and thereby good reliability in initiation systems, this quality is significantly more thermally stable than stipulated in the military specifications.

USES

Owing to its stability at high temperature and its excellent performance, HNS has several applications in the aerospace, ammunition and oil and gas industries when thermal and/or vacuum stability are required:

Space and military pyrotechnics
HNS is used in cap relays, detonating cords, transmission cords and booster charges for I.M. applications by bringing heat resistance, low sensibility and high performance.

Artillery ammunition filling
HNS is used as anti-crack additive in TNT or TNT-RDX charges; it improves the fine crystalline structure of the composition and prevents from crack formation.

Oil and gas drilling
Thanks to its excellent thermal stability, HNS is used in perforating and cutting charges for oil and gas industry when the requirement of high temperature resistance is important. This HNS is extra purified and produced in special formulations leading to an increased thermal resistance and good handling characteristics, which are critical for this type of high mass production rate.

Slapper detonators
Owing to its high sensitivity and good reliability characteristics, this HNS is used as initiation explosive in slapper detonators (the surface area is above 10 m²/g). A purification process makes it significantly more thermally stable than stipulated in military specifications.

EURENCO
Explosive Charges & Additives Business Unit
12 quai Henri IV - 75004 Paris – France
Tel.: +33 (0) 1 49 96 74 00 - Fax: +33 (0) 1 49 96 74 03
E-mail: eca.bu@eurenco.com - www.eurenco.com

EURENCO
GROUPE SNPE

MSD 6.7. N-Methy-4-nitroaniline (MNA)

SIGMA-ALDRICH *sigma-aldrich.com*

SAFETY DATA SHEET
Version 3.8
Revision Date 07/01/2014
Print Date 11/07/2014

1. PRODUCT AND COMPANY IDENTIFICATION

1.1 Product identifiers

Product name :	Epoxy embedding medium, hardener MNA
Product Number :	45347
Brand :	Fluka
CAS-No. :	25134-21-8

1.2 Relevant identified uses of the substance or mixture and uses advised against

Identified uses : Laboratory chemicals, Manufacture of substances

1.3 Details of the supplier of the safety data sheet

Company : Sigma-Aldrich
3050 Spruce Street
SAINT LOUIS MO 63103
USA
Telephone : +1 800-325-5832
Fax : +1 800-325-5052

1.4 Emergency telephone number

Emergency Phone # : (314) 776-6555

---

2. HAZARDS IDENTIFICATION

2.1 Classification of the substance or mixture

GHS Classification in accordance with 29 CFR 1910 (OSHA HCS)

Acute toxicity, Oral (Category 4), H302
Skin corrosion (Category 1C), H314
Serious eye damage (Category 1), H318
Respiratory sensitisation (Category 1), H334
Skin sensitisation (Category 1), H317

For the full text of the H-Statements mentioned in this Section, see Section 16.

2.2 GHS Label elements, including precautionary statements

Pictogram

Signal word Danger

Hazard statement(s)

H302	Harmful if swallowed.
H314	Causes severe skin burns and eye damage.
H317	May cause an allergic skin reaction.
H334	May cause allergy or asthma symptoms or breathing difficulties if inhaled.

Precautionary statement(s)

P261	Avoid breathing dust/ fume/ gas/ mist/ vapours/ spray.
P264	Wash skin thoroughly after handling.
P270	Do not eat, drink or smoke when using this product.
P272	Contaminated work clothing should not be allowed out of the workplace.
P280	Wear protective gloves/ protective clothing/ eye protection/ face
P301 + P312	IF SWALLOWED: Call a POISON CENTER or doctor/ physician if you feel unwell.
P301 + P330 + P331	IF SWALLOWED: rinse mouth. Do NOT induce vomiting.
P303 + P361 + P353	IF ON SKIN (or hair): Remove/ Take off immediately all contaminated clothing. Rinse skin with water/ shower.
P304 + P340	IF INHALED: Remove victim to fresh air and keep at rest in a position comfortable for breathing.
P305 + P351 + P338	IF IN EYES: Rinse cautiously with water for several minutes. Remove contact lenses, if present and easy to do. Continue rinsing.
P310	Immediately call a POISON CENTER or doctor/ physician.
P321	Specific treatment (see supplemental first aid instructions on this label).
P333 + P313	If skin irritation or rash occurs: Get medical advice/ attention.
P363	Wash contaminated clothing before reuse.
P405	Store locked up.
P501	Dispose of contents/ container to an approved waste disposal plant.

2.3 Hazards not otherwise classified (HNOC) or not covered by GHS – none

---

3. COMPOSITION/INFORMATION ON INGREDIENTS

3.1 Substances

Synonyms : Methyl nadic anhydride
Methyl-5-norbornene-2,3-dicarboxylic anhydride
Epon® MNA substitute
Methylnorbornene-2,3-dicarboxylic acid anhydride
MNA

Formula :	C10H10O3
Molecular Weight :	178.18 g/mol
CAS-No. :	25134-21-8
EC-No. :	246-644-8

Hazards Components

Component	Classification	Concentration
Methyl-5-norbornene-2,3-dicarboxylicanhydride		
	Acute Tox. 4; Skin Corr. 1C; Eye Dam. 1; Resp. Sens. 1; Skin Sens. 1; H302, H314, H317, H334	-

For the full text of the H-Statements mentioned in this Section, see Section 16

.

4. FIRST AID MEASURES

4.1 Description of first aid measures

General advice

Move out of dangerous area.Consult a physician. Show this safety data sheet to the doctor in attendance.

If inhaled

If breathed in, move person into fresh air. If not breathing, give artificial resp ration. Consult a physician.

In case of skin contact

Take off contaminated clothing and shoes immediately. Wash off with soap and plenty of water. Consult a physician.

In case of eye contact

Rinse thoroughly with plenty of water for at least 15 minutes and consult a phys cian.Continue rinsing eyes during transport to hospital.

If swallowed

Do NOT induce vomiting. Never give anything by mouth to an unconscious person. Rinse mouth with water. Consult a physician.

4.2 Most important symptoms and effects, both acute and delayed

The most important known symptoms and effects are described in the labelling (see section 2.2) and/or in section 11

4.3 Indication of any immediate medical attention and special treatmenneeded

no data available

---

5. FIREFIGHTING MEASURES

5.1 Extinguishing media

Suitable extinguishing media

Use water spray, alcohol-resistant foam, dry chemical or carbon dioxide.

5.2 Special hazards arising from the substance or mixture

Carbon oxides

5.3 Advice for firefighters

Wear self contained breathing apparatus for fire fighting if necessary.

5.4 Further information

no data available

---

6. ACCIDENTAL RELEASE MEASURES

6.1 Personal precautions, protective equipment and emergency procedures

Use personal protective equipment. Avoid breathing vapours, mist or gas. En sure adequate ventilation. Evacuate personnel to safe areas.
For personal protection see section 8.

6.2 Environmental precautions

Do not let product enter drains.

6.3 Methods and materials for containment and cleaning up

Soak up with inert absorbent material and dispose of as hazardous waste. Keep in suitable, closed containers for disposal.

6.4 Reference to other sections

For disposal see section 13.

---

7. HANDLING AND STORAGE

7.1 Precautions for safe handling

Avoid contact with skin and eyes. Avoid inhalation of vapour or mist.
For precautions see section 2.2.

7.2 Conditions for safe storage, including any incompatibilities

Keep container tightly closed in a dry and well-ventilated place. Containers which are opened must be carefully resealed and kept upright to prevent leakage.

7.3 Specific end use(s)

Apart from the uses mentioned in section 1.2 no other specific uses are stipulated

---

8. EXPOSURE CONTROLS/PERSONAL PROTECTION

8.1 Control parameters

Components with workplace control parameters

Contains no substances with occupational exposure limit values.

8.2 Exposure controls

Appropriate engineering controls

Handle in accordance with good industrial hygiene and safety practice. Wash hands before breaks and at the end of workday.

Personal protective equipment

Eye/face protection

Tightly fitting safety goggles. Faceshield (8-inch minimum). Use equipment for eye protection tested and approved under appropriate government standards such as NIOSH (US) or EN 166(EU).

Skin protection

Handle with gloves. Gloves must be inspected prior to use. Use proper glove removal technique (without touching glove's outer surface) to avoid skin contact with this product. Dispose of contaminated gloves after use in accordance with applicable laws and good laboratory practices. Wash and dry hands.

Full contact
Material: Nitrile rubber
Minimum layer thickness: 0.4 mm
Break through time: 480 min
Material tested:Camatril® (KCL 730 / Aldrich Z677442, Size M)

Splash contact
Material: Nitrile rubber
Minimum layer thickness: 0.11 mm
Break through time: 30 min
Material tested:Dermatril® (KCL 740 / Aldrich Z677272, Size M)

data source: KCL GmbH, D-36124 Eichenzell, phone +49 (0)6659 87300, e-mail sales@kcl.de, test method:
EN374
If used in solution, or mixed with other substances, and under conditions which differ from EN 374, contact the supplier of the CE approved gloves. This recommendation is advisory only and must be evaluated by an industrial hygienist and safety officer familiar with the specific situation of anticipated use by our customers. It should not be construed as offering an approval for any specific use scenario.

Body Protection
Complete suit protecting against chemicals, The type of protective equipment must be selected according to the concentration and amount of the dangerous substance at the specific workplace.

Respiratory protection
Where risk assessment shows air-purifying respirators are appropriate use a full-face respirator with multipurpose combination (US) or type ABEK (EN 14387) respirator cartridges as a backup to engineering controls. If the respirator is the sole means of protection, use a full-face supplied air respirator. Use respirators and components tested and approved under appropriate government standards such as NIOSH (US) or CEN (EU).

Control of environmental exposure
Do not let product enter drains.

---

9. PHYSICAL AND CHEMICAL PROPERTIES

9.1 Information on basic physical and chemical properties

a)	Appearance	Form: viscous liquid
	Colour: light yellow	
b)	Odour	no data available
c)	Odour Threshold	no data available
d)	pH	no data available
e)	Melting point/freezing point	no data available
f)	Initial boiling point and boiling range	no data available

g)	Flash point	135 °C (275 °F)
h)	Evapouration rate	no data available
i)	Flammability (solid, gas)	no data available
j)	Upper/lower flammability or explosive limits	no data available
k)	Vapour pressure	no data available
l)	Vapour density	no data available
m)	Relative density	1.232 g/mL at 25 °C (77 °F)
n)	Water solubility	no data available
o)	Partition coefficient: o-noctanol/water	no data available
p)	Auto-ignition temperature	no data available
q)	Decomposition Temperature	no data available
r)	Viscosity	no data available
s)	Explosive properties	no data available
t)	Oxidizing properties	no data available

9.2 Other safety information

no data available

10. STABILITY AND REACTIVITY

10.1 Reactivity

no data available

10.2 Chemical stability

Stable under recommended storage conditions.

10.3 Possibility of hazardous reactions

no data available

10.4 Conditions to avoid

no data available

10.5 Incompatible materials

no data available

10.6 Hazardous decomposition products

Other decomposition products - no data available
In the event of fire: see section 5

---

11. TOXICOLOGICAL INFORMATION

11.1 Information on toxicological effects

Acute toxicity

LD50 Oral - rat - 914 mg/kg
Remarks: Behavioral:Somnolence (general depressed activity). Kidney, Ureter, Bladder:Hematuria. Nutritional and

Gross Metabolic:Weight loss or decreased weight gain.

Inhalation: no data available

LD50 Dermal - rat - 4,290 mg/kg
Remarks: Behavioral:Somnolence (general depressed activity). Lungs, Thorax, or Respiration:Other changes.

no data available

Skin corrosion/irritation
no data available

Serious eye damage/eye irritation
no data available

Respiratory or skin sensitisation
Prolonged or repeated exposure may cause allergic reactions in certain sensitive individuals.

Germ cell mutagenicity
no data available

Carcinogenicity

IARC: No component of this product present at levels greater than or equal to 0.1% is identified as probable, possible or confirmed human carcinogen by IARC.
ACGIH: No component of this product present at levels greater than or equal to 0.1% is identified as a carcinogen or potential carcinogen by ACGIH.
NTP: No component of this product present at levels greater than or equal to 0.1% is identified as a known or anticipated carcinogen by NTP.
OSHA: No component of this product present at levels greater than or equal to 0.1% is identified as a carcinogen or potential carcinogen by OSHA.

Reproductive toxicity
no data available

no data available

Specific target organ toxicity - single exposure
no data available

Specific target organ toxicity - repeated exposure
no data available

Aspiration hazard
no data available

Additional Information
RTECS: RB9100000

To the best of our knowledge, the chemical, physical, and toxicological proper ties have not been thoroughly investigated.

---

12. ECOLOGICAL INFORMATION

12.1 Toxicity

no data available

12.2 Persistence and degradability

no data available

12.3 Bioaccumulative potential

no data available

12.4 Mobility in soil

no data available

12.5 Results of PBT and vPvB assessment

PBT/vPvB assessment not available as chemical safety assessment not r quired/not conducted

12.6 Other adverse effects

no data available

13. DISPOSAL CONSIDERATIONS

13.1 Waste treatment methods

Product

Offer surplus and non-recyclable solutions to a licensed disposal company. Contact a censed professional waste disposal service to dispose of this material. Dissolve or mix the material with a combustible solvent and burn in a chemical incinerator equipped with an afterburner and scrubber.

Contaminated packaging

Dispose of as unused product.

14. TRANSPORT INFORMATION

DOT (US)

UN number: 3265 Class: 8 Packing group: III

Proper shipping name: Corrosive liquid, acidic, organic, n.o.s. (Methyl-5-norbornene-2,3-dicarboxylicanhydride) Reportable Quantity (RQ):

Marine pollutant: No

Poison Inhalation Hazard: No

IMDG

UN number: 3265 Class: 8 Packing group: III EMS-No: F-A, S-B

Proper shipping name: CORROSIVE LIQUID, ACIDIC, ORGANIC, N.O.S. (Methyl-5-norbornene-2,3-dicarboxylicanhydride)

Marine pollutant: No

IATA

UN number: 3265 Class: 8 Packing group: III

Proper shipping name: Corrosive liquid, acidic, organic, n.o.s. (Methyl-5-norbornene-2,3-dicarboxylicanhydride)

15. REGULATORY INFORMATION

SARA 302 Components

SARA 302: No chemicals in this material are subject to the reporting requirements of SARA Title III, Section 302.

SARA 313 Components

SARA 313: This material does not contain any chemical components with known CAS numbers that exceed the threshold (De Minimis) reporting levels established by SARA Title III, Section 313.

SARA 311/312 Hazards

Acute Health Hazard

Massachusetts Right To Know Components

No components are subject to the Massachusetts Right to Know Act.

Pennsylvania Right To Know Components

	CAS-No.	Revision Date
Methyl-5-norbornene-2,3-Dicarboxylicanhydride	25134-21-8	1989-12-01

New Jersey Right To Know Components

	CAS-No.	Revision Date
Methyl-5-norbornene-2,3-dicarboxylicanhydride	25134-21-8	1989-12-01

California Prop. 65 Components

This product does not contain any chemicals known to State of California to cause cancer, birth defects, or any other reproductive harm.

---

16. OTHER INFORMATION

Full text of H-Statements referred to under sections 2 and 3.

Acute Tox.	Acute toxicity
Eye Dam.	Serious eye damage
H302	Harmful if swallowed.
H314	Causes severe skin burns and eye damage.
H317	May cause an allergic skin reaction.
H318	Causes serious eye damage.
	H334 May cause allergy or asthma symptoms or breathing difficulties if inhaled.
Resp. Sens.	Respiratory sensitisation
Skin Corr.	Skin corrosion

HMIS Rating

Health hazard:	3
Chronic Health Hazard:	*
Flammability:	1
Physical Hazard	0

NFPA Rating

Health hazard:	3
Fire Hazard:	1
Reactivity Hazard:	0

Further information

Preparation Information

Product Safety ó Americas Region
1-800-521-8956

Version: 3.8 Revision Date: 07/01/2014 Print Date: 12/01/2014

MSD 6.8. 1-azido-2-nitro-2-azapropane (ANAP)

ARTEC CHEMICAL CO., LTD

Material Safety Data Sheet

1. IDENTIFICATION OF THE SUBSTANCE AND THE COMPANY INFORMATION

Product Name:	ANAP
Supplier:	Artec Chemical Co., Ltd. 1401-03, Crocodile House 2, 55 Connaught Rd. Central, Hong Kong
Emergency Phone No.:	852-25432233 / 25422082 Fax: 852-25431883 / 25451036

2. COMPOSITION / INFORMATION ON INGREDIENTS

INCI Name:	1-NAPHTHOL
CAS No.:	90-15-3
ENIECS No.:	201-969-4
C.I. NO.:	76605
Molecular Formula:	C10H8O

3. HAZARD IDENTIFICATION

Most Important Hazards:

DANGER! May cause respiratory tract irritation. Harmful if absorbed through the skin. Corrosive. Light sensitive. Air sensitive. May be harmful if swallowed. Cause digestive tract irritation. Cause eye and skin burns. May cause liver and kidney damage. May cause reproductive and fetal effects. May cause blood abnormalities.

Potential Health Effects:

Eye: Cause eye burns. May cause eye injury.
Skin: Harmful is absorbed through the skin. Cause skin burns.
Inhalation: May cause severe irritation of the upper respiratory tract with pain, burns and inflammation. May cause effects similar to those described for ingestion.
Ingestion: May be harmful if swallowed. Overexposure may result in hemolytic anemia, leading to kidney failure. Symptoms include diarrhea, headache, perspiration, listlessness and confusion

4. First Aid Measures

Eye Contact: Rinse immediately with plenty of water for at least 15 min. Get medical aid immediately. Do not allow victim to rub or keep eyes closed
Skin Contact: Get medical aid immediately. Flush skin with soap and water for at least 15 min. Discard contaminated clothing.
Skin Contact: Get medical aid immediately. Flush skin with soap and water for at least 15 min. Discard contaminated clothing.
Ingestion: Move to fresh air, get medical help immediately. If breathing is difficult, give oxygen.
Inhalation: Do not induce vomiting. Do not give anything by mouth to an unconscious person. Get immediate medical attention

5. Fire Fighting Measures

Extinguishing Media:
Carbon dioxide, dry chemical, chemical foam or water spray recommended.
Special Equipment for Firefighters:
Self-contained breathing apparatus and full protective gear recommended.

6. Accidental Release Measures

Personal Precautions:
Wear self-contained breathing apparatus, appropriate protective gloves and clothing.
Methods for Cleaning Up:
Take up mechanically and collect in suitable container for disposal. Ventilate area and wash off with plenty of water.
Environmental Precautions:
Do not flush into surface water or sanitary sewer system.

7. Handling and Storage

Handling:
Avoid contact with skin and eyes, wear personal protective equipment. Avoid ingestion and inhalation. Use with adequate ventilation.
Storage:
Keep container tightly closed in a dry and well-ventilated place. Keep away from heat.

8. Exposure Controls/Personal Protection

Engineering Control:
Ensure adequate local ventilation to control airborne level.
Personal Protection:
NIOSH approved dust respirators are recommended when handling in areas of organic chemical dusting. Safety glasses are also recommended. Impervious clothing should be worn when gross contact is likely, such as cleaning up spills of large amounts.

9. Physical and Chemical Properties

Appearance:	Off-white flakes
Melting Point:	95–96 °C
Boiling Point:	278–280 °C @760.00 mm Hg
Molecular Weight:	144.2

10. Stability and Reactivity

Stability:
Stable under normal temperatures and pressures. Substance undergoes color change upon exposure to light and air.
Hazardous Decomposition Products:
Carbon monoxide, carbon dioxide, acid smoke and fumes.
Incompatibilities:
Strong oxidizing agents, strong bases, acid chlorides, acid anhydrides, halogens.

11. Toxicological Information

Carcinogenicity:
Mutation has been observed in cases where 1-naphthol was administered to microorganisms and E. Coli and Bacillus subtilis bacteria.

12. Ecological Information

No data available.

13. Disposal Consideration

Waste from Residue/Unused Products:
Dispose of as special waste in compliance with local and national regulations.
Contaminated Packaging:
Triple rinse containers. Dispose of as special waste in compliance with local and national regulations.

14. Transport Regulations

UN- number:	2811
ADR/RID:	
Shipping Name:	Toxic Solid, Organic, N.O.S.
Class:	6.1
Packing Group:	III
IMO:	
Shipping Name:	Toxic Solid, Organic, N.O.S.
Class:	6.1
Packing Group:	III
ICAO:	
Shipping Name:	Toxic Solid, Organic, N.O.S.
Class:	6.1
Packing Group:	III

15. Regulatory Information

Classification according to European directive on classification of hazardous preparations 90/492/EEC	
Hazard Symbol (s):	Xn—Harmful
Risk Phrase(s):	R21/22- Harmful in contact with skin and if swal lowed
	R37/38- Irritating to respiratory system and skin
	R41- Risks of serious damage to eyes

(continued)

(continued)

Classification according to European directive on classification of hazardous preparations 90/492/EEC	
Safety Phrase (s):	S22- Do not inhale dust
	S26- In case of contact with eyes, rinse immediately with plenty of water and seek medical advice
	S37/39- Wear suitable gloves and eye/face protection
Water Hazard Class:	Class 1 (German Regulation): slightly hazardous for water

16. Other Information

The information provided in this material safety data sheet is correct to the best of our knowledge. No warranty is expressed or implied regarding the accuracy of these data or the results to be obtained from the use thereof. Artec Chemical Co., Ltd. assumed no responsibility for any personal injury or property damage caused by the materials. Users assume all risks associated with the use of the materials.

MSD 6.9. 1,3,5-Triamino-2,4,6-trinitrobenzene (TATB)

SIGMA-ALDRICH

sigma-aldrich.com
SAFETY DATA SHEET
Version 5.10
Revision Date 11/04/2014
Print Date 11/07/2014

---

1. PRODUCT AND COMPANY IDENTIFICATION

1.1 Product identifiers

Product name :	4,4′,4″-*s*-Triazine-2,4,6-triyl-tribenzoic acid
Product Number :	741175
Brand :	Aldrich
CAS-No. :	61414-16-2

1.2 Relevant identified uses of the substance or mixture and uses advised against

Identified uses : Laboratory chemicals, Manufacture of substances

1.3 Details of the supplier of the safety data sheet

Company :	Sigma-Aldrich 3050 Spruce Street SAINT LOUIS MO 63103 USA
Telephone :	+1 800-325-5832
Fax :	+1 800-325-5052

1.4 Emergency telephone number

Emergency Phone # : (314) 776-6555

---

2. HAZARDS IDENTIFICATION

2.1 Classification of the substance or mixture

GHS Classification in accordance with 29 CFR 1910 (OSHA HCS)
Acute toxicity, Oral (Category 4), H302

Skin irritation (Category 2), H315
Eye irritation (Category 2A), H319
Reproductive toxicity (Category 1B), H360
Specific target organ toxicity—single exposure (Category 3), Respiratory system, H335
Chronic aquatic toxicity (Category 4), H413
For the full text of the H-Statements mentioned in this Section, see Section 16.

2.2 GHS Label elements, including precautionary statements

Pictogram

Signal word Danger

Hazard statement(s)

H302	Harmful if swallowed.
H315	Causes skin irritation.
H319	Causes serious eye irritation.
H335	May cause respiratory irritation.
H360	May damage fertility or the unborn child.
H413	May cause long lasting harmful effects to aquatic life

Precautionary statement(s)

P201	Obtain special instructions before use.
P202	Do not handle until all safety precautions have been read and understood.
P261	Avoid breathing dust/ fume/ gas/ mist/ vapours/ spray.
P264	Wash skin thoroughly after handling.
P270	Do not eat, drink or smoke when using this product.
P271	Use only outdoors or in a well-ventilated area.
P273	Avoid release to the environment.
P280	Wear protective gloves/ eye protection/ face protection.
P301 + P312	IF SWALLOWED: Call a POISON CENTER or doctor/ physician if you feel unwell.
P302 + P352	IF ON SKIN: Wash with plenty of soap and water.
P304 + P340	IF INHALED: Remove victim to fresh air and keep at rest in a position comfortable for breathing.
P305 + P351 + P338	IF IN EYES: Rinse cautiously with water for several minutes. Remove contact lenses, if present and easy to do. Continue rinsing.

P308 + P313	IF exposed or concerned: Get medical advice/ attention.
P321	Specific treatment (see supplemental first aid instructions on this label).
P330	Rinse mouth.
P332 + P313	If skin irritation occurs: Get medical advice/ attention.
P337 + P313	If eye irritation persists: Get medical advice/ attention.
P362	Take off contaminated clothing and wash before reuse.
P403 + P233	Store in a well-ventilated place. Keep container tightly closed.
P405	Store locked up.
P501	Dispose of contents/ container to an approved waste disposal plant

2.3 Hazards not otherwise classified (HNOC) or not covered by GHS

Rapidly absorbed through skin.

3. COMPOSITION/INFORMATION ON INGREDIENTS

3.1 Substances

Formula : C24H15N3O6
Molecular weight : 441.39 g/mol
CAS-No.: 61414-16-2

Hazardous Components

Component	Classification	Concentration
4,4′,4″-s-Triazine-2,4,6-triyl-tribenzoic acid		
	Skin Irrit. 2; Eye Irrit. 2A; STOT SE 3; Aquatic Chronic 4; H315, H319, H335, H413	<=100%
N,N-Dimethylformamide Included in the Candidate List of Substances of Very High Concern (SVHC) according to Regulation (EC) No. 1907/2006 (REACH)		
	Flam. Liq. 3; Acute Tox. 4; Eye Irrit. 2A; Repr. 1B; H226, H312 + H332, H319, H360	>=30–<50%

For the full text of the H-Statements mentioned in this Section, see Section 16

4. FIRST AID MEASURES

4.1 Description of first aid measures

General advice
Consult a physician. Show this safety data sheet to the doctor in attendance.Move out of dangerous area.

If inhaled
If breathed in, move person into fresh air. If not breathing, give artificial respiration. Consult a physician.

In case of skin contact
Wash off with soap and plenty of water. Consult a physician.

In case of eye contact
Rinse thoroughly with plenty of water for at least 15 minutes and consult a physician.
Aldrich - 741175 Page 3 of 8

If swallowed
Never give anything by mouth to an unconscious person. Rinse mouth with water. Consult a physician.

4.2 Most important symptoms and effects, both acute and delayed

The most important known symptoms and effects are described in the labelling (see section 2.2) and/or in section 11

4.3 Indication of any immediate medical attention and special treatment needed

No data available

5. FIREFIGHTING MEASURES

5.1 Extinguishing media

Suitable extinguishing media
Use water spray, alcohol-resistant foam, dry chemical or carbon dioxide.

5.2 Special hazards arising from the substance or mixture

Carbon oxides, Nitrogen oxides (NOx)

5.3 Advice for firefighters

Wear self-contained breathing apparatus for firefighting if necessary.

5.4 Further information

No data available

6. ACCIDENTAL RELEASE MEASURES

6.1 Personal precautions, protective equipment and emergency procedures

Use personal protective equipment. Avoid dust formation. Avoid breathing vapours, mist or gas. Ensure adequate
ventilation. Evacuate personnel to safe areas. Avoid breathing dust.
For personal protection see section 8.

6.2 Environmental precautions

Prevent further leakage or spillage if safe to do so. Do not let product enter drains.

6.3 Methods and materials for containment and cleaning up

Pick up and arrange disposal without creating dust. Sweep up and shovel. Keep in suitable, closed containers for
disposal.

6.4 Reference to other sections

For disposal see section 13.

7. HANDLING AND STORAGE

7.1 Precautions for safe handling

Avoid contact with skin and eyes. Avoid formation of dust and aerosols.
Provide appropriate exhaust ventilation at places where dust is formed.
For precautions see section 2.2.

7.2 Conditions for safe storage, including any incompatibilities

Keep container tightly closed in a dry and well-ventilated place.

7.3 Specific end use(s)

Apart from the uses mentioned in section 1.2 no other specific uses are stipulated

8. Exposure Controls/Personal Protection

8.1 Control parameters

Components with workplace control parameters

Component	CAS-No.	Value parameters	Control	Basis
N, N-Dimethylformamide	68-12-2	TWA	10 ppm	USA. ACGIH Threshold Limit Values (TLV)
	Remarks	Liver damage Substances for which there is a Biological Exposure Index or Indice (see BEI® section) Not classifiable as a human carcinogen Danger f cutaneous absorption		
		TWA	10 ppm, 30 mg/m^3	USA. OSHA—TABLE Z-1 Limits for Air Contaminants—1910.1000
Skin notation				
		TWA	10 ppm 30 mg/m^3	USA. Occupational Exposure Limits (OSHA)—Table Z-1 Limits for Air Contaminants
		Skin designation The value in mg/m^3 is approximate		
		TWA	10 ppm 30 mg/m^3	USA. NIOSH Recommended Exposure Limits
		Potential for dremal absorption		

Biological occupational exposure limits

Component	CAS-No.	Parameters	Value	Biological specimen	Basis
N, NDimethylformamide	68-12-2	N-Methylformamide	150,000 mg/l	In urine	ACGIH—Biological Exposure Indices (BEI)
	Remarks	End of shift (As soon as possible after exposure ceases)			
		N-Acetyl-S-(Nmethylcarbamoyl)cysteine	40.0000 mg/l	In urine	ACGIH—Biological Exposure Indices (BEI)
		Prior to last shift of workweek			

8.2 Exposure controls

Appropriate engineering controls

Handle in accordance with good industrial hygiene and safety practice. Wash hands before breaks and at the end of workday.

Personal protective equipment

Eye/face protection

Safety glasses with side-shields conforming to EN166 Use equipment for eye protection tested and approved under appropriate government standards such as NIOSH (US) or EN 166(EU).

Skin protection

Handle with gloves. Gloves must be inspected prior to use. Use proper glove removal technique (without touching glove's outer surface) to avoid skin contact with this product. Dispose of contaminated gloves after use in accordance with applicable laws and good laboratory practices. Wash and dry hands.

Body Protection

Impervious clothing, The type of protective equipment must be selected according to the concentration and amount of the dangerous substance at the specific workplace.

Respiratory protection

Where risk assessment shows air-purifying respirators are appropriate use a full-face particle respirator type N100 (US) or type P3 (EN 143) respirator cartridges as a backup to engineering controls. If the respirator is the sole means of protection, use a full-face supplied air respirator. Use respirators and components tested and approved under appropriate government standards such as NIOSH (US) or CEN (EU).

Control of environmental exposure

Prevent further leakage or spillage if safe to do so. Do not let product enter drains.

---

9. PHYSICAL AND CHEMICAL PROPERTIES

9.1 Information on basic physical and chemical properties

a) Appearance	Form: solid
b) Odour	No data available
c) Odour Threshold	No data available
d) pH	No data available
e) Melting point/freezing point	Melting point/range: 83 - 88 °C (181 - 190 °F)
f) Initial boiling point and boiling range	No data available
g) Flash point	No data available
h) Evaporation rate	No data available
i) Flammability (solid, gas)	No data available
j) Upper/lower flammability or explosive limits	No data available
k) Vapour pressure	No data available
l) Vapour density	No data available
m)	Relative density No data available
n) Water solubility	No data available
o) Partition coefficient: noctanol/water	log Pow: 4.412
p) Auto-ignition temperature	No data available
q) Decomposition temperature	No data available
r) Viscosity	No data available
s) Explosive properties	No data available
t) Oxidizing properties	No data available

9.2 Other safety information

No data available

10. STABILITY AND REACTIVITY

10.1 Reactivity

No data available

10.2 Chemical stability

Stable under recommended storage conditions.

10.3 Possibility of hazardous reactions

No data available

10.4 Conditions to avoid

No data available

10.5 Incompatible materials

Strong oxidizing agents

10.6 Hazardous decomposition products

Other decomposition products - No data available

In the event of fire: see section 5

---

11. TOXICOLOGICAL INFORMATION

11.1 Information on toxicological effects

Acute toxicity

No data available
Inhalation: No data available
Dermal: No data available
No data available

Skin corrosion/irritation
No data available

Serious eye damage/eye irritation
No data available

Respiratory or skin sensitisation
No data available

Germ cell mutagenicity
No data available

Carcinogenicity
IARC: 3 - Group 3: Not classifiable as to its carcinogenicity to humans (N,N-Dimethylformamide)
NTP: No component of this product present at levels greater than or equal to 0.1% is identified as a known or anticipated carcinogen by NTP.
OSHA: No component of this product present at levels greater than equal to 0.1% is identified as a carcinogen or potential carcinogen by OSHA.

Reproductive toxicity
No data available

No data available

Specific target organ toxicity - single exposure
Inhalation - May cause respiratory irritation.

Specific target organ toxicity - repeated exposure
No data available

Aspiration hazard
No data available

Additional Information
RTECS: Not available

Warning: intolerance for alcohol can occur up to 4 days after dimethylformamide exposure. N,N-dimethylformamide is considered to be a potent liver toxin., Vomiting, Diarrhoea, Abdominal pain, To the best of our knowledge, the chemical, physical, and toxicological properties have not been thoroughly investigated

To the best of our knowledge, the chemical, physical, and toxicological properties have not been thoroughly investigated.

12. ECOLOGICAL INFORMATION

12.1 Toxicity

No data available

12.2 Persistence and degradability

No data available

12.3 Bioaccumulative potential

No data available

12.4 Mobility in soil

No data available

12.5 Results of PBT and vPvB assessment

PBT/vPvB assessment not available as chemical safety assessment not required/not conducted

12.6 Other adverse effects

No data available

13. DISPOSAL CONSIDERATIONS

13.1 Waste treatment methods

Product

Offer surplus and non-recyclable solutions to a licensed disposal company. Contact a licensed professional waste disposal service to dispose of this material.

Contaminated packaging

Dispose of as unused product.

14. TRANSPORT INFORMATION

DOT (US)

Not dangerous goods

IMDG

Not dangerous goods

IATA

Not dangerous goods

15. REGULATORY INFORMATION

SARA 302 Components

No chemicals in this material are subject to the reporting requirements of SARA Title III, Section 302.

SARA 313 Components

The following components are subject to reporting levels established by SARA Title III, Section 313:

	CAS-No.	Revision Date
N,N-Dimethylformamide	68-12-2	2007-07-01

SARA 311/312 Hazards

Acute Health Hazard, Chronic Health Hazard

Massachusetts Right To Know Components

	CAS-No.	Revision Date
N,N-Dimethylformamide	68-12-2	2007-07-01

Pennsylvania Right To Know Components

	CAS-No.	Revision Date
4,4′,4′′-s-Triazine-2,4,6-triyl-tribenzoic acid	61414-16-2	
N,N-Dimethylformamide	68-12-2	2007-07-01

New Jersey Right To Know Components

	CAS-No	Revision Date
4,4′,4′′-s-Triazine-2,4,6-triyl-tribenzoic acid	61414-16-2	
N,N-Dimethylformamide	68-12-2	2007-07-01

California Prop. 65 Components

This product does not contain any chemicals known to State of California to cause cancer, birth defects, or any other reproductive harm.

16. Other Information

Full text of H-Statements referred to under sections 2 and 3.

Acute Tox.	Acute toxicity
Aquatic Chronic	Chronic aquatic toxicity
Eye Irrit.	Eye irritation
Flam. Liq.	Flammable liquids

H226	Flammable liquid and vapour.
H302	Harmful if swallowed.
H302	Harmful if swallowed.
H312 + H332	Harmful in contact with skin or if inhaled
H315	Causes skin irritation.
H319	Causes serious eye irritation.
H335	May cause respiratory irritation.
H360	May damage fertility or the unborn child.
H413	May cause long lasting harmful effects to aquatic life.
Repr.	Reproductive toxicity
Skin Irrit.	Skin irritation
STOT SE	Specific target organ toxicity—single exposure

HMIS Rating

Health hazard:	2
Chronic Health Hazard:	*
Flammability:	0
Physical Hazard	0

NFPA Rating

Health hazard:	2
Fire Hazard:	0
Reactivity	Hazard: 0

Further information

The above information is believed to be correct but does not purport to be all inclusive and shall be used only as a guide. The information in this document is based on the present state of our knowledge and is applicable to the product with regard to appropriate safety precautions. It does not represent any guarantee of the properties of the product. Sigma-Aldrich Corporation and its Affiliates shall not be held liable for any damage resulting from handling or from contact with the above product. See www.sigma-aldrich.com and/or the reverse side of invoice or packing slip for additional terms and conditions of sale.

Preparation Information

Sigma-Aldrich Corporation
Product Safety—Americas Region
1-800-521-8956
Version: 5.10 Revision Date: 11/04/2014 Print Date: 12/09/2014

MSD 6.10. Triacetone triperoxide (TATP)

ChemSpectra, Inc.
2599 Still Meadow Lane
Lancaster, CA 93536
(661) 860-9014

Section 1—Identity

Product Name: YELLOW CAPPED SOLUTION
Test Mix for Peroxide, TATP, HMTD, and Chlorate

Section 2—Typical Composition

Component[a]	CAS #	% (by wt)
Ethyl Alcohol	64-17-5	40–70%
Water	7732-18-5	30–60%

[a] Carcinogenic components <0.1% and non-carcinogenic components <1% not considered hazardous and not listed

Section 3—Health Hazards

Warning Statement
Caution: Flammable liquid. May irritate eyes. May cause birth defects.
Routes of Absorption
Accidental ingestion, inhalation of vapor of aerosol, contact with the skin and eye.
Eye
May irritate eyes.
Skin
May dehydrate and/or defat skin.
Acute Toxicity
Ethyl Alcohol: Oral rat, LD_{50}: 7060 mg/kg; Inhalation rat, LC_{50}: 20,000 ppm/10-hour.

Organ System Toxicity

Ethyl Alcohol: May cause CNS depression, liver toxicity.

Reproductive and Developmental Toxicity

Ethyl Alcohol: May cause birth defects (fetal alcohol syndrome).

Carcinogenicity and Mutagenicity

None of the components are listed as a carcinogen under NTP, OSHA, or IARC.

Occupational Exposure Limits

Ethyl alcohol: OSHA Permissible Exposure Limits (PEL)—1000 ppm. American Conference of Governmental Industrial Hygienists (ACGIH) Threshold Limit Values (TLV)—1000 ppm.

Section 4—First Aid Precautions

Eye Contact

Flush eyes thoroughly with water for at least 15 min; notify medical personnel and supervisor if redness or irritation develops.

Skin Contact

Wash thoroughly with soap and water for 15 min; notify medical personnel and supervisor if redness or irritation develops.

Inhalation

Remove from exposure source; notify medical personnel and supervisor if breathing difficulties develop.

Ingestion

Rinse mouth thoroughly with water; notify medical personnel and supervisor to determine if vomiting should be induced.

Section 5—Fire Protection

Flammability/Explosivity

Product is considered a flammable liquid with flammable vapors (based on 70% ethyl alcohol content). Above its flash point (21 °C or 70 °F), vapor-air mixtures of alcohol between 3.3% by volume (the Lower Explosive Limit or LEL) and 19% by volume (the Upper Explosive Limit or UEL) are explosive in the presence of an ignition source.

Extinguishing Media

For packaging material, use water fog or fire extinguishing media suitable for Class B fires (e.g., dry chemical, carbon dioxide or foam).

Special Fire Fighting Procedures

Wear appropriate personal protective equipment. Decontaminate all equipment after use.

Section 6—Spill and Release Measures

If material is released or spilled, cordon off spill area. Limit the spread of the liquid with absorbent materials. Dispose of collected material in accordance with applicable waste disposal regulations.

Section 7—Handling and Storage

Avoid contact with skin, eyes or clothing. Store in accordance with material specifications. Wash thoroughly after handling.

Section 8—Exposure Control/Personal Protection

Eye Protection
Use safety glasses if eye contact is possible. Base the choice of protection on the job activity and potential for contact with eyes or face.
Respiratory Protection
Required use of respiratory protective equipment is not anticipated when product is used in a room with adequate mechanical ventilation.
Skin Protection
Use gloves if skin contact is possible. Wear lab coat or other protective over-garment if splashing is possible. Base the choice of protection on the job activity and potential for skin contact.
Engineering Controls
Use of local exhaust ventilation or a laboratory hood to mitigate exposure to volatile components of the mixture (principally ethyl alcohol) is not anticipated if adequate general room ventilation is available.
Other
Wash hands, face and other potentially exposed areas immediately in the event of physical contact with contents.

Section 9—Physical/Chemical Properties

For Ethyl Alcohol:

Appearance and Odor:	Clear, colorless liquid; mild pleasant whiskey-like odor.
Solubility:	Miscible in water.
Density:	0.79 g/mL @ 20 °C/4 °C
pH:	No information found.
% Volatiles (v @ 21 °C):	100
Boiling Point:	78 °C (172 °F)
Melting Point:	−114 °C (−173 °F)
Vapor Density (Air = 1):	1.6 g/L
Vapor Pressure (mm Hg):	40 @ 19 °C (66 °F)
Evaporation Rate:	~1.4 (CCl_4 = 1)

Section 10—Stability/Reactivity

Stability:	Stable chemically
Hazardous Polymerization:	Will not occur
Hazardous Decomposition Products:	Carbon monoxide, carbon dioxide
Conditions to Avoid:	Heat, flames, ignition sources

Section 11—Toxicological Information

Section 12—Environmental Information

Persistence and Degradability

Ethyl Alcohol: Expected to readily degrade.

Aquatic Toxicity

Ethyl Alcohol: Not expected to be toxic to aquatic life; 96-h LC_{50} values in fish exceeded 100 mg/L

Section 13—Waste Disposal Methods

All wastes containing the product should be properly labeled. Dispose of wastes in accordance to prescribed federal, state, and local guidelines, e.g., appropriately permitted chemical waste incinerator. Rinse waters resulting from spill cleanups should be discharged in an environmentally safe manner, e.g., appropriately permitted municipal or on-site wastewater treatment facility.

Section 14—Transportation Information

In addition to the identity label, containers of this material should have affixed the following:
UN1170, Ethanol Solution, 3, II

Section 15—Labeling/Regulatory Information

European Union (EU) Risk and Safety Phrases
R10: Flammable
R36: Irritating to the eyes
R61: May cause harm to the unborn child
California Proposition 65
None of the components are listed.

Section 16—Other Information

No additional information.

——

The above information is offered in good faith and with the belief that it is accurate. As of the date of issuance, we are providing all information relevant to the foreseeable handling of the material. However, in the event of an adverse incident associated with this product, this Material Safety Data Sheet is not, and is not intended to be, a substitute for consultation with appropriately trained personnel.
Date of Issue: November 11, 2010

MSD 6.11. 1,3,3-Trinitroazetidine (TNAZ)

MATERIAL SAFETY DATA SHEET

MSDS D0582
Issue 1
Latest Revision: February 19, 2003

ATK Thiokol Propulsion P.O. Box 707 Brigham City, UT 84302-0707	Emergency Phone No. (435) 863-8545 Product Information (435) 863-3325

Section 1. CHEMICAL PRODUCT IDENTIFICATION

NAME: 1,3,3-Trinitroazetidine
SYNONYMS: TNAZ

NOTICE: Under TSCA regulations this chemical material is for Research and Development Use Only under the supervision of a technically qualified individual.

Section 2. COMPOSITION AND INFORMATION ON INGREDIENTS

Ingredients	CAS #	Percent	PEL (TWA)	STEL	TLV
1,3,3-Trinitroazetidine	97645-24-4	100	NE	NE	NE
NE: Not Established					

Section 3. HAZARDS IDENTIFICATION

Exposure Limits: Have not been established for this material.
Inhalation: Unknown. Avoid inhalation or breathing particulate. May be toxic if inhaled.
Eyes: Unknown. Avoid eye contact. May cause eye irritation.
Skin: Unknown. Avoid skin contact. May cause skin irritation.
Ingestion: Unknown. Avoid ingestion. May be toxic if ingested.
Existing conditions that may be aggravated:

Section 4. FIRST AID MEASURES

Inhalation: Move to fresh air. Administer artificial respiration or oxygen. Contact physician.
Eyes: Flush with water for 15 minutes while holding eyelids open.
Skin: Remove contaminated clothing and wash with soap and water. Contact physician.
Ingestion: Induce vomiting if conscious. Contact poison control center or physician immediately.

Section 5. FIREFIGHTING MEASURES

SPECIAL FIRE FIGHTING PROCEDURES: DOT 1.1, Explosive! Do not attempt to fight fire. If ignited, this material may detonate. If this material detonates, thrust and overpressure may result with uncontrollable ballistic property. Fire Fighting should belimited to evacuating an area proportional to the amount of explosive that may burn or detonate, and to preventing the spread of fire beyond the isolated area.
EXTINGUISHING MEDIA: Use sprinkler or deluge system where available to prevent the spread of fire to other areas.

UNUSUAL FIRE AND EXPLOSIONS HAZARDS: Material liberates toxic products when subjected to fire or heat. Material carries 1.1 explosive classification; may deflagrate or detonate and containers may rupture in a fire.

Section 6. ACCIDENTAL RELEASE MEASURES

Precautions if Container is Damaged or Material Spilled: Avoid open flame,sparks, heat, impact, shock, friction, and temperatures above 100°C (212°F). If accidentally ignited, a detonation should be anticipated, causing a shock wave and spreading of burning material with the release of toxic decomposition gases. Contact proper authorities.

Section 7. HANDLING AND STORAGE

Avoid eye contact. Store material in an approved container in a cool, dry place. Building and transportation equipment must be protected from lightning and other forms of static discharge. Do not store at temperatures above 100°C.

Section 8. EXPOSURE CONTROLS - PERSONAL PROTECTION

VENTILATION: Provide sufficient mechanical ventilation to limit material inhalation.

RESPIRATORY PROTECTION: In the absence of adequate mechanical ventilation, an approval NIOSH particulate respirator (P100) may be necessary when handling this material.

PROTECTIVE GLOVES: Use impervious gloves such as neoprene.

EYE PROTECTION: Chemical goggles.

OTHER PROTECTIVE EQUIPMENT: flame resistant clothing and conductive safety shoes.

Section 9. PHYSICAL AND CHEMICAL PROPERTIES

VAPOR DENSITY:	<1
SPECIFIC GRAVITY:	1.83
SOLUBILITY IN WATER:	Low
VAPOR PRESSURE:	<0.01
EVAPORATION RATE:	<1
MELTING POINT:	101°C
BOILING POINT:	>200°C
APPEARANCE AND COLOR:	White solid, no odor.
DETECTION METHODS:	NE
pH:	NE
FLASHPOINT:	NE

Section 10. STABILITY AND REACTIVITY

STABILITY: Stable under normal conditions of storage and use.

Conditions to Avoid: Open flame, sparks, heat, impact, shock, friction, and temperatures above 100°C.

INCOMPATIBILITY (Materials to Avoid): Strong caustic

HAZARDOUS DECOMPOSITION PRODUCTS: Dinitrogen tetroxide, oxides of nitrogen (NOX).

HAZARDOUS POLYMERIZATION: Will not occur.

OTHER HAZARDS: Unknown.

Section 11. TOXICOLOGICAL INFORMATION

ACUTE EFFECTS: Moderately toxic orally, TNAZ caused transitory irritation to the conjuctive of the eye.

CHRONIC EFFECTS: Not known. May affect internal organ systems.

TARGET ORGAN(s): Not known

Section 12. ECOLOGICAL INFORMATION

Data not available.

Section 13. DISPOSAL CONSIDERATIONS

Dispose of in accordance with federal, state, and local regulations.

Section 14. TRANSPORTATION INFORMATION

Transport in accordance with federal, state, and local regulations. See 49 CFR – rules governing transportation.

TNAZ can only be shipped in **25 gram quantities or less** in accordance with **DOT-E 8451** until an Interim Hazard Classification (IHC) from a DoD or DOE agency or an EX number from the USDOT Competent Authority for the United States is obtained for this material. This material can be transported for developmental testing in accordance with the requirements set forth in 49 CFR 173.56(e).

Section 15. REGULATORY INFORMATION

1,3,3-Trinitroazetidine (TNAZ) is a "new chemical" as defined by the Toxic Substance Control Act (TSCA) and is not listed on the TSCA Inventory. It is **"For Research and Development Use Only"** and can only be used by or under the supervision of a **Technically Qualified Individual** (TQI).

NOTICE: Under TSCA regulations this chemical material is for Research and Development Use Only under the supervision of a technically qualified individual.

Section 16. OTHER INFORMATION

For R&D use only. To the best of our knowledge the information contained herein is correct. All chemicals may present unknown health hazards and must be used withcaution. Although certain hazards are described herein, we cannot guarantee that these are the only hazards that exist. Final determination of the suitability of the chemical is the sole responsibility of the user. Users of any chemical should satisfy themselves that the conditions and methods of use assure that the chemical is used safely.

NO REPRESENTATIONS OR WARRANTIES, EITHER EXPRESS OR IMPLIED, TO INCLUDE WARRANTIES OF MERCHANTABILITY, FITNESS FOR A PARTICULAR PURPOSE, OR ANY OTHER NATURE ARE MADE HEREUNDER WITH RESPECT TO THE INFORMATION CONTAINED HEREIN OR THE CHEMICAL TO WHICH THE INFORMATION REFERS.